NASA
Reference
Publication
1179

1988

Tip Aerodynamics and Acoustics Test

A Report and Data Survey

Jeffrey L. Cross
and Michael E. Watts
Ames Research Center
Moffett Field, California

National Aeronautics
and Space Administration

**Scientific and Technical
Information Division**

TABLE OF CONTENTS

Page

SYMBOLS

A_z	azimuth
a_0	steady term in harmonic analysis
a_1	diameter of rotating cylinder
C	blade chord length, in.
C_c	chordwise force coefficient
C_d	drag coefficient
CG	longitudinal center of gravity
C_k	amplitude at kth harmonic of series
C_ℓ	lift coefficient
C_m	pitching-moment coefficient
C_n	normal force coefficient
C_p	pressure coefficient
C_T	thrust coefficient
D	drag
FS,%	percent full scale
GW	aircraft gross weight
g	acceleration caused by Earth's gravity
IAS	indicated airspeed
KTAS	true airspeed, knots
L	lift
M	advancing-tip Mach number
M_c	critical Mach number

OAT	outside air temperature
psia	pounds per square inch absolute
psid	pounds per square inch dynamic
R	total blade radial length, in.
r	partial blade radial length, in.
r_1	radial distance from center of rotating cylinder
T_o	starting point of measured data, sec
V_h	maximum velocity achievable in level flight
x	blade chord location from leading edge
y	vertical distance from two-dimensional airfoil centerline
Γ	circulation of rotating cylinder
γ	ratio of specific heats
μ	rotor advance ratio
σ	rotor solidity
ϕ_k	phase at kth harmonic of series
ψ	slip stream function

1. SUMMARY

In a continuing effort to understand helicopter rotor tip aerodynamics and acoustics, a flight test was conducted by NASA Ames Research Center. The test was performed using the NASA White Cobra and a set of highly instrumented blades. All aspects of the flight test instrumentation and test procedures will be explained. Additionally, complete data sets for selected test points will be presented and analyzed. Because of the high volume of data acquired, only select data points can be presented here. However, access to the entire data set is available to the researcher upon request.

2. INTRODUCTION

This report describes a flight test conducted at the NASA Ames Research Center to study rotor tip aerodynamics and acoustics. The Tip Aerodynamics and Acoustics Test (TAAT), conducted on an AH-1G Cobra, used the highly instrumented rotor blades and instrumentation hardware developed for the U.S. Army Operational Loads Survey (OLS) test. The OLS test, flown using performance flight testing techniques, measured the rotor airloads on a set of blades equipped with instrumentation arrays at five radial stations. For the TAAT, three new radial stations were added in the tip region of the blade. The total number of data streams in the rotating system remained 314, of which 188 were absolute pressure transducers. Flight testing was divided into four phases: performance, air-to-air acoustics, air-to-ground acoustics, and aerodynamics.

Each of the four flight-test phases of the TAAT concentrated on different areas of investigation. The first phase, performance, was mainly concerned with duplicating the flight conditions flown during the OLS test for the purpose of determining data repeatability. The second phase, air-to-air acoustics, obtained rotor noise data from microphones that were stationary with respect to the helicopter. The microphones used for this phase were mounted on the YO-3A which was flown in formation with the Cobra. This method of testing simplified the analysis required in both prediction and correlation of the data. Air-to-ground noise data were taken during Phase III for correlation of flyover acoustics analysis with blade loads. In the fourth and final phase, aerodynamics, several specific thrust coefficients, tip Mach numbers, and advance ratios were flown to study the correlation between these parameters and pressure distributions.

The data accumulated from both OLS and TAAT reside at Ames Research Center and are accessible through the Data from Aeromechanics Test and Analytics - Management and Analysis Package (DATAMAP). These two data bases are currently being used by approximately nine agencies or companies to conduct correlations of flight data with theory. Technical areas being addressed vary from blade-vortex interaction, encountered primarily in low-speed flight, to high-speed compressibility effects. These efforts include such two-dimensional aerodynamic codes as C81, Comprehensive Analytical Model of Rotorcraft Aerodynamics and Dynamics (CAMRAD) and TRANDES and the three-dimensional aerodynamic code ROT22. The investigations include such specialized areas as full- and model-scale acoustic comparisons as well as autorotation phenomenon. Results of some of those studies are presented in references 1-3.

A data survey is presented here covering a sample of each of the sensor types included in this test. The survey includes data plots, summary tables and selected tables of data harmonics. Data accuracy and data-base limitations are discussed. A data analysis section is included which addresses the aerodynamic phenomena presented in the data survey section. Appendices provide reference information on the following: TAAT flight test plan (appendix A); TAAT annotated flight cards (appendix B); TAAT instrumentation set-up sheets (appendix C); acoustic test microphone gain settings and calibration charts (appendix D); DATAMAP information file for the TAAT data (appendix E); TAAT undigitized data list (appendix F); and OLS/TAAT full-scale airfoil coordinates (appendix G). A separate report is being compiled which will present a data table of up to 15 harmonics for a large representative sample of available test points.

3. BACKGROUND

Since the beginning of vertical flight, engineers have attempted to analytically model the lifting rotor. The aim of this modeling has been to accurately predict aircraft performance and vibration, such that improvements could be made in subsequent aircraft designs. To accomplish this goal the aerodynamic loading of the rotor was required, as it is both the forcing function behind the vibration and the heart of the rotor's performance. The accuracy of the models developed could be measured easily enough by comparing the model predictions with measured values. However, when the comparisons were not good, as was the rule rather than the exception, improvements to the models were difficult. The engineer was always stymied by the inability to measure the intermediate step in the modeling procedure, rotor airloads. To fill this void a number of flight tests and wind tunnel tests were conducted to attempt to measure the complex aerodynamic flow associated with helicopter flight. Technical areas investigated included a complex combination of three-dimensional, transonic, unsteady, and reversed-flow aerodynamics.

A number of tests have been conducted since the late 1950s to measure helicopter rotor airloads. Two of the earliest studies were conducted on an H-34 rotor system outfitted with differential pressure transducers, strain gages, and a full assortment of hub sensors. The first test was conducted in flight (ref. 4), while the second was conducted in the NASA 40- by 80-Foot Full-Scale Wind Tunnel (ref. 5). Subsequent tests were conducted on CH-47, XH-51A, NH-3A and CH-53A aircraft (refs. 6-9). The majority of these tests used differential pressure transducers, had a limited number of sensor locations, and limited frequency response. These tests have all helped to improve the understanding of rotor loading distributions. However, because of the use of differential pressure transducers, the data could not address the individual mechanisms which produced the loads. Additionally, comprehensive knowledge of the airload distributions was limited by the low-frequency rates at which the data were presented and the limited number of sensors available, specifically in the chordwise sense.

A test of three airfoils was conducted at NASA Langley Research Center in the mid-1970s (refs. 10-16). This test, conducted on the NASA White Cobra, included an assortment of strain gages and a single chordwise array of pressure transducers on each of the three instrumented blades. Absolute pressures were measured and the recording system had better data resolution than that of previous tests. The data instrumentation and recording system for this series of tests was quite unorthodox (ref. 17), in that the data were radioed from the rotating system to the fixed system, as opposed to conditioning the data and then sending them through slip rings mounted on the rotor shaft to the fixed system.

A second flight test, conducted by Bell Helicopter for the U.S. Army, was undertaken at about the same time. This test, the Operational Loads Survey (ref. 18), like the Langley tests, was also flown on an AH-1G. The OLS blades were slightly modified standard 540 blades. The OLS blades contained 144 absolute-pressure sensors arranged in five chordwise arrays on one blade, and a mix of strain gages, accelerometers, hot-wire annenometers, and flow meters on the other blade. The total number of sensors in the rotating system was 314, some of which had a frequency response to 400 Hz. The test addressed flight regimes that included autorotations, accelerations, hovers, high-gravity (g) turns, partial power descents and maneuvers. Acoustic measurements were also recorded by mounting several microphones externally on the aircraft and by flying over a ground microphone array. This test has produced a large number of technical reports, covering both aeromechanics and acoustics, some of which are given in references 19-24. A fuselage shake test was also conducted as a part of the OLS test (ref. 25).

Several instrumented rotors have been tested by the Royal Aircraft Establishment in the United Kingdom (ref. 26). These tests have been conducted on Sea King, Lynx, and Puma aircraft and have generally included several chordwise instrumentation arrays concentrated in the tip regions of the blades. Often, these tests have used standard blades with a glove attached over a short span segment with the instrumentation embedded in the glove. Several airfoil and tip shape studies have been conducted in this manner.

The French have also begun conducting rotorcraft airloads tests. One such test was conducted on a Gazelle equipped with an advanced geometry three-bladed rotor. Due to data acquisition limitations, each test point requires up to 24 consecutive rotor rotations to acquire one complete data-acquisition cycle. This test and sample data tables are presented in reference 27.

The Tip Aerodynamics and Acoustics Test is a follow-on to the OLS test. Three chordwise arrays of absolute pressure transducers were added in the tip region of the OLS pressure blade, increasing the total number of pressure transducers to 188. The flight test plan for the TAAT, presented in appendix A, had an expanded test matrix. Several scale model wind tunnel tests have been conducted of the OLS blades in the ONERA and DNW wind tunnels (refs. 28 and 29). A two-dimensional wind tunnel test of the OLS airfoil was also conducted by NASA Langley Research Center (ref. 30).

Plans are currently under way to construct and test two highly instrumented, four-bladed rotor systems. These tests, to be conducted on the Boeing Vertol model 360 and a Sikorsky UH-60A, will have an increased number of pressure transducers, and more chordwise and radial arrays as well as higher aggregate frequency responses (ref. 31). The results of these tests have already improved, and will continue to improve, our understanding of rotorcraft aerodynamics, dynamics, and acoustics.

4. TEST EQUIPMENT

The TAAT involved the following four sets of test systems: the NASA AH-1G White Cobra, the YO-3A Acoustics Research Aircraft, the Ames Moffett Ground Station system, and the NASA Crows Landing facility. With the exception of the ground station, each system was self-contained, with only broadcast time code available as the common link. Primary flight data were recorded aboard the AH-1G and YO-3A, with flyover acoustics and radar tracking data being recorded at Crows Landing. The ground station was used to monitor safety-of-flight data streams in the first test phase and for postflight data which were stripped out for all test phases.

4.1 AH-1G Cobra

The AH-1G Cobra used during the TAAT (fig. 1) was the first production Cobra built, serial number 20004. Included in its past were hard landing tests for the Cobra series and research flights at Langley Research Center (refs. 10-16, 18). The physical characteristics of the AH-1G are presented in table I. The TAAT test equipment included on the Cobra can be divided into the following categories: fuselage, rotor system, and data recording.

4.1.1 Fuselage- The airframe was instrumented to monitor fuselage attitudes and rates, control stick positions, vertical accelerations at both the aircraft center of gravity and the pilot's seat, engine speed and torque, main rotor shaft torque and perpendicular and parallel bending, and both main and tail rotor rpms. The aircraft was also equipped with an instrumentation boom to monitor static and dynamic pressure, outside air temperature, and angles of attack and sideslip. The item codes for the aircraft state sensors are presented in table II. The static pressure and outside air temperature (OAT) sensors proved to be erratic throughout the test. However, altitude and OAT readings were manually recorded during the test, so although the sensor losses were inconvenient it was not a major impediment.

During the TAAT, the flight test engineer kept extensive notes on each flight condition. The resultant flight cards, presented in appendix B, contain altitude, OAT, airspeed, main rotor speed, fuel readings, and elapsed time data, as well as comments on test point quality. During most of Phase IV, gage readings of engine torque, engine speed, and exhaust temperature were recorded in addition to those items just mentioned.

Of some interest is that the side-slip and angle-of-attack vanes on the instrumentation boom may have reduced data accuracy on the early flights. This reduction of accuracy is due to the balsa wood angle vanes being shredded on the early flights. However, when reinforced with a fiberglass skin, the vanes remained intact.

4.1.2 Rotor system- The instrumented blades used for this test were the original OLS blades (ref. 18). The blades had been modified from the production standards by the addition of a 0.1-in.-thick honeycomb glove. The glove was glued onto the blade so that the blade could be instrumented, yet retain its aerodynamic shape. The standard thickness to chord ratio was maintained by extending the trailing edge 1.36 in. Adjustments to the weight in the leading edge and tip were required in order for the blade dynamics of the instrumented blade to closely match the production blades. Appendix G presents the airfoil coordinates of the OLS blade. Five chordwise sensor arrays had been buried in the glove of each blade for the OLS test. The white blade contained 144 pressure transducers (fig. 2), and the red blade held an assortment of strain gages, leading-edge hot-wire anemometer arrays, accelerometers, and flow-field magnitude and direction sensors (fig. 3).

For the TAAT, three additional radial stations of pressure transducers were added to the white blade in the tip region (fig. 4). The pressure transducer layout on the white blade for the TAAT is shown in figure 5. The original OLS pressure instrumentation was housed in chordwise channels with an aluminum cover strip (fig. 6). The additional pressure sensor locations for the TAAT were obtained by routing out the nomex honeycomb glove at the desired sensor locations (fig. 7). Table III shows the item codes for the TAAT pressure transducer locations by chordwise array. Also note that at the 91% radius, 92% chord station, the trailing-edge sensor was not installed because of the trailing-edge tab and the wire routing for the outboard sensor arrays.

As part of the preparations for TAAT all pressure transducers from the OLS test were first cataloged by serial number, then removed from the blades, recalibrated, and reinstalled in their original locations. Transducers that did not meet specifications were replaced. The new sensor location transducers were cataloged, calibrated, and installed.

The amount of instrumentation on the red blade was reduced from the OLS test to compensate for the added pressure transducers on the white blade. The instrumentation locations on the red blade for the TAAT are shown in figure 8. The corresponding sensor locations and associated item codes for the blade accelerometers, strain gages, boundary-layer buttons (BLBs), and hot-wire gages are presented in tables IV-VII, respectively.

The strain gages and miniature accelerometers were installed on the red blade to measure blade loading and motion (fig. 9). The accelerometers, temperature compensated piezoresistive types, were epoxied directly to the blade surface and were then potted over with plastic filler to maintain the airfoil contour. The accelerometers were aligned so as to measure blade beamwise or chordwise acceleration. The strain gage and associated wiring were attached to the blade before the installation of the blade glove. The strain gages, which included redundant spares, measured blade beamwise and chordwise bending and blade torsion.

The hot-wire anemometer arrays were designed to measure the local blade-stagnation points. Angle of attack was then to have been deduced from the location of the stagnation point using hot wires on a two-dimensional airfoil wind tunnel model. However, because of size restrictions, the two-dimensional data obtained by Langley Research Center in the 6- by 28-in. tunnel did not include hot wires.

The hot-wire sensors consist of an array of from 10 to 19 temperature sensing elements. The array consisted of a flexible 0.004-in.-thick printed circuit, bonded to the blade's leading edge with 0.0020-in.-wide conductors aligned parallel with the chord and 0.110 in. apart. Hot-wire filaments of 0.0012-in. diam were soldered across the gaps on the printed circuit at staggered stations around the leading edge. Figure 10 shows the wiring arrangement and the array installation of the hot wires on the blade.

The flow-field sensors are referred to as BLBs, although they extend slightly above the boundary layer. The BLBs measure both magnitude and direction of the local airflow. Each BLB consists of two pipettes, which measure total pressure, and a static port. Each pipette delivers flow from the slip stream to a separate differential pressure transducer. The static port was connected to the backside of each differential pressure transducer, and is the reference pressure. The resultant measurement is the airflow's dynamic pressure. The pipettes are geometrically arranged at 90° to each other, and 45° to the blade chord. An exploded view of a BLB is shown in figure 11. An algorithm that computes flow velocities and directions from these data is included in the data analysis program.

The sensors on the red blade were all recalibrated prior to the test. The strain gages on the red blade were recalibrated and the primary gages of the redundant sets were identified. The BLBs were given functional and leak checks, the pitot probes were calibrated in a wind tunnel, and the final assemblage was given a five-point calibration. Accelerometers were given a simple 2-g variation check which consisted of hanging the blade, taking a reading, inverting the blade, and taking a second reading. This was the limit of the calibration, as the accelerometers were glued in place, and hence could not be removed for individual testing. Hub instrumentation included blade feathering and flapping, yoke loads, and pitch-link loads.

Appendix C is a collection of the instrumentation set-up sheets used during the TAAT, as well as the sign convention for the sensors. The set-up sheets provide the general pretest calibration values of each sensor, with the detailed sensor calibration results being presented in reference 32. New set-up sheets were issued after any alteration of the instrumentation occurred. Alterations could include recalibration or replacement of a gage. However, the hot-wire anemometers were repaired frequently without new set-up sheets being issued.

The sensors were all wired to multiple prong plugs located at the blade root ends (fig. 12). This configuration facilitated blade removal. The blades were removed on two separate occasions: once when the main rotor transmission was replaced, and a second time when the feathering bearings were replaced.

At the completion of the TAAT the blades were determined to be no longer flightworthy. The loss of airworthiness was due to the following: (1) the blades had been manufactured 8 yr earlier, (2) the blades were not visually inspectable because of the installed glove, (3) the blades had accumulated 28 flight hr during the OLS test and 35 hr during the TAAT, and (4) the blades had spent 4 yr not in an atmospheric controlled storage. As a result the instrumentation was removed for use on other programs and the blades were scrapped.

4.1.3 Data recording system- The 314 data streams from the rotating system were picked up at the hub and fed to the multiplex (mux) bucket (fig. 13). The mux bucket, originally designed and used on the OLS test (ref. 32), was mounted atop the teetering hub. The 314 analog data streams were multiplexed onto twenty 16-band data channels using frequency modulation (FM). Data were brought down out of the rotating system, via slip rings, to the recording instrument package. The mux bucket is 21 in. in diameter, 9 in. tall, and weighs 55 lb. The bucket was bolted directly to the main rotor hub and teetered with it. The slip-ring assemblage was attached to the shaft and passed through a 6-in. by 12-in. channel in the center of the bucket. Data were fed into the mux bucket via 20 radio-frequency filtered plugs located on the bottom plate. Two of this type plug, located at the top of the bucket, passed the data to the slip-ring assembly. The bucket contained twenty 16-band FM multiplexers, two transducer bridge voltage regulators, five hot-wire excitation and monitor assemblies, interfacing circuits and signal filters. Each of the FM multiplexer units consisted of a 16-signal-conditioning amplifier and oscillator, a mixer amplifier and a connector plug. This hardware was also equipped with externally accessible adjustment pots which controlled bridge balance, amplifier balance, and excitation voltages for the hot-wire anemometers and the two bridge voltage regulators.

The recording instrumentation package (fig. 14), located in the Cobra ammunition bay, consisted of a 28-track FM recorder, time-code generator, power supplies, attitude and rate gyros and discriminators for the fixed-system sensors. For the acoustic tests, a time-code receiver was installed for time alignment between remotely recorded and aircraft recorded data. The recording package was mounted on a sliding rack for ease of access during preflight calibration and maintenance. The recorder used 1-in.-wide magnetic tape on 14-in.-diam reels, and was recorded at 15 ips. The time-code generator provided a combined time and run number data stream to the recorder and pilot comments were also recorded on this data channel. Two power supplies were included, each supplying power to half of the sensors in the rotating systems. The sensors recorded on tracks 1-10 were powered by one power supply and tracks 11-20 by the second. Prior to being recorded, the gyro, instrumentation-boom, and control-position data were processed by the stationary multiplex unit.

4.2 YO-3A Acoustic Research Aircraft

During the TAAT, the YO-3A Acoustic Research Aircraft (fig. 15) was flown in formation with the AH-1G to record the air-to-air acoustic data. The Acoustic Research Aircraft is a specially instrumented version of the low-speed observation aircraft manufactured for the military by the Lockheed Aircraft Corporation. The Acoustic Research Aircraft is used as a flying microphone platform for the study of rotorcraft noise. The YO-3A is equipped with a special instrumentation package which includes the following: three one-half inch microphones, one on each wing tip and one atop the vertical tail; gain adjustable microphone power supplies; an instrumentation boom; a radio link with the test helicopter that carries the main rotor contactor signal; an IRIG-B time-code receiver; and a 14-track FM tape recorder.

The YO-3A is powered by a highly modified Continental 210 horsepower engine and a three-bladed wide-chord wooden propellor. The engine is equipped with a very effective muffler which combines with the low tip-speed propellor to produce a very quiet aircraft. The physical characteristics of the YO-3A are presented in table VIII. A more thorough discussion of the Acoustic Research Aircraft is presented in references 33 and 34.

4.3 Ground-Based Acoustic Test Range

The ground-based acoustic test range, located at NASA's Crows Landing Facility in the San Joaquin Valley, was used for the flyover acoustic testing phase of the TAAT. The test range consists of three instrumentation packages: acoustics, meteorological, and tracking (fig. 16). The acoustics package contains tower and tripod mounted microphones, amplifier line drivers, and a tape recorder. The tracking package includes radar and laser trackers and a computerized data handling system. The meteorological package consists of aerial and ground-based temperature, humidity, and wind-velocity measurements. The ground-based acoustics package is itemized in table IX.

The microphone layout, corresponding to the FAA standard, had a microphone on the centerline of the flightpath with additional microphones 150 m on either side of the centerline, as shown in figure 16. These microphones, shown in figure 17, were mounted on tripods, 4 ft above ground level. Two additional microphones, located along the centerline and right stations, were mounted atop 40-ft towers, shown in figure 18. All microphones were adjusted such that their diaphragms were coplaner with the expected nominal flightpath. The flightpath centerline was set up along the right shoulder of the runway. This configuration kept all test hardware, except the cable to the left microphone, off the runway, thus leaving the runway available for emergency use.

The tracking package consisted of two radar trackers and one laser tracker, shown in figure 19. The radar trackers are improved models of the Nike Hercules X-Band monopulse radars. Their range was from 250 to 20,000 yards, with an average accuracy of 7 ft at 1 sigma out to 15,000 ft and 7 ft plus 1% past 15,000 ft. The accuracy of the radar azimuth measurement was 0.3 milliradians at 1 sigma. Video cameras augmented the tracking system, providing visual verification of proper tracking. The radar trackers were designed for use with a radar beacon mounted on the target, although they work acceptably with skin tracking. The laser, mounted on the south radar tracker, is a 1 MW pulsed Ni-Yag which emitted a pulsed beam that reflected off a corner reflector mounted on the Cobra. The laser tracker typically began tracking only after a positive radar lock-on had been achieved. The laser tracker had an average accuracy of 1 ft at 1 sigma out to 30,000 ft and 2 ft at 2 sigma beyond that distance.

The meteorological data were obtained from two sources. The first source, mounted on a platform 24 ft above ground level, measured windspeed, direction, and air temperature. The platform was located between the two radar trackers. Humidity readings were taken manually at ground level. The automated meteorological data were processed, along with the tracking data, on a pair of PDP 11-45 computers and stored on digital tape. The second atmospheric measurement source involved manually recording humidity and temperature readings taken at various altitudes over the ground array. These readings were obtained by flying hand-held instruments in a fixed-wing aircraft at selected intervals throughout the test.

4.4 Ground Station

The ground station at the Ames Research Center was used during the TAAT for monitoring aircraft telemetry and for postflight data-integrity checks. A complete set of FM discriminators was housed in the ground station (fig. 20). They were used both for the telemetry monitoring and postflight strip-outs. A calibration rack was used for all preflight calibration checks on the aircraft instrumentation (fig. 21).

5. TEST DESCRIPTION

The TAAT was conducted to obtain an extensive detailed data base of rotor loads and acoustics. To accomplish this goal, the test was divided into four phases with several support tests also conducted. Phase I involved gathering data using aircraft performance testing techniques which would allow comparison and correlation with the OLS data. Phase II obtained acoustic data of the Cobra by flying formation with the YO-3A for identification of acoustic sources on the rotor blades. Phase III consisted of low-altitude flybys of the Cobra over the acoustic ground array which allowed comparison of acoustic detection and the responsible aerodynamic source. Phase IV gathered aerodynamic data while varying key nondimensional parameters. The pilot cards, presented in appendix B, list the individual flight conditions with run numbers for these four phases. Because of instrumentation problems, not all of the conditions flown produced complete data sets. However, all flights flown are included in the pilot cards, with data restrictions so noted.

Three separate support tests were conducted after the completion of the flight test. The pressure-instrumented blade was tested for transducer integrity during the Supplemental Calibration Test (ref. 34). A two-dimensional wind tunnel model of the OLS/TAAT blade airfoil section was tested at the Langley Research Center, the results of which are presented in reference 30. Two separate airspeed calibration tests were conducted, one prior to testing, the other upon completion of testing.

5.1 Phase I: Performance

Phase I of the TAAT gathered aircraft performance data. The test matrix (table X) was obtained by selecting test conditions from the OLS test matrix. The aim of the performance phase was to gather test data with the upgraded OLS equipment that would closely match the original OLS data. This replication of flight conditions would help verify the authenticity of the aerodynamic phenomena displayed in the OLS data and would also provide tip airload measurements for such flight conditions as hovers, accelerations, high-g turns, and autorotations. The test points for Phase I were conducted at two nominal gross weights, 8500 lb and 9500 lb, and three center of gravity (CG) configurations: forward, mid, and aft.

Safety of flight sensors were monitored at the ground station during Phase I. Once the test envelope was bounded and the established safety limits not exceeded, the in-flight monitoring of the safety of flight sensors was dispensed with. In an attempt to repeat the OLS results as closely as possible, the rotor speeds and test altitudes were varied with each test point. The rotor speeds were adjusted to maintain a similar advance ratio and the altitudes were varied to maintain the same density ratio as that of the OLS test. A program, run on a hand-held calculator, was used to calculate the appropriate rotor speed and altitude, considering the atmospheric conditions at the time of the test.

The test matrix for Phase I was not as complete as had been hoped as the monitored hub loads were found to be excessive during 2-g turns and quick stops. These two maneuvers were, therefore, not performed for other than the aft CG, 8600-lb aircraft configuration.

5.2 Phase II: Air-to-Air Acoustic

Phase II of the TAAT gathered acoustic data obtained with the YO-3A Acoustic Research Aircraft while flying formation with the Cobra (fig. 22). The goal of Phase II was to obtain simultaneous in-flight acoustic and blade pressure data of a rotor system. The test point matrix (table XI) consists of speed sweeps and partial power descents. The flight test techniques used here were patterned after those pioneered by Schmitz and Boxwell (refs. 36 and 37) and detailed in references 33 and 34. Analysis of data obtained in this phase will lead to a better understanding of the relationship between rotor acoustics and airloads.

For the first time, full-scale in-flight airloads and measured far field acoustic results, without the complications of doppler, atmospheric, and reflective effects, are available for correlation with predictive codes. A programmable hand calculator was again used, much as in Phase I, to set up test conditions to maintain a constant rotor thrust coefficient and obtain specific advancing tip Mach numbers and rotor advance ratios. The test matrix flown was partitioned by four different aircraft formations. In the first position, the helicopter flew in trail formation (fig. 23) with the rotor disk in the same plane as the tail microphone on the YO-3A. In the second and third positions, the helicopter flew above the plane of the YO-3A while behind the left and right wing tips, respectively (figs. 24(a) and 24(b)). The fourth formation began in the first formation position, and ended with the helicopter having flown an arc to a position directly above the YO-3A (fig. 25). The first formation measured predominantly the high-speed thickness noise emanating off of the advancing blade. The second and third positions measured the blade-vortex interaction noise, found predominantly at lower speeds during descent. The last formation was primarily used to measure the acoustic directivity. A small set of data was taken at higher altitudes which resulted in a higher nondimensional thrust coefficient, to measure the effects of rotor loading on acoustics.

5.3 Phase III: Flyover Acoustics

Phase III of the TAAT gathered acoustic data from ground-based microphones during aircraft flyovers. The test matrix (table XII) consisted of level speed sweeps, approaches, climbouts, and hovers. The goal of Phase III was to simultaneously obtain flyover acoustics data and rotor loads data. By measuring the perceived noise signals at ground level and comparing them with the rotor loads that produced the noise, an improved understanding of helicopter detectability can be gained. In an attempt to correlate the flyover acoustic data with the in-flight acoustic data of Phase II, several test points were flown over the ground microphone array with the Cobra in formation with the YO-3A.

The level, constant speed flybys were conducted down the right shoulder of the runway, over the center of the microphone array with the altitude being adjusted with the aid of the tracking network. Approach descents were begun upon crossing the runway threshold, with sufficient altitude such that the aircraft would pass over the center microphone array at the prescribed altitude. Radar altitude readings, checked at microphone crossover, were typically within ±25 ft of the target altitude. Climbout runs were begun from both standing and running starts. The standing starts began 1600 ft from the microphone array at a 3-ft skid height while the running starts began 2600 ft from the microphone array at a 65-ft skid height, with the climbout maneuver initiated at 1600 ft from the microphone array, at a velocity of V_y. The hover conditions tested were taken at a nominal skid height of

3 ft and at four azimuthal headings. The test began with the aircraft pointed at the center microphone arrays referred to as the 0° azimuth condition. The aircraft was then turned in 90° increments clockwise, to obtain the remaining three test points.

5.4 Phase IV: Aerodynamic Survey

The goal of Phase IV was to obtain a comprehensive data base geared toward a thorough aerodynamic effects analysis. The test matrix (table XIII) consists of level flight test points flown so as to achieve desired nondimensional aerodynamic coefficients. Each test point was established with the use of a programmable hand-held calculator, much as in Phases I and II. The desired nondimensional parameters and aircraft state information (OAT and fuel reading) were used to calculate the required airspeed, altitude, and rotor speed for each test point. The calculation of rotor thrust coefficient was based on the assumption that rotor thrust equaled aircraft gross weight. Phase IV was conducted at three thrust coefficients, the lower in the clean configuration, and the higher with two rocket launcher pods mounted on the aircraft. The test matrix values of μ, Mach number, and C_t were set by the following rotor speed limits: 294 and 324 rpm at speeds below 70 knots and 314 and 324 rpm at flight speeds above 70 knots. The temperature gradients encountered during Phase IV occasionally dictated the test points that could be achieved. As a result, the final test matrix is somewhat altered from the original planned matrix.

5.5 Support Tests

Three separate tests were conducted in support of the TAAT: the Supplementary Calibration Test, two airspeed tests, and a two-dimensional wind tunnel test of the modified airfoil section. The Supplementary Calibration Test (ref. 35) was conducted after the completion of the TAAT to ascertain the condition of the pressure transducers. The test consisted of placing the pressure instrumented blade in a pressure chamber (fig. 26) and measuring each transducer's output voltage as the chamber pressure was lowered. The data provided information on each transducer's calibration slope. From the results, discussed in section 7 under slope change, several transducers were determined to have either failed, or to have altered calibration slopes at some time during the test. Procedures for potential correction of some of these transducer problems are also discussed in section 7 of this report.

Two airspeed calibrations were conducted to obtain airspeed correction curves. The first calibration test, conducted before the TAAT, consisted of flying a pace aircraft equipped with a calibrated speed bomb. The second test was conducted after the TAAT was completed, and involved making low altitude passes over the runway at Crows Landing Naval Air Facility while both radar and laser trackers calculated the relative ground speeds. Wind corrections were then added to the relative ground speeds to determine the true airspeeds. Results from these calibrations have been included in DATAMAP for use in data analysis.

A two-dimensional wind tunnel model of the OLS blade was tested in the NASA Langley Research Center 6- by 8-in. wind tunnel. The test, performed at Mach numbers of 0.34 to 0.88 and angles of attack of +12 to -4°, measured chordwise pressure distributions as well as C_ℓ, C_d, and C_m coefficients. The results, presented in reference 30, have been incorporated into the airfoil tables of the C-81 OLS Cobra model. The two-dimensional data have also been compared with flight test data, and the predictions of TRANDES (a two-dimensional transonic aerodynamic predictive code). A semi-empirical three-dimensional correction method has been developed, and is presented in reference 3.

6. DATA DESCRIPTION AND PROCESSING

The data obtained during the TAAT were recorded on four different systems using three distinct formats, requiring three separate processing procedures. Ultimately, all three are to be converted for use with DATAMAP, so as to facilitate future data analysis. The acoustic tapes from both the YO-3A and ground microphone array at Crows Landing used the same analog tape formats, while the Cobra analog tape used an FM multiplexed analog format. The Crows Landing tracking tapes were recorded digitally. The Cobra analog tapes were digitized into the Bell Ground Data Center (GDC) standard digitized format (ref. 41) by Bell Helicopter Textron. Selected test points from the acoustic phases have been digitized by Langley Research Center with further test points to be processed by Ames Research Center.

6.1 Acoustic Tapes

The acoustic data were recorded at 30 ips on 1-in.-wide analog tape mounted on 10-in.-diam reels, with 14 wideband II FM format channels. The channel assignments for the YO-3A and ground array are presented in tables XIV and XV, respectively. Voice comments and IRIG-B time code were used to identify the test conditions during playback for analysis. Both tapes were started and stopped for each test condition. Listings of the microphone gain settings for both Phases II and III are provided in appendix D.

6.2 Cobra Analog Tapes

The Cobra analog data tapes contained 28 channels, each channel consisting of 16 multiplexed bands. The data were recorded at 15 ips on 1-in.-wide, 14-in.-diam reels. The band frequency information is presented in table XVI. Because this hardware was from the OLS test, conducted by Bell Helicopter under an Army contract, the discriminator center frequencies were all Bell standard. Unfortunately, several of those frequencies were not common with other systems, thus hampering the current ability to retrieve the data from the flight tapes. Each multiplex signal also contained two additional carriers, a 68-kHz crystal-derived-frequency provided a basis for electronic flutter correction and a 560-Hz voltage controlled oscillator provided a level code.

Unlike the acoustic tapes, the Cobra analog tapes were generally run continuously during the flight with a VCO level code used as a prime data indicator. Generally, the test procedure was for the flight test engineer to begin the prime data record once the proper test condition had been set up by the pilot, and to end the prime data record at the termination of the test point. At the end of each prime data record a two-point, three-cycle, automatic calibration sequence was initiated. This sequence served two functions, one to update the test point counter and the second to provide calibration levels for use during digitization. The test point counter number was encoded in the aircraft time code signal and displayed to the flight test engineer. This enabled the flight test engineer to refer to the maneuver by number during voice comments, and allowed accurate recording of the maneuver number on the flight cards.

6.3 Tracking Tapes

The data from the laser/radar tracker were stored on one-half inch, nine track, 1600 BPI, 125 IPS magnetic tapes. The data format consisted of a 47-word frame: 3 words for time, 16 words for data, 10 words for laser tracking, 16 words for radar tracking, and 2 words for system status. Hard copy results can be obtained as trajectory plots or tabulations with sample rate being user selectable.

6.4 Ground Station Monitoring

The Ames Research Center ground station served the dual purpose of allowing in-flight monitoring of telemetered signals and postflight data quality checks. The ground station housed a complete set of discriminators, an L-band transceiver, and strip charts.

The in-flight monitoring of the safety of flight parameters involved transmitting one of the 20 groups of multiplexed signals obtained from the rotating system to the ground station via an L-band transmitter. The transmitted signal was demultiplexed and the 16 recovered channels were then recorded on two strip charts and were monitored by flight test personnel.

Due to the specialized equipment required, most of the data from the TAAT were not reduced until after completion of testing. In an attempt to ensure that sensors were properly scaled, properly working and free of noise, "quick look" spot checks of the data were performed after each flight by individually stripping out each of the multiplexed tracks from the 28-track flight tape. A test point near the end of each flight was selected so as to catch any sensors that failed during that day's test. The same equipment was used for this operation as was used for the in-flight safety of flight monitoring. This monitoring enabled some sensor failures to be caught and corrected. However, due to the limited number of channels surveyed, and the limited frequency response of the strip charts, a number of errors evaded detection. The section on data anomalies in this report discusses these errors in detail.

6.5 Cobra Digital Tapes

The data taken on board the AH-1G aircraft during the TAAT were recorded onto 23 analog flight tapes. When digitized, these data were stored on 350 digital tapes (at 1600 bpi). This collection of data is accessible through the DATAMAP program. The process of getting access to the data requires that the researcher identify a specific data set of interest. This data set is then read from the storage tapes onto a computer disk file. It is this disk file that DATAMAP accesses interactively. While this technique has the advantage of requiring only a relatively moderate file space for data storage, it has the drawback that only a small portion of the data base is accessible at any one time.

During testing, the duration of each test point depended on the test phase. Phase I and IV test points were typically 20 sec long for all but the maximum acceleration and high-g turn points. Test points from Phase II were typically 30 sec long, while those from Phase III varied depending on the test condition. Pilot comments were used to select the best 5 sec of steady state data to be digitized from Phases I and IV, while maneuver test points were digitized in their entirety. Phase II and III data were digitized for 15 sec with pilot comments used to select the appropriate starting times. The sensor signals that were not digitized are listed, by flight number, in appendix F. Since the frequency response of each sensor is dependent on its track and channel assignment on the analog tape, the frequency responses for the white and red blades are presented in tables XVII and XVIII, respectively.

6.6 DATAMAP/Search

The principal data management and analysis tool used with the TAAT data, as well as the original OLS data, is DATAMAP (refs. 38-40). The DATAMAP provides easy access to large data groups (e.g., the pressure transducer arrays) with single command sequences contained in the information files. Appendix E presents the information file for the TAAT data. This single-command-sequence feature eliminates the need for the engineer to know and input each sensor identification label and location separately when handling the data. The DATAMAP also incorporates a large number of analysis tools and coefficient derivations which can be applied to the raw data, as shown in table XIX. With the exception of figures 31, 32, and 116-123, all data plots presented in this report have been produced by the DATAMAP program.

A second program, Search, has been developed to assist the engineer in locating test points of interest out of the 338 total taken during the TAAT. Search will collate and tabulate the test points by selected ranges of true airspeed, gross weight, CG location, advance ratio, rotor thrust coefficient, or tip Mach number. The Search program is used when attempting to locate specific test conditions of interest. Once the desired test conditions are located, the corresponding time history data are first pulled from the digital storage tapes, then stored on the master file where it is accessible by DATAMAP.

7. DATA SURVEY

This section presents samples of every major instrumentation category and a thorough discussion of data qualities from the TAAT. The pressure data presented in this report have been cycle averaged over two complete rotor revolutions. The consecutive cycles used were those whose control inputs and aircraft states were the closest to steady state of the time histories available. The sensor signals from the red blade (nonpressure instrument blade) have only been cycle averaged over a single complete revolution. The use of only one revolution allows that the data from the two blades, red and white, would more closely correspond to the same instants in time. The authors admit to a bias towards the pressure data, being aerodynamicists; a dynamicist would likely have made the opposite choice given the chance. The logic behind cycle averaging the data is to eliminate the transients contained in any one cycle. If too many cycles are averaged, however, phenomena can be blurred, such that the resultant data are not representative.

Plots of pressure, strain gage, BLB, accelerometer, and hot-wire data are presented. A table of aircraft parameters, including blade flapping and feathering is presented for each test condition. Harmonics of pressure sensor and strain gage data are presented for the high speed flight case only. Data that are presented in this section consist of a speed sweep and an in-ground effect hover case from Phase I. Each of the data sets will be discussed. A thorough analysis of the aerodynamic phenomena identified in this section will be discussed in section 8.

7.1 Data Anomalies

The data from the TAAT have been found to contain anomalies that take several guises; however, most of them are readily identifiable and correctable. Individual sensors can exhibit any of the following errors: band edge, constant value responses, spikes, and value shifts. This section discusses how each of these anomalies is addressed. In addition, discussions are provided on methods for obtaining values for reference static pressure and ensuring that the data are correctly aligned azimuthally.

7.1.1 Band edge- During each preflight, the gains of each data stream were adjusted so as to compensate for any drift and ensure the use of the full frequency band. Occasionally, however, errors were made and gains were incorrectly set or sensor channels were skipped. When the signal exceeded the upper or lower limit on these channels a flattened area in the curve would result (fig. 27). That portion of the signal exceeding the band edges is not recoverable. Because of the variance of the amplitude of the signal between flight conditions, each sensor must be checked at each test point and for each flight being investigated. Depending on the cause of the contamination a sensor may well be band-edged at only a single, several contiguous, or several intermittent test points and/or flights. The DATAMAP allows the output of any sensors to be masked during analysis, so that the results are not contaminated by the erroneous signal.

7.1.2 Constant value response- Sensors that have only a constant DC value are easily recognized, and their signals are not recoverable. This situation is caused by one of two reasons: either the sensor failed, or the gain adjustment was such that the sensor's output was continually band edged. In either event, the sensor may have been subsequently replaced or readjusted, such that on later flights the sensor was functional again. Due to the nature of this problem it need be checked at only the first and last test point of a flight. Regardless of the reason for its condition, such a sensor will not regain its function during the flight. Preflight checks would reveal failed sensors going into the flight, and postflight checks would reveal the sensors which failed during that flight.

7.1.3 Spikes- The data contain intermittent spikes which are easily identified as being from one of three groups. The first group appears as a pulsed increase in value that occurs only on those sensors powered by the power supply that serviced the pressure transducers on the blade's top surface. These spikes occur at the same instant in time on all affected sensors resulting in a ripple effect in the data from the leading to the trailing edge of the blade. An example is shown in figure 27 at 0.154 sec. When a time history of several revolutions for one test point is plotted, the spikes will occur at the same azimuth location for each revolution. When data from two different test points are compared, however, the spikes will not necessarily align across test points. Indeed, one test point may have multiple spikes while another, such as shown in figure 27, will contain only one spike. While the precise cause of this spike has not been proven, an indication of the cause of the spike is provided by the fact that it only appears on sensors powered by a common power supply. The transducer manufacturer was contacted regarding possible causes of such transducer behavior. Their opinion, which supports the authors', was that the most likely cause was either the power supply or one of several power converters housed in the mux bucket.

The second type of spike appears as a sharp increase followed by a sharp decrease in signal level, followed by a damped oscillation back to the correct signal. This type of spike, shown in figure 28 at 0.13 sec, does not affect all transducers on the top surface, as does the first spike variety. Rather, this type is found on those sensors whose signal is contained on a common tape track of the shipboard recorder. These spikes further differ from the previously mentioned type in that they are intermittent. When looking at a time history, several revolutions may be completed without a spike, or there may be several spikes in one revolution. These spikes are less well understood than the first variety, but are equally obvious. An especially puzzling trait of this type of spike is that the data track upon which they are found varied from flight to flight. They have been found on pressure transducers recorded on tracks 6, 7, and 8. Postflight digitizing is the leading contender for the source for these spikes.

The third variety of spike, shown in figure 29 at 0.169 sec, is identified by the fact that a single digitized point has a DC shift. Furthermore, like the second variety of spikes, the companion sensors on that tape track, of like sensors, are affected at the same instant. This spike phenomenon is the least understood of the three. It has so far only been observed in the hot-wire data.

The DATAMAP has been modified by Ames Research Center to include an algorithm which deletes spikes from data to be analyzed, yet maintaining their original values in the stored data. The result of using the spike routine is shown in figure 30. For this figure, the raw data have been cycle averaged over two revolutions and is shown on the left. The data contain one spike of the first type and four spikes of the second type. The data were then processed by the spike routine and are plotted on the right. It should be noted that all data presented in this report have had all spikes which fit the first two descriptions removed. It should also be noted that the contamination illustrated in figure 30 represents the worst case of all the data presented in this report.

7.1.4 Value shifts- Another form of data anomalies that have been found in the data for this report involves zero shifts. Detection of zero shift anomalies in pressure instrumentation requires plotting coefficients of pressure versus blade chord. Transducers that have undergone a shift in the zero reference value appear as those which add a saw toothed character to the plot. If a constant delta value can be found for all azimuthal stations then the data in question may be adjusted by this amount using DATAMAP. In most instances, however, this is not the case, and the sensor in question must be checked for slope change as well. This test should be performed on the first data set from a given flight to assure data integrity. While there are several possible causes for this phenomenon, the two most prevalent are a permanent shift in the transducer's basic characteristic or the improper entry of the calibration factor during digitization. Blade feathering, item code P111, is a sensor which is affected by value shifts. While the zero shift changes from flight to flight, P111 can still be used for the derivation of longitudinal and lateral cyclic pitch. Collective pitch should be calculated from collective stick position, D023, using equation (1), where D023 is in percent and collective pitch is in degrees. The resultant accuracy of this equation is ±0.75°.

$$\text{Collective Pitch} = (\text{D023} \times 0.2069) + 8 \tag{1}$$

7.1.5 Slope change- The final data anomaly found concerns changes in the calibration slopes of individual transducers. The Supplementary Calibration Test, performed at the conclusion of the TAAT, involved testing the pressure blade for slope changes by installing it in an environmental pressure chamber and monitoring transducer response to pressure changes. The results of this test are documented in reference 35. The summary results are presented in figure 31 and table XX. While the majority of the transducers showed no slope change, some indicate that adjustments may be required. The adjustment procedure involves using the adjust command in DATAMAP to apply the slope correction, of which a sample case is presented in figure 32. Since this procedure is somewhat controversial, it has not been applied to the data presented in this report; instead, the affected item codes have been masked.

7.1.6 Static pressure and OAT- Unfortunately, both the static pressure sensor and OAT sensors were inoperative during the TAAT. The OAT is obtained from the flight cards (appendix B). Postflight calibration of the OAT sensor indicated that a correction factor of -1.5°C must be applied to the flight card OAT readings. Two methods exist for derivation of the static pressure. The first method involves using the pressure altitude, obtained from the flight cards in appendix B, to calculate the static pressure. The second method involves taking the mean of the trailing-edge pressure sensors on the white blade and using that value for static pressure. Typically, the inboard and tip-trailing-edge sensors are excluded from this procedure as they are often affected by aerodynamic phenomena not conducive to maintaining the Kutta condition, which is required for this method to be valid.

These two techniques have been compared with the expectation of finding good agreement. Agreement, however, is not as good as hoped for, nor is it especially consistent. The values have been as close as 50 ft and as far apart as 250 ft in resultant pressure altitude. The second technique was used in preparing the results presented in this report.

7.1.7 Blade azimuth- The aircraft's main rotor contactor signal was originally aligned to trigger when the pressure blade was over the tail boom, 0° azimuth. During the test, however, the rotor was disassembled and reassembled twice. The first time the hardware was reassembled, the signal was inadvertently set to trigger 180° out of phase with the original setup. This offset was discovered and corrected during the second rotor removal; thus the data for counters 2336-2833 must be adjusted to correct for the resultant phase shift. When using DATAMAP as the analysis tool, this is done by inserting the change in the information file (appendix E).

7.2 Data Survey Plots

The data presented in this survey are arranged by airspeed, blade location, and sensor type. The pressure data are presented first, followed by the strain gage, accelerometer, BLB, and finally the hot-wire anemometer data. The test points presented are from a level flight speed sweep followed by an in-ground effect hover test point conducted during Phase I of the TAAT. The speed sweep begins at V_h with subsequent speeds reduced by 0.1 V_h increments down to 0.5 V_h. All sensors that meet any of the aforementioned data anomalies have been corrected or removed, with the exception of the hot-wire anemometer data. The reason for this is explained in the following paragraph.

Figures 33-39 present cycle averaged plots of pressure versus azimuth. Each page contains two plots, the top surface presented on the left and the bottom surface presented on the right. The figures proceed from the 40% radial station outboard to the tip. Figures 40-46 present plots of blade bending and torsion for the speed sweep mentioned in the preceding paragraph. Each page contains three plots, beamwise and chordwise bending, and blade torsion. The figures proceed from the inboard to the outboard radial stations. Blade vibration data are presented in figures 47-53 as beamwise and chordwise pairs. The raw pressure data from the BLBs are shown in figures 54-60. The inboard element is presented atop the outboard element. Hot-wire data are presented in figures 61-67. Data contamination is found in the hot-wire data plots, consisting principally of two types of data spikes. These spikes have not been removed, however, because the data reduction done on this type of data is tolerant of the contamination (sect. 8.8). Blade flapping data are presented in figure 68.

7.3 Data Survey Tables

The aircraft states for the data just presented are given in table XXI. Tables XXII-XXV present harmonics of the pressure transducer data, as well as beamwise, chordwise, and blade-torsion strain-gage data for the V_h flight condition only. These data are presented out to the highest possible harmonic value; the cutoff value is dictated by each sensor's filter frequency and the rotor revolution rate. The harmonic analysis, using DATAMAP's capabilities, uses equation (1), where the series amplitude is given by C_k and the phase by ϕ_k.

$$x(t) = \frac{a_0}{2} + \sum_{k=1}^{\infty} C_k \cos\left(\frac{2\pi k}{T} - \phi_k\right) \qquad (2)$$

8. DATA SURVEY ANALYSIS

This section will discuss various aerodynamic phenomena and derivation techniques that relate to the data survey just presented. The aerodynamic phenomena addressed include integrated blade airloads, shock formation, blade vortex interaction (BVI), tip effects, retreating blade stall, and several miscellaneous effects. The techniques include the derivation of leading-edge stagnation points, airflow magnitude and direction, and blade vibration. A cross reference of aerodynamic phenomena and test conditions is presented in table XXVI. The following discussions will often refer to the figures presented in section 7.2.

8.1 Blade Airloads

The raw pressures presented in section 7 have been integrated to produce both nondimensional normal forces and pitching moments (figs. 69-80). While chordwise forces can be derived, they are not presented here, as they have been shown to be of low accuracy. This inaccuracy is due to the neglect of skin friction in the airload's integration routine used in DATAMAP.

8.2 Shock Effects

The pressure data presented in section 7 reveal the presence of strong shock waves on the advancing side of the rotor disk. The intensity of the shock diminishes at lower local speed locations (e.g., inboard radial stations) and at lower aircraft airspeeds. The presence of shocks is denoted by a sharp pressure decrease upon shock formation and a sharp pressure rise upon dissipation of the shock. The shocks appear first, and tend to be strongest, on the upper surface. The pressure taps from the leading edge to near the quarter chord are most influenced by the shocks on this symmetrical airfoil. The following discussion will follow the reduction of shock strength as airspeed is reduced from $1.0\ V_h$ to $0.5\ V_h$. The discussion of the 159 KTAS case includes presentation of chordwise pressure coefficients on the advancing side.

Indication of local transonics begins at the 75% spanwise station for 159 KTAS and become much more pronounced farther outboard where fully developed shocks are encountered. These effects are first evident on the transducers at the 8% and 15% chord positions between 50 and 120° azimuth. The region of supersonic flow is identified by the steep-sided bucket on the rotor's advancing side (fig. 33(c)) on the upper surface. Shock effects are delayed on the lower surface until 86% span (fig. 33(d)) where the first indications are seen at 15% chord. The comparable stage of shock development on the upper surface is just outboard of the 60% radial station. The lower surface has fully developed shock patterns by 91% radius (fig. 33(e)) although they are still lagging in development when compared with the upper surface.

At 91% radius on the upper surface, the supersonic region extends from before the 8% chord past the 25% chord, but not aft to the 35% chord location. The bottom surface at 91% radius encounters supersonic flow from 8% chord past 20% chord; however, the phenomenon is delayed azimuthally, from near 60 through 150° on the top surface to near 100 through 145° on the lower surface. The magnitude of the bucket is also smaller for the lower than the upper surface, 2 psi versus 3 psi, respectively. For the 159 KTAS test point, these general trends continue out to the blade tip. Note the overshoot that accompanies the steep rise during pressure recovery.

Figures 81-88 present the chordwise pressure coefficient distributions for the same data just discussed. The figures present the C_p distributions at 90° azimuth, from the root station to the tip. Figure 84, however, presents data at 86% radius for azimuth angles 45 to 130° in 10° increments. The symbols used represent the pressure sensor locations used in producing the curves. The critical pressure coefficients, defined by equation (2), have also been included on the C_p plots.

$$C_p^* = \frac{2}{\gamma M_{cr}}\left\{\left[\frac{(1 + 0.2M_{cr}^2)}{(\gamma + 1)/2}\right]^{\gamma/(\gamma-1)} - 1\right\} \qquad (3)$$

The progression from 40% to 75% radius shows the reduction in C_p^*, caused by the increased velocity and the movement of the pressure peak from the leading edge aft to 15% chord. This aft shift corresponds to the development of the shock region. The azimuthal development and dissipation of the shock at 86% radius is shown in figure 84. At 50° azimuth the pressure peak is shifting aft from the leading edge, with a smooth shallow pressure gradient returning the curve to subcritical pressures. By 60° the pressure peak is building in girth, with the 25% chord sensor measuring decreased pressure, resulting in a steepening gradient aft of quarter chord.

At 70° the peak pressure now occurs at the 25% chord sensor with a fully developed shock behind returning the pressure coefficient to subcritical values. This trend continues to the 110° azimuth, where the lower surface C_p's have increased to very near upper surface values. The 25% chord C_p value at 120° azimuth has fallen below the peak value indicating the lessening of the shock intensity and the return of a moderate pressure gradient. At 130° azimuth, the leading edge pressure for the upper surface has dropped off from its equivalent value at the 50° azimuthal location, while the lower surface has not yet recovered to its preshock contour.

Continuing out the blade from 91% to 99% radius, at the 90° azimuth position, the aspects of the upper surface coefficient of pressure distribution change little. While the intensity of the shock diminishes as the blade tip is neared on the upper surface, the lower surface magnitudes continue to increase, appropaching to within 0.1 of the upper surface magnitudes. At 99% radius the effect of the tip relief on the shock is evident, although the mechanism behind the kink at 20% chord is not well understood. However, the kink is observed in unsteady calculations and is usually attributed to flow over supercritical airfoils.

The development of shock effects at 146 KTAS can be seen from 60% through 99% span on the upper surface (figs. 34(b)-(h)). the development of shock effects on the lower surface can be seen from 86% to 99% radius (figs. 34(d)-(h)). As expected, the events parallel those mentioned above for the 159 KTAS case, although at somewhat reduced intensity.

Shock locations at 129 KTAS (figs. 35(a)-(h)) parallel those at higher speeds on the upper surface. The bottom surface, however, does not contain shock effects until the 96% radial position, with the full steep-sided bucket only present at the 97% spanwise location. The magnitude of the pressure drop is seen to be much reduced at this slower speed.

The set of plots for 116 KTAS (figs. 36(a)-(h)) continue to show the shock effects of the previous sets on the upper surface, but at a much reduced magnitude, as would be expected for the reduced airspeed. The lower surface is devoid of the bucket at all radial locations, leaving only a smooth dip in the pressures near the quarter chord in the advancing quadrant. An item of note here is that the shock phenomenon on the upper surface, 15% chord, 99% span, never fully develops (fig. 36(h)), while the slopes of the pressure dips on the lower surface lessen from those at 97% radius. The tip relief effect reduces shock strength near the blade tip. In the extreme tip region near 99% span, the reduction changes the aerodynamic character.

The set of plots covering 98 KTAS (figs. 37(a)-(h)) show the continued reduction of shock effects to the extent that the fully developed shock phenomenon of the higher speeds is not seen. Figures 38(f)-(h) exhibit only weak shock effects, and where they do appear, the BVI effects are not dominated as they are at the higher speeds. The shock effects are still present on the upper surface in the 82 KTAS data set (figs. 38(f)-(h)). Evidence of shocks is first encountered at 86% radius, is strongest at 91%, and then weakens near the tip. The lower surface shows no indication of shock at all.

8.3 Blade-Vortex Interaction

Blade-vortex interaction has become a focus for both acoustic and vibration studies in rotorcraft. The BVI event occurs over such a small time step that it is generally regarded that data recording frequencies must be at least 2000 Hz to fully capture the event. Although the precise nature of BVI cannot be studied with the 400 Hz resolution of the TAAT data, the locations of the event can be determined, and their relative strengths ascertained.

Indications of BVI do not become apparent in the speed sweep pressure data presented until the airspeed is reduced to 129 KTAS (fig. 35). While vortex intersections occur at other azimuths, only those that are predominant will be discussed here. The characteristic shapes of the BVIs can differ markedly depending on where they are encountered azimuthally because of the fact that the vortex, relative to the blade, is spinning in the opposite direction. This spin causes the blade to encounter a downwash followed by an upwash on the advancing side of the disk, with the reverse being true on the retreating side.

The data at 129 KTAS (fig. 35) contain a slight pressure pulse at the first three chordwise sensors of the lower surface at 120° azimuth, with no corresponding pulse on the upper surface at this radial station. A much smaller effect can be seen at the leading edge of the lower surface at 60% R (fig. 35). This pulse is much less noticeable than in the previous plot, and has moved forward to 100° azimuth. In the vicinity of 90° azimuth, the 75% radial station encounters an effect similar in strength to that at the 40% radius station. This effect, again, is not seen on the upper surface. There are only subtle indications of BVI encounters over the rest of the blade out to the tip, including an indication near 70° azimuth on the upper surface leading edge sensor at 99% span. The BVIs discussed were generated by the preceding blade and are three-quarters of a revolution old. That the blade is not parallel with the vortex at intersection is evident in the azimuthal staggering of the encounters at the affected radial stations. Azimuthal locations in the vicinity of 60°, where parallel encounters are expected, show no signs of BVI as the wake in level flight has been blown away from the rotor disk.

As the airspeed is reduced to 116 KTAS, the BVI effects generated by the opposite blade's three-quarters-revolution old wake become more pronounced. The lower surface of the blade at 40% span (Fig. 36(a)) exhibits the effects of BVI from the leading edge to 8% chord, at 120° azimuth. As at the higher speeds, the upper surface appears unaffected by the encounter at this radial station. The next radial station (fig. 36(b)) exhibits the effects of BVI on both surfaces. On the lower surface the encounter extends back to 15% chord and occurs at 100° azimuth. This encounter extends farther back on the blade chord than it does at the inboard chordwise array and precedes that event by some 20°. The effect appears at the same azimuthal location on the upper surface at the first two chordwise stations, but is larger in magnitude.

The 75% radial station (fig. 36(c)) shows that BVI has moved forward to 90° azimuth on both the upper and lower surfaces. The magnitudes are comparable to those found in fig. 36(b)), with the same sensors affected. The notable exception to this is the 8% chordwise station on the upper surface. It registers a 1.8 psi drop in pressure, which may be due to a combination of BVI and shock formation. The corresponding sensor at the 86% span (fig. 36(d)) exhibits the smooth-sided pressure bucket. The BVI at the 86% radial location has proceeded to near 80° azimuth, with the 35% and 40% chordwise lower surface stations beginning to experience the effects. Curiously, the leading-edge sensor on the upper surface does not record the BVI as prominently as have the corresponding sensors around it. The reason for this is not well understood.

The 91% span sensors (fig. 36(e)) display both shock and BVI, the lower surface only BVI. The BVI on the lower surface is located near 80°, slightly earlier than for the 86% span station. The shock phenomenon at 91% span occurs between 8% chord and 25% chord. At the 95% radial station (fig. 36(f)) again both shock and BVI are present. At 75° azimuth, the lower surface displays only BVI effects, while the upper surface contains both shock and BVI effects. The BVI is present only at the first two sensors while the shock effects are between 8% and 25% chord. Since BVI effects are most noticeable at the 8% chord locations on the inboard radial arrays, it is most likely that the BVI effects at the 8% chord on the outboard locations are masked by the shock effects at this test condition. It seems unlikely that the BVI effects should diminish at the higher rotational speed of this radial position, nor has the vortex much changed, as the other leading-edge sensors attest. Both shock and BVI effects are evident at the 97% spanwise array (fig. 36(g)). The lower surface shows the approach of shock, but not the steep slopes of fully developed shock. The BVI is also present, from the leading edge to quarter chord, near 75° azimuth. The upper surface contains BVI near the leading edge, and shock forward of the quarter chord. The tip array (fig. 36(h)) contains both shock and BVI, along with the tip rollup which will be discussed separately in section 8.4.

The set of plots covering 98 KTAS (figs. 37(a)-(h)) show the continued reduction of shock effects and a number of new BVI phenomena. One new phenomenon displayed in this set is found in the fourth quadrant of the rotor disk. The magnitude of the BVI encounter on the retreating side is significantly larger than that of the advancing side. This variation in strength is due to the relative strengths of each vortex element. Both encounters are due to passage of the blade past the opposite blade's three-quarters revolution old wake; however, little lift is carried on the advancing tip, while the retreating tip carries considerable lift. Hence, the vortex on the advancing side is weaker than on the retreating side. Of importance also is the susceptibility of the airfoil to external disturbances such as BVI. The retreating blade, with its moderate angle of attack, is more responsive to excitation than the low angle of attack advancing side blade.

The BVI that corresponds to those discussed previously for the higher airspeeds exhibits some unusual tendencies at 98 KTAS. The vortex is now encountered at 130° azimuth at the inboard radial station (fig. 37(a)). At the 60% span chordwise array the encounter has proceeded to 95°. This is the first large azimuthal change in BVI location encountered during the speed sweep. The shape of the BVI on the top surface at 60% radius (fig. 37(b)) has changed from that seen previously in that there appears to be a double encounter at the three inboard chordwise arrays (figs. 37(a)-(c)). Outboard of these arrays (figs. 37(d)-(h)) the shape returns to the characteristic shape found earlier. The double encounter shown at the 60% radius location is the first major appearance of the intersection of the blade with both its own and the opposite blade's wakes. The blade's interaction with its own wake is not seen in the outer radial stations because it has been blown down away from the sensor arrays by the increased downwash.

The final data set of this airspeed sweep is for 82 KTAS and is presented in figures 38(a)-(h). At the 60% spanwise station (fig. 38(b)) there are again two BVIs on the advancing side, as was the case for 98 KTAS (fig. 37(b)). However, the relative strengths have reversed from the previous test condition, as the second BVI is now the stronger one. At 75% radius (fig. 37(c)) the double encounter, first seen in figures 37(a)-(c), appears as the two BVIs approach each other. The overlay of these two BVIs into one single BVI encounter is not completed at any of the radial stations at this test point. The BVI in the fourth quadrant is seen in all plots at this speed with the magnitude being greater than at 98 KTAS and the azimuthal location having moved little. Figures 37(f)-(h) exhibit only weak shock effects and where they do appear, the BVI effects are not dominated as they are at the higher speeds.

8.4 Tip Rollup

One of the principal objectives of the TAAT was to obtain pressure data in the blade tip region. The pressure sensors in the tip region show evidence of the aerodyanmic phenomenon of tip rollup in the forward half of the rotor disk. Figure 33(h) indicates a suction occurring on the lower surface trailing edge between 120 and 200° azimuth. A similar effect is seen on the upper surface from 60% chord to the trailing edge. The trailing edge first encounters the suction at 130° azimuth and does not recover until 295°. The trailing-edge curve is interesting in that both ends of the event have low pressure lobes, while the center is relatively flat with a slightly positive slope. The tip effect is not present at 60% chord until 190° azimuth and it only lasts until 280°. Its shape, single lobed, is similar in character to that found on the lower surface.

Not presented in figure 33(h), because it exceeded the band edge, is the top sensor located at 70% chord. It also measured the suction, although its pressure change was much more pronounced (fig. 89). While its exact shape is not known due to band edging, the shape appears to closely resemble the single-lobed characteristics.

The mechanism of the tip rollup phenomenon is the result of the tip vortex being blown back over the blade tip due to the aircraft's forward velocity inducing an inboard pointing radial airflow. The general single-lobed shape is similar to that found in regions of the suction lobes. What is seen here is perhaps the passing of the low-pressure area of the forming vortex moving over the blade's extreme tip region. The effects of BVI rarely extend much past the leading-edge region of the airfoil; similarly the effects of the suction lobes do not extend radially inboard to the 97% spanwise station.

As the aircraft speed decreases (figs. 33(h)-37(h)), the suction lobes are lost on the bottom surface. At 82 KTAS (figs. 34(h)-37(h)) the tip effect is only observed at the trailing-edge sensor on the top surface. Its magnitude is much reduced and its two-lobed shape has reverted to the single-lobed shape. This is all consistent with the proposed explanation of its source. As the radial velocity has been greatly reduced, the shed vortex is less influenced and the low pressure of the vortex remains off the tip of the blade. The suction lobe, found at the extreme tip, is present, but it too is less prominent.

8.5 Blade Stall

The phenomenon of blade stall can be seen both inboard and outboard of the retreating side of the rotor disk. The inboard stall is the result of a high angle of attack and low speed, while the outboard section approaches stall due to high angle of attack and high speed.

It can be seen in figure 33(a) that the rotor blade, at 40% radius, is producing essentially no lift on the retreating side. The median pressure for the upper surface is above 13.5 psia from 260 to 320° azimuth, while corresponding pressures for the lower surface extend from 210 to 320°. The lower surface has a median pressure of 13.35 psia from 260 to 320°, 0.15 psi lower than that of the top surface.

To better illustrate the issue, the chordwise distributions of the retreating blade pressures and pressure coefficients will now be examined at specific azimuthal locations. Figure 90 shows the upper surface chordwise pressure distribution for the 40% spanwise location at both 90 and 270° azimuth. It can be seen that while the advancing side exhibits a typical lifting airfoil pressure distribution, the retreating side is essentially a straight line, approximately 0.15 psi below static pressure. The corresponding plots at 60% and 75% span (figs. 91 and 92) show that the upper surface on the retreating side is recovering from the low-speed, upper-surface stall.

A look at the chordwise C_p distributions for both the upper and lower surface (fig. 93) shows the development of the inboard retreating blade stall at 40% span from 230° azimuth to 330°. The large values of C_p result from the low relative velocities inboard on the retreating side of the rotor disk. At 230°, the leading quarter of the blade is lifting while the aft three-quarters is producing a download. At 250°, only the extreme leading edge is producing lift, while the rest of the blade section is producing a download. At 270° the entire blade section produces a substantial download which continues through 290°; however, the pressure difference on the two surfaces has lessened. By 310°, the blade section has very nearly returned to neutral lift and by the time the blade has proceeded to 330°, the section is once again a lifting surface, as the suction on the upper surface is greater than that on the lower surface.

Comparing the chordwise pressure distributions at 60% radius (fig. 94) with those just presented at 40% shows that the surface is lifting throughout the azimuthal sweep. It should be noted that the plots reveal a large adverse pressure gradient at the upper surface leading edge at 250 and 270°, which is indicative of potential, incipient leading edge stall.

Figures 95-97 present the chordwise C_p distributions at 270° azimuth for 75%, 86% and 91% radius, respectively. At 75% span, the large adverse pressure gradient is evident, while at 86% span the gradient appears to be much reduced. This reduction is perhaps an optical illusion caused by the loss of the leading-edge sensor. The large pressure gradient returns at the 91% radius station.

The C_p distributions at 96% span for azimuths 230-330° are presented in figure 98. The leading-edge pressure gradient can be seen to build between 230 and 250°, stabilize between 270 and 290°, and subside between 270 and 330°. The general curve shapes at 270° for 91% and 96% radius are very similar. The chordwise C_p distribution at 97% radius and 270° azimuth (fig. 99) shows that the leading-edge upper-surface pressure values have declined from those at 96% radius. The C_p distribution at 99% span (fig. 100) displays a further reduction in leading-edge pressure as the result of tip relief. The splitting of the trailing-edge pressure coefficients is the result of the tip rollup discussed at length previously.

At the next slower test condition, 146 KTAS, the inboard chordwise array, 40% radius, is producing no lift (fig. 34(a)). This situation is similar to that pointed out at the higher airspeed, as previously discussed. Upon inspecting the corresponding plots at lower speeds, it can be seen that the reverse flow region has progressed inboard of the 40% radial station before 129 KTAS is reached (fig. 35(a)).

The resultant conclusions from the above discussions are that at 159 KTAS, the blade is in a low speed stalled region inboard on the retreating side and the rest of the blade is approaching a condition of leading-edge stall. The tip relief effect alleviates the sharp leading-edge pressure gradient from 97% radius outboard. At 146 KTAS the inboard station is still stalled; however, the slopes of the pressure traces outboard have lessened. The stalled region has progressed inboard of the 40% radial station before the 129 KTAS test point is encountered.

8.6 Hub Wake

Figures 33(a)-36(a) reveal that the 40% radial station encounters turbulence (note the rapid pressure fluctuation) near 10° azimuth. As indicated in figures 33(b)-36(b) this turbulence does not extend out past this radial array. It has been surmised that this phenomenon is the blade impinging on the shed wake of the mux bucket, mounted on the rotor hub. The 10° shift of this impingement from 0° is caused by the rotating bucket acting as a lifting surface, deflecting the wake away from the geometrical trailing location. A simple rotating cylinder calculation using the appropriate flight parameters for the 159 KTAS test point as inputs to equation (3) was performed. It was found that at the 40% radius station, the streamline from the stagnation point is deflected 8.9° (fig. 101). This close correlation between analysis and test, plus the turbulence decrease with airspeed (figs. 36(a)-38(a)), tends to confirm that the hub wake is the source of this phenomenon.

$$\psi = V_\infty y \frac{1 - a_1^2}{r_1^2} + \frac{\Gamma}{2\pi} \log \left(\frac{r_1}{a_1}\right) \tag{4}$$

8.7 Leading-Edge Sinusoid

An interesting phenomenon occurs at the leading-edge pressure sensors on both upper and lower surfaces for 159 KTAS (fig. 33). The leading-edge pressure transducers on the inboard, lower surface display a pseudo-sinusoidal wave form, much as would be expected from a rotating dynamic pressure sensor, in a uniform airflow. This shape appears to make a transition to the upper surface at the 75% radial station and remains on that surface out to the tip. Figure 102 presents a sample case for three radial locations, in which each of the three radial station plots has had a curve added representing the total dynamic pressure. The amplitude of these dynamic pressure curves has been normalized to match that of the 1% chord transducer signal. It can be seen that at the 60% radius location the two curves match very closely, while the two outboard locations show a distinct phase shift. The generating mechanism of the sinusoid could be the leading-edge stagnation pressure being influenced by the total dynamic pressure. However, due to the presence of the airfoil, the flow field is not at free-stream conditions and the measured magnitude is less than the free-stream magnitude. Pressure transducers very near the stagnation point are affected by this local phenomenon, thus the presence of such sinusoids on a leading-edge transducer is indicative that the stagnation point is very near that location. Presumably the closer the waveform is to the normalized q curve, the nearer the stagnation point is to that transducer.

8.8 Stagnation Point Determination

Meaningful interpretation of the hot-wire anemometer data (figs. 61-67) is not immediately obvious. The nature of the sensor, a high-resistance wire cooled by airflow, requires that the data be reprocessed to yield the stagnation point locations. As the stagnation point approaches a hot-wire element, the reduction in airflow produces a corresponding reduction of element cooling, thus leading to a temperature rise of that element. This temperature rise results in an increase in resistance of the wire, resulting in a measurable voltage drop.

The hot-wire plots in section 7 present the hot-wire voltages as a percentage of the nominal voltages. The specific value of any one curve is of no importance; what matters is the trend of each curve relative to those of the other curves. When the stagnation point either passes over an element or nears then turns away and retreats from the element, the resistance reaches a minimum. Thus, the nearness of the stagnation point is observed by noting the curve shapes of all the elements, relative to their neighbors. The estimated stagnation points for the speed sweep are presented in figures 103-108 and were obtained by tabulating the azimuths at which each element's response peaked.

As mentioned in section 7, the data spikes have not been removed from the raw traces from which the stagnation point plots have been produced. Engineering judgment must be used in selecting the peak locations of sensors.

A related problem in selecting sensor peaks occurs routinely on the retreating side of the rotor disk where many of the hot-wires on the lower surface peak. The stagnation point only passes over a few of the wires with the rest reacting to its approach and retreat. Engineering judgment must be used in determining which of these peaks to include on the stagnation point plots. Basically, the criterion used has been to include only those elements which respond with a steep slope before and after the peak. Unfortunately, the limited number of sensors on the airfoil surface and the unsteadiness of the flow make interpretation of the graphs difficult.

8.9 Airflow Magnitude and Direction

Each BLB contains two pitot probes which measure the dynamic pressure at ±45° from the blade's direction of rotation. As presented in section 7 (figs. 54-60) they offer little insight into the blade's aerodynamic environment. However, DATAMAP contains a routine which takes these dynamic pressures, plus the pertinent geometric information, and calculates the flow field magnitude and direction. The direction values are limited to ±25° due to the calibration limits of the sensors.

Figures 109-111 present the output of the DATAMAP algorithm for the speed sweep test points. Each figure consists of two plots, with the left side representing the upper surface and the right side the lower surface. Nominally, there are three chordwise sensor locations per radial station plot. However, on occasion, one transducer of the BLB sensor was lost, thus eliminating that BLB from processing. The results of having one sensor giving a low output (fig. 54(b)) produces the symptomatic curve in figure 109(b). The clipping noted in figure 109(a) is the result of the 25° limit on calculated direction. Figure 111(a) has an interesting feature on the direction plot where the curve displays a step function to 0° because of the corresponding velocity reaching 0.

While the pitot probes have been shown to be slightly above the boundary layer, their use can still yield a significant amount of information pertaining to the three-dimensional aspects of the airflow.

8.10 Blade Vibration

The data from the blade accelerometers (figures 47-53) present situations that, taken at face value, are physically impossible. The data indicate that both the beamwise and chordwise accelerations are oscillating about mean values which are greater than the nominally anticipated value of 1 g. Considering that the accelerometers are mounted in an accelerated reference frame, some such indications are not totally unexpected. The accelerometers measure accelerations relative to their axis, which are in turn aligned with the blade. Any motion of the blade that alters the transducer's orientation with relation to the shaft axis will result in misleading signals. Precone, coning, flapping, feathering, and lead-lag are the primary blade motions that must be considered. In addition, the sensor itself is susceptible to axis crosstalk.

Coning and precone of the rotor system offer two sources of steady acceleration. The transducer, being oriented along the blade, measures accelerations relative to the blade axis. As the rotor cones, a component of the radial acceleration is aligned with the transducer axis. The rotational acceleration effects on the chordwise accelerometers have the same sources, except that the blade must feather such that the transducer is oriented out of the rotor disk. Calculations were performed for the 159 KTAS case, assuming rigid blades and a precone of 2.75°, the results of which are presented in table XXVII. The calculations assumed rigid blades, no coning, and took into account the angle of blade incidence based on the collective setting and blade twist.

Two sources of oscillatory acceleration are blade flapping and feathering. As the rotor flaps and feathers, the transducers are oriented out of the rotational disk which results in much the same loading of the accelerometers as coning. The key difference is that while the coning is relatively constant, flapping and feathering are cyclic. Calculations, not presented here, were made to account for the effect of flapping on the accelerometer readings. The effects of lead-lag motion were not calculated, as this would have increased the offset correction and would likely have been rather small in any event.

These results, when compared to the mean of the accelerometer data, overpredict the effects being modeled. The currently accepted means of adjusting the raw data is to calculate the mean and subtract that value from the data, thereby forcing the data to oscillate about 1 g. Work continues on devising improved correction techniques.

Cross plots were made to study the relationship between blade flapping and beamwise and chordwise accelerations (figs. 112-116). Each of the cross plots presents the beamwise data on the left and the chordwise on the right. The accelerometer data have been adjusted so that they cycle about 1.0 g, as previously mentioned. This was done by calculating the mean at each flight condition and subtracting that from each data history. The cross plots also contain azimuth information, as each symbol represents an increment of 10° with the square being 0°.

The beamwise plots tend to exhibit a similar character at all radial locations, except at the hub and near the tip. The general character is multiple reversals near the maximum flapping angle in the third azimuthal quadrant, with a single reversal at the minimum flapping angle. The mid-flapping values tend to have similar values, with a moderate amount of hysteresis. The hub response has many reversals throughout the flapping range. The tip response consists of a clockwise procession with reversals in the vicinity of the advancing and retreating azimuthal areas.

The chordwise plots show two variations of a distinct pattern. The inboard locations are open, much like the tip beamwise plot, except that they proceed counterclockwise. The outer two stations have the same counterclockwise orientation; however, each deviation from the general trend is amplified from that of the inner locations. There are two very peculiar reversals where the vibration changes direction while the flapping remains essentially constant. These occur between 170 and 210° at both of the outer radial stations.

It should be noted that these cross plots do not converge because a single cycle was used. Had several revolutions been averaged together, the plots would close.

8.11 Harmonic Content

The use of harmonic tables have long been a means of presenting the results of tests such as the TAAT. Tables of pressure transducer and strain gage output have been presented in this report for the 159 KTAS test point. while data reports have traditionally contained only the first 10 harmonics, this report presents all harmonics available. Figures 117 and 118 graphically present the results of omitting harmonics. The solid curves in figure 117 are the output from item code P636, staggered by 1.0 psi. The dashed lines that are paired with the multiple curves of P636 are the reconstructed curves including only that number of harmonics listed to the right of each set of lines. It can be seen that with only five harmonics the shock phenomena present in the data are lost. When the first 15 harmonics are used the fit is much improved; however, the slopes of the bucket are not correct. To properly capture the slopes, the first 45 harmonics must be included.

Figure 118 presents the item code P663 in an identical manner at a speed of 82 KTAS. Here it can be seen that the effects of BVI are not captured adequately with any less than 65 harmonics. This plot does contain two data spikes, one at 205° and the second at 310°.

The decision to include all harmonics, up to the sensor frequency cutoff, in the tables was based upon the results previously shown. So as not to require an environmental impact study of the deforestation of our national timberland to provide enough paper, only the harmonics from a single test condition are presented.

9. CONCLUSIONS

It is the intent of this report that it serve not only as a data survey, but also as the reference source for all matters relating to the Tip Aerodynamic and Acoustic Test. As such, in addition to the presentation of sample data, this report contains detailed descriptions of the instrumentation, test hardware, and test procedures used during the test, as well as brief descriptions of the pertinent data formats and data analysis tools. A large number of appendices have been included in the report so as to complete the documentation on TAAT. To better place the TAAT in proper perspective, a background section has been included that briefly discusses and references the significant reports of other pressure instrumented airload surveys.

The sample data presented here include examples of all the various sensor types for a level flight speed sweep and an in-ground-effect hover. The data are presented as azimuthal plots and harmonic tables. A thorough discussion of data anomalies that exist in the data base has been presented. Techniques and methodology for correcting, removing, or minimizing the effects of the anomalies have been discussed and example figures have been provided to assist the user in reviewing and correcting data for analysis. The more prominent aerodynamic phenomena that are in the data set presented in this report have been highlighted and discussed. These phenomena include retreating blade stall, advancing blade shock, and tip rollup.

The data base currently resides on digital storage tapes formatted for use with DATAMAP. Access to the data can be obtained in a variety of ways; among them are the following: use of DATAMAP at Ames Research Center; transfer of data partitions to the user's computer for use with DATAMAP; transfer of digital tapes containing harmonics, in a NASA-specified format, of selected sensors and for selected test conditions, to the user. It is important to note that when using the TAAT data base, checks must be made to ensure that all sensors are corrected. Data anomalies from several sources, including test hardware and postflight digitizing, are in the data base. These must be addressed when using the data.

The data obtained during the TAAT have been used in correlation studies with two- and three-dimensional aerodynamic predictive codes. Studies of comprehensive predictive codes, notably C-81 and CAMRAD, have been undertaken using the TAAT data base. The combination of the OLS and TAAT flight data, combined with the scale model tunnel data (both two-dimensional and rotating scale), present one of the most comprehensive and detailed descriptions of a rotor system obtained to date. Much work can still be done using this vast data base in the technical areas of aerodynamics, acoustics, performance, handling qualities, and dynamics.

APPENDIX A

FLIGHT TEST PLAN FOR AH-1G TIP AERO/ACOUSTICS

TEST AT AMES RESEARCH CENTER

The flight test plan that was used, and followed during the conduct of the TAAT, is presented.

TEST OBJECTIVES

A. Obtain detailed aerodynamic data of the flow on a helicopter rotor tip in forward flight and for maneuvers within the normal AH-1G Cobra flight envelope.

B. Measure external helicopter noise for a wide envelope of flight conditions while simultaneously measuring aerodynamic data.

TEST DESCRIPTION

A. The flight test program will consist of approximately 20 flights of 1, 1.5, and 2 hr each on the AH-1G. The flight program will be divided into four phases.

1. Phase I- Performance: At 324 rpm data will be recorded matching a selected set of data points taken in the OLS test.

2. Phase II- Air-to-Air Noise: Measurements will be recorded on the YO-3A instrument system simultaneously with the blade data being recorded on the Cobra. This phase will be flown with the YO-3A and Cobra in formation of various relative positions similar to previous air-to-air acoustics tests flown by NASA and Army. Flight conditions will be set up based on four nondimensional parameters, V/R, C_T/σ, M, and μ.

3. Phase III- Air-to-Ground Noise: Measurements of flyover noise will be taken in this phase. Approximately 25% of the records will be flown with the YO-3A so that air-to-air and air-to-ground measurements are recorded simultaneously with the blade data.

4. Phase IV- Rotor Aerodynamics: Data will be recorded based on the same variables listed in Phase II. This phase will require revolutions per minute and altitude changes between records, to maintain prescribed nondimensional parameters.

B. Ames Research Center, Langley Research Center, and ATL will participate in the program. In addition, Bell Helicopter Textron will provide instrumentation support to the Cobra and will digitize the data from the Cobra instrumentation system.

C. Phases I and IV will be flown out of Moffett Field; Phases II and III will be flown out of Crows Landing.

AIRCRAFT CONFIGURATION

Phases I and IV of the flight test program will include both the "clean" and "hog" configurations for the AH-1G. There will be a mid, fore, and aft center of gravity condition for each configuration. The clean configuration consists of the Cobra without external stores (at a gross weight of approximately 8200 lb); the hog configuration is with rocket pods on the stub wings and a gross weight of approximately 9000 lb.

Phases II and III will be flown in clean configuration, mid center of gravity, and approximately 8100 lb gross weight. The YO-3A will have external microphones on each wing tip and on the vertical stabilizer.

The exact weight will be obtained by weighing the aircraft at the start of the flight and reading the fuel counts during flight.

INSTRUMENTATION SETUP AND DATA REQUIREMENTS

The Tip Aero/Acoustics Test (TAAT) will use a variety of transducers and several data acquisition systems. The instrument can be divided into the following groups:

Instrumentation:

A. Rotating system, helicopter

1. Blade instrumentation

   Absolute pressure transducers (188)
   Differential pressure transducers (36)
   Strain gages (33)
   Accelerometers (12)
   Hot-wire anemometers (47)

2. Hub and control system

   Strain gages (11)
   Accelerometers (1)

Position and rate potentiometers (4)
Azimuth encoder (2)

B. Stationary system, helicopter

Strain gages
Gyros (rate and positions) (12)
Accelerometers (1)
Pressure
Temperature (2)

C. Airborne acoustics YO-3A

Microphones (3)
Temperature (1)
Pressure (1)
Position (2)

D. Ground-based instrumentation

Microphones (5)
Radar tracking (2)
Time code (1)
Telemetry (16)
Pressure (1)
Temperature (19)

Recording Requirements:

A. All helicopter instrumentation will be recorded on an on-board 28-track tape deck.

B. Airborne acoustics will be recorded on 14-track tape deck in YO-3A.

C. Ground-based acoustics will be recorded on ground based 14-track tape deck.

D. Telemetry and radar tracking will be recorded by the facilities instrumentation system. (Telemetry at Ames Research Center when flying out of Moffett Field, tracking at Crows site when flying out of Crows Landing.)

E. All recorders will be synchronized via a time code simultaneously transmitted to all recorders. The time code generator at Ames Research Center or Crows Landing will be used as appropriate.

RESPONSIBILITIES AND CONTROL FUNCTIONS

Responsibility assignments are:

Ames Research Center's Test Director	Gerald Shockey
Cobra Aircraft Manager	Steve Haff
YO-3A Aircraft Manager	Jeffrey Cross
Project Pilot	Robert Merrill
Ames Research Center's Instrumentation	Vard Holland
Contractor Instrumentation	Aaron Whitener
Crows Site Manager	Doug Wilner
Langley Research Center's Project Manager	Andy Conner
ATL Project Manager	Don Merkley
Ground Data Center	David Glass

The responsibilities and control functions are given in tables AI and AII.

OPERATING LIMITS

Parameter Limits

All flight conditions will be within the established operating limits of the standard AH-1G helicopter. Flight regimes that are known to be potentially hazardous, such as those areas in the H-V diagram where no successful autorotation can be executed, will be avoided except for the Phase III hover points at 492 ft. In addition to the standard operating limits, the maximum dive airspeed for the TAAT rotor is 165 KIAS. The load limit for the TAAT rotor is established at 1.8 g at 165 knots and 2.2 g at 132 knots. These limits were established in the envelope expansion phase of a flight test program with this rotor in 1976. The limiting item was beam bending at station 132. For power-on flight conditions, the parameter limits are:

GW	5800 to 9500 lb
CGMAX	Sta. 190 to 201
ROTOR RPM	314 to 324 over 70 knots, 294 to 324 under 70 knots; 339 rpm power-off limit
V_d	165 knots, $V_{lateral}$ = 35 knots, $V_{rearward}$ = 30 knots

Telemetered safety-of-flight information will be a primary consideration in determining whether a maneuver may be conducted.

Flight Envelope

The flight envelope for the TAAT is given. This envelope is within the usual operating limits of the AH-1G. Any maneuver will be terminated when any limit, as specified by the AH-1G Operating Manual, is attained or when any endurance limit is reached as indicated by telemetry of safety-of-flight items.

Weather Restrictions

All prime data flights will be flown in moderate atmospheric conditions. Visibility will be daylight, with at least 3 miles, with a well defined horizon. Wind limits are: Phase I and IV surface winds less than 10 knots, and Phase II and III surface winds less than 5 knots. Special care will be taken to protect the blade instrumentation from moisture.

OPERATING PROCEDURES

Pre/Postflight Briefing

The procedures for each of the four phases of the test are given. The pilots, test director, test engineers and instrumentation engineers will attend a preflight briefing prior to each flight. These will be held after the aircraft and instrumentation preflight checks have been conducted. The flight card will be reviewed for the flight, and each record will be discussed as required. Test areas, communication channels, and emergency procedures will also be reviewed.

A postflight debriefing including the aforementioned personnel will be held at the conclusion of each flight. The preceding flight will be discussed and plans for the next flight will be made.

Special Inspection

An instrumentation preflight calibration and functional check will be conducted prior to each flight to ensure proper functioning of all installed instrumentation. Included in this check will be a telemetry system checkout. Following each flight a helicopter safety inspection will be conducted. Special attention will be given to the attachment of the instrumentation sleeves to the blades. The table below shows the list of special inspection items.

A. Check for loose harnesses and cables.

B. Check for unevenness of filling material in beamwise wiring trough (between L.E. abrasion strip and fiberglass panels).

C. Check for loose screws in chordwise aluminum pressure port strips.

D. Check for crack at T.E. of blade where aluminum pressure port strips intersect T.E.

DATA REVIEWS

Data reviews will be conducted after each flight. After the initial flight, the test tape will be returned to BHT for digitizing as an end-to-end functional check. The routine data review will be a sample of data from each prime data record of the flight. The sampling criteria to determine the quality of recorded data will consist of:

A. Examination of strip chart from bands 1-8 of track 8 and 9-16 of track 17 for all records.

B. Examination of strip chart from all tracks and bands of the last record of the flight.

Voltage monitors are on track 6, band 6 and track 20, band 13. Examination of the strip chart of these items will indicate the reliability of the instrumentation system. A review of all items of the last record of a flight will ensure the operation of all the transducers during the flight.

TABLE AI.- TAAT FLIGHT OPERATIONS RESPONSIBILITY MATRIX

Function responsibility	Ames Ins. (FOX)	Ames test Dir. (FHI)	Cobra A/C Mgr. (FHI)	YO-3A A/C Mgr. (FHI)	Project Plts (FOF)
Test requirements		X[a]			
Test plan		X			X
Safety of flight plan		X	0[b]	0	0
Instrument requirements	0	X			
A/C test schedule		0	X	X	0
Flight test W.O.			X	X	
Instr. preflight	X		0	0	
TM	X				
Flight card		X			X
Preflight briefing		X			0
Perform flight	0	0			X
Fly-no-fly operation			X	X	X
Fly-no-fly tech.		X			X
Postflight debriefing	0	X	0	0	0
Data verification		0			
Ground based operation, Crows Site		0			
Data processing					
Start flight prop. sequence			X	X	

[a] X = primary responsibility
[b] 0 = secondary responsibility

TABLE AII.- TAAT FLIGHT OPERATIONS RESPONSIBILITY MATRIX

Ames Instr. (FOX)	Contract Inst. (BHT)	Crows Site Mgr. (FOX)	LaRC Proj. Mgr.	Alt. Proj. Mgr.	Gr. data Ctr. (BHT)
Test requirement			0[a]	0	
Test plan			0	0	
Safety of flight plan					
Instrument requirements	0		0	0	
A/C test schedule					
Flight test W.O.					
Instr. preflight	0	0			
TM	0	X[b]			
Flight card					
Preflight briefing					
Perform flight		0			
Fly-no-fly operation					
Fly-no-fly tech.					
Postflight debriefing					
Data verification			(acous.) X	X	
Ground based operation Crows Site		X	0		
Data processing			0	0	X
Start flight prop. sequence					

[a] 0 = secondary responsibility
[b] X = primary responsibility

APPENDIX B

ORIGINAL PAGE IS OF POOR QUALITY

FLIGHT CARDS OF TAAT

The flight cards present a synopsis of each test flight on a counter by counter basis. Each flight card lists the run number (or counter number), the target and obtained indicated airspeeds, rate of descents, rotor speeds, and pressure altitudes; and the fuel readings, the OAT gage readings, the run starting time, and test point comments. The test flight tape number, flight number, flight date, aircraft takeoff gross weight, and aircraft CG position are recorded in the upper right-hand corner. The lower right-hand corner records the flight crew of the chase and test aircraft. During the majority of Phase IV flights, the cockpit gage readings of engine torque, exhaust temperature, and engine speed were recorded in the comments column of the flight cards.

The key to reading the flight cards is presented below. In the event that only one numerical entry is present in a row column space, the value shown is coded as A for the airspeed and altitude columns and B for the rate of descent and rotor speed columns.

Airspeeds, rate of descent, and rotor speed

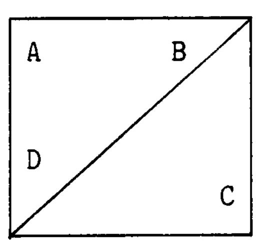

or

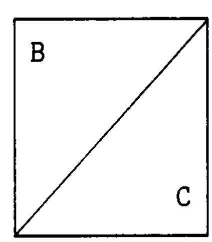

where

A reference airspeed used as computation input
B calculated target condition
C condition actually flown
D approximate condition used by pilot for initial setup

Altitudes

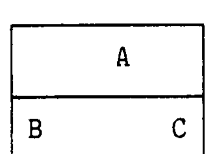

where

A target altitude
B starting altitude
C ending altitude

During the majority of Phase IV flights, the cockpit gage readings of engine torque, exhaust temperature, and engine speed were recorded in the comments column of the flight cards.

The units for the values presented on the flight cards are as follows:

Airspeed - knots
Rate of sink - feet per minute
Rotor speed - rotations per minute
Altitude - feet
Fuel - pounds
Outside ambient temperature - degrees Centigrade, except for flights 14A, 15A, 22A, 22B, and 23A which are in degrees Fahrenheit
Time - hours:minutes local time

Flight: 1A Data tape: 006 Date: 4/30/81 CG location: N/A
Takeoff gross weight (lb): 8100 Fuel weight (lb): N/A Turning: N/A

Run	Indicated Huey airspeed	Rate of sink	Test engineer	Huey pressure altitude	Pilot airspeed	Test engineer altitude	Pilot altitude	Bomb airspeed	Bomb altitude	Comments
	40	0	39	2000	35	2000	1960	43	1960	1st run
	60	0	58	2000	58	1900	1960	57.5	1960	2nd run
	60	0	58	2000	58	--	2020	59	2000	
61	70	0	68	2000	67	--	2000	67.5	2000	
62	80	0	74	2000	74	2000	1980	73	1980	
63	100	0	93	2000	94	2000	1960	93	1960	
64	100	0	92	2000	95	2010	2040	95	2010	
65	110	0	104	2000	105	2000	2020	103.5	2010	
66	110	0	104	2000	106	2000	2030	104	2010	
67	80	0	76	2000	77	--	1970	76.5	1970	
68	70	0	66	2000	67	--	1970	67.5	1970	
69	40	0	35	2000	36	1930	1940	41	1950	
70	60	500↑	59	3000	58	--	600	60	2600	
71	70	500↑	67	3000	67	--	500	67.5	3000	
72	80	0	78	5000	78	5020	4990	77	4960	
73	100	0	95	5000	96	--	4990	93.5	4950	
74	82	0	78	5000	76	5020	5020	74.5	5000	
75	60	0	55	5000	56	5000	5000	57	5000	
76	60 450↓	500↓	65	3000	65	--	300↓ 5800	66.5	4800	

Flight 1A (Concluded)

Run	Indicated Huey airspeed	Rate of sink	Test engineer	Huey pressure altitude	Pilot airspeed	Test engineer altitude	Pilot altitude	Bomb airspeed	Bomb altitude	Comments
77	80	500↓	75	3000	75	--	400↓ 4000	74.5	4250	
78	90	500↓	86	3000	82	--	300↓ 3600	84.5	3750	
	69	1000↑	69	3000	70	--	900↑	68.5	4100 900↑	
	80	1000↓	75	3000	75	--	950↓ 2300	74	950↓	
	70	1000↓	65	3000	66	--	800↓ 1400	67	950↓	

UH-1H test: George Tucker
Jack Brilla AH-1G: Bob Merrill
Jeff Cross OH-6: Gordon Hardy

Flight: 3A Data tape: 009 Date: 5/12/81 CG location: 192 Fwd
Takeoff gross weight (lb): 8645 Fuel weight (lb): 1650 Turning: N/A

Run	Position	Indicated airspeed	Rate of sink	Rotor speed	Pressure altitude	Fuel	OAT	Time	Comments
126	--	--	--	--		--	--	8:02	Ground run
127	--	Hover	--	--	4'	--	--	8:15	
128	--	$1.0V_h$ 146	0	320 320	1803 1850	1450	20	8:30	
129	--	$0.9V_h$ 130	0	320 320	1884 1880	1425	20	8:36	
130	--	$0.8V_h$ 117	0	320 320	2046 2040	1375	20	8:40	50↓
132	--	$0.7V_h$ 102	0	320 320	2127 2140	1350	20	8:42	131 abort-in climb and wrong RPM
133	--	$0.6V_h$ 88	0	320 320	2209 2220	1325	20	8:45	100↓
134	--	$0.5V_h$ 73	0	320 320	2291 2380	1300	19	8:50	3/4 through the test hit a 20-ft climb and decelerated
135	--	120 Power to auto	--	328	2373 3500	1275	19	8:55	
136	--	Auto to power	--	--	2000	--	--	8:55	
137	--	Hover to Max V_h accel	0	324	2620 2600	1200	19	8:59-9:02	
138	--	$0.6V_h$ 88	0	319 319	2766 2750	1150	19	9:06	
139	--	Power to auto	--	--	1750	1100	19	9:10	

Flight 3A (Concluded)

Run	Posi-tion	Indicated airspeed	Rate of sink	Rotor speed	Pressure altitude	Fuel	OAT	Time	Comments
140	--	Auto to power	--	--	500	--	--	9:10	70% RPM

731 Chase: George Tucker

736 Cobra: Bob Merrill
Jeff Cross

Flight: 4A Data tape: 010 Date: 5/13/81 CG location: 200.48 Aft
Takeoff gross weight (lb): 8191 Fuel weight (lb): 1700 Turning: 7:23

Run	Position	Indicated airspeed	Rate of sink	Rotor speed	Pressure altitude	Fuel	OAT	Time	Comments
150	--	--	--	--	--	--	--	--	Ground zero
151	--	Hover	--	324	4'	--	16	7:34	32 PSI torque, 94% RPM
152	--	$1.0V_h$ / 152	0	315 / 315	2346 / 2340	1575	13	7:45	
153	--	$0.9V_h$ 137 / 137	0	319 / 319	2654 / 2640	1500	20	7:50	
154	--	$0.8V_h$ 122 / 122	0	319 / 319	2765 / 2760	1450	20	7:54	
155	--	$0.7V_h$ 106 / 106	0	319 / 319	2910 / 2910	1425	20	7:58	10-ft variation
156	--	$0.6V_h$ 91 / 91	0	319 / 319	2996 / 3000	1400	20	8:01	
157	--	$0.5V_h$ 76 / 76	0	319 / 319	3062 / 3060	1375	20	8:03	
158	--	Power to auto	--	--	3814 / 3800	1350	20	8:08	
159	--	Auto to power	--	--	2900	--	--	8:08	
160	--	Max accel Hover to V_h / 142	--	324	3986 / 3990	1300	20	8:14	40↓ 42 PSI torque Top power at 100 H
161	--	Decel 50 to hover	--	--	3750	1225	20	8:21	6° nose up, steady
163	--	Decel 50 to hover	--	--	3700	1175	20	8:25	15° nose up, full down collective

Flight 4A (Concluded)

Run	Posi-tion	Indicated airspeed	Rate of sink	Rotor speed	Pressure altitude	Fuel	OAT	Time	Comments
162	Bogus point								
164	Telemetry check on pitch link and drag brace								

734 Chase: George Tucker
Jerry Shockey, observer
Dick Clayton, photographer

736 Cobra: Bob Merrill
Jeff Cross

Flight: 5A Data tape: 011 Date: 5/15/81 CG location: Aft
Takeoff gross weight (lb): 8969 Fuel weight (lb): 1700 Turning: N/A

Run	Position	Indicated airspeed	Rate of sink	Rotor speed	Pressure altitude	Fuel	OAT	Time	Comments
180	--	--	--	--	--	--	16	8:12	Ground run
181	--	$1.0V_h$ / 142	0	315/315	3041/3040	1575	10	8:38	Smooth, last quarter bumpy
183	--	$0.9V_h$ 126/127	0	315/315	3483/3480	1425	10	8:48	Gain 20 ft
184	--	$0.8V_h$ 112/112	0	314/314	3678/3680	1375	11	8:53	
185	--	$0.7V_h$ 98/98	0	314/314	3756/3760	1350	10	8:55	Airspeed good, 30-ft climb
186	--	$0.6V_h$ 84/84	0	314/314	3834/3840	1325	11	8:58	
187	--	$0.5V_h$ 70/70	0	313/313	3912/3900	1300	10	9:01	±2 knots
188	--	Power to auto / 120	--	324	4633/4600	1275	11	9:04	40 lb·torque, 4700, 71% RPM
189	--	Auto to power / 90	--	--	3400	--	--	9:04	
190	--	Max accel Hover to V_h / 142	--	324	4869/4900	1200	11	9:10	Slight 30-ft climb at 110 knots, 99.8%, 48 lb·torque, early pt gained alt., then level
182	Abort								

731 Chase: Tex Ritter
Jerry Shockey, observer

736 Cobra: Bob Merrill
Jeff Cross

Flight: 12A Data tape: 021 Date: 6/10/81 CG location: N/A
Takeoff gross weight (lb): 8480 Fuel weight (lb): 1750 Turning: N/A

Run	Position	Indicated airspeed	Rate of sink	Rotor speed	Pressure altitude	Fuel	OAT	Time	Comments
336	Trail	67.8 60 63/64	0	320	3080	1400	62	9:04	50 ft/min climb, drift back in middle, position good at begin and end
337	Left	67.8 60 63/64	0	321	3416/3400	1300	64 21	9:09	Lost 1/rev on YO + head set, position good, except last 5 sec
338	Left	67.8 60 63/64	200 210	320	3584/3600	1250	63	9:13	±10 R/S, 2200 RPM on YO, 1/rev in heads, position good, then high last 10 sec
339	Left	67.8 60 63/63	400 400-450	320	3754	1200	63	9:22	±5 ft, not stable early (first 10 sec)
340	Trail	67.8 60 63/64	400 400	320	3924/3850	1150	63	9:27	Position good last two-thirds
342	Trail	67.8 60 63/63	600	320	4181	1075	63	9:34	Good stable point, position good, vitals good
344	Left	67.8 60 62/64	600	321	4267	1050	64	9:40	Far early, inside a bit, last half good
347	Left	67.8 60 62/--	800	320	4439	1000	62	9:45	Wing rocking, last quarter good, #345 on YO tape
349	OAT voice interference test							10:05	
350-352								10:08	
354	1/sec mic. key intervals								
360	Back seat prime data switch								

734: George Tucker, Jerry Shockey, Dave Conner, Doug Hunt
736: Bob Merrill, Jeff Cross
718: Warren Hall, Mike Watts

Flight: 13A Data tape: 022 Date: 7/1/71 CG location: Mid
Takeoff gross weight (lb): 9195 Fuel weight (lb): 1600 Turning: 7:37

Run	Posi- tion	Indicated airspeed	Rate of sink	Rotor speed	Pressure altitude	Fuel	OAT	Time	Comments
370	--	Hover	--	--	--	1520	18	7:45	
371	--	Transition to 60 knots	--	--	--	1520	18	7:46	
372	--	Climb 100 knots	--	--	--	1475	18	7:49	Max shaft hp
373	--	$1.0V_h$ / 142	30↓	317	2316/2320	1425	20	7:58	100% engine RPM, 49 lb·torque
374	--	$0.9V_h$ 128/128	--	320/320	2657/2660	1375	24	8:01	40 lb·torque, stable point
375	--	$0.8V_h$ 114/114	10↑	320/320	2733/2740	1350	24	8:04	Lost 1 knot, fairly stable
376	--	$0.7V_h$ 99/99	10↓	320/320	2869/2870	1325	24	8:06	Lost 1 knot, 30 lb·torque
377	--	$0.6V_h$ 85/85	--	322/322	2905/2910	1300	24	8:08	26 lb·torque, good point
378	--	$0.5V_h$ 71/71	--	322/322	2921/2920	1275	23	8:12	21 lb·torque, good point
379	--	125/123	Left turn 1.5 g	321/322	2383/2390	1225	23	8:17	1.5-g spiral, good point
380	--	120	1.7	321/322	1994/2010	1200	23	8:21	Lost ɔ knots, 1.6- to 1.5-g spiral
381	--	120	Right turn 1.5 g	317/320	2130/2100	1150	23	8:24	1.5-g spiral, good point
382	--	--	1.7 g	319/320	2324/2330	1125	23	8:27	Vibration, 1.5 g early on, 1.7 g last half
383	--	Power to auto 120	--	324	2500	1075	23	8:30	6000 RPM

Flight 13A (Concluded)

Run	Position	Indicated airspeed	Rate of sink	Rotor speed	Pressure altitude	Fuel	OAT	Time	Comments
384	--	Auto to power 105	--	322	1800	--	--	8:30	
385	--	Hover to V_h / Max accel 141	--	324	2500	1050	23	8:36	600°C exh. temp., 49 lb·torque, lost 30 ft last 10 sec
369	Turning on pad								

734: Warren Hall
Rich Young

736: Bob Merrill
Jeff Cross

Flight: 13B Data tape: 023 Date: 7/1/81 CG location: Fwd
Takeoff gross weight (lb): 9039 Fuel weight (lb): 1200 Turning: 10:45

Run	Posi-tion	Indicated airspeed	Rate of sink	Rotor speed	Pressure altitude	Fuel	OAT	Time	Comments		
									Engine RPM, %	lb·torque	Exhaust tempera-ture, °C
388	--	Hover	--	--	--	1125	22	10:54	Steady 3-knot wind		
389	--	$1.0V_h$ / 131	20↓	321 / 321	4298 / 4300	1000	21	11:08	100	45	600
390	--	$0.9V_h$ 118 / 118	50↓	321	4374 / 4380	975	23	11:14	--	--	--
391	--	$0.8V_h$ 105 / 105	20↓	322	4527 / 4530	925	23	11:17	96	32	595
392	--	$0.7V_h$ 92 / 92	--	322 / 322	4680 / 4680	875	23	11:20	94	24	570
393	--	$0.6V_h$ 79 / 79	20↓	322 / 322	4834 / 4830	825	23	11:23	93	25	--
394	--	$0.5V_h$ 66 / 66	10↓	321 / 322	4988 / 4990	775	22	11:26	92 Last half best	21	--
395	--	Power to auto / 120	--	324	3500	725	23	11:29	70	--	--
396	--	Auto to power	--	--	2400	--	23	11:29	--	--	--
397	--	Max accel Hover to V_h / 132	50↓	324	3500	675	23	11:34	100 15 sec of last point is extra	45	600

734: Warren Hall
Rich Young
Doug Hunt

736: Bob Merrill
Jeff Cross

Flight: 14A Data tape: 024 Date: 7/7/81 CG location: N/A
Takeoff gross weight (lb): 8480 Fuel weight (lb): 1725 Turning: 8:18

Run	Position	Indicated airspeed	Rate of sink	Rotor speed	Pressure altitude	Fuel	OAT	Time	Comments
806	Trail	123 110 115/109	0	321	3165/3170	1350	67/22	9:11	Position good
808	Trail	123 110 115/117	200/250	321	3500	1250	66	9:21	Good point
810	Left	123 110 114/115	200/320	321	3840	1150	64	9:27	Close in middle, then back
811	Trail	123 110 114/114	600/600	320	4004	1100	62	9:30	Good position
812	Trail	99.6 90 92/92-94	0	321	4095/4060	1075	64/20	9:35	Good position, last half excellent
813	Trail	99.6 90 92/91	800/450	319	4267	1025	60/19	9:40	Out of position
814	Trail	99.6 90/92	800/800	319	--	--	--	9:44	Position good early part
815	Trail	135 120 124/125	600/650	320	4526	950	62/20	9:47	10 ft back most of run
816	Trail	135 120 124/124	800/800	319	4700	900	59/19	9:55	Position good, then back last quarter
817	Trail	135 123 120/123-128	1000/1000	320	4963	825	61/19	10:00	Position 6 yd back consistently, airspeed gained last quarter
818	Left	135 120 122/123	1000/1000	320	5140	775	62/20	10:05	Position good, R/S dropped last quarter
807 809	Bogus point								

718: Glen Stinet, Rich Young

731: Gordon Hardy, Jerry Shockey, Doug Hunt

736: Bob Merrill, Jeff Cross

Flight: 15A Data tape: 025 Date: 7/8/81 CG location: N/A
Takeoff gross weight (lb): 8480 Fuel weight (lb): 1725 Turning: 7:45

Run	Position	Indicated airspeed	Rate of sink	Rotor speed	Pressure altitude	Fuel	OAT	Time	Comments
825	Left	89.1 80 84/84	800 800	321	3160	1350	66	8:28	Power changes at end, close early, then OK
826	Trail	89.1 80 83/83	0	323	3330/3300	1300	72	8:35	Close early, then OK
827	Left	89.1 80 83/83-85	--	323	3500/3480	1250	71/23	8:38	Power change at end, a little close early, then very close (21 yd)
828	Left	89.1 80 83/83-53	200/250	322	3600	1225	68	8:43	Good position early, then outside
829	Left	89.1 80 82/80-82	400/450	322	3750	1175	69	8:47	Position really good
830	Trail	89.1 80 82/82	400/400	322	3750	1150	70	8:52	Early OK, end lagged, last 20 sec good
831	Trail	89.1 80 82/82	600/600	322	3900	1125	70/65	8:58	First 90% excellent, good run
832	Left	89.1 80 82/82	600/650	322	4100	1075	68	9:03	Close, then good position
833	Trail	89.1 80 82/82	800/800	321	4200	1050	67	9:08	Really close early, then ±1 yd
834	Trail	110.1 100 101/101	0	321	4450/4500	975	67	9:15	Good position early, drifted back, small inputs

734: Jim Martin
Tex Ritter
Jerry Shockey
Doug Hunt

718: Glen Stinnett
Rich Young

736: Dan Dugan
Jeff Cross

Flight: 16A Data tape: 026 Date: 7/9/81 CG location: N/A
Takeoff gross weight (lb): 8480 Fuel weight (lb): 1700 Turning: 7:40

Run	Position	Indicated airspeed	Rate of sink	Rotor speed	Pressure altitude	Fuel	OAT	Time	Comments: Engine RPM, %	Comments: lb·torque	Comments: Exhaust temperature, °C
842	--	64/65	0	314/315	2834/2840	1475	24	8:15	Smooth air, good point		
843	--	75/74	0	315/315	3779/3750	1425	26	8:20	90	20	510
844	--	86/86	0	314/314	3244/3250	1375	25	8:26	92	24	510
845	--	109/109	0	314/314	3605/3600	1375	25	8:28	94	28	540
846	--	129/129	0	315/315	3856/3850	1325	26	8:32	97 Vibration levels up	37	560
847	--	143/141	0	315/315	4262/4270	1300	26	8:36	100 Slower by 1 knot in middle	45	600
848	--	142/141	0	318/316	4124/4130	1200	22	8:45	100 Topped engine	45	600
849	--	132/132	0	322	5100/5130	1150	22	8:47	98	38	580
850	--	132/131	0	323/325	5414/5400	1125	23	8:49	99	40	590
851	--	129/128	0	323/323	5515/5400	1100	22	8:56	98	38	580
852	--	110/110	0	323/323	5576/5580	1075	23	9:00	95	29	540
853	--	109/109	0	319/319	4919/4920	1025	22	9:04	95	28	540
854	--	101/101-100	0	319/319	5203/5200	1000	23	9:06	92 Slight deceleration	23	530

Flight 16A (Concluded)

Run	Posi-tion	Indicated airspeed	Rate of sink	Rotor speed	Pressure altitude	Fuel	OAT	Time	Comments		
									Engine RPM, %	lb·torque	Exhaust tempera-ture, °C
855	--	95/95	0	323/323	5852/5860	950	22	9:11	92	21	520
856	--	88/86-85	0	323/323	5906/5900	925	22	9:14	92 Lose 1 knot	21	520
857	--	87/86	0	319/319	5471/5480	875	21	9:18	92 Slight climb	21	520
859	--	88/88	0	321/321	5750/5760	825	20	9:24	92	20	520
860	--	65/65	0	319/319	5296/5300	775	20	9:27	90 Descent last quarter run	18	510
861	--	62	0	322	5537	725	21	9:32	91 Wrong altitude	17	500
862	--	62/60	0	322/322	6376/6380	675	21	9:35	92 Slight climb, tape remaining	19	510
863	--	61/61	0	301/301	3600/3690	575	24	9:45	90	18	500

731: Dave Barth
Doug Hunt

736: Dan Dugan
Jeff Cross

Ames Moffett: Jerry Shockey
Mike Watts

Flight: 16B   Data tape: 027   Date: 7/9/81   CG location: N/A
Takeoff gross weight (lb): 8480   Fuel weight (lb): 1700   Turning: 11:35

Run	Position	Indicated airspeed	Rate of sink	Rotor speed	Pressure altitude	Fuel	OAT	Time	Comments: Engine RPM, %	Comments: lb·torque	Comments: Exhaust temperature, °C
866	--	61/61	0	299/299	2866/2950	1575	24	11:52	90	21	530
867	--	64/64	0	314/314	5100/5170	1500	21	12:00	91	20	510
868	--	75/75-77	0	313/313	4941/4960-5000	1475	21	12:04	92	21	510
869	--	85/85	0	313/314	5377/5400	1450	22	12:07	93 Accelerated during last half	25	520
870	--	109/110	0	314/314	5303/5280	1425	22	12:11	94	28	540
871	--	128/128	0	314	5550/5550	1400	22	12:14	97 Slowed to 126 at end	36	560
872	--	142/140	0	314/304	5605/5560	1375	22	12:17	100	46	600
873	--	131/130	0	321/319	6500/6500	1275	19	12:26	99	39	590
874	--	128/124	0	322	6728/6760	1225	19	12:30	98	35	570
875	--	110/110	0	322	6990/6960	1225	19	12:35	95	29	545
876	--	108/107	0	317/317	6424/6390	1150	20	12:39	94	27	540
877	--	100/101	0	318/318	6750/6750	1150	20	12:43	94 Climbed 20 ft	26	530
878	--	100/100	0	317/317	6697/6700	1125	19	12:46	94 Gusts yaw oscillation	26	530

Flight 16B (Concluded)

Run	Posi-tion	Indicated airspeed	Rate of sink	Rotor speed	Pressure altitude	Fuel	OAT	Time	Comments: Engine RPM, %	Comments: lb·torque	Comments: Exhaust tempera-ture, °C
879	--	95/95	0	321/321	7076/7090	1100	20	12:49	93 Stable	24	530
880	--	87/87	0	321/321	7128/7150	1075	19	12:51	93 Climb in middle	24	520
881	--	86/86-84	0	321/321	6608/6600	1050	18	12:56	91	19	520
882	--	61/86-84	0	320	7132/7150	975	19	12:59	91	19	510
883	--	65/63	0	317/317	7000/7020	950	18	1:05	91	18	505

731: Dave Barth
Doug Hunt

736: Dan Dugan
Jeff Cross

Ames Moffett: Jerry Shockey
Mike Watts

Flight: 17A Data tape: 028 Date: 7/10/81 CG location: Mid
Takeoff gross weight (lb): 9258 Fuel weight (lb): 1700 Turning: 7:45

Run	Position	Indicated airspeed	Rate of sink	Rotor speed	Pressure altitude	Fuel	OAT	Time	Comments: Engine RPM, %	Comments: lb·torque	Comments: Exhaust temperature, °C
890	--	148/120	0	314/314	6356/6500	1425	18	8:14	100	45	600
891	--	127/121	0	314/314	6912/6920	1400	19	8:18	100	44	600
892	--	106/106-107	0	314/314	6835/6840	1360	19	8:24	97	34	560
893	--	120/117	0	320/320	7976/7950	1300	19	8:27	100	40	590
894	--	108/105	0	316/316	7839/7900	1275	18	8:32	96 Very stable point	31	550
895	--	109/109	0	320/320	8165/8130	1200	15	8:39	98	35	560
896	--	100/101	0	315/315	7591/7600	1160	16	8:42	96	31	550
897	--	94/95	0	319/319	8073/8150	1130	16	8:46	94 Climb 20 ft	29	530
898	--	87/87	0	320/320	8534/8570	1100	15	8:49	94 Stable point	26	530
899	--	86/85	0	316/316	7946/7940	1075	15	8:53	94 Stable point	26	530
900	--	85/84	0	314/314	7356/7330	1040	16	8:55	93	25	520
901	--	75/76	0	314/314	7480/7500	1000	16	8:58	92 Lose 50 ft	22	520
902	--	65/66	0	317/317	8200/8220	980	16	9:02	92 Gain 20 ft	24	520

Flight 17A (Concluded)

Run	Position	Indicated airspeed	Rate of sink	Rotor speed	Pressure altitude	Fuel	OAT	Time	Comments: Engine RPM, %	Comments: lb·torque	Comments: Exhaust temperature, °C
903	--	65/66-65	0	319/322	8634/8660	950	15	9:06	92 Lost 20 ft	21	515
904	--	65/65	0	318/318	8359/8400	910	14	9:12	92	24	520
905	--	61/61	0	318/318	8640/8650	850	14	9:14	92	21	515
906	--	61/61	0	296/298	6000/6000	775	18	9:22	91 First half good	21	500

731: Gordon Hardy
Doug Hunt

736: Dan Dugan
Jeff Cross

Ames Moffett: Jerry Shockey
Mike Watts

Flight: 19A Data tape: 031 Date: 7/15/81 CG location: N/A
Takeoff gross weight (lb): 8480 Fuel weight (lb): 1700 Turning: N/A

Run	Position	Indicated airspeed	Rate of sink	Rotor speed	Pressure altitude	Fuel	OAT	Time	Comments
3061	--	Hover	--	--	--	--	--	9:55	0° azimuth, 3 ft height
3062	--	West 90°	--	--	3	--	30°	9:57	
3063	--	South 180°	--	--	3	--	--	9:58	
3064	--	East 270°	--	--	3	--	--	9:59	
3065	--	75	--	--	190	--	--	10:00	Standing start departure
3066	--	70	--	--	340	--	--	10:06	3-knot winds at 50 ft, 330°
3067	--	65	--	--	450	--	--	10:09	5 knots on ground, 10 knots at 50 ft
3068	--	V_h/150	--	--	460	--	30°	10:12	
3069	--	60/58	320↓ 3°/300↓	--	380	--	30°	10:22	Fairly stable, at two-thirds way into run hit gust
3070	--	60 61	640↓ 6°/600↓	--	430	--	--	10:27	Fairly stable, at 500 ft hit a gust
3071	--	60 59	950↓ 9°/900↓	--	480	980	--	10:31	Fairly stable, collective input early in data
3072	--	60 58	1260↓ 12°/1260↓	--	470	870	30° at 1700	10:38	
3073	--	60/60	1260↓ 12°/1200↓	--	530	800	--	10:45	
3074	--	60/60	950↓ 9°/950↓	--	470	775	--	10:48	

Flight 19A (Concluded)

Run	Position	Indicated airspeed	Rate of sink	Rotor speed	Pressure altitude	Fuel	OAT	Time	Comments
3075	--	60/57	640↓ 6° / 650↓	--	400	725	--	10:53	Prime data ran long
3076	--	60/59	320↓ 3° / 300↓	--	390	680	--	10:58	
3077	--	$0.9V_h$/135	--	--	500/530	--	--	11:02	First three-fourths were steady at 500 ft
3078	--	$0.8V_h$/120	--	--	500/490	600	--	11:05	Very stable, some bumps
3079	--	$0.7V_h$/105	--	--	500/505	570	30° at 500	11:08	
3080	--	$0.6V_h$/94	--	--	500/505	540	--	11:12	ECU on
3081	--	$0.5V_h$/75 ±1	--	--	500/490	500	--	11:16	
3082	--	V_h/151	--	--	500/520	475	--	11:21	RPM limit

736: Dan Dugan
Jeff Cross

Flight: 20A Data tape: 032 Date: 7/16/81 CG location: N/A
Takeoff gross weight (lb): 8480 Fuel weight (lb): 1700 Turning: 9:35

Run	Position	Indicated airspeed	Rate of sink	Rotor speed	Pressure altitude	Fuel	OAT	Time	Comments
3091	--	V_h/149	--	360	480	1320	25	10:15	RPM topped bumpy
3092	--	$0.9V_h$/135	--	458	520	1260	25	10:21	
3093	--	$0.9V_h$/136	--	475	540	1225	--	10:25	Slight yaw
3094	--	$0.8V_h$/120	--	545	570	1175	25	10:29	Slight yaw
3095	--	$0.7V_h$/105	--	480	530	1150	25	10:31	Slight yaw
3096	--	$0.5V_h$/77	--	--	580	1030	--	10:42	Small inputs
3097	--	$0.6V_h$	--	--	620	1000	--	10:45	Gust/aft then OK
3098	--	$0.7V_h$/105 ±2	--	--	610	--	--	10:49	Continual inputs, gusts
3100	--	60/61	--	--	680	890	--	10:54	Large inputs, gusts
3101	--	Max dive/120	1000	--	680	700	--	11:07	Close over microphone
3102	--	130	1000	--	700	--	--	--	Off to right, behind and bouncing all over
3102'	--	60/75	--	--	--	--	--	--	YO-3A alone
3102"	--	Max V	--	--	--	--	--	--	11:34

718: Jim Martin
Rich Young

736: Warren Hall
Jeff Cross

Flight: 21A Data tape: 033 Date: 7/21/81 CG location: Aft
Takeoff gross weight (lb): 9245 Fuel weight (lb): N/A Turning: N/A

Run	Position	Indicated airspeed	Rate of sink	Rotor speed	Pressure altitude	Fuel	OAT	Time	Comments: Engine RPM, %	Comments: lb·torque	Comments: Exhaust temperature, °C
3111	--	142/105	0	314	7806	1475	23	11:08	100	36	620
3112	--	108/108	0	317	8277/8280	1375	20	11:14	Vibration		610
3113	--	106/105	0	323	9000/9000	1350	20	11:20	Vibration		610
3114	--	100/100	0	317	8478/8480	1300	20	11:24	97 Moderate vibration	32	600
3115	--	95/95	0	321	8959/8980	1250	20	11:27	96	29	600
3116	--	88	0	321	9300	1200	20	11:31	95 Smoother	26	580
3117	--	86/86	10↑	314	8230/8230	1175	20	11:37	95 Smooth V right on	26	580
3118	--	73/73	10↑	314	8253/8260	1150	20	11:41	94 Good point	23	560
3119	--	65/65	10↑	318	9000/9000	1100	20	11:45	93 Good point	21	560
3120	--	61/61	10↑	321	9200/9200	1075	19	11:48	94 Excellent point	21	560
3121	--	63/63	20↑	309	8200/8000	1050	21	11:54	93 Some shaking going on	22	560
3122	--	61	20↑	299	6700/6700	1000	23	11:58	92 Steady point, shaking	21	550

731: Warren Hall, Doug Hunt 736: Bob Merrill, Jeff Cross Ames Moffett: **Jerry Shockey**, **Mike Watts**

Flight: 21B Data tape: 034 Date: 7/21/81 CG location: Aft
Takeoff gross weight (lb): 8381 Fuel weight (lb): 1700 Turning: 2:20

Run	Position	Indicated airspeed	Rate of sink	Rotor speed	Pressure altitude	Fuel	OAT	Time	Comments: Engine RPM, %	Comments: lb·torque	Comments: Exhaust temperature, °C
3126	--	133/131	--	324	5300/5350	1550	23	2:42	99	40	600
3127	--	132/134	--	324	5664/5650	1525	28	2:45	100 Air getting rough	41	610
3128	--	130/130	--	324	5900/5900	1500	27	2:50	99	39	600
3129	--	143/140	--	316	4600/4560	1450	28	2:55	100	43	610
3130	--	130/129	--	317	5000/5000	1400	28	2:58	98 A little rough	35	580
3131	--	108/110	--	317	5017/4990	1375	28	3:02	95	27	550
3132	--	111/110-109	10↓	324	6026/6020	1340	26	3:06	96	28	560
3133	--	96/96-97	10↑	324	6132/6130	1300	26	3:08	94	25	550
3134	--	89/88	0	324	6184/6180	1290	26	3:09	94	21	540
3135	--	86/80	0	316	5040/5060	1275	27	3:15	93	21	530
3136	--	86/86	0	316	5209/5250	1225	28	3:19	93	20	530
3137	--	75/76	0	316	5300/5300	1200	28	3:21	92	19	530
3138	--	66/66	0	322	6172/6230	1180	26.5	3:25	92	18	530

Flight 21B (Concluded)

Run	Position	Indicated airspeed	Rate of sink	Rotor speed	Pressure altitude	Fuel	OAT	Time	Comments: Engine RPM, %	Comments: lb·torque	Comments: Exhaust temperature, °C
3139	--	62/62	0	324	6500/6500	1150	26	3:28	92	17	520
									Lost speed last 5 sec		
3140	--	65/65	0	315	5470/5530	1125	27	3:33	91	18	520
3141	--	62/63	0	302	3695/3700	1075	29.5	3:38	91	19	510

731: Ron Gerdes
Doug Hunt

736: Dan Dugan
Jeff Cross

Ames Moffett: Jerry Shockey
Mike Watts

Flight: 22A Data tape: 035 Date: 7/22/81 CG location: N/A
Takeoff gross weight (lb): 8381 Fuel weight (lb): 1663 Turning: N/A

Run	Position	Indicated airspeed	Rate of sink	Rotor speed	Pressure altitude	Fuel	OAT	Time	Comments
3149	Trail	73.1 68 / 65 68	0 / 80+	324	3416 / 3410	1400	78	8:55	
3150	Left	73.1 67 / 65 67	0	324	3593 / 3590	1350	78	9:00	Close early, last half good
3151	Left	73.1 67 / 65 67	200	324	3655 / 3750 3600	1325	77	9:05	Back, then good
3152	Left	73.1 67 / 65 66	400 / 400	324	3834 / 3800 3650	1275	78	9:10	Pretty good
3153	Trail	73.1 67 / 65 67-68	400 / 400-450	324	3919 / 4000 3800	1250	78	9:13	Last part the best
3154	Trail	73.1 67 / 65 67	600 / 600	324	4000 / 4050 3700	1225	78	9:16	Back early, then good
3155	Left	73.1 67 / 65 67	600 / 600	324	4100 / 4250 3900	1200	78	9:19	Really good point
3156	Trail	-- 62 / 60 62	800 / 750-800	324	4173 / 4150 3600	1175	78	9:25	Moderate control inputs, back throughout
3157	Left	144 130 / 130 124-130	1000 / 900-1000	324	4429 / 4500 3900	1100	78	9:31	Not good, position poor
3158	Left	144 130 / 130 125-130	1000 / 900-1200	324	4600 / 4800 4200	1050	76	9:37	Repeat of 3157, position better, some inputs
3159	Trail	144 130 / 130 124-128	1000 / 1100-1150	324	4773 / 4900 4350	1000	77	9:43	Back early, last two-thirds good
3160	Trail	135 121 / 120 121-123	1000 / 750-1000	324	5034 / 5350 4800	925	77	9:49	Last half best, may be a little high
3161	Trail	123 110 / 110 102-105	0 / 50+	323	5297 / 5300	850	74	9:53	Fairly good and stable
3162	Experimental	89.1 79 / 80 79	400 / 400	323	5473 / 5600 5400	800	74	9:58	Stable, good point

Flight 22A (Concluded)

Run	Position	Indicated airspeed	Rate of sink	Rotor speed	Pressure altitude	Fuel	OAT	Time	Comments
3163	Experimental	89.1 79 / 80 78-79	600 / 650	323	5650 / 5650 5400	750	72	10:03	Good
3164	Experimental	67.8 60 / 60 60	400 / 400-450	323	5830 / 5950 5650	700	74	10:07	Good point, slightly high at end
3165	Experimental	67.8 60 / 60 60	600 / 600	323	5920 / 5950 5650	675	72	10:10	Slightly low, good point
3166	Experimental	-- 119 / 120 117-121	1000 / 850-1000	323	6100 / 6150 5700	625	73	10:17	Good point
3167	Left	-- 64 / 65 64	800	322	6280 / 6300 5800	575	71	10:22	Good point
3168	Trail	-- 64 / 65 64-63	800 / 800	323	6460 / 6500 6100	525	73	10:27	Good point

718: Dave Barth
Jeff Cross

731: Gordon Hardy
Jerry Shockey

736: Bob Merrill
Doug Hunt

Flight: 22B Data tape: 036 Date: 7/22/81 CG location: N/A
Takeoff gross weight (lb): 8381 Fuel weight (lb): 1725 Turning: 11:47 +.0.

Run	Position	Indicated airspeed	Rate of sink	Rotor speed	Pressure altitude	Fuel	OAT	Time	Comments
3171	Trail	67.8 59/ 60 /59	0	323	6574 / 6500	1575	71	12:08	Drift back
3172	Left	67.8 59/ 60 /59-58	0	321	6900 / 6900	1450	68	12:12	Good point
3173	Left	67.8 58/ 60 /59	200/ /200	321	7060 / 7200 7100	1425	66	12:18	3 to 4 ft back consistently
3174	Left	67.8 58/ 60 /59	400/ /400-350	321	7140 / 7100 6800	1400	65	12:21	2 to 3 ft back
3175	Trail	67.8 58/ 60 /58	400/ /400	321	7222 / 7400 7100	1375	66	12:25	First three-fourths good, then back
3176	Trail	67.8 58/ 60 /58	600/ /650-700	321	7386 / 7500 7200	1325	65	12:30	Fairly good, then back at end
3177	Left	67.8 58/ 60 /58	600/ /600	321	7550 / 7600 7200	1275	65	12:35	Last 4-5 sec best, earlier OK
3178	Left	67.8 58/ 60 /59	800/ /800-900	321	7716 / 7750 7200	1225	66	12:42	10 ft back throughout
3179	Left	67.8 58/ 60 /60	800/ /800	321	7800 / 7800 7300	1200	66	12:48	Repeat of 178, good point
3180	Trail	67.8 57/ 60 /60	800/ /800-820	321	7966 / 8200 7750	1150	66	12:55	Distance good, some drift up and down
3181	Left	67.8 71/ 70 /71	800/ /800-850	323	4728 / 5000 4400	1075	74	1:03	Good point
3182	Left	110.1 99/ 100 /99	0	324	4815 / 4820	1050	78	1:09	Middle good, back at end
3183	Left	110.1 99/ 100 /99	400/ /400	324	4990 / 5220 4975	1000	76	1:13	Middle best, back early and late
3184	Left	110.1 94/ 100 /99	600/ /550-650	323	5165 / 5450 5050	950	74	1:16	Good

Flight 22B (Concluded)

Run	Position	Indicated airspeed	Rate of sink	Rotor speed	Pressure altitude	Fuel	OAT	Time	Comments
3185	Trail	110.1 98 / 100 /98	600 / /650-675	323	5340 / 5500 5100	900	74	1:19	Good
3186	Trail	-- 70 / 70 /70	0	323	5515 / 5520	850	74	1:23	Good, plus/minus a few feet
3187	Left	-- 69 / 70 /69	0 / /20↑	323	5604 / 5610	825	73	1:25	Close early, then good
3188	Left	-- 69 / 70 /69-68	400 / /400	323	5780 / 5900 5600	775	72	1:28	Close early, last 10 sec best
3189	Right	-- 60 / 60 /60	400 / /400-600	323	5960 / 6200 5700	725	71	1:34	Drifted back, then last 5 sec good

731: Gordon Hardy
Jerry Shockey

718: Dave Barth
Jeff Cross

736: Bob Merrill
Doug Hunt

Note: runs 3171 through 3180 have ref. gross weight of 10,500 lb

Flight: 23A Data tape: 037 Date: 7/23/81 CG location: N/A
Takeoff gross weight (lb): 8480 Fuel weight (lb): N/A Turning: N/A

Run	Position	Indicated airspeed	Rate of sink	Rotor speed	Pressure altitude	Fuel	OAT	Time	Comments
3196	Left	89.1 78/ 80 /78	400/ /400	322	6580	1450	68	11:10	Good position last one-third of run
3197	Left	89.1 78/ 80 /78	0	322	6660 6660	1425	68	11:16	Right on point
3198	Trail	89.1 78/ 80 /78-77	400/ /450	322	6820 6900 6500	1375	68	11:20	Lost position at end
3199	Trail	89.1 78/ 80 /77	400/ /420	321	6900 7000 6700	1350	67	11:25	Last 10 sec best, rest back
3200	Trail	89.1 78/ 80 /78-77	800/ /780-820	321	7070 7100 6700	1300	66	11:30	Good point
3201	Left	89.1 77/ 80 /77-75	800/ /850	321	7225 7350 6700	1250	67	11:39	Last half good
3202	Left	89.1 77/ 80 /76-77	800/ /790	321	7390 7500 7000	1200	67	11:46	Last half good, repeat of 3201
3203	Right	89.1 81/ 80 /81-82	400/ /400	323	4130 4250 4050	1125	71	11:55	Good, last half best
3204	Right	89.1 81/ 81 /81	600/ /600	324	4300 4400 4000	1075	75	11:59	Excellent, last 55 sec the best
3205	Right	89.1 81/ 80 /82-81	800/ /790-810	324	4390 4450 4000	1050	75	12:04	Last half good
3206	Right	67.8 61/ 60 /60	0	324	4560 4550	1000	76	12:08	Back slightly
3207	Right	67.8 61/ 60 /61	600/ /600	323	4730 4800 4500	950	73	12:12	Good point
3208	Right	67.8 61/ 60 /61	800/ /800	323	4905 5100 4700	900	74	12:15	Position OK, no record by Cobra

Flight 23A (Concluded)

Run	Position	Indicated airspeed	Rate of sink	Rotor speed	Pressure altitude	Fuel	OAT	Time	Comments
3208'	Right	67.8 61/ 60 /61	800/ /800	323	5080 5200 4850	850	73	12:21	Good point

731: Gordon Hardy
Jerry Shockey

718: Warren Hall
Jeff Cross

736: Bob Merrill
Doug Hunt

Note: runs 3196 through 3202 at ref. gross weight of 10,500 lb.

Flight: 23B Data tape: 038 Date: 7/23/81 CG location: Fwd
Takeoff gross weight (lb): 8381 Fuel weight (lb): 1700 Turning: 2:43

Run	Position	Indicated airspeed	Rate of sink	Rotor speed	Pressure altitude	Fuel	OAT	Time	Comments: Engine RPM	Comments: lb·torque	Comments: Exhaust temperature, °C
3211	--	Pylon mount check	--	--	3'	1625	--	2:49			
3212	--	Pylon mount check	--	--	3'	1625	--	2:50	Better run than 211		
3213	--	70	--	--	3500	1550	25	2:58	Long. step aft, slowed to 40 knots		
3214	--	70	--	--	3500	--	--	2:59	Long. step forward, up to 95 knots		
3215	--	70	--	--	3500	--	--	3:00	Left lateral step input		
3216	--	70	--	--	3580	--	26	3:00	Right lateral step input		
3217	--	143/137-140	0	315	3055/3060	1500	26	3:07	64000 Rough ride	45	620
3218	--	129/128	20↑	316	3513/3510	1450	27	3:10	64200	39	610
3219	--	132/132	0	323	4604/4600	1425	27	3:14	64700	41	620
3220	--	111/110	10↓	324	4990/4990	1400	27	3:17	65900	29	600
3221	--	108/108	0	317	4139/4000	1350	27	3:21	64900	28	590
3222	--	96/96	0	324	5336/5340	1300	27	3:25	65900	24	580
3224	--	89/89	10↑	324	5385/5390	1275	26	3:28	66000	24	570

Flight 23B (Concluded)

Run	Posi-tion	Indicated airspeed	Rate of sink	Rotor speed	Pressure altitude	Fuel	OAT	Time	Comments		
									Engine RPM	lb·torque	Exhaust tempera-ture, °C
3225	--	86/86	10↑	315	3884/3885	1250	26	3:33	63700	24	570
3226	--	75/75	10↑	316	4300/4300	1200	27	3:35	64000	21	560
3227	--	66 66	0	322	5297/5300	1175	27	3:39	64700	20	560
3228	--	64/64	10↓	315	4200/4200	1150	25	3:44	63800	19	550
3229	--	62/62	0	302	2500/2690	1100	27	3:48	60100	20	550

731: Dan Dugan
Doug Hunt

736: Bob Merrill
Jeff Cross

Ames Moffett: Jerry Shockey
Mike Watts

Flight: 24A   Data tape: 039   Date: 7/24/81   CG location: Fwd
Takeoff gross weight (lb): 9039   Fuel weight (lb): 1200   Turning: N/A

Run	Position	Indicated airspeed	Rate of sink	Rotor speed	Pressure altitude	Fuel	OAT	Time	Comments: Engine RPM	Comments: lb·torque	Comments: Exhaust temperature, °C
3237	--	87/87	--	320	8444/8440	1025	20	9:50	64400	28	540
3238	--	61/60	--	320	8483/8480	975	17	9:53	64300	22	520
3239	--	61/61	--	320	8383/8380	950	17	9:54	64400	21	520
3241	--	61/61	--	324	8385/8400	950	17	9:55	65400	22	520
3242	--	109/109	20↑	320	8497/8500	925	17	10:00	64300 Vibration light	39	580
3243	--	94/94-93	10↑	320	8531/8530	900	17	10:01	64200	30	545
3244	--	100/100	0	316	8174/8170	850	18	10:07	64000	31	550
3245	--	108/108	0	316	8344/8340	800	18	10:09	64000	36	570
3246	--	72/72	30↓	314	8000/8000	775	18	10:15	63900	22	520
3247	--	85/85	20↓	314	8200/8200	700	19	10:19	63300	26	535
3248	--	63/62-63	0	307	7509/7510	675	18	10:24	62100	23	515
3249	--	61/61	0	299	6863/6860	625	19	10:28	60400	22	510

731: Gordon Hardy
Doug Hunt

736: Bob Merrill
Jeff Cross

Ames Moffett: Jerry Shockey
Mike Watts

APPENDIX C

TAAT INSTRUMENTATION SHEETS AND SIGN CONVENTIONS

The instrumentation setup sheets are comprised of two sections. The first section deals only with sensors in the rotating system; the second section deals with all sensors on the aircraft, both rotating and nonrotating. A list of sign conventions for all the sensors follow the setup sheets.

The first section lists by sensor type and physical location the magnetic flight tape track and channel number, the wiring bundle cable number and the associated unit calibration value. The track number indicates which of the 28 tracks on the tape recorder the signal used. The band number denotes which of the 16 multiplex center frequencies was used by the sensor. The "item" column defines what type of sensor is being identified. The abbreviations used are:

ABS PRESS	absolute pressure transducer
HWS SGMT	hot-wire segment
VIBR BEAM/CHORD	blade vibration in beamwise or chordwise sense
BLADE BEAM/CH/TORS	blade bending in beamwise, chordwise, or torsional sense
YOKE BEAM/CH/TORS	hub or yoke bending in beamwise, chordwise, or torsional sense
MAST PARA	mast bending parallel to the blades
MAST PERP	mast bending perpendicular to the blades

The "location" column code varies depending on the sensor type. For the absolute pressure transducers, the code indicates which surface of the blade the transducer is located on (upper or lower surface) and what its chordwise location is. The chordwise location numbering system begins at the upper-surface leading edge as 1, and continues aft, around the trailing edge back to the leading edge on the lower surface. The code for the HWS SGMT starts its numbering at the aftmost segment on the lower surface, and then proceeds around the leading edge to the upper surface. The BLB code denotes the surface, the chordwise location from the leading edge and the directional orientation (inboard or outboard).

The "station" column gives the radial station location (inches) from the shaft as well as the blade (white or red). The "cable" column indicates which input plug the signal used to enter the multiplex bucket, and which pin in the plug was used.

The second section presents information for every sensor on the aircraft. This information includes the item code, sensor description, balance value, track and band or channel number, the unit calibration, and reference values, the engineering unit equivalence, and the excitation voltage.

TRACK	BAND	ITEM	LOCATION	STA	CABLE	UNIT CAL
5	4	ABS PRESS	UPR#1	W106	A1	2.56
6	1	ABS PRESS	UPR#2	W106	A3	1.22
7	1	ABS PRESS	UPR#3	W106	A5	2.38
9	6	ABS PRESS	UPR#4	W106	A7	2.61
9	8	ABS PRESS	UPR#5	W106	A9	1.96
9	9	ABS PRESS	UPR#6	W106	A11	3.37
9	10	ABS PRESS	UPR#7	W106	A13	1.74
19	11	ABS PRESS	LWR#8	W106	E1	2.91
19	12	ABS PRESS	LWR#9	W106	E3	2.66
19	13	ABS PRESS	LWR#10	W106	E5	2.36
20	7	ABS PRESS	LWR#11	W106	E7	1.43
20	8	ABS PRESS	LWR#12	W106	E9	1.52
20	9	ABS PRESS	LWR#13	W106	E11	1.90
20	10	ABS PRESS	LWR#14	W106	E13	1.99

TRACK	BAND	ITEM	LOCATION	STA	CABLE	UNIT CAL
7	12	ABS PRESS	UPR#1	W158	A15	2.9
7	13	ABS PRESS	UPR#2	W158	A17	2.84
8	7	ABS PRESS	UPR#3	W158	A19	2.27
8	8	ABS PRESS	UPR#4	W158	A21	2.55
8	9	ABS PRESS	UPR#5	W158	A23	2.50
8	10	ABS PRESS	UPR#6	W158	A25	2.01
8	11	ABS PRESS	UPR#7	W158	A27	2.07
8	12	ABS PRESS	UPR#8	W158	A29	3.00
8	13	ABS PRESS	UPR#9	W158	A31	1.61
9	7	ABS PRESS	UPR#10	W158	A33	1.66
18	8	ABS PRESS	LWR#11	W158	E15	2.83
18	9	ABS PRESS	LWR#12	W158	E17	2.18
18	10	ABS PRESS	LWR#13	W158	E19	2.06
18	11	ABS PRESS	LWR#14	W158	E21	2.62
18	12	ABS PRESS	LWR#15	W158	E23	1.94
18	13	ABS PRESS	LWR#16	W158	E25	1.41
19	7	ABS PRESS	LWR#17	W158	E27	2.87
19	8	ABS PRESS	LWR#18	W158	E29	2.75
19	9	ABS PRESS	LWR#19	W158	E31	1.85
19	10	ABS PRESS	LWR#20	W158	E33	3.04

TRACK	BAND	ITEM	LOCATION	STA	CABLE	UNIT CAL
6	8	ABS PRESS	UPR#1	W198	A35	2.02
6	9	ABS PRESS	UPR#2	W198	A37	2.65
6	10	ABS PRESS	UPR#3	W198	A39	2.15
6	11	ABS PRESS	UPR#4	W198	A41	2.42
6	12	ABS PRESS	UPR#6	W198	A43	2.85
6	13	ABS PRESS	UPR#7	W198	A45	2.83
7	7	ABS PRESS	UPR#8	W198	A47	2.19
7	8	ABS PRESS	UPR#9	W198	B1	1.85
7	9	ABS PRESS	UPR#10	W198	B3	2.28
7	10	ABS PRESS	UPR#11	W198	B5	1.69
7	11	ABS PRESS	UPR#12	W198	B7	3.23
16	10	ABS PRESS	LWR#13	W198	E35	2.80
16	11	ABS PRESS	LWR#14	W198	E37	2.99
16	12	ABS PRESS	LWR#15	W198	E39	2.79
16	13	ABS PRESS	LWR#16	W198	E41	1.81
17	7	ABS PRESS	LWR#18	W198	E43	1.72
17	8	ABS PRESS	LWR#19	W198	E45	1.89
17	10	ABS PRESS	LWR#20	W198	E47	1.40
17	11	ABS PRESS	LWR#21	W198	F1	2.08
17	12	ABS PRESS	LWR#22	W198	F3	2.31
17	13	ABS PRESS	LWR#23	W198	F5	2.79
18	7	ABS PRESS	LWR#24	W198	F7	1.95

TRACK	BAND	ITEM	LOCATION	STA	CABLE	UNIT CAL
4	9	ABS PRESS	UPR#1	W228	B9	2.56
4	10	ABS PRESS	UPR#2	W228	B11	2.70
4	11	ABS PRESS	UPR#3	W228	B13	2.17
4	12	ABS PRESS	UPR#4	W228	B15	2.23
4	13	ABS PRESS	UPR#6	W228	B17	1.74
5	7	ABS PRESS	UPR#7	W228	B19	2.27

5	8	ABS PRESS	UPR#8	W228	B21	2.70
5	9	ABS PRESS	UPR#9	W228	B23	2.88
5	10	ABS PRESS	UPR#10	W228	B25	2.41
5	11	ABS PRESS	UPR#11	W228	B27	2.89
5	12	ABS PRESS	UPR#12	W228	B29	3.05
5	13	ABS PRESS	UPR#13	W228	B31	1.42
6	7	ABS PRESS	UPR#14	W228	B33	1.92
14	10	ABS PRESS	LWR#15	W228	F9	2.31
14	11	ABS PRESS	LWR#16	W228	F11	2.78
14	12	ABS PRESS	LWR#17	W228	F13	2.36
14	13	ABS PRESS	LWR#18	W228	F15	2.79
15	8	ABS PRESS	LWR#20	W228	F17	1.74
15	9	ABS PRESS	LWR#21	W228	F19	1.60
15	10	ABS PRESS	LWR#22	W228	F21	1.62
15	11	ABS PRESS	LWR#23	W228	F23	1.86
15	12	ABS PRESS	LWR#24	W228	F25	1.82
15	13	ABS PRESS	LWR#25	W228	F27	1.83
16	7	ABS PRESS	LWR#26	W228	F29	2.15
16	8	ABS PRESS	LWR#27	W228	F31	1.99
16	9	ABS PRESS	LWR#28	W228	F33	2.00
TRACK	BAND	ITEM	LOCATION	STA	CABLE	UNIT CAL
2	10	ABS PRESS	UPR#1	W240	B35	1.64
2	11	ABS PRESS	UPR#2	W240	B37	1.62
2	12	ABS PRESS	UPR#3	W240	B39	2.04
2	13	ABS PRESS	UPR#4	W240	B41	1.97
3	7	ABS PRESS	UPR#5	W240	B43	2.08
3	8	ABS PRESS	UPR#6	W240	B45	2.06
3	9	ABS PRESS	UPR#7	W240	B47	1.97
3	10	ABS PRESS	UPR#8	W240	C1	1.82
3	11	ABS PRESS	UPR#9	W240	C3	2.03
3	12	ABS PRESS	UPR#10	W240	C5	2.05
3	13	ABS PRESS	UPR#11	W240	C7	1.91
4	7	ABS PRESS	UPR#12	W240	C9	2.39
4	8	ABS PRESS	UPR#13	W240	C11	1.56
12	10	ABS PRESS	LWR#15	W240	F35	2.08
12	11	ABS PRESS	LWR#16	W240	F37	2.15
12	12	ABS PRESS	LWR#17	W240	F39	2.05
12	13	ABS PRESS	LWR#18	W240	F41	1.61
13	7	ABS PRESS	LWR#19	W240	F43	2.08
13	8	ABS PRESS	LWR#20	W240	F45	1.50
13	9	ABS PRESS	LWR#21	W240	F47	1.52
13	10	ABS PRESS	LWR#22	W240	G1	1.90
13	11	ABS PRESS	LWR#23	W240	G3	1.91
13	12	ABS PRESS	LWR#24	W240	G5	1.95
13	13	ABS PRESS	LWR#25	W240	G7	1.44
14	7	ABS PRESS	LWR#26	W240	G9	1.49
14	8	ABS PRESS	LWR#27	W240	G11	1.60
TRACK	BAND	ITEM	LOCATION	STA	CABLE	UNIT CAL
1	7	ABS PRESS	UPR#1	W252	C13	2.7
1	8	ABS PRESS	UPR#2	W252	C15	1.6
1	9	ABS PRESS	UPR#3	W252	C17	2.29
1	10	ABS PRESS	UPR#4	W252	C19	2.50
1	11	ABS PRESS	UPR#5	W252	C21	2.84
1	12	ABS PRESS	UPR#6	W252	C23	2.75
1	13	ABS PRESS	UPR#7	W252	C25	2.76
2	7	ABS PRESS	UPR#8	W252	C27	3.13
2	8	ABS PRESS	UPR#9	W252	C29	2.97
2	9	ABS PRESS	UPR#10	W252	C31	2.56
9	11	ABS PRESS	UPR#11	W252	C33	2.89
9	12	ABS PRESS	UPR#12	W252	C35	2.35
11	7	ABS PRESS	LWR#13	W252	G13	1.45
11	8	ABS PRESS	LWR#14	W252	G15	2.14
11	9	ABS PRESS	LWR#15	W252	G17	2.25
11	10	ABS PRESS	LWR#16	W252	G19	2.60
11	11	ABS PRESS	LWR#17	W252	G21	1.65
11	12	ABS PRESS	LWR#18	W252	G23	2.54

11	13	ABS PRESS	LWR#19	W252	G25	2.00
12	7	ABS PRESS	LWR#20	W252	G27	1.85
12	8	ABS PRESS	LWR#21	W252	G29	1.57
12	9	ABS PRESS	LWR#22	W252	G31	1.85
20	15	ABS PRESS	LWR#23	W252	G33	2.15
20	16	ABS PRESS	LWR#24	W252	G35	1.77
TRACK	BAND	ITEM	LOCATION	STA	CABLE	UNIT CAL
5	16	ABS PRESS	UPR#1	W256	C37	1.72
6	14	ABS PRESS	UPR#2	W256	C39	2.09
6	15	ABS PRESS	UPR#3	W256	C41	1.94
6	16	ABS PRESS	UPR#4	W256	C43	1.98
7	14	ABS PRESS	UPR#5	W256	C45	1.99
7	15	ABS PRESS	UPR#6	W256	C47	2.08
7	16	ABS PRESS	UPR#7	W256	D1	2.06
8	14	ABS PRESS	UPR#8	W256	D3	1.97
8	15	ABS PRESS	UPR#9	W256	D5	1.71
8	16	ABS PRESS	UPR#10	W256	D7	1.94
9	13	ABS PRESS	UPR#11	W256	D9	1.93
9	14	ABS PRESS	UPR#12	W256	D11	1.99
9	15	ABS PRESS	UPR#13	W256	D13	1.58
9	16	ABS PRESS	UPR#14	W256	D15	1.71
15	16	ABS PRESS	LWR#15	W256	G37	1.37
16	14	ABS PRESS	LWR#16	W256	G39	1.57
16	15	ABS PRESS	LWR#17	W256	G41	2.06
16	16	ABS PRESS	LWR#18	W256	G43	1.86
17	14	ABS PRESS	LWR#19	W256	G45	1.80
17	15	ABS PRESS	LWR#20	W256	G47	2.13
17	16	ABS PRESS	LWR#21	W256	H1	2.05
18	14	ABS PRESS	LWR#22	W256	H3	1.85
18	15	ABS PRESS	LWR#23	W256	H5	2.28
18	16	ABS PRESS	LWR#24	W256	H7	1.89
19	14	ABS PRESS	LWR#25	W256	H9	2.06
19	15	ABS PRESS	LWR#26	W256	H11	1.44
19	16	ABS PRESS	LWR#27	W256	H13	2.05
20	14	ABS PRESS	LWR#28	W256	H15	1.84
TRACK	BAND	ITEM	LOCATION	STA	CABLE	UNIT CAL
1	14	ABS PRESS	UPR#1	W261	D17	1.99
1	15	ABS PRESS	UPR#2	W261	D19	1.91
1	16	ABS PRESS	UPR#3	W261	D21	2.18
2	14	ABS PRESS	UPR#4	W261	D23	1.99
2	15	ABS PRESS	UPR#5	W261	D25	2.05
2	16	ABS PRESS	UPR#6	W261	D27	1.79
3	14	ABS PRESS	UPR#7	W261	D29	1.75
3	15	ABS PRESS	UPR#8	W261	D31	2.05
3	16	ABS PRESS	UPR#9	W261	D33	1.99
4	14	ABS PRESS	UPR#10	W261	D35	2.07
4	15	ABS PRESS	UPR#11	W261	D37	2.08
4	16	ABS PRESS	UPR#12	W261	D39	2.28
5	14	ABS PRESS	UPR#13	W261	D41	1.97
5	15	ABS PRESS	UPR#14	W261	D43	2.1
11	14	ABS PRESS	LWR#15	W261	H17	2.05
11	15	ABS PRESS	LWR#16	W261	H19	1.88
11	16	ABS PRESS	LWR#17	W261	H21	2.48
12	14	ABS PRESS	LWR#18	W261	H23	2.05
12	15	ABS PRESS	LWR#19	W261	H25	1.83
12	16	ABS PRESS	LWR#20	W261	H27	1.91
13	14	ABS PRESS	LWR#21	W261	H29	1.94
13	15	ABS PRESS	LWR#22	W261	H31	1.98
13	16	ABS PRESS	LWR#23	W261	H33	1.85
14	14	ABS PRESS	LWR#24	W261	H35	1.62
14	15	ABS PRESS	LWR#25	W261	H37	1.43
14	16	ABS PRESS	LWR#26	W261	H39	2.04
15	14	ABS PRESS	LWR#27	W261	H41	2.07
15	15	ABS PRESS	LWR#28	W261	H43	2.04

TOTAL NUMBER OF ABS P = 188

TRACK	BAND	ITEM	LOCATION	STA	CABLE	UNIT CAL
15	7	HWS SGMT	#7	R198	J1	5.839
17	9	HWS SGMT	#8	R198	J3	5.839
20	2	HWS SGMT	#9	R198	J5	5.839
20	3	HWS SGMT	#10	R198	J7	5.839
20	4	HWS SGMT	#11	R198	J9	5.839
20	5	HWS SGMT	#12	R198	J11	5.839
20	6	HWS SGMT	#13	R198	J13	5.839
20	11	HWS SGMT	#14	R198	J15	5.839
20	12	HWS SGMT	#15	R198	J17	5.839
TRACK	BAND	ITEM	LOCATION	STA	CABLE	UNIT CAL
1	1	HWS SGMT	#1	R228	J19	5.839
1	2	HWS SGMT	#2	R228	J21	5.839
1	3	HWS SGMT	#3	R228	J23	5.839
1	4	HWS SGMT	#4	R228	J25	5.839
1	5	HWS SGMT	#5	R228	J27	5.839
1	6	HWS SGMT	#6	R228	J29	5.839
2	1	HWS SGMT	#7	R228	J31	5.839
2	2	HWS SGMT	#8	R228	J33	5.839
2	3	HWS SGMT	#9	R228	J35	5.839
2	4	HWS SGMT	#10	R228	J37	5.839
2	5	HWS SGMT	#11	R228	J39	5.839
2	6	HWS SGMT	#12	R228	J41	5.839
3	1	HWS SGMT	#13	R228	J43	5.839
3	2	HWS SGMT	#14	R228	J45	5.839
3	3	HWS SGMT	#15	R228	J47	5.839
3	4	HWS SGMT	#16	R228	K1	5.839
3	5	HWS SGMT	#17	R228	K3	5.839
3	6	HWS SGMT	#18	R228	K5	5.839
4	1	HWS SGMT	#19	R228	K7	5.839
TRACK	BAND	ITEM	. LOCATION	STA	CABLE	UNIT CAL
17	1	HWS SGMT	#1	R252	K9	5.839
17	2	HWS SGMT	#2	R252	K11	5.839
17	3	HWS SGMT	#3	R252	K13	5.839
17	4	HWS SGMT	#4	R252	K15	5.839
17	5	HWS SGMT	#5	R252	K17	5.839
17	6	HWS SGMT	#6	R252	K19	5.839
18	1	HWS SGMT	#7	R252	K21	5.839
18	2	HWS SGMT	#8	R252	K23	5.839
18	3	HWS SGMT	#9	R252	K25	5.839
18	4	HWS SGMT	#10	R252	K27	5.839
18	5	HWS SGMT	#11	R252	K29	5.839
18	6	HWS SGMT	#12	R252	K31	5.839
19	1	HWS SGMT	#13	R252	K33	5.839
19	2	HWS SGMT	#14	R252	K35	5.839
19	3	HWS SGMT	#15	R252	K37	5.839
19	4	HWS SGMT	#16	R252	K39	5.839
19	5	HWS SGMT	#17	R252	K41	5.839
19	6	HWS SGMT	#18	R252	K43	5.839
20	1	HWS SGMT	#19	R252	K45	5.839

TOTAL NUMBER OF HWS S = 47

TRACK	BAND	ITEM	LOCATION	STA	CABLE	UNIT CAL
11	1	BL BUTTON	UPR#1-I	R198	L1	1.39
11	2	BL BUTTON	UPR#2-I	R198	L3	2.03
11	3	BL BUTTON	UPR#3-I	R198	L5	2.09
11	4	BL BUTTON	LWR#4-I	R198	L7	3.34
11	5	BL BUTTON	LWR#5-I	R198	L9	3.73
11	6	BL BUTTON	LWR#6-I	R198	L11	4.63
12	1	BL BUTTON	UPR#1-O	R198	L13	1.10
12	2	BL BUTTON	UPR#2-O	R198	L15	1.83
12	3	BL BUTTON	UPR#3-O	R198	L17	1.85
12	4	BL BUTTON	LWR#4-O	R198	L19	2.98
12	5	BL BUTTON	LWR#5-O	R198	L21	2.01
12	6	BL BUTTON	LWR#6-O	R198	L23	2.40
TRACK	BAND	ITEM	LOCATION	STA	CABLE	UNIT CAL
13	1	BL BUTTON	UPR#1-I	R228	L25	2.50
13	2	BL BUTTON	UPR#2-I	R228	L27	1.81
13	3	BL BUTTON	UPR#3-I	R228	L29	1.99
13	4	BL BUTTON	LWR#4-I	R228	L31	2.41
13	5	BL BUTTON	LWR#5-I	R228	L33	2.18
13	6	BL BUTTON	LWR#6-I	R228	L35	2.47
14	1	BL BUTTON	UPR#1-O	R228	L37	2.66
14	2	BL BUTTON	UPR#2-O	R228	L39	1.40
14	3	BL BUTTON	UPR#3-O	R228	L41	2.79
14	4	BL BUTTON	LWR#4-O	R228	L43	2.42
14	5	BL BUTTON	LWR#5-O	R228	L45	2.40
14	6	BL BUTTON	LWR#6-O	R228	L47	2.46
TRACK	BAND	ITEM	LOCATION	STA	CABLE	UNIT CAL
15	1	BL BUTTON	UPR#1-I	R252	M1	2.65
15	2	BL BUTTON	UPR#2-I	R252	M3	2.54
15	3	BL BUTTON	UPR#3-I	R252	M5	3.12
15	4	BL BUTTON	LWR#4-I	R252	M7	1.99
15	5	BL BUTTON	LWR#5-I	R252	M9	2.26
15	6	BL BUTTON	LWR#6-I	R252	M11	2.69
16	1	BL BUTTON	UPR#1-O	R252	M13	2.59
16	2	BL BUTTON	UPR#2-O	R252	M15	2.59
16	3	BL BUTTON	UPR#3-O	R252	M17	2.62
16	4	BL BUTTON	LWR#4-O	R252	M19	2.00
16	5	BL BUTTON	LWR#5-O	R252	M21	1.65
16	6	BL BUTTON	LWR#6-O	R252	M23	2.40

TOTAL NUMBER OF BL BU = 36

TRACK	BAND	ITEM	LOCATION	STA	CABLE	UNIT CAL
8	5	VIBR-BEAM	-	R3.5	Q39	2.902
8	6	VIBR-CHORD	-	R3.5	Q41	2.341
TRACK	BAND	ITEM	LOCATION	STA	CABLE	UNIT CAL
5	6	VIBR-BEAM	-	R132	N9	2.38
9	5	VIBR-CHORD	-	R132	N11	2.266
TRACK	BAND	ITEM	LOCATION	STA	CABLE	UNIT CAL
9	3	VIBR-BEAM	-	R156	N13	2.11
9	4	VIBR-CHORD	-	R156	N15	2.179
TRACK	BAND	ITEM	LOCATION	STA	CABLE	UNIT CAL
9	1	VIBR-BEAM	-	R184	N5	2.131
9	2	VIBR-CHORD	-	R184	N7	2.192
TRACK	BAND	ITEM	LOCATION	STA	CABLE	UNIT CAL
8	1	VIBR-BEAM	-	R238	N17	2.182
8	3	VIBR-CHORD	-	R238	N19	2.069
TRACK	BAND	ITEM	LOCATION	STA	CABLE	UNIT CAL
8	2	VIBR-BEAM	-	R263	N21	2.484
8	4	VIBR-CHORD	-	R263	N23	2.186

TOTAL NUMBER OF VIBR- = 12

TRACK	BAND	ITEM	LOCATION	STA	CABLE	UNIT CAL
6	2	BLADE BEAM	-	R 60	P1	31453
7	2	BLADE CH	-	R 60	P3	156852
TRACK	BAND	ITEM	LOCATION	STA	CABLE	UNIT CAL
10	7	BLADE BEAM	-	R 82	P5	23813
10	10	BLADE CH	-	R 82	P7	140175
10	13	BLADE TORS	-	R 82	P9	32420
TRACK	BAND	ITEM	LOCATION	STA	CABLE	UNIT CAL
10	9	BLADE BEAM	-	R103	P11	21716
10	12	BLADE CH	-	R103	P13	164813
TRACK	BAND	ITEM	LOCATION	STA	CABLE	UNIT CAL
4	4	BLADE TORS	-	R132	P15	17022
10	8	BLADE BEAM	-	R132	P17	18944
10	11	BLADE CH	-	R132	P19	142634
TRACK	BAND	ITEM	LOCATION	STA	CABLE	UNIT CAL
4	5	BLADE TORS	-	R185	P21	23511
6	3	BLADE BEAM	-	R185	P23	17427
7	3	BLADE CH	-	R185	P25	110529
TRACK	BAND	ITEM	LOCATION	STA	CABLE	UNIT CAL
6	4	BLADE BEAM	-	R212	P27	10093
7	4	BLADE CH	-	R212	P29	108833
TRACK	BAND	ITEM	LOCATION	STA	CABLE	UNIT CAL
4	6	BLADE TORS	-	R238	P31	19790
6	5	BLADE BEAM	-	R238	P33	18123
7	5	BLADE CH	-	R238	P35	160905

TOTAL NUMBER OF BLADE = 18

TRACK	BAND	ITEM	LOCATION	STA	CABLE	UNIT CAL
4	2	YOKE TORS	-	R6.0	Q1	58.63
4	3	YOKE TORS	-	W6.0	Q3	58.63
5	1	YOKE BEAM	-	W6.0	Q5	15054
5	2	YOKE BEAM	-	R 11	Q7	12015
5	3	YOKE CHORD	-	R6.0	Q9	411767
5	5	YOKE CHORD	-	W6.0	Q11	410113
6	6	VOLT MON A	-	-	Q13	-
7	6	PITCH LINK	AX WHITE	-	Q15	3228
10	1	FLAPPING	-	-	Q17	2.1078
10	2	MAST TORQUE	-	21.0	Q19	39198
10	3	PITCH LINK	AX RED	-	Q21	3236
10	4	DRAG BRACE	RED	-	Q23	14041
10	5	YOKE BEAM	-	R6.0	Q25	14178
10	6	GRIP BM BD	-	R 38	Q27	75150
10	14	YOKE CHORD	-	R 11	Q29	12015
10	15	MAST PARA	-	47.2	Q31	34124
10	16	MAST PERP	-	47.2	Q33	33942
14	9	FEATHERING	-	-	Q35	1.6513
20	13	VOLT MON B	-	-	Q37	-

TOTAL NUMBER OF OTHER = 19

ORIGINAL PAGE IS
OF POOR QUALITY

Program No.: F0620 Model: AH-1G S/N: 20004 Date: 27 Feb. 81 Rec: 2001
Track: 1 Box: 1 Multiplex: 1 Data coordinator: Goodfellow Engineer: Whitener
Technician: Gray Program: OLS Rotor System (ARC)

Band	Balance	Item code	Item Location station	Lab No. Bridge No.	Sensor code (SCM)	Unit calibration Ref.	Units Excitation	Cable No.	Remarks
			Position	--		854	%		
1	50	D021	Fore/aft stick	--	KP	50	5.92	1/6	
			Position	--		779	%		
2	50	D022	Lateral stick	--	KP	50	5.92	1/7	
			Position	--		773	%		
3	10	D024	Pedal	--	KG	0*	5.92	1/8	*Full lt pedal
			Position	--		1002	%		
4	10	D023	Collective stick	--	KP	0*	5.92	1/5	*Full down stick
			Position	--		352.5	deg		
7	50	D007	Angle of sideslip	--	KG	0	5.92	1/1	
			Position	--		357.2	deg		
8	50	D008	Angle of attack	--	KG	0	5.92	1/2	
			Pitch attitude	H-32		177.66	deg		
9	50	D010	Gyro	--	KP	0	5.96	/1	
			Roll attitude	H-32		359.81	deg		
10	50	D009	Gyro	--	KT	0	5.96	/2	
			Yaw attitude	H-26		367.22	deg		
11	50	D011	Gyro	--	KG	0	5.96	/3	
			Pitch rate	206		30.0	deg/sec		
12	50	V013	Gyro	--	KB	--	1.0	/4	

Track 1 (Concluded)

Band	Balance	Item code	Item / Location station	Lab No. / Bridge No.	Sensor code (SCM)	Unit calibration / Ref.	Units / Excitation	Cable No.	Remarks
			Roll rate	206		29.99	deg/sec		
13	50	V012	Gyro	--	KB	--	1.0	/5	
			Yaw rate	206		29.9	deg/sec		
14	50	V014	Gyro	--	KB	29.9	1.0	/6	

Program No.: F0620 Model: AH-1G S/N: 20004 Date: 27 Feb 81 Rec: 2001
Track: 2 Box: 1 Multiplex: 2 Data coordinator: Goodfellow Engineer: Whitener
Technician: Gray Program: OLS Rotor System (ARC)

Band	Balance	Item code	Item Location station	Lab No. Bridge No.	Sensor code (SCM)	Unit calibration Ref.	Units Excitation	Cable No.	Remarks
1	20	T004	Temperature	R0580-10	KR	0.0294		1/4	
			OAT	--		0	1.0		
2	10	P002	Airspeed	11443	HR	18,090	$(knots)^2$	1/3	
			--	--		0	5.92		
3	20	P506	Pressure	3352	HP	28.9	psi	3/4	
			Engine torque	--		0	5.99		
4	20	P030	Pressure	11440	HR	0.308	psi	1/10	
			Ship'd static	--		14.7	5.92		
7	50	F100	Axial force	13150AF	HB	4350	lb	3/3	
			Fore/aft cyclic boost tube	01		0	5.94		
8	50	F101	Axial force	13151AF	HB	4923	lb	3/2	
			Lateral cyclic boost tube	01		0	5.94		
9	50	F102	Axial force	13152AF	HB	4749	lb	3/1	
			Collective boost tube	01		0	5.94		
10	50	A019	Vertical acceleration	13935	HP	0.986	g	1/9	
			Pilot seat	--		1	5.92		
11	30	R018	Main rotor RPM	--	KW	--	RPM	Rear PB	
			--	--		0	--		

Track 2 (Concluded)

Band	Balance	Item code	Item / Location station	Lab No. / Bridge No.	Sensor code (SCM)	Unit calibration / Ref.	Units / Excitation	Cable No.	Remarks
12	30	R025	Tail rotor RPM	--	KW	--	RPM	Rear PB	
			--	--		0	--		
13	50	A005	Vertical acceleration	13932	HP	0.993	g	3/7	
			CG	--		1	5.94		

ORIGINAL PAGE IS
OF POOR QUALITY

Program No.: W056 Model: OLS S/N: WT Date: 3/10/81 Rec: 001
Track: 5 Box: N/A Multiplex: 1 Data coordinator: Goodfellow Engineer: Whitener
Technician: Gray Program: OLS Modification

Band	Balance	Item code	Item		Lab No.	Sensor code (SCM)	Unit calibration	Units	Cable No.	Remarks
			Location station		Bridge No.		Ref.	Excitation		
			Hws sgmt		--		5.839	% full scale		
1	40	V866	#1	R228	--	FG	0	6.00	J19	
			Hws sgmt		--		5.839	% full scale		
2	40	V867	#2	R228	--	FG	0	6.00	J21	
			Hws sgmt		--		5.839	% full scale		
3	40	V878	#3	R228	--	FG	0	6.00	J23	
			Hws sgmt		--		5.839	% full scale		
4	40	V879	#4	R228	--	FG	0	6.00	J25	
			Hws sgmt		--		5.839	% full scale		
5	40	V880	#5	R228	--	FG	0	6.00	J27	
			Hws sgmt		--		5.839	% full scale		
6	40	V881	#6	R228	--	FG	0	6.00	J29	
			Abs press		--		2.7	psia		
7	70	P908	Upper #1	W252	--	FO	14.7	5.500	C13	
			Abs press		--		1.6	psia		
8	70	P909	Upper #2	W252	--	FO	14.7	5.500	C15	

Track 5 (Concluded)

Band	Balance	Item code	Item Location station	Lab No. Bridge No.	Sensor code (SCM)	Unit calibration Ref.	Units Excitation	Cable No.	Remarks
			Abs press	--		2.29	psia		
9	70	P919	Upper #3 W252	--	FO	14.7	5.500	C17	
			Abs press	--		2.50	psia		
10	70	P920	Upper #4 W252	--	FO	14.7	5.500	C19	
			Abs press	--		2.84	psia		
11	70	P921	Upper #5 W252	--	FO	14.7	5.500	C21	
			Abs press	--		2.75	psia		
12	70	P926	Upper #6 W252	--	FO	14.7	5.500	C23	
			Abs press	--		2.76	psia		
13	70	P927	Upper #7 W252	--	FO	14.7	5.500	C25	
			Abs press	--		1.99	psia		
14	70	P661	Upper #1 W261	--	FO	14.7	5.500	D17	
			Abs press	--		1.91	psia		
15	70	P662	Upper #2 W261	--	FO	14.7	5.500	D19	
			Abs press	--		2.18	psia		
16	70	P663	Upper #3 W261	--	FO	14.7	5.500	D21	

Program No.: W056 Model: OLS S/N: WT Date: 3/10/81 Rec: 001
Track: 6 Box: N/A Multiplex: 2 Data coordinator: Goodfellow Engineer: Whitener
Technician: Gray Program: OLS Modification

Band	Balance	Item code	Item		Lab No.	Sensor code (SCM)	Unit calibration	Units	Cable No.	Remarks
			Location	station	Bridge No.		Ref.	Excitation		
1	40	V894	Hws sgmt		--	FG	5.839	% Full scale	J31	
			#7	R228	--		0	6.00		
2	40	V895	Hws sgmt		--	FG	5.839	% Full scale	J33	
			#8	R228	--		0	6.00		
3	40	V896	Hws sgmt		--	FG	5.839	% Full scale	J35	
			#9	R228	--		0	6.00		
4	40	V897	Hws sgmt		--	FG	5.839	% Full scale	J37	
			#10	R228	--		0	6.00		
5	40	V898	Hws sgmt		--	FG	5.839	% Full scale	J39	
			#11	R228	--		0	6.00		
6	40	V899	Hws sgmt		--	FG	5.839	% Full scale	J41	
			#12	R228	--		0	6.00		
7	70	P928	Abs press		--	FO	3.13	psia	C27	
			Upper #8	W252	--		14.7	5.500		
8	70	P941	Abs press		--	FW	2.97	psia	C29	
			Upper #9	W252	--		14.7	5.500		

Track 6 (Concluded)

Band	Balance	Item code	Item Location station		Lab No. Bridge No.	Sensor code (SCM)	Unit calibration Ref.	Units Excitation	Cable No.	Remarks
9	70	P942	Abs press		--	FW	2.56	psia	C31	
			Upper #10	W252	--		14.7	5.500		
10	70	P601	Abs press		--	FO	1.64	psia	B35	
			Upper #1	W240	--		14.7	5.500		
11	70	P602	Abs press		--	FO	1.62	psia	B37	
			Upper #2	W240	--		14.7	5.500		
12	70	P603	Abs press		--	FO	2.04	psia	B39	
			Upper #3	W240	--		14.7	5.500		
13	70	P604	Abs press		--	FO	1.97	psia	B41	
			Upper #4	W240	--		14.7	5.500		
14	70	P664	Abs press		--	FO	1.99	psia	D23	
			Upper #4	W261	--		14.7	5.500		
15	70	P665	Abs press		--	FO	2.05	psia	D25	
			Upper #5	W261	--		14.7	5.500		
16	70	P666	Abs press		--	FO	1.79	psia	D27	
			Upper #6	W261	--		14.7	5.500		

Program No.: W056 Model: OLS S/N: WT Date: 3/10/81 Rec: 001
Track: 7 Box: N/A Multiplex: 3 Data coordinator: Goodfellow Engineer: Whitener
Technician: Gray Program: OLS Modification

Band	Balance	Item code	Item / Location station		Lab No. / Bridge No.	Sensor code (SCM)	Unit calibration / Ref.	Units / Excitation	Cable No.	Remarks
1	40	V910	Hws sgmt		--	FG	5.839	% Full scale	J43	
			#13	R228	--		0	6.00		
2	40	V911	Hws sgmt		--	FG	5.839	% Full scale	J45	
			#14	R228	--		0	6.00		
3	40	V912	Hws sgmt		--	FG	5.839	% Full scale	J47	
			#15	R228	--		0	6.00		
4	40	V913	Hws sgmt		--	FG	5.839	% Full scale	K1	
			#16	R228	--		0	6.00		
5	40	V914	Hws sgmt		--	FG	5.839	% Full scale	K3	
			#17	R228	--		0	6.00		
6	40	V915	Hws sgmt		--	FG	5.839	% Full scale	K5	
			#18	R228	--		0	6.00		
7	70	P605	Abs press		--	FO	2.08	psia	B43	
			Upper #5	W240	--		14.7	5.500		
8	70	P606	Abs press		--		2.06	psia	B45	
			Upper #6	W240	--		14.7	5.500		

Track 7 (Concluded)

Band	Balance	Item code	Item Location station	Lab No. Bridge No.	Sensor code (SCM)	Unit calibration Ref.	Units Excitation	Cable No.	Remarks
			Abs press	--		1.97	psia		
9	70	P607	Upper #7 W240	--	FO	14.7	5.500	B47	
			Abs press	--		1.82	psia		
10	70	P608	Upper #8 W240	--	FO	14.7	5.500	C1	
			Abs press	--		2.03	psia		
11	70	P609	Upper #9 W240	--	FW	14.7	5.500	C3	
			Abs press	--		2.05	psia		
12	70	P610	Upper #10 W240	--	FW	14.7	5.500	C5	
			Abs press	--		1.91	psia		
13	70	P611	Upper #11 W240	--	FW	14.7	5.500	C7	
			Abs press	--		1.75	psia		
14	70	P667	Upper #7 W261	--	FO	14.7	5.500	D29	
			Abs press	--		2.05	psia		
15	70	P668	Upper #8 W261	--	FO	14.7	5.500	D31	
			Abs press	--		1.99	psia		
16	70	P669	Upper #9 W261	--	FW	14.7	5.500	D33	

Program No.: W056 Model: OLS S/N: WT Date: 3/10/81 Rec: 001
Track: 8 Box: N/A Multiplex: 4 Data coordinator: Goodfellow Engineer: Whitener
Technician: Gray Program: OLS Modification

Band	Balance	Item code	Item / Location	station	Lab No. / Bridge No.	Sensor code (SCM)	Unit calibration / Ref.	Units / Excitation	Cable No.	Remarks
			Hws sgmt		--		5.839	% Full scale		
1	40	V922	#19	R228	--	FG	0	6.00	K7	
			Yoke tors		09323BM		58.63	in.-lb		
2	50	M906	--	R6.0	05	FB	50	6.00	Q1	
			Yoke tors		09323BM		58.63	in.-lb		
3	50	M918	--	W6.0	09	FB	50	6.00	Q3	
			Blade tors		09449BM		17022	in.-lb		
4	70	M935	--	R132	38	FB	0	5.500	P15	
			Blade tors		09449BM		23511	in.-lb		
5	70	M936	--	R185	39	FB	0	5.500	P21	
			Blade tors		09449BM		19790	in.-lb		
6	70	M937	--	R238	40	FR	0	5.500	P31	
			Abs press		--		2.39	psia		
7	70	P612	Upper #12	W240	--	FW	14.7	5.500	C9	
			Abs press		--		1.56	psia		
8	30	P613	Upper #13	W240	--	FW	14.7	5.500	C11	
			Abs press		--		2.56	psia		
9	70	P164	Upper #1	W228	--	FO	14.7	5.500	B9	

Track 8 (Concluded)

Band	Balance	Item code	Item Location station		Lab No. Bridge No.	Sensor code (SCM)	Unit calibration Ref.	Units Excitation	Cable No.	Remarks
			Abs press		--		2.70	psia		
10	70	P165	Upper #2	W228	--	FO	14.7	5.500	B11	
			Abs press		--		2.17	psia		
11	70	P166	Upper #3	W228	--	FO	14.7	5.500	B13	
			Abs press		--		2.23	psia		
12	70	P180	Upper #4	W228	--	FW	14.7	5.500	B15	
			Abs press		--		1.74	psia		
13	70	P182	Upper #6	W228	--	FO	14.7	5.500	B17	
			Abs press		--		2.07	psia		
14	70	P670	Upper #10	W261	--	FW	14.7	5.500	D35	
			Abs press		--		2.08	psia		
15	70	P671	Upper #11	W261	--	FW	14.7	5.500	D37	
			Abs press		--		2.28	psia		
16	70	P672	Upper #12	W261	--	FW	14.7	5.500	D39	

Program No.: W056 Model: OLS S/N: WT Date: 3/10/81 Rec: 001
Track: 9 Box: N/A Multiplex: 5 Data coordinator: Goodfellow Engineer: Whitener
Technician: Gray Program: OLS Modification

Band	Balance	Item code	Item Location station	Lab No. Bridge No.	Sensor code (SCM)	Unit calibration Ref.	Units Excitation	Cable No.	Remarks
			Yoke beam	09323BM		15054	in.-lb		
1	25	B916	-- W6.0	08	FO	-41,158	5.500	Q5	
			Yoke beam	09323BM		12015	in.-lb		
2	15	B114	-- R 11	04	FO	-38,531	5.500	Q7	
			Yoke chord	09323BM		411767	in.-lb		
3	20	B113	-- R6.0	01	FB	0	5.500	Q9	
			Abs press	--		2.56	psia		
4	70	P157	Upper #1 W106	--	FO	14.7	5.500	A1	
			Yoke chord	09323BM		410113	in.-lb		
5	40	B917	-- W6.0	07	FB	0	5.500	Q11	
			Vibr-beam	--		2.38	g		
6	50	A950	-- R132	--	FG	+1	5.500	N9	
			Abs press	--		2.27	psia		
7	70	P194	Upper #7 W228	--	FO	14.7	5.500	B19	
			Abs press	--		2.70	psia		
8	70	P195	Upper #8 W228	--	FO	14.7	5.500	B21	
			Abs press	--		2.88	psia		
9	70	P196	Upper #9 W228	--	FW	14.7	5.500	B23	
			Abs press	--		2.41	psia		
10	70	P813	Upper #10 W228	--	FW	14.7	5.500	B25	

Track 9 (Concluded)

Band	Balance	Item code	Item Location station	Lab No. Bridge No.	Sensor code (SCM)	Unit calibration Ref.	Units Excitation	Cable No.	Remarks
			Abs press	--		2.89	psia		
11	70	P814	Upper #11 W228	--	FW	14.7	5.500	B27	
			Abs press	--		3.05	psia		
12	70	P815	Upper #12 W228	--	FW	14.7	5.500	B29	
			Abs press	--		1.42	psia		
13	70	P829	Upper #13 W228	--	FW	14.7	5.500	B31	
			Abs press	--		1.97	psia		
14	30	P673	Upper #13 W261	--	FW	14.7	5.500	D41	
			Abs press	--		2.1	psia		
15	70	P674	Upper #14 W261	--	FW	14.7	5.500	D43	
			Abs press	--		1.72	psia		
16	70	P631	Upper #1 W256	--	FO	14.7	5.500	C37	

Program No.: W056 Model: OLS S/N: WT Date: 3/10/81 **Rec:** 001
Track: 10 Box: N/A Multiplex: 6 Data coordinator: Goodfellow **Engineer:** Whitener
Technician: Gray Program: OLS Modification

Band	Balance	Item code	Item Location	Item station	Lab No. Bridge No.	Sensor code (SCM)	Unit calibration Ref.	Units Excitation	Cable No.	Remarks
			Abs press		--		1.22	psia		
1	70	P158	Upper #2	W106	--	FO	14.7	5.500	A3	
			Blade beam		09449BM		31453	in.-lb		
2	30	B120	--	R 60	22	FW	-23,126	5.500	P1	
			Blade beam		09449BM		17427	in.-lb		
3	40	B132	--	R185	32	FW	-3,993	5.500	P23	
			Blade beam		09449BM		18093	in.-lb		
4	50	B124	--	R212	34	FW	-1,729	5.500	P27	
			Blade beam		09449BM		18123	in.-lb		
5	40	B134	--	R238	36	FB	-429	5.500	P33	
			Volt monitor A		--		--	--		
6	70	V016	--	--	--	BB	--	5.500	Q13	FG mod, 80 mV
			Abs press		--		1.92	psia		
7	70	P830	Upper #14	W228	--	FO	14.7	5.500	B33	
			Abs press		--		2.02	psia		
8	70	P828	Upper #1	W198	--	FO	14.7	5.500	A35	
			Abs press		--		2.65	psia		
9	70	P836	Upper #2	W198	--	FO	14.7	5.500	A37	
			Abs press		--		2.15	psia		
10	70	P837	Upper #3	W198	--	FY	14.7	5.500	A39	

Track 10 (Concluded)

Band	Balance	Item code	Item / Location	station	Lab No. / Bridge No.	Sensor code (SCM)	Unit calibration / Ref.	Units / Excitation	Cable No.	Remarks
			Abs press		--		2.42	psia		
11	90	P838	Upper #4	W198	--	FO	14.7	5.500	A41	
			Abs press		--		2.85	psia		
12	70	P840	Upper #6	W198	--	FO	14.7	5.500	A43	
			Abs press		--		2.83	psia		
13	70	P841	Upper #7	W198	--	FW	14.7	5.500	A45	
			Abs press		--		2.09	psia		
14	70	P632	Upper #2	W256	--	FO	14.7	5.500	C39	
			Abs press		--		1.94	psia		
15	70	P633	Upper #3	W256	--	FO	14.7	5.500	C41	
			Abs press		--		1.98	psia		
16	70	P634	Upper #4	W256	--	FO	14.7	5.500	C43	

Program No.: W056 Model: OLS S/N: WT Date: 3/10/81 Rec: 001
Track: 11 Box: N/A Multiplex: 7 Data coordinator: Goodfellow Engineer: Whitener
Technician: Gray Program: OLS Modification

Band	Balance	Item code	Item Location station	Lab No. Bridge No.	Sensor code (SCM)	Unit calibration Ref.	Units Excitation	Cable No.	Remarks
			Abs press	--		2.38	psia		
1	70	P159	Upper #3 W106	--	FW	14.7	5.500	A5	
			Blade chord	09449BM		156852	in.-lb		
2	40	B121	-- R 60	21	FW	0	5.500	P3	
			Blade chord	09449BM		110529	in.-lb		
3	30	B133	-- R185	31	FR	0	5.500	P25	
			Blade chord	09449BM		108833	in.-lb		
4	50	B125	-- R212	33	FB	0	5.500	P29	
			Blade chord	09449BM		160905	in.-lb		
5	60	B135	-- R238	35	FB	0	5.500	P35	
			Pitch link	13149AF		3228	lb		
6	50	F104	Axis white --	--	FW	0	5.500	Q15	
			Abs press	--		2.19	psia		
7	70	P842	Upper #8 W198	--	FO	14.7	5.500	A47	
			Abs press	--		1.85	psia		
8	70	P852	Upper #9 W198	--	FW	14.7	5.500	B1	
			Abs press	--		2.28	psia		
9	70	P853	Upper #10 W198	--	FW	14.7	5.500	B3	
			Abs press	--		1.69	psia		
10	70	P854	Upper #11 W198	--	FW	14.7	5.500	B5	

Track 11 (Concluded)

Band	Balance	Item code	Item Location station		Lab No. Bridge No.	Sensor code (SCM)	Unit calibration Ref.	Units Excitation	Cable No.	Remarks
			Abs press		--		3.23	psia		
11	70	P855	Upper #12	W198	--	FW	14.7	5.500	B7	
			Abs press		--		2.9	psia		
12	70	P187	Upper #1	W158	--	FW	14.7	5.500	A15	
			Abs press		--		2.84	psia		
13	70	P188	Upper #2	W158	--	FO	14.7	5.500	A17	
			Abs press		--		1.99	psia		
14	70	P635	Upper #5	W256	--	FO	14.7	5.500	C45	
			Abs press		--		2.08	psia		
15	70	P636	Upper #6	W256	--	FO	14.7	5.500	C47	
			Abs press		--		2.06	psia		
16	70	P637	Upper #7	W256	--	FO	14.7	5.500	D1	

Program No.: W056 Model: OLS S/N: WT Date: 3/10/81 Rec: 001
Track: 12 Box: N/A Multiplex: 8 Data coordinator: Goodfellow Engineer: Whitener
Technician: Gray Program: OLS Modification

Band	Balance	Item code	Item		Lab No.	Sensor code (SCM)	Unit calibration	Units	Cable No.	Remarks
			Location	station	Bridge No.		Ref.	Excitation		
			Vibr beam		--		2.182	g		
1	50	A953	--	R238	--	FG	+1	5.500	N17	
			Vibr beam		--		2.484	g		
2	50	A954	--	R263	--	FG	+1	5.500	N21	
			Vibr chord		--		2.069	g		
3	30	A971	--	R238	--	FY	0	5.500	N19	
			Vibr chord		--		2.186	g		
4	50	A972	--	R263	--	FY	0	5.500	N23	
			Vibr beam		--		2.902	g		
5	50	A889	--	R3.5	--	FO	+1	5.500	Q39	
			Vibr chord		--		2.341	g		
6	30	A905	--	R3.5	--	FO	0	5.500	Q41	
			Abs press		--		2.27	psia		
7	70	P189	Upper #3	W158	--	FO	14.7	5.500	A19	
			Abs press		--		2.55	psia		
8	70	P190	Upper #4	W158	--	FW	14.7	5.500	A21	
			Abs press		--		2.50	psia		
9	70	P191	Upper #5	W158	--	FW	14.7	5.500	A23	
			Abs press		--		2.01	psia		
10	70	P192	Upper #6	W158	--	FW	14.7	5.500	A25	

Track 12 (Concluded)

Band	Balance	Item code	Item Location station	Lab No. Bridge No.	Sensor code (SCM)	Unit calibration Ref.	Units Excitation	Cable No.	Remarks
			Abs press	--		2.07	psia		
11	70	P193	Upper #7 W158	--	FW	14.7	5.500	A27	
			Abs press	--		3.00	psia		
12	70	P806	Upper #8 W158	--	FW	14.7	5.500	A29	
			Abs press	--		1.61	psia		
13	70	P807	Upper #9 W158	--	FW	14.7	5.500	A31	
			Abs press	--		1.97	psia		
14	70	P638	Upper #8 W256	--	FO	14.7	5.500	D3	
			Abs press	--		1.71	psia		
15	70	P639	Upper #9 W256	--	FW	14.7	5.500	D5	
			Abs press	--		1.94	psia		
16	70	P640	Upper #10 W256	--	FW	14.7	5.500	D7	

Program No.: W056 Model: OLS S/N: WT Date: 3/10/81 Rec: 001
Track: 15 Box: N/A Multiplex: 9 Data coordinator: Goodfellow Engineer: Whitener
Technician: Gray Program: OLS Modification

Band	Balance	Item code	Item / Location	station	Lab No. / Bridge No.	Sensor code (SCM)	Unit calibration / Ref.	Units / Excitation	Cable No.	Remarks
			Vibr beam		--		2.131	g		
1	50	A952	--	R084	--	FY	+1	5.500	N5	
			Vibr chord		--		2.192	g		
2	50	A970	--	R034	--	FO	0	5.500	N7	
			Vibr beam		--		2.11	g		
3	50	A951	--	R156	--	FG	+1	5.500	N13	
			Vibr chord		--		2.179	g		
4	50	A969	--	R156	--	FY	0	5.500	N15	
			Vibr chord		--		2.266	g		
5	50	A968	--	R132	--	FY	0	5.500	N11	
			Abs press		--		2.61	psia		
6	80	P160	Upper #4	W106	--	FB	14.7	5.500	A7	
			Abs press		--		1.66	psia		
7	70	P808	Upper #10	W158	--	FW	14.7	5.500	A33	
			Abs press		--		1.96	psia		
8	70	P161	Upper #5	W106	--	FB	14.7	5.500	A9	
			Abs press		--		3.37	psia		
9	70	P162	Upper #6	W106	--	FB	14.7	5.500	A11	
			Abs press		--		1.74	psia		
10	70	P163	Upper #7	W106	--	FB	14.7	5.500	A13	

Track 15 (Concluded)

Band	Balance	Item code	Item		Lab No.	Sensor	Unit calibration	Units	Cable	Remarks
			Location	station	Bridge No.	code (SCM)	Ref.	Excitation	No.	
			Abs press		--		2.89	psia		
11	70	P943	Upper #11	W252	--	FW	14.7	5.500	C33	
			Abs press		--		2.35	psia		
12	70	P957	Upper #12	W252	--	FW	14.7	5.500	C35	
			Abs press		--		1.93	psia		
13	70	P614	Upper #11	W256	--	FW	14.7	5.500	D9	
			Abs press		--		1.99	psia		
14	70	P642	Upper #12	W256	--	FW	14.7	5.500	D11	
			Abs press		--		1.58	psia		
15	30	P643	Upper #13	W256	--	FW	14.7	5.500	D13	
			Abs press		--		1.71	psia		
16	70	P644	Upper #14	W256	--	FW	14.7	5.500	D15	

Program No.: W056 Model: OLS S/N: WT Date: 3/10/81 Rec: 991
Track: 16 Box: N/A Multiplex: 10 Data coordinator: Goodfellow Engineer: Whitener
Technician: Gray Program: OLS Modification

Band	Balance	Item code	Item / Location	station	Lab No. / Bridge No.	Sensor code (SCM)	Unit calibration Ref.	Units / Excitation	Cable No.	Remarks
1	50	D110	Flapping		12898AF	FY	2.1078	deg	Q17	
			--	--	--		0	5.500		
2	20	M107	Mast torque		13157AF	FY	39198	in.-lb	Q19	
			--	21.0	03		0	5.500		
3	50	F103	Pitch link		13148AF	FW	3236	lb	Q21	
			Ax red	--	--		0	5.500		
4	20	F105	Drag brace		09493A	FW	14041	lb	Q23	
			Red	--	01		0	5.500		
5	25	B112	Yoke beam		09323BM	FO	14178	in.-lb	Q25	
			--	R6.0	02		-41,158	5.500		
6	30	B118	Grip beam bending		09369A	FW	75150	in.-lb	Q27	
			--	R 38	01		0	5.500		
7	40	B126	Blade beam		09449BM	FW	23813	in.-lb	P5	
			--	R 82	24		-19,725	5.500		
8	40	B122	Blade beam		09449BM	FW	18944	in.-lb	P17	
			--	R132	28		-11,098	5.500		
9	20	B128	Blade beam		09449BM	FW	21716	in.-lb	P11	
			--	R103	26		-14,425	5.500		
10	40	B127	Blade chord		09449BM	FW	140175	in.-lb	P7	
			--	R 82	23		0	5.500		

Track 16 (Concluded)

Band	Balance	Item code	Item / Location station	Lab No. / Bridge No.	Sensor code (SCM)	Unit calibration / Ref.	Units / Excitation	Cable No.	Remarks
			Blade chord	09449BM		142634	in.-lb		
11	40	B123	-- R132	27	FW	0	5.500	P19	
			Blade chord	09449BM		164813	in.-lb		
12	20	B129	-- R103	25	FB	0	5.500	P13	
			Blade tors	09449BM		32420	in.-lb		
13	70	M150	-- R 82	37	FB	0	5.500	P9	
			Yoke chord	09323BM		12015	in.-lb		
14	40	B115	-- R 11	04	FB	0	5.500	Q29	
			Mast parallel	13157AF		34124	in.-lb		
15	50	B108	-- 47.2	02	FB	0	5.500	Q31	
			Mast perpendicular	13157AF		33942	in.-lb		
16	50	B109	-- 47.2	01	FB	0	5.500	Q33	

Program No.: W056 Model: OLS S/N: WT Date: 3/10/81 Rec: 001
Track: 17 Box: N/A Multiplex: 11 Data coordinator: Goodfellow Engineer: Whitener
Technician: Gray Program: OLS Modification

Band	Balance	Item code	Item Location station		Lab No. Bridge No.	Sensor code (SCM)	Unit calibration Ref.	Units Excitation	Cable No.	Remarks
			Bl button		--		1.39	psid		
1	40	P750	Upper #1-I	R198	--	FO	0	5.500	L1	
			Bl button		--		2.03	psid		
2	30	P752	Upper #2-I	R198	--	FW	0	5.500	L3	
			Bl button		--		2.09	psid		
3	40	P754	Upper #3-I	R198	--	FW	0	5.500	L5	
			Bl button		--		3.34	psid		
4	30	P726	Lower #4-I	R198	--	FW	0	5.500	L7	
			Bl button		--		3.73	psid		
5	30	P728	Lower #5-I	R198	--	FW	0	5.500	L9	
			Bl button		--		4.63	psid		
6	40	P730	Lower #6-I	R198	--	FW	--	5.500	L11	
			Abs press		--		1.45	psia		
7	30	P958	Lower #13	W252	--	FW	14.7	5.500	G13	
			Abs press		--		2.14	psia		
8	70	P959	Lower #14	W252	--	FW	14.7	5.500	G15	
			Abs press		--		2.25	psia		
9	70	P973	Lower #15	W252	--	FO	14.7	5.500	G17	
			Abs press		--		2.60	psia		
10	70	P974	Lower #16	W252	--	FO	14.7	5.500	G19	

Track 17 (Concluded)

Band	Balance	Item code	Item / Lab No.			Sensor code (SCM)	Unit calibration / Units		Cable No.	Remarks
			Location	station	Bridge No.		Ref.	Excitation		
			Abs press		--		1.65	psia		
11	70	P975	Lower #17	W252	--	FO	14.7	5.500	G21	
			Abs press		--		2.54	psia		
12	90	P989	Lower #18	W252	--	FO	14.7	5.500	G23	
			Abs press		--		2.00	psia		
13	80	P990	Lower #19	W252	--	FO	14.7	5.500	G25	
			Abs press		--		2.05	psia		
14	70	P675	Lower #15	W261	--	FO	14.7	5.500	H17	
			Abs press		--		1.88	psia		
15	70	P676	Lower #16	W261	--	FO	14.7	5.500	H19	
			Abs press		--		2.48	psia		
16	70	P677	Lower #17	W261	--	FO	14.7	5.500	H21	

Program No.: W056 Model: OLS S/N: WT Date: 3/10/81 Rec: 001
Track: 18 Box: N/A Multiplex: 12 Data coordinator: Goodfellow Engineer: Whitener
Technician: Gray Program: OLS Modification

Band	Balance	Item code	Item Location station	Lab No. Bridge No.	Sensor code (SCM)	Unit calibration Ref.	Units Excitation	Cable No.	Remarks
			Bl button	--		1.10	psid		
1	40	P751	Upper #1-0 R198	--	FO	0	5.500	L13	
			Bl button	--		1.83	psid		
2	40	P753	Upper #2-0 R198	--	FO	0	5.500	L15	
			Bl button	--		1.85	psid		
3	40	P725	Upper #3-0 R198	--	FW	0	5.500	L17	
			Bl button	--		2.98	psid		
4	30	P727	Lower #4-0 R198	--	FW	0	5.500	L19	
			Bl button	--		2.01	psid		
5	30	P729	Lower #5-0 R198	--	FY	0	5.500	L21	
			Bl button	--		2.40	psid		
6	40	P731	Lower #6-0 R198	--	FW	0	5.500	L23	
			Abs press	--		1.85	psia		
7	80	P991	Lower #20 W252	--	FW	14.7	5.500	G27	
			Abs press	--		1.57	psia		
8	50	P738	Lower #21 W252	--	FW	14.7	5.500	G29	
			Abs press	--		1.85	psia		
9	50	P739	Lower #22 W252	--	FW	14.7	5.500	G31	
			Abs press	--		2.08	psia		
10	70	P615	Lower #15 W240	--	FO	14.7	5.500	F35	

Track 18 (Concluded)

Band	Balance	Item code	Item		Lab No.	Sensor	Unit calibration	Units	Cable	Remarks
			Location	station	Bridge No.	code (SCM)	Ref.	Excitation	No.	
			Abs press		--		2.15	psia		
11	70	P616	Lower #16	W240	--	FO	14.7	5.500	F37	
			Abs press		--		2.05	psia		
12	70	P617	Lower #17	W240	--	FO	14.7	5.500	F39	
			Abs press		--		1.61	psia		
13	90	P618	Lower #18	W240	--	FO	14.7	5.500	F41	
			Abs press		--		2.05	psia		
14	90	P678	Lower #18	W261	--	FO	14.7	5.500	H23	
			Abs press		--		1.83	psia		
15	80	P679	Lower #19	W261	--	FO	14.7	5.500	H25	
			Abs press		--		1.91	psia		
16	80	P680	Lower #20	W2611	--	FW	14.7	5.500	H27	

Program No.: W056 Model: OLS S/N: WT Date: 3/10/81 Rec: 001
Track: 19 Box: N/A Multiplex: 13 Data coordinator: Goodfellow Engineer: Whitener
Technician: Gray Program: OLS Modification

Band	Balance	Item code	Item Location station		Lab No. Bridge No.	Sensor code (SCM)	Unit calibration Ref.	Units Excitation	Cable No.	Remarks
			B1 button		--		2.50	psid		
1	40	P732	Upper #1-I	R228	--	FO	0	5.500	L25	
			B1 button		--		1.81	psid		
2	40	P734	Upper #2-I	R228	--	FO	0	5.500	L27	
			B1 button		--		1.99	psid		
3	40	P736	Upper #3-I	R228	--	FO	0	5.500	L29	
			B1 button		--		2.41	psid		
4	40	P976	Lower #4-I	R228	--	FO	0	5.500	L31	
			B1 button		--		2.18	psid		
5	40	P978	Lower #5-I	R228	--	FO	0	5.500	L33	
			B1 button		--		2.47	psid		
6	40	P980	Lower #6-I	R228	--	FO	0	5.500	L35	
			Abs press		--		2.08	psia		
7	80	P619	Lower #19	W240	--	FO	14.7	5.500	F43	
			Abs press		--		1.50	psia		
8	80	P620	Lower #20	W240	--	FW	14.7	5.500	F45	
			Abs press		--		1.52	psia		
9	50	P621	Lower #21	W240	--	FW	14.7	5.500	F47	
			Abs press		--		1.90	psia		
10	50	P622	Lower #22	W240	--	FW	14.7	5.500	G1	

Track 19 (Concluded)

Band	Balance	Item code	Item Location	station	Lab No. Bridge No.	Sensor code (SCM)	Unit calibration Ref.	Units Excitation	Cable No.	Remarks
			Abs press		--		1.91	psia		
11	50	P623	Lower #23	W240	--	FW	14.7	5.500	G3	
			Abs press		--		1.95	psia		
12	50	P624	Lower #24	W240	--	FB	14.7	5.500	G5	
			Abs press		--		1.44	psia		
13	50	P625	Lower #25	W240	--	FB	14.7	5.500	G7	
			Abs press		--		1.94	psia		
14	50	P681	Lower #21	W261	--	FW	14.7	5.500	H29	
			Abs press		--		1.98	psia		
15	50	P682	Lower #22	W261	--	FW	14.7	5.500	H31	
			Abs press		--		1.85	psia		
16	50	P683	Lower #23	W261	--	FW	14.7	5.500	H33	

Program No.: W056 Model: OLS S/N: WT Date: 3/10/81 Rec: 001
Track: 20 Box: N/A Multiplex: 14 Data coordinator: Goodfellow Engineer: Whitener
Technician: Gray Program: OLS Modification

Band	Balance	Item code	Item Location station	Lab No. Bridge No.	Sensor code (SCM)	Unit calibration Ref.	Units Excitation	Cable No.	Remarks
			Bl button	--		2.66	psid		
1	40	P733	Upper #1-0 R228	--	FO	0	5.500	L37	
			Bl button	--		1.40	psid		
2	40	P735	Upper #2-0 R228	--	FO	0	5.500	L39	
			Bl button	--		2.79	psid		
3	40	P737	Upper #3-0 R228	--	FO	0	5.500	L41	
			Bl button	--		2.42	psid		
4	40	P977	Lower #4-0 R228	--	FO	0	5.500	L43	
			Bl button	--		2.40	psid		
5	50	P979	Lower #5-0 R228	--	FO	0	5.500	L45	
			Bl button	--		2.46	psid		
6	40	P981	Lower #6-0 R228	--	FO	0	5.500	L47	
			Abs press	--		1.49	psia		
7	50	P626	Lower #26 W240	--	FB	14.7	5.500	G9	
			Abs press	--		1.60	psia		
8	50	P627	Lower #27 W240	--	FB	14.7	5.500	G11	
			Feathering	12899QR		1.6513	deg		
9	20	P111	-- --	--	FY	--	5.500	Q35	
			Abs press	--		2.31	psia		
10	50	P831	Lower #15 W228	--	FW	14.7	5.500	F9	

Track 20 (Concluded)

Band	Balance	Item code	Item Location station		Lab No. Bridge No.	Sensor code (SCM)	Unit calibration Ref.	Units Excitation	Cable No.	Remarks
			Abs press		--		2.78	psia		
11	70	P843	Lower #16	W228	--	FW	14.7	5.500	F11	
			Abs press		--		2.36	psia		
12	80	P844	Lower #17	W228	--	FO	14.7	5.500	F13	
			Abs press		--		2.79	psia		
13	70	P845	Lower #18	W228	--	FO	14.7	5.500	F15	
			Abs press		--		1.62	psia		
14	50	P684	Lower #24	W261	--	FB	14.7	5.500	H35	
			Abs press		--		1.43	psia		
15	50	P685	Lower #25	W261	--	FB	14.7	5.500	H37	
			Abs press		--		2.04	psia		
16	50	P686	Lower #26	W261	--	FB	14.7	5.500	H39	

Program No.: W056 Model: OLS S/N: WT Date: 3/10/81 Rec: 001
Track: 21 Box: N/A Multiplex: 15 Data coordinator: Goodfellow Engineer: Whitener
Technician: Gray Program: OLS Modification

Band	Balance	Item code	Item Location station		Lab No. Bridge No.	Sensor code (SCM)	Unit calibration Ref.	Units Excitation	Cable No.	Remarks
			Bl button		--		2.65	psid		
1	30	P982	Upper #1-I	R252	--	FO	0	5.500	M1	
			Bl button		--		2.54	psid		
2	40	P984	Upper #2-I	R252	--	FO	0	5.500	M3	
			Bl button		--		3.12	psid		
3	45	P986	Upper #3-I	R252	--	FO	0	5.500	M5	
			Bl button		--		1.99	psid		
4	40	P988	Lower #4-I	R252	--	FO	0	5.500	M7	
			Bl button		--		2.26	psid		
5	40	P965	Lower #5-I	R252	--	FO	0	5.500	M9	
			Bl button		--		2.69	psid		
6	40	P755	Lower #6-I	R252	--	FO	0	5.500	M11	
			Hws sgmt		--		5.839	% Full scale		
7	40	V846	#7	R198	--	FG	0	6.00	J1	
			Abs press		--		1.74	psia		
8	70	P860	Lower #20	W228	--	FO	14.7	5.500	F17	
			Abs press		--		1.60	psia		
9	70	P861	Lower #21	W228	--	FO	14.7	5.500	F19	

Track 21 (Concluded)

Band	Balance	Item code	Item Location station	Lab No. Bridge No.	Sensor code (SCM)	Unit calibration Ref.	Units Excitation	Cable No.	Remarks
10	70	P875	Abs press	--	FW	1.62	psia	F21	
			Lower #22 W228	--		14.7	5.500		
11	70	P876	Abs press	--	FW	1.86	psia	F23	
			Lower #23 W228	--		14.7	5.500		
12	70	P877	Abs press	--	FW	1.82	psia	F25	
			Lower #24 W228	--		14.7	5.500		
13	70	P891	Abs press	--	FW	1.83	psia	F27	
			Lower #25 W228	--		14.7	5.500		
14	50	P687	Abs press	--	FB	2.07	psia	H41	
			Lower #27 W261	--		14.7	5.500		
15	50	P688	Abs press	--	FB	2.04	psia	H43	
			Lower #28 W261	--		14.7	5.500		
16	70	P645	Abs press	--	FO	1.37	psia	G37	
			Lower #15 W256	--		14.7	5.500		

Program No.: W056 Model: OLS S/N: WT Date: 3/10/81 Rec: 001
Track: 22 Box: N/A Multiplex: 16 Data coordinator: Goodfellow Engineer: Whitener
Technician: Gray Program: OLS Modification

Band	Balance	Item code	Item Location station		Lab No. Bridge No.	Sensor code (SCM)	Unit calibration Ref.	Units Excitation	Cable No.	Remarks
			Bl button		--		2.59	psid		
1	30	P983	Upper #1-0	R252	--	FO	0	5.500	M13	
			BL button		--		2.59	psid		
2	40	P985	Upper #2-0	R252	--	FO	0	5.500	M15	
			Bl button		--		2.62	psid		
3	30	P987	Upper #3-0	R252	--	FO	0	5.500	M17	
			Bl button		--		2.00	psid		
4	40	P964	Lower #4-0	R252	--	FY	0	5.500	M19	
			Bl button		--		1.65	psid		
5	40	P966	Lower #5-0	R252	--	FO	0	5.500	M21	
			Bl button		--		2.40	psid		
6	40	P756	Lower #6-0	R252	--	FO	0	5.500	M23	
			Abs press		--		2.15	psia		
7	50	P892	Lower #26	W228	--	FW	14.7	5.500	F29	
			Abs press		--		1.99	psia		
8	70	P893	Lower #27	W228	--	FW	14.7	5.500	F31	
			Abs press		--		2.00	psia		
9	70	P907	Lower #28	W228	--	FW	14.7	5.500	F33	
			Abs press		--		2.80	psia		
10	50	P856	Lower #13	W198	--	FW	14.7	5.500	E35	

Track 22 (Concluded)

Band	Balance	Item code	Item Location	station	Lab No. Bridge No.	Sensor code (SCM)	Unit calibration Ref.	Units Excitation	Cable No.	Remarks
			Abs press		--		2.99	psia		
11	70	P857	Lower #14	W198	--	FW	14.7	5.500	E37	
			Abs press		--		2.79	psia		
12	70	P858	Lower #15	W198	--	FY	14.7	5.500	E39	
			Abs press		--		1.81	psia		
13	70	P868	Lower #16	W198	--	FO	14.7	5.500	E41	
			Abs press		--		1.57	psia		
14	70	P646	Lower #16	W256	--	FO	14.7	5.500	G39	
			Abs press		--		2.06	psia		
15	70	P647	Lower #17	W256	--	FO	14.7	5.500	G41	
			Abs press		--		1.86	psia		
16	90	P648	Lower #18	W256	--	FO	14.7	5.500	G43	

Program No.: W056 Model: OLS S/N: WT Date: 3/10/81 Rec: 001
Track: 23 Box: N/A Multiplex: 17 Data coordinator: Goodfellow Engineer: Whitener
Technician: Gray Program: OLS Modification

Band	Balance	Item code	Item		Lab No.	Sensor	Unit calibration	Units	Cable	Remarks
			Location	station	Bridge No.	code (SCM)	Ref.	Excitation	No.	
			Hws sgmt		--		5.839	% Full scale		
1	40	V923	#1	R252	--	FG	0	6.00	K9	
			Hws sgmt		--		5.839	% Full scale		
2	40	V924	#2	R252	--	FG	0	6.00	K11	
			Hws sgmt		--		5.839	% Full scale		
3	40	V925	#3	R252	--	FG	0	6.00	K13	
			Hws sgmt		--		5.839	% Full scale		
4	40	V929	#4	R252	--	FG	0	6.00	K15	
			Hws sgmt		--		5.839	% Full scale		
5	40	V930	#5	R252	--	FG	0	6.00	K17	
			Hws sgmt		--		5.839	% Full scale		
6	40	V931	#6	R252	--	FG	0	6.00	K19	
			Abs press.		--		1.72	psia		
7	70	P869	Lower #17	W198	--	FO	14.7	5.500	E43	
			Abs press		--		1.89	psia		
8	80	P870	Lower #18	W198	--	FW	14.7	5.500	E45	

Track 23 (Concluded)

Band	Balance	Item code	Item Location station	Lab No. Bridge No.	Sensor code (SCM)	Unit calibration Ref.	Units Excitation	Cable No.	Remarks
			Hws sgmt	--		5.839	% Full scale		
9	40	V847	#8 R198	--	FG	0	6.00	J3	
			Abs press	--		1.40	psia		
10	70	P872	Lower #20 W198	--	FW	14.7	5.500	E47	
			Abs press	--		2.08	psia		
11	70	P873	Lower #21 W198	--	FW	14.7	5.500	F1	
			Abs press	--		2.31	psia		
12	70	P874	Lower #22 W198	--	FW	14.7	5.500	F3	
			Abs press	--		2.79	psia		
13	50	P884	Lower #23 W198	--	FW	14.7	5.500	F5	
			Abs press	--		1.80	psia		
14	80	P649	Lower #19 W256	--	FO	14.7	5.500	G45	
			Abs press	--		2.13	psia		
15	80	P650	Lower #20 W256	--	FW	14.7	5.500	G47	
			Abs press	--		2.05	psia		
16	50	P651	Lower #21 W256	--	FW	14.7	5.500	H1	

Program No.: W056 Model: OLS S/N: WT Date: 3/10/81 Rec: 001
Track: 24 Box: N/A Multiplex: 18 Data coordinator: Goodfellow Engineer: Whitener
Technician: Gray Program: OLS Modification

Band	Balance	Item code	Item		Lab No.	Sensor	Unit calibration	Units	Cable	Remarks
			Location	station	Bridge No.	code (SCM)	Ref.	Excitation	No.	
			Hws sgmt		--		5.839	% Full scale		
1	40	V932	#7	R252	--	FG	0	6.0	K21	
			Hws sgmt		--		5.839	% Full scale		
2	40	V933	#8	R252	--	FG	0	6.00	K23	
			Hws sgmt		--		5.839	% Full scale		
3	40	V934	#9	R252	--	FG	0	6.00	K25	
			Hws sgmt		--		5.839	% Full scale		
4	40	V944	#10	R252	--	FG	0	6.00	K27	
			Hws sgmt		--		5.839	% Full scale		
5	40	V945	#11	R252	--	FG	0	6.00	K29	
			Hws sgmt		--		5.839	% Full scale		
6	40	V946	#12	R252	--	FG	0	6.00	K31	
			Abs press		--		1.95	psia		
7	50	P885	Lower #24	W198	--	FW	14.7	5.500	F7	
			Abs press		--		2.83	psia		
8	70	P809	Lower #11	W158	--	FW	14.7	5.500	E15	

Track 24 (Concluded)

Band	Balance	Item code	Item		Lab No.	Sensor	Unit calibration	Units	Cable	Remarks
			Location	station	Bridge No.	code (SCM)	Ref.	Excitation	No.	
			Abs press		--		2.18	psia		
9	70	P810	Lower #12	W158	--	FW	14.7	5.500	E17	
			Abs press		--		2.06	psia		
10	70	P811	Lower #13	W158	--	FW	14.7	5.500	E19	
			Abs press		--		2.62	psia		
11	70	P812	Lower #14	W158	--	FW	14.7	5.500	E21	
			Abs press		--		1.94	psia		
12	70	P822	Lower #15	W158	--	FW	14.7	5.500	E23	
			Abs press		--		1.41	psia		
13	70	P823	Lower #16	W158	--	FW	14.7	5.500	E25	
			Abs press		--		1.85	psia		
14	50	P652	Lower #22	W256	--	FW	14.7	5.500	H3	
			Abs press		--		2.28	psia		
15	50	P653	Lower #23	W256	--	FW	14.7	5.500	H5	
			Abs press		--		1.89	psia		
16	50	P654	Lower #24	W256	--	FB	14.7	5.500	H7	

Program No.: W056 Model: OLS S/N: WT Date: 3/10/81 Rec: 001
Track: 25 Box: N/A Multiplex: 19 Data coordinator: Goodfellow Engineer: Whitener
Technician: Gray Program: OLS Modification

Band	Balance	Item code	Item Location station		Lab No. Bridge No.	Sensor code (SCM)	Unit calibration Ref.	Units Excitation	Cable No.	Remarks
			Hws sgmt		--		5.839	% Full scale		
1	40	V947	#13	R252	--	FG	0	6.00	K33	
			Hws sgmt		--		5.839	% Full scale		
2	40	V948	#14	R252	--	FG	0	6.00	K35	
			Hws sgmt		--		5.839	% Full scale		
3	40	V949	#15	R252	--	FG	0	6.00	K37	
			Hws sgmt		--		5.839	% Full scale		
4	40	V960	#16	R252	--	FG	0	6.00	K39	
			Hws sgmt		--		5.839	% Full scale		
5	40	V961	#17	R252	--	FG	0	6.00	K41	
			Hws sgmt		--		5.839	% Full scale		
6	40	V962	#18	R252	--	FG	0	6.00	K43	
			Abs press		--		2.87	psia		
7	70	P824	Lower #17	W158	--	FW	14.7	5.500	E27	
			Abs press		--		2.75	psia		
8	70	P825	Lower #18	W158	--	FW	14.7	5.500	E29	

Track 25 (Concluded)

Band	Balance	Item code	Item Location station	Lab No. Bridge No.	Sensor code (SCM)	Unit calibration Ref.	Units Excitation	Cable No.	Remarks
			Abs press	--		1.85	psia		
9	70	P826	Lower #19 W158	--	FW	14.7	5.500	E31	
			Abs press	--		3.04	psia		
10	20	P827	Lower #20 W158	--	FW	14.7	5.500	E33	
			Abs press	--		2.91	psia		
11	70	P173	Lower #8 W106	--	FW	14.7	5.500	E1	
			Abs press	--		2.66	psia		
12	70	P174	Lower #9 W106	--	FW	14.7	5.500	E3	
			Abs press	--		2.36	psia		
13	70	P175	Lower #10 W106	--	FW	14.7	5.500	E5	
			Abs press	--		2.06	psia		
14	50	P655	Lower #25 W256	--	FB	14.7	5.500	H9	
			Abs press	--		1.44	psia		
15	50	P656	Lower #26 W256	--	FB	14.7	5.500	H11	
			Abs press	--		2.05	psia		
16	50	P657	Lower #27 W256	--	FB	14.7	5.500	H13	

Program No.: W056 Model: OLS S/N: WT Date: 3/10/81 Rec: 001
Track: 26 Box: N/A Multiplex: 20 Data coordinator: Goodfellow Engineer: Whitener
Technician: Gray Program: OLS Modification

Band	Balance	Item code	Item Location station		Lab No. Bridge No.	Sensor code (SCM)	Unit calibration Ref.	Units Excitation	Cable No.	Remarks
			Hws sgmt		--		5.839	% Full scale		
1	40	V963	#19	R252	--	FG	0	6.00	K45	
			Hws sgmt		--		5.839	% Full scale		
2	90	V848	#9	R198	--	FG	0	6.00	J5	
			Hws sgmt		--		5.839	% Full scale		
3	40	V849	#10	R198	--	FG	0	6.00	J7	
			Hws sgmt		--		5.839	% Full scale		
4	40	V850	#11	R198	--	FG	0	6.00	J9	
			Hws sgmt		--		5.839	% Full scale		
5	40	V851	#12	R198	--	FG	0	6.0	J11	
			Hws sgmt		--		5.839	% Full scale		
6	40	V862	#13	R198	--	FG	0	6.00	J13	
			Abs press		--		1.43	psia		
7	70	P176	Lower #11	W106	--	FW	14.7	5.500	E7	
			Abs press		--		1.52	psia		
8	70	P177	Lower #12	W106	--	FW	14.7	5.500	E9	

Track 26 (Concluded)

Band	Balance	Item code	Item: Location	Item: station	Lab No.: Bridge No.	Sensor code (SCM)	Unit calibration: Ref.	Units: Excitation	Cable No.	Remarks
			Abs press		--		1.90	psia		
9	70	P178	Lower #13	W106	--	FW	14.7	5.500	E11	
			Abs press		--		1.99	psia		
10	70	P179	Lower #14	W106	--	FW	14.7	5.500	E13	
			Hws sgmt		--		5.839	% Full scale		
11	40	V863	#14	R198	--	FG	0	6.00	J15	
			Hws sgmt		--		5.839	% Full scale		
12	40	V844	#15	R198	--	FG	0	6.00	J17	
			Volt monitor B		--		--	volts		
13	70	V015	--	--	--	BB	--	5.500	Q37	FG mod, 80 mV
			Abs press		--		1.84	psia		
14	50	P658	Lower #28	W256	--	FB	14.7	5.500	H15	
			Abs press		--		2.15	psia		
15	50	P740	Lower #23	W252	--	FW	14.7	5.500	G33	
			Abs press		--		1.77	psia		
16	50	P757	Lower #24	W252	--	FB	14.7	5.500	G35	

INSTRUMENTATION SIGN CONVENTION

Stick positions	Positive direction or motion
Fore/aft cyclic	Stick motion forward of center
Lateral cyclic	Stick motion to the right of center
Pedal	Right pedal forward
Collective	Stick motion up from full down
Aircraft state	
Side slip	Nose left from wind axis
Angle of attack	Nose up from wind axis
Pitch attitude	Nose above horizon
Roll attitude	Right wing down from behind aircraft
Yaw attitude	Nose right from behind aircraft
Pitch rate	Nose up angular velocity
Roll rate	Right wing down angular velocity
Yaw rate	Nose right angular velocity
Vertical center of gravity acceleration	Upward acceleration at aircraft center of gravity
Vertical pilot seat acceleration	Upward acceleration at pilot's seat
Control linkages	
Fore/aft cyclic boost tube	Aft side in tension
Lateral cyclic boost tube	Left side in tension
Collective cyclic boost tube	Bottom in tension
Pitch link	Link in tension
Hub and shaft	
Mast parallel bending	Top of mast bending away from red blade
Mast perpendicular bending	Top of mast toward red blade trailing edge
Drag brace	Axial tension
Grip beam bending	Lower side in tension
Mast torque	With base fixed, counterclockwise loading at mast top
Yoke chord	Leading edge in tension
Yoke beam	Lower side in tension
Flapping	Red blade moves upward
Feathering	Blade angle increasing
Blade	
Beam bending	Lower surface in tension
Chord bending	Leading edge in tension
Torsion	Leading edge up and trailing edge down

APPENDIX D

ACOUSTIC TEST PHASE II: ACOUSTIC TEST MICROPHONE

GAIN SETTINGS AND CALIBRATION CHARTS

The microphone power supply gain settings were recorded by the YO-3A flight test engineer in a similar manner to the flight cards. These cards detail the counter numbers, the target airspeeds, helicopter rotor speed, rate of descent, and pressure altitude, the aircraft formation, and the gain settings for the left, tail, and right microphones.

The calibration sheets were made during each pre- or postflight calibration of the YO-3A aircraft.

Tape No.: YO-5A Date: 6/5/81 Flight: 12A

Run	Indicated airspeed, knots	Rate of sink	Rotor speed	Pressure altitude	Position	OAT	Gain, setting, dB			Tape time
							Left	Tail	Right	
2336	60/64	0	--	3081	Trail	--	10	10	10	--
2337	60/64	0	--	3416	Left	--	10	10	10	--
2338	60/64	200	--	3584	Left	--	10	10	10	--
2339	60/63	400	--	3754	Left	--	10	10	10	
2340	60/63	400	--	3924	Trail	--	10	10	10	--
2342	60/63	600	--	4181	Trail	--	0	0	0	--
2344	60/62	600	--	4267	Left	--	0	0	0	--
2347	60/62	800	--	4439	Left	--	0	0	0	--
2348	60/62	800	--	4613	Trail	--	--	--	--	--

YO-3A CALIBRATION SHEET

Flight: 12A   Date: 6/10/81   Tape: YO-5A

Total pressure, psi	Angle of attack, deg	Temperature, °F
0.1	0	57*
0.3	+15	57*
0.55	-15	57*
Static pressure, psi	Sideslip, deg	
0.55	0	24
1.0	+5	24
2.0	-5	24
Microphone		
Gain setting, dB	Signal strength, volts peak to peak	
Left 0	1	105
Tail 0	1	105
Right 0	1	105

*Ambient

Tape No.: YO-7A Date: 7/7/81 Flight: 14A

Run	Indicated airspeed, knots	Rate of sink	Rotor speed	Pressure altitude	Position	OAT	Gain setting, dB			Tape time
							Left	Tail	Right	
806	110/109	0	320	2998	Trail	69	0	0	0	3:12
808	110/117	200	--	3500	Trail	64	0	0	0	4:00
810	110/115	200	--	3840	Left	62	0	0	0	7:20
811	110/114	600	320	4009	Trail	64	0	0	0	10:54
812	90/92	0	321	4095	Trail	62	0	0	0	--
813 814	90/92	800	319	4267	Trail	62	0	0	0	13:13
815	120/124	600	320	4526	Trail	65	0	0	0	14:15
816	120/124	800	--	4700	Trail	62	0	0	0	15:26
817	120/123	1000	320	4963	Trail	61	0	0	0	16:26
818	120/122	1000	320	5140	Left	61	0	0	0	17:33

YO-3A CALIBRATION SHEET

Flight: 14A Date: 7/7/81 Tape: YO-7A

Total pressure, psi	Angle of attack, deg	Temperature, °F
0.1	0	63*
0.3	+15	63*
0.55	-15	63*
Static pressure, psi	Sideslip, deg	
0.55	0	24
1.0	+5	24
2.0	-5	24
Microphone		
Gain setting, dB	Signal strength, volts peak to peak	
Left 0	1	105
Tail 0	1	105
Right 0	1	105

*Ambient

Note: First 3 records on tape are not part of calibration.

Tape No.: YO-8 Date: 7/8/81 Flight: 15A

Run	Indicated airspeed, knots	Rate of sink	Rotor speed	Pressure altitude	Position	OAT	Gain setting, dB			Tape time
							Left	Tail	Right	
825	80/84	800	321	3165	Left	70	0	0	0	3:26
826	80/83	0	323	3330	Trail	72	0	0	0	4:20
827	80/83	0	323	3500	Left	71	10	10	10	--
828	80/83	200	322	3600	Left	68	0	0	0	6:42
829	80/82	400	322	3700	Left	69	0	0	0	7:37
830	80/82	400	322	3750	Trail	70	0	0	0	8:49
831	80/82	600	322	3900	Trail	65	0	0	0	9:49
832	80/82	600	322	4100	Left	68	0	0	0	10:50
833	80/82	800	321	4200	Trail	67	0	0	0	11:47
834	100/101	0	321	4450	Trail	67	0	0	0	12:57

YO-3A CALIBRATION SHEET

Flight: 15A Date: 7/8/81 Tape: YO-8

Total pressure, psi	Angle of attack, deg	Temperature, °F
0.1 0.3 0.55	0 +15 -15	82* 82* 82*
Static pressure, psi	Sideslip, deg	
0.55 1.0 2.0	0 +5 -5	25 25 25
	Microphone	
Gain setting, dB	Signal strength, volts peak to peak	
Left 0 Tail 0 Right 0	1 1 1	105 105 105

*Ambient

Tape time: 2:30

Flight: 19A Date: 7/15/81 Tape: 4

Test point	Counter	Channel gain settings					Wind direction	Channel attenuation					Signal strength, mV	Tape counter	
		1	2	3	4	5		1	2	3	4	5		Start	Stop
Tape introduction	--	0	0	0	0	0								0000	0020
Calibration of #1 microphone	--	0			0			0	0	0	0	0		0020	0116
Calibration of #4 microphone	--	40			0									116	186
Calibration of #2 microphone	--				40								178	188	255
Repeat #2 microphone	--												181	255	333
Calibration of #5 microphone	--		40										179	333	411
Calibration of #3 microphone	-					40							177	411	476
Background noise	--			40				10	10	10	10	10		476	585
Gun shot position #1	--							0	0	0	0	0		585	807
Gun shot position #1	--							0	0	0	0	0		807	857
Gun shot position #1	--							10	10	10	10	10		857	907
Gun shot position #2	--							10	10	10	10	10		907	1071
Gun shot position #2	--							0	0	0	0	0		1074	1122
Gun shot position #2	--							0	0	0	0	0		1124	1161
Background	--							10	10	10	10	10		1164	1234
Hover 0° in-ground effect	3061													1263	1301
Hover 90° in-ground effect	3062													1302	1337
Hover 180° in-ground effect	3063													1339	1367
Hover 270° in-ground effect	3064													1367	1406
Takeoff at maximum climb	3065						3 at 320							1408	1489
Takeoff at maximum climb	3066													1491	1585
Takeoff at maximum climb	3067													1585	1700
V_h	3068													1702	1751
3° approach 60 knots	Practice													1752	1891
3° approach 60 knots	3069													1894	2018
6° approach 60 knots	3070													2021	2170
9° approach 60 knots	3071													2170	2355
12° approach 60 knots	3072													2357	2483
12° approach 60 knots	3073													2486	2603
9° approach 60 knots	3074													2606	2793
6° approach 60 knots	3075													2795	2947
3° approach 60 knots	3076													2950	3099
0.9 V_h	3077													3110	3206
0.8 V_h	3078													3208	3293

Flight 19A (Concluded)

Test point	Counter	Channel gain settings					Wind direction	Channel attenuation					Signal strength, mV	Tape counter	
		1	2	3	4	5		1	2	3	4	5		Start	Stop
0.7 V_h	3079	40	40	40	40	40		10	10	10	10	10		3293	3401
0.6 V_h	3080													3404	3518
Background							4 at 320							3520	3569
0.5 V_h	3081													3572	3714
V_h	3082													3716	3808
Background	--						3 knots							3810	3858
Calibration of #1 microphone	--	0						0					177	3860	3920
Calibration of #4 microphone	--				0						0		182	3922	
Repeat #4 microphone	--												182		4059
Calibration of #2 microphone	--		0						0				182	4061	4139
Calibration of #5 microphone	--		0			0			0			0	178	4141	4217
Calibration of #3 microphone	--		0	0		0			0	0		0	181	4219	

Flight: 20A Date: 7/16/81 Tape: 5

Test point	Counter	Channel gain settings 1	2	3	4	5	Wind direction	Channel attenuation 1	2	3	4	5	Signal strength, mV	Tape counter Start	Stop
Tape introduction														0000	0024
Calibration of #3 microphone		0	0	0	0	0		0	0	0	0	0	181	0026	0123
Calibration of #5 microphone				40		0							182	0125	0210
Calibration of #2 microphone						40							185	0212	0299
--													--	0301	0381
Calibration of #4 microphone (called #3 on tape)			40										183	0383	0466
Calibration of #1 microphone					40								178	0468	0557
Background noise		40					4-5 knots	10	10	10	10	10		0557	0643
V_h	3091													0645	0745
0.9 V_h	3092													0747	0815
0.9 V_h	3093						10 at 310							0818	0908
0.8 V_h	3094													0910	1050
0.7 V_h	3095													1052	1181
Background														1183	1266
75 knots with YO-3A	3096													1268	1437
90 knots with YO-3A	3097						11							1439	1621
105 knots with YO-3A	3098													1623	1752
60 knots with YO-3A	3099													1755	2017
Practice $V_{maximum}$ dive	3101													2017	2097
$V_{maximum}$ dive with YO-3A	3102						6 at 310							2099	2237
75 knots YO-3A only								0	0	0	0	0		2239	2400
120 knots YO-3A only														2400	2539
Background							7-9 knots	10	10	10	10	10		2541	26__
Calibration of #1 microphone		0						0	0	0	0	0	179	26__	2720
Calibration of #4 microphone					0								178	2724	2797
Calibration of #2 microphone			0										181	2800	2881
Calibration of #3 microphone			0	0									178	2883	2963
Calibration of #5 microphone			0	0		0							--	2966	3053

Tape No.: YO-11 Date: 7/16/81 Flight: 20A

Run	Indicated airspeed, knots	Rate of sink	Rotor speed	Pressure altitude*	Position	OAT	Gain setting, dB			Tape time
							Left	Tail	Right	
3095	0.5 V_h/75	--	--	500	Trail	--	10	10	10	--
3096	0.5 V_h/75	--	--	500	Trail	--	0	0	0	--
3097	0.6 V_h/90	--	--	500	Trail	--	0	0	0	--
3098	0.7 V_h/105	--	--	500	Trail	--	10	10	10	6:57
3100	60	--	--	500	Trail	--	10	10	10	--
3101	Maximum velocity of YO-3A	--	--	500	Trail	--	--	--	--	--
3102	130-knot dive	1000	--	--	Trail	--	0	0	0	--
3102'	Maximum velocity of YO-3A	--	--	500	N/A	--	-	-	-	11:34
3102"	60/75	--	--	500	N/A	--	--	--	--	--
--	130-knot dive	1000	--	--	N/A	--	--	--	--	--

*Relative to ground

YO-3A CALIBRATION SHEET

Flight: 20A Date: 7/16/81 Tape: YO-11

Total pressure, psi	Angle of attack, deg	Temperature, °F
0.1 0.3 0.55	0 +15 -15	70* 70* 70*
Static pressure, psi	Sideslip, deg	
0.55 1.0 2.0	0 +5 -5	25 25 25
	Microphone	
Gain setting, dB	Signal strength, volts peak to peak	
Left 0 Tail 0 Right 0	1 1 1	105 105 105

*Ambient
Tape time: 2:26

Tape No.: YO-12 Date: 7/22/81 Flight: 22A

Run	Indicated airspeed, knots	Rate of sink	Rotor speed	Pressure altitude	Position	OAT	Gain setting, dB			Tape time*
							Left	Tail	Right	
3149	65 68/68	0	324	3416	Trail	78	10	10	10	4:29
3150	65 67/67	0	324	3593	Left	78	10	10	10	5:18
3151	65 67/67	200	324	3655	Left	77	10	10	10	6:17
3152	65 67/66	400	324	3834	Left	78	10	10	10	7:08
3153	65 67/67-68	400	324	3919	Trail	78	10	10	10	8:05
3154	65 67/67	600	324	4000	Trail	78	10	10	10	9:01
3155	65 67/67	600	324	4100	Left	78	10	10	10	9:51
3156	60 62/62	800	324	4173	Trail	77	10	10	10	11:00
3157	130 130/124-130	1000	324	4429	Left	76	10-0	10-0	10-0	12:17
3158	130 130/125-130	1000	324	4600	Left	76	0	0	0	13:20
3159	130 130/124-128	1000	324	4773	Trail	77	0	0	0	14:23
3160	120 121/121-123	1000	324	5034	Trail	75	0	0	0	15:38

Flight 22A (Concluded)

Run	Indicated airspeed, knots	Rate of sink	Rotor speed	Pressure altitude	Position	OAT	Gain setting, dB			Tape time
							Left	Tail	Right	
3161	110 110/102-105	0	323	5297	Trail	74	10-0	10-0	10-0	16:53
3162	80 79/79	400	323	5473	Experi-mental	74	10	10	10	17:54
3163	80 79 78-79	600	323	5650	Experi-mental	72	10	10	10	18:48
3164	60 60/60	400	323	5830	Experi-mental	74	10	10	10	19:44
3165	60 60/60	600	323	5920	Experi-mental	72	10	10	10	20:42
3166	120 119/117-121	1000	323	6100	Experi-mental	72	0	0	0	21:53
3167	65 64/64	800	322	6280	Left	71	10	10	10-0 -10	22:54
3168	65 64/64-63	800	323	6400	Trail	73	10	10	10	23:50

*The end time of the run.

YO-3A CALIBRATION SHEET

Flight: 22A   Date: 7/22/81   Tape: YO-12

Total pressure, psi	Temperature, °F
0.1 0.3 0.55	64* 64* 64*
Static pressure, psi	
0.55 1.0 2.0	24 24 24
Angle of attack, deg	
0 +15 -15	105 105 105
Sideslip, deg	
0 +5 -5	63* 62* 63*

Microphone		
Gain setting, dB	Signal strength, volts peak to peak	Temperature, °C
Left 0 Tail 0 Right 0	1 1 1	-- -- --

*Ambient

Tape time: 3:35:5

Tape No.: YO-13 Date: 7/22/81 Flight: 22B

Run	Indicated airspeed, knots	Rate of sink	Rotor speed	Pressure altitude	Position	OAT	Gain setting, dB			Tape time
							Left	Tail	Right	
3171	60/59	0	323	6574 6500	Trail	71	10	10	10	1:08
3172	60/59	0	321	6900 6900	Left	68	10	10	10	1:52
3173	60/59	200 200	321	7060 7200-7100	Left	66	10	10	10	2:50
3174	60/59	400 400- 350	321	7140 7100-6800	Left	65	10	10	10	3:54
3175	60/58	400 400	321	7222 7400-7100	Trail	66	10	10	10	4:52
3176	60/58	600 650- 700	321	7386 7500-7200	Trail	65	10	10	10	5:48
3177	60/58	600 600	321	7550 7600-7200	Left	65	10	10	10	7:20
3178	60/59	800 800- 900	321	7716 7750-7200	Left	66	10	10	10	8:42
3179	60/60	800 800	321	7800 7800-7300	Left	66	10	10	10	9:58
3180	60/60	800 800- 820	321	7966 8200-7250	Trail	66	10	10	10	10:52
3181	70/71	800 800- 850	323	4728 5000-4400	Left	74	10	10	10	11:51
3182	100/99	0	324	4815 4820	Left	78	10-0	10-0	10-0	12:47

Flight 22B (Concluded)

Run	Indicated airspeed, knots	Rate of sink	Rotor speed	Pressure altitude	Position	OAT	Gain setting, dB			Tape time
							Left	Tail	Right	
3183	100/99	400 400	324	4990 5220-4975	Left	76	10-0	10-0	10-0	13:49
3184	100/99	600 550-650	323	5165 5450-5050	Left	74	10-0	10-0	10-0	14:56
3185	100/98	600 650-625	323	5340 5500-5100	Trail	74	0	0	0	15:57
3186	70/70	0	323	5515 5520	Trail	74	10	10	10	16:39
3187	70/69	0 20↑	323	5604 5610	Left	74	10	10	10	17:30
3188	70/69-68	400 400	323	5780 5900-5600	Left	72	10	10	10	18:40
3199	60/60	400 400-600	323	5960 6200-5700	Right	70	10	10	10	19:57

YO-3A CALIBRATION SHEET

Flight: 22B   Date: 7/22/81   Tape: YO-13

Total pressure, psi	Temperature, °F
0.1	70*
0.3	70*
0.55	71*
Static pressure, psi	
0.55	24
1.0	24
2.0	24
Angle of attack, deg	
0	105
+15	105
-15	105
Sideslip, deg	
0	71*
+5	71*
-5	71*

Microphone

Gain setting, dB	Signal strength, volts peak to peak	Temperature, °C
Left 0	1	--
Tail 0	1	--
Right 0	1.3	--

*Ambient

Tape No.: YO-14 Date: 7/23/81 Flight: 23A

Run	Indicated airspeed, knots	Rate of sink	Rotor speed	Pressure altitude	Position	OAT	Gain setting, dB			Tape time
							Left	Tail	Right	
3196	80/78	400/400	322	6580	**Left**	**68**	10-0	10-0	10-0	4:15
3197	80/78	0	322	6660 6660	**Left**	**68**	10	20-10	10	5:20
3198	80/78-77	400/450	322	6820 6900-6500	**Trail**	**68**	10	10	10	6:31
3199	80/77	400/420	321	6900 7000-6700	**Trail**	**66**	10	10	10	7:34
3200	80 78/78-77	800/780-820	321	7070 7100-6700	**Trail**	**67**	10	10	10	8:49
3201	80 77/77-75	800/850	321	7225 7350-6700	**Left**	**67**	10	10-0	10	9:59
3202	80 77/76-77	800/790	321	7390 7500-7000	**Left**	**67**	10	10	10	11:09
3203	80/81-82	400/400	323	4130 4250-4050	**Right**	**71-75**	10	10	10	12:15
3204	80/81	600/600	324	4300 4400-4000	**Right**	**75**	10	10	10	13:13
3205	80/82-81	800/790-810	324	4390 4450-4000	**Right**	**75**	10	10	10	14:18
3206	60/60	0	324	4560 4550	**Right**	**76**	10	10	10	15:28
3207	60/61	600/600	323	4730 4800-4500	**Right**	**73**	10	10	10	16:24

Flight 23A (Concluded)

Run	Indicated airspeed, knots	Rate of sink	Rotor speed	Pressure altitude	Position	OAT	Gain setting, dB			Tape time
							Left	Tail	Right	
3208	60/61	800/800	323	4905 5100-4700	Right	74	10	10	10	17:26
3208'	60/61	800/800	323	5080 5200-4850	Right	73	10	10	10	18:28

YO-3A CALIBRATION SHEET

Flight: 23A Date: 7/23/81 Tape: YO-14

Total pressure, psi	Temperature, °F
0.1	70*
0.3	70*
0.55	70*
Static pressure, psi	
0.55 ±0.1	70
1.0 ±0.1	24
2.0 ±0.2	24
Angle of attack, deg	
0	105
+15	105
-15	105
Sideslip, deg	
0	70*
+5	70*
-5	70*

Microphone		
Gain setting, dB	Signal strength, volts peak to peak	Temperature, °C
Left 0	1	--
Tail 0	1	--
Right 0	1	--

*Ambient
Tape time: 3:30

APPENDIX E

DATAMAP INFORMATION FILE FOR TAAT DATA

The data analysis computer program DATAMAP uses information that is stored in the information file to facilitate computation and display of related data sets. The file contains related sets of sensor item codes that are organized by their physical location, and are given four character group names. Each group can be a one-, two-, or three-dimensional array. The third dimension is limited to only two values. Each group name is followed by a description of that sensor set. This description is included on any plot produced using this group name. The next line identifies the azimuthal offset of that sensor group with the main rotor once per rev contactor. The next two lines are the labels applied to the first two dimensions of the sensor array. These are followed by the physical locations of the sensors and the orientation of the first entrant, for the first-array dimension. If this is a two- or three-dimensional array the information for the second-array dimension follows. Next is a four character code unique to the type of sensors included in the group. If the group is a three-dimensional array these codes are followed by the orientation of the third dimension. The item codes that comprise the group are listed last. In the information file, the item codes are presented in the reverse order just discussed; that is, the third dimension is varied first, then after a slash the second dimension is incremented and the third dimension is again varied. When the second dimension has been completely varied a double slash denotes that the first dimension is incremented. The other two dimensions are then varied as before. Each group information section is terminated with the word END. A more thorough explanation of the structure of the information file can be found in the DATAMAP manuals.

PRECEDING PAGE BLANK NOT FILMED

```
MRAZ R992 338.0,R049 0.0,R200 0.0,R001 0.0,I500 0.0/
TRAZ R025 45.0/
MDEG A320 0.0, R002 0.0, R990 0.0, Y001 0.0,AZIM 0.0/
TDEG A333 0.0/
TIAS P042  0.0 0.0  35. 36.  57. 57.
 67. 67.  76. 76.3  94. 94.7
 105. 105.4  200. 200.
 P002  0.0 0.0  70.2 72.5  99.5 104.5
 130. 134.  171. 169./
TASK A173/
OATM T004 T001/
STAT P030 P001/
MTOR M107/
MFLP D110 180./
MFTH P111 180. D111 180./
END
FLAP  OFFSET D110 TO ALIGN WITH PRESSURE BLADE
AZIMUTH 180.0
FLAPPING
FLAPPING
BLADE HUB
0.0//
FLAP//
D110//
END
NFBV  BLADE AND YOKE BEAMWISE VIBRATION, TAAT
AZIMUTH 180.0
FRACTN OF RADIUS
R/RADIUS
BLADE ROOT
.0133,.5000,.5902,.7000,.9020,.9962//
BLBV//
A889/A950/A951/A952/A953/A954//
END
NFCV  BLADE AND YOKE CHORDWISE VIBRATION, TAAT
AZIMUTH 180.0
FRACTN OF RADIUS
R/RADIUS
BLADE ROOT
.0133,.5000,.5902,.7000,.9020,.9962//
BLCV//
A905/A968/A969/A970/A971/A972//
END
S2FT  BL BUTTONS  UPPER SURFACE, TAAT
AZIMUTH 180.0
FRACTN OF RADIUS
R/RADIUS
BLADE ROOT
.75,.864,.955//
FRACTN OF CHORD
X/CHORD
LEADING EDGE
.30,.60,.90//
BLBI,BLBO//
```

```
INBOARD POINTING
OUTBOARD POINTING
P750,.789,P751,-.858/P732,-.927,P733,-.907/
P982,-.945,P983,-1.034//
P752,-.912,P753,.880/P734,.951,P735,-.967/
P984,-.866,P985,.872//
P754,-.922,P725,.912/P736,.862,P737,-.925/
P986,-.932,P987,.901//
END
S2FB  BL BUTTONS   LOWER SURFACE, TAAT
AZIMUTH 180.0
FRACTN OF RADIUS
R/RADIUS
BLADE ROOT
.75,.864,.955//
FRACTN OF CHORD
X/CHORD
LEADING EDGE
.30,.60,.90//
BLBI,BLBO//
INBOARD POINTING
OUTBOARD POINTING
P726,-.975,P727,.966/P976,.754,P977,-.722/
P988,-.833,P964,.883//
P728,-.874,P729,.915/P978,-.926,P979,.845/
P965,-.998,P966,.941//
P730,-.944,P731,.957/P980,.975,P981,-.859/
P755,-.901,P756,-.926//
END
S2HA  HOT-WIRE ATTENUATION SENSORS, TAAT
AZIMUTH 180.0
FRACTN OF RADIUS
R/RADIUS
BLADE ROOT
.7500,.8639,.9545//
CONTOUR POSITION
INCHES
LEADING EDGE
-1.56,-1.44,-1.32,-1.20,-1.08,-.96,-.84,-.72,-.60,
-.48,-.36,-.24,-.18,-.12,-.06,.0,.06,.12,.15,.18,.24//
HWAT//
NULL/V866/V923//NULL/V867/V924//NULL/V878/V925//
NULL/V879/V929//NULL/V880/V930//NULL/V881/V931//
V846/V894/V932//V847/V895/V933//V848/V896/V934//
V849/V897/V944//V850/V898/V945//V851/V899/V946//
NULL/V910/NULL//V862/V911/V947//NULL/V912/V948//
V863/V913/V949//NULL/V914/V960//NULL/V915/V961//
V844/NULL/NULL//NULL/NULL/V962//NULL/V922/V963//
END
NBBB  BLADE BEAMWISE BENDING, TAAT
AZIMUTH 180.0
FRACTN OF RADIUS
R/RADIUS
BLADE ROOT
```

```
.2273,.3087,.3902,.5000,.7000,.8042,.9020//
BLBB//
B120/B126/B128/B122/B132/B124/B134//
END
NFBB  BLADE AND YOKE BEAMWISE BENDING, TAAT
AZIMUTH 180.0
FRACTN OF RADIUS
R/RADIUS
BLADE ROOT
.0227,.0436,.2273,.3087,.3902,.5000,.7000,.8042,.9020//
BLBB//
B112/B114/B120/B126/B128/B122/B132/B124/B134//
END
NBCB  BLADE CHORDWISE BENDING, TAAT
AZIMUTH 180.0
FRACTN OF RADIUS
R/RADIUS
BLADE ROOT
.2273,.3087,.3902,.5000,.7000,.8042,.9020//
BLCB//
B121/B127/B129/B123/B133/B125/B135//
END
NFCB  BLADE AND YOKE CHORDWISE BENDING, TAAT
AZIMUTH 180.0
FRACTN OF RADIUS
R/RADIUS
BLADE ROOT
.0227,.0436,.2273,.3087,.3902,.5000,.7000,.8042,.9020//
BLCB//
B113/B115/B121/B127/B129/B123/B133/B125/B135//
END
NBLT  BLADE TORSION, TAAT
AZIMUTH 180.0
FRACTN OF RADIUS
R/RADIUS
BLADE ROOT
.3087,.5000,.7000,.9020//
BLTR//
M150/M935/M936/M937//
END
S2PT  BLADE PRESSURES, TAAT DATA, .864 AND OUT R/R
FRACTN OF RADIUS
R/RADIUS
BLADE ROOT
.864,.910,.955,.970,.990//
FRACTN OF CHORD
X/CHORD
LEADING EDGE
.009991,.029972,.079930,.149869,.199825,.249782,.349694,
.399651,.449607,.499563,.549520,.599476,.699389,.919196//
BLAP,BLAM//
TOP SURFACE
BOTTOM SURFACE
NULL,.016697,P831,-.016697/P601,.016697,P615,-.016697/
```

```
P908,.016697,P958,-.016697/P631,.016697,P645,-.016697/
P661,.016697,P675,-.016697//
P165,.026953,P843,-.026953/P602,.026953,P616,-.026953/
P909,.026953,P959,-.026953/P632,.026953,P646,-.026953/
P662,.026953,P676,-.026953//
P166,.039120,P844,-.039120/P603,.039120,P617,-.039120/
P919,.039120,NULL,-.039120/P633,.039120,P647,-.039120/
P663,.039120,NULL,-.039120//
P180,.046362,P845,-.046362/P604,.046362,P618,-.046362/
P920,.046362,P974,-.046362/P634,.046362,P648,-.046362/
P664,.046362,P678,-.046362//
NULL,.048165,NULL,-.048165/P605,.048165,P619,-.048165/
NULL,.048165,NULL,-.048165/NULL,.048165,P649,-.048165/
P665,.048165,P679,-.048165//
P182,.048164,NULL,-.048164/P606,.048164,P620,-.048164/
P921,.048164,P975,-.048164/P636,.048164,P650,-.048164/
P666,.048164,P680,-.048164//
P194,.044446,P861,-.044446/P607,.044446,P621,-.044446/
P926,.044446,P989,-.044446/P637,.044446,P651,-.044446/
P667,.044446,P681,-.044446//
P195,.041355,NULL,-.041355/P608,.041355,P622,-.041355/
P927,.041355,P990,-.041355/NULL,.041355,P652,-.041355/
P668,.041355,P682,-.041355//
P196,.038071,P876,-.038071/P609,.038071,P623,-.038071/
NULL,.038071,NULL,-.038071/P639,.038071,P653,-.038071/
NULL,.038071,P683,-.038071//
P813,.034788,P877,-.034788/P610,.034788,P624,-.034788/
P941,.034788,P738,-.034788/P640,.034788,P654,-.034788/
P670,.034788,P684,-.034788//
P814,.031504,P891,-.031504/P611,.031504,P625,-.031504/
P942,.031504,NULL,-.031504/P614,.031504,NULL,-.031504/
NULL,.031504,P685,-.031504//
P815,.028220,NULL,-.028220/P612,.028220,P626,-.028220/
NULL,.028220,NULL,-.028220/P642,.028220,P656,-.028220/
P672,.028220,P686,-.028220//
P829,.021653,P893,-.021653/P613,.021653,P627,-.021653/
P943,.021653,P740,-.021653/P643,.021653,P657,-.021653/
P673,.021653,P687,-.021653//
P830,.007205,P907,-.007205/NULL,.007205,NULL,-.007205/
P957,.007205,P757,-.007205/P644,.007205,P658,-.007205/
P674,.007205,P688,-.007205//
END
S2PO  BLADE ABSOLUTE PRESSURE, OUTER BLADE, TAAT DATA
FRACTN OF RADIUS
R/RADIUS
BLADE ROOT
.75,.864,.910,.955,.970,.990//
FRACTN OF CHORD
X/CHORD
LEADING EDGE
.009991,.029972,.079930,.149869,.199825,.249782,.349694,
.399651,.449607,.499563,.549520,.599476,.699389,.919196//
BLAP,BLAM//
TOP SURFACE
```

```
BOTTOM SURFACE
P828,.016697,P856,-.016697/NULL,.016697,P831,-.016697/
P601,.016697,P615,-.016697/P908,.016697,P958,-.016697/
P631,.016697,P645,-.016697/P661,.016697,P675,-.016697//
P836,.026953,P857,-.026953/P165,.026953,P843,-.026953/
P602,.026953,P616,-.026953/P909,.026953,P959,-.026953/
P632,.026953,P646,-.026953/P662,.026953,P676,-.026953//
P837,.039120,P858,-.039120/P166,.039120,P844,-.039120/
P603,.039120,P617,-.039120/P919,.039120,NULL,-.039120/
P633,.039120,P647,-.039120/P663,.039120,NULL,-.039120//
P838,.046362,P868,-.046362/P180,.046362,P845,-.046362/
P604,.046362,P618,-.046362/P920,.046362,P974,-.046362/
P634,.046362,P648,-.046362/P664,.046362,P678,-.046362//
NULL,.048165,NULL,-.048165/NULL,.048165,NULL,-.048165/
P605,.048165,P619,-.048165/NULL,.048165,NULL,-.048165/
NULL,.048165,P649,-.048165/P665,.048165,P679,-.048165//
P840,.048164,P869,-.048164/P182,.048164,NULL,-.048164/
P606,.048164,P620,-.048164/P921,.048164,P975,-.048164/
P636,.048164,P650,-.048164/P666,.048164,P680,-.048164//
P841,.044446,P870,-.044446/P194,.044446,P861,-.044446/
P607,.044446,P621,-.044446/P926,.044446,P989,-.044446/
P637,.044446,P651,-.044446/P667,.044446,P681,-.044446//
P842,.041355,P872,-.041355/P195,.041355,NULL,-.041355/
P608,.041355,P622,-.041355/P927,.041355,P990,-.041355/
NULL,.041355,P652,-.041355/P668,.041355,P682,-.041355//
NULL,.038071,P873,-.038071/P196,.038071,P876,-.038071/
P609,.038071,P623,-.038071/NULL,.038071,NULL,-.038071/
P639,.038071,P653,-.038071/NULL,.038071,P683,-.038071//
NULL,.034788,NULL,-.034788/P813,.034788,P877,-.034788/
P610,.034788,P624,-.034788/P941,.034788,P738,-.034788/
P640,.034788,P654,-.034788/P670,.034788,P684,-.034788//
P853,.031504,P874,-.031504/P814,.031504,P891,-.031504/
P611,.031504,P625,-.031504/P942,.031504,NULL,-.031504/
P614,.031504,NULL,-.031504/NULL,.031504,P685,-.031504//
NULL,.028220,NULL,-.028220/P815,.028220,NULL,-.028220/
P612,.028220,P626,-.028220/NULL,.028220,NULL,-.028220/
P642,.028220,P656,-.028220/P672,.028220,P686,-.028220//
P854,.021653,P884,-.021653/P829,.021653,P893,-.021653/
P613,.021653,P627,-.021653/P943,.021653,P740,-.021653/
P643,.021653,P657,-.021653/P673,.021653,P687,-.021653//
P855,.007205,P885,-.007205/P830,.007205,P907,-.007205/
NULL,.007205,NULL,-.007205/P957,.007205,P757,-.007205/
P644,.007205,P658,-.007205/P674,.007205,P688,-.007205//
END
S2PA  TAAT DATA, ALL SENSORS EXCEPT BAD ONES
FRACTN OF RADIUS
R/RADIUS
BLADE ROOT
.40,.60,.75,.864,.910,.955,.970,.990//
FRACTN OF CHORD
X/CHORD
LEADING EDGE
.009991,.029972,.079930,.149869,.199825,.249782,.349694,
.399651,.449607,.499563,.549520,.599476,.699389,.919196//
```

ORIGINAL PAGE IS
OF POOR QUALITY

```
BLAP,BLAM//
TOP SURFACE
BOTTOM SURFACE
P157,.016697,P173,-.016697/P187,.016697,P809,-.016697/
P828,.016697,P856,-.016697/NULL,.016697,P831,-.016697/
P601,.016697,P615,-.016697/P908,.016697,P958,-.016697/
P631,.016697,P645,-.016697/P661,.016697,P675,-.016697//
P158,.026953,P174,-.026953/P188,.026953,NULL,-.026953/
P836,.026953,P857,-.026953/P165,.026953,P843,-.026953/
P602,.026953,P616,-.026953/P909,.026953,P959,-.026953/
P632,.026953,P646,-.026953/P662,.026953,P676,-.026953//
P159,.039120,P175,-.039120/P189,.039120,P811,-.039120/
P837,.039120,P858,-.039120/P166,.039120,P844,-.039120/
P603,.039120,P617,-.039120/P919,.039120,NULL,-.039120/
P633,.039120,P647,-.039120/P663,.039120,NULL,-.039120//
NULL,.046362,NULL,-.046362/P190,.046362,P812,-.046362/
P838,.046362,P868,-.046362/P180,.046362,P845,-.046362/
P604,.046362,P618,-.046362/P920,.046362,P974,-.046362/
P634,.046362,P648,-.046362/P664,.046362,P678,-.046362//
NULL,.048165,NULL,-.048165/NULL,.048165,NULL,-.048165/
NULL,.048165,NULL,-.048165/NULL,.048165,NULL,-.048165/
P605,.048165,P619,-.048165/NULL,.048165,NULL,-.048165/
NULL,.048165,P649,-.048165/P665,.048165,P679,-.048165//
P160,.048164,P176,-.048164/P191,.048164,P822,-.048164/
P840,.048164,P869,-.048164/P182,.048164,NULL,-.048164/
P606,.048164,P620,-.048164/P921,.048164,P975,-.048164/
P636,.048164,P650,-.048164/P666,.048164,P680,-.048164//
NULL,.044446,NULL,-.044446/P192,.044446,NULL,-.044446/
P841,.044446,P870,-.044446/P194,.044446,P861,-.044446/
P607,.044446,P621,-.044446/P926,.044446,P989,-.044446/
P637,.044446,P651,-.044446/P667,.044446,P681,-.044446//
NULL,.041355,NULL,-.041355/NULL,.041355,NULL,-.041355/
P842,.041355,P872,-.041355/P195,.041355,NULL,-.041355/
P608,.041355,P622,-.041355/P927,.041355,P990,-.041355/
NULL,.041355,P652,-.041355/P668,.041355,P682,-.041355//
P161,.038071,P177,-.038071/P193,.038071,P824,-.038071/
NULL,.038071,P873,-.038071/P196,.038071,P876,-.038071/
P609,.038071,P623,-.038071/NULL,.038071,NULL,-.038071/
P639,.038071,P653,-.038071/NULL,.038071,P683,-.038071//
NULL,.034788,NULL,-.034788/NULL,.034788,NULL,-.034788/
NULL,.034788,NULL,-.034788/P813,.034788,P877,-.034788/
P610,.034788,P624,-.034788/P941,.034788,P738,-.034788/
P640,.034788,P654,-.034788/P670,.034788,P684,-.034788//
NULL,.031504,NULL,-.031504/P806,.031504,P825,-.031504/
P853,.031504,P874,-.031504/P814,.031504,P891,-.031504/
P611,.031504,P625,-.031504/P942,.031504,NULL,-.031504/
P614,.031504,NULL,-.031504/NULL,.031504,P685,-.031504//
NULL,.028220,NULL,-.028220/NULL,.028220,NULL,-.028220/
NULL,.028220,NULL,-.028220/P815,.028220,NULL,-.028220/
P612,.028220,P626,-.028220/NULL,.028220,NULL,-.028220/
P642,.028220,P656,-.028220/P672,.028220,P686,-.028220//
NULL,.021653,P178,-.021653/P807,.021653,P826,-.021653/
P854,.021653,P884,-.021653/P829,.021653,P893,-.021653/
P613,.021653,P627,-.021653/P943,.021653,P740,-.021653/
```

```
P643,.021653,P657,-.021653/P673,.021653,P687,-.021653//
P163,.007205,P179,-.007205/P808,.007205,P827,-.007205/
P855,.007205,P885,-.007205/P830,.007205,P907,-.007205/
NULL,.007205,NULL,-.007205/P957,.007205,P757,-.007205/
P644,.007205,P658,-.007205/P674,.007205,P688,-.007205//
END
S2BV TAAT DATA, 0 TO .25 X/C EXCEPT BAD ONES
FRACTN OF RADIUS
R/RADIUS
BLADE ROOT
.40,.60,.75,.864,.910,.955,.970,.990//
FRACTN OF CHORD
X/CHORD
LEADING EDGE
.009991,.029972,.079930,.149869,.199825,.249782//
BLAP,BLAM//
TOP SURFACE
BOTTOM SURFACE
P157,.016697,P173,-.016697/P187,.016697,P809,-.016697/
P828,.016697,P856,-.016697/NULL,.016697,P831,-.016697/
P601,.016697,P615,-.016697/P908,.016697,P958,-.016697/
P631,.016697,P645,-.016697/P661,.016697,P675,-.016697//
P158,.026953,P174,-.026953/P188,.026953,NULL,-.026953/
P836,.026953,P857,-.026953/P165,.026953,P843,-.026953/
P602,.026953,P616,-.026953/P909,.026953,P959,-.026953/
P632,.026953,P646,-.026953/P662,.026953,P676,-.026953//
P159,.039120,P175,-.039120/P189,.039120,P811,-.039120/
P837,.039120,P858,-.039120/P166,.039120,P844,-.039120/
P603,.039120,P617,-.039120/P919,.039120,NULL,-.039120/
P633,.039120,P647,-.039120/P663,.039120,NULL,-.039120//
NULL,.046362,NULL,-.046362/P190,.046362,P812,-.046362/
P838,.046362,P868,-.046362/P180,.046362,P845,-.046362/
P604,.046362,P618,-.046362/P920,.046362,P974,-.046362/
P634,.046362,P648,-.046362/P664,.046362,P678,-.046362//
NULL,.048165,NULL,-.048165/NULL,.048165,NULL,-.048165/
NULL,.048165,NULL,-.048165/NULL,.048165,NULL,-.048165/
P605,.048165,P619,-.048165/NULL,.048165,NULL,-.048165/
NULL,.048165,P649,-.048165/P665,.048165,P679,-.048165//
P160,.048164,P176,-.048164/P191,.048164,P822,-.048164/
P840,.048164,P869,-.048164/P182,.048164,NULL,-.048164/
P606,.048164,P620,-.048164/P921,.048164,P975,-.048164/
P636,.048164,P650,-.048164/P666,.048164,P680,-.048164//
END
S2PF FULL TAAT BLADE WITH ALL SENSORS
FRACTN OF RADIUS
R/RADIUS
BLADE ROOT
.40,.60,.75,.864,.910,.955,.970,.990//
FRACTN OF CHORD
X/CHORD
LEADING EDGE
.009991,.029972,.079930,.149869,.199825,.249782,.349694,
.399651,.449607,.499563,.549520,.599476,.699389,.919196//
BLAP,BLAM//
```

TOP SURFACE
BOTTOM SURFACE
P157,.016697,P173,-.016697/P187,.016697,P809,-.016697/
P828,.016697,P856,-.016697/P164,.016697,P831,-.016697/
P601,.016697,P615,-.016697/P908,.016697,P958,-.016697/
P631,.016697,P645,-.016697/P661,.016697,P675,-.016697//
P158,.026953,P174,-.026953/P188,.026953,P810,-.026953/
P836,.026953,P857,-.026953/P165,.026953,P843,-.026953/
P602,.026953,P616,-.026953/P909,.026953,P959,-.026953/
P632,.026953,P646,-.026953/P662,.026953,P676,-.026953//
P159,.039120,P175,-.039120/P189,.039120,P811,-.039120/
P837,.039120,P858,-.039120/P166,.039120,P844,-.039120/
P603,.039120,P617,-.039120/P919,.039120,P973,-.039120/
P633,.039120,P647,-.039120/P663,.039120,P677,-.039120//
NULL,.046362,NULL,-.046362/P190,.046362,P812,-.046362/
P838,.046362,P868,-.046362/P180,.046362,P845,-.046362/
P604,.046362,P618,-.046362/P920,.046362,P974,-.046362/
P634,.046362,P648,-.046362/P664,.046362,P678,-.046362//
NULL,.048165,NULL,-.048165/NULL,.048165,NULL,-.048165/
NULL,.048165,NULL,-.048165/NULL,.048165,NULL,-.048165/
P605,.048165,P619,-.048165/NULL,.048165,NULL,-.048165/
P635,.048165,P649,-.048165/P665,.048165,P679,-.048165//
P160,.048164,P176,-.048164/P191,.048164,P822,-.048164/
P840,.048164,P869,-.048164/P182,.048164,P860,-.048164/
P606,.048164,P620,-.048164/P921,.048164,P975,-.048164/
P636,.048164,P650,-.048164/P666,.048164,P680,-.048164//
NULL,.044446,NULL,-.044446/P192,.044446,P823,-.044446/
P841,.044446,P870,-.044446/P194,.044446,P861,-.044446/
P607,.044446,P621,-.044446/P926,.044446,P989,-.044446/
P637,.044446,P651,-.044446/P667,.044446,P681,-.044446//
NULL,.041355,NULL,-.041355/NULL,.041355,NULL,-.041355/
P842,.041355,P872,-.041355/P195,.041355,P875,-.041355/
P608,.041355,P622,-.041355/P927,.041355,P990,-.041355/
P638,.041355,P652,-.041355/P668,.041355,P682,-.041355//
P161,.038071,P177,-.038071/P193,.038071,P824,-.038071/
P852,.038071,P873,-.038071/P196,.038071,P876,-.038071/
P609,.038071,P623,-.038071/P928,.038071,P991,-.038071/
P639,.038071,P653,-.038071/P669,.038071,P683,-.038071//
NULL,.034788,NULL,-.034788/NULL,.034788,NULL,-.034788/
NULL,.034788,NULL,-.034788/P813,.034788,P877,-.034788/
P610,.034788,P624,-.034788/P941,.034788,P738,-.034788/
P640,.034788,P654,-.034788/P670,.034788,P684,-.034788//
NULL,.031504,NULL,-.031504/P806,.031504,P825,-.031504/
P853,.031504,P874,-.031504/P814,.031504,P891,-.031504/
P611,.031504,P625,-.031504/P942,.031504,P739,-.031504/
P614,.031504,P655,-.031504/P671,.031504,P685,-.031504//
NULL,.028220,NULL,-.028220/NULL,.028220,NULL,-.028220/
NULL,.028220,NULL,-.028220/P815,.028220,P892,-.028220/
P612,.028220,P626,-.028220/NULL,.028220,NULL,-.028220/
P642,.028220,P656,-.028220/P672,.028220,P686,-.028220//
P162,.021653,P178,-.021653/P807,.021653,P826,-.021653/
P854,.021653,P884,-.021653/P829,.021653,P893,-.021653/
P613,.021653,P627,-.021653/P943,.021653,P740,-.021653/
P643,.021653,P657,-.021653/P673,.021653,P687,-.021653//

```
P163,.007205,P179,-.007205/P808,.007205,P827,-.007205/
P855,.007205,P885,-.007205/P830,.007205,P907,-.007205/
NULL,.007205,NULL,-.007205/P957,.007205,P757,-.007205/
P644,.007205,P658,-.007205/P674,.007205,P688,-.007205//
END
S1BT  BLADE BEAMWISE VIBRATION, TAAT
AZIMUTH 180.0
FRACTN OF RADIUS
R/RADIUS
BLADE ROOT
.2273,.3087,.3902,.5000,.5902,.7000,.9020,.9962//
BLBV//
NULL/A939/A940/A950/A951/A952/A953/A954//
END
S1CT  BLADE CHORDWISE VIBRATION, TAAT
AZIMUTH 180.0
FRACTN OF RADIUS
R/RADIUS
BLADE ROOT
.2273,.3087,.3902,.5000,.5902,.7000,.9020,.9962//
BLCV//
A955/A956/A967/A968/A969/A970/A971/A972//
END
```

APPENDIX F

TAAT DATA NOT DIGITIZED

During postflight data processing and digitization, various sensors were found that for a variety of reasons were not recoverable. These sensors are listed here by flight. Correlation of this list with counters of flight conditions can be done by cross referencing flights and counters with the use of the flight cards. For each flight, the flight tape track and channel assignment, the physical location, the sensor identification code, sensor type, and item code are presented.

Flight	Track/channel	Location	I.D	Type	Item code
1A	5-8	W252	UPR#2	ABS PRESS	P909
	8-3	W6.0	--	YOKE TORS	M918
	12-14	W256	UPR#8	ABS PRESS	P638
	12-4	R263	--	VIBR-CHORD	A972
	20-5	R228	LWR#5-0	BL BUTTON	P979
	21-6	R252	LWR#6-I	BL BUTTON	P755
	21-11	W228	LWR#23	ABS PRESS	P876
	25-3	R252	#15	HWS SGMT	V949
	5-14	W261	UPR#1	ABS PRESS	P661
	9-1	W6.0	--	YOKE BEAM	B916
	22-2	R252	UPR#2-0	BL BUTTON	P985
	24-13	W158	LWR#16	ABS PRESS	P823
	26-4	R198	#11	HWS SGMT	V850
	26-15	W252	LWR#23	ABS PRESS	P740
	19-1	R228	UPR#1-I	BL BUTTON	P732
	19-2	R228	UPR#2-I	BL BUTTON	P734
	19-3	R228	UPR#3-I	BL BUTTON	P736
	19-4	R228	LWR#4-I	BL BUTTON	P976
	19-5	R228	LWR#5-I	BL BUTTON	P978
	19-6	R228	LWR#6-I	BL BUTTON	P980
	19-7	W240	LWR#19	ABS PRESS	P619
	19-8	W240	LWR#20	ABS PRESS	P620
	19-9	W240	LWR#21	ABS PRESS	P621
	19-10	W240	LWR#22	ABS PRESS	P622
	19-11	W240	LWR#23	ABS PRESS	P623
	19-12	W240	LWR#24	ABS PRESS	P624
	19-13	W240	LWR#25	ABS PRESS	P625
	19-14	W261	LWR#21	ABS PRESS	P681
	19-15	W261	LWR#22	ABS PRESS	P682
	19-16	W261	LWR#23	ABS PRESS	P683

Flight	Track/channel	Location	I.D	Type	Item code
3A	8-1	R228	#19	HWS-SGMT	V922
	18-1	R198	UPR#1-0	BL BUTTON	P751
	18-2	R198	UPR#2-0	BL BUTTON	P753
	18-3	R198	UPR#3-0	BL BUTTON	P725
	18-4	R198	LWR#4-0	BL BUTTON	P727
	18-5	R198	LWR#5-0	BL BUTTON	P729
	18-6	R198	LWR#6-0	BL BUTTON	P731
	18-7	W252	LWR#20	ABS PRESS	P991
	18-8	W252	LWR#21	ABS PRESS	P738
	18-9	W252	LWR#22	ABS PRESS	P739
	18-10	P615	LWR#15	ABS PRESS	P615
	18-11	P616	LWR#16	ABS PRESS	P616
	18-12	W240	LWR#17	ABS PRESS	P617
	18-13	W240	LWR#18	ABS PRESS	P618
	18-14	W261	LWR#18	ABS PRESS	P678
	18-15	W261	LWR#19	ABS PRESS	P679
	18-16	W261	LWR#20	ABS PRESS	P680
	22-10	W198	LWR#13	ABS PRESS	P856
	23-7	W198	LWR#17	ABS PRESS	P869
	24-5	R252	#11	HWS SGMT	V945
	24-6	R252	#12	HWS SGMT	V946
4A	12-4	R263	--	VIBR-CHORD	A972
	19-14	W261	LWR#21	ABS PRESS	P681
	22-10	W198	LWR#13	ABS PRESS	P856
	24-5	R252	#11	HWS SGMT	V945
	24-6	R252	#12	HWS SGMT	V946
5A	12-4	R263	--	VIBR-CHORD	A972
	19-4	W261	LWR#21	ABS PRESS	P681
	22-10	W198	LWR#13	ABS PRESS	P856
	24-5	R252	#11	HWS SGMT	V945
	24-6	R252	#12	HWS SGMT	V946
12A	22-10	W198	LWR#13	ABS PRESS	P856
	25-3	R252	#15	HWS SGMT	V949
	25-13	W106	LWR#10	ABS PRESS	P175
13A	11-11	W198	UPR#12	ABS PRESS	P855
	21-14	W261	LWR#27	ABS PRESS	P687
	22-10	W198	LWR#13	ABS PRESS	P856
	25-4	R252	#16	HWS SGMT	V960
	25-8	W158	LWR#18	ABS PRESS	P825
	25-15	W256	LWR#26	ABS PRESS	P656

Flight	Track/channel	Location	I.D	Type	Item code
13B	11-11	W198	UPR#12	ABS PRESS	P855
	25-4	R252	#16	HWS SGMT	V960
	25-8	W158	LWR#18	ABS PRESS	P825
	21-14	W261	LWR#27	ABS PRESS	P687
	25-15	W256	LWR#26	ABS PRESS	P656
14A	9-14	W261	UPR#13	ABS PRESS	P673
	16-1	--	--	FLAPPING	D110
	16-15	47.2	--	MAST PARA	B108
	17-11	W252	LWR#17	ABS PRESS	P975
	20-2	R228	UPR#2-0	BL BUTTON	P735
	20-4	R228	LWR#4-0	BL BUTTON	P977
	20-9	--	--	FEATHERING	P111
	22-10	W198	LWR#13	ABS PRESS	P856
	25-4	R252	#16	HWS SGMT	V960
	25-8	W158	LWR#18	ABS PRESS	P825
15A	20-2	R228	UPR#2-0	BL BUTTON	P735
	20-4	R228	LWR#4-0	BL BUTTON	P977
	20-9	--	--	FEATHERING	P111
	21-7	R198	#7	HWS SGMT	V846
	26-1	R252	#19	HWS SGMT	V963
	26-2	R198	#9	HWS SGMT	V848
	26-3	R198	#10	HWS SGMT	V849
	26-4	R198	#11	HWS SGMT	V850
	26-5	R198	#12	HWS SGMT	V851
	26-6	R198	#13	HWS SGMT	V862
	26-11	R198	#14	HWS SGMT	V863
	26-12	R198	#15	HWS SGMT	V844
16A,16B	20-2	R228	UPR#2-0	BL BUTTON	P735
	20-4	R228	LWR#4-0	BL BUTTON	P977
	22-10	W198	LRW#13	ASB PRESS	P856
	25-7	W158	LWR#17	ABS PRESS	P824
	11-11	W198	UPR#12	ABS PRESS	P855
17A	1-13	--	--	ROLL RATE GYRO	VO12
	9-1	W6.0	--	YOKE BEAM	B916
	11-11	W198	UPR#12	ABS PRESS	P855
	20-4	R228	LWR#4-0	BL BUTTON	P977
19A	22-10	W198	LWR#13	ABS PRESS	P856
	25-8	W158	LWR#18	ABS PRESS	P825

Flight	Track/channel	Location	I.D	Type	Item code
20A	25-8	W158	LWR#18	ABS PRESS	P825
	26-1	R252	#19	HWS SGMT	V963
	26-3	R198	#10	HWS SGMT	V849
21A,21B	20-2	R228	UPR#2-0	BL BUTTON	P735
	26-15	W252	LWR#23	ABS PRESS	P740
22A,22B	7-15	W261	UPR#8	ABS PRESS	P668
	22-10	W198	LWR#13	ABS PRESS	P856
	23-1	R252	#1	HWS SGMT	V923
	23-2	R252	#2	HWS SGMT	V924
	26-15	W252	LWR#23	ABS PRESS	P740
	5-1	R228	#1	HWS SGMT	V866
	5-2	R228	#2	HWS SGMT	V867
	5-3	R228	#3	HWS SGMT	V878
	5-4	R228	#4	SWS SGMT	V879
	5-5	R228	#5	HWS SGMT	V880
	5-6	R228	#6	SWS SGMT	V881
	5-7	W252	UPR#1	ABS PRESS	P908
	5-8	W252	UPR#2	ABS PRESS	P909
	5-9	W252	UPR#3	ABS PRESS	P919
	5-10	W252	UPR#4	ABS PRESS	P920
	5-11	W252	UPR#5	ABS PRESS	P921
	5-12	W252	UPR#6	ABS PRESS	P926
	5-13	W252	UPR#7	ABS PRESS	P927
	5-14	W261	UPR#1	ABS PRESS	P661
	5-15	W261	UPR#2	ABS PRESS	P662
	5-16	W261	UPR#3	ABS PRESS	P663
23A,23B	7-1	R228	#13	HWS SGMT	V910
	7-2	R228	#14	HWS SGMT	V911
	7-3	R228	#15	HWS SGMT	V912
	7-4	R228	#16	HWS SGMT	V913
	7-5	R228	#17	HWS SGMT	V914
	7-6	R228	#18	HWS SGMT	V915
	7-7	W240	UPR#5	ABS PRESS	P605
	7-8	W240	UPR#6	ABS PRESS	P606
	7-9	W240	UPR#7	ABS PRESS	P607
	7-10	W240	UPR#8	ABS PRESS	P608
	7-11	W240	UPR#9	ABS PRESS	P609
	7-12	W240	UPR#10	ABS PRESS	P610
	7-13	W240	UPR#11	ABS PRESS	P611
	7-14	W261	UPR#7	ABS PRESS	P667
	7-15	W261	UPR#8	ABS PRESS	P668

Flight	Track/channel	Location	I.D	Type	Item code
	7-16	W261	UPR#9	ABS PRESS	P669
	22-10	W198	LWR#13	ABS PRESS	P856
24A	7-15	W261	UPR#8	ABS PRESS	P668
	26-15	W252	LWR#23	ABS PRESS	P740

APPENDIX G

OLS/TAAT FULL SCALE AIRFOIL COORDINATES

Appendix G contains the upper surface ordinates of the OLS/TAAT full scale airfoil in inches. The X dimension is distance along the chord mean line with 0.0 being the leading edge and Z is the distance from the mean line. The airfoil is symmetrical; therefore, the lower surface ordinates are the negative of the Z value.

X, in.	Z, in.	X, in.	Z, in.
0.0	0.0	3.71950	1.29306
0.12969	0.33318	3.82004	1.30099
0.24679	0.44944	3.92057	1.30851
0.35811	0.53187	4.02107	1.31562
0.46632	0.59781	4.12157	1.32234
0.57262	0.65363	4.22204	1.32869
0.67767	0.70244	4.32251	1.33466
0.78185	0.74604	4.42296	1.34029
0.88538	0.78554	4.52340	1.34556
0.98843	0.82172	4.62383	1.35049
1.09110	0.85512	4.72425	1.35510
1.19346	0.88613	4.82465	1.35939
1.29558	0.91508	4.92505	1.36337
1.39750	0.94222	5.02544	1.36704
1.49925	0.96772	5.12582	1.37042
1.60085	0.99177	5.22618	1.37351
1.70233	1.01448	5.32654	1.37531
1.80371	1.03598	5.42690	1.37885
1.90499	1.05636	5.52724	1.38111
2.00618	1.07571	5.62757	1.38311
2.10731	1.09409	5.72790	1.38486
2.20837	1.11157	5.82822	1.38636
2.30937	1.12820	5.92854	1.38760
2.41032	1.14404	6.02884	1.38861
2.51122	1.15913	6.12914	1.38939
2.61208	1.17350	6.22944	1.38994
2.71290	1.18720	6.32973	1.39026
2.81368	1.20026	6.43001	1.39036
2.91443	1.21271	6.53029	1.39024
3.01515	1.22457	6.63056	1.38992
3.11585	1.23587	6.73082	1.38938
3.21651	1.24663	6.83108	1.38865
3.31715	1.25687	6.93134	1.38771
3.41777	1.26662	7.03159	1.38658
3.51837	1.27589	7.13184	1.38526
3.61894	1.28470	7.23208	1.38375

PRECEDING PAGE BLANK NOT FILMED

PAGE 166 INTENTIONALLY BLANK

X, in.	Z, in.	X, in.	Z, in.
7.33231	1.38206	11.63853	1.17606
7.43255	1.38018	11.73853	1.16949
7.53277	1.37813	11.83853	1.16292
7.63300	1.37590	11.93853	1.15634
7.73322	1.37351	12.03853	1.14977
7.83343	1.37094	12.13853	1.14320
7.93364	1.36821	12.23853	1.13662
8.03385	1.36532	12.33853	1.13005
8.13406	1.36227	12.43853	1.12348
8.23426	1.35907	12.53853	1.11691
8.33446	1.35571	12.63853	1.11033
8.43465	1.35220	12.73853	1.10376
8.53484	1.34854	12.83853	1.09719
8.63503	1.34473	12.93853	1.09061
8.73521	1.34079	13.03853	1.08404
8.83539	1.33670	13.13853	1.07747
8.93557	1.33247	13.23853	1.07089
9.03574	1.32811	13.33853	1.06432
9.13592	1.32361	13.43853	1.05775
9.23608	1.31898	13.53853	1.05117
9.33625	1.31423	13.63853	1.04460
9.43641	1.30934	13.73853	1.03803
9.53658	1.30433	13.83853	1.03145
9.63673	1.29920	13.93853	1.02488
9.73689	1.29394	14.03853	1.01831
9.83704	1.28857	14.13853	1.01173
9.93719	1.28308	14.23853	1.00516
10.03734	1.27747	14.33853	0.99859
10.13749	1.27174	14.43853	0.99202
10.23763	1.26591	14.53853	0.98544
10.33778	1.25996	14.63853	0.97887
10.43792	1.25391	14.73853	0.97230
10.53805	1.24775	14.83853	0.96572
10.63819	1.24148	14.93853	0.95915
10.73832	1.23511	15.03853	0.95258
10.83845	1.22864	15.13853	0.94600
10.89478	1.22495	15.23853	0.93943
10.93853	1.22208	15.33853	0.93286
11.03853	1.21550	15.43853	0.92628
11.13853	1.20893	15.53853	0.91971
11.23853	1.20236	15.63853	0.91314
11.33853	1.19578	15.73853	0.90656
11.43853	1.18921	15.83853	0.89999
11.53853	1.18264	15.93853	0.89342

X, in.	Z, in.	X, in.	Z, in.
16.03853	0.88684	20.43851	0.59762
16.13850	0.88027	20.53850	0.59105
16.23849	0.87370	20.63850	0.58448
16.33850	0.86713	20.73849	0.57791
16.43851	0.86055	20.83850	0.57133
16.53850	0.85398	20.93851	0.56476
16.63850	0.84741	21.03850	0.55819
16.73849	0.84083	21.13850	0.55161
16.83850	0.83426	21.23849	0.54504
16.93851	0.82769	21.33850	0.53847
17.03850	0.82111	21.43851	0.53189
17.13850	0.81454	21.53850	0.52532
17.23849	0.80797	21.63850	0.51875
17.33850	0.80139	21.73849	0.51217
17.43851	0.79482	21.83850	0.50560
17.53850	0.78825	21.93851	0.49903
17.63850	0.78167	22.03850	0.49245
17.73849	0.77510	22.13850	0.48588
17.83850	0.76853	22.23849	0.47931
17.93851	0.76195	22.33850	0.47273
18.03850	0.75538	22.43851	0.46616
18.13850	0.74881	22.53850	0.45959
18.23849	0.74224	22.63850	0.45302
18.33850	0.73566	22.73849	0.44644
18.43851	0.72909	22.83850	0.43987
18.53850	0.72252	22.93851	0.43330
18.63850	0.71594	23.03850	0.42672
18.73849	0.70937	23.13850	0.42015
18.83850	0.70280	23.23849	0.41358
18.93851	0.69622	23.33850	0.40700
19.03850	0.68965	23.43851	0.40043
19.13850	0.68308	23.53850	0.39386
19.23849	0.67650	23.63850	0.38728
19.33850	0.66993	23.73849	0.38071
19.43851	0.66336	23.83850	0.37414
19.53850	0.65678	23.93851	0.36756
19.63850	0.65021	24.03850	0.36099
19.73849	0.64364	24.13850	0.35442
19.83850	0.63706	24.23849	0.34784
19.93851	0.63049	24.33850	0.34127
20.03850	0.62392	24.43851	0.33470
20.13850	0.61734	24.53850	0.32813
20.23849	0.61077	24.63850	0.32155
20.33850	0.60420	24.73849	0.31498

X, in.	Z, in.	X, in.	Z, in.
24.83850	0.30841	26.83850	0.17694
24.93851	0.30183	26.93851	0.17037
25.03850	0.29526	27.03850	0.16380
25.13850	0.28869	27.13850	0.15722
25.23849	0.28211	27.23851	0.15065
25.33850	0.27554	27.33850	0.14408
25.43851	0.26897	27.43851	0.13750
25.53850	0.26239	27.53850	0.13093
25.63850	0.25582	27.63850	0.12438
25.73851	0.24925	27.73851	0.11778
25.83850	0.24267	27.83850	0.11121
25.93851	0.23610	27.93851	0.10464
26.03850	0.22953	28.03850	0.09806
26.13850	0.22295	28.13850	0.09149
26.23851	0.21638	28.23851	0.08492
26.33850	0.20981	28.33850	0.07834
26.43851	0.20323	28.43851	0.07177
26.53850	0.19666	28.53850	0.06520
26.63850	0.19009	28.63850	0.05862
26.73851	0.18351		

REFERENCES

1. Shenoy, K. R.; Waak, T.; and Brieger, J. T.: Development of a Rot22-DATAMAP Interface. NASA CR-177403, April 1986.

2. Miley, S. J.; Hall, G. F.; and von Lavente, E.: Investigation of Helicopter Rotor Blade/Wake Interactive Impulsive Noise. NASA CR-177435, 1987.

3. Schillings, J. J.: Mach Number Correlation for a Two-Dimensional Helicopter Rotor-Blade Analysis in the Tip Region. NASA CR-177430, 1986.

4. Scheiman, J.: A Tabulation of Helicopter Rotor-Blade Differential Pressures, Stresses, and Motions as Measured in Flight. NASA TM X-952, 1964.

5. Rabbott, J. P., Jr.; Lizak, A. A.; and Paglino, V. M.: A Presentation of Measured and Calculated Full-Scale Rotor Blade Aerodynamic and Structural Loads. USAAVLABS TR-66-31, Sikorsky Aircraft, July 1966.

6. Pruyn, R. R.: In-Flight Measurement of Rotor Blade Airloads, Bending Moments, and Motions, Together with Rotor Shaft Loads and Fuselage Vibration, on a Tandem Rotor Helicopter. USAAVLABS TR-67-9, May 1967.

7. Beno, E.: CH-53a Main Rotor and Stabilizer Vibratory Airloads and Forces. Department of the Navy SER 65593, Sikorsky Aircraft, June 1970.

8. Bartsch, E. A.: In-Flight Measurement and Correlation with Theory of Blade Airloads and Resources in the XH-51A Compound Helicopter Rotor. USAAVLABS TR 68-22A through D, May 1967.

9. Fenaughty, R.; and Beno, E.: NH-3A Vibratory Airloads and Vibratory Rotor Loads. Department of the Navy SER 611493, Sikorsky Aircraft, Jan. 1970.

10. Morris, C. E. K., Jr.: Rotor-Airfoil Flight Investigation: Preliminary Results. AHS 78-05, presented at 34th American Helicopter Society Annual National Forum, May 1978.

11. Morris, C. E. K., Jr.; Tomaine, R. L.; and Stevens, D. D.: A Flight Investigation of Performance and Loads for a Helicopter with NLR-1T Main-Rotor Blade Sections. NASA TM-80165, 1979.

12. Morris, C. E. K., Jr.; Tomaine, R. L.; and Stevens, D. D.: A Flight Investigation of Performance and Loads for a Helicopter with RC-SC2 Main-Rotor Blade Sections. NASA TM-81898, 1980.

13. Morris, C. E. K., Jr.; Tomaine, R. L.; and Stevens, D. D.: A Flight Investigation of Performance and Loads for a Helicopter with 10-64C Main-Rotor Blade Sections. NASA TM-81871, 1980.

14. Morris, C. E. K., Jr.: A Flight Investigation of Blade-Section Aerodynamics for a Helicopter Main Rotor Having 10-64C Airfoil Sections. NASA TM 83226, 1981.

15. Morris, C. E. K., Jr.; Stevens, D. D.; and Tomaine, R. L.: A Flight Investigation of Blade-Section Aerodynamics for a Helicopter Main Rotor Having NLR-1T Airfoil Sections. NASA TM 80166, 1980.

16. Morris, C. E. K., Jr.: A Flight Investigation of Blade-Section Aerodynamics for a Helicopter Main Rotor Having RC-SC2 Airfoil Sections. NASA TM 83298, 1982.

17. Knight, V. H., Jr.; Haywood, W. S., Jr.; and Williams, M. L.: A Rotor-Mounted Digital Instrumentation System for Helicopter Blade Flight Research Measurements. NASA TP 1146, 1978.

18. Shockey, G. A.; Williamson, J. W.; and Cox, C. R.: AH-1G Helicopter Aerodynamic and Structural Loads Survey. USAAMRDL-TR-76-39, Bell Helicopter Textron, Feb. 1977.

19. Brieger, J. T.: Validation of Helicopter Noise Prediction Techniques--Data Base. Bell Report 699-099-119, Bell Helicopter Textron, Jan. 1980.

20. Sakowski, P. C., Jr.; and Charles, B. D.: Noise Measurement Test Results for AH-1G Operational Loads Survey, Vol. 1 - Engineering Report. Bell Report 299-099-831, Bell Helicopter Textron, Feb. 1976.

21. Sakowski, P. C., Jr.; and Charles, B. D.: Noise Measurement Test Results for AH-1G Operational Loads Survey, Vol. 2 - Appendices A and B. Bell Report 299-099-831, Bell Helicopter Textron, Feb. 1976.

22. Sakowski, P. C., Jr.; and Cox, C. R.: AH-1G Helicopter Rotor Aerodynamic and Acoustic Data Analysis for Descent and High Forward Speeds, Vol. 1. NASA CR-159036, Bell Helicopter Textron, June 1979.

23. Sakowski, P. C., Jr.; and Cox, C. R.: AH-1G Helicopter Rotor Aerodynamics and Acoustics Data Analysis for Descent and High Forward Speeds, Vol. Two. NASA CR-159037, Bell Helicopter Textron, June 1979.

24. Nakamura, Y.: Prediction of Blade-Vortex Interaction Noise from Measured Blade Pressure. Paper No. 32, presented at the 7th European Rotorcraft and Powered Lift Aircraft Forum, Sept. 1981.

25. White, J. A.: Model AH-1G Airframe and Control System Ground Vibration Test Results. Bell Report 299-099-819, Bell Helicopter Textron, April 1976.

26. Merkley, D. J.; Riley, M. J.; and Young, C.: Summary Report of the Second TTCP/Htp-6 Joint Working Session on Rotor Loads. USAAVRADCOM-TR-83-D-29, Fort Eusstis, Va., Oct. 1983.

27. Heffernan, R. M.; and Gaubert, M.: Structural and Aerodynamic Loads and Performance Measurements of a SA349/2 Helicopter with an Advanced Geometry Rotor. NASA TM 88370, 1986.

28. Splettstoesser, W. R.; Schultz, K. J.; Schmitz, F. H.; and Boxwell, D. A.: Model Rotor High-Speed Impulsive Noise - Parametric Variations and Full-Scale Comparisons. AHS paper, presented at American Helicopter Society 39th Annual Forum, May 1983, St. Louis, Mo.

29. Boxwell, D. A.; Schmitz, F. H.; Splettstoesser, W. R.; and Schultz, K. J.: Model Helicopter Rotor High-Speed Impulsive Noise: Measured Acoustics and Blade Pressures. NASA TM 85850, USAAVRADCOM TR-83-A-14, 1983.

30. Watts, M. E.; and Cross, J. L.: Two-Dimensional Characteristics of the OLS/TAAT Airfoil. NASA TM 89435, 1987.

31. Watts, M. E.; and Cross, J. L.: The NASA Modern Technology Rotors Program. AIAA paper 86-9788 presented at the 3rd Flight Testing Conference, April 1986.

32. Anon.: Instrumentation Report for the Operational Loads Survey Rotor and the BHT Model 576 Wind Tunnel Test Stand. Bell Report 576-099-065, Bell Helicopter Textron, March 1980.

33. Cross, J. L.; and Watts, M. E.: In-Flight Acoustic Testing Techniques Using the YO-3A Acoustic Research Aircraft. NASA TM-85895, 1984.

34. Cross, J. L.: YO-3A Acoustic Research Aircraft Systems Manual. NASA TM 85968, 1984.

35. Watts, M. E.: Supplementary Calibration Test of the Tip-Aerodynamics and Acoustics-Test Pressure Transducers. NASA TM 88312, 1986.

36. Boxwell, D. A.; and Schmitz, F. H.: Full-Scale Measurements of Blade-Vortex Interaction Noise. AHS paper, presented at American Helicopter Society 36th Annual Forum, May 1980, Washington, D.C.

37. Schmitz, F. H.; and Boxwell, D. A.: In-Flight Far-Field Measurement of Helicopter Impulsive Noise. Journal of the AHS, vol. 21, no. 4, Oct. 1976, pp. 2-16.

38. Philbrick, R. B.: The Data from Aeromechanics Test and Analytics, Management and Analysis Package (DATAMAP) - Vol. One: User's Manual. USAAVRADCOM TR-80-D-30A, Bell Helicopter Textron, Dec. 1980.

39. Philbrick, R. B.: The Data from Aeromechanics Test and Analytics, Management and Analysis Package (DATAMAP) - Vol. Two: Systems Manual. USAAVRADCOM TR-80-D-30B, Bell Helicopter Textron, Dec. 1980.

40. Philbrick, R. B.: DATAMAP Installation at NASA Ames Research Center. Bell Report 299-099-021, Bell Helicopter Textron, Oct. 1980.

41. Tieman, L. J.: Ground Data Center Standard Digital Tape Format. Bell Report 699-099-020, Bell Helicopter Textron, April 1976.

42. Hooper, W. E.: The Vibratory Airloading of Helicopter Rotors. Paper No. 46 presented at 9th European Rotorcraft Forum, Boeing Vertol Company, Sept. 1983. (Also Vertica, vol. 8, no. 2, 1984.)

TABLE I.- AH-1G AIRCRAFT CHARACTERISTICS

Empty weight	5600 lb
Maximum gross weight	9500 lb
Crew	2
Maximum speed	160 knots
Number of blades (main rotor/tail rotor)	2/2
Diameter	44 ft/8.5 ft
Chord	28.63 in./8.4 in.
RPM (nominal)	324/1654 rpm
Gearbox rating	1000 hp
Maximum horsepower	1400 hp
Power plant	Lycoming T53-L-13

TABLE II.- AIRCRAFT STATE VARIABLE ITEM CODES

CG vertical acceleration	A005	Roll rate	V012
Pilot vertical acceleration	A019	Pitch rate	V013
Aircraft sideslip	D007	Yaw rate	V014
Aircraft angle of attack	D008	Lateral stick	D022
Pitch attitude	D010	Longitudinal stick	D021
Roll attitude	D009	Collective stick	D023
Yaw attitude	D011	Pedal position	D024
Airspeed	P042	Flapping	D110
Fore/aft axial boost tube	F100	Feathering	P111
Lateral cyclic boost tube	F101	Engine Q pressure	P506
Collective boost tube	F102	Main rotor 1/rev	R049
Static pressure	P030	Tail rotor 1/rev	R048

TABLE III.- PRESSURE TRANSDUCER LOCATION/ITEM CODE LIST

Chord, %	Surface	Radial location, r/R							
		0.40	0.60	0.75	0.864	0.91	0.955	0.97	0.99
1	Upper	P157	P187	P828	P164	P601	P908	P631	P661
	Lower	P173	P809	P856	P831	P615	P958	P645	P675
3	Upper	P158	P188	P836	P165	P602	P909	P632	P662
	Lower	P174	P810	P857	P843	P616	P959	P646	P676
8	Upper	P159	P189	P837	P166	P603	P919	P633	P663
	Lower	P175	P811	P858	P844	P617	P973	P647	P677
15	Upper	--	P190	P838	P180	P604	P920	P634	P664
	Lower	--	P812	P868	P845	P618	P974	P648	P678
20	Upper	--	--	--	--	P605	--	P635	P665
	Lower	--	--	--	--	P619	--	P649	P679
25	Upper	P160	P191	P840	P182	P606	P921	P636	P666
	Lower	P176	P822	P869	P860	P620	P975	P650	P680
35	Upper	--	P192	P841	P194	P607	P926	P637	P667
	Lower	--	P823	P870	P861	P621	P989	P651	P681
40	Upper	--	--	P842	P195	P698	P927	P638	P668
	Lower	--	--	P872	P875	P622	P990	P652	P682
45	Upper	P161	P193	P852	P106	P609	P928	P639	P669
	Lower	P171	P824	P873	P876	P623	P991	P653	P683
50	Upper	--	--	--	P813	P610	P941	P640	P670
	Lower	--	--	--	P877	P624	P738	P654	P684
55	Upper	--	P806	P853	P814	P611	P942	P614	P671
	Lower	--	P825	P874	P891	P625	P739	P655	P685
60	Upper	--	--	--	P815	P612	--	P642	P672
	Lower	--	--	--	P892	P626	--	P656	P686
70	Upper	P162	P807	P854	P829	P613	P943	P643	P673
	Lower	P178	P826	P884	P893	P627	P740	P657	P687
92	Upper	P167	P808	P855	P830	--	P957	P644	P674
	Lower	P179	P827	P885	P907	--	P757	P658	P688

TABLE IV.- ACCELEROMETER LOCATION/ITEM CODE LIST

Location, r/R	Beamwise	Chordwise
0.013	A889	A905
0.500	A950	A968
0.591	A951	A969
0.697	A952	A970
0.902	A953	A971
0.996	A954	A972

TABLE V.- STRAIN GAGE LOCATION/ITEM CODE LIST

Location, r/R	Beamwise	Chordwise	Torsion
0.023	B112/B916	B113/B917	M906/M918
0.042	B114	B115	--
0.227	B120	B121	--
0.311	B126	B127	M150
0.390	B128	B129	--
0.500	B122	B123	M935
0.701	B132	B133	M936
0.803	B124	B125	--
0.902	B134	B135	M937
Red blade pitch link			F103
White blade pitch link			F104
Mast bending perpendicular			B109
Mast bending parallel			B108
Shaft torque			M107

Note: The second Item Code values are for sensors on the white blade yoke.

TABLE VI.- BOUNDARY LAYER BUTTON LOCATION/ITEM CODE LIST

Chord, %	0.75 r/R Inboard/Outboard	0.866 r/R Inboard/Outboard	0.955 r/R Inboard/Outboard
30 Upper	P750/P751	P732/P733	P982/P983
Lower	P726/P727	P976/P977	P988/P964
60 Upper	P752/P753	P734/P735	P984/P985
Lower	P728/P729	P978/P979	P965/P966
90 Upper	P754/P755	P736/P737	P986/P987
Lower	P730/P731	P980/P981	P755/P756

TABLE VII.- HOT-WIRE LOCATION/ITEM CODE LIST

Station	Location, in.	0.75 r/R	0.866 r/R	0.955 r/R
1	-1.56	--	V866	V923
2	-1.44	--	V867	V924
3	-1.32	--	V878	V925
4	-1.20	--	V879	V929
5	-1.08	--	V880	V930
6	-0.96	--	V881	V931
7	-0.84	V846	V894	V932
8	-0.72	V847	V895	V933
9	-0.60	V848	V896	V934
10	-0.48	V849	V897	V944
11	-0.36	V850	V898	V945
12	-0.24	V851	V899	V946
13	-0.18	--	V910	--
14	-0.12	V862	V911	V947
15	-0.06	--	V912	V948
16	0.00	V863	V913	V949
17	0.06	--	V914	V960
18	0.12	--	V915	V961
19	0.15	V844	--	--
20	0.18	--	--	V962
21	0.24	--	V922	V963

TABLE VIII.- YO-3A PHYSICAL CHARACTERISTICS

Wing span	57.0 ft
Length	29.3 ft
Height	9.1 ft
Maximum gross weight	3800 lb
Power plant	210 hp
Propeller diameter	100 in.
Stall speed	60 knots
Maximum level speed	110 knots
Blades	3
Crew	2
Flaps	Fixed

TABLE IX.- GROUND-BASED ACOUSTICS PACKAGE

1/2 in. condenser microphones	5
Preamplifier	5
Amplifier-line divers	5
1000 ft shielded cable reels	8
5-channel remote gain unit	1
14-track FM recorder	1
Oscilloscope	1
Oscillator/attenuator	1

TABLE X.- PHASE ONE TEST MATRIX

Condition	Clean			Hog		
	Forward	Mid	Aft	Forward	Mid	Aft
IGE hover	2127	--	2151	2388'	2370'	--
0.5 V_h	2134	--	2157	2394'	2378'	2187
0.6 V_h	2133/2138	--	2156	2393'	2377'	2186
0.7 V_h	2132	--	2155	2392'	2376'	2185
0.8 V_h	2130	--	2154	2391'	2375'	2184
0.9 V_h	2129	--	2153	2390'	2374'	2183
1.0 V_h	2128	--	2152	2389'	2373'	2181
Accelerate to V_h	2137	--	2160	2397'	2385'	2190
Maximum climb	--	--	--	--	2372'	--
Left 1.5 g	--	--	--	--	2379'	--
Left 1.7 g	--	--	--	--	2380'	--
Left 2.0 g	--	--	--	--	--	--
Right 1.5 g	--	--	--	--	2381'	--
Right 1.7 g	--	--	--	--	2382'	--
Right 2.0 g	--	--	--	--	--	--
Transition	--	--	--	--	2371'	--
Auto entry	2135/2139	--	2158	2395'	2383'	2188
Auto recovery	2136/2140	--	2159	2396'	2384'	2189
Flair to hover	--	--	2163	--	--	--
Stop to hover	--	--	2161	--	--	--
Climbout	--	--	--	--	--	--
Ground run	2126	--	2150	--	--	--
Pylon mount check	3211/3212					
Left lateral step	3215					
Right lateral step	3216					
Longitudinal aft step	3213					
Longitudinal forward step	3214					

Note: The symbol ' above denotes a test point where the rotating sensors are shifted by 180°. See explanation in section 7.1.7.

TABLE XI.- PHASE TWO TEST MATRIX: a) 9200 lb reference aircraft gross weight; b) 10,500 lb reference aircraft gross weight

Airspeed, knots	Rate of descent, ft/min					
	0	200	400	600	800	1000
A. Left position						
60	2337'	2338'	2339'	2344'	2347'	--
65	3150	3151	3152	3155	3167	--
70	3187	--	3188	--	3181	--
80	2827'	2828'	2829'	2832'	2825'	--
90	--	--	--	--	--	--
100	3182	--	3183	3184	--	--
110	--	2810'	--	--	--	--
120	--	--	--	--	--	2818'
130	--	--	--	--	--	3158
Right position						
60	3206	--	3189	3207	3208	--
80	--	--	3203	3204	3205	--
120	--	--	--	--	--	--
Trail position						
60	2336'	--	2340'	2342'	3156	--
65	3149	--	3153	3154	3168	--
70	3186	--	--	--	--	--
80	2826'	--	2830'	2831'	2833'	--
90	2812'	--	--	--	2814'	--
100	2834'	--	--	3185	--	--
110	3161/2806'	2808'	--	2811'	--	--
120	--	--	--	2815'	2816'	3160/2817'
130	--	--	--	--	--	3159
Experimental position						
60	--	--	3164	3165	--	--
80	--	--	3162	3163	--	--
120	--	--	--	--	--	3166
B. Left position						
60	3172	3173	3174	3177	3179	--
80	3197	--	3196	--	3202	--
Trail position						
60	3171	--	3175	3176	3180	--
80	--	--	3199/3198	--	3200/3201	--

Note: The symbol ' above denotes a test point where the rotating sensors are shifted by 180°. See explanation in section 7.1.7.

TABLE XII.- GROUND-BASED ACOUSTIC TEST MATRIX

Condition	W/YO-3A	W/O YO-3A
V_h level	--	3091/3068/3082
0.9 V_h	--	3092/3093/3077
.8 V_h	--	3094/3078
.7 V_h	3098	3095/3079
.6 V_h	3097	3080
.5 V_h	3096	3081
60 knots	3100	--
120 dive	3101/3012	--

IGE hover[a]	0°	90°	180°	270°
	3061	3062	3063	3064

Descent run	3° Glide slope	3069
	6° Glide slope	3070
	9° Glide slope	3071/3074
	12° Glide slope	3072/3073
Takeoff	Standing start	3065
	Running start	3066/3067

[a]Azimuth angle to center line.

TABLE XIII.- PHASE 4 AERODYNAMIC TEST MATRIX

a) $C_t = 0.0050$

Advance Ratio, μ

M	.11	.14	.15	.16	.17	.18	.19	.20
0.66								
0.70		0M2863						
0.71	0F3217				+1F3229			
					+3A3141			
0.72								
0.73		-1M2842						
0.74				+2A3140				
0.75				+4M2867	-1F3228	+1M2843		
0.76			-2M2862	-2M2860	+1A3138		+4M2868	
			+2M2882	+2M2883			+2A3137	
			+1A3139					
0.77				-2F3215	-2F3213	0F3227		0F3226
					-2F3214			+2A3135
					-2F3216			
0.78							+2A3136	
0.79								
0.80								-1M2856

LEGEND

+2 F 9999

- 9999 — Counter number
- F — C.G. location, (F) forward, (M) mid, (A) aft
- +2 — Deviation from optimum C_t value x 0.0001, i.e. 0.0052 actual C_t for 0.0050 table

TABLE XIII.- CONTINUED

a) C_t = 0.0050 (continued)

M	Advance Ratio, μ .21	.22	.23	.24	.25	.26	.27	.28
0.77	0M2844							
0.78								
0.79			+4M2869					
			0F3225					
0.80		+1A3134						
		-1M2857						
		-2M2859						
		+1M2881						
0.81			+2M2880	0F3224			+1M2845	
0.82			-1M2855	+2M2879		-1M2854	+3M2878	+2A3131
				+1A3133				
0.83								-1M2853
								+3M2876
								0F3221
0.84								-1M2852
								+1A3132
0.85								+2M2875

LEGEND

+2 F 9999

- 9999 — Counter number
- F — C.G. location, (F) forward, (M) mid, (A) aft
- +2 — Deviation from optimum C_t value x 0.0001 i.e. 0.0052 actual C_t for 0.0050 table

TABLE XIII.- CONTINUED

a) $C_t = 0.0050$ (concluded)

M	Advance Ratio, μ: .29	.30	.31	.32	.33	.34	.35	.36
0.83	+4M2870							
0.84								
0.85	0F3220			+1M2846	+4M2871			
					0F3218			
0.86					+2A3130			
0.87					+3M2873			+1M2847
								+2A3129
0.88				+2M2874	-1M2849	0F3219	-1M2848	
					-1M2850	+2A3127		
					-1M2851			
					+1A3126			
					-2A3128			

LEGEND

+2 F 9999

- 9999 — Counter number
- F — C.G. location, (F) forward, (M) mid, (A) aft
- +2 — Deviation from optimum C_t value x 0.0001
  i.e. 0.0052 actual C_t for 0.0050 table

TABLE XIII.- CONTINUED

b) $C_t = 0.0062$

Advance Ratio, μ

M	.11	.14	.15	.16	.17	.18	.19	.20
0.70								
0.71				+2F3249				
0.72					-1M2906	+3A3122		
0.73								
0.74								
0.75						+2A3121		
0.76				-3M2905				
				+0F3238				
				-1F3239				
0.77				-2F3241	-2M2902		+1A3119	+1A3118
					-3M2904			
					0A3120			
0.78					-3M2903			-2M2901

LEGEND

+2 F 9999

- 9999 — Counter number
- F — C.G. location, (F) forward, (M) mid, (A) aft
- +2 — Deviation from optimum C_t value x 0.0001
  i.e. 0.0052 actual C_t for 0.0050 table

TABLE XIII.- CONCLUDED

b) C_t = 0.0062 (continued)

M	Advance Ratio, μ .21	.22	.23	.24	.25	.26	.27	.28
0.80		-2M2899	-2M2900					
0.81			-2M2898					
			0F3237					
0.82					-2M2897			
					-2A3116			
0.83							-1M2896	-1M2892
							+1A3115	0M2894
0.84								+2A3114

b) C_t = 0.0062 (concluded)

M	Advance Ratio, μ .29	.30	.31	.32	.33	.34	.35	.36
0.85	-2M2895		+2A3112	0M2891	+3A3111			
0.86		+1A3113	-1M2893	-1M2890				

(c) Additional C_t's

Ct	Advance Ratio, μ	M	Record
0.0043	0.00	0.66	0F3211
	0.00	0.81	0F3212
	0.23	0.81	-1F3222
0.0056	0.17	0.71	0M2866
	0.37	0.85	-1M2872

LEGEND

+2 F 9999

9999 — Counter number

F — C.G. location, (F) forward, (M) mid, (A) aft

+2 — Deviation from optimum C_t value x 0.0001
i.e. 0.0052 actual C_t for 0.0050 table

TABLE XIV.- YO-3A TAPE RECORDER CHANNEL ASSIGNMENTS

Channel	Sensor
1	Port microphone (unfiltered)
2	1/rev pulse
3	Tail microphone (unfiltered)
4	Time code
5	Starboard microphone (unfiltered)
6	Starboard microphone (filtered)
7	Port microphone (filtered)
8	Reproduction channel (blank)
9	Altimeter
10	Airspeed
11	OAT (°F)
12	Angle of attack
13	Angle of sideslip
14	Voice track
30 ips tape speed	

TABLE XV.- CHANNEL ASSIGNMENTS FOR THE GROUND ACOUSTICAL ARRAY

Microphone number	Tape recorder channel number	Microphone physical location	Comment
1	1 6	4 ft tripod nearest radar complex	ch 1, highest gain ch 6, lowest gain (-10 dB)
2	2 7	4 ft tripod on flight centerline (on runway edge nearest radar complex)	ch 2, highest gain ch 7, lowest gain
3	3 8	4 ft tripod farthest from radar complex (in bean field)	ch 3, highest gain ch 8, lowest gain (-10 dB)
4	4 9	40 ft tower nearest radar complex	ch 4, highest gain ch 9, lowest gain (-10 dB)
5	5 10	40 ft tower, 10 ft off flight centerline away from microphone #3	ch 5, highest gain ch 10, lowest gain (-10 dB)

TABLE XVI.- MULTIPLEXER BAND DATA FREQUENCY INFORMATION

Band	Center frequency, kHz	Bandwidth	Maximum data frequency, Hz
1	1.5	±250 Hz	50
2	2.5		
3	3.5		
4	4.5		
5	5.5		
6	6.5		
7	10.0	±1 kHz	200
8	14.0		
9	18.0		
10	22.0		
11	26.0		
12	30.0		
13	34.0		
14	44.0	±2 kHz	400
15	52.0		
16	60.0		

TABLE XVII.- WHITE BLADE INSTRUMENTATION FREQUENCY RESPONSE, Hz

Chord, %	40% R Top/Bot	60% R Top/Bot	75% R Top/Bot	86.4% R Top/Bot	91% R Top/Bot	95.5% R Top/Bot	97% R Top/Bot	99% R Top/Bot
1	50/200	200/200	200/200	200/200	200/200	200/200	400/400	400/400
3	50/200	200/200	200/200	200/200	200/200	200/200	400/400	400/400
8	50/200	200/200	200/200	200/200	200/200	200/200	400/400	400/400
15	--/--	200/200	200/200	200/200	200/200	200/200	400/400	400/400
20	--/--	--/--	--/--	--/--	200/200	--/--	400/400	400/400
25	50/200	200/200	200/200	200/200	200/200	200/200	400/400	400/400
35	--/--	200/200	200/200	200/200	200/200	200/200	400/400	400/400
40	--/--	--/--	200/200	200/200	200/200	200/200	400/400	400/400
45	200/200	200/200	200/200	200/200	200/200	200/200	400/400	400/400
50	--/--	--/--	--/--	200/200	200/200	200/200	400/400	400/400
55	--/--	200/200	200/200	200/200	200/200	200/200	200/400	400/400
60	--/--	--/--	--/--	200/200	200/200	--/--	400/400	400/400
70	200/200	200/200	200/200	200/200	200/200	200/400	400/400	400/400
92	200/200	200/200	200/200	200/200	--/--	200/400	400/400	400/400

TABLE XVIII.- RED BLADE INSTRUMENTATION FREQUENCY RESPONSE, Hz

r/R	Strain gages, in.-lb			Boundary Layer Buttons[a]			Hot wire	Accelerometers, g	
	Beam	Chord	Torsion	0.3 X/C	0.6 X/C	0.9 X/C		Beam	Chord
0.02	50	50	50	--	--	--	--	--	--
.23	50	50	--	--	--	--	--	--	--
.31	200	200	200	--	--	--	--	--	--
.39	200	200	--	--	--	--	--	--	--
.50	50	200	200	--	--	--	--	50	50
.59	--	--	--	--	--	--	--	50	50
.70	50	50	50	--	--	--	--	50	50
.75	--	--	--	50/50	50/50	50/50	50[b]	--	--
.80	50	50	--	--	--	--	--	--	--
.85	--	--	--	50/50	50/50	50/50	50	--	--
.90	50	50	50	--	--	--	--	50	50
.95	--	--	--	50/50	50/50	50/50	50	--	--
.996	--	--	--	--	--	--	--	50	50

[a]Inboard/outboard pointing elements, psid.
[b]Elements #7, 14, 15 @ 200.

TABLE XIX.- DATAMAP PROCESSING CAPABILITIES

Analysis	Derivation	Plot
Amplitude spectra	True airspeed	Single X-Y plot
Harmonic analysis	Rotor speed	Multiple X-Y plot
Minimum/maximum analysis	Rotor azimuth	Contour plot
Digital filtering	Shaft horsepower	Surface plot
Cycle averaging	Density altitude	Cross plot
Moving black damping	Blade flapping	Log or semi-log
Numeric integration	Blade feathering	Tabulated printout
Radially	Mach number	
Azimuthally	Blade loading coefficient	
Time	Normal	
Numeric Difference	Chordwise	
Radially	Moment	
Azimuthally	Pressure	
Time	Blade loading force	
Stochastic analysis	Normal	
Cross-correlation	Chordwise	
Auto-correlation	Moment	
Cross-spectral density	Blade displacement	
Auto-spectral density	Blade slope	
Coherence function	Local flow magnitude	
Frequency response function	Local flow direction	
Statistical analysis		
Mean		
Variance		
Standard deviation		
Normal distribution test		
Acoustic analysis		
Narrow band		
Octave		
Third octave		
PNL		
Network weighted		

TABLE XX.- SUMMARY OF PRESSURE TRANSDUCERS WITH EXCESSIVE SLOPE CHANGES

Item code	Radial station %	Chord station %	Surface
P162	40	70	Upper
P163	40	92	Upper
P167	40	92	Upper
P620	91	25	Lower
P638	97	40	Upper
P639	97	45	Upper
P655	97	55	Lower
P677	99	8	Lower
P739	95.5	55	Lower
P823	60	35	Lower
P875	86.4	40	Lower
P928	95.5	45	Upper
P973	95.5	8	Lower
P974	95.5	15	Lower
P989	95.5	35	Lower
P991	95.5	45	Lower

TABLE XXI.- AIRCRAFT STATES FOR SPEED SWEEP

Variable	Test points (counter)						
	2152	2153	2154	2155	2156	2157	2370
RPM	307.2	315.0	314.7	315.2	315.5	315.9	321.0
OAT, °C	11.5	18.5	18.5	18.5	18.5	18.5	16.5
Static pressure, psia	13.65	13.60	13.45	13.30	13.24	13.18	14.75
Airspeed, KTAS	159	146	129	116	98	82	0
Gross weight, lb	8066	8000	7941	7920	7890	7870	9115
μ	0.377	0.341	0.303	0.268	0.230	0.189	0.000
Longitudinal flapping, deg	-1.13	-1.87	-2.20	-2.38	-2.29	-2.13	5.05
Lateral flapping, deg	-1.11	-0.60	-0.51	-0.19	-0.01	0.15	-4.12
Fuselage α, deg	-3.9	-1.7	-0.5	1.4	3.4	4.0	--
C_T	0.00474	0.00460	0.00462	0.00464	0.00464	0.00464	0.00485
T_0, sec	1.6	2.6	2.9	2.5	2.0	1.2	0.5
Main rotor torque, in.-lb	224,310	184,126	152,109	130,789	105,313	93,472	--
Pitch attitude, deg	-4.56	-2.36	-2.51	0.37	-0.16	0.89	-4.21
Roll attitude, deg	0.97	0.96	0.25	0.92	0.30	0.32	-0.37
Sideslip, deg	-0.51	-1.12	-1.34	-1.90	-1.69	-2.24	0.00
Collective, %	48.1	37.8	31.3	25.9	20.4	18.1	31.0
Longitudinal cyclic stick position, %	84.2	81.4	78.6	75.9	71.8	67.8	33.6
Lateral cyclic stick position, %	47.7	51.6	53.3	54.2	54.4	55.4	50.2
Pedal, %	37.2	41.4	44.2	45.5	48.3	50.4	15.1
Pitch rate, deg/sec	0.44	0.58	0.01	-0.31	-0.09	0.02	0.20
Yaw rate, deg/sec	-0.11	0.81	-0.27	-0.13	-0.21	0.01	-3.21
Roll rate, deg/sec	-0.23	-0.37	-0.07	-0.76	-0.46	0.20	0.16
Longitudinal cyclic blade pitch, deg	11.8	10.2	8.9	7.9	6.5	5.5	1.9
Lateral cyclic blade pitch, deg	-3.6	-2.4	-2.4	-2.1	-1.8	-1.7	2.4
Collective blade pitch, deg	18.0	15.8	14.5	13.4	12.2	11.7	14.4

TABLE XXII.- HARMONICS OF PRESSURE VALVES AT 159 KTAS

	BOTTOM SURFACE					
	RADIUS= 0.400 CHORD= 0.010		RADIUS= 0.400 CHORD= 0.030		RADIUS= 0.400 CHQRD= 0.080	
HARM	AMPLITUDE	PHASE	AMPLITUDE	PHASE	AMPLITUDE	PHASE
0.	0.1416E+02	0.0000E+00	0.1365E+02	0.0000E+00	0.1341E+02	0.0000E+00
1.	0.1039E+01	0.1010E+03	0.3766E+00	0.1325E+03	0.1630E+00	-0.1622E+03
2.	0.2905E+00	-0.1266E+03	0.1838E+00	-0.6050E+02	0.1761E+00	-0.2938E+02
3.	0.8443E-01	0.8918E+02	0.5366E-01	0.9732E+02	0.2879E-01	0.1165E+03
4.	0.2406E-02	0.5153E+01	0.2844E-01	0.1010E+03	0.2421E-01	0.1052E+03
5.	0.3650E-01	0.1611E+03	0.4247E-01	-0.1718E+03	0.2931E-01	-0.1623E+03
6.	0.1283E-01	0.1486E+03	0.2014E-01	0.1387E+03	0.1773E-01	0.1366E+03
7.	0.2715E-01	0.1591E+03	0.4014E-01	0.1709E+03	0.3380E-01	0.1768E+03
8.	0.7664E-02	-0.1640E+03	0.1838E-01	0.1739E+03	0.1516E-01	0.1747E+03
9.	0.1014E-01	0.1409E+03	0.1988E-01	0.1501E+03	0.1673E-01	0.1559E+03
10.	0.1476E-01	0.1472E+03	0.2543E-01	0.1510E+03	0.1998E-01	0.1538E+03
11.	0.1270E-01	0.1574E+03	0.1803E-01	0.1601E+03	0.1374E-01	0.1612E+03
12.	0.9770E-02	0.1596E+03	0.1306E-01	0.1644E+03	0.9794E-02	0.1625E+03
13.	0.7260E-02	0.1523E+03	0.9466E-02	0.1749E+03	0.5671E-02	0.1698E+03
14.	0.4388E-02	0.1744E+03	0.3854E-02	-0.1369E+03	0.3455E-02	-0.1070E+03
15.	0.2736E-02	-0.1652E+03	0.2749E-02	-0.8477E+02	0.4902E-02	-0.8113E+02
16.	0.3678E-02	0.1476E+03	0.2389E-02	-0.1424E+03	0.3492E-02	-0.9429E+02
17.	0.1683E-02	0.1357E+03	0.3846E-02	-0.7929E+02	0.3816E-02	-0.6054E+02
18.	0.1923E-02	0.1192E+03	0.2278E-02	-0.6932E+02	0.1505E-02	-0.4942E+02
19.	0.5500E-02	0.4956E+02	0.2666E-02	0.8812E+01	0.2863E-02	0.1814E+02
20.	0.2760E-02	-0.4880E+02	0.5008E-02	-0.6506E+02	0.3502E-02	-0.6817E+02
21.	0.6389E-02	0.6710E+01	0.6506E-02	-0.9195E+01	0.4666E-02	0.1533E+02
22.	0.8309E-02	-0.2353E+00	0.6453E-02	0.5827E+01	0.4914E-02	0.6004E+01
23.	0.8277E-02	0.6630E+01	0.9914E-02	-0.5172E+01	0.6200E-02	0.1163E+02
24.	0.6388E-02	-0.1363E+01	0.7439E-02	0.9526E+01	0.4580E-02	0.3221E+02
25.	0.7672E-02	-0.6433E+01	0.9983E-02	0.3783E+01	0.4727E-02	0.9937E+01
26.	0.9053E-02	0.5063E+02	0.1101E-01	0.5086E+02	0.9268E-02	0.6526E+02
27.	0.6784E-02	0.3965E+02	0.9015E-02	0.3807E+02	0.6080E-02	0.5582E+02
28.	0.6530E-02	0.3840E+02	0.1036E-01	0.5121E+02	0.4708E-02	0.5601E+02
29.	0.5325E-02	0.6705E+02	0.7142E-02	0.6524E+02	0.3774E-02	0.6252E+02
30.	0.5893E-02	0.8564E+02	0.7617E-02	0.7603E+02	0.4663E-02	0.6816E+02
31.	0.8281E-02	0.9529E+02	0.9190E-02	0.1111E+03	0.6110E-02	0.1087E+03
32.	0.5810E-02	0.9839E+02	0.7019E-02	0.1130E+03	0.3229E-02	0.1373E+03
33.	0.5134E-02	0.1188E+03	0.8008E-02	0.1417E+03	0.4762E-02	0.1531E+03
34.	0.3793E-02	0.1403E+03	0.6368E-02	0.1508E+03	0.5162E-02	-0.1762E+03
35.	0.4712E-02	0.1194E+03	0.5385E-02	0.1563E+03	0.3325E-02	-0.1624E+03
36.	0.1764E-02	0.1277E+03	0.2919E-02	0.1635E+03	0.1766E-02	-0.1445E+03
37.	0.3445E-02	0.1525E+03	0.4361E-02	0.1650E+03	0.2856E-02	0.1719E+03
38.	0.3916E-02	-0.1732E+03	0.4005E-02	-0.1547E+03	0.3952E-02	-0.1507E+03
39.	0.4944E-03	-0.4400E+02	0.1681E-02	-0.1684E+03	0.1007E-02	-0.1300E+03

ORIGINAL PAGE IS
OF POOR QUALITY

TABLE XXII.- CONTINUED

BOTTOM SURFACE

	RADIUS= Ø.4ØØ CHORD= Ø.25Ø		RADIUS= Ø.4ØØ CHORD= Ø.45Ø		RADIUS= Ø.4ØØ CHORD= Ø.699	
HARM	AMPLITUDE	PHASE	AMPLITUDE	PHASE	AMPLITUDE	PHASE
Ø.	Ø.132ØE+Ø2	Ø.ØØØØE+ØØ	Ø.1333E+Ø2	Ø.ØØØØE+ØØ	Ø.135ØE+Ø2	Ø.ØØØØE+ØØ
1.	Ø.2664E+ØØ	-Ø.1Ø92E+Ø3	Ø.94Ø3E-Ø1	-Ø.145ØE+Ø3	Ø.8187E-Ø1	Ø.1467E+Ø3
2.	Ø.1887E+ØØ	-Ø.1962E+Ø2	Ø.1332E+ØØ	-Ø.2772E+Ø2	Ø.7548E-Ø1	-Ø.3487E+Ø2
3.	Ø.1955E-Ø1	Ø.1388E+Ø3	Ø.2321E-Ø1	-Ø.1552E+Ø3	Ø.2Ø43E-Ø1	-Ø.1593E+Ø3
4.	Ø.1315E-Ø1	Ø.1Ø31E+Ø3	Ø.6474E-Ø2	Ø.1Ø42E+Ø3	Ø.6891E-Ø2	Ø.1664E+Ø3
5.	Ø.2114E-Ø1	-Ø.1577E+Ø3	Ø.1719E-Ø1	-Ø.17Ø1E+Ø3	Ø.1387E-Ø1	-Ø.1715E+Ø3
6.	Ø.9855E-Ø2	Ø.141ØE+Ø3	Ø.1Ø71E-Ø1	Ø.1165E+Ø3	Ø.9585E-Ø2	Ø.1249E+Ø3
7.	Ø.2293E-Ø1	-Ø.1756E+Ø3	Ø.1752E-Ø1	Ø.1739E+Ø3	Ø.1273E-Ø1	Ø.1787E+Ø3
8.	Ø.1143E-Ø1	-Ø.1787E+Ø3	Ø.7585E-Ø2	Ø.1561E+Ø3	Ø.6241E-Ø2	Ø.1652E+Ø3
9.	Ø.12Ø8E-Ø1	Ø.1679E+Ø3	Ø.5747E-Ø2	Ø.1432E+Ø3	Ø.4899E-Ø2	Ø.1643E+Ø3
1Ø.	Ø.13Ø8E-Ø1	Ø.1618E+Ø3	Ø.86Ø5E-Ø2	Ø.1341E+Ø3	Ø.7854E-Ø2	Ø.1467E+Ø3
11.	Ø.839ØE-Ø2	Ø.1655E+Ø3	Ø.4472E-Ø2	Ø.1295E+Ø3	Ø.4736E-Ø2	Ø.1598E+Ø3
12.	Ø.5483E-Ø2	Ø.16Ø7E+Ø3	Ø.2889E-Ø2	Ø.1448E+Ø3	Ø.4844E-Ø2	Ø.1756E+Ø3
13.	Ø.2524E-Ø2	-Ø.162ØE+Ø3	Ø.2424E-Ø2	Ø.1689E+Ø3	Ø.3152E-Ø2	-Ø.1518E+Ø3
14.	Ø.3452E-Ø2	-Ø.7738E+Ø2	Ø.2ØØ8E-Ø2	-Ø.9187E+Ø2	Ø.3476E-Ø2	-Ø.1Ø25E+Ø3
15.	Ø.4569E-Ø2	-Ø.5819E+Ø2	Ø.3343E-Ø2	-Ø.8Ø57E+Ø2	Ø.5611E-Ø2	-Ø.8594E+Ø2
16.	Ø.3133E-Ø2	-Ø.675ØE+Ø2	Ø.2213E-Ø2	-Ø.7Ø87E+Ø2	Ø.4215E-Ø2	-Ø.6811E+Ø2
17.	Ø.431ØE-Ø2	-Ø.4953E+Ø2	Ø.2875E-Ø2	-Ø.4Ø14E+Ø2	Ø.435ØE-Ø2	-Ø.45Ø6E+Ø2
18.	Ø.2137E-Ø2	-Ø.4921E+Ø2	Ø.1333E-Ø2	-Ø.3216E+Ø2	Ø.2532E-Ø2	-Ø.4ØØ9E+Ø2
19.	Ø.2173E-Ø2	Ø.1723E+Ø2	Ø.2Ø91E-Ø2	Ø.1617E+Ø2	Ø.3874E-Ø2	-Ø.1236E+Ø2
2Ø.	Ø.9266E-Ø3	-Ø.1Ø96E+Ø2	Ø.1ØØ7E-Ø2	-Ø.4736E+Ø1	Ø.2894E-Ø2	-Ø.2488E+Ø2
21.	Ø.2194E-Ø2	Ø.55ØØE+Ø2	Ø.145ØE-Ø2	Ø.8571E+Ø2	Ø.2486E-Ø2	Ø.2Ø7ØE+ØØ
22.	Ø.2124E-Ø2	Ø.4629E+Ø2	Ø.1477E-Ø2	Ø.1179E+Ø3	Ø.2247E-Ø2	Ø.15Ø5E+Ø2
23.	Ø.252ØE-Ø2	Ø.3988E+Ø2	Ø.14Ø9E-Ø2	Ø.4863E+Ø2	Ø.3545E-Ø2	-Ø.3743E+Ø1
24.	Ø.1234E-Ø2	Ø.8227E+Ø2	Ø.139ØE-Ø2	-Ø.1799E+Ø3	Ø.1228E-Ø2	-Ø.5Ø14E+Ø2
25.	Ø.594ØE-Ø3	-Ø.1Ø29E+Ø3	Ø.19Ø2E-Ø2	-Ø.126ØE+Ø3	Ø.2768E-Ø2	-Ø.9125E+Ø2
26.	Ø.2484E-Ø2	Ø.5754E+Ø2	Ø.3957E-Ø3	Ø.5225E+Ø2	Ø.2Ø9ØE-Ø2	-Ø.27Ø9E+Ø2
27.	Ø.3Ø15E-Ø2	Ø.1123E+Ø3	Ø.1593E-Ø2	Ø.1286E+Ø3	Ø.3Ø62E-Ø3	-Ø.6311E+Ø2
8.	Ø.2418E-Ø2	Ø.1416E+Ø3	Ø.1525E-Ø2	Ø.1764E+Ø3	Ø.1369E-Ø2	-Ø.3584E+Ø2
29.	Ø.1266E-Ø2	-Ø.1629E+Ø3	Ø.24Ø4E-Ø2	-Ø.12Ø7E+Ø3	Ø.1874E-Ø2	-Ø.6465E+Ø2
3Ø.	Ø.1414E-Ø2	Ø.6545E+Ø2	Ø.8296E-Ø3	-Ø.8922E+Ø2	Ø.2Ø66E-Ø2	-Ø.5182E+Ø2
31.	Ø.1718E-Ø2	Ø.1439E+Ø3	Ø.6989E-Ø3	Ø.5913E+Ø2	Ø.2397E-Ø2	-Ø.1576E+Ø2
32.	Ø.1228E-Ø2	-Ø.1477E+Ø3	Ø.16Ø7E-Ø2	-Ø.81Ø1E+Ø2	Ø.2976E-Ø2	-Ø.4Ø62E+Ø2
33.	Ø.874ØE-Ø3	-Ø.133ØE+Ø3	Ø.284ØE-Ø3	Ø.1Ø61E+Ø3	Ø.2669E-Ø2	-Ø.6732E+Ø1
34.	Ø.2534E-Ø2	-Ø.1577E+Ø3	Ø.1344E-Ø2	Ø.1454E+Ø3	Ø.1571E-Ø2	Ø.4643E+Ø2
35.	Ø.3Ø81E-Ø2	-Ø.1242E+Ø3	Ø.2333E-Ø2	-Ø.1393E+Ø3	Ø.155ØE-Ø2	Ø.1142E+Ø3
36.	Ø.2518E-Ø2	-Ø.65Ø4E+Ø2	Ø.2475E-Ø2	-Ø.8118E+Ø2	Ø.4255E-Ø3	-Ø.7279E+Ø2
37.	Ø.47Ø3E-Ø3	-Ø.1126E+Ø1	Ø.1686E-Ø2	-Ø.6222E+Ø1	Ø.1414E-Ø2	-Ø.7228E+Ø1
38.	Ø.24Ø3E-Ø2	-Ø.156ØE+Ø3	Ø.134ØE-Ø2	-Ø.1653E+Ø3	Ø.6855E-Ø3	Ø.1622E+Ø3
39.	Ø.144ØE-Ø2	-Ø.1115E+Ø3	Ø.2221E-Ø2	-Ø.1195E+Ø3	Ø.127ØE-Ø2	-Ø.1398E+Ø3

TABLE XXII.- CONTINUED

TOP SURFACE

	RADIUS= Ø.4ØØ CHORD= Ø.Ø1Ø		RADIUS= Ø.4ØØ CHORD= Ø.Ø3Ø		RADIUS= Ø.4ØØ CHORD= Ø.Ø8Ø	
HARM	AMPLITUDE	PHASE	AMPLITUDE	PHASE	AMPLITUDE	PHASE
Ø.	Ø.1182E+Ø2	Ø.ØØØØE+ØØ	Ø.12Ø9E+Ø2	Ø.ØØØØE+ØØ	Ø.1241E+Ø2	Ø.ØØØØE+ØØ
1.	Ø.2Ø33E+Ø1	-Ø.46Ø7E+Ø2	Ø.17Ø5E+Ø1	-Ø.6129E+Ø2	Ø.1248E+Ø1	-Ø.6576E+Ø2
2.	Ø.3762E+ØØ	Ø.1324E+Ø3	Ø.2272E+ØØ	Ø.7143E+Ø2	Ø.2Ø73E+ØØ	Ø.5328E+Ø2
3.	Ø.5Ø9ØE-Ø1	Ø.4796E+Ø2	Ø.3767E-Ø1	Ø.8525E+Ø2	Ø.3228E-Ø1	Ø.9482E+Ø2
4.	Ø.1373E+ØØ	-Ø.8613E+Ø2	Ø.831ØE-Ø1	-Ø.8893E+Ø2	Ø.39Ø9E-Ø1	-Ø.8731E+Ø2
5.	Ø.1156E+ØØ	Ø.2983E+Ø2	Ø.6659E-Ø1	Ø.18Ø5E+Ø2	Ø.3568E-Ø1	Ø.1953E+Ø2
6.	Ø.7619E-Ø1	-Ø.7Ø12E+Ø2	Ø.4Ø32E-Ø1	-Ø.6341E+Ø2	Ø.1926E-Ø1	-Ø.5174E+Ø2
7.	Ø.9672E-Ø1	-Ø.1554E+Ø2	Ø.5561E-Ø1	-Ø.2Ø89E+Ø2	Ø.246ØE-Ø1	-Ø.2Ø33E+Ø2
8.	Ø.4Ø75E-Ø1	-Ø.3126E+Ø2	Ø.2677E-Ø1	-Ø.1899E+Ø2	Ø.1238E-Ø1	-Ø.5251E+ØØ
9.	Ø.5Ø59E-Ø1	-Ø.3681E+Ø2	Ø.22ØØE-Ø1	-Ø.335ØE+Ø2	Ø.1316E-Ø1	-Ø.3Ø49E+Ø2

TABLE XXII.- CONTINUED

	RADIUS= 0.400 CHORD= 0.250		TOP SURFACE RADIUS= 0.400 CHORD= 0.450	
HARM	AMPLITUDE	PHASE	AMPLITUDE	PHASE
0.	0.1289E+02	0.0000E+00	0.1323E+02	0.0000E+00
1.	0.6978E+00	-0.7337E+02	0.3113E+00	-0.7705E+02
2.	0.1345E+00	0.4188E+02	0.6282E-01	0.6041E+02
3.	0.2346E-01	0.6489E+02	0.1927E-01	0.4600E+02
4.	0.1086E-01	-0.1061E+03	0.1400E-02	-0.1183E+03
5.	0.1813E-01	0.3051E+01	0.1162E-01	-0.5141E+00
6.	0.8715E-02	-0.5057E+02	0.4890E-02	-0.5423E+02
7.	0.1288E-01	-0.3431E+02	0.6654E-02	-0.4223E+02
8.	0.4141E-02	-0.4070E+02	0.1537E-02	-0.3619E+02
9.	0.3914E-02	-0.1343E+02	0.1841E-02	-0.2846E+02
10.			0.5072E-02	-0.1370E+02
11.			0.3850E-02	-0.1469E+02
12.			0.2125E-02	-0.4841E+02
13.			0.1146E-02	-0.8716E+01
14.			0.3366E-02	0.6461E+02
15.			0.2922E-02	0.4494E+02
16.			0.1338E-02	0.9725E+01
17.			0.1362E-02	-0.1094E+03
18.			0.1609E-02	0.1514E+03
19.			0.1446E-02	0.1196E+03
20.			0.8604E-03	0.5243E+02
21.			0.1740E-02	0.4233E+02
22.			0.1480E-02	-0.1236E+03
23.			0.1935E-02	-0.1419E+03
24.			0.1099E-02	0.1626E+03
25.			0.6895E-03	0.6792E+02
26.			0.9759E-03	-0.2488E+01
27.			0.8035E-03	-0.8192E+02
28.			0.1272E-02	0.1778E+03
29.			0.1377E-02	-0.1422E+03
30.			0.9460E-03	-0.1643E+02
31.			0.1133E-02	0.9088E+02
32.			0.6962E-03	-0.1422E+03
33.			0.1892E-03	0.1363E+03
34.			0.1114E-02	0.1545E+03
35.			0.4717E-03	-0.1161E+03
36.			0.7500E-03	0.4978E+02
37.			0.1142E-02	0.8534E-01
38.			0.5186E-03	-0.1159E+03
39.			0.6206E-03	-0.5672E+02

TABLE XXII.- CONTINUED

BOTTOM SURFACE

HARM	RADIUS= 0.600 CHORD= 0.010 AMPLITUDE	PHASE	RADIUS= 0.600 CHORD= 0.080 AMPLITUDE	PHASE	RADIUS= 0.600 CHORD= 0.150 AMPLITUDE	PHASE
0.	0.14[illegible]2E+02	0.0000E+00	0.1329E+02	0.0000E+00	0.1331E+02	0.0000E+00
1.	0.1459E+01	0.9554E+02	0.5816E+00	-0.8724E+02	0.5827E+00	-0.8871E+02
2.	0.4229E-01	-0.1192E+03	0.2832E+00	0.1367E+02	0.2452E+00	0.1046E+02
3.	0.7489E-01	-0.1395E+03	0.1172E+00	-0.9638E+02	0.7691E-01	-0.1015E+03
4.	0.8999E-01	0.1964E+02	0.5380E-01	0.1825E+02	0.3328E-01	0.1718E+02
5.	0.9851E-02	0.1694E+03	0.2310E-01	-0.1486E+03	0.1702E-01	-0.1422E+03
6.	0.5433E-02	-0.5495E+02	0.1464E-01	-0.1058E+03	0.1042E-01	-0.1277E+03
7.	0.1112E-01	-0.7897E+02	0.1736E-01	-0.8543E+02	0.1614E-01	-0.8744E+02
8.	0.1053E-01	-0.5646E+01	0.4984E-02	-0.4558E+01	0.4200E-02	-0.2793E+02
9.	0.1348E-02	-0.6092E+01	0.6014E-02	-0.1419E+03	0.6383E-02	-0.1332E+03
10.	0.3370E-02	0.1120E+03	0.4697E-02	-0.1326E+03	0.4279E-02	-0.1642E+03
11.	0.3139E-02	0.8164E+02	0.9425E-03	-0.1589E+03	0.7508E-04	0.4533E+02
12.	0.2873E-02	0.1389E+03	0.4809E-02	0.1734E+03	0.4059E-02	0.1549E+03
13.	0.1118E-02	0.1732E+03	0.2773E-02	-0.1455E+03	0.1627E-02	-0.1425E+03
14.	0.1387E-02	0.6381E+01	0.3531E-02	-0.9790E+02	0.2343E-02	-0.6867E+02
15.	0.2921E-02	-0.5208E+02	0.3488E-02	-0.7334E+02	0.3919E-02	-0.5381E+02
16.	0.1708E-02	-0.5472E+01	0.2620E-02	-0.5029E+02	0.3335E-02	-0.3349E+02
17.	0.2025E-02	0.4441E+02	0.7421E-03	0.8827E+01	0.1640E-02	-0.4463E+00
18.	0.2285E-02	0.1180E+03	0.1277E-02	-0.1759E+03	0.7994E-03	0.1394E+03
19.	0.2334E-02	0.6670E+02	0.1371E-02	0.3455E+02	0.1879E-02	0.3613E+02
20.	0.7343E-03	0.1683E+03	0.7941E-03	-0.6299E+01	0.1247E-02	-0.3881E+01
21.	0.4375E-02	0.1026E+03	0.4137E-02	0.8663E+02	0.4905E-02	0.7973E+02
22.	0.3456E-02	0.1003E+03	0.3397E-02	0.1123E+03	0.2992E-02	0.8290E+02
23.	0.1387E-02	0.7334E+02	0.5962E-03	-0.2601E+02	0.1606E-02	0.2561E+02
24.	0.4138E-03	-0.1409E+03	0.1921E-02	-0.6493E+02	0.9787E-03	-0.9780E+02
25.	0.2112E-02	-0.3505E+02	0.1451E-02	-0.3335E+02	0.1306E-02	-0.4150E+02
26.	0.2866E-02	0.1135E+03	0.2688E-02	0.1380E+03	0.2789E-02	0.1214E+03
27.	0.8456E-03	0.1233E+03	0.1016E-02	0.1827E+02	0.4692E-03	-0.5648E+02
28.	0.1637E-02	-0.9054E+02	0.7226E-03	-0.2092E+02	0.9292E-04	0.1006E+03
29.	0.1040E-02	-0.3152E+02	0.8368E-03	0.1283E+03	0.1112E-02	0.1612E+03
30.	0.2216E-02	-0.5138E+02	0.1459E-02	-0.7175E+02	0.1286E-02	-0.1660E+03
31.	0.1357E-02	0.1240E+03	0.8664E-03	0.5175E+00	0.2100E-02	0.6262E+02
32.	0.2726E-02	-0.6195E+02	0.3143E-02	-0.6205E+02	0.4077E-02	-0.3917E+02
33.	0.6772E-03	0.1557E+03	0.5804E-03	0.5569E+02	0.1377E-02	0.1059E+03
34.	0.1561E-02	-0.1203E+03	0.1265E-02	-0.12[illegible]7E+03	0.1673E-02	-0.9780E+02
35.	0.2668E-02	-0.1453E+03	0.1493E-02	-0.1503E+03	0.5026E-03	-0.1644E+03
36.	0.2189E-02	-0.2409E+02	0.3108E-02	-0.1779E+02	0.2412E-02	-0.5763E+02
37.	0.2534E-02	0.4312E+02	0.1380E-02	0.3154E+02	0.9204E-03	0.2413E+02
38.	0.1284E-02	-0.9927E+02	0.1398E-02	-0.1142E+03	0.2636E-02	-0.9419E+02
39.	0.9071E-03	-0.7022E+01	0.2582E-03	0.5202E+00	0.1513E-02	0.5196E+01

ORIGINAL PAGE IS OF POOR QUALITY

TABLE XXII.- CONTINUED

BOTTOM SURFACE

HARM	RADIUS= 0.600 CHORD= 0.250 AMPLITUDE	PHASE	RADIUS= 0.600 CHORD= 0.450 AMPLITUDE	PHASE	RADIUS= 0.600 CHORD= 0.550 AMPLITUDE	PHASE
0.	0.1327E+02	0.0000E+00	0.1331E+02	0.0000E+00	0.1344E+02	0.0000E+00
1.	0.5984E+00	-0.9025E+02	0.2623E+00	-0.1016E+03	0.1734E+00	-0.1119E+03
2.	0.2375E+00	0.7479E+01	0.1340E+00	-0.3603E+00	0.1065E+00	-0.3518E+01
3.	0.6205E-01	-0.1091E+03	0.4026E-01	-0.1186E+03	0.3448E-01	-0.1243E+03
4.	0.2096E-01	0.2464E+02	0.8179E-02	0.3680E+02	0.6594E-02	0.5270E+02
5.	0.1584E-01	-0.1361E+03	0.1146E-01	-0.1158E+03	0.1022E-01	-0.1167E+03
6.	0.6011E-02	-0.1278E+03	0.4836E-02	0.1576E+03	0.5543E-02	0.1299E+03
7.	0.1256E-01	-0.9279E+02	0.1045E-01	-0.1090E+03	0.9854E-02	-0.1095E+03
8.	0.2819E-02	-0.9023E+01	0.3366E-02	-0.3276E+02	0.3378E-02	-0.3921E+02
9.	0.4953E-02	-0.1331E+03	0.4234E-02	-0.9434E+02	0.3535E-02	-0.8136E+02
10.	0.2951E-02	-0.1515E+03	0.2536E-02	-0.1677E+03	0.2705E-02	-0.1744E+03
11.	0.3756E-03	-0.1086E+03	0.6408E-03	0.5404E+02	0.5115E-03	0.1284E+03
12.	0.2597E-02	0.1541E+03	0.2355E-02	0.1657E+03	0.2967E-02	0.1712E+03
13.	0.1335E-02	-0.1215E+03	0.8708E-03	0.1888E+01	0.2729E-03	-0.1895E+01
14.	0.1794E-02	-0.7669E+02	0.1339E-02	-0.4369E+02	0.7821E-03	-0.1240E+03
15.	0.3164E-02	-0.4847E+02	0.4375E-02	-0.7315E+02	0.3416E-02	-0.8267E+02
16.	0.2633E-02	-0.2663E+02	0.1332E-02	-0.3218E+01	0.7799E-03	-0.3116E+02
17.	0.1034E-02	-0.1139E+02	0.1109E-02	-0.2076E+01	0.1006E-02	0.1252E+02
18.	0.2511E-03	0.1603E+03	0.1991E-02	0.1426E+03	0.2291E-02	0.1554E+03
19.	0.1702E-02	0.2949E+02	0.2478E-02	0.6640E+02	0.2217E-02	0.7479E+02
20.	0.1479E-02	-0.2085E+02	0.1504E-02	-0.5853E+02	0.1093E-02	-0.6005E+02
21.	0.3779E-02	0.6928E+02	0.4433E-02	0.5687E+02	0.3820E-02	0.6483E+02
22.	0.3293E-02	0.8360E+02	0.2246E-02	0.6053E+02	0.2596E-02	0.4726E+02
23.	0.7890E-03	0.4217E+02	0.2459E-02	0.6658E+02	0.3265E-02	0.3422E+02
24.	0.1018E-02	-0.9863E+02	0.9298E-03	0.1500E+03	0.1637E-02	0.1476E+03
25.	0.4323E-03	-0.9822E+02	0.2455E-02	-0.9951E+02	0.2028E-02	-0.1044E+03
26.	0.2227E-02	0.1486E+03	0.2300E-02	0.1201E+03	0.2674E-02	0.1287E+03
27.	0.1205E-02	-0.5148E+02	0.1494E-02	0.3093E+02	0.1492E-02	0.1742E+02
28.	0.1350E-02	0.6773E+02	0.2332E-02	0.1899E+02	0.1451E-02	-0.2452E+02
29.	0.1817E-02	0.1521E+03	0.3954E-03	0.9867E+02	0.1032E-02	0.6040E+02
30.	0.2500E-02	-0.1676E+03	0.8733E-03	0.1136E+03	0.7975E-03	0.1470E+03
31.	0.1654E-02	0.7316E+02	0.3173E-02	0.1138E+03	0.2613E-02	0.1095E+03
32.	0.2341E-02	-0.5409E+02	0.1274E-02	-0.1030E+03	0.9935E-03	-0.1084E+03
33.	0.1145E-03	-0.1486E+03	0.9386E-03	0.1134E+02	0.6642E-03	-0.4184E+02
34.	0.9581E-03	-0.1085E+03	0.2168E-02	-0.6619E+02	0.7862E-03	-0.1758E+03
35.	0.1017E-02	0.8845E+02	0.7476E-03	0.7916E+02	0.7184E-03	0.3504E+00
36.	0.8806E-03	-0.1197E+03	0.2516E-02	-0.2444E+02	0.1357E-02	-0.8900E+01
37.	0.1135E-02	-0.1069E+01	0.7544E-03	-0.2757E+02	0.2241E-02	0.3581E+02
38.	0.2267E-02	-0.1190E+03	0.2101E-02	-0.1671E+03	0.8004E-03	-0.1262E+03
39.	0.1818E-03	0.7260E+01	0.1799E-02	0.2157E+02	0.1645E-02	-0.2261E+02

TABLE XXII.- CONTINUED

			BOTTOM SURFACE	
	RADIUS= 0.600		RADIUS= 0.600	
	CHORD= 0.699		CHORD= 0.919	
HARM	AMPLITUDE	PHASE	AMPLITUDE	PHASE
0.	0.1369E+02	0.0000E+00	0.1353E+02	0.0000E+00
1.	0.9906E-01	-0.1310E+03	0.1265E+00	0.1318E+03
2.	0.6250E-01	-0.1261E+02	0.2563E-01	-0.5387E+02
3.	0.2278E-01	-0.1229E+03	0.1474E-01	-0.1189E+03
4.	0.5254E-02	0.6724E+02	0.4625E-02	0.1301E+03
5.	0.7260E-02	-0.1136E+03	0.5150E-02	-0.8141E+02
6.	0.4823E-02	0.1219E+03	0.6664E-02	0.1324E+03
7.	0.6395E-02	-0.1249E+03	0.7638E-02	-0.1254E+03
8.	0.1692E-02	-0.3750E+02	0.3219E-02	-0.4842E+02
9.	0.2678E-02	-0.6973E+02	0.3958E-02	-0.6288E+02
10.	0.1294E-02	0.1716E+03	0.1751E-02	0.1763E+03
11.	0.6522E-03	-0.1635E+03	0.1749E-02	0.1081E+03
12.	0.1797E-02	0.1522E+03	0.2579E-02	0.1754E+03
13.	0.6574E-03	0.6834E+02	0.2066E-02	0.2187E+02
14.	0.7136E-03	-0.1601E+03	0.5956E-03	-0.9079E+02
15.	0.3373E-02	-0.7888E+02	0.3946E-02	-0.8364E+02
16.	0.1265E-02	-0.7178E+02	0.2166E-03	-0.7851E+02
17.	0.1517E-02	-0.2135E+02	0.1182E-02	0.3124E+02
18.	0.1066E-02	0.1215E+03	0.2242E-02	0.1433E+03
19.	0.2035E-02	0.9910E+02	0.3384E-02	0.5842E+02
20.	0.1802E-02	-0.1096E+03	0.1916E-02	-0.1230E+03
21.	0.2536E-02	0.5004E+02	0.3698E-02	0.6262E+02
22.	0.2064E-02	0.4750E+02	0.3278E-02	0.1822E+02
23.	0.2283E-02	0.3251E+02	0.2860E-02	0.4903E+02
24.	0.1109E-02	0.1167E+03	0.1842E-02	0.1107E+03
25.	0.1217E-02	-0.1324E+03	0.2945E-02	-0.7270E+02
26.	0.1404E-02	0.1060E+03	0.3844E-02	0.1176E+03
27.	0.6085E-03	-0.4209E+02	0.9826E-03	0.6467E+02
28.	0.1833E-02	-0.1838E+02	0.2377E-02	-0.3508E+02
29.	0.1137E-02	-0.2681E+00	0.2851E-03	0.3551E+02
30.	0.8804E-04	0.8718E+01	0.7712E-03	-0.1048E+03
31.	0.1358E-02	0.1235E+03	0.2081E-02	0.9006E+02
32.	0.6735E-03	-0.1235E+03	0.3867E-03	0.2783E+02
33.	0.1195E-03	0.1208E+03	0.1113E-02	0.4656E+02
34.	0.1126E-02	-0.1367E+03	0.1904E-02	-0.1728E+03
35.	0.3841E-03	-0.1481E+02	0.2902E-03	0.1317E+03
36.	0.1328E-02	-0.4557E+02	0.1161E-02	-0.2085E+01
37.	0.1045E-02	0.1421E+02	0.3561E-03	-0.3679E+02
38.	0.1626E-02	-0.1189E+03	0.1490E-02	0.1708E+03
39.	0.1988E-02	0.1620E+02	0.4829E-03	0.1223E+03

ORIGINAL PAGE IS
OF POOR QUALITY

TABLE XXII.- CONTINUED

TOP SURFACE

HARM	RADIUS= 0.600 CHORD= 0.010 AMPLITUDE	PHASE	RADIUS= 0.600 CHORD= 0.030 AMPLITUDE	PHASE	RADIUS= 0.600 CHORD= 0.080 AMPLITUDE	PHASE
0.	0.1108E+02	0.0000E+00	0.1096E+02	0.0000E+00	0.1136E+02	0.0000E+00
1.	0.4102E+00	-0.8563E+01	0.1490E+01	-0.7323E+02	0.1515E+01	-0.7617E+02
2.	0.4084E+00	-0.1437E+03	0.1863E+00	-0.1933E+02	0.2596E+00	0.3185E+01
3.	0.4338E+00	0.1019E+03	0.4059E+00	0.9810E+02	0.2575E+00	0.9418E+02
4.	0.7275E-01	0.1627E+03	0.9436E-01	-0.1790E+03	0.7428E-01	-0.1797E+03
5.	0.5542E-01	0.5498E+02	0.4416E-01	0.2196E+02	0.1941E-01	-0.5382E+01
6.	0.6160E-01	0.8654E+02	0.6318E-01	0.5512E+02	0.3138E-01	0.4483E+02
7.	0.5207E-01	0.9923E+02	0.5122E-01	0.1105E+03	0.2547E-01	0.9440E+02
8.	0.1272E-01	0.7844E+02	0.1774E-02	-0.1487E+02	0.1663E-02	-0.7621E+02
9.	0.1190E-01	0.1778E+02	0.2025E-01	-0.1833E+02	0.6754E-02	-0.7751E+02
10.	0.9005E-02	-0.4375E+01	0.1861E-01	-0.1103E+02	0.1028E-01	-0.5191E+02
11.	0.1874E-01	0.7317E+02	0.1371E-01	0.7678E+02	0.1133E-01	0.6134E+02
12.	0.1150E-01	0.1998E+02	0.2388E-02	-0.2320E+02	0.7007E-02	-0.2216E+02
13.	0.1877E-01	0.3643E+02	0.1551E-01	0.6969E+01	0.6319E-02	-0.9204E+01
14.	0.1020E-01	0.4178E+01	0.8294E-02	0.2652E+01	0.5651E-02	-0.3466E+02
15.	0.8837E-02	0.5855E+02	0.4465E-02	0.6922E+02	0.6128E-02	0.2108E+02
16.	0.1828E-02	-0.1411E+03	0.9502E-02	-0.1710E+03	0.3550E-02	0.1110E+03
17.	0.3524E-02	0.7633E+02	0.8934E-02	-0.9641E+02	0.2946E-02	0.1163E+03
18.	0.2466E-02	-0.5668E+02	0.8002E-02	-0.1218E+03	0.3225E-02	-0.1459E+03
19.	0.4571E-02	0.5812E+02	0.1086E-01	0.5523E+02	0.5764E-02	0.6126E+02
20.	0.1918E-02	-0.1662E+03	0.5818E-02	-0.1309E+03	0.4273E-02	-0.1392E+03
21.	0.1566E-02	-0.7142E+02	0.7324E-02	0.1445E+03	0.1813E-02	0.1775E+03
22.	0.6143E-02	-0.1121E+02	0.3260E-02	0.2187E+02	0.7663E-02	-0.8095E+02
23.	0.3614E-02	0.1288E+03	0.1099E-01	-0.1195E+03	0.1195E-02	0.9440E+02
24.	0.1451E-02	0.6103E+02	0.8315E-02	0.5424E+02	0.5680E-02	0.7643E+01
25.	0.2585E-02	-0.1132E+03	0.2593E-02	-0.1496E+03	0.1564E-02	-0.1120E+03
26.	0.2000E-02	-0.1869E+02	0.1505E-01	0.1595E+03	0.2873E-02	0.1110E+02
27.	0.4694E-02	0.4877E+02	0.3940E-02	-0.9006E+02	0.3157E-02	0.6223E+02
28.	0.2305E-02	0.1793E+03	0.1858E-02	-0.1365E+03	0.2562E-02	0.1623E+03
29.	0.8519E-02	-0.7345E+02	0.1419E-01	-0.3535E+02	0.6808E-02	-0.1126E+03
30.	0.1019E-01	0.4969E+02	0.1400E-01	0.6537E+02	0.3651E-02	0.1290E+03
31.	0.4757E-02	0.9525E+02	0.8330E-02	0.4076E+02	0.2159E-02	-0.8668E+01
32.	0.4444E-02	-0.1712E+03	0.1236E-01	0.1425E+03	0.6072E-02	-0.1215E+03
33.	0.3536E-02	-0.6063E+02	0.3408E-02	-0.5243E+02	0.2435E-02	-0.1098E+03
34.	0.2278E-02	0.1595E+03	0.1198E-01	-0.1750E+03	0.2710E-02	-0.1132E+03
35.	0.6451E-02	-0.8067E+02	0.1728E-02	0.5460E+02	0.5823E-02	-0.1260E+03
36.	0.2774E-02	-0.1612E+03	0.5050E-02	-0.1727E+03	0.1305E-01	-0.1370E+03
37.	0.1866E-02	-0.5265E+02	0.5264E-02	-0.6201E+02	0.7708E-02	-0.5643E+02
38.	0.2695E-02	-0.1770E+03	0.7269E-02	-0.1496E+03	0.5771E-02	-0.5657E+02
39.	0.1210E-02	-0.1120E+03	0.6529E-02	0.1806E+01	0.8159E-02	0.9351E+02

TABLE XXII.- CONTINUED

TOP SURFACE

HARM	RADIUS= 0.600 CHORD= 0.150 AMPLITUDE	PHASE	RADIUS= 0.600 CHORD= 0.250 AMPLITUDE	PHASE	RADIUS= 0.600 CHORD= 0.350 AMPLITUDE	PHASE
0.	0.1182E+02	0.0000E+00	0.1230E+02	0.0000E+00	0.1252E+02	0.0000E+00
1.	0.1335E+01	-0.7755E+02	0.9545E+00	-0.7841E+02	0.7031E+00	-0.7927E+02
2.	0.2336E+00	0.7070E+01	0.1565E+00	0.3944E+01	0.9028E-01	0.6028E+01
3.	0.1698E+00	0.8897E+02	0.9898E-01	0.7987E+02	0.7387E-01	0.6586E+02
4.	0.4721E-01	0.1713E+03	0.2877E-01	0.1625E+03	0.1661E-01	0.1570E+03
5.	0.9182E-02	0.1811E+02	0.5232E-02	0.2397E+01	0.3470E-02	-0.5733E+01
6.	0.1717E-01	0.4460E+02	0.9794E-02	0.3560E+02	0.2672E-02	0.3509E+02
7.	0.1544E-01	0.7991E+02	0.6340E-02	0.8765E+02	0.5265E-02	0.7284E+02
8.	0.2513E-02	-0.1804E+02	0.2483E-02	0.9109E+02	0.3289E-03	-0.1511E+03
9.	0.5292E-02	-0.6003E+02	0.4164E-02	-0.8415E+02	0.2925E-02	-0.4358E+02
10.	0.6926E-02	-0.5290E+02	0.6613E-02	-0.4428E+02	0.6555E-02	-0.6337E+02
11.	0.7259E-02	0.1915E+02	0.5140E-02	0.3771E+02	0.2822E-02	0.1653E+02
12.	0.4008E-02	0.1614E+02	0.1479E-02	-0.1326E+01	0.3839E-03	-0.1089E+03
13.	0.3153E-02	-0.2450E+02	0.4185E-02	0.3575E+00	0.2716E-02	-0.3369E+02
14.	0.3313E-02	-0.2047E+02	0.4784E-02	-0.6274E+01	0.2683E-02	-0.6480E+01
15.	0.1846E-02	0.5545E+02	0.7089E-03	0.1186E+03	0.1914E-02	0.5175E+02
16.	0.3188E-02	0.1763E+03	0.3266E-02	0.1063E+03	0.2740E-02	0.9885E+02
17.	0.2698E-02	0.2311E+02	0.2396E-02	-0.1724E+03	0.1538E-02	-0.1616E+03
18.	0.8891E-03	-0.8472E+02	0.1676E-02	-0.1524E+03	0.4603E-02	-0.1470E+03
19.	0.2221E-02	-0.2069E+02	0.3193E-02	0.6298E+02	0.1115E-02	0.6214E+02
20.	0.1540E-02	-0.1026E+03	0.5883E-03	0.7785E+02	0.2916E-02	-0.1217E+03
21.	0.5899E-03	0.2957E+02	0.1965E-02	0.5028E+01	0.9686E-03	0.3811E+02
22.	0.4999E-03	0.5960E+02	0.9244E-03	0.1425E+02	0.9398E-03	0.2998E+02
23.	0.2251E-02	-0.1165E+03	0.3302E-02	0.9603E+02	0.3570E-02	0.1729E+03
24.	0.1157E-02	0.6062E+02	0.1467E-02	-0.1009E+03	0.2124E-02	0.2001E+01
25.	0.4012E-02	0.3203E+02	0.2480E-02	-0.1238E+03	0.4871E-02	-0.9581E+02
26.	0.1977E-02	-0.3265E+01	0.9591E-03	0.2182E+02	0.2552E-02	-0.1662E+03
27.	0.4389E-02	-0.5759E+02	0.7616E-03	0.1513E+03	0.2775E-02	-0.1516E+01
28.	0.3700E-02	0.4337E+02	0.4611E-02	-0.2826E+02	0.2967E-03	-0.1134E+03
29.	0.1805E-02	0.9376E+02	0.1037E-02	-0.3624E+01	0.1249E-02	0.1388E+03
30.	0.1247E-02	-0.1232E+03	0.1300E-02	0.4651E+02	0.1209E-02	-0.1529E+03
31.	0.5635E-02	0.2433E+01	0.3328E-02	-0.2919E+02	0.1945E-02	-0.4821E+00
32.	0.4972E-02	0.9876E+02	0.2235E-02	-0.2129E+02	0.4120E-03	0.2996E+02
33.	0.1990E-02	0.1447E+03	0.2921E-02	-0.4445E+02	0.3005E-02	-0.1292E+03
34.	0.2689E-02	-0.2687E+02	0.2009E-03	-0.1131E+03	0.7225E-03	-0.7078E+02
35.	0.2605E-02	-0.1375E+03	0.1301E-02	0.9467E+01	0.1626E-02	0.1679E+03
36.	0.3763E-02	0.1283E+03	0.4094E-02	-0.9935E+02	0.2857E-02	-0.1744E+03
37.	0.3287E-02	-0.1289E+03	0.1341E-02	0.1285E+03	0.2219E-02	-0.8392E+02
38.	0.1132E-02	-0.4310E+02	0.5252E-02	-0.2823E+02	0.2685E-02	0.1651E+03
39.	0.2271E-02	0.1092E+03	0.1338E-02	-0.1414E+03	0.2410E-02	0.8193E+01

TABLE XXII.- CONTINUED

	TOP SURFACE					
	RADIUS= 0.600		RADIUS= 0.600		RADIUS= 0.600	
	CHORD= 0.450		CHORD= 0.550		CHORD= 0.699	
HARM	AMPLITUDE	PHASE	AMPLITUDE	PHASE	AMPLITUDE	PHASE
0.	0.1286E+02	0.0000E+00	0.1305E+02	0.0000E+00	0.1323E+02	0.0000E+00
1.	0.4316E+00	-0.7917E+02	0.3015E+00	-0.7809E+02	0.1465E+00	-0.7997E+02
2.	0.3207E-01	0.1512E+02	0.2679E-01	0.7823E+01	0.1288E-01	0.1671E+03
3.	0.5936E-01	0.5603E+02	0.4221E-01	0.3838E+02	0.2865E-01	0.3149E+02
4.	0.1231E-01	0.1341E+03	0.1526E-01	0.1209E+03	0.8359E-02	0.1167E+03
5.	0.8207E-02	0.4631E+02	0.2263E-02	-0.2606E+02	0.4562E-02	0.2905E+02
6.	0.7680E-03	0.4573E+01	0.4108E-02	0.4399E+02	0.1763E-02	-0.4012E+02
7.	0.4164E-02	0.3365E+02	0.4652E-02	-0.1073E+03	0.1056E-02	-0.3934E+02
8.	0.3005E-02	-0.6332E+02	0.2717E-02	0.2323E+02	0.1706E-02	-0.4716E+02
9.	0.3500E-02	-0.7424E+02	0.6814E-02	-0.1278E+03	0.2280E-02	-0.8921E+02
10.	0.3418E-02	-0.5431E+02	0.4046E-02	-0.6821E+02	0.3733E-02	-0.7762E+02
11.	0.2934E-02	-0.6035E+02	0.1660E-02	-0.4974E+02	0.2980E-02	-0.9575E+01
12.	0.1878E-02	0.1098E+03	0.4766E-02	0.8909E+02	0.3289E-03	-0.1706E+03
13.	0.2524E-02	-0.6742E+02	0.2564E-02	-0.4961E+02	0.5794E-03	-0.6273E+02
14.	0.3058E-02	0.7564E+01	0.3667E-02	0.2681E+02	0.2126E-02	-0.2702E+02
15.	0.3464E-02	0.1202E+03	0.2625E-02	0.8304E+02	0.1280E-02	0.1973E+02
16.	0.2149E-02	0.1051E+03	0.2559E-02	0.6686E+02	0.1380E-03	0.1280E+03
17.	0.1959E-02	0.1005E+03	0.2301E-02	-0.9910E+02	0.7345E-03	-0.1473E+03
18.	0.5141E-02	-0.1760E+03	0.1809E-02	-0.5339E+02	0.1709E-02	0.1718E+03
19.	0.1065E-02	-0.3426E+02	0.1750E-02	-0.1716E+03	0.1118E-02	0.1147E+03
20.	0.1246E-02	-0.1721E+03	0.3572E-02	-0.1082E+03	0.1413E-02	-0.9605E+02
21.	0.1825E-02	0.8354E+02	0.2305E-02	0.6468E+02	0.1469E-02	0.1191E+03
22.	0.9796E-03	0.7425E+02	0.5590E-02	-0.2242E+02	0.2494E-02	-0.2304E+02
23.	0.6078E-02	0.1141E+03	0.3890E-02	0.1473E+03	0.2319E-02	0.8714E+02
24.	0.1853E-02	0.7357E+02	0.5028E-02	0.2970E+02	0.2002E-02	0.6042E+02
25.	0.2909E-02	-0.1750E+03	0.4232E-02	-0.8639E+02	0.1944E-02	-0.6273E+02
26.	0.4362E-02	-0.1465E+02	0.3941E-03	-0.8611E+02	0.3016E-02	0.1127E+03
27.	0.2690E-02	-0.4415E+01	0.5297E-02	-0.1323E+03	0.1418E-02	-0.1726E+03
28.	0.2838E-02	0.3804E+02	0.3364E-02	-0.9063E+02	0.2121E-02	-0.6239E+02
29.	0.1908E-02	0.3237E+02	0.1626E-02	-0.9671E+02	0.1967E-02	0.4912E+02
30.	0.1603E-02	0.9867E+02	0.4703E-03	0.1432E+03	0.3160E-02	-0.1370E+03
31.	0.3265E-02	0.7979E+02	0.4432E-02	0.7624E+02	0.1393E-02	0.2025E+02
32.	0.9220E-03	0.6639E+02	0.5940E-02	-0.9224E+02	0.1527E-02	-0.1371E+02
33.	0.2740E-02	-0.1054E+03	0.2512E-02	0.1603E+03	0.3536E-02	-0.1159E+03
34.	0.7312E-02	0.2358E+02	0.3929E-02	0.8550E+01	0.4733E-02	-0.4248E+02
35.	0.7507E-03	-0.1037E+02	0.5517E-02	-0.1241E+03	0.1741E-02	0.3545E+02
36.	0.4581E-02	-0.1796E+03	0.5183E-02	0.1388E+03	0.9201E-03	-0.1147E+03
37.	0.1913E-02	-0.6794E+02	0.7961E-02	0.1677E+03	0.3598E-02	-0.6015E+02
38.	0.1439E-02	-0.1213E+03	0.1489E-02	-0.1369E+03	0.3073E-02	0.5173E+02
39.	0.1659E-02	0.8254E+02	0.2368E-02	0.1572E+03	0.1620E-02	0.1211E+03

TABLE XXII.- CONTINUED

TOP SURFACE

RADIUS= 0.600

CHORD= 0.919

HARM	AMPLITUDE	PHASE
0.	0.1348E+02	0.0000E+00
1.	0.5437E-01	0.1138E+03
2.	0.2106E-01	-0.1708E+03
3.	0.1483E-01	0.6061E+01
4.	0.5705E-02	0.1041E+03
5.	0.2821E-02	0.5025E+02
6.	0.8788E-03	0.7074E+02
7.	0.4687E-03	-0.1431E+03
8.	0.5632E-03	0.1706E+03
9.	0.8684E-03	-0.1131E+03
10.	0.1283E-02	-0.1339E+03
11.	0.1342E-03	-0.7677E+02
12.	0.1960E-02	0.8461E+02
13.	0.4317E-03	-0.1958E+02
14.	0.3756E-03	-0.8362E+02
15.	0.1825E-03	-0.1704E+02
16.	0.1478E-03	0.3909E+02
17.	0.1898E-02	-0.6266E+02
18.	0.1052E-02	-0.1571E+03
19.	0.1070E-02	-0.4062E+02
20.	0.7927E-03	-0.8011E+02
21.	0.1102E-02	0.6053E+02
22.	0.1199E-02	-0.2444E+02
23.	0.4293E-03	-0.2699E+02
24.	0.2690E-03	0.8565E+02
25.	0.3116E-03	0.8857E+02
26.	0.1284E-02	-0.1268E+03
27.	0.1336E-02	-0.1077E+03
28.	0.8700E-03	-0.1005E+03
29.	0.1291E-02	-0.1360E+02
30.	0.1231E-02	-0.3704E-01
31.	0.5843E-03	0.8962E+02
32.	0.3626E-03	-0.2688E+02
33.	0.1556E-02	0.1155E+03
34.	0.2056E-02	-0.1416E+03
35.	0.1710E-02	-0.8690E+02
36.	0.1348E-02	0.1170E+02
37.	0.5227E-03	0.1120E+03
38.	0.4954E-03	-0.7719E+02
39.	0.4755E-03	0.6098E+02

TABLE XXII.- CONTINUED

	BOTTOM SURFACE					
	RADIUS= 0.750 CHORD= 0.030		RADIUS= 0.750 CHORD= 0.080		RADIUS= 0.750 CHORD= 0.150	
HARM	AMPLITUDE	PHASE	AMPLITUDE	PHASE	AMPLITUDE	PHASE
0.	0.1410E+02	0.0000E+00	0.1314E+02	0.0000E+00	0.1282E+02	0.0000E+00
1.	0.5534E+00	-0.4425E+02	0.1199E+01	-0.7117E+02	0.1289E+01	-0.7709E+02
2.	0.4089E+00	0.4965E+02	0.4526E+00	0.3457E+02	0.4210E+00	0.2646E+02
3.	0.2610E+00	-0.9796E+02	0.1830E+00	-0.1061E+03	0.1436E+00	-0.1129E+03
4.	0.1209E+00	-0.8503E+01	0.8290E-01	-0.2838E+02	0.6425E-01	-0.3463E+02
5.	0.3064E-01	-0.5109E+01	0.2989E-01	-0.1377E+02	0.2769E-01	-0.5164E+01
6.	0.6401E-02	-0.5803E+02	0.1822E-01	0.1240E+03	0.7135E-02	0.1296E+03
7.	0.1887E-01	-0.5151E+02	0.2655E-01	-0.8574E+02	0.2170E-01	-0.6459E+02
8.	0.1422E-01	-0.2326E+02	0.2287E-01	-0.3035E+02	0.1828E-01	-0.1450E+02
9.	0.1359E-01	-0.1663E+02	0.1683E-01	-0.4324E+02	0.7135E-02	-0.3629E+00
10.	0.6399E-02	0.1004E+03	0.1561E-01	0.1255E+03	0.7384E-02	0.1266E+03
11.	0.2698E-02	-0.1645E+03	0.5528E-02	0.1439E+03	0.1569E-02	-0.1422E+03
12.	0.3091E-02	-0.1034E+03	0.1603E-01	0.1653E+03	0.3335E-02	-0.1700E+03
13.	0.5167E-02	-0.1444E+02	0.1266E-01	-0.2621E+02	0.5450E-02	-0.7151E+01
14.	0.3877E-02	-0.1220E+02	0.1009E-01	0.2250E+02	0.4142E-02	0.9428E+01
15.	0.6434E-03	-0.1277E+03	0.1387E-01	-0.9042E+02	0.2391E-02	-0.9570E+02
16.	0.8982E-03	-0.9283E+02	0.2038E-02	-0.8668E+02	0.2048E-02	-0.4947E+02
17.	0.4926E-02	-0.7563E+01	0.1287E-01	-0.1857E+02	0.5254E-02	-0.5818E+01
18.	0.1039E-02	0.7280E+02	0.2722E-02	0.5000E+02	0.3732E-02	0.7627E+02
19.	0.4047E-02	0.1852E+02	0.1685E-01	0.3816E+02	0.5001E-02	0.5813E+02
20.	0.2709E-02	0.4534E+02	0.1997E-02	0.1798E+01	0.8911E-03	0.2502E+02
21.	0.2705E-02	0.6737E+02	0.1259E-01	0.5447E+02	0.4532E-02	0.4973E+02
22.	0.3615E-02	-0.2399E+02	0.1784E-01	0.2777E+02	0.1046E-01	0.2987E+02
23.	0.4676E-02	0.6531E+01	0.1426E-01	0.1770E+02	0.5389E-02	0.2330E+02
24.	0.2639E-02	0.1226E+03	0.9496E-02	0.1526E+03	0.2725E-02	0.1388E+03
25.	0.3501E-02	-0.1262E+03	0.1204E-01	-0.1174E+03	0.3900E-02	-0.1288E+03
26.	0.3795E-02	0.1472E+02	0.4716E-02	0.5873E+02	0.2745E-02	0.9025E+01
27.	0.3716E-02	0.4400E+02	0.1168E-01	0.4285E+02	0.4899E-02	0.2133E+02
28.	0.2158E-02	-0.1642E+03	0.7736E-02	0.1319E+03	0.9819E-03	-0.1780E+03
29.	0.2399E-02	-0.9464E+02	0.1494E-01	-0.1349E+03	0.2150E-02	-0.9457E+02
30.	0.6310E-03	0.1386E+03	0.5213E-02	-0.1551E+03	0.2670E-02	0.1565E+03
31.	0.1417E-02	0.4284E+02	0.9630E-02	0.6306E+02	0.4436E-02	0.7947E+02
32.	0.1522E-02	-0.9575E+02	0.1400E-01	-0.8832E+02	0.1817E-02	-0.1008E+03
33.	0.7685E-03	0.7552E+02	0.1023E-01	0.1540E+03	0.3942E-02	0.1568E+03
34.	0.6425E-03	-0.1030E+03	0.1523E-01	-0.1376E+03	0.4247E-02	-0.1748E+03
35.	0.2085E-02	-0.8050E+02	0.1538E-01	-0.9936E+02	0.3438E-02	-0.8420E+02
36.	0.2347E-02	-0.7689E+02	0.1414E-01	-0.1052E+03	0.9112E-03	0.1567E+03
37.	0.8562E-03	0.1808E+02	0.1962E-01	0.8573E+01	0.6428E-03	0.1239E+03
38.	0.4408E-02	0.9894E+02	0.1470E-01	0.1678E+03	0.4400E-02	0.8250E+02
39.	0.2425E-02	0.1710E+03	0.7409E-02	0.6142E+02	0.3452E-02	0.8293E+02

TABLE XXII.- CONTINUED

BOTTOM SURFACE

HARM	RADIUS= 0.750 CHORD= 0.400 AMPLITUDE	PHASE	RADIUS= 0.750 CHORD= 0.450 AMPLITUDE	PHASE	RADIUS= 0.750 CHORD= 0.550 AMPLITUDE	PHASE
0.	0.1335E+02	0.0000E+00	0.1335E+02	0.0000E+00	0.1351E+02	0.0000E+00
1.	0.6161E+00	-0.8419E+02	0.5037E+00	-0.8670E+02	0.3176E+00	-0.9422E+02
2.	0.1955E+00	0.1605E+02	0.1597E+00	0.1441E+02	0.1186E+00	0.8747E+01
3.	0.4928E-01	-0.1046E+03	0.4290E-01	-0.1076E+03	0.3954E-01	-0.1090E+03
4.	0.1243E-01	-0.3069E+02	0.9891E-02	-0.3142E+02	0.4943E-02	-0.4811E+02
5.	0.1158E-01	-0.2974E+02	0.1149E-01	-0.4131E+02	0.1123E-01	-0.4597E+02
6.	0.3110E-02	0.1012E+03	0.3928E-02	0.9574E+02	0.3604E-02	0.1155E+03
7.	0.8512E-02	-0.5946E+02	0.7851E-02	-0.7385E+02	0.7895E-02	-0.7593E+02
8.	0.7452E-02	-0.1579E+01	0.6756E-02	-0.7463E+01	0.6001E-02	-0.1979E+02
9.	0.3502E-02	0.4916E+01	0.4367E-02	-0.1878E+02	0.3442E-02	-0.2589E+02
10.	0.2062E-02	0.1162E+03	0.3213E-02	0.1042E+03	0.1311E-02	0.1277E+03
11.	0.4208E-03	-0.1200E+03	0.6710E-03	0.1507E+03	0.1044E-02	0.9988E+02
12.	0.1613E-02	-0.1124E+03	0.1966E-02	-0.1520E+03	0.2696E-02	-0.1285E+03
13.	0.2432E-02	0.1020E+02	0.1868E-02	-0.7553E+01	0.2760E-02	0.4764E+01
14.	0.2046E-02	0.4761E+02	0.2068E-02	0.5341E+02	0.2101E-02	0.1315E+02
15.	0.1716E-03	-0.5704E+01	0.1476E-02	-0.3606E+02	0.9993E-03	-0.5133E+02
16.	0.3543E-03	-0.1659E+02	0.2467E-03	0.3536E+02	0.4796E-03	0.5228E+02
17.	0.1849E-02	0.2535E+02	0.2052E-02	0.2353E+02	0.1748E-02	0.1901E+02
18.	0.2323E-02	0.1061E+03	0.2420E-02	0.1063E+03	0.2453E-02	0.8834E+02
19.	0.1973E-02	0.1198E+03	0.2985E-02	0.1204E+03	0.2967E-02	0.9377E+02
20.	0.1873E-02	-0.8929E+02	0.1157E-02	-0.5717E+02	0.1982E-02	-0.9870E+02
21.	0.5437E-03	0.1538E+03	0.1392E-02	0.1142E+03	0.1931E-02	0.1263E+03
22.	0.2799E-02	0.2395E+02	0.2427E-02	0.4543E+02	0.2461E-02	-0.1290E+01
23.	0.4090E-02	0.6660E+02	0.4880E-02	0.6035E+02	0.4519E-02	0.4653E+02
24.	0.2402E-02	0.1486E+03	0.2515E-02	0.1392E+03	0.3452E-02	0.1449E+03
25.	0.2319E-02	-0.1115E+03	0.2538E-02	-0.1184E+03	0.2160E-02	-0.8932E+02
26.	0.2917E-03	0.1730E+03	0.4555E-03	0.1272E+03	0.1574E-02	0.1091E+03
27.	0.3997E-03	-0.1106E+02	0.8901E-03	-0.1481E+03	0.7348E-03	0.1745E+03
28.	0.1029E-02	-0.4174E+02	0.8648E-03	0.1854E+02	0.1579E-02	-0.3582E+02
29.	0.4149E-03	-0.1377E+02	0.6560E-03	-0.2638E+02	0.1408E-02	0.5824E+02
30.	0.1091E-02	0.6423E+02	0.1328E-02	0.6879E+02	0.1716E-02	0.5650E+02
31.	0.6901E-03	0.8581E+02	0.9105E-03	0.1206E+03	0.1915E-02	0.1077E+03
32.	0.1276E-02	0.5567E+01	0.1510E-02	0.4985E+01	0.1664E-02	-0.4391E+02
33.	0.1049E-02	0.1300E+03	0.9957E-03	0.1547E+03	0.9785E-03	0.1659E+03
34.	0.2382E-03	0.8032E+02	0.1015E-02	0.8764E+02	0.6064E-03	0.5139E+01
35.	0.9145E-03	-0.9343E+02	0.1088E-02	0.1793E+03	0.8492E-03	-0.8374E+02
36.	0.1420E-02	0.5957E+02	0.1321E-02	0.7320E+02	0.2772E-02	0.6787E+02
37.	0.9381E-03	0.9011E+02	0.5253E-03	0.3128E+02	0.7926E-03	-0.1640E+03
38.	0.1648E-02	-0.1220E+03	0.2346E-02	-0.1682E+03	0.2958E-02	-0.1331E+03
39.	0.9099E-03	0.3590E+02	0.5586E-03	-0.1450E+02	0.1236E-02	-0.2020E+02

TABLE XXII.- CONTINUED

			BOTTOM SURFACE	
	RADIUS= 0.750		RADIUS= 0.750	
	CHORD= 0.699		CHORD= 0.919	
HARM	AMPLITUDE	PHASE	AMPLITUDE	PHASE
0.	0.1358E+02	0.0000E+00	0.1352E+02	0.0000E+00
1.	0.1766E+00	-0.1089E+03	0.8268E-01	0.1440E+03
2.	0.7362E-01	0.1705E+01	0.1246E-01	-0.9458E+02
3.	0.2727E-01	-0.1180E+03	0.1282E-01	-0.1145E+03
4.	0.1441E-02	-0.1402E+03	0.3185E-02	0.1208E+03
5.	0.9232E-02	-0.6113E+02	0.4390E-02	-0.7883E+02
6.	0.5774E-02	0.1088E+03	0.3173E-02	0.1033E+03
7.	0.7034E-02	-0.8583E+02	0.4720E-02	-0.1067E+03
8.	0.5245E-02	-0.2219E+02	0.3194E-02	-0.5990E+02
9.	0.4447E-02	-0.5544E+02	0.2456E-02	-0.7636E+02
10.	0.2099E-02	0.9178E+02	0.1641E-02	0.1582E+03
11.	0.1836E-02	0.9405E+02	0.1782E-02	0.9804E+02
12.	0.3959E-02	-0.1612E+03	0.1835E-02	-0.1739E+03
13.	0.1253E-02	-0.1735E+02	0.1024E-02	-0.5925E+01
14.	0.2092E-02	0.1862E+02	0.1610E-02	-0.2910E+02
15.	0.2732E-02	-0.3372E+02	0.1571E-02	-0.3618E+02
16.	0.2746E-03	0.1323E+02	0.1236E-02	0.1446E+02
17.	0.1963E-02	0.2275E+02	0.6412E-03	0.1881E+02
18.	0.2499E-02	0.1114E+03	0.9711E-03	0.1108E+03
19.	0.2984E-02	0.1065E+03	0.2800E-02	0.7455E+02
20.	0.6808E-03	-0.1195E+03	0.9002E-03	-0.1398E+03
21.	0.3341E-02	0.1379E+03	0.2522E-02	0.1114E+03
22.	0.2641E-02	0.1232E+02	0.1642E-02	0.3660E+02
23.	0.5396E-02	0.3374E+02	0.2509E-02	0.1211E+02
24.	0.1489E-02	0.1409E+03	0.1245E-02	0.6279E+02
25.	0.2160E-02	-0.7728E+02	0.1499E-02	-0.5572E+02
26.	0.3209E-02	0.1223E+03	0.2419E-02	0.9934E+02
27.	0.7113E-03	-0.1650E+03	0.4874E-03	0.8287E+02
28.	0.1305E-02	-0.6323E+02	0.8264E-03	-0.7689E+02
29.	0.1521E-02	-0.9332E+02	0.2081E-03	0.6057E+02
30.	0.9494E-03	-0.1844E+02	0.1273E-02	-0.5292E+02
31.	0.2620E-02	0.1149E+03	0.1207E-02	0.1027E+03
32.	0.2673E-02	-0.3364E+02	0.2808E-02	-0.5393E+02
33.	0.1169E-02	-0.1265E+03	0.1480E-02	0.1389E+03
34.	0.1286E-02	-0.3414E+01	0.8657E-03	-0.1143E+03
35.	0.8209E-03	0.8342E+02	0.1138E-02	-0.1013E+03
36.	0.4007E-03	-0.1627E+03	0.1320E-02	0.2008E+02
37.	0.9376E-03	-0.3502E+02	0.3181E-03	0.2137E+02
38.	0.7732E-03	0.1680E+03	0.3245E-03	-0.1793E+02
39.	0.1063E-02	0.1476E+03	0.3547E-03	-0.1730E+03

TABLE XXII.- CONTINUED

	TOP SURFACE					
	RADIUS= 0.750 CHORD= 0.010		RADIUS= 0.750 CHORD= 0.030		RADIUS= 0.750 CHORD= 0.080	
HARM	AMPLITUDE	PHASE	AMPLITUDE	PHASE	AMPLITUDE	PHASE
0.	0.9678E+01	0.0000E+00	0.9837E+01	0.0000E+00	0.1033E+02	0.0000E+00
1.	0.2892E+01	0.1177E+03	0.5779E+00	-0.1604E+03	0.1720E+01	-0.9372E+02
2.	0.5713E+00	-0.1686E+03	0.3224E+00	-0.1155E+03	0.6357E+00	-0.1549E+02
3.	0.9865E+00	0.1077E+03	0.4313E+00	0.9621E+02	0.5914E+00	0.8592E+02
4.	0.3560E+00	0.9296E+02	0.1462E+00	0.1018E+03	0.2561E+00	0.1519E+03
5.	0.2019E+00	0.1134E+03	0.1279E+00	0.1230E+03	0.6765E-01	-0.1516E+03
6.	0.1373E+00	0.9160E+02	0.6313E-01	0.1296E+03	0.1079E-01	0.1528E+03
7.	0.8274E-01	0.1020E+03	0.4914E-01	0.1383E+03	0.4180E-01	-0.1121E+03
8.	0.4967E-01	0.1218E+03	0.3006E-01	0.1365E+03	0.6981E-01	-0.4731E+00
9.	0.4565E-01	0.1612E+03	0.2737E-01	0.1732E+03	0.9131E-01	0.9203E+02
10.	0.2630E-01	0.1705E+03	0.9666E-02	-0.1379E+03	0.7254E-01	0.1764E+03
11.	0.3443E-01	0.1301E+03	0.1612E-01	0.9018E+02	0.3020E-01	-0.9189E+02
12.	0.3447E-01	0.1145E+03	0.1308E-01	0.1056E+03	0.1717E-01	0.2511E+02
13.	0.2172E-01	0.1300E+03	0.5736E-02	0.1187E+03	0.1695E-01	-0.1067E+03
14.	0.1927E-01	0.1561E+03	0.5290E-02	0.1454E+03	0.4163E-01	-0.1856E+02
15.	0.1008E-01	0.1489E+03	0.6683E-02	-0.1613E+03	0.4851E-01	0.6997E+02
16.	0.1892E-01	0.1228E+03	0.7502E-02	0.1394E+03	0.5392E-01	0.1528E+03
17.	0.1599E-01	0.1263E+03	0.4402E-02	0.1542E+03	0.3603E-01	-0.1082E+03
18.	0.1150E-01	0.1599E+03	0.5954E-02	0.8672E+02	0.1195E-01	-0.2414E+02
19.	0.6561E-02	0.1752E+03	0.3023E-02	0.1548E+03	0.1032E-01	-0.1490E+03
20.	0.1005E-01	-0.1613E+03	0.5319E-02	0.1590E+03	0.2189E-01	-0.3659E+02
21.	0.7936E-02	0.8419E+02	0.6026E-02	0.1085E+03	0.4210E-01	0.7912E+02
22.	0.7683E-02	0.1306E+03	0.9053E-03	0.1051E+03	0.2680E-01	0.1521E+03
23.	0.7556E-02	0.1795E+03	0.9085E-02	0.1768E+03	0.2221E-01	-0.1366E+03
24.	0.5484E-02	-0.1594E+03	0.5609E-02	-0.1271E+03	0.8252E-02	-0.6842E+02
25.	0.2744E-02	0.8300E+02	0.2966E-03	-0.6000E+02	0.5293E-02	0.2387E+02
26.	0.4104E-02	0.1045E+03	0.1924E-02	-0.1095E+03	0.1574E-01	-0.3178E+02
27.	0.2029E-03	0.5569E+02	0.8830E-02	0.8692E+02	0.1977E-01	0.8365E+02
28.	0.9613E-02	0.1736E+03	0.9940E-02	-0.1607E+03	0.1940E-01	0.1601E+03
29.	0.4039E-02	0.9073E+02	0.4945E-03	-0.1500E+03	0.1093E-01	-0.2030E+02
30.	0.1009E-01	-0.2489E+02	0.3925E-02	0.1273E+03	0.1087E-01	0.4230E+02
31.	0.2455E-02	-0.8412E+02	0.4963E-02	0.1528E+03	0.4041E-02	-0.4763E+02
32.	0.8227E-02	0.8152E+02	0.4732E-02	0.3574E+01	0.1524E-01	-0.2544E+02
33.	0.1170E-01	-0.1359E+03	0.5877E-02	0.1510E+03	0.2798E-01	0.5662E+02
34.	0.5238E-02	-0.1062E+02	0.5111E-02	0.1535E+03	0.1025E-01	0.1662E+03
35.	0.5821E-02	-0.1173E+03	0.8079E-02	-0.6485E+00	0.3467E-02	-0.9915E+01
36.	0.6292E-02	0.1315E+03	0.8021E-02	-0.1489E+03	0.1275E-01	-0.1730E+03
37.	0.4187E-02	-0.8950E+02	0.4785E-02	-0.1705E+03	0.1284E-01	0.9254E+02
38.	0.8775E-02	-0.9726E+02	0.3903E-02	0.1829E+02	0.2138E-01	-0.8058E+02
39.	0.8021E-02	0.5120E+02	0.4293E-02	0.1553E+03	0.1608E-01	0.4705E+02

TABLE XXII.- CONTINUED

	TOP SURFACE					
	RADIUS= 0.750 CHORD= 0.150		RADIUS= 0.750 CHORD= 0.250		RADIUS= 0.750 CHORD= 0.350	
HARM	AMPLITUDE	PHASE	AMPLITUDE	PHASE	AMPLITUDE	PHASE
0.	0.1114E+02	0.0000E+00	0.1160E+02	0.0000E+00	0.1213E+02	0.0000E+00
1.	0.1766E+01	-0.8933E+02	0.1198E+01	-0.8771E+02	0.7360E+00	-0.8805E+02
2.	0.6426E+00	-0.8873E+01	0.2655E+00	-0.1763E+02	0.1391E+00	-0.2781E+02
3.	0.5609E+00	0.8852E+02	0.1798E+00	0.7275E+02	0.1059E+00	0.5832E+02
4.	0.3220E+00	0.1645E+03	0.6567E-01	0.1131E+03	0.3652E-01	0.9613E+02
5.	0.1920E+00	-0.9660E+02	0.3686E-01	0.1314E+03	0.2367E-01	0.1219E+03
6.	0.1618E+00	-0.2687E+01	0.1303E-01	-0.1357E+03	0.5441E-02	0.1795E+03
7.	0.1109E+00	0.9768E+02	0.3914E-02	-0.2826E+02	0.3920E-02	0.1452E+03
8.	0.1077E+00	-0.1691E+03	0.1725E-01	0.6827E+02	0.4795E-02	0.8696E+02
9.	0.6315E-01	-0.7426E+02	0.1460E-01	0.1396E+03	0.5706E-02	0.1417E+03
10.	0.3320E-01	-0.4044E+02	0.1222E-01	-0.1172E+03	0.3707E-02	-0.1341E+03
11.	0.1375E+00	0.9541E+02	0.8133E-02	-0.6353E+02	0.1220E-02	0.7765E+02
12.	0.1097E-01	-0.2506E+02	0.1221E-01	0.5403E+02	0.2338E-02	-0.2615E+01
13.	0.5566E-01	0.5317E+02	0.3256E-02	0.8137E+02	0.2295E-02	0.3070E+02
14.	0.5717E-01	0.1143E+03	0.1851E-02	0.3444E+02	0.6407E-03	0.5377E+02
15.	0.2315E-01	-0.1348E+03	0.3283E-02	-0.1073E+03	0.2469E-02	-0.1188E+03
16.	0.2597E-01	-0.1627E+02	0.4231E-02	0.1395E+03	0.1206E-02	0.1010E+03
17.	0.2619E-01	0.1072E+03	0.1252E-02	0.2484E+02	0.1435E-02	0.6614E+02
18.	0.2224E-01	-0.1696E+03	0.1275E-02	-0.8918E+02	0.2251E-02	-0.1598E+03
19.	0.2968E-01	-0.9096E+01	0.8311E-02	-0.1319E+03	0.3012E-02	-0.1217E+03
20.	0.3839E-01	0.7658E+02	0.7216E-02	-0.6489E+02	0.3135E-02	0.1784E+03
21.	0.3482E-01	-0.1793E+03	0.4560E-02	0.1678E+02	0.3157E-02	0.2166E+02
22.	0.3786E-01	-0.8055E+02	0.6917E-02	0.1058E+03	0.1831E-02	0.7204E+02
23.	0.4096E-01	0.2574E+02	0.6672E-02	0.1579E+03	0.2762E-02	0.1614E+03
24.	0.3382E-01	0.1054E+03	0.6995E-02	-0.1372E+03	0.2071E-02	-0.1138E+03
25.	0.1803E-01	0.1522E+03	0.5805E-02	0.1309E+03	0.3728E-02	0.8265E+01
26.	0.1740E-01	-0.4551E+02	0.5922E-02	0.4225E+01	0.1367E-02	0.4240E+01
27.	0.1750E-01	0.6516E+02	0.1646E-02	0.8233E+02	0.3932E-02	0.9903E+02
28.	0.1808E-02	-0.5927E+02	0.5172E-02	-0.4393E+02	0.2917E-03	0.1387E+03
29.	0.1498E-01	0.1538E+02	0.4415E-02	0.1559E+02	0.2762E-02	0.3741E+02
30.	0.1389E-01	0.9366E+02	0.6469E-02	-0.1076E+02	0.1300E-02	-0.3265E+02
31.	0.2235E-01	-0.1550E+03	0.1260E-01	-0.4717E+02	0.2177E-02	-0.1388E+02
32.	0.4154E-01	-0.4156E+02	0.8407E-02	0.9689E+02	0.4593E-02	-0.1578E+03
33.	0.3755E-01	0.5582E+02	0.1604E-02	-0.1698E+03	0.6833E-03	-0.1128E+03
34.	0.2510E-01	0.1274E+03	0.5474E-02	-0.2219E+01	0.1405E-02	0.1105E+03
35.	0.1109E-01	-0.1684E+03	0.8103E-02	0.7930E+02	0.2093E-02	0.1007E+03
36.	0.7101E-02	-0.1072E+03	0.4725E-02	-0.1660E+03	0.5238E-02	0.1610E+03
37.	0.1075E-01	0.6034E+02	0.4972E-02	-0.6297E+02	0.3343E-02	0.5962E+01
38.	0.8570E-02	-0.8776E+02	0.6390E-02	-0.2256E+02	0.2830E-02	-0.4296E+01
39.	0.4306E-02	0.1577E+02	0.9828E-02	0.1313E+03	0.1706E-02	0.3970E+02

TABLE XXII.- CONTINUED

TOP SURFACE

	RADIUS= 0.750 CHORD= 0.400		RADIUS= 0.750 CHORD= 0.550		RADIUS= 0.750 CHORD= 0.699	
HARM	AMPLITUDE	PHASE	AMPLITUDE	PHASE	AMPLITUDE	PHASE
0.	0.1226E+02	0.0000E+00	0.1275E+02	0.0000E+00	0.1320E+02	0.0000E+00
1.	0.6310E+00	-0.8703E+02	0.2722E+00	-0.8509E+02	0.1789E+00	-0.7786E+02
2.	0.1132E+00	-0.3331E+02	0.4355E-01	-0.7107E+02	0.2195E-01	-0.1184E+03
3.	0.8931E-01	0.5475E+02	0.6110E-01	0.3651E+02	0.3833E-01	0.2842E+02
4.	0.3772E-01	0.9439E+02	0.1798E-01	0.7945E+02	0.1179E-01	0.6262E+02
5.	0.2707E-01	0.1212E+03	0.1554E-01	0.1165E+03	0.9763E-02	0.1126E+03
6.	0.4620E-02	0.9112E+02	0.2102E-02	0.1478E+03	0.2180E-02	0.1371E+03
7.	0.5301E-02	0.1349E+03	0.5256E-02	0.1238E+03	0.2802E-02	0.1442E+03
8.	0.3495E-02	0.5654E+02	0.4096E-02	0.1126E+03	0.1456E-02	0.4340E+02
9.	0.3018E-02	-0.1622E+03	0.1885E-02	-0.1597E+03	0.8709E-03	-0.8934E+02
10.	0.4059E-02	-0.1496E+03	0.3517E-02	-0.1264E+03	0.3164E-02	-0.1193E+03
11.	0.5476E-02	0.9840E+02	0.1027E-02	0.1745E+03	0.1274E-02	0.1472E+02
12.	0.2297E-02	0.1220E+02	0.1680E-02	0.7963E+02	0.2257E-02	0.9164E+02
13.	0.4426E-02	-0.3729E+02	0.2926E-02	-0.3167E+01	0.1664E-02	-0.4186E+01
14.	0.2188E-02	0.5092E+02	0.1116E-02	0.2343E+02	0.8376E-03	0.1338E+02
15.	0.3449E-02	0.4056E+02	0.2861E-02	-0.1514E+03	0.1268E-02	-0.1699E+03
16.	0.3370E-02	0.1772E+03	0.1050E-02	0.1259E+03	0.8728E-03	0.1030E+03
17.	0.7630E-03	0.1521E+03	0.1920E-03	-0.4283E+02	0.1140E-02	0.4771E+02
18.	0.3953E-02	-0.5713E+02	0.5952E-03	0.1155E+03	0.9896E-03	-0.1757E+03
19.	0.2775E-02	-0.2055E+02	0.8461E-03	0.8505E+02	0.4314E-03	-0.1533E+03
20.	0.6480E-02	-0.9253E+02	0.2285E-02	-0.1189E+03	0.1528E-02	-0.9868E+02
21.	0.7819E-02	0.3858E+02	0.2482E-03	-0.1200E+03	0.1632E-02	-0.8011E+02
22.	0.1101E-02	0.1083E+03	0.2055E-02	-0.1681E+02	0.1975E-03	0.6335E+02
23.	0.6368E-02	-0.1750E+03	0.4828E-02	0.1789E+03	0.2323E-02	0.1794E+03
24.	0.3241E-02	0.8051E+02	0.2501E-02	0.1346E+02	0.6169E-03	0.1278E+02
25.	0.3065E-02	0.1391E+02	0.2016E-02	-0.5126E+02	0.2250E-02	0.1325E+02
26.	0.3533E-02	-0.9968E+02	0.2083E-03	0.2585E+01	0.1407E-02	-0.1384E+03
27.	0.3310E-02	0.1425E+03	0.1532E-02	-0.4218E+02	0.1521E-02	0.6183E+02
28.	0.1886E-02	-0.1303E+03	0.2730E-02	-0.1576E+03	0.3661E-02	-0.1419E+03
29.	0.1058E-02	-0.2433E+02	0.3223E-02	-0.2476E+02	0.3610E-02	-0.3858E+02
30.	0.6816E-02	0.7382E+02	0.4769E-02	0.7139E+02	0.3750E-02	0.5596E+02
31.	0.7089E-02	0.9814E+02	0.4280E-02	0.5153E+02	0.2105E-02	0.5359E+02
32.	0.7708E-02	0.1388E+03	0.2815E-02	0.1157E+03	0.2648E-03	0.1609E+03
33.	0.1967E-02	0.8766E+02	0.1689E-02	-0.7810E+01	0.1635E-02	0.1170E+01
34.	0.2182E-02	-0.5694E+02	0.2614E-02	0.1668E+03	0.1550E-02	-0.1652E+03
35.	0.4092E-02	-0.1568E+03	0.1586E-02	-0.7362E+02	0.1879E-02	-0.4974E+02
36.	0.3157E-02	0.1379E+03	0.3101E-02	0.1477E+03	0.2802E-02	0.1409E+03
37.	0.6578E-02	-0.5611E+02	0.1147E-02	0.1434E+03	0.2992E-02	-0.3487E+02
38.	0.3541E-02	0.7700E+02	0.2735E-02	0.1147E+03	0.1367E-02	0.1417E+03
39.	0.4309E-02	0.1148E+03	0.2549E-02	-0.1634E+03	0.2156E-02	-0.7699E+02

TABLE XXII.- CONTINUED

TOP SURFACE

RADIUS= Ø.75Ø
CHORD= Ø.919

HARM	AMPLITUDE	PHASE
Ø.	Ø.1352E+Ø2	Ø.ØØØØE+ØØ
1.	Ø.1341E+ØØ	Ø.1Ø32E+Ø3
2.	Ø.56Ø2E-Ø1	-Ø.1541E+Ø3
3.	Ø.2246E-Ø1	-Ø.4575E+Ø1
4.	Ø.1Ø36E-Ø1	Ø.5435E+Ø2
5.	Ø.4378E-Ø2	Ø.8753E+Ø2
6.	Ø.3Ø92E-Ø2	Ø.788ØE+Ø2
7.	Ø.3Ø5ØE-Ø2	Ø.1254E+Ø3
8.	Ø.3183E-Ø2	Ø.8338E+Ø2
9.	Ø.41Ø2E-Ø2	-Ø.5Ø92E+Ø2
1Ø.	Ø.3863E-Ø2	-Ø.1Ø62E+Ø3
11.	Ø.2ØØ5E-Ø2	Ø.1685E+Ø3
12.	Ø.2618E-Ø2	Ø.1295E+Ø3
13.	Ø.2751E-Ø2	-Ø.4747E+Ø1
14.	Ø.213ØE-Ø2	Ø.468ØE+Ø2
15.	Ø.7863E-Ø3	-Ø.23Ø6E+Ø2
16.	Ø.463ØE-Ø2	-Ø.1453E+Ø3
17.	Ø.199ØE-Ø2	-Ø.1276E+Ø3
18.	Ø.1945E-Ø2	Ø.2823E+Ø2
19.	Ø.13Ø7E-Ø2	Ø.3115E+Ø2
2Ø.	Ø.2483E-Ø2	-Ø.139ØE+Ø3
21.	Ø.2877E-Ø2	Ø.1767E+Ø3
22.	Ø.1Ø8ØE-Ø2	Ø.1438E+Ø1
23.	Ø.2269E-Ø2	Ø.1736E+Ø3
24.	Ø.1Ø5ØE-Ø2	Ø.9Ø53E+Ø2
25.	Ø.1585E-Ø2	-Ø.6444E+ØØ
26.	Ø.1843E-Ø2	-Ø.179ØE+Ø3
27.	Ø.2968E-Ø2	-Ø.7Ø51E+Ø2
28.	Ø.4487E-Ø2	-Ø.9384E+Ø2
29.	Ø.1Ø94E-Ø2	-Ø.1438E+Ø3
3Ø.	Ø.5Ø89E-Ø2	Ø.8141E+Ø2
31.	Ø.8144E-Ø2	Ø.2591E+Ø2
32.	Ø.4649E-Ø2	Ø.99Ø2E+Ø2
33.	Ø.19Ø3E-Ø2	-Ø.9912E+Ø2
34.	Ø.1775E-Ø2	Ø.1347E+Ø3
35.	Ø.1721E-Ø2	-Ø.9532E+Ø1
36.	Ø.7Ø75E-Ø2	Ø.14Ø2E+Ø3
37.	Ø.2231E-Ø2	Ø.1762E+Ø3
38.	Ø.8348E-Ø2	Ø.1259E+Ø3
39.	Ø.2854E-Ø2	Ø.2621E+Ø2

	BOTTOM SURFACE					
	RADIUS= 0.864		RADIUS= 0.864		RADIUS= 0.864	
	CHORD= 0.010		CHORD= 0.030		CHORD= 0.080	
HARM	AMPLITUDE	PHASE	AMPLITUDE	PHASE	AMPLITUDE	PHASE
0.	0.1549E+02	0.0000E+00	0.1415E+02	0.0000E+00	0.1281E+02	0.0000E+00
1.	0.1110E+01	0.6623E+02	0.1086E+01	-0.4670E+02	0.2099E+01	-0.6610E+02
2.	0.6934E+00	0.7422E+02	0.5079E+00	0.6626E+02	0.6039E+00	0.4917E+02
3.	0.3416E+00	-0.8675E+02	0.3559E+00	-0.8990E+02	0.2811E+00	-0.1093E+03
4.	0.1509E+00	0.2820E+01	0.1404E+00	-0.1219E+02	0.1476E+00	-0.2396E+02
5.	0.8150E-01	-0.2626E+02	0.6287E-01	-0.1285E+02	0.4427E-01	0.2064E+02
6.	0.3561E-01	0.3080E+02	0.2842E-01	0.1420E+02	0.1363E-01	-0.1308E+02
7.	0.1569E-01	0.3445E+02	0.1910E-01	0.8362E+01	0.2458E-01	0.1062E+02
8.	0.7204E-02	0.4454E+02	0.1830E-01	0.1648E+02	0.1049E-01	-0.3692E+01
9.	0.1205E-01	0.9238E+01	0.1271E-01	0.1411E+02	0.2492E-01	-0.7639E+01
10.	0.1069E-01	0.7748E+02	0.1184E-01	0.4803E+02	0.2404E-01	0.8391E+02
11.	0.9931E-02	0.9410E+02	0.1221E-01	0.8907E+02	0.1234E-01	0.1201E+03
12.	0.6778E-02	0.1578E+03	0.1989E-02	0.1626E+03	0.4962E-02	-0.1429E+03
13.	0.3388E-03	0.7183E+02	0.5944E-02	0.5149E+02	0.5495E-02	0.3480E+02
14.	0.1020E-02	-0.6040E+00	0.1802E-02	-0.1664E+02	0.5368E-02	0.3307E+02
15.	0.1397E-02	-0.4490E+02	0.2930E-02	0.3055E+02	0.9802E-03	-0.4685E+02
16.	0.3522E-02	0.1057E+03	0.6627E-02	0.1088E+03	0.5256E-02	0.1289E+03
17.	0.1524E-02	-0.1717E+03	0.1991E-02	0.1534E+03	0.2754E-02	-0.5575E+02
18.	0.1149E-02	-0.1712E+03	0.2520E-02	-0.1548E+03	0.4558E-02	0.9732E+02
19.	0.1794E-02	0.1647E+02	0.3894E-02	0.4476E+02	0.7916E-02	0.7605E+02
20.	0.1852E-02	-0.6828E+01	0.1844E-02	-0.1369E+02	0.3692E-02	-0.3321E+02
21.	0.3335E-02	0.8792E+02	0.5316E-02	0.8390E+02	0.9926E-02	0.1015E+03
22.	0.2478E-02	0.1145E+03	0.3261E-02	0.1202E+03	0.5523E-02	0.1219E+03
23.	0.2796E-03	0.1774E+03	0.1730E-02	0.1117E+03	0.4732E-02	0.7803E+01
24.	0.1451E-02	-0.9762E+02	0.2322E-02	-0.1109E+03	0.1716E-02	-0.1427E+03
25.	0.1637E-02	-0.3741E+02	0.1863E-02	-0.8100E+02	0.3942E-02	-0.8491E+02
26.	0.2490E-02	0.1275E+03	0.5841E-02	0.1065E+03	0.8231E-02	0.1042E+03
27.	0.9706E-03	0.1296E+03	0.2960E-02	0.1624E+03	0.5514E-02	0.1726E+03
28.	0.1418E-02	-0.1238E+03	0.3053E-02	-0.9968E+02	0.2910E-02	-0.5627E+02
29.	0.2044E-02	-0.5439E+02	0.2925E-02	-0.4780E+02	0.4057E-02	-0.4432E+02
30.	0.1186E-02	0.1295E+02	0.1057E-02	0.2653E+02	0.5039E-03	-0.1053E+02
31.	0.2099E-02	0.6398E+02	0.1970E-02	0.6530E+02	0.2148E-02	0.3933E+02
32.	0.2746E-02	-0.1050E+03	0.3652E-02	-0.1182E+03	0.6654E-02	-0.1230E+03
33.	0.1440E-02	-0.1325E+03	0.4559E-03	-0.1400E+03	0.4075E-02	-0.1244E+03
34.	0.2073E-02	-0.3589E+02	0.4270E-02	-0.1488E+02	0.2702E-02	-0.1521E+02
35.	0.1802E-02	0.7249E+01	0.1753E-02	0.2350E+02	0.6453E-02	0.9513E+02
36.	0.9889E-03	0.5094E+01	0.2984E-02	0.4184E+02	0.4826E-02	-0.6965E+01
37.	0.8536E-03	-0.1579E+03	0.1853E-02	-0.1553E+03	0.6742E-03	0.1348E+03
38.	0.1207E-02	0.5474E+02	0.2099E-02	0.8324E+02	0.4845E-02	0.3766E+02
39.	0.1967E-03	-0.1693E+03	0.1088E-02	-0.7868E+02	0.3337E-02	-0.4083E+02

ORIGINAL PAGE IS
OF POOR QUALITY

TABLE XXII.- CONTINUED

BOTTOM SURFACE

HARM	RADIUS= 0.864 CHORD= 0.150 AMPLITUDE	PHASE	RADIUS= 0.864 CHORD= 0.350 AMPLITUDE	PHASE	RADIUS= 0.864 CHORD= 0.450 AMPLITUDE	PHASE
0.	0.1227E+02	0.0000E+00	0.1282E+02	0.0000E+00	0.1318E+02	0.0000E+00
1.	0.2268E+01	-0.7142E+02	0.1176E+01	-0.7986E+02	0.7035E+00	-0.8338E+02
2.	0.7327E+00	0.3731E+02	0.2933E+00	0.1516E+02	0.1506E+00	0.1094E+02
3.	0.2282E+00	-0.1578E+03	0.2368E-01	-0.9558E+02	0.3939E-01	-0.8336E+02
4.	0.1850E+00	-0.6510E+02	0.8337E-02	-0.1578E+03	0.3058E-02	0.1243E+03
5.	0.1292E+00	0.2508E+02	0.2642E-01	-0.5743E+02	0.1639E-01	-0.6370E+02
6.	0.7343E-01	0.1444E+03	0.1569E-01	0.3605E+02	0.8627E-02	0.1429E+02
7.	0.6774E-01	-0.7663E+02	0.2100E-02	-0.3879E+02	0.3875E-02	-0.3982E+02
8.	0.6198E-01	0.2632E+02	0.9223E-02	-0.4245E+02	0.5750E-02	-0.4147E+02
9.	0.2285E-01	0.1477E+03	0.1335E-01	-0.8225E+01	0.8870E-02	-0.1730E+02
10.	0.1315E-01	-0.5119E+02	0.1239E-01	0.9199E+02	0.7407E-02	0.8058E+02
11.	0.3597E-01	0.7780E+02	0.7012E-02	0.1288E+03	0.4030E-02	0.1066E+03
12.	0.2730E-01	-0.1642E+03	0.7305E-02	-0.1458E+03	0.4469E-02	-0.1626E+03
13.	0.2545E-01	-0.2872E+02	0.3721E-02	-0.2311E+02	0.2298E-02	-0.6319E+02
14.	0.2305E-01	0.6843E+02	0.5208E-02	0.2604E+02	0.2622E-02	0.4231E+01
15.	0.1727E-01	-0.1402E+03	0.2549E-02	-0.4780E+02	0.9135E-03	-0.2023E+02
16.	0.1322E-01	0.1453E+02	0.2328E-02	0.1101E+03	0.1813E-02	0.8354E+02
17.	0.1334E-01	0.1193E+03	0.1686E-02	0.4211E+02	0.2213E-02	0.9265E+02
18.	0.9717E-02	-0.9910E+02	0.2497E-02	0.1026E+03	0.1516E-02	0.1291E+03
19.	0.2118E-01	0.5474E+02	0.5158E-02	0.9240E+02	0.2529E-02	0.9026E+02
20.	0.1633E-01	0.1718E+03	0.1434E-03	-0.5407E+01	0.1432E-02	0.1325E+03
21.	0.8178E-02	-0.4244E+02	0.2018E-02	0.1128E+03	0.3950E-03	0.8617E+02
22.	0.2190E-01	0.6826E+02	0.4477E-02	0.5001E+02	0.2084E-02	0.1560E+01
23.	0.7228E-02	0.1591E+03	0.6085E-02	0.5570E+02	0.3073E-02	0.4867E+02
24.	0.8956E-02	-0.4498E+02	0.2882E-02	-0.1565E+03	0.1031E-02	-0.1744E+03
25.	0.8139E-02	0.9701E+02	0.2148E-02	-0.7904E+02	0.1257E-02	-0.1792E+03
26.	0.1221E-01	0.1600E+03	0.2738E-02	0.1433E+03	0.2328E-02	0.1532E+03
27.	0.5319E-02	-0.2132E+02	0.1185E-02	0.1266E+03	0.1836E-02	-0.1199E+03
28.	0.8666E-02	0.1645E+03	0.1350E-02	0.9310E+01	0.6627E-03	-0.1487E+02
29.	0.1298E-01	-0.5980E+02	0.1517E-02	-0.1536E+03	0.2907E-03	-0.7443E+02
30.	0.9862E-02	0.3729E+02	0.2098E-02	-0.2244E+02	0.9474E-03	0.7296E+02
31.	0.9371E-02	0.1388E+03	0.5680E-02	0.1405E+03	0.3116E-02	0.1614E+03
32.	0.1979E-01	-0.8588E+02	0.1013E-02	-0.4096E+02	0.1868E-02	-0.1039E+03
33.	0.8316E-02	0.1070E+03	0.2784E-02	0.1395E+03	0.7274E-03	-0.1612E+03
34.	0.9153E-02	-0.1529E+03	0.2128E-02	-0.8292E+01	0.9766E-03	-0.1678E+02
35.	0.6115E-02	-0.1479E+02	0.3450E-02	0.5449E+02	0.1122E-02	0.1295E+03
36.	0.1064E-01	0.9588E+02	0.3502E-02	-0.1077E+03	0.1424E-02	-0.1215E+03
37.	0.1112E-01	-0.1218E+03	0.1419E-02	-0.4899E+02	0.8091E-03	-0.1613E+03
38.	0.1162E-01	0.2932E+02	0.3115E-02	-0.3545E+02	0.8643E-03	-0.1029E+03
39.	0.9528E-02	0.1397E+03	0.1970E-02	0.7466E+02	0.1268E-02	0.1034E+03

TABLE XXII.- CONTINUED

BOTTOM SURFACE

	RADIUS= 0.864	CHORD= 0.500	RADIUS= 0.864	CHORD= 0.550	RADIUS= 0.864	CHORD= 0.699
HARM	AMPLITUDE	PHASE	AMPLITUDE	PHASE	AMPLITUDE	PHASE
0.	0.1314E+02	0.0000E+00	0.1334E+02	0.0000E+00	0.1357E+02	0.0000E+00
1.	0.5667E+00	-0.8717E+02	0.4573E+00	-0.8866E+02	0.2580E+00	-0.1032E+03
2.	0.1226E+00	0.6207E+01	0.9156E-01	0.4276E+01	0.5323E-01	-0.3127E+01
3.	0.3915E-01	-0.9062E+02	0.3490E-01	-0.8930E+02	0.2412E-01	-0.1118E+03
4.	0.2249E-02	0.1453E+03	0.3027E-02	0.1301E+03	0.4167E-02	0.1681E+03
5.	0.1585E-01	-0.6284E+02	0.1277E-01	-0.6477E+02	0.1113E-01	-0.8290E+02
6.	0.8654E-02	0.1867E+02	0.5265E-02	0.2009E+02	0.3353E-02	0.1192E+02
7.	0.4481E-02	-0.2967E+02	0.4552E-02	-0.5164E+02	0.3586E-02	-0.9728E+02
8.	0.3879E-02	-0.3398E+02	0.3539E-02	-0.3007E+02	0.2258E-02	-0.5996E+02
9.	0.8517E-02	-0.2335E+02	0.6680E-02	-0.3200E+02	0.5581E-02	-0.5825E+02
10.	0.7423E-02	0.7613E+02	0.5489E-02	0.6759E+02	0.3200E-02	0.5924E+02
11.	0.4339E-02	0.9894E+02	0.3564E-02	0.1005E+03	0.2770E-02	0.5931E+02
12.	0.5082E-02	-0.1747E+03	0.3986E-02	-0.1700E+03	0.4539E-02	0.1573E+03
13.	0.2101E-02	-0.8690E+02	0.2488E-02	-0.7533E+02	0.1317E-02	-0.1196E+03
14.	0.3251E-02	0.6753E+01	0.2248E-02	0.1710E+01	0.2247E-02	-0.2215E+02
15.	0.1284E-02	-0.1409E+02	0.1038E-02	-0.7027E+02	0.1560E-02	-0.9746E+02
16.	0.1444E-02	0.8553E+02	0.1513E-02	0.5622E+02	0.1515E-02	0.1499E+02
17.	0.1377E-02	0.7449E+02	0.1815E-02	0.6509E+02	0.2014E-02	0.2711E+02
18.	0.1936E-02	0.1083E+03	0.1391E-02	0.1139E+03	0.1295E-02	0.5795E+02
19.	0.3012E-02	0.6948E+02	0.3093E-02	0.8330E+02	0.2651E-02	0.5510E+02
20.	0.1140E-02	0.1485E+03	0.2179E-02	0.1510E+03	0.1110E-02	0.6059E+02
21.	0.1475E-02	0.9689E+02	0.1199E-02	0.1307E+03	0.1312E-02	0.6358E+02
22.	0.1613E-02	0.4012E+02	0.7700E-03	0.3498E+02	0.1845E-02	0.1233E+02
23.	0.3055E-02	0.3043E+02	0.3019E-02	0.1729E+02	0.2926E-02	-0.9435E+01
24.	0.3429E-03	0.3868E+02	0.6877E-03	0.1077E+03	0.1009E-02	-0.7407E+02
25.	0.2159E-03	-0.8460E+02	0.6402E-03	-0.1456E+03	0.1347E-02	-0.2723E+02
26.	0.3342E-02	0.1272E+03	0.2806E-02	0.1144E+03	0.2540E-02	0.3989E+02
27.	0.3742E-03	-0.7426E+02	0.4552E-03	-0.1681E+03	0.1763E-02	0.1128E+03
28.	0.1239E-02	-0.5040E+02	0.1689E-02	-0.2598E+02	0.1259E-02	-0.1627E+03
29.	0.9883E-03	-0.8601E+02	0.1594E-02	-0.8954E+02	0.1386E-02	-0.9194E+02
30.	0.6234E-03	-0.2250E+02	0.5953E-03	0.1722E+03	0.1534E-02	0.1183E+03
31.	0.1808E-02	0.1177E+03	0.3040E-02	0.1297E+03	0.2784E-02	0.5469E+02
32.	0.5604E-03	-0.5018E+02	0.1132E-02	-0.1358E+03	0.4954E-03	0.1703E+03
33.	0.8758E-03	-0.1100E+03	0.1308E-02	-0.1687E+03	0.7144E-03	0.1280E+03
34.	0.1192E-02	-0.1997E+02	0.4220E-03	-0.1295E+03	0.1770E-02	-0.1557E+03
35.	0.9743E-03	0.8519E+02	0.6668E-03	0.7738E+02	0.1436E-02	-0.8037E+02
36.	0.1121E-02	-0.1179E+03	0.1625E-02	-0.3955E+02	0.1739E-02	-0.6464E+02
37.	0.1222E-02	-0.1656E+03	0.1355E-02	-0.1387E+03	0.1773E-02	0.6650E+02
38.	0.1426E-02	-0.7647E+02	0.2285E-02	-0.7716E+02	0.1200E-02	0.1343E+03
39.	0.1325E-02	0.1135E+03	0.1661E-02	0.4379E+02	0.1039E-02	-0.1507E+03

TABLE XXII.- CONTINUED

BOTTOM SURFACE

RADIUS= Ø.864
CHORD= Ø.919

HARM	AMPLITUDE	PHASE
Ø.	Ø.1353E+Ø2	Ø.ØØØØE+ØØ
1.	Ø.6323E-Ø1	Ø.1448E+Ø3
2.	Ø.1512E-Ø1	-Ø.1479E+Ø3
3.	Ø.1357E-Ø1	-Ø.11Ø5E+Ø3
4.	Ø.3137E-Ø2	Ø.1426E+Ø3
5.	Ø.7444E-Ø2	-Ø.8569E+Ø2
6.	Ø.2575E-Ø2	Ø.6195E+Ø2
7.	Ø.2662E-Ø2	-Ø.1Ø24E+Ø3
8.	Ø.1246E-Ø2	-Ø.2762E+Ø2
9.	Ø.3595E-Ø2	-Ø.7767E+Ø2
1Ø.	Ø.1558E-Ø2	Ø.7279E+Ø2
11.	Ø.1375E-Ø2	Ø.4388E+Ø2
12.	Ø.344ØE-Ø2	Ø.1487E+Ø3
13.	Ø.6935E-Ø3	-Ø.1679E+Ø3
14.	Ø.1Ø8ØE-Ø2	-Ø.1975E+Ø2
15.	Ø.16Ø7E-Ø2	-Ø.914ØE+Ø2
16.	Ø.8329E-Ø3	-Ø.7736E+Ø1
17.	Ø.2185E-Ø2	Ø.9Ø37E+Ø1
18.	Ø.9199E-Ø3	Ø.2915E+Ø2
19.	Ø.2612E-Ø2	Ø.4577E+Ø2
2Ø.	Ø.9551E-Ø3	Ø.1Ø66E+Ø3
21.	Ø.19Ø4E-Ø2	Ø.8131E+Ø2
22.	Ø.38Ø4E-Ø3	Ø.639ØE+Ø2
23.	Ø.2441E-Ø2	-Ø.3117E+Ø2
24.	Ø.1716E-Ø2	-Ø.1117E+Ø3
25.	Ø.1368E-Ø2	-Ø.387ØE+Ø2
26.	Ø.165ØE-Ø2	Ø.2861E+Ø2
27.	Ø.1215E-Ø2	Ø.5658E+Ø2
28.	Ø.1284E-Ø2	Ø.7586E+Ø2
29.	Ø.1Ø16E-Ø2	-Ø.121ØE+Ø3
3Ø.	Ø.1449E-Ø2	Ø.9Ø75E+Ø2
31.	Ø.1278E-Ø2	Ø.3Ø8ØE+Ø2
32.	Ø.1721E-Ø2	-Ø.3724E+Ø2
33.	Ø.947ØE-Ø3	Ø.8Ø29E+Ø2
34.	Ø.93Ø8E-Ø3	-Ø.1Ø44E+Ø3
35.	Ø.9859E-Ø3	-Ø.1372E+Ø3
36.	Ø.1Ø2ØE-Ø2	-Ø.4413E+Ø2
37.	Ø.1546E-Ø2	Ø.4349E+Ø2
38.	Ø.1766E-Ø2	Ø.1257E+Ø3
39.	Ø.2579E-Ø3	Ø.1768E+Ø3

TABLE XXII.- CONTINUED

TOP SURFACE

HARM	RADIUS= 0.864 CHORD= 0.030 AMPLITUDE	PHASE	RADIUS= 0.864 CHORD= 0.080 AMPLITUDE	PHASE	RADIUS= 0.864 CHORD= 0.250 AMPLITUDE	PHASE
0.	0.9699E+01	0.0000E+00	0.9804E+01	0.0000E+00	0.1061E+02	0.0000E+00
1.	0.1431E+01	0.1373E+03	0.1369E+01	-0.1134E+03	0.2174E+01	-0.9183E+02
2.	0.4189E+00	-0.1610E+03	0.4023E+00	-0.4570E+02	0.1023E+01	-0.7896E+01
3.	0.3189E+00	0.1136E+03	0.3131E+00	0.6452E+02	0.7393E+00	0.8211E+02
4.	0.7625E-01	0.1037E+03	0.1703E+00	0.8103E+02	0.4124E+00	0.1691E+03
5.	0.1125E+00	0.1518E+03	0.1593E+00	0.1203E+03	0.1868E+00	-0.9957E+02
6.	0.4416E-01	0.1763E+03	0.9653E-01	0.1562E+03	0.6075E-01	0.2288E+02
7.	0.4088E-01	0.1685E+03	0.6665E-01	-0.1698E+03	0.5475E-01	-0.1231E+03
8.	0.2774E-01	0.1749E+03	0.2693E-01	-0.1379E+03	0.1364E+00	-0.1921E+01
9.	0.4537E-01	-0.1553E+03	0.2757E-01	-0.1292E+03	0.1749E+00	0.9566E+02
10.	0.3327E-01	-0.1275E+03	0.2537E-01	-0.6947E+02	0.1734E+00	-0.1701E+03
11.	0.1967E-01	-0.1435E+03	0.2445E-01	0.2178E+02	0.1132E+00	-0.6981E+02
12.	0.9298E-02	-0.1378E+03	0.2309E-01	0.8596E+02	0.5802E-01	0.4946E+02
13.	0.9830E-02	-0.9810E+02	0.1056E-01	0.1213E+03	0.5241E-01	-0.1351E+03
14.	0.9344E-02	-0.1086E+03	0.1592E-01	0.1459E+03	0.9311E-01	-0.1023E+02
15.	0.9165E-02	-0.1448E+03	0.2745E-01	-0.1658E+03	0.1142E+00	0.9842E+02
16.	0.8671E-02	-0.1337E+03	0.2071E-01	-0.1100E+03	0.1131E+00	-0.1601E+03
17.	0.5353E-02	-0.8030E+02	0.9328E-02	-0.5634E+02	0.8506E-01	-0.5783E+02
18.	0.2900E-02	0.7923E+02	0.9635E-02	-0.4320E+02	0.4711E-01	0.6949E+02
19.	0.1660E-02	0.1554E+03	0.1184E-01	-0.2158E+02	0.4916E-01	-0.1332E+03
20.	0.4129E-02	0.1643E+03	0.7323E-02	0.6692E+02	0.6054E-01	-0.1075E+02
21.	0.4767E-02	0.2810E+02	0.8787E-02	0.7427E+02	0.7427E-01	0.9823E+02
22.	0.8380E-02	-0.2343E+01	0.8015E-02	0.1215E+03	0.6390E-01	-0.1552E+03
23.	0.6056E-02	0.9682E+02	0.1347E-01	0.1549E+03	0.4125E-01	-0.4678E+02
24.	0.9045E-02	0.1368E+03	0.1104E-01	-0.1471E+03	0.3084E-01	0.8577E+02
25.	0.4613E-02	0.1179E+03	0.4800E-02	-0.1146E+02	0.2456E-01	-0.1145E+03
26.	0.3353E-02	-0.1956E+02	0.6060E-02	-0.1061E+03	0.4364E-01	0.6103E+01
27.	0.1973E-02	-0.1488E+03	0.1467E-01	-0.4279E+02	0.4815E-01	0.1147E+03
28.	0.2737E-02	-0.8058E+02	0.1184E-01	0.1726E+02	0.4402E-01	-0.1435E+03
29.	0.3728E-02	-0.6449E+02	0.8328E-02	0.6379E+02	0.3158E-01	-0.2769E+02
30.	0.4871E-02	0.4129E+02	0.2317E-02	-0.6330E+01	0.1743E-01	0.9665E+02
31.	0.8145E-02	-0.1033E+03	0.8434E-02	0.7628E+02	0.2154E-01	-0.9431E+02
32.	0.7965E-02	0.1600E+03	0.1073E-01	-0.1676E+03	0.3886E-01	0.2821E+02
33.	0.1328E-02	0.1452E+03	0.6757E-02	-0.8470E+02	0.4029E-01	0.1161E+03
34.	0.3053E-02	-0.6777E+02	0.2142E-02	-0.1587E+03	0.3816E-01	-0.1252E+03
35.	0.1278E-01	-0.8380E+02	0.1201E-01	-0.5274E+02	0.3094E-01	-0.1073E+02
36.	0.7460E-02	-0.9057E+01	0.3392E-02	-0.9142E+00	0.1539E-01	0.1159E+03
37.	0.5400E-02	-0.1030E+03	0.1530E-01	0.6037E+02	0.1249E-01	-0.6720E+02
38.	0.7743E-02	-0.6215E+02	0.3124E-02	-0.1027E+03	0.2154E-01	0.3542E+02
39.	0.1670E-01	-0.1046E+03	0.9896E-02	0.7639E+02	0.3031E-01	0.1570E+03

TABLE XXII.- CONTINUED

	TOP SURFACE					
	RADIUS= 0.864		RADIUS= 0.864		RADIUS= 0.864	
	CHORD= 0.350		CHORD= 0.400		CHORD= 0.450	
HARM	AMPLITUDE	PHASE	AMPLITUDE	PHASE	AMPLITUDE	PHASE
0.	0.1223E+02	0.0000E+00	0.1232E+02	0.0000E+00	0.1256E+02	0.0000E+00
1.	0.6528E+00	-0.9225E+02	0.3940E+00	-0.9192E+02	0.2439E+00	-0.9030E+02
2.	0.1428E+00	-0.6286E+02	0.1144E+00	-0.1106E+03	0.9393E-01	-0.1265E+03
3.	0.1095E+00	0.2436E+02	0.8020E-01	-0.2049E+02	0.6742E-01	-0.2804E+02
4.	0.8323E-01	0.8415E+02	0.9380E-01	0.3995E+02	0.7268E-01	0.2578E+02
5.	0.4889E-01	0.1788E+03	0.6742E-01	0.1132E+03	0.6026E-01	0.1084E+03
6.	0.4432E-01	-0.2115E+02	0.1800E-01	-0.1434E+03	0.2489E-01	-0.1703E+03
7.	0.6352E-01	0.8904E+02	0.1312E-01	0.9229E+02	0.2305E-02	-0.1279E+02
8.	0.5766E-01	0.1763E+03	0.1758E-01	0.1509E+03	0.4768E-02	0.1048E+03
9.	0.4139E-01	-0.8844E+02	0.9535E-02	-0.1152E+03	0.4192E-02	-0.1756E+03
10.	0.2903E-01	0.1263E+02	0.9391E-02	-0.2242E+02	0.7414E-03	0.1200E+03
11.	0.2497E-01	0.1181E+03	0.1116E-01	0.1150E+03	0.7427E-02	0.1442E+03
12.	0.8389E-02	-0.1429E+03	0.5318E-02	-0.1093E+03	0.5202E-02	-0.7355E+02
13.	0.4633E-02	0.1432E+02	0.6939E-02	-0.2719E+02	0.4543E-02	-0.1453E+02
14.	0.4247E-02	-0.1458E+03	0.7136E-02	0.2715E+02	0.8503E-03	0.4053E+02
15.	0.9528E-02	-0.4286E+02	0.1632E-02	0.4952E+02	0.2183E-02	-0.1697E+03
16.	0.5067E-02	0.9979E+02	0.5953E-02	0.1785E+03	0.2206E-02	0.1434E+03
17.	0.9446E-02	0.1548E+03	0.2063E-02	0.2855E+02	0.3391E-02	-0.1229E+03
18.	0.7116E-02	-0.1503E+03	0.3722E-02	0.9007E+02	0.7619E-03	-0.1643E+03
19.	0.8181E-02	-0.7573E+02	0.3167E-02	-0.3718E+02	0.1876E-02	-0.5052E+02
20.	0.4514E-02	0.2926E+02	0.6186E-02	-0.5892E+02	0.2413E-02	-0.7968E+02
21.	0.6816E-02	0.6814E+02	0.3543E-02	0.5374E+02	0.8669E-03	0.1313E+03
22.	0.2593E-02	0.1984E+02	0.3343E-02	0.3846E+02	0.2368E-02	-0.8960E+02
23.	0.5423E-02	-0.6997E+02	0.3187E-02	-0.1492E+03	0.1373E-02	0.1642E+03
24.	0.6324E-02	-0.2839E+02	0.1633E-02	-0.8674E+02	0.1922E-02	0.8494E+02
25.	0.3790E-02	0.2500E+02	0.1427E-01	0.1106E+03	0.2618E-02	0.1327E+03
26.	0.4011E-02	-0.5138E+02	0.5590E-02	-0.1105E+02	0.1561E-02	0.1132E+03
27.	0.4280E-02	-0.1209E+03	0.3203E-02	0.1470E+03	0.6082E-02	-0.1011E+03
28.	0.3966E-02	0.1303E+03	0.3588E-02	0.3743E+02	0.3003E-02	-0.1144E+03
29.	0.4373E-02	-0.6648E+02	0.2855E-02	0.1759E+03	0.3447E-02	-0.6628E+02
30.	0.5804E-02	0.3430E+02	0.4232E-02	0.6412E+02	0.1759E-02	-0.3175E+02
31.	0.9947E-02	0.8196E+02	0.9825E-02	0.1670E+03	0.6205E-02	-0.1515E+03
32.	0.3975E-02	-0.5310E+02	0.5681E-02	-0.1691E+03	0.3048E-02	-0.3179E+02
33.	0.1136E-02	0.1759E+03	0.6150E-02	0.9920E+02	0.4162E-02	-0.1257E+03
34.	0.6192E-02	-0.1678E+02	0.5878E-02	-0.8666E+02	0.4933E-02	0.1661E+02
35.	0.4627E-02	-0.3921E+01	0.4869E-02	0.4512E+02	0.2715E-02	0.1249E+03
36.	0.8959E-02	-0.1671E+03	0.2413E-02	0.1788E+03	0.3803E-02	-0.3663E+02
37.	0.5239E-02	-0.6219E+02	0.1117E-01	-0.5836E+02	0.3467E-02	0.9686E+02
38.	0.4206E-02	-0.4433E+02	0.4790E-02	-0.4643E+02	0.3675E-02	0.5751E+01
39.	0.2909E-02	0.1393E+03	0.6641E-02	0.1470E+02	0.4611E-02	-0.2845E+02

TABLE XXII.- CONTINUED

TOP SURFACE

HARM	RADIUS= 0.864 CHORD= 0.500 AMPLITUDE	PHASE	RADIUS= 0.864 CHORD= 0.550 AMPLITUDE	PHASE	RADIUS= 0.864 CHORD= 0.599 AMPLITUDE	PHASE
0.	0.1274E+02	0.0000E+00	0.1298E+02	0.0000E+00	0.1310E+02	0.0000E+00
1.	0.1971E+00	-0.8562E+02	0.1369E+00	-0.7811E+02	0.1003E+00	-0.8059E+02
2.	0.7747E-01	-0.1269E+03	0.7020E-01	-0.1264E+03	0.7799E-01	-0.1264E+03
3.	0.5318E-01	-0.2439E+02	0.4522E-01	-0.2038E+02	0.4401E-01	-0.1727E+02
4.	0.5910E-01	0.2428E+02	0.4525E-01	0.2458E+02	0.3547E-01	0.1775E+02
5.	0.4878E-01	0.1077E+03	0.3668E-01	0.1015E+03	0.2902E-01	0.9310E+02
6.	0.1959E-01	-0.1734E+03	0.1244E-01	0.1701E+03	0.9848E-02	0.1588E+03
7.	0.2564E-02	-0.1103E+03	0.1183E-02	0.3497E+02	0.2702E-02	0.7379E+02
8.	0.4748E-02	0.7266E+02	0.3799E-02	0.6348E+02	0.4712E-02	0.5229E+02
9.	0.3996E-02	0.1284E+03	0.5288E-02	0.1390E+03	0.3290E-02	0.1479E+03
10.	0.2878E-02	0.1497E+03	0.4847E-02	0.1639E+03	0.3778E-02	-0.1178E+03
11.	0.6099E-02	0.1605E+03	0.3334E-02	0.1363E+03	0.4299E-02	0.1340E+03
12.	0.3685E-02	-0.9049E+02	0.5292E-02	-0.6880E+02	0.2632E-02	-0.4526E+02
13.	0.3021E-02	0.1591E+02	0.1207E-02	-0.4591E+02	0.4455E-02	0.1346E+02
14.	0.1119E-02	0.2201E+02	0.1947E-02	0.9041E+02	0.2718E-02	0.3144E+02
15.	0.1392E-02	0.2794E+02	0.3335E-02	-0.6505E+02	0.1440E-02	0.8578E+02
16.	0.2813E-02	0.1565E+03	0.1227E-02	-0.1672E+03	0.3074E-02	-0.1624E+03
17.	0.6802E-03	0.1499E+03	0.2282E-02	-0.5681E+02	0.4282E-02	-0.1525E+03
18.	0.1425E-02	0.1380E+03	0.2967E-02	0.1634E+03	0.1107E-02	-0.1336E+03
19.	0.8478E-03	-0.6321E+02	0.4060E-02	-0.1255E+03	0.3446E-02	-0.1101E+03
20.	0.1781E-02	-0.9570E+02	0.3401E-02	-0.7112E+02	0.2412E-02	-0.5423E+02
21.	0.1078E-02	0.1452E+02	0.2168E-02	0.1078E+03	0.2578E-02	0.1126E+03
22.	0.6486E-03	-0.3162E+02	0.2675E-02	0.4157E+02	0.2385E-02	-0.8653E+02
23.	0.2210E-02	-0.7370E+02	0.1079E-02	0.7884E+02	0.2293E-02	0.1754E+03
24.	0.5038E-03	0.1107E+03	0.1274E-02	-0.4497E+02	0.4702E-02	0.4153E+02
25.	0.2685E-02	0.8557E+02	0.3243E-02	0.1132E+03	0.2750E-02	0.1137E+03
26.	0.2365E-02	0.1044E+03	0.1382E-02	0.1752E+03	0.2325E-02	0.7215E+02
27.	0.1343E-02	-0.7573E+02	0.2859E-02	-0.1412E+03	0.3661E-02	-0.1488E+03
28.	0.1554E-02	0.7585E+01	0.1660E-02	0.1445E+03	0.3217E-02	-0.1121E+03
29.	0.2392E-02	-0.2381E+02	0.3144E-03	0.8702E+02	0.2986E-02	-0.9278E+02
30.	0.1843E-02	0.7021E+02	0.1843E-02	-0.4149E+01	0.2616E-03	0.1773E+02
31.	0.3235E-02	-0.4767E+02	0.1859E-02	-0.6450E+02	0.2257E-02	0.1003E+03
32.	0.2083E-02	-0.7984E+02	0.2477E-02	-0.1866E+02	0.5370E-02	-0.6416E+00
33.	0.2407E-02	-0.1201E+03	0.2249E-02	-0.1595E+03	0.1923E-02	0.1766E+03
34.	0.1303E-02	-0.5987E+02	0.1856E-02	-0.5767E+02	0.4233E-02	-0.2717E+02
35.	0.2131E-02	-0.2166E+02	0.4005E-02	0.5740E+02	0.3015E-02	0.1250E+02
36.	0.4757E-02	-0.1547E+03	0.2005E-02	-0.1592E+03	0.3367E-02	-0.1717E+03
37.	0.1308E-02	-0.7825E+02	0.2390E-02	-0.8166E+02	0.4343E-02	-0.9933E+02
38.	0.1121E-02	0.5681E+02	0.4297E-02	0.2670E+02	0.2627E-02	-0.1500E+02
39.	0.1128E-02	0.7990E+02	0.2300E-02	-0.9954E+01	0.5716E-02	0.1492E+02

ORIGINAL PAGE IS
OF POOR QUALITY

TABLE XXII.- CONTINUED

			TOP SURFACE	
	RADIUS= Ø.864		RADIUS= Ø.864	
	CHORD= Ø.699		CHORD= Ø.919	
HARM	AMPLITUDE	PHASE	AMPLITUDE	PHASE
Ø.	Ø.13ØØE+Ø2	Ø.ØØØØE+ØØ	Ø.1376E+Ø2	Ø.ØØØØE+ØØ
1.	Ø.7338E-Ø1	-Ø.5966E+Ø2	Ø.1918E+ØØ	Ø.9217E+Ø2
2.	Ø.7Ø9ØE-Ø1	-Ø.1432E+Ø3	Ø.7378E-Ø1	-Ø.1516E+Ø3
3.	Ø.3421E-Ø1	-Ø.2438E+Ø2	Ø.2382E-Ø1	-Ø.26Ø3E+Ø2
4.	Ø.2754E-Ø1	Ø.8874E+Ø1	Ø.116ØE-Ø1	Ø.3Ø91E+Ø2
5.	Ø.1724E-Ø1	Ø.8552E+Ø2	Ø.9665E-Ø2	Ø.6156E+Ø2
6.	Ø.4466E-Ø2	Ø.1439E+Ø3	Ø.6157E-Ø2	Ø.4474E+Ø2
7.	Ø.3347E-Ø2	Ø.1261E+Ø3	Ø.4661E-Ø2	Ø.7Ø25E+Ø2
8.	Ø.1637E-Ø2	Ø.1156E+Ø3	Ø.13Ø7E-Ø2	Ø.78Ø1E+Ø2
9.	Ø.2355E-Ø2	Ø.1Ø24E+Ø3	Ø.3518E-Ø2	-Ø.1386E+Ø3
1Ø.	Ø.2217E-Ø2	-Ø.1771E+Ø3	Ø.271ØE-Ø2	-Ø.7838E+Ø2
11.	Ø.2Ø59E-Ø2	Ø.1499E+Ø3	Ø.3476E-Ø2	Ø.5666E+Ø2
12.	Ø.2311E-Ø2	-Ø.8875E+Ø2	Ø.3246E-Ø2	-Ø.3627E+Ø2
13.	Ø.2252E-Ø2	Ø.5956E+Ø2	Ø.3982E-Ø2	Ø.1482E+Ø2
14.	Ø.125ØE-Ø2	Ø.4Ø37E+Ø2	Ø.5313E-Ø3	-Ø.2724E+Ø2
15.	Ø.7396E-Ø3	Ø.3844E+Ø2	Ø.1799E-Ø2	-Ø.1812E+Ø1
16.	Ø.1634E-Ø2	-Ø.1772E+Ø3	Ø.38ØØE-Ø2	Ø.1518E+Ø3
17.	Ø.9816E-Ø3	-Ø.8419E+Ø2	Ø.5271E-Ø2	-Ø.1Ø57E+Ø3
18.	Ø.318ØE-Ø2	Ø.5893E+Ø2	Ø.1617E-Ø2	-Ø.1659E+Ø3
19.	Ø.1849E-Ø2	Ø.1657E+Ø3	Ø.3783E-Ø2	-Ø.2584E+Ø2
2Ø.	Ø.1397E-Ø3	Ø.6165E+Ø2	Ø.2655E-Ø2	-Ø.1299E+Ø3
21.	Ø.116ØE-Ø2	Ø.1218E+Ø3	Ø.28Ø4E-Ø2	Ø.4451E+Ø2
22.	Ø.4685E-Ø3	-Ø.4117E+Ø2	Ø.2Ø33E-Ø2	-Ø.1749E+Ø3
23.	Ø.6833E-Ø3	Ø.9714E+Ø2	Ø.2491E-Ø2	-Ø.8943E+Ø2
24.	Ø.1833E-Ø2	-Ø.5292E+Ø2	Ø.1287E-Ø2	Ø.8693E+Ø2
25.	Ø.2196E-Ø2	Ø.136ØE+Ø3	Ø.4Ø18E-Ø2	Ø.217ØE+Ø2
26.	Ø.1Ø66E-Ø2	Ø.1Ø77E+Ø3	Ø.139ØE-Ø2	Ø.2217E+Ø2
27.	Ø.938ØE-Ø3	-Ø.1ØØ9E+Ø3	Ø.1517E-Ø2	Ø.1368E+Ø2
28.	Ø.127ØE-Ø2	-Ø.8Ø58E+Ø2	Ø.1393E-Ø2	Ø.1363E+Ø3
29.	Ø.9227E-Ø3	Ø.1793E+Ø3	Ø.1416E-Ø2	-Ø.1189E+Ø3
3Ø.	Ø.1173E-Ø2	Ø.467ØE+Ø2	Ø.3685E-Ø3	Ø.8712E+Ø2
31.	Ø.8533E-Ø3	-Ø.1299E+Ø3	Ø.3156E-Ø2	Ø.9988E+Ø2
32.	Ø.1133E-Ø2	Ø.1728E+Ø3	Ø.823ØE-Ø3	Ø.599ØE+Ø2
33.	Ø.9Ø89E-Ø3	-Ø.13Ø2E+Ø3	Ø.8299E-Ø2	Ø.1293E+Ø3
34.	Ø.22Ø5E-Ø2	-Ø.5561E+Ø2	Ø.3451E-Ø2	Ø.9375E+Ø2
35.	Ø.1254E-Ø2	Ø.2696E+Ø2	Ø.2294E-Ø2	Ø.1427E+Ø2
36.	Ø.1525E-Ø2	-Ø.6368E+Ø2	Ø.7187E-Ø2	Ø.173ØE+Ø3
37.	Ø.1578E-Ø2	-Ø.1Ø66E+Ø3	Ø.3827E-Ø2	Ø.6438E+Ø2
38.	Ø.7342E-Ø3	Ø.281ØE+Ø2	Ø.96Ø2E-Ø2	-Ø.6969E+Ø2
39.	Ø.7822E-Ø3	-Ø.1664E+Ø3	Ø.2132E-Ø2	Ø.1633E+Ø2

TABLE XXII.- CONTINUED

BOTTOM SURFACE

	RADIUS= 0.910 CHORD= 0.150		RADIUS= 0.910 CHORD= 0.200		RADIUS= 0.910 CHORD= 0.350	
HARM	AMPLITUDE	PHASE	AMPLITUDE	PHASE	AMPLITUDE	PHASE
0.	0.1231E+02	0.0000E+00	0.1257E+02	0.0000E+00	0.1300E+02	0.0000E+00
1.	0.2244E+01	-0.7145E+02	0.2410E+01	-0.7403E+02	0.1125E+01	-0.8166E+02
2.	0.6270E+00	0.3760E+02	0.7976E+00	0.3150E+02	0.1956E+00	0.5622E+01
3.	0.1775E+00	-0.1467E+03	0.2190E+00	0.1683E+03	0.8028E-01	-0.2558E+02
4.	0.1259E+00	-0.6197E+02	0.1592E+00	-0.7599E+02	0.6137E-01	0.9183E+02
5.	0.8715E-01	0.6124E+01	0.1041E+00	0.3648E+02	0.4981E-01	-0.1395E+03
6.	0.4210E-01	0.8403E+02	0.6726E-01	-0.1751E+03	0.4079E-01	-0.3348E+02
7.	0.1405E-01	-0.1631E+03	0.8633E-01	-0.3839E+02	0.2115E-01	0.7246E+02
8.	0.3142E-01	-0.7663E+02	0.7291E-01	0.7660E+02	0.1911E-01	-0.1562E+03
9.	0.4846E-01	-0.2583E+01	0.4719E-01	-0.1456E+03	0.2382E-01	-0.3160E+02
10.	0.4672E-01	0.9424E+02	0.3658E-01	-0.1055E+02	0.1780E-01	0.7211E+02
11.	0.3544E-01	0.1738E+03	0.4073E-01	0.1105E+03	0.8648E-02	0.1469E+03
12.	0.2796E-01	-0.8185E+02	0.2869E-01	-0.1156E+03	0.4761E-02	-0.1386E+03
13.	0.2366E-01	0.2938E+02	0.2718E-01	0.4727E+02	0.2159E-02	-0.2318E+02
14.	0.1278E-01	0.1147E+03	0.2727E-01	-0.1645E+03	0.3837E-02	-0.3562E+02
15.	0.9081E-02	-0.1361E+03	0.4109E-01	-0.3370E+02	0.4984E-02	-0.3120E+01
16.	0.6405E-02	-0.9264E+02	0.4294E-01	0.9533E+02	0.5062E-02	0.1052E+03
17.	0.1289E-01	0.9651E+01	0.3882E-01	-0.1413E+03	0.2494E-02	-0.1525E+03
18.	0.1746E-01	0.1102E+03	0.3261E-01	-0.1336E+02	0.9271E-03	0.1004E+02
19.	0.1594E-01	-0.1473E+03	0.3289E-01	0.1104E+03	0.2320E-02	0.9763E+02
20.	0.1564E-01	-0.2998E+02	0.2809E-01	-0.1054E+03	0.1082E-02	-0.1087E+03
21.	0.1925E-01	0.8518E+02	0.2353E-01	0.3875E+02	0.2345E-03	-0.1761E+03
22.	0.2389E-02	0.1415E+03	0.2047E-01	0.1529E+03	0.2007E-02	0.7332E+02
23.	0.5396E-02	0.4932E+02	0.1570E-01	-0.2914E+02	0.1462E-02	0.2782E+02
24.	0.1119E-01	-0.1267E+03	0.1532E-01	0.9977E+02	0.1825E-02	-0.1394E+02
25.	0.1782E-01	-0.1002E+02	0.2055E-01	-0.1015E+03	0.4090E-03	0.4188E+02
26.	0.2650E-01	0.1144E+03	0.2145E-01	0.3182E+02	0.1882E-02	-0.1796E+03
27.	0.2001E-01	-0.1192E+03	0.2697E-01	0.1499E+03	0.8243E-03	-0.2031E+01
28.	0.1709E-01	-0.5212E+01	0.2767E-01	-0.7700E+02	0.2610E-03	0.1352E+03
29.	0.1241E-01	0.1515E+03	0.2313E-01	0.4710E+02	0.1227E-02	-0.9373E+02
30.	0.1129E-01	-0.6351E+02	0.1946E-01	-0.1773E+03	0.1352E-02	0.4451E+02
31.	0.1358E-01	0.8489E+02	0.1524E-01	-0.3253E+02	0.1844E-02	0.1777E+03
32.	0.1415E-01	-0.1228E+03	0.1358E-01	0.9387E+02	0.2024E-02	-0.4290E+02
33.	0.1753E-01	0.6947E+01	0.1647E-01	-0.1087E+03	0.7645E-03	0.1142E+03
34.	0.2075E-01	0.1228E+03	0.1668E-01	0.4491E+02	0.7429E-03	-0.1675E+03
35.	0.1963E-01	-0.9174E+02	0.1725E-01	-0.1711E+03	0.2603E-03	-0.1435E+03
36.	0.1153E-01	0.1531E+02	0.1856E-01	-0.2342E+02	0.1313E-02	0.1587E+03
37.	0.4657E-02	-0.1729E+03	0.1974E-01	0.1133E+03	0.1722E-02	-0.8910E+02
38.	0.9612E-02	-0.1975E+02	0.2080E-01	-0.1184E+03	0.6681E-03	-0.9088E+02
39.	0.4615E-02	0.1341E+03	0.1798E-01	0.2234E+02	0.5771E-03	-0.7866E+02

TABLE XXII.- CONTINUED

BOTTOM SURFACE

HARM	RADIUS= 0.910 CHORD= 0.010 AMPLITUDE	PHASE	RADIUS= 0.910 CHORD= 0.030 AMPLITUDE	PHASE	RADIUS= 0.910 CHORD= 0.080 AMPLITUDE	PHASE
0.	0.1523E+02	0.0000E+00	0.1378E+02	0.0000E+00	0.1214E+02	0.0000E+00
1.	0.7922E+00	0.4678E+02	0.1523E+01	-0.5300E+02	0.2702E+01	-0.6748E+02
2.	0.5912E+00	0.8083E+02	0.4448E+00	0.7214E+02	0.7187E+00	0.4903E+02
3.	0.3669E+00	-0.7870E+02	0.3914E+00	-0.7926E+02	0.3055E+00	-0.1143E+03
4.	0.1104E+00	-0.2138E+01	0.1090E+00	-0.3463E+01	0.1677E+00	-0.2088E+02
5.	0.9639E-01	-0.3274E+02	0.8508E-01	-0.3576E+02	0.2806E-01	0.3597E+02
6.	0.4606E-01	0.3149E+02	0.5638E-01	0.2336E+02	0.4663E-01	-0.2218E+02
7.	0.2172E-01	0.2668E+02	0.1754E-01	0.3739E+02	0.4301E-01	0.5789E+02
8.	0.1421E-01	0.2293E+02	0.1748E-01	-0.1266E+02	0.2446E-01	-0.1145E+03
9.	0.1131E-01	0.1085E+02	0.2187E-01	0.2385E+02	0.4729E-01	0.1584E+01
10.	0.9051E-02	0.1014E+03	0.1103E-01	0.1021E+03	0.3554E-01	0.1158E+03
11.	0.1274E-01	0.1122E+03	0.1608E-01	0.8067E+02	0.5567E-02	-0.1237E+03
12.	0.9914E-02	0.1612E+03	0.1288E-01	0.1622E+03	0.1264E-01	0.8686E+02
13.	0.2760E-02	0.1461E+03	0.1089E-02	-0.1767E+03	0.1032E-01	-0.1767E+03
14.	0.2714E-02	0.5122E+02	0.3601E-02	0.1483E+02	0.1415E-01	-0.3195E+02
15.	0.2061E-02	-0.1288E+01	0.2803E-02	-0.4692E+02	0.8190E-02	0.7388E+02
16.	0.4736E-02	0.1094E+03	0.1897E-02	0.1481E+03	0.4409E-02	0.1642E+03
17.	0.1694E-02	0.9204E+02	0.1897E-02	0.1799E+03	0.3928E-02	0.1035E+03
18.	0.2688E-02	0.1571E+03	0.6456E-02	0.1464E+03	0.1115E-01	-0.1738E+03
19.	0.1197E-02	0.1200E+03	0.2083E-02	0.2186E+02	0.1106E-01	-0.1646E+02
20.	0.4120E-02	0.8557E+02	0.1726E-02	0.1074E+03	0.1392E-01	0.9862E+02
21.	0.6517E-02	0.6233E+02	0.8503E-02	0.1198E+03	0.5613E-02	0.1530E+03
22.	0.6527E-02	0.8268E+02	0.5258E-02	0.9616E+02	0.1091E-01	0.5124E+02
23.	0.5557E-02	0.3576E+02	0.6121E-02	-0.6541E+01	0.8915E-02	0.7429E+02
24.	0.4423E-02	-0.1384E+03	0.3623E-02	-0.6759E+02	0.1033E-01	-0.1042E+03
25.	0.1902E-02	-0.1047E+03	0.3962E-02	-0.1055E+03	0.4111E-02	0.5484E+02
26.	0.3115E-02	0.8456E+02	0.4257E-02	0.9975E+02	0.5530E-02	-0.1668E+03
27.	0.3447E-02	-0.1651E+02	0.8989E-03	-0.1983E+02	0.3256E-02	0.7707E+02
28.	0.1375E-02	-0.1610E+03	0.2951E-02	-0.1108E+03	0.5829E-02	0.1742E+03
29.	0.2505E-02	-0.3973E+02	0.2229E-03	0.1368E+03	0.6322E-02	-0.6815E+02
30.	0.5755E-02	0.1338E+02	0.8130E-02	0.5161E+01	0.5573E-02	0.3666E+02
31.	0.1092E-02	0.1590E+03	0.2079E-02	0.5271E+02	0.5637E-02	-0.1775E+03
32.	0.4221E-02	-0.1961E+02	0.3927E-02	0.3522E+02	0.1017E-01	-0.7566E+01
33.	0.2217E-02	-0.8803E+01	0.7755E-02	0.3503E+01	0.8529E-02	0.1423E+03
34.	0.3805E-02	-0.3417E+02	0.2545E-02	-0.3036E+01	0.4739E-02	-0.1089E+03
35.	0.2574E-02	-0.6822E+02	0.3725E-02	-0.9868E+02	0.4351E-02	0.1097E+03
36.	0.4222E-02	0.8383E+01	0.4203E-02	0.4622E+02	0.2435E-02	-0.1235E+03
37.	0.1660E-02	0.7484E+02	0.4185E-02	0.1689E+03	0.3166E-02	0.2485E+02
38.	0.2672E-02	-0.1043E+03	0.1956E-02	0.4538E+01	0.7100E-02	0.1732E+03
39.	0.1219E-02	0.1314E+03	0.2062E-02	-0.1589E+03	0.7237E-02	-0.5263E+02

TABLE XXII.- CONTINUED

BOTTOM SURFACE

HARM	RADIUS= 0.910 CHORD= 0.400 AMPLITUDE	PHASE	RADIUS= 0.910 CHORD= 0.450 AMPLITUDE	PHASE	RADIUS= 0.910 CHORD= 0.500 AMPLITUDE	PHASE
0.	0.1349E+02	0.0000E+00	0.1318E+02	0.0000E+00	0.1352E+02	0.0000E+00
1.	0.8956E+00	-0.8288E+02	0.6512E+00	-0.8501E+02	0.5226E+00	-0.8792E+02
2.	0.1381E+00	0.3504E+01	0.8843E-01	0.6563E+01	0.6344E-01	0.4083E+01
3.	0.7102E-01	-0.4647E+02	0.4744E-01	-0.5088E+02	0.4437E-01	-0.6464E+02
4.	0.3952E-01	0.8475E+02	0.2543E-01	0.8592E+02	0.1791E-01	0.8614E+02
5.	0.2802E-01	-0.1368E+03	0.1951E-01	-0.1307E+03	0.1520E-01	-0.1211E+03
6.	0.2602E-01	-0.3801E+02	0.1513E-01	-0.3852E+02	0.1202E-01	-0.3552E+02
7.	0.1296E-01	0.4599E+02	0.1823E-02	0.2018E+02	0.3131E-02	-0.1877E+01
8.	0.1003E-01	-0.1546E+03	0.7927E-02	-0.1391E+03	0.5454E-02	-0.1421E+03
9.	0.1685E-01	-0.3525E+02	0.1473E-01	-0.3838E+02	0.1101E-01	-0.3668E+02
10.	0.1238E-01	0.6179E+02	0.9049E-02	0.6135E+02	0.7669E-02	0.5559E+02
11.	0.8036E-02	0.1196E+03	0.6755E-02	0.1020E+03	0.4846E-02	0.9501E+02
12.	0.6107E-02	-0.1507E+03	0.5175E-02	-0.1663E+03	0.3997E-02	-0.1758E+03
13.	0.3382E-02	-0.3888E+02	0.3761E-02	-0.4334E+02	0.2252E-02	-0.6458E+02
14.	0.2972E-02	-0.2229E+02	0.3056E-02	-0.7176E+01	0.2159E-02	-0.2037E+02
15.	0.3527E-02	-0.1763E+02	0.3970E-02	-0.3160E+02	0.3177E-02	-0.3076E+02
16.	0.3257E-02	0.8597E+02	0.2641E-02	0.6753E+02	0.2516E-02	0.5431E+02
17.	0.1763E-02	0.1335E+03	0.1247E-02	0.8289E+02	0.1303E-02	0.9353E+02
18.	0.1310E-02	0.1205E+03	0.3011E-02	0.1171E+03	0.1738E-02	0.1033E+03
19.	0.1831E-02	0.8486E+02	0.2273E-02	0.1091E+03	0.1711E-02	0.1018E+03
20.	0.1202E-02	-0.1333E+03	0.1568E-02	-0.8348E+02	0.1640E-02	-0.1110E+03
21.	0.9180E-03	0.9286E+02	0.2645E-02	0.1220E+03	0.5272E-03	0.1008E+03
22.	0.4290E-03	0.4968E+02	0.1226E-02	0.1316E+03	0.1314E-02	0.1251E+03
23.	0.1468E-02	0.2760E+02	0.2756E-02	0.1324E+02	0.9043E-03	0.1602E+02
24.	0.1067E-02	0.8964E+01	0.1860E-02	0.1916E+02	0.1795E-02	0.5454E+01
25.	0.7275E-03	0.6829E+02	0.1317E-02	-0.3012E+01	0.8652E-03	0.6207E+02
26.	0.2384E-02	0.1459E+03	0.1228E-02	0.1409E+03	0.1227E-02	0.1622E+03
27.	0.8469E-03	0.5646E+02	0.1375E-02	0.1089E+03	0.8298E-03	0.1199E+02
28.	0.6458E-03	-0.1563E+03	0.1554E-02	-0.1588E+03	0.8930E-03	0.1283E+03
29.	0.1283E-02	-0.6886E+02	0.1632E-02	-0.8441E+02	0.8278E-03	-0.1163E+03
30.	0.1976E-02	0.2371E+02	0.2241E-02	0.2996E+02	0.1235E-02	0.2283E+02
31.	0.1873E-02	0.1521E+03	0.3190E-02	0.1420E+03	0.1788E-02	0.1531E+03
32.	0.1083E-02	-0.4205E+02	0.2418E-02	-0.5672E+02	0.1079E-02	-0.3344E+02
33.	0.7810E-03	0.1777E+03	0.6861E-03	0.1334E+03	0.6603E-03	-0.1476E+03
34.	0.6921E-03	-0.1704E+03	0.1808E-02	0.1518E+03	0.2023E-03	-0.6485E+02
35.	0.5484E-03	-0.1377E+03	0.5594E-03	-0.1211E+03	0.7822E-03	-0.1603E+03
36.	0.4441E-03	0.5712E+02	0.1332E-02	0.1262E+03	0.7493E-03	0.1223E+03
37.	0.1274E-02	-0.1304E+03	0.9979E-03	-0.1116E+03	0.1023E-02	-0.1318E+03
38.	0.2155E-02	-0.8836E+02	0.1575E-02	-0.1287E+03	0.1724E-02	-0.9817E+02
39.	0.1206E-02	-0.6336E+02	0.1662E-02	-0.8002E+02	0.1379E-02	-0.5559E+02

TABLE XXII.- CONTINUED

	BOTTOM SURFACE					
	RADIUS= 0.910		RADIUS= 0.910		RADIUS= 0.910	
	CHORD= 0.550		CHORD= 0.599		CHORD= 0.699	
HARM	AMPLITUDE	PHASE	AMPLITUDE	PHASE	AMPLITUDE	PHASE
0.	0.1320E+02	0.0000E+00	0.1357E+02	0.0000E+00	0.1348E+02	0.0000E+00
1.	0.4525E+00	-0.9148E+02	0.3290E+00	-0.9341E+02	0.1908E+00	-0.1112E+03
2.	0.5516E-01	-0.1528E+01	0.3433E-01	-0.1136E+02	0.1287E-01	-0.2956E+02
3.	0.4799E-01	-0.7774E+02	0.4429E-01	-0.9137E+02	0.2851E-01	-0.9799E+02
4.	0.1363E-01	0.8603E+02	0.7641E-02	0.1110E+03	0.8248E-02	0.1234E+03
5.	0.1308E-01	-0.1092E+03	0.9551E-02	-0.9303E+02	0.1043E-01	-0.1044E+03
6.	0.9218E-02	-0.2989E+02	0.8409E-02	-0.4562E+02	0.4938E-02	-0.4015E+02
7.	0.4807E-02	-0.1427E+02	0.7275E-02	-0.2847E+02	0.3893E-02	-0.6993E+02
8.	0.1566E-02	-0.1161E+03	0.1732E-02	-0.8977E+02	0.1358E-02	-0.1233E+03
9.	0.8477E-02	-0.3757E+02	0.6059E-02	-0.4918E+02	0.6090E-02	-0.6149E+02
10.	0.5645E-02	0.4964E+02	0.4503E-02	0.4467E+02	0.4054E-02	0.4122E+02
11.	0.3286E-02	0.8624E+02	0.3157E-02	0.6879E+02	0.2558E-02	0.4553E+02
12.	0.4144E-02	-0.1751E+03	0.2144E-02	0.1778E+03	0.2468E-02	0.1524E+03
13.	0.2062E-02	-0.1063E+03	0.1083E-02	-0.9968E+02	0.1253E-02	-0.1248E+03
14.	0.2178E-02	-0.2482E+02	0.1458E-02	-0.1775E+02	0.1289E-02	-0.3000E+02
15.	0.1491E-02	-0.3734E+02	0.1772E-02	-0.8654E+02	0.1745E-02	-0.8520E+02
16.	0.1835E-02	0.2832E+02	0.1753E-02	0.2061E+02	0.1424E-02	0.9629E+01
17.	0.1694E-02	0.8372E+02	0.2351E-02	0.6283E+02	0.1541E-02	0.3131E+02
18.	0.3653E-03	0.5107E+02	0.1112E-02	0.5862E+02	0.1425E-02	0.3809E+02
19.	0.1411E-02	0.1019E+03	0.2319E-02	0.6799E+02	0.1496E-02	0.5585E+02
20.	0.1222E-02	-0.1481E+03	0.1530E-02	0.1630E+03	0.1009E-02	0.1265E+03
21.	0.7685E-03	-0.3099E+02	0.4119E-03	0.1167E+03	0.8352E-03	0.1340E+03
22.	0.3841E-03	0.3469E+02	0.2674E-03	-0.1227E+03	0.3839E-03	0.1280E+03
23.	0.9159E-03	-0.6178E+02	0.6070E-03	-0.5576E+02	0.2846E-03	-0.7611E+02
24.	0.2246E-02	-0.3801E+02	0.1113E-02	-0.6366E+02	0.2079E-02	-0.7254E+02
25.	0.1844E-02	0.4176E+02	0.1417E-02	-0.2393E+02	0.1138E-02	0.6789E+01
26.	0.1395E-02	0.1295E+03	0.1403E-02	0.9312E+02	0.1064E-02	0.8056E+02
27.	0.5711E-03	0.1452E+01	0.1419E-03	0.4848E+02	0.5126E-03	0.1461E+03
28.	0.1032E-02	0.1373E+03	0.6239E-03	0.9651E+02	0.7409E-03	0.7510E+02
29.	0.1228E-02	-0.9991E+02	0.3388E-03	0.1770E+03	0.4663E-03	0.1680E+03
30.	0.7358E-03	0.1713E+01	0.4271E-03	0.2857E+00	0.7113E-03	-0.1339E+03
31.	0.2060E-02	0.1465E+03	0.1261E-02	0.9959E+02	0.1338E-02	0.5594E+02
32.	0.1313E-02	-0.1044E+03	0.6697E-03	-0.1216E+03	0.7899E-03	-0.1527E+03
33.	0.1148E-02	-0.1173E+03	0.7166E-03	0.1699E+03	0.3981E-03	0.1249E+03
34.	0.1033E-02	-0.4080E+02	0.8688E-03	-0.4968E+02	0.3570E-03	-0.1153E+03
35.	0.5934E-03	0.1721E+03	0.1229E-02	0.1029E+03	0.5507E-03	0.2366E+02
36.	0.2401E-03	-0.3893E+02	0.2516E-03	-0.1119E+03	0.6475E-03	0.8045E+02
37.	0.6397E-03	0.1764E+03	0.6311E-03	-0.1605E+03	0.6563E-03	0.1612E+03
38.	0.1555E-02	-0.1527E+03	0.8832E-03	0.1627E+03	0.3474E-03	-0.1634E+03
39.	0.1043E-02	-0.5695E+02	0.6870E-03	-0.1390E+03	0.8208E-03	0.1528E+03

TABLE XXII.- CONTINUED

TOP SURFACE

HARM	RADIUS= 0.910 CHORD= 0.010 AMPLITUDE	PHASE	RADIUS= 0.910 CHORD= 0.030 AMPLITUDE	PHASE	RADIUS= 0.910 CHORD= 0.080 AMPLITUDE	PHASE
0.	0.9591E+01	0.0000E+00	0.8903E+01	0.0000E+00	0.9345E+01	0.0000E+00
1.	0.5206E+01	0.1188E+03	0.1739E+01	0.1392E+03	0.1399E+01	-0.1149E+03
2.	0.8110E+00	0.1182E+03	0.5445E+00	-0.1741E+03	0.2378E+00	-0.4300E+02
3.	0.7604E+00	0.8951E+02	0.3952E+00	0.1209E+03	0.1224E+00	0.5992E+02
4.	0.3056E+00	0.8431E+02	0.1591E+00	0.1142E+03	0.2016E+00	0.1337E+02
5.	0.2365E+00	0.1219E+03	0.1701E+00	0.1439E+03	0.1682E+00	0.8468E+02
6.	0.1259E+00	0.1151E+03	0.6958E-01	0.1470E+03	0.6243E-01	0.1462E+03
7.	0.9757E-01	0.1118E+03	0.8037E-01	0.1503E+03	0.4284E-01	0.1160E+03
8.	0.4552E-01	0.8665E+02	0.6014E-01	0.1468E+03	0.5333E-01	0.1465E+03
9.	0.4726E-01	-0.1728E+03	0.5966E-01	0.1626E+03	0.3079E-01	-0.1595E+03
10.	0.3970E-01	0.1642E+03	0.2988E-01	0.1528E+03	0.1480E-01	-0.1584E+03
11.	0.1183E-01	0.8068E+02	0.2047E-01	0.1319E+03	0.2645E-01	-0.1433E+03
12.	0.2458E-01	-0.4389E+02	0.1716E-01	0.6625E+02	0.2781E-01	-0.4248E+02
13.	0.1569E-01	-0.1193E+03	0.1307E-01	0.3477E+02	0.1599E-01	0.3627E+02
14.	0.1334E-01	0.1378E+03	0.1083E-01	-0.1306E+02	0.3771E-02	-0.3087E+02
15.	0.1211E-01	0.1060E+02	0.1157E-01	-0.4340E+02	0.6444E-02	0.3510E+02
16.	0.1822E-01	-0.6239E+02	0.1088E-01	-0.6171E+02	0.7954E-02	0.1359E+03
17.	0.1474E-01	-0.1008E+03	0.1164E-01	-0.8717E+02	0.7395E-02	-0.1112E+03
18.	0.2704E-02	-0.6543E+02	0.1351E-01	-0.1082E+03	0.5119E-02	0.9161E+01
19.	0.6627E-02	-0.8290E+01	0.1171E-01	-0.1304E+03	0.6145E-02	-0.1644E+03
20.	0.6400E-02	-0.8607E+02	0.1725E-01	-0.1614E+03	0.7919E-02	-0.9630E+02
21.	0.6989E-02	-0.9241E+02	0.1376E-01	0.1734E+03	0.5351E-02	0.8657E+02
22.	0.7628E-02	-0.1344E+03	0.1371E-01	0.1572E+03	0.3273E-02	-0.5177E+02
23.	0.3467E-02	0.1377E+03	0.1251E-01	0.1244E+03	0.9581E-02	0.4365E+02
24.	0.5680E-02	0.7352E+02	0.1037E-01	0.1090E+03	0.7410E-02	0.9334E+02
25.	0.5820E-02	-0.2491E+02	0.8510E-02	0.7849E+02	0.1681E-02	0.7209E+02
26.	0.6533E-02	-0.1172E+03	0.8524E-02	0.6043E+02	0.5927E-02	0.8814E+02
27.	0.7338E-02	-0.1710E+03	0.5043E-02	-0.1252E+02	0.7761E-02	-0.1291E+03
28.	0.4182E-02	0.9389E+02	0.6043E-02	-0.1625E+02	0.3068E-02	-0.6299E+02
29.	0.4443E-02	-0.1067E+03	0.3993E-02	-0.3433E+02	0.6716E-02	-0.1618E+03
30.	0.8238E-02	-0.1719E+03	0.6239E-02	-0.3161E+02	0.9120E-02	-0.7775E+02
31.	0.7910E-02	0.1294E+03	0.4878E-02	-0.4531E+02	0.5226E-02	-0.8612E+01
32.	0.4194E-02	0.1097E+03	0.7257E-02	-0.7421E+02	0.2522E-02	-0.7135E+02
33.	0.1843E-02	-0.7523E+02	0.5529E-02	-0.6418E+02	0.9187E-02	0.3577E+01
34.	0.8706E-02	-0.1467E+03	0.9080E-02	-0.7323E+02	0.5761E-02	0.6436E+02
35.	0.1014E-01	0.1374E+03	0.3176E-02	-0.6451E+02	0.7075E-02	0.5756E+02
36.	0.1032E-01	0.1335E+03	0.4245E-02	-0.1023E+03	0.1033E-01	0.1150E+03
37.	0.4596E-02	-0.1669E+03	0.8260E-02	-0.1153E+03	0.7214E-02	-0.1671E+03
38.	0.3973E-02	-0.1769E+03	0.3916E-02	-0.7866E+02	0.1300E-02	-0.1503E+03
39.	0.3583E-02	-0.1551E+03	0.6031E-02	-0.8859E+02	0.5582E-02	-0.1625E+03

ORIGINAL PAGE IS
OF POOR QUALITY

TABLE XXII.- CONTINUED

TOP SURFACE

HARM	RADIUS= 0.910 CHORD= 0.150 AMPLITUDE	PHASE	RADIUS= 0.910 CHORD= 0.200 AMPLITUDE	PHASE	RADIUS= 0.910 CHORD= 0.250 AMPLITUDE	PHASE
0.	0.1039E+02	0.0000E+00	0.1092E+02	0.0000E+00	0.1078E+02	0.0000E+00
1.	0.1974E+01	-0.9866E+02	0.2099E+01	-0.9318E+02	0.2200E+01	-0.9065E+02
2.	0.7925E+00	-0.2052E+02	0.9254E+00	-0.9504E+01	0.1075E+01	-0.6317E+01
3.	0.3408E+00	0.6052E+02	0.4893E+00	0.7699E+02	0.6477E+00	0.8410E+02
4.	0.1580E+00	0.6232E+02	0.1527E+00	0.1164E+03	0.2788E+00	0.1628E+03
5.	0.2433E+00	0.1038E+03	0.2001E+00	0.1228E+03	0.5905E-01	0.1786E+03
6.	0.1677E+00	0.1680E+03	0.2085E+00	-0.1684E+03	0.1314E+00	-0.1654E+03
7.	0.4044E-01	-0.1339E+03	0.1560E+00	-0.7845E+02	0.1953E+00	-0.7381E+02
8.	0.5239E-01	-0.1679E+03	0.7674E-01	0.1725E+02	0.2067E+00	0.1824E+02
9.	0.8731E-01	-0.9346E+02	0.2379E-01	-0.1074E+03	0.1555E+00	0.1165E+03
10.	0.6019E-01	-0.1909E+01	0.8616E-01	0.1527E+02	0.6390E-01	-0.1446E+03
11.	0.1243E-01	0.1470E+03	0.1172E+00	0.1097E+03	0.4828E-01	0.9426E+02
12.	0.4984E-01	-0.1012E+02	0.7756E-01	-0.1578E+03	0.1106E+00	-0.1621E+03
13.	0.6982E-01	0.9307E+02	0.2224E-01	-0.5132E+02	0.1373E+00	-0.6408E+02
14.	0.4813E-01	-0.1648E+03	0.4534E-01	-0.1715E+03	0.1146E+00	0.3434E+02
15.	0.2076E-01	-0.7882E+01	0.8014E-01	-0.7003E+02	0.5689E-01	0.1382E+03
16.	0.4109E-01	0.1540E+03	0.7097E-01	0.2855E+02	0.2177E-01	-0.1436E+02
17.	0.5091E-01	-0.1011E+03	0.3450E-01	0.1361E+03	0.7213E-01	0.1174E+03
18.	0.3398E-01	0.2403E+02	0.1760E-01	-0.1224E+02	0.9718E-01	-0.1400E+03
19.	0.2357E-01	0.1753E+03	0.4960E-01	0.1143E+03	0.7716E-01	-0.4122E+02
20.	0.2998E-01	-0.4974E+02	0.5710E-01	-0.1384E+03	0.3216E-01	0.6913E+02
21.	0.3142E-01	0.7880E+02	0.3463E-01	-0.3544E+02	0.2654E-01	-0.6788E+02
22.	0.2264E-01	-0.1497E+03	0.1112E-01	0.1584E+03	0.5775E-01	0.4703E+02
23.	0.1984E-01	-0.9178E+00	0.3671E-01	-0.6129E+02	0.7453E-01	0.1532E+03
24.	0.1911E-01	0.1280E+03	0.4634E-01	0.5624E+02	0.5609E-01	-0.1029E+03
25.	0.1436E-01	-0.7835E+02	0.3668E-01	0.1684E+03	0.2549E-01	0.2503E+02
26.	0.1836E-01	0.7464E+02	0.2031E-01	-0.4534E+02	0.2950E-01	-0.1449E+03
27.	0.2009E-01	-0.1502E+03	0.2642E-01	0.1328E+03	0.5085E-01	-0.2598E+02
28.	0.1596E-01	-0.2043E+02	0.3986E-01	-0.1130E+03	0.5627E-01	0.8015E+02
29.	0.1550E-01	0.1581E+03	0.4225E-01	0.2559E+01	0.3787E-01	-0.1653E+03
30.	0.2585E-01	-0.7907E+02	0.2583E-01	0.1314E+03	0.2100E-01	-0.3165E+02
31.	0.2570E-01	0.4046E+02	0.2244E-01	-0.5058E+02	0.2014E-01	0.1388E+03
32.	0.1547E-01	-0.1689E+03	0.3435E-01	0.8034E+02	0.3324E-01	-0.9377E+02
33.	0.2456E-01	-0.7944E+01	0.2764E-01	-0.1607E+03	0.3932E-01	0.1586E+02
34.	0.3326E-01	0.1102E+03	0.2536E-01	-0.3943E+02	0.2610E-01	0.1191E+03
35.	0.2241E-01	-0.1376E+03	0.1973E-01	0.1409E+03	0.1384E-01	-0.1091E+03
36.	0.1392E-01	0.5450E+02	0.2523E-01	-0.7986E+02	0.1532E-01	0.9419E+02
37.	0.2984E-01	-0.1693E+03	0.2310E-01	0.5958E+02	0.2593E-01	-0.1450E+03
38.	0.3056E-01	-0.5206E+02	0.2135E-01	-0.1737E+03	0.3196E-01	-0.4107E+02
39.	0.1540E-01	0.7694E+02	0.1034E-01	-0.1073E+02	0.2332E-01	0.7388E+02

TABLE XXII.- CONTINUED

TOP SURFACE

HARM	RADIUS= 0.910 CHORD= 0.350 AMPLITUDE	PHASE	RADIUS= 0.910 CHORD= 0.400 AMPLITUDE	PHASE	RADIUS= 0.910 CHORD= 0.450 AMPLITUDE	PHASE
0.	0.1189E+02	0.0000E+00	0.1208E+02	0.0000E+00	0.1308E+02	0.0000E+00
1.	0.7791E+00	-0.8932E+02	0.3562E+00	-0.8744E+02	0.1384E+00	-0.7716E+02
2.	0.2811E+00	-0.2209E+02	0.9922E-01	-0.8153E+02	0.1170E+00	-0.1403E+03
3.	0.2143E+00	0.6911E+02	0.6896E-01	0.1016E+02	0.9219E-01	-0.6030E+02
4.	0.1644E+00	0.1595E+03	0.5534E-01	0.8847E+02	0.8048E-01	0.2080E+02
5.	0.1461E+00	-0.9977E+02	0.3557E-01	-0.1436E+03	0.4531E-01	0.1048E+03
6.	0.1544E+00	0.3918E+01	0.6164E-01	-0.1096E+02	0.5213E-02	-0.1386E+03
7.	0.1408E+00	0.9570E+02	0.7357E-01	0.8365E+02	0.2129E-01	0.6821E+02
8.	0.8708E-01	-0.1695E+03	0.6033E-01	0.1718E+03	0.1765E-01	0.1655E+03
9.	0.4107E-01	-0.6916E+02	0.3699E-01	-0.1008E+03	0.1317E-01	-0.1103E+03
10.	0.1969E-01	0.1089E+03	0.2092E-01	0.9242E+01	0.9715E-02	0.3375E+02
11.	0.2852E-01	-0.1257E+03	0.1143E-01	0.1094E+03	0.1330E-01	0.1252E+03
12.	0.4239E-01	0.4797E-01	0.7469E-02	0.1894E+02	0.3710E-02	-0.1380E+03
13.	0.3734E-01	0.9158E+02	0.9046E-02	0.1296E+03	0.1206E-02	-0.1225E+03
14.	0.2607E-01	-0.1672E+03	0.1047E-01	-0.1540E+03	0.2578E-02	-0.6464E+02
15.	0.1248E-01	-0.6804E+02	0.1015E-01	-0.4417E+02	0.3805E-02	0.5225E+02
16.	0.4377E-02	-0.1743E+03	0.3418E-02	0.4450E+02	0.4642E-02	0.1535E+03
17.	0.5808E-02	-0.8323E+02	0.2630E-02	0.9887E+02	0.1355E-02	-0.1660E+03
18.	0.7183E-02	0.2697E+02	0.7284E-02	-0.1658E+03	0.3278E-02	-0.1319E+03
19.	0.8680E-02	0.1328E+03	0.6964E-02	-0.1189E+03	0.1856E-02	-0.1345E+03
20.	0.8705E-02	-0.1210E+03	0.6937E-02	-0.6501E+02	0.1730E-02	-0.6165E+02
21.	0.7897E-02	-0.3720E+02	0.6735E-02	0.4101E+01	0.3646E-02	-0.4254E+02
22.	0.8863E-02	-0.4831E+02	0.2490E-02	0.1790E+01	0.3124E-02	-0.1562E+02
23.	0.2410E-02	-0.1644E+03	0.3342E-02	-0.1693E+03	0.3244E-02	0.1584E+03
24.	0.1283E-02	0.5154E+02	0.6956E-02	-0.1152E+03	0.3664E-02	-0.1202E+03
25.	0.3528E-02	0.1461E+03	0.5536E-03	-0.1183E+03	0.1913E-02	-0.1582E+01
26.	0.7447E-02	-0.1034E+03	0.5117E-02	-0.1496E+03	0.5296E-03	0.1096E+03
27.	0.5987E-02	-0.5463E+02	0.3676E-02	-0.1110E+03	0.2700E-02	0.1647E+03
28.	0.4002E-02	0.1064E+03	0.4183E-02	0.9997E+02	0.1697E-02	0.1253E+03
29.	0.7121E-02	-0.5355E+02	0.2086E-02	-0.4920E+02	0.3712E-02	-0.3991E+02
30.	0.2258E-02	0.7924E+02	0.1750E-02	0.1287E+03	0.2461E-02	0.2499E+02
31.	0.2019E-02	0.1352E+03	0.1974E-02	0.1243E+03	0.1133E-02	-0.1413E+03
32.	0.4160E-02	-0.1095E+03	0.4646E-02	0.7601E+02	0.1274E-02	-0.3922E+02
33.	0.3544E-02	0.4165E+02	0.3220E-02	0.6316E+02	0.1889E-02	0.8456E+01
34.	0.2261E-02	-0.3166E+02	0.3432E-02	0.8400E+02	0.1636E-02	-0.8735E+02
35.	0.7902E-02	0.1255E+03	0.3025E-02	0.1734E+03	0.1268E-02	0.1534E+03
36.	0.8849E-02	-0.1301E+03	0.6791E-02	-0.1366E+03	0.2599E-02	-0.9869E+02
37.	0.5198E-02	0.4603E+02	0.1279E-02	-0.1217E+03	0.2666E-03	-0.4989E+02
38.	0.5238E-02	-0.9379E+02	0.6234E-02	-0.1761E+03	0.1966E-02	-0.1160E+03
39.	0.4804E-02	0.5838E+02	0.5594E-02	0.1406E+03	0.3543E-03	-0.1286E+03

TABLE XXII.- CONTINUED

TOP SURFACE

	RADIUS= 0.910		RADIUS= 0.910		RADIUS= 0.910	
	CHORD= 0.500		CHORD= 0.550		CHORD= 0.599	
HARM	AMPLITUDE	PHASE	AMPLITUDE	PHASE	AMPLITUDE	PHASE
0.	0.1312E+02	0.0000E+00	0.1370E+02	0.0000E+00	0.1289E+02	0.0000E+00
1.	0.6763E-01	-0.4167E+02	0.4763E-01	0.8547E-01	0.5164E-01	-0.1329E+02
2.	0.1167E+00	-0.1462E+03	0.1010E+00	-0.1528E+03	0.8363E-01	-0.1517E+03
3.	0.9169E-01	-0.6747E+02	0.6685E-01	-0.6195E+02	0.4939E-01	-0.5781E+02
4.	0.7917E-01	0.1120E+02	0.6492E-01	0.7771E+01	0.5287E-01	0.4655E+01
5.	0.5224E-01	0.9198E+02	0.4472E-01	0.9020E+02	0.3610E-01	0.8040E+02
6.	0.1645E-01	0.1783E+03	0.1459E-01	0.1685E+03	0.1012E-01	0.1509E+03
7.	0.8648E-02	0.1433E+02	0.4122E-02	0.1114E+02	0.1450E-02	0.4314E+02
8.	0.3437E-02	0.9935E+02	0.2661E-02	0.6483E+02	0.2158E-02	0.6647E+02
9.	0.4454E-02	0.1583E+03	0.4293E-02	0.1607E+03	0.3893E-02	0.1214E+03
10.	0.2841E-02	0.1095E+03	0.4936E-02	0.1399E+03	0.3870E-02	0.1280E+03
11.	0.9733E-02	0.1625E+03	0.7076E-02	0.1619E+03	0.6294E-02	0.1520E+03
12.	0.3178E-02	-0.8915E+02	0.1822E-02	-0.3914E+02	0.9444E-03	-0.7045E+02
13.	0.8850E-03	0.8276E+02	0.1545E-02	0.1488E+02	0.3239E-02	0.4770E+02
14.	0.2674E-02	0.3104E+02	0.9193E-03	0.9623E+02	0.9759E-03	0.1014E+03
15.	0.2058E-02	0.4374E+02	0.1149E-02	0.1071E+03	0.1569E-02	0.8908E+02
16.	0.4759E-02	0.1750E+03	0.3210E-02	-0.1619E+03	0.2571E-02	0.1709E+03
17.	0.1825E-02	-0.8454E+02	0.8127E-03	-0.1254E+03	0.1870E-02	-0.1031E+03
18.	0.3466E-02	-0.1323E+03	0.2575E-03	-0.1436E+03	0.1941E-03	0.3994E+02
19.	0.2274E-02	-0.7119E+02	0.9392E-03	-0.1325E+03	0.9513E-03	-0.1100E+03
20.	0.1336E-02	0.4618E+02	0.8245E-03	-0.3869E+02	0.1265E-02	0.7882E+02
21.	0.1400E-02	-0.7086E+02	0.5618E-03	-0.1055E+03	0.2569E-02	-0.1627E+03
22.	0.3445E-02	-0.8058E+02	0.5698E-02	-0.7556E+02	0.2896E-02	-0.1672E+01
23.	0.2659E-02	-0.4588E+02	0.2500E-02	-0.1313E+03	0.3282E-02	0.1357E+03
24.	0.1524E-02	-0.1513E+03	0.6946E-03	0.3906E+02	0.1059E-02	0.1178E+03
25.	0.7346E-03	-0.7248E+02	0.1026E-02	-0.3982E+02	0.1328E-02	-0.3140E+01
26.	0.4832E-02	-0.1789E+03	0.1351E-02	-0.1708E+03	0.2368E-02	0.1210E+03
27.	0.2095E-02	-0.1294E+03	0.9023E-03	-0.1461E+03	0.2575E-02	-0.9430E+02
28.	0.1543E-02	0.1167E+03	0.3264E-02	0.1269E+03	0.1853E-02	0.6811E+02
29.	0.1817E-02	-0.1058E+03	0.2604E-02	-0.4967E+02	0.2943E-02	-0.7988E+02
30.	0.2225E-02	0.1794E+02	0.9617E-03	-0.2042E+02	0.1280E-02	0.3385E+02
31.	0.1530E-02	0.2732E+02	0.1786E-02	0.1692E+03	0.1261E-02	0.5149E+02
32.	0.7745E-03	0.1347E+03	0.1989E-02	-0.4735E+02	0.1932E-02	-0.1112E+03
33.	0.7344E-03	0.9302E+02	0.9322E-03	-0.8251E+00	0.2214E-02	0.3958E+01
34.	0.2381E-02	-0.1590E+03	0.1702E-02	-0.1156E+03	0.4077E-02	0.1777E+03
35.	0.1416E-02	0.1640E+03	0.1670E-02	0.1282E+03	0.3063E-02	-0.3553E+02
36.	0.9745E-03	-0.1221E+03	0.1634E-02	0.3527E+02	0.2659E-02	-0.9190E+02
37.	0.1529E-02	0.7433E+02	0.3177E-02	0.8210E+02	0.1483E-02	0.1742E+03
38.	0.1532E-02	-0.1555E+03	0.1151E-02	-0.1013E+03	0.1219E-02	0.1144E+02
39.	0.3113E-02	-0.2210E+02	0.2033E-02	0.4115E+02	0.1887E-02	-0.1436E+03

TABLE XXII.- CONTINUED

TOP SURFACE

RADIUS= 0.910
CHORD= 0.699

HARM	AMPLITUDE	PHASE
0.	0.1355E+02	0.0000E+00
1.	0.1135E+00	0.6073E+02
2.	0.7625E-01	-0.1572E+03
3.	0.3047E-01	-0.5387E+02
4.	0.3268E-01	-0.2444E+01
5.	0.2262E-01	0.6659E+02
6.	0.4870E-02	0.1087E+03
7.	0.3716E-02	0.4146E+02
8.	0.2446E-02	0.6870E+02
9.	0.2913E-02	0.1219E+03
10.	0.1618E-02	0.1447E+03
11.	0.3219E-02	0.1205E+03
12.	0.1886E-02	-0.7031E+02
13.	0.7410E-03	0.2433E+02
14.	0.5270E-03	0.1776E+03
15.	0.3139E-03	-0.6485E+02
16.	0.1752E-02	0.1600E+03
17.	0.7078E-03	-0.1045E+03
18.	0.4311E-03	0.1645E+03
19.	0.7001E-03	-0.1590E+03
20.	0.5604E-03	0.1797E+03
21.	0.1013E-02	0.1522E+03
22.	0.1558E-02	-0.1085E+03
23.	0.6847E-03	0.1695E+03
24.	0.8917E-03	0.3606E+02
25.	0.1311E-02	-0.2776E+02
26.	0.1097E-02	0.1152E+03
27.	0.9552E-03	-0.1246E+03
28.	0.2864E-03	0.5710E+02
29.	0.1314E-02	-0.8086E+02
30.	0.1273E-02	-0.1078E+02
31.	0.1299E-02	0.1101E+03
32.	0.6981E-03	-0.5963E+02
33.	0.9871E-03	0.1420E+03
34.	0.1124E-02	0.1560E+03
35.	0.7402E-04	-0.7829E+02
36.	0.2289E-03	-0.7255E+02
37.	0.1292E-02	-0.7697E+02
38.	0.3266E-03	0.3395E+02
39.	0.7343E-03	-0.1150E+03

TABLE XXII.- CONTINUED

	BOTTOM SURFACE					
	RADIUS= 0.955		RADIUS= 0.955		RADIUS= 0.955	
	CHORD= 0.010		CHORD= 0.030		CHORD= 0.250	
HARM	AMPLITUDE	PHASE	AMPLITUDE	PHASE	AMPLITUDE	PHASE
0.	0.1510E+02	0.0000E+00	0.1295E+02	0.0000E+00	0.1190E+02	0.0000E+00
1.	0.8097E+00	0.2191E+02	0.2190E+01	-0.5670E+02	0.2654E+01	-0.8009E+02
2.	0.5539E+00	0.9192E+02	0.4778E+00	0.7475E+02	0.9680E+00	0.1542E+02
3.	0.4235E+00	-0.6927E+02	0.4568E+00	-0.7946E+02	0.3832E+00	0.1159E+03
4.	0.1118E+00	-0.1472E+02	0.1493E+00	-0.1285E+02	0.2532E+00	-0.1384E+03
5.	0.1242E+00	-0.2772E+02	0.9691E-01	-0.2362E+02	0.1412E+00	-0.1867E+02
6.	0.5278E-01	0.2552E+02	0.6501E-01	0.2451E+02	0.8138E-01	0.1477E+03
7.	0.2797E-01	0.2614E+02	0.2219E-01	0.4072E+02	0.1411E+00	-0.6860E+02
8.	0.1464E-01	0.3673E+02	0.1346E-01	0.2376E+01	0.1569E+00	0.3762E+02
9.	0.1448E-01	0.2493E+02	0.1907E-01	0.2276E+02	0.1212E+00	0.1455E+03
10.	0.8133E-02	0.5176E+02	0.9704E-02	0.6738E+02	0.7198E-01	-0.1046E+03
11.	0.1546E-01	0.9567E+02	0.1479E-01	0.8098E+02	0.3331E-01	0.6297E+02
12.	0.8632E-02	0.1761E+03	0.8423E-02	0.1566E+03	0.5113E-01	-0.1187E+03
13.	0.1903E-02	0.1621E+03	0.2064E-02	0.1451E+03	0.8092E-01	0.6356E+01
14.	0.3540E-02	-0.1032E+03	0.1960E-02	-0.8366E+02	0.8563E-01	0.1198E+03
15.	0.4318E-02	-0.4088E+02	0.3360E-02	-0.4902E+02	0.7926E-01	-0.1163E+03
16.	0.1292E-02	0.1000E+03	0.1365E-02	0.1599E+03	0.6058E-01	0.1333E+02
17.	0.9340E-03	-0.5637E+02	0.1404E-02	-0.2251E+02	0.5104E-01	0.1499E+03
18.	0.1539E-02	-0.9148E+02	0.1568E-02	-0.1181E+03	0.5004E-01	-0.7189E+02
19.	0.2182E-02	-0.1169E+02	0.3564E-02	0.6238E+01	0.5695E-01	0.6369E+02
20.	0.2979E-02	-0.2363E+02	0.4082E-02	0.5658E-01	0.5149E-01	-0.1619E+03
21.	0.2455E-02	0.4428E+02	0.4446E-02	0.7445E+02	0.4476E-01	-0.2908E+02
22.	0.1946E-02	0.8373E+02	0.3388E-02	0.8671E+02	0.4950E-01	0.1021E+03
23.	0.1489E-02	0.3489E+02	0.2691E-02	0.5806E+02	0.4108E-01	-0.1230E+03
24.	0.2674E-03	0.8889E+02	0.1188E-02	-0.1911E+02	0.4542E-01	0.4499E+01
25.	0.2720E-02	-0.5261E+02	0.3359E-02	0.4553E+01	0.3875E-01	0.1282E+03
26.	0.2550E-02	0.3666E+02	0.3381E-02	0.6377E+02	0.2994E-01	-0.1039E+03
27.	0.1636E-02	0.6147E+02	0.3547E-02	0.6690E+02	0.2332E-01	0.4442E+02
28.	0.2210E-02	0.3016E+02	0.1914E-02	0.6562E+02	0.2123E-01	0.1724E+03
29.	0.5302E-03	0.4333E+02	0.2136E-02	0.9039E+02	0.1814E-01	-0.5658E+02
30.	0.3613E-03	-0.3734E+02	0.2351E-02	0.9952E+02	0.1606E-01	0.7838E+02
31.	0.2212E-02	0.4630E+02	0.2766E-02	0.9623E+02	0.1136E-01	-0.1551E+03
32.	0.2702E-02	0.4364E+02	0.1281E-02	0.1007E+03	0.1472E-01	-0.2526E+01
33.	0.1410E-02	0.7703E+02	0.1155E-02	0.1577E+03	0.1272E-01	0.1197E+03
34.	0.1401E-02	0.1025E+03	0.1405E-02	0.1715E+03	0.1446E-01	-0.1372E+03
35.	0.2941E-02	0.1471E+03	0.1171E-02	-0.8705E+02	0.9895E-02	-0.2553E+02
36.	0.5010E-03	-0.2121E+02	0.1783E-02	0.2021E+02	0.3346E-02	0.1060E+03
37.	0.1462E-02	0.1380E+03	0.1324E-02	0.1596E+03	0.3817E-02	0.3172E+02
38.	0.1736E-02	-0.1196E+03	0.1828E-02	0.1706E+03	0.4225E-02	0.1413E+03
39.	0.8564E-03	0.1734E+03	0.1428E-02	-0.1116E+03	0.8544E-02	-0.1343E+03

TABLE XXII.- CONTINUED

BOTTOM SURFACE

HARM	RADIUS= 0.955 CHORD= 0.400 AMPLITUDE	PHASE	RADIUS= 0.955 CHORD= 0.500 AMPLITUDE	PHASE	RADIUS= 0.955 CHORD= 0.699 AMPLITUDE	PHASE
0.	0.1300E+02	0.0000E+00	0.1307E+02	0.0000E+00	0.1349E+02	0.0000E+00
1.	0.7558E+00	-0.8495E+02	0.5339E+00	-0.9178E+02	0.1830E+00	-0.1017E+03
2.	0.1636E-01	0.9178E+01	0.2071E-01	0.8299E+02	0.4360E-01	0.9824E+02
3.	0.1226E+00	-0.6117E+02	0.6959E-01	-0.6986E+02	0.1565E-01	-0.1172E+03
4.	0.6593E-01	0.6373E+02	0.2979E-01	0.7361E+02	0.1354E-01	0.1419E+03
5.	0.3793E-01	-0.1772E+03	0.1939E-01	-0.1570E+03	0.1303E-01	-0.1277E+03
6.	0.2535E-01	-0.8426E+02	0.1244E-01	-0.7468E+02	0.4789E-02	-0.9940E+02
7.	0.1717E-01	0.1186E+01	0.5693E-02	-0.3770E+01	0.4610E-02	-0.9317E+02
8.	0.2568E-02	0.1760E+03	0.4988E-02	0.1728E+03	0.1547E-02	-0.1331E+03
9.	0.1412E-01	-0.5388E+02	0.8959E-02	-0.6318E+02	0.6146E-02	-0.6781E+02
10.	0.5301E-02	0.9554E+02	0.5561E-02	0.3543E+02	0.2408E-02	0.5420E+02
11.	0.8116E-02	0.1041E+03	0.4798E-02	0.7593E+02	0.2215E-02	0.4203E+02
12.	0.5315E-02	0.1681E+03	0.4488E-02	-0.1789E+03	0.4007E-02	0.1531E+03
13.	0.5681E-03	0.3180E+02	0.1132E-02	-0.1088E+03	0.1457E-02	-0.1044E+03
14.	0.3983E-02	-0.2402E+02	0.1335E-02	-0.4019E+02	0.1915E-02	-0.5051E+02
15.	0.8119E-02	-0.6507E+02	0.2558E-02	-0.6931E+02	0.3085E-02	-0.1170E+03
16.	0.4331E-02	0.6420E+02	0.2957E-02	0.1455E+02	0.1385E-02	-0.2471E+02
17.	0.3135E-02	0.7319E+02	0.3249E-02	0.5003E+02	0.2433E-02	-0.2361E+01
18.	0.5961E-02	0.1664E+03	0.2609E-02	0.9296E+02	0.2052E-02	0.3597E+02
19.	0.4770E-02	0.9037E+02	0.9967E-03	0.9827E+02	0.3775E-02	0.4768E+02
20.	0.3207E-02	-0.1220E+03	0.7426E-03	-0.1492E+03	0.1316E-02	0.1499E+03
21.	0.5778E-02	0.1136E+03	0.1395E-02	0.6939E+02	0.1925E-02	0.4640E+02
22.	0.5971E-02	0.1048E+03	0.1402E-02	0.9788E+02	0.1962E-02	0.6648E+02
23.	0.6028E-02	0.6937E+02	0.1818E-02	-0.4579E+01	0.1088E-02	0.2603E+02
24.	0.2109E-02	0.1321E+02	0.5680E-03	-0.4964E+01	0.1336E-02	-0.1387E+03
25.	0.3675E-02	-0.5390E+02	0.1162E-02	-0.1199E+03	0.1448E-02	-0.1083E+03
26.	0.3726E-02	0.1280E+03	0.1497E-02	0.1076E+03	0.1995E-02	0.9268E+02
27.	0.4117E-02	0.1116E+03	0.2510E-02	0.4034E+02	0.1276E-02	-0.2759E+01
28.	0.2541E-02	-0.1454E+03	0.4779E-03	0.1702E+03	0.6575E-03	0.8880E+01
29.	0.3163E-02	-0.1295E+03	0.3640E-03	-0.3494E+02	0.1065E-02	-0.1407E+03
30.	0.5424E-02	0.1274E+03	0.1233E-02	0.1450E+03	0.1108E-02	-0.1215E+02
31.	0.1531E-02	0.1136E+03	0.1879E-02	-0.1785E+03	0.2190E-02	0.5718E+02
32.	0.1323E-02	0.2385E+02	0.1502E-02	0.2052E+01	0.2594E-02	-0.1156E+03
33.	0.2249E-02	-0.5060E+02	0.5011E-03	-0.7906E+02	0.1052E-02	0.1095E+03
34.	0.1118E-02	0.1354E+03	0.1252E-02	-0.5868E+02	0.5729E-03	-0.1553E+03
35.	0.3419E-02	0.1162E+03	0.8823E-03	-0.7590E+02	0.2357E-03	-0.1501E+03
36.	0.1543E-02	-0.1100E+01	0.3345E-03	-0.1739E+03	0.7648E-03	-0.9707E+02
37.	0.4548E-02	0.2430E+02	0.8367E-03	0.1583E+03	0.2999E-03	0.2024E+02
38.	0.2263E-02	0.1602E+03	0.1593E-02	0.1315E+03	0.7149E-03	0.7115E+02
39.	0.2335E-02	-0.1042E+03	0.5330E-03	-0.1653E+03	0.4447E-03	0.1078E+03
					0.6499E-03	0.6160E+02
					0.2496E-03	0.9097E+02
					0.1124E-02	0.1453E+03
					0.1615E-02	0.1290E+03
					0.6270E-03	0.9406E+02
					0.8295E-03	0.5597E+02
					0.7559E-03	-0.1564E+03
					0.1569E-02	-0.8582E+02
					0.1590E-03	-0.1524E+03
					0.5248E-03	-0.3153E+02
					0.3382E-03	0.3856E+02
					0.1651E-02	-0.8055E+02
					0.5464E-03	0.5514E+01
					0.8669E-03	-0.1796E+02
					0.6154E-03	-0.2196E+02
					0.1099E-02	-0.1171E+02
					0.1787E-02	-0.2393E+02
					0.9253E-03	-0.9201E+02
					0.1104E-02	-0.4376E+02
					0.1790E-02	-0.8546E+02
					0.1823E-02	-0.6973E+02
					0.1348E-02	-0.2365E+02
					0.1255E-02	0.1073E+03
					0.7007E-03	-0.7329E+02
					0.6440E-03	0.6404E+02
					0.3065E-02	-0.2830E+02
					0.1834E-02	0.1987E+02
					0.4023E-03	-0.4282E+02
					0.1952E-02	-0.7204E+02
					0.2417E-02	-0.3218E+02
					0.1550E-02	-0.1194E+03
					0.1792E-02	-0.9600E+02
					0.1949E-02	-0.1006E+03
					0.8898E-03	-0.4966E+02
					0.2244E-03	·0.7446E+02
					0.1569E-02	0.1665E+03
					0.1166E-02	0.1534E+03
					0.1242E-02	-0.4901E+02
					0.1348E-02	-0.1890E+02

ORIGINAL PAGE IS
OF POOR QUALITY

TABLE XXII.- CONTINUED

BOTTOM SURFACE

RADIUS= Ø.955
CHORD= Ø.919

HARM	AMPLITUDE	PHASE
Ø.	Ø.138ØE+Ø2	Ø.ØØØØE+ØØ
1.	Ø.2323E+ØØ	Ø.1Ø6ØE+Ø3
2.	Ø.5597E-Ø1	Ø.1766E+Ø3
3.	Ø.1ØØ3E-Ø1	Ø.1674E+Ø1
4.	Ø.7625E-Ø2	Ø.14Ø9E+Ø3
5.	Ø.9952E-Ø2	-Ø.116ØE+Ø3
6.	Ø.3525E-Ø2	-Ø.1729E+Ø2
7.	Ø.197ØE-Ø2	Ø.1648E+Ø3
8.	Ø.1795E-Ø2	Ø.1495E+Ø3
9.	Ø.3493E-Ø2	-Ø.1111E+Ø3
1Ø.	Ø.1411E-Ø2	-Ø.3728E+Ø2
11.	Ø.1255E-Ø2	-Ø.41Ø9E+Ø2
12.	Ø.2Ø78E-Ø2	Ø.1478E+Ø3
13.	Ø.6854E-Ø3	-Ø.1554E+Ø3
14.	Ø.3741E-Ø3	-Ø.1Ø44E+Ø3
15.	Ø.1Ø87E-Ø2	-Ø.11Ø5E+Ø3
16.	Ø.5Ø58E-Ø3	-Ø.147ØE+Ø2
17.	Ø.168ØE-Ø2	-Ø.2349E+Ø2
18.	Ø.9495E-Ø3	Ø.1945E+Ø1
19.	Ø.1182E-Ø2	Ø.2142E+Ø2
2Ø.	Ø.8Ø42E-Ø3	Ø.6544E+Ø2
21.	Ø.84Ø2E-Ø3	Ø.9969E+Ø2
22.	Ø.9874E-Ø3	Ø.9193E+Ø2
23.	Ø.137ØE-Ø2	Ø.6641E+Ø2
24.	Ø.1295E-Ø2	-Ø.16Ø3E+Ø3
25.	Ø.1396E-Ø2	-Ø.1317E+Ø3
26.	Ø.1285E-Ø2	Ø.6337E+Ø2
27.	Ø.44Ø5E-Ø3	-Ø.1Ø33E+Ø3
28.	Ø.86Ø9E-Ø3	-Ø.8787E+Ø2
29.	Ø.2Ø24E-Ø3	-Ø.1Ø33E+Ø3
3Ø.	Ø.6Ø29E-Ø3	Ø.1535E+Ø3
31.	Ø.1344E-Ø2	Ø.8375E+Ø2
32.	Ø.2168E-Ø2	-Ø.1681E+Ø3
33.	Ø.534ØE-Ø3	Ø.1249E+Ø3
34.	Ø.8488E-Ø3	Ø.1768E+Ø3
35.	Ø.4448E-Ø3	Ø.1465E+Ø3
36.	Ø.5499E-Ø3	Ø.1582E+Ø3
37.	Ø.5559E-Ø3	-Ø.1579E+Ø3
38.	Ø.2963E-Ø3	-Ø.4Ø34E+Ø1
39.	Ø.9354E-Ø4	Ø.1755E+Ø3
4Ø.	Ø.5785E-Ø4	Ø.1Ø4ØE+Ø3
41.	Ø.2Ø61E-Ø3	Ø.3111E+Ø2
42.	Ø.1238E-Ø2	-Ø.1786E+Ø3
43.	Ø.11Ø5E-Ø2	Ø.1496E+Ø3
44.	Ø.3377E-Ø3	-Ø.1449E+Ø3
45.	Ø.36Ø1E-Ø3	Ø.7483E+Ø2
46.	Ø.5269E-Ø3	-Ø.1424E+Ø3
47.	Ø.1759E-Ø2	-Ø.1152E+Ø3
48.	Ø.6275E-Ø3	-Ø.7238E+Ø2
49.	Ø.2952E-Ø3	-Ø.1757E+Ø3
5Ø.	Ø.142ØE-Ø2	-Ø.2183E+Ø2
51.	Ø.5578E-Ø3	-Ø.5518E+Ø2
52.	Ø.8856E-Ø3	-Ø.11ØØE+Ø2
53.	Ø.8913E-Ø3	Ø.57Ø6E+Ø2
54.	Ø.2117E-Ø3	-Ø.219ØE+Ø2
55.	Ø.8173E-Ø3	-Ø.3539E+Ø1
56.	Ø.3575E-Ø3	-Ø.5133E+Ø2
57.	Ø.7249E-Ø3	-Ø.7822E+Ø2
58.	Ø.5226E-Ø3	-Ø.3975E+Ø2
59.	Ø.9766E-Ø3	-Ø.1233E+Ø3
6Ø.	Ø.6459E-Ø3	-Ø.6455E+Ø2
61.	Ø.6Ø26E-Ø3	Ø.59Ø2E+Ø1
62.	Ø.7467E-Ø3	Ø.2562E+Ø2
63.	Ø.4372E-Ø3	-Ø.1214E+Ø3
64.	Ø.3315E-Ø3	-Ø.125ØE+Ø3
65.	Ø.1Ø29E-Ø2	-Ø.1Ø84E+Ø2
66.	Ø.5766E-Ø3	-Ø.1626E+Ø2
67.	Ø.435ØE-Ø3	-Ø.1767E+Ø2
68.	Ø.9699E-Ø3	-Ø.6739E+Ø2
69.	Ø.489ØE-Ø3	-Ø.278ØE+Ø2
7Ø.	Ø.4617E-Ø3	Ø.1734E+Ø3
71.	Ø.8229E-Ø3	-Ø.1665E+Ø3
72.	Ø.7633E-Ø3	-Ø.7887E+Ø2
73.	Ø.4294E-Ø3	Ø.1595E+Ø3
74.	Ø.6832E-Ø3	-Ø.9352E+Ø2
75.	Ø.7Ø41E-Ø3	Ø.1591E+Ø3
76.	Ø.2831E-Ø3	-Ø.7995E+Ø1
77.	Ø.3177E-Ø3	-Ø.584ØE+Ø2
78.	Ø.7266E-Ø3	-Ø.7588E+Ø2

TABLE XXII.- CONTINUED

TOP SURFACE

HARM	RADIUS= 0.955 CHORD= 0.010 AMPLITUDE	PHASE	RADIUS= 0.955 CHORD= 0.030 AMPLITUDE	PHASE	RADIUS= 0.955 CHORD= 0.080 AMPLITUDE	PHASE
0.	0.1051E+02	0.0000E+00	0.8126E+01	0.0000E+00	0.9567E+01	0.0000E+00
1.	0.5673E+01	0.1160E+03	0.2363E+01	0.1650E+03	0.1146E+01	-0.1361E+03
2.	0.4798E+00	0.9692E+02	0.6781E+00	-0.1582E+03	0.1051E+00	-0.9636E+02
3.	0.4482E+00	0.8921E+02	0.6843E+00	0.1301E+03	0.1212E+00	0.5844E+02
4.	0.1799E+00	0.1042E+03	0.4861E+00	0.1308E+03	0.1617E+00	-0.9667E+01
5.	0.2066E+00	0.1505E+03	0.3771E+00	0.1282E+03	0.5908E-01	-0.9071E+01
6.	0.1013E+00	0.1439E+03	0.2119E+00	0.7835E+02	0.3656E-01	-0.4280E+01
7.	0.5831E-01	0.1502E+03	0.1590E+00	0.5718E+02	0.5810E-01	0.8639E+02
8.	0.4418E-01	0.1733E+03	0.6504E-01	0.2009E+01	0.6765E-01	0.9244E+02
9.	0.6732E-01	-0.1702E+03	0.8625E-01	-0.5869E+02	0.4078E-01	0.1241E+03
10.	0.3340E-01	-0.1739E+03	0.8416E-01	-0.7318E+02	0.1126E-01	-0.1617E+03
11.	0.1836E-01	-0.1682E+03	0.7394E-01	-0.1122E+03	0.1437E-01	0.1421E+03
12.	0.4277E-02	-0.1527E+03	0.6887E-01	-0.1244E+03	0.2134E-01	0.1558E+03
13.	0.6016E-02	0.1711E+03	0.6272E-01	-0.1422E+03	0.4202E-02	-0.8804E+02
14.	0.9593E-02	0.1219E+03	0.5489E-01	0.1777E+03	0.6447E-02	0.4540E+02
15.	0.6895E-02	0.1012E+03	0.3462E-01	0.1456E+03	0.7761E-02	-0.1420E+03
16.	0.2524E-02	-0.1129E+03	0.2805E-01	0.1245E+03	0.2409E-02	-0.5256E+02
17.	0.1148E-01	-0.9073E+02	0.1859E-01	0.7208E+02	0.9542E-02	0.1084E+03
18.	0.4997E-02	-0.1501E+03	0.2581E-01	0.1930E+02	0.5897E-02	0.2507E+02
19.	0.8622E-02	0.1534E+03	0.2342E-01	0.6052E+01	0.1866E-01	0.1085E+02
20.	0.7729E-02	0.1176E+03	0.2228E-01	-0.2121E+02	0.9649E-02	-0.3814E+02
21.	0.3128E-02	0.1159E+03	0.3119E-01	-0.5318E+02	0.1410E-01	-0.6150E+02
22.	0.3183E-02	-0.1483E+03	0.3022E-01	-0.7467E+02	0.3851E-02	0.2010E+02
23.	0.6335E-02	-0.1727E+03	0.1758E-01	-0.1151E+03	0.9940E-02	0.1356E+03
24.	0.3847E-02	0.1560E+03	0.2310E-01	-0.1325E+03	0.4164E-02	0.4636E+02
25.	0.4355E-02	0.6315E+02	0.1519E-01	-0.1723E+03	0.1460E-01	0.3871E+02
26.	0.5399E-02	0.1557E+03	0.1377E-01	0.1252E+03	0.2511E-02	0.1325E+03
27.	0.4842E-02	-0.1174E+03	0.9257E-02	0.9527E+02	0.6581E-02	-0.1286E+03
28.	0.4908E-02	-0.1369E+03	0.1081E-01	0.6575E+02	0.1097E-01	-0.1706E+03
29.	0.3178E-02	-0.5523E+02	0.1656E-01	0.8055E+01	0.9400E-02	0.1737E+03
30.	0.1391E-02	-0.1427E+03	0.1392E-01	-0.1480E+01	0.1585E-01	0.1273E+03
31.	0.6613E-02	-0.1327E+03	0.7526E-02	-0.4235E+02	0.8712E-02	0.1273E+03
32.	0.6805E-02	-0.1500E+03	0.7142E-02	-0.7391E+02	0.7899E-02	0.2246E+02
33.	0.2093E-02	-0.1715E+03	0.3323E-02	-0.7442E+02	0.9584E-02	-0.4448E+02
34.	0.1908E-03	-0.4517E+02	0.2249E-02	0.2336E+02	0.1406E-01	-0.7066E+02
35.	0.3079E-02	-0.8238E+02	0.6044E-03	0.1564E+03	0.1135E-01	-0.1348E+03
36.	0.5071E-02	-0.7360E+02	0.7739E-02	-0.4135E+02	0.7276E-02	-0.1642E+03
37.	0.3870E-02	-0.9378E+02	0.5044E-02	-0.1143E+03	0.1099E-01	0.1202E+03
38.	0.7281E-02	-0.9074E+02	0.4958E-02	-0.1673E+03	0.7135E-02	0.7614E+02
39.	0.2667E-02	-0.1992E+02	0.4873E-02	0.1644E+03	0.1342E-01	0.3664E+02

TABLE XXII.- CONTINUED

TOP SURFACE

HARM	RADIUS= 0.955 CHORD= 0.150 AMPLITUDE	PHASE	RADIUS= 0.955 CHORD= 0.250 AMPLITUDE	PHASE	RADIUS= 0.955 CHORD= 0.350 AMPLITUDE	PHASE
0.	0.1015E+02	0.0000E+00	0.1046E+02	0.0000E+00	0.1211E+02	0.0000E+00
1.	0.2217E+01	-0.9896E+02	0.2545E+01	-0.9006E+02	0.7583E+00	-0.8339E+02
2.	0.6918E+00	-0.2324E+02	0.1341E+01	-0.8438E+01	0.2320E+00	-0.2837E+02
3.	0.1991E+00	0.4201E+02	0.8233E+00	0.7998E+02	0.1930E+00	0.6496E+02
4.	0.2221E+00	0.1329E+02	0.3647E+00	0.1529E+03	0.1815E+00	0.1419E+03
5.	0.2137E+00	0.8825E+02	0.1326E+00	0.1596E+03	0.1588E+00	-0.1262E+03
6.	0.1197E+00	0.1625E+03	0.2295E+00	-0.1641E+03	0.1604E+00	-0.2623E+02
7.	0.5473E-01	0.1498E+03	0.2894E+00	-0.8420E+02	0.1240E+00	0.6210E+02
8.	0.7600E-01	0.1694E+03	0.2470E+00	-0.2782E+00	0.5527E-01	0.1416E+03
9.	0.5131E-01	-0.9701E+02	0.1186E+00	0.7647E+02	0.1178E-01	0.1493E+03
10.	0.2854E-01	0.8485E+01	0.5784E-01	0.5804E+02	0.4313E-01	0.1682E+03
11.	0.8737E-02	-0.7448E+02	0.1542E+00	0.1093E+03	0.5742E-01	-0.1162E+03
12.	0.3099E-01	0.1161E+02	0.1727E+00	-0.1668E+03	0.6304E-01	-0.2821E+02
13.	0.2519E-01	0.1200E+03	0.1344E+00	-0.8477E+02	0.4705E-01	0.5637E+02
14.	0.1195E-01	-0.1784E+03	0.4445E-01	-0.1571E+02	0.2347E-01	0.1153E+03
15.	0.1705E-01	0.1522E+03	0.5475E-01	-0.4906E+02	0.1288E-01	0.1576E+03
16.	0.3168E-01	-0.1365E+03	0.1042E+00	0.2575E+02	0.2282E-01	-0.1625E+03
17.	0.2641E-01	-0.5840E+02	0.1038E+00	0.1119E+03	0.2350E-01	-0.9700E+02
18.	0.1929E-01	-0.2895E+02	0.6659E-01	-0.1606E+03	0.1931E-01	-0.2146E+02
19.	0.3305E-01	-0.4184E+01	0.1612E-01	-0.1346E+03	0.1924E-01	0.3695E+02
20.	0.3184E-01	0.5061E+02	0.5545E-01	-0.1311E+03	0.1055E-01	0.1066E+03
21.	0.1119E-01	0.1402E+03	0.7252E-01	-0.4895E+02	0.1044E-01	0.1706E+03
22.	0.1669E-01	0.9345E+02	0.6153E-01	0.4268E+02	0.1061E-01	-0.1069E+03
23.	0.3790E-01	0.1556E+03	0.2682E-01	0.1218E+03	0.8147E-02	-0.7958E+02
24.	0.2431E-01	-0.1437E+03	0.2243E-01	0.8202E+02	0.5481E-02	0.3583E+02
25.	0.6629E-02	-0.1595E+03	0.4621E-01	0.1566E+03	0.1051E-01	0.7067E+02
26.	0.2566E-01	-0.1141E+03	0.5204E-01	-0.1132E+03	0.6251E-02	0.1650E+03
27.	0.3252E-01	-0.2460E+02	0.2990E-01	-0.2314E+02	0.4407E-02	-0.1427E+03
28.	0.1837E-01	0.3427E+02	0.3047E-02	0.1073E+02	0.2809E-02	-0.7411E+02
29.	0.2464E-01	-0.4697E+01	0.2805E-01	-0.2505E+01	0.8389E-02	-0.6732E+01
30.	0.3499E-01	0.6812E+02	0.4023E-01	0.9557E+02	0.2500E-02	0.1351E+03
31.	0.2116E-01	0.1436E+03	0.2990E-01	-0.1745E+03	0.3893E-02	0.2057E+01
32.	0.2983E-02	-0.1633E+03	0.1918E-01	-0.9092E+02	0.7372E-02	-0.1181E+03
33.	0.1946E-01	0.1573E+03	0.4591E-02	-0.1263E+03	0.4874E-02	0.1276E+03
34.	0.2513E-01	-0.1106E+03	0.2268E-01	-0.4132E+02	0.2306E-02	-0.7308E+02
35.	0.1172E-01	-0.6522E+02	0.2618E-01	0.4313E+02	0.7131E-02	-0.1615E+03
36.	0.9924E-02	-0.8392E+02	0.2174E-01	0.1410E+03	0.2280E-02	-0.1051E+03
37.	0.1432E-01	0.4045E+01	0.1617E-01	-0.1146E+03	0.3367E-02	-0.1105E+03
38.	0.1221E-01	0.9164E+02	0.8992E-02	0.1720E+03	0.4954E-02	-0.3261E+02
39.	0.9005E-02	0.5196E+02	0.2414E-01	-0.1041E+03	0.2206E-02	0.4761E+02

TABLE XXII.- CONTINUED

	TOP SURFACE					
	RADIUS= 0.955		RADIUS= 0.955		RADIUS= 0.955	
	CHORD= 0.400		CHORD= 0.500		CHORD= 0.550	
HARM	AMPLITUDE	PHASE	AMPLITUDE	PHASE	AMPLITUDE	PHASE,
0.	0.1254E+02	0.0000E+00	0.1288E+02	0.0000E+00	0.1296E+02	0.0000E+00
1.	0.3916E+00	-0.7004E+02	0.1919E+00	-0.1717E+02	0.1813E+00	-0.8622E+01
2.	0.7363E-01	-0.6882E+02	0.1450E+00	-0.1761E+03	0.1070E+00	-0.1780E+03
3.	0.7480E-01	0.4529E+02	0.1010E+00	-0.9853E+02	0.7587E-01	-0.1018E+03
4.	0.9016E-01	0.1281E+03	0.8998E-01	-0.1060E+02	0.7233E-01	-0.1571E+02
5.	0.9753E-01	-0.1295E+03	0.6489E-01	0.7035E+02	0.5413E-01	0.6370E+02
6.	0.1320E+00	-0.2622E+02	0.2025E-01	0.1408E+03	0.2104E-01	0.1357E+03
7.	0.1287E+00	0.5941E+02	0.3786E-02	-0.1603E+03	0.8596E-02	-0.1476E+03
8.	0.9822E-01	0.1415E+03	0.2076E-02	-0.1423E+03	0.4380E-02	-0.7996E+02
9.	0.7372E-01	-0.1379E+03	0.2974E-02	0.1672E+03	0.6380E-02	0.4363E+02
10.	0.4072E-01	-0.6517E+02	0.2727E-02	-0.1552E+02	0.5048E-02	0.8609E+02
11.	0.2587E-01	0.1764E+02	0.4295E-02	0.5092E+02	0.3976E-02	0.1162E+03
12.	0.2566E-01	0.3969E+02	0.3386E-02	0.8129E+02	0.3578E-02	-0.7027E+02
13.	0.1408E-01	0.1011E+03	0.7774E-02	0.1512E+03	0.2702E-02	0.1456E+03
14.	0.1322E-01	0.1688E+03	0.5192E-02	-0.8771E+02	0.2038E-02	-0.4640E+02
15.	0.1523E-01	-0.1319E+03	0.8821E-02	-0.1640E+02	0.4332E-02	0.1715E+02
16.	0.1686E-01	-0.8729E+02	0.3717E-02	0.4638E+02	0.2180E-02	0.1191E+03
17.	0.1042E-01	0.1212E+01	0.3719E-02	0.1592E+03	0.3211E-02	0.1725E+03
18.	0.1226E-01	0.9900E+02	0.5159E-02	-0.1664E+03	0.3341E-02	-0.1362E+03
19.	0.1102E-01	0.1490E+03	0.2069E-02	-0.6535E+02	0.2517E-02	0.8391E+00
20.	0.7322E-02	-0.1375E+03	0.6808E-03	-0.1040E+03	0.1057E-02	-0.1295E+03
21.	0.5152E-02	-0.8102E+02	0.1900E-02	0.1284E+03	0.2077E-02	0.1540E+03
22.	0.8052E-02	-0.1877E+02	0.1643E-02	0.1799E+03	0.2061E-02	-0.1481E+03
23.	0.2671E-02	0.9337E+02	0.5232E-03	-0.8460E+02	0.6363E-03	-0.1420E+03
24.	0.6119E-02	0.1251E+03	0.2873E-02	-0.7918E+01	0.2095E-02	-0.1710E+02
25.	0.4504E-02	0.1327E+03	0.1353E-02	0.8535E+02	0.1906E-02	0.5543E+02
26.	0.2048E-03	-0.1110E+03	0.1766E-02	0.1591E+03	0.6145E-03	0.1471E+03
27.	0.2494E-02	-0.2233E+02	0.1077E-02	-0.1195E+03	0.8408E-03	-0.5770E+02
28.	0.6319E-02	0.1296E+02	0.4291E-03	0.3917E+02	0.1508E-02	0.3415E+02
29.	0.2539E-02	-0.5531E+01	0.1023E-02	0.4117E+02	0.1282E-02	-0.7929E+02
30.	0.4731E-02	0.1455E+03	0.9829E-03	0.1390E+03	0.3059E-03	0.1355E+03
31.	0.2653E-02	-0.1190E+03	0.2857E-02	-0.1196E+03	0.1195E-02	-0.1270E+03
32.	0.7017E-03	-0.8413E+02	0.1659E-02	0.8218E+02	0.1431E-02	0.7334E+02
33.	0.4176E-02	0.8659E+02	0.1935E-02	0.1362E+03	0.9802E-03	-0.1449E+03
34.	0.5465E-02	0.1320E+03	0.1663E-02	-0.3371E+02	0.1876E-02	0.3382E+01
35.	0.4043E-02	-0.7911E+02	0.3074E-02	0.9065E+02	0.1448E-02	0.1303E+02
36.	0.5316E-02	0.3860E+01	0.2658E-02	0.1038E+03	0.1598E-02	0.1134E+03
37.	0.5498E-02	-0.1751E+03	0.1607E-02	-0.1413E+03	0.1880E-02	-0.1325E+03
38.	0.3436E-02	-0.9358E+02	0.1028E-02	-0.6546E+02	0.1768E-02	-0.1284E+03
39.	0.2340E-02	0.6816E+02	0.2055E-02	-0.9525E+02	0.2018E-02	-0.4957E+02

TABLE XXII.- CONTINUED

			TOP SURFACE	
	RADIUS= 0.955		RADIUS= 0.955	
	CHORD= 0.699		CHORD= 0.919	
HARM	AMPLITUDE	PHASE	AMPLITUDE	PHASE
0.	0.1314E+02	0.0000E+00	0.1374E+02	0.0000E+00
1.	0.1844E+00	0.1548E+02	0.2444E+00	0.7026E+02
2.	0.4749E-01	-0.1774E+03	0.4390E-01	-0.1706E+03
3.	0.2826E-01	-0.8803E+02	0.1262E-01	-0.1008E+03
4.	0.3367E-01	-0.1254E+02	0.1387E-01	-0.3261E+02
5.	0.2686E-01	0.6645E+02	0.9293E-02	0.4326E+02
6.	0.9144E-02	0.1104E+03	0.5086E-02	0.3658E+02
7.	0.3594E-02	0.1468E+03	0.2573E-02	0.7708E+02
8.	0.4463E-02	-0.4757E+02	0.2786E-02	-0.6140E+02
9.	0.2858E-02	0.1018E+03	0.2045E-02	-0.1519E+03
10.	0.3852E-02	0.1308E+03	0.1099E-02	0.1216E+03
11.	0.3440E-02	0.1553E+03	0.1751E-02	0.1497E+03
12.	0.2965E-02	-0.2628E+00	0.8064E-03	-0.2745E+01
13.	0.2724E-02	0.7712E+02	0.2901E-02	0.7341E+02
14.	0.2569E-02	0.2132E+02	0.3032E-02	0.3906E+02
15.	0.1798E-02	0.4399E+01	0.4593E-03	-0.3042E+02
16.	0.2299E-02	0.1702E+03	0.1819E-02	-0.1136E+03
17.	0.2500E-02	-0.1068E+03	0.3031E-02	-0.9210E+02
18.	0.9489E-03	-0.5959E+02	0.1201E-03	0.2386E+02
19.	0.1461E-02	0.3546E+02	0.1940E-02	0.5411E+02
20.	0.6195E-03	-0.8846E+02	0.3857E-03	0.1698E+03
21.	0.9420E-03	0.1149E+03	0.1764E-02	0.8121E+02
22.	0.1079E-02	-0.3014E+02	0.1781E-02	-0.2511E+01
23.	0.9394E-03	0.1720E+03	0.1306E-02	-0.1482E+03
24.	0.2923E-03	0.1267E+02	0.5399E-03	-0.5298E+01
25.	0.1338E-02	0.5813E+02	0.9372E-03	-0.1992E+02
26.	0.1639E-02	-0.6265E+02	0.1427E-02	-0.5306E+02
27.	0.9838E-03	-0.3431E+02	0.2801E-03	0.3458E+02
28.	0.2873E-02	-0.1791E+03	0.9039E-03	0.1611E+03
29.	0.2406E-02	-0.6815E+02	0.2045E-02	-0.7226E+02
30.	0.2484E-02	0.6801E+02	0.2161E-02	0.1262E+02
31.	0.8955E-03	0.7954E+02	0.5259E-03	0.1376E+03
32.	0.2334E-02	0.1064E+03	0.4546E-03	-0.1676E+03
33.	0.1144E-02	0.6384E+02	0.1699E-02	0.1237E+03
34.	0.2774E-02	0.8337E+02	0.3114E-03	0.1797E+03
35.	0.2831E-02	-0.1447E+03	0.1319E-02	0.1242E+03
36.	0.7784E-03	0.9598E+02	0.1181E-02	0.9421E+02
37.	0.2304E-03	-0.6191E+02	0.1209E-02	-0.1286E+03
38.	0.3059E-03	-0.1234E+03	0.1143E-02	-0.6670E+02
39.	0.1649E-02	0.2702E+02	0.1458E-02	0.2079E+02

ORIGINAL PAGE IS OF POOR QUALITY

TABLE XXII.- CONTINUED

BOTTOM SURFACE

HARM	AMPLITUDE (RADIUS= 0.970, CHORD= 0.010)	PHASE (RADIUS= 0.970, CHORD= 0.010)	AMPLITUDE (RADIUS= 0.970, CHORD= 0.030)	PHASE (RADIUS= 0.970, CHORD= 0.030)	AMPLITUDE (RADIUS= 0.970, CHORD= 0.080)	PHASE (RADIUS= 0.970, CHORD= 0.080)
0.	0.1534E+02	0.0000E+00	0.1342E+02	0.0000E+00	0.1172E+02	0.0000E+00
1.	0.7677E+00	0.3358E+02	0.1882E+01	-0.6047E+02	0.2869E+01	-0.7343E+02
2.	0.4273E+00	0.9933E+02	0.2952E+00	0.7873E+02	0.5809E+00	0.3376E+02
3.	0.3671E+00	-0.7303E+02	0.4251E+00	-0.8140E+02	0.2809E+00	-0.1058E+03
4.	0.9493E-01	-0.3302E+02	0.1049E+00	-0.2463E+02	0.1829E+00	-0.1309E+02
5.	0.1194E+00	-0.3783E+02	0.1040E+00	-0.4813E+02	0.4986E-01	0.9370E+02
6.	0.4911E-01	0.1332E+02	0.6445E-01	0.8197E+01	0.4727E-01	-0.8001E+02
7.	0.2386E-01	0.5520E+01	0.2161E-01	0.1022E+02	0.3898E-01	0.1440E+02
8.	0.1402E-01	0.1022E+02	0.1543E-01	-0.1003E+02	0.1757E-01	-0.1220E+03
9.	0.1488E-01	0.3814E+00	0.1728E-01	-0.7851E+01	0.4455E-01	-0.1530E+02
10.	0.5374E-02	0.4394E+02	0.8189E-02	0.5386E+02	0.3372E-01	0.9890E+02
11.	0.1321E-01	0.6461E+02	0.1459E-01	0.5278E+02	0.4274E-02	-0.1369E+03
12.	0.6835E-02	0.1471E+03	0.9748E-02	0.1387E+03	0.1290E-01	0.8331E+02
13.	0.2371E-02	0.1213E+03	0.2253E-03	-0.1296E+03	0.1313E-01	-0.1704E+03
14.	0.3372E-02	-0.8493E+02	0.2433E-02	-0.1096E+03	0.1839E-01	-0.5378E+02
15.	0.4968E-02	-0.7963E+02	0.6816E-02	-0.9321E+02	0.6438E-02	0.1249E+02
16.	0.5827E-03	-0.9895E+01	0.3264E-02	-0.4687E+02	0.1793E-02	-0.1775E+03
17.	0.4464E-02	-0.3392E+01	0.4635E-02	-0.3417E+02	0.6929E-02	0.2429E+02
18.	0.3071E-02	0.1198E+03	0.2925E-02	0.2876E+02	0.8098E-02	0.1494E+03
19.	0.2767E-02	0.3932E+02	0.4737E-02	0.2053E+02	0.8218E-02	-0.4349E+02
20.	0.2524E-02	-0.4180E+02	0.2254E-02	-0.9930E+02	0.6415E-02	0.1965E+02
21.	0.2551E-02	0.4277E+02	0.3616E-02	0.1175E+02	0.2976E-02	0.3727E+02
22.	0.4033E-02	0.2446E+02	0.6349E-02	0.7866E+00	0.1175E-01	0.2741E+01
23.	0.5340E-02	0.1501E+02	0.6565E-02	-0.1222E+02	0.4914E-02	0.4652E+02
24.	0.3170E-03	0.1429E+03	0.1948E-02	0.1350E+03	0.5535E-02	-0.9357E+02
25.	0.2093E-02	-0.8828E+02	0.1467E-02	-0.7817E+02	0.2718E-02	0.9982E+01
26.	0.2869E-02	0.8168E+02	0.1990E-02	0.1435E+02	0.1050E-02	0.1214E+03
27.	0.2453E-02	0.2304E+01	0.3271E-02	0.9833E+01	0.8762E-02	-0.1030E+02
28.	0.2790E-02	-0.1287E+02	0.6527E-03	-0.6505E+02	0.3951E-02	0.1319E+03
29.	0.1547E-02	-0.5256E+02	0.1061E-02	-0.1128E+03	0.5192E-02	-0.9508E+02
30.	0.9438E-03	0.4870E+02	0.3033E-02	0.6497E+02	0.7452E-02	0.6489E+02
31.	0.1814E-02	0.7974E+02	0.2967E-02	0.8855E+01	0.2413E-02	0.1434E+03
32.	0.1648E-02	-0.5178E+02	0.7764E-03	-0.5359E+02	0.6426E-02	-0.5123E+02
33.	0.1544E-02	0.9176E+02	0.1806E-02	0.1252E+03	0.6869E-02	0.6899E+02
34.	0.1865E-02	0.6207E+02	0.1625E-02	0.1605E+03	0.1111E-02	-0.1024E+03
35.	0.2685E-03	0.9866E+02	0.1948E-02	0.1373E+03	0.4980E-02	0.9436E+02
36.	0.6469E-03	-0.1197E+03	0.1777E-02	-0.1444E+03	0.8336E-02	-0.1423E+03
37.	0.2244E-02	0.1436E+03	0.1058E-02	-0.2884E+02	0.6658E-02	-0.9631E+01
38.	0.1705E-02	-0.1740E+03	0.2943E-02	0.5032E+02	0.7939E-02	0.1026E+03
39.	0.3119E-02	0.6442E+02	0.1738E-02	0.5179E+02	0.2429E-02	-0.6394E+02
40.	0.3062E-02	0.1157E+03	0.3270E-02	0.5742E+02	0.6488E-02	0.7764E+02
41.	0.9927E-03	0.1392E+03	0.1291E-02	0.1319E+03	0.4861E-02	-0.1729E+03
42.	0.2744E-02	0.9001E+02	0.2531E-02	0.1608E+03	0.3155E-02	0.4710E+02
43.	0.7121E-03	0.1561E+02	0.2373E-02	0.1639E+03	0.8077E-02	0.1703E+03
44.	0.1703E-02	0.1094E+02	0.1354E-02	0.6125E+02	0.6029E-02	-0.3403E+02
45.	0.2199E-02	0.1730E+03	0.3810E-02	0.7826E+02	0.6103E-02	0.6248E+02
46.	0.1007E-02	0.2916E+02	0.1663E-02	-0.1565E+03	0.6991E-02	-0.1247E+03
47.	0.9721E-03	0.1059E+03	0.2436E-02	0.2531E+00	0.4614E-02	-0.6068E+01
48.	0.1243E-02	0.7602E+02	0.2640E-02	-0.1153E+03	0.5081E-02	-0.1524E+03
49.	0.7809E-03	0.1269E+03	0.2635E-02	-0.1557E+03	0.3062E-02	-0.9978E+02
50.	0.1161E-02	-0.2824E+01	0.1709E-02	-0.1556E+03	0.3731E-02	0.1265E+03
51.	0.1189E-02	-0.2689E+02	0.1794E-02	-0.1160E+03	0.3280E-02	-0.1154E+03
52.	0.6753E-03	0.1666E+03	0.2011E-02	0.1518E+03	0.1492E-02	0.6092E+02
53.	0.1446E-02	-0.6572E+02	0.1379E-02	-0.3952E+02	0.8376E-03	0.9607E+02
54.	0.2119E-02	-0.1797E+03	0.2684E-02	0.1609E+03	0.4556E-02	0.1360E+03
55.	0.2062E-02	-0.7690E+02	0.4071E-02	-0.1368E+03	0.4752E-02	-0.1358E+03
56.	0.1316E-02	0.8351E+02	0.1377E-02	-0.1466E+03	0.2012E-02	-0.8141E+02
57.	0.1533E-02	-0.8084E+02	0.1211E-02	0.7274E+02	0.9592E-03	0.1392E+02
58.	0.8756E-03	-0.1235E+03	0.2424E-02	0.3838E+02	0.6600E-03	0.1549E+03
59.	0.4442E-03	-0.3893E+02	0.9317E-03	0.1429E+03	0.2319E-02	0.1670E+03
60.	0.2031E-02	0.9429E+02	0.1713E-02	-0.5912E+01	0.7894E-02	0.1771E+02
61.	0.6659E-03	0.3423E+02	0.2572E-02	0.1473E+03	0.7408E-02	0.1294E+03
62.	0.2799E-02	0.1634E+02	0.1015E-02	-0.7696E+01	0.3846E-02	-0.7916E+02
63.	0.1944E-02	-0.4651E+02	0.7489E-03	-0.7285E+01	0.3535E-02	0.6650E+02
64.	0.1456E-02	0.4930E+02	0.3609E-02	-0.1291E+03	0.6745E-02	-0.1026E+03
65.	0.2865E-02	0.1306E+03	0.1793E-02	0.1104E+03	0.2967E-02	0.7977E+02
66.	0.2812E-02	-0.1097E+03	0.2177E-02	-0.1327E+02	0.7157E-03	-0.1725E+03
67.	0.1820E-02	-0.1918E+02	0.1320E-02	-0.2191E+01	0.7953E-02	-0.3282E+02
68.	0.8837E-03	0.1300E+03	0.3202E-02	-0.8669E+02	0.4281E-02	0.1615E+03
69.	0.4083E-02	0.7035E+02	0.3731E-02	-0.7178E+02	0.9195E-02	-0.8926E+02
70.	0.8037E-03	0.4075E+01	0.4217E-02	0.1634E+03	0.9848E-02	0.7978E+02
71.	0.3593E-02	0.1647E+03	0.2594E-02	-0.6419E+00	0.9613E-02	-0.1461E+03
72.	0.2101E-02	0.1507E+03	0.9596E-03	0.1155E+02	0.1042E-01	0.1247E+02
73.	0.2871E-02	-0.5834E+02	0.2445E-02	0.1739E+03	0.1082E-01	0.1677E+03
74.	0.3629E-02	0.4793E+02	0.3943E-02	0.2431E+02	0.1008E-01	-0.1429E+02
75.	0.3933E-03	-0.9216E+02	0.8700E-04	0.2750E+02	0.8759E-02	0.1018E+03
76.	0.3150E-02	-0.1466E+03	0.4400E-02	0.3360E+02	0.5975E-02	-0.1032E+03
77.	0.1552E-02	0.2993E+02	0.8179E-03	0.9497E+02	0.8210E-02	0.3356E+02
78.	0.6086E-03	0.1235E+03	0.3774E-02	0.1266E+03	0.9074E-02	0.1696E+03

ORIGINAL PAGE IS
OF POOR QUALITY

TABLE XXII.- CONTINUED

BOTTOM SURFACE

	RADIUS= Ø.97Ø CHORD= Ø.15Ø		RADIUS= .Ø.97Ø CHORD= Ø.2ØØ		RADIUS= Ø.97Ø CHORD= Ø.35Ø	
HARM	AMPLITUDE	PHASE	AMPLITUDE	PHASE	AMPLITUDE	PHASE
Ø.	Ø.1169E+Ø2	Ø.ØØØØE+ØØ	Ø.1142E+Ø2	Ø.ØØØØE+ØØ	Ø.1261E+Ø2	Ø.ØØØØE+ØØ
1.	Ø.2586E+Ø1	-Ø.7897E+Ø2	Ø.2968E+Ø1	-Ø.8Ø57E+Ø2	Ø.9462E+ØØ	-Ø.8365E+Ø2
2.	Ø.7412E+ØØ	Ø.1995E+Ø2	Ø.9318E+ØØ	Ø.1623E+Ø2	Ø.4252E-Ø1	Ø.5886E+Ø2
3.	Ø.1839E+ØØ	Ø.1538E+Ø3	Ø.2ØØ8E+ØØ	Ø.1249E+Ø3	Ø.136ØE+ØØ	-Ø.6857E+Ø2
4.	Ø.1745E+ØØ	-Ø.1Ø73E+Ø3	Ø.7918E-Ø1	-Ø.9327E+Ø2	Ø.6555E-Ø1	Ø.4958E+Ø2
5.	Ø.1347E+ØØ	-Ø.1645E+Ø2	Ø.7864E-Ø1	Ø.6Ø46E+Ø2	Ø.2657E-Ø1	Ø.1713E+Ø3
6.	Ø.59Ø5E-Ø1	Ø.819ØE+Ø2	Ø.9121E-Ø1	-Ø.1796E+Ø3	Ø.11ØØE-Ø1	-Ø.5Ø59E+Ø2
7.	Ø.1953E-Ø1	-Ø.98Ø1E+Ø2	Ø.7746E-Ø1	-Ø.8734E+Ø2	Ø.5357E-Ø2	Ø.1194E+Ø3
8.	Ø.1539E-Ø1	Ø.3592E+Ø2	Ø.5457E-Ø1	-Ø.438ØE+Ø2	Ø.1811E-Ø1	-Ø.11Ø9E+Ø3
9.	Ø.1273E-Ø1	-Ø.1442E+Ø3	Ø.7616E-Ø1	Ø.37Ø8E+Ø1	Ø.22Ø4E-Ø1	-Ø.1228E+Ø2
1Ø.	Ø.15Ø3E-Ø1	-Ø.5676E+Ø2	Ø.8462E-Ø1	Ø.8846E+Ø2	Ø.1559E-Ø1	Ø.9593E+Ø2
11.	Ø.23ØØE-Ø1	Ø.3532E+Ø2	Ø.5475E-Ø1	Ø.1721E+Ø3	Ø.3621E-Ø2	Ø.1643E+Ø3
12.	Ø.21ØØE-Ø1	Ø.1191E+Ø3	Ø.175ØE-Ø1	-Ø.1Ø25E+Ø3	Ø.2219E-Ø2	Ø.14Ø5E+Ø3
13.	Ø.1249E-Ø1	-Ø.17Ø4E+Ø3	Ø.1973E-Ø1	-Ø.1729E+Ø3	Ø.359ØE-Ø2	Ø.1783E+Ø3
14.	Ø.1556E-Ø1	-Ø.6675E+Ø2	Ø.4295E-Ø1	-Ø.7622E+Ø2	Ø.5359E-Ø2	-Ø.5274E+Ø2
15.	Ø.8529E-Ø2	-Ø.73Ø4E+ØØ	Ø.4552E-Ø1	Ø.1295E+Ø2	Ø.49Ø7E-Ø2	-Ø.1999E+Ø2
16.	Ø.3365E-Ø2	Ø.1653E+Ø3	Ø.28Ø3E-Ø1	Ø.1Ø57E+Ø3	Ø.2626E-Ø2	Ø.6648E+Ø2
17.	Ø.1384E-Ø1	Ø.5Ø74E+Ø1	Ø.3764E-Ø2	Ø.1341E+Ø3	Ø.1144E-Ø2	Ø.5558E+Ø2
18.	Ø.2245E-Ø1	Ø.1174E+Ø3	Ø.17ØØE-Ø1	Ø.14Ø6E+Ø3	Ø.2297E+Ø2	Ø.9119E+Ø2
19.	Ø.2351E-Ø1	-Ø.1254E+Ø3	Ø.1263E-Ø1	-Ø.1Ø85E+Ø3	Ø.171ØE-Ø2	Ø.8162E+Ø2
2Ø.	Ø.2642E-Ø1	-Ø.2347E+Ø2	Ø.27Ø1E-Ø2	Ø.9899E+Ø2	Ø.2Ø81E-Ø2	-Ø.9554E+Ø2
21.	Ø.2193E-Ø1	Ø.8136E+Ø2	Ø.2333E-Ø1	-Ø.1222E+Ø3	Ø.2568E-Ø2	Ø.5929E+Ø2
22.	Ø.7414E-Ø2	-Ø.8417E+Ø2	Ø.4528E-Ø1	-Ø.1297E+Ø2	Ø.126ØE-Ø2	Ø.7187E+Ø2
23.	Ø.1379E-Ø1	Ø.4128E+Ø2	Ø.4798E-Ø1	Ø.8374E+Ø2	Ø.28Ø3E-Ø2	-Ø.5355E+ØØ
24.	Ø.2Ø85E-Ø1	-Ø.1696E+Ø3	Ø.32Ø9E-Ø1	-Ø.1549E+Ø3	Ø.4949E-Ø3	Ø.1452E+Ø3
25.	Ø.264ØE-Ø1	-Ø.5878E+Ø2	Ø.2Ø51E-Ø1	-Ø.6117E+Ø1	Ø.3Ø72E-Ø2	-Ø.9232E+Ø2
26.	Ø.26Ø4E-Ø1	Ø.5483E+Ø2	Ø.32Ø5E-Ø1	Ø.1539E+Ø3	Ø.2488E-Ø2	Ø.3855E+Ø2
27.	Ø.1375E-Ø1	Ø.17Ø7E+Ø3	Ø.3788E-Ø1	-Ø.764ØE+Ø2	Ø.2961E-Ø2	Ø.8237E+Ø2
28.	Ø.8898E-Ø2	-Ø.674ØE+Ø2	Ø.384ØE-Ø1	Ø.4131E+Ø2	Ø.5697E-Ø3	-Ø.6789E+Ø2
29.	Ø.7952E-Ø2	Ø.1182E+Ø3	Ø.29Ø6E-Ø1	Ø.1757E+Ø3	Ø.1485E-Ø2	Ø.7598E+Ø2
3Ø.	Ø.1Ø15E-Ø1	-Ø.115ØE+Ø3	Ø.258ØE-Ø1	-Ø.3676E+Ø2	Ø.179ØE-Ø2	Ø.1512E+Ø3
31.	Ø.1524E-Ø1	Ø.652ØE+Ø1	Ø.2878E-Ø1	Ø.8575E+Ø2	Ø.14ØØE-Ø2	-Ø.29Ø5E+Ø2
32.	Ø.1182E-Ø1	Ø.1Ø1ØE+Ø3	Ø.1985E-Ø1	-Ø.1415E+Ø3	Ø.1982E-Ø2	Ø.2252E+Ø2
33.	Ø.8638E-Ø2	-Ø.1693E+Ø3	Ø.5932E-Ø2	Ø.4Ø51E+Ø1	Ø.1446E-Ø2	-Ø.1759E+Ø3
34.	Ø.4937E-Ø2	-Ø.3282E+Ø2	Ø.1Ø6ØE-Ø1	-Ø.1317E+Ø3	Ø.9693E-Ø3	Ø.2852E+Ø2
35.	Ø.4591E-Ø2	Ø.1157E+Ø3	Ø.1649E-Ø1	-Ø.13Ø1E+Ø2	Ø.1791E-Ø2	Ø.1528E+Ø3
36.	Ø.7494E-Ø2	-Ø.9732E+Ø2	Ø.1398E-Ø1	Ø.1197E+Ø3	Ø.13Ø2E-Ø2	-Ø.4894E+Ø2
37.	Ø.1Ø56E-Ø1	Ø.3637E+Ø2	Ø.9474E-Ø2	-Ø.7323E+Ø2	Ø.62Ø4E-Ø3	Ø.61Ø1E+Ø2
38.	Ø.16Ø2E-Ø1	Ø.141ØE+Ø3	Ø.1674E-Ø1	Ø.9497E+Ø2	Ø.2Ø7ØE-Ø2	Ø.1646E+Ø3
39.	Ø.1337E-Ø1	-Ø.861ØE+Ø2	Ø.2ØØ5E-Ø1	-Ø.1526E+Ø3	Ø.4722E-Ø3	-Ø.5425E+Ø2
4Ø.	Ø.1555E-Ø1	Ø.476ØE+Ø2	Ø.1562E-Ø1	-Ø.1743E+Ø2	Ø.7415E-Ø3	Ø.1254E+Ø3
41.	Ø.1238E-Ø1	-Ø.1754E+Ø3	Ø.1364E-Ø1	Ø.1326E+Ø3	Ø.8551E-Ø3	-Ø.1171E+Ø3
42.	Ø.916ØE-Ø2	-Ø.6Ø86E+Ø1	Ø.1279E-Ø1	-Ø.7757E+Ø2	Ø.7437E-Ø3	-Ø.1776E+Ø3
43.	Ø.1694E-Ø1	Ø.1355E+Ø3	Ø.1267E-Ø1	Ø.6612E+Ø2	Ø.9753E-Ø3	-Ø.1478E+Ø3
44.	Ø.141ØE-Ø1	-Ø.9116E+Ø2	Ø.12Ø6E-Ø1	-Ø.1525E+Ø3	Ø.7999E-Ø3	-Ø.1764E+Ø3
45.	Ø.17ØØE-Ø1	Ø.3Ø52E+Ø2	Ø.955ØE-Ø2	Ø.112ØE+Ø2	Ø.1152E-Ø2	-Ø.1332E+Ø3
46.	Ø.1Ø29E-Ø1	-Ø.1792E+Ø3	Ø.14Ø6E-Ø1	Ø.1625E+Ø3	Ø.1625E-Ø2	-Ø.625ØE+Ø1
47.	Ø.1142E-Ø1	-Ø.1ØØ7E+Ø2	Ø.234ØE-Ø1	-Ø.6716E+Ø2	Ø.1967E-Ø2	-Ø.5Ø95E+Ø2
48.	Ø.1171E-Ø1	Ø.1455E+Ø3	Ø.1628E-Ø1	Ø.5476E+Ø2	Ø.6253E-Ø3	-Ø.4349E+Ø2
49.	Ø.1282E-Ø1	-Ø.9227E+Ø2	Ø.8335E-Ø2	-Ø.1717E+Ø3	Ø.4396E-Ø3	Ø.1568E+Ø2
5Ø.	Ø.9511E-Ø2	Ø.5338E+Ø2	Ø.8662E-Ø2	Ø.4763E+Ø1	Ø.1272E-Ø2	-Ø.561ØE+Ø1
51.	Ø.7833E-Ø2	-Ø.1549E+Ø3	Ø.75Ø1E-Ø2	Ø.1494E+Ø3	Ø.5893E-Ø3	-Ø.7344E+Ø2
52.	Ø.7823E-Ø2	Ø.2343E+Ø2	Ø.9172E-Ø2	-Ø.8523E+Ø2	Ø.9635E-Ø3	Ø.1155E+Ø3
53.	Ø.7733E-Ø2	Ø.1549E+Ø3	Ø.1Ø78E-Ø1	Ø.3764E+Ø2	Ø.13Ø2E-Ø2	Ø.3152E+Ø1
54.	Ø.6228E-Ø2	-Ø.7922E+Ø2	Ø.54Ø5E-Ø2	Ø.1689E+Ø3	Ø.6Ø28E-Ø3	Ø.9847E+Ø2
55.	Ø.5326E-Ø2	Ø.1Ø1ØE+Ø3	Ø.8832E-Ø2	-Ø.4293E+Ø2	Ø.158ØE-Ø2	-Ø.9Ø63E+Ø2
56.	Ø.7138E-Ø2	-Ø.1267E+Ø3	Ø.7327E-Ø2	Ø.8472E+Ø2	Ø.1833E-Ø2	Ø.3518E+Ø2
57.	Ø.8689E-Ø2	Ø.2184E+Ø2	Ø.1468E-Ø2	-Ø.1146E+Ø3	Ø.9598E-Ø3	Ø.5131E+Ø2
58.	Ø.1Ø37E-Ø1	-Ø.17Ø4E+Ø3	Ø.4646E-Ø2	Ø.4295E+Ø2	Ø.6331E-Ø3	-Ø.4588E+Ø2
59.	Ø.189ØE-Ø2	-Ø.2828E-Ø2	Ø.4179E-Ø2	Ø.1467E+Ø3	Ø.1161E-Ø2	Ø.1274E+Ø3
6Ø.	Ø.6845E-Ø2	Ø.361ØE+Ø2	Ø.4458E-Ø2	-Ø.9872E+Ø1	Ø.1578E-Ø2	Ø.4531E+Ø2
61.	Ø.7631E-Ø3	Ø.2229E+Ø2	Ø.1775E-Ø2	Ø.1532E+Ø3	Ø.1137E-Ø2	-Ø.1384E+Ø3
62.	Ø.1421E-Ø2	Ø.15Ø2E+Ø3	Ø.4173E-Ø2	-Ø.7Ø54E+Ø2	Ø.12Ø1E-Ø2	Ø.377ØE+Ø2
63.	Ø.3496E-Ø2	-Ø.1686E+Ø3	Ø.7669E-Ø2	Ø.2713E+Ø2	Ø.14Ø8E-Ø2	-Ø.8554E+Ø2
64.	Ø.41Ø1E-Ø2	-Ø.9999E+Ø2	Ø.659ØE-Ø2	Ø.147ØE+Ø3	Ø.1623E-Ø2	-Ø.3515E+Ø1
65.	Ø.2399E-Ø2	-Ø.1696E+Ø3	Ø.656ØE-Ø2	-Ø.2861E+Ø2	Ø.1873E-Ø2	Ø.4772E+Ø2
66.	Ø.8652E-Ø2	Ø.1176E+Ø2	Ø.8ØØØE-Ø2	Ø.1Ø3ØE+Ø3	Ø.1632E-Ø2	Ø.6572E+Ø2
67.	Ø.4354E-Ø2	-Ø.1599E+Ø3	Ø.79Ø5E-Ø2	-Ø.1Ø44E+Ø3	Ø.1482E-Ø2	-Ø.4167E+Ø2
68.	Ø.8136E-Ø2	-Ø.8266E+Ø2	Ø.6Ø81E-Ø2	Ø.7465E+Ø1	Ø.1136E-Ø2	-Ø.5159E+Ø2
69.	Ø.363ØE-Ø2	Ø.1466E+Ø3	Ø.5583E-Ø2	-Ø.179ØE+Ø3	Ø.3813E-Ø3	-Ø.3239E+Ø1
7Ø.	Ø.3587E-Ø3	-Ø.3763E+Ø2	Ø.1288E-Ø1	-Ø.5Ø27E+Ø2	Ø.1836E-Ø2	-Ø.1292E+Ø3
71.	Ø.1184E-Ø2	-Ø.21Ø8E+Ø2	Ø.1229E-Ø1	Ø.88Ø2E+Ø2	Ø.1628E-Ø2	-Ø.4116E+Ø2
72.	Ø.5996E-Ø2	Ø.126ØE+Ø3	Ø.1196E-Ø1	-Ø.1414E+Ø3	Ø.3969E-Ø3	-Ø.891ØE+Ø2
73.	Ø.2155E-Ø2	-Ø.87Ø4E+Ø2	Ø.8459E-Ø2	Ø.518ØE+Ø1	Ø.1961E-Ø2	Ø.6555E+ØØ
74.	Ø.6857E-Ø2	Ø.472ØE+Ø2	Ø.41Ø6E-Ø2	-Ø.1746E+Ø3	Ø.1793E-Ø2	-Ø.6991E+Ø2
75.	Ø.5158E-Ø2	Ø.142ØE+Ø3	Ø.6532E-Ø2	-Ø.3938E+Ø2	Ø.492ØE-Ø3	-Ø.926ØE+Ø2
76.	Ø.2284E-Ø2	-Ø.3883E+Ø2	Ø.4168E-Ø2	Ø.826ØE+Ø2	Ø.1561E-Ø2	-Ø.6642E+Ø2
77.	Ø.2841E-Ø2	Ø.1148E+Ø3	Ø.7419E-Ø2	-Ø.1145E+Ø3	Ø.1139E-Ø2	-Ø.834ØE+Ø2
78.	Ø.33Ø5E-Ø2	Ø.1364E+Ø3	Ø.4365E-Ø2	-Ø.1898E+Ø2	Ø.235ØE-Ø2	-Ø.1Ø13E+Ø3

TABLE XXII.- CONTINUED

BOTTOM SURFACE

HARM	RADIUS= 0.970 CHORD= 0.400 AMPLITUDE	PHASE	RADIUS= 0.970 CHORD= 0.450 AMPLITUDE	PHASE	RADIUS= 0.970 CHORD= 0.500 AMPLITUDE	PHASE
0.	0.1295E+02	0.0000E+00	0.1329E+02	0.0000E+00	0.1316E+02	0.0000E+00
1.	0.6891E+00	-0.8662E+02	0.5755E+00	-0.8701E+02	0.3129E+00	-0.9326E+02
2.	0.4884E-01	0.9232E+02	0.6613E-01	0.1009E+03	0.7188E-01	0.1536E+03
3.	0.9936E-01	-0.7508E+02	0.8120E-01	-0.7925E+02	0.5540E-01	-0.7019E+02
4.	0.4582E-01	0.5638E+02	0.3437E-01	0.7106E+02	0.2306E-01	0.1631E+03
5.	0.2498E-01	0.1777E+03	0.2101E-01	-0.1730E+03	0.1825E-01	-0.5492E+02
6.	0.1380E-01	-0.8012E+02	0.1201E-01	-0.8526E+02	0.4959E-02	0.1390E+03
7.	0.6874E-02	-0.5526E+01	0.6380E-02	-0.3271E+02	0.1110E-01	-0.6263E+02
8.	0.7362E-02	-0.1541E+03	0.5463E-02	-0.1558E+03	0.3964E-02	0.1271E+03
9.	0.1013E-01	-0.5218E+02	0.9182E-02	-0.6749E+02	0.5493E-02	-0.6467E+02
10.	0.6444E-02	0.6429E+02	0.4138E-02	0.6508E+02	0.3538E-02	0.1156E+03
11.	0.5083E-02	0.7088E+02	0.5098E-02	0.6370E+02	0.2576E-02	-0.4986E+02
12.	0.5887E-02	0.1388E+03	0.5164E-02	0.1586E+03	0.1773E-02	0.9905E+02
13.	0.1810E-02	-0.1583E+03	0.7570E-03	-0.6638E+02	0.8098E-03	-0.3557E+02
14.	0.3094E-02	-0.4157E+02	0.2445E-02	-0.3455E+02	0.1866E-02	0.2005E+02
15.	0.3409E-02	-0.5449E+02	0.3898E-02	-0.6871E+02	0.1885E-02	-0.1054E+03
16.	0.2446E-02	0.7041E+01	0.2731E-02	-0.1075E+02	0.1074E-02	0.5712E+02
17.	0.1908E-02	0.3723E+02	0.2418E-02	0.2758E+02	0.7017E-03	-0.1268E+03
18.	0.2050E-02	0.4033E+02	0.2417E-02	0.6473E+02	0.1612E-02	0.4828E+02
19.	0.2648E-02	0.6592E+02	0.3635E-02	0.5632E+02	0.6788E-03	-0.3393E+02
20.	0.2097E-02	-0.1462E+03	0.1271E-02	-0.1722E+03	0.6358E-03	0.1307E+02
21.	0.2491E-02	0.4151E+02	0.2844E-02	0.5165E+02	0.7458E-03	0.9052E+02
22.	0.2944E-02	0.7925E+02	0.2019E-02	0.7735E+02	0.1505E-02	0.1066E+02
23.	0.1928E-02	-0.3838E+02	0.2215E-02	-0.2866E+02	0.2036E-03	0.3042E+02
24.	0.1223E-02	-0.2077E+01	0.9137E-03	0.9518E+01	0.9603E-03	-0.1335E+02
25.	0.5058E-03	-0.1249E+03	0.1272E-02	-0.1367E+03	0.3324E-03	-0.1684E+03
26.	0.7409E-03	0.4580E+02	0.1392E-02	0.4892E+02	0.2280E-03	0.6877E+02
27.	0.2319E-02	0.1860E+02	0.3064E-02	0.1781E+02	0.8190E-03	0.6081E+02
28.	0.7065E-03	0.1327E+02	0.4309E-04	-0.1574E+03	0.6938E-03	-0.4509E+02
29.	0.1173E-02	0.4090E+02	0.8026E-03	-0.8785E+02	0.6845E-03	0.6570E+02
30.	0.1474E-02	0.1126E+03	0.2100E-03	0.1615E+03	0.7655E-03	-0.4764E+02
31.	0.2746E-03	-0.1127E+03	0.7221E-03	0.4735E+02	0.1135E-02	0.5682E+02
32.	0.1994E-02	-0.4615E+02	0.2987E-02	-0.4784E+02	0.1805E-02	-0.4398E+02
33.	0.1048E-02	0.1379E+03	0.5215E-03	0.1648E+03	0.2985E-03	0.1378E+03
34.	0.1039E-02	-0.3912E+02	0.2228E-02	-0.3161E+02	0.1077E-02	-0.3251E+02
35.	0.2227E-02	0.1241E+03	0.1796E-02	0.1225E+03	0.4175E-03	0.1316E+03
36.	0.2246E-02	-0.3155E+02	0.2289E-02	-0.5153E+02	0.1082E-02	-0.3798E+01
37.	0.9403E-03	0.2291E+02	0.1760E-02	0.1385E+02	0.5734E-03	-0.1253E+03
38.	0.1741E-02	0.1535E+03	0.2353E-02	0.1377E+03	0.6759E-03	0.1190E+03
39.	0.1049E-02	0.2216E+02	0.1060E-02	0.1681E+01	0.6968E-03	0.8088E+02
40.	0.2119E-02	0.8277E+02	0.1678E-02	0.7561E+02	0.5730E-03	0.9045E+02
41.	0.5458E-03	-0.1302E+03	0.1500E-03	-0.1184E+02	0.9133E-03	0.7562E+02
42.	0.1153E-02	0.1943E+02	0.9682E-03	0.6164E+02	0.6281E-03	0.3106E+02
43.	0.7376E-03	-0.6102E+02	0.1742E-02	-0.1132E+03	0.1700E-03	-0.1158E+03
44.	0.8853E-03	0.5751E+02	0.1250E-02	0.4960E+01	0.7788E-03	0.1437E+03
45.	0.1068E-02	0.9084E+02	0.2354E-02	0.1078E+03	0.6717E-03	0.8051E+02
46.	0.1444E-02	-0.5355E+02	0.1811E-02	-0.4696E+02	0.2554E-04	0.8334E+02
47.	0.7517E-03	0.1590E+03	0.8363E-03	0.8028E+02	0.2591E-03	0.1640E+03
48.	0.3380E-03	-0.1255E+03	0.1080E-02	0.1699E+03	0.3284E-03	0.1512E+03
49.	0.1408E-02	0.5945E+02	0.1161E-02	0.1298E+03	0.1942E-03	0.1091E+03
50.	0.3369E-03	-0.1686E+03	0.3844E-03	-0.4835E+02	0.7086E-04	0.3367E+02
51.	0.1871E-02	-0.6079E+02	0.1953E-02	-0.4455E+02	0.3754E-03	-0.3771E+02
52.	0.1189E-02	-0.2803E+02	0.6342E-03	-0.1271E+03	0.6288E-03	-0.9754E+02
53.	0.1519E-02	-0.1452E+03	0.2533E-02	-0.1437E+03	0.2339E-03	-0.1451E+03
54.	0.8417E-03	-0.4943E+02	0.8356E-03	-0.4659E+02	0.4024E-03	-0.6378E+02
55.	0.1068E-02	-0.6532E+02	0.7425E-03	-0.1069E+03	0.3255E-03	-0.1064E+03
56.	0.4932E-03	-0.7408E+01	0.1067E-02	0.3094E+02	0.2288E-03	-0.4662E+02
57.	0.8083E-03	0.3800E+02	0.1446E-02	0.1106E+03	0.4154E-03	-0.3584E+02
58.	0.5340E-03	-0.8170E+02	0.2089E-02	-0.1281E+03	0.6079E-03	-0.6851E+02
59.	0.5071E-03	-0.5171E+02	0.1327E-02	-0.2247E+02	0.1972E-03	-0.8601E+02
60.	0.5622E-03	-0.1081E+03	0.2261E-03	-0.4730E+02	0.2937E-03	-0.6549E+02
61.	0.6627E-03	0.1039E+03	0.6551E-03	0.6308E+02	0.2928E-03	0.5777E+02
62.	0.1193E-02	-0.3414E+02	0.1083E-02	-0.9270E+02	0.6799E-03	-0.1360E+02
63.	0.8484E-03	-0.1321E+02	0.1266E-02	-0.7120E+00	0.4296E-03	-0.1420E+02
64.	0.1551E-02	-0.5007E+02	0.2484E-02	-0.2415E+02	0.7106E-03	-0.4478E+02
65.	0.1011E-02	0.1069E+03	0.2014E-02	0.6868E+02	0.4924E-04	-0.1142E+01
66.	0.3935E-03	0.7603E+02	0.1549E-02	0.1263E+03	0.9196E-03	-0.1467E+02
67.	0.1318E-02	-0.6350E+02	0.2929E-02	-0.7146E+02	0.9693E-03	-0.7277E+02
68.	0.4677E-03	-0.9412E+02	0.5083E-03	-0.4097E+02	0.6744E-03	-0.9805E+02
69.	0.1329E-02	-0.9204E+02	0.4465E-03	-0.1273E+03	0.7890E-03	-0.1057E+03
70.	0.1038E-02	-0.1659E+03	0.2069E-02	0.1692E+03	0.9713E-03	-0.1527E+03
71.	0.8955E-03	0.9130E+02	0.1127E-02	0.7347E+02	0.4526E-03	0.1242E+03
72.	0.1416E-02	0.1471E+02	0.6041E-03	0.1804E+02	0.3759E-03	-0.4290E+02
73.	0.3390E-03	-0.2835E+02	0.1607E-02	-0.7777E+02	0.5438E-03	-0.6694E+02
74.	0.1398E-02	-0.2993E+02	0.3107E-02	-0.7667E+02	0.9448E-03	-0.8510E+02
75.	0.1392E-02	-0.1255E+03	0.1236E-02	-0.9631E+02	0.1102E-02	-0.1146E+03
76.	0.4701E-03	-0.1627E+03	0.2396E-02	0.1428E+03	0.8445E-03	-0.1638E+03
77.	0.1318E-02	0.5465E+02	0.8874E-03	0.1250E+03	0.2759E-03	0.4432E+02
78.	0.2028E-02	-0.1152E+03	0.1153E-02	-0.1114E+03	0.6175E-03	-0.4295E+02

TABLE XXII.- CONTINUED

BOTTOM SURFACE

	RADIUS= 0.970 CHORD= 0.599		RADIUS= 0.970 CHORD= 0.699		RADIUS= 0.970 CHORD= 0.919	
HARM	AMPLITUDE	PHASE	AMPLITUDE	PHASE	AMPLITUDE	PHASE
0.	0.1328E+02	0.0000E+00	0.1340E+02	0.0000E+00	0.1340E+02	0.0000E+00
1.	0.2719E+00	-0.9048E+02	0.1439E+00	-0.1018E+03	0.2182E+00	0.9663E+02
2.	0.8429E-01	0.1021E+03	0.7421E-01	0.1045E+03	0.6015E-01	0.1412E+03
3.	0.3657E-01	-0.9054E+02	0.2174E-01	-0.9787E+02	0.5392E-02	-0.1678E+03
4.	0.2061E-01	0.1044E+03	0.1884E-01	0.1199E+03	0.9357E-02	0.1127E+03
5.	0.1662E-01	-0.1494E+03	0.1515E-01	-0.1430E+03	0.1148E-01	-0.1409E+03
6.	0.6660E-02	-0.8244E+02	0.6206E-02	-0.8694E+02	0.3312E-02	-0.5323E+02
7.	0.3206E-02	-0.5817E+02	0.3387E-02	-0.7342E+02	0.7457E-03	-0.7013E+02
8.	0.3555E-02	-0.1748E+03	0.2067E-02	-0.1621E+03	0.1863E-02	0.1658E+03
9.	0.5640E-02	-0.6727E+02	0.5036E-02	-0.7711E+02	0.3777E-02	-0.9600E+02
10.	0.1806E-02	0.2145E+02	0.7036E-03	0.1269E+02	0.8573E-03	0.2146E+02
11.	0.2119E-02	0.2298E+02	0.1517E-02	0.1678E+02	0.1675E-02	-0.1737E+02
12.	0.2952E-02	0.1590E+03	0.1941E-02	0.1483E+03	0.2347E-02	0.1268E+03
13.	0.8532E-03	-0.7845E+02	0.1127E-03	0.1915E+02	0.9505E-03	0.1710E+03
14.	0.1178E-02	-0.1173E+02	0.1273E-02	-0.2155E+02	0.7778E-03	0.4866E+01
15.	0.2007E-02	-0.9666E+02	0.1930E-02	-0.1045E+03	0.1463E-02	-0.9572E+02
16.	0.1639E-02	-0.1685E+02	0.1001E-02	-0.1731E+02	0.9024E-03	-0.5026E+02
17.	0.1709E-02	0.1972E+02	0.1560E-02	0.5133E+01	0.1330E-02	-0.3519E+02
18.	0.1577E-02	0.4475E+02	0.1152E-02	0.2129E+02	0.1083E-02	0.1649E+02
19.	0.1510E-02	0.6804E+02	0.2728E-02	0.4557E+02	0.1088E-02	0.1971E+02
20.	0.1187E-02	-0.1653E+03	0.8338E-03	0.1677E+03	0.7723E-03	0.6702E+02
21.	0.8863E-03	0.1338E+02	0.1013E-02	0.4074E+02	0.9405E-03	0.7314E+02
22.	0.9191E-03	0.1071E+03	0.1022E-02	0.9279E+02	0.1295E-02	0.8206E+02
23.	0.1002E-02	-0.1041E+03	0.7415E-03	-0.1202E+03	0.5769E-03	0.9981E+02
24.	0.1097E-02	-0.1661E+02	0.7496E-03	-0.4971E+02	0.1230E-02	-0.1431E+03
25.	0.4910E-03	-0.1442E+03	0.5912E-03	-0.7551E+02	0.1199E-02	-0.1150E+03
26.	0.3321E-03	-0.5831E+02	0.1094E-02	0.1373E+03	0.1066E-02	0.3698E+02
27.	0.1669E-02	0.1183E+02	0.1202E-02	-0.2918E+01	0.1997E-03	0.6970E+02
28.	0.5881E-03	0.5820E+02	0.8300E-03	0.1009E+02	0.1473E-02	-0.8044E+02
29.	0.8661E-03	-0.3924E+02	0.8235E-03	-0.1131E+03	0.7364E-03	0.5886E+02
30.	0.8733E-03	0.3609E+02	0.7548E-03	-0.2272E+02	0.8640E-03	0.1726E+03
31.	0.1040E-02	0.1256E+03	0.8701E-03	0.5682E+02	0.1055E-02	0.1191E+02
32.	0.1444E-02	-0.4763E+02	0.8625E-03	-0.2873E+02	0.9285E-03	-0.1560E+03
33.	0.5362E-03	-0.1702E+03	0.3679E-03	0.1413E+03	0.4429E-03	0.1156E+03
34.	0.6395E-03	-0.4425E+02	0.3169E-03	-0.1227E+03	0.1225E-02	0.1109E+03
35.	0.1905E-03	0.1544E+03	0.3751E-03	-0.1486E+03	0.4488E-03	-0.1228E+03
36.	0.8111E-03	-0.5331E+02	0.8901E-03	-0.7266E+02	0.8150E-03	0.1692E+03
37.	0.7947E-03	0.1008E+02	0.8495E-03	-0.3431E+02	0.5774E-03	-0.1162E+03
38.	0.6935E-03	0.1110E+03	0.5583E-03	0.9044E+02	0.5946E-03	-0.1039E+03
39.	0.1849E-03	-0.2702E+02	0.6070E-04	0.1358E+03	0.7686E-03	0.8668E+02
40.	0.3535E-03	0.7102E+02	0.5545E-03	0.4437E+02	0.2011E-03	0.4209E+02
41.	0.6710E-03	0.1300E+03	0.6430E-03	0.1318E+03	0.1065E-02	0.7671E+02
42.	0.2678E-03	0.1837E+02	0.1333E-03	0.2104E+02	0.3814E-03	0.1775E+03
43.	0.3089E-03	-0.1748E+03	0.5295E-03	-0.1335E+03	0.6371E-03	0.1241E+03
44.	0.3182E-03	0.1787E+03	0.6828E-03	0.8835E+02	0.9775E-03	-0.1424E+03
45.	0.5476E-03	0.1268E+03	0.5933E-03	0.8390E+02	0.5438E-03	-0.6587E+02
46.	0.1088E-03	0.1643E+03	0.5400E-03	0.1249E+03	0.2891E-03	0.1167E+03
47.	0.7256E-03	0.1406E+03	0.5633E-03	0.1746E+03	0.1408E-02	-0.1133E+03
48.	0.5961E-03	-0.1265E+03	0.1770E-03	-0.3358E+02	0.4039E-03	-0.1528E+03
49.	0.2060E-03	-0.8808E+02	0.6981E-03	0.1160E+03	0.3845E-03	-0.5744E+02
50.	0.3448E-03	-0.1155E+03	0.1199E-02	-0.1080E+03	0.4931E-03	0.6489E+02
51.	0.5185E-03	-0.2674E+02	0.7110E-03	0.6544E+01	0.5288E-03	-0.9899E+02
52.	0.7347E-03	0.1728E+02	0.9769E-03	0.5831E+02	0.4278E-03	-0.2002E+01
53.	0.4386E-03	-0.1384E+02	0.4244E-04	0.1393E+02	0.3772E-03	0.3906E+01
54.	0.4265E-03	-0.3290E+02	0.3740E-03	-0.1368E+03	0.1162E-02	-0.2290E+02
55.	0.8036E-03	-0.6356E+02	0.1058E-02	-0.3267E+02	0.3266E-03	-0.1623E+02
56.	0.5444E-03	0.1122E+02	0.3299E-03	0.1218E+03	0.7661E-03	0.1310E-01
57.	0.3065E-03	0.7401E+02	0.3532E-03	-0.6921E+01	0.7060E-03	-0.6761E+02
58.	0.5878E-03	-0.3178E+02	0.4014E-03	-0.3929E+02	0.4821E-03	0.3701E+01
59.	0.8158E-03	0.4123E+01	0.5222E-03	0.7225E+02	0.9713E-03	-0.1034E+03
60.	0.3714E-03	0.1773E+03	0.6433E-04	0.1166E+03	0.3237E-03	-0.2859E+02
61.	0.2215E-03	0.1503E+03	0.1139E-02	0.6575E+02	0.1261E-02	-0.2097E+02
62.	0.5415E-03	-0.1274E+03	0.5500E-03	-0.1331E+03	0.1088E-03	0.1590E+03
63.	0.5493E-03	-0.2711E+02	0.8085E-03	-0.9646E+02	0.5228E-03	0.1399E+03
64.	0.1657E-03	0.3900E+02	0.3031E-03	0.1258E+03	0.2953E-03	0.2947E+02
65.	0.2436E-03	-0.1501E+02	0.5654E-03	0.5187E+02	0.4371E-03	-0.3517E+02
66.	0.6387E-03	0.4569E+02	0.1161E-02	-0.7013E+01	0.5977E-03	0.2055E+02
67.	0.6130E-03	-0.7823E+02	0.8175E-03	-0.3829E+02	0.3541E-03	-0.1387E+02
68.	0.1029E-02	-0.6115E+02	0.9714E-03	-0.6894E+02	0.4310E-03	-0.1003E+03
69.	0.7124E-03	-0.2634E+02	0.8808E-03	-0.3251E+02	0.1038E-02	-0.8418E+02
70.	0.6245E-03	-0.1120E+03	0.1194E-02	-0.1200E+03	0.4096E-03	-0.8793E+02
71.	0.1110E-02	-0.8858E+02	0.1824E-02	-0.1056E+03	0.5023E-03	-0.1560E+03
72.	0.9420E-03	-0.1408E+03	0.1051E-02	-0.1218E+03	0.9888E-03	-0.6954E+02
73.	0.7336E-03	-0.1405E+03	0.4251E-03	-0.1111E+03	0.1347E-03	-0.5784E+02
74.	0.1147E-03	-0.9553E+02	0.1017E-02	0.7168E+02	0.4568E-03	-0.1290E+03
75.	0.4716E-03	-0.5861E+02	0.4828E-03	-0.1756E+03	0.5010E-03	-0.1691E+03
76.	0.4072E-03	-0.4803E+02	0.5802E-03	-0.1666E+02	0.6580E-03	0.1121E+03
77.	0.1710E-03	0.4627E+02	0.1032E-02	-0.7063E+01	0.5986E-03	-0.9047E+02
78.	0.5927E-03	-0.5662E+02	0.3567E-03	0.5341E+02	0.7572E-03	-0.7589E+02

TABLE XXII.- CONTINUED

TOP SURFACE

HARM	RADIUS= Ø.97Ø CHORD= Ø.Ø1Ø AMPLITUDE	PHASE	RADIUS= Ø.97Ø CHORD= Ø.Ø3Ø AMPLITUDE	PHASE	RADIUS= Ø.97Ø CHORD= Ø.Ø8Ø AMPLITUDE	PHASE
Ø.	Ø.1Ø4ØE+Ø2	Ø.ØØØØE+ØØ	Ø.8857E+Ø1	Ø.ØØØØE+ØØ	Ø.916ØE+Ø1	Ø.ØØØØE+ØØ
1.	Ø.4892E+Ø1	Ø.12Ø7E+Ø3	Ø.2176E+Ø1	Ø.15Ø5E+Ø3	Ø.1483E+Ø1	-Ø.1213E+Ø3
2.	Ø.7912E+ØØ	Ø.1226E+Ø3	Ø.71Ø3E+ØØ	Ø.1753E+Ø3	Ø.2429E+ØØ	-Ø.1Ø41E+Ø3
3.	Ø.7616E+ØØ	Ø.7655E+Ø2	Ø.5251E+ØØ	Ø.1212E+Ø3	Ø.724ØE-Ø1	-Ø.1314E+Ø3
4.	Ø.3483E+ØØ	Ø.4151E+Ø2	Ø.3683E+ØØ	Ø.1171E+Ø3	Ø.1281E+ØØ	-Ø.1681E+Ø2
5.	Ø.4192E-Ø1	-Ø.7938E+Ø2	Ø.342ØE+ØØ	Ø.1263E+Ø3	Ø.5354E-Ø1	Ø.857ØE+Ø2
6.	Ø.1533E+ØØ	-Ø.1367E+Ø3	Ø.1977E+ØØ	Ø.1176E+Ø3	Ø.2382E-Ø1	-Ø.4739E+Ø2
7.	Ø.1634E+ØØ	-Ø.1797E+Ø3	Ø.1643E+ØØ	Ø.1ØØ7E+Ø3	Ø.3416E-Ø1	Ø.6448E+Ø2
8.	Ø.1179E+ØØ	Ø.1445E+Ø3	Ø.1237E+ØØ	Ø.8176E+Ø2	Ø.2Ø33E-Ø1	Ø.1165E+Ø3
9.	Ø.6295E-Ø1	Ø.14Ø2E+Ø3	Ø.73Ø9E-Ø1	Ø.7341E+Ø2	Ø.6ØØØE-Ø2	-Ø.1314E+Ø3
1Ø.	Ø.2426E-Ø1	-Ø.1671E+Ø3	Ø.4Ø82E-Ø1	Ø.192ØE+Ø2	Ø.1766E-Ø1	-Ø.4899E+Ø2
11.	Ø.4Ø54E-Ø1	-Ø.169ØE+Ø3	Ø.3841E-Ø1	-Ø.4Ø28E+Ø2	Ø.1133E-Ø1	-Ø.5718E+Ø2
12.	Ø.3513E-Ø1	Ø.1522E+Ø3	Ø.5383E-Ø1	-Ø.5785E+Ø2	Ø.7369E-Ø2	-Ø.8313E+Ø1
13.	Ø.29Ø9E-Ø1	Ø.1Ø55E+Ø3	Ø.5934E-Ø1	-Ø.7659E+Ø2	Ø.7239E-Ø2	Ø.1726E+Ø2
14.	Ø.2581E-Ø1	Ø.77Ø7E+Ø2	Ø.5573E-Ø1	-Ø.9478E+Ø2	Ø.1436E-Ø1	Ø.217ØE+Ø2
15.	Ø.1795E-Ø1	Ø.6114E+Ø2	Ø.55Ø1E-Ø1	-Ø.1186E+Ø3	Ø.1156E-Ø1	Ø.17ØØE+Ø2
16.	Ø.11Ø9E-Ø1	Ø.53Ø9E+Ø2	Ø.5968E-Ø1	-Ø.1429E+Ø3	Ø.884ØE-Ø2	Ø.6525E+Ø2
17.	Ø.1385E-Ø1	-Ø.76Ø9E+Ø1	Ø.5733E-Ø1	-Ø.1545E+Ø3	Ø.8128E-Ø2	Ø.117ØE+Ø3
18.	Ø.1358E-Ø1	-Ø.27Ø9E+Ø2	Ø.4368E-Ø1	-Ø.1749E+Ø3	Ø.72Ø3E-Ø2	Ø.1216E+Ø3
19.	Ø.9888E-Ø2	-Ø.8659E+Ø2	Ø.3548E-Ø1	Ø.1593E+Ø3	Ø.3443E-Ø2	Ø.1345E+Ø3
2Ø.	Ø.8663E-Ø2	-Ø.1Ø86E+Ø3	Ø.2794E-Ø1	Ø.1346E+Ø3	Ø.4Ø85E-Ø2	-Ø.14Ø5E+Ø3
21.	Ø.7714E-Ø2	Ø.1615E+Ø3	Ø.259ØE-Ø1	Ø.9288E+Ø2	Ø.318ØE-Ø2	Ø.1695E+Ø3
22.	Ø.84Ø1E-Ø2	Ø.1414E+Ø3	Ø.2533E-Ø1	Ø.5339E+Ø2	Ø.4546E-Ø2	Ø.1768E+Ø3
23.	Ø.3417E-Ø2	Ø.1189E+Ø3	Ø.3Ø4ØE-Ø1	Ø.32Ø9E+Ø2	Ø.6Ø43E-Ø2	Ø.1776E+Ø3
24.	Ø.6756E-Ø2	-Ø.9743E+Ø2	Ø.2693E-Ø1	-Ø.1434E+Ø1	Ø.7593E-Ø2	-Ø.738ØE+Ø2
25.	Ø.1269E-Ø1	-Ø.1717E+Ø3	Ø.3ØØ7E-Ø1	-Ø.1742E+Ø2	Ø.7556E-Ø2	-Ø.2247E+Ø2
26.	Ø.1713E-Ø1	Ø.1716E+Ø3	Ø.2552E-Ø1	-Ø.3642E+Ø2	Ø.2836E-Ø2	Ø.6279E+Ø1
27.	Ø.17Ø1E-Ø1	Ø.1355E+Ø3	Ø.2Ø36E-Ø1	-Ø.5577E+Ø2	Ø.2933E-Ø2	Ø.3296E+Ø2
28.	Ø.7631E-Ø2	Ø.1174E+Ø3	Ø.1654E-Ø1	-Ø.7993E+Ø2	Ø.4174E-Ø2	-Ø.3223E+Ø1
29.	Ø.2Ø47E-Ø2	Ø.3641E+Ø2	Ø.165ØE-Ø1	-Ø.1245E+Ø3	Ø.6125E-Ø2	-Ø.4395E+Ø2
3Ø.	Ø.4873E-Ø2	Ø.1619E+Ø3	Ø.1386E-Ø1	-Ø.1738E+Ø3	Ø.3859E-Ø2	-Ø.216ØE+Ø2
31.	Ø.95Ø2E-Ø2	Ø.1476E+Ø3	Ø.1832E-Ø1	Ø.1524E+Ø3	Ø.1944E-Ø2	-Ø.9269E+Ø2
32.	Ø.432ØE-Ø2	Ø.1134E+Ø3	Ø.2431E-Ø1	Ø.13Ø6E+Ø3	Ø.7359E-Ø2	Ø.4457E+Ø2
33.	Ø.3719E-Ø2	Ø.1567E+Ø3	Ø.2695E-Ø1	Ø.1Ø96E+Ø3	Ø.731ØE-Ø2	Ø.5352E+Ø2
34.	Ø.7385E-Ø2	-Ø.1321E+Ø3	Ø.2311E-Ø1	Ø.9689E+Ø2	Ø.2945E-Ø2	-Ø.1233E+Ø3
35.	Ø.4695E-Ø2	-Ø.1146E+Ø3	Ø.2717E-Ø1	Ø.9335E+Ø2	Ø.5787E-Ø2	Ø.12Ø6E+Ø3
36.	Ø.4512E-Ø2	Ø.124ØE+Ø3	Ø.223ØE-Ø1	Ø.7157E+Ø2	Ø.5351E-Ø2	Ø.1283E+Ø3
37.	Ø.2435E-Ø2	-Ø.114ØE+Ø3	Ø.1514E-Ø1	Ø.5678E+Ø2	Ø.2778E-Ø2	Ø.4921E+Ø2
38.	Ø.65Ø1E-Ø2	-Ø.1Ø13E+Ø3	Ø.815ØE-Ø2	Ø.4424E+Ø2	Ø.3Ø7ØE-Ø2	-Ø.1327E+Ø3
39.	Ø.8782E-Ø2	-Ø.174ØE+Ø3	Ø.4799E-Ø2	Ø.6923E+Ø2	Ø.3Ø7ØE-Ø2	-Ø.6775E+Ø2
4Ø.	Ø.4899E-Ø2	Ø.1299E+Ø3	Ø.5252E-Ø2	-Ø.1375E+Ø3	Ø.1813E-Ø2	-Ø.2152E+Ø2
41.	Ø.76ØØE-Ø2	Ø.96Ø5E+Ø2	Ø.5816E-Ø2	-Ø.1483E+Ø3	Ø.3963E-Ø2	Ø.1985E+Ø2
42.	Ø.2899E-Ø2	-Ø.6498E+Ø2	Ø.1124E-Ø1	-Ø.15Ø3E+Ø3	Ø.4983E-Ø2	-Ø.137ØE+Ø2
43.	Ø.2596E-Ø2	-Ø.1466E+Ø3	Ø.1817E-Ø1	Ø.177ØE+Ø3	Ø.8784E-Ø3	Ø.1444E+Ø3
44.	Ø.7663E-Ø2	-Ø.1735E+Ø3	Ø.19Ø6E-Ø1	-Ø.1769E+Ø3	Ø.5611E-Ø2	Ø.1794E+Ø3
45.	Ø.953ØE-Ø2	Ø.1Ø68E+Ø3	Ø.1226E-Ø1	Ø.1695E+Ø3	Ø.2422E-Ø2	Ø.7721E+Ø2
46.	Ø.377ØE-Ø2	-Ø.1934E+Ø2	Ø.128ØE-Ø1	Ø.1695E+Ø3	Ø.1937E-Ø2	Ø.146ØE+Ø3
47.	Ø.2593E-Ø2	-Ø.8315E+Ø2	Ø.1275E-Ø1	-Ø.1779E+Ø3	Ø.6229E-Ø2	-Ø.1449E+Ø3
48.	Ø.8286E-Ø2	-Ø.1166E+Ø2	Ø.8794E-Ø2	Ø.1473E+Ø3	Ø.3911E-Ø2	-Ø.132ØE+Ø3
49.	Ø.386ØE-Ø2	Ø.1564E+Ø3	Ø.5484E-Ø2	-Ø.1177E+Ø3	Ø.16Ø8E-Ø2	-Ø.16Ø1E+Ø3
5Ø.	Ø.5674E-Ø2	Ø.155ØE+Ø3	Ø.3366E-Ø2	-Ø.9618E+Ø2	Ø.6414E-Ø2	-Ø.125ØE+Ø3
51.	Ø.15Ø3E-Ø2	Ø.1746E+Ø3	Ø.423ØE-Ø2	-Ø.6382E+Ø2	Ø.5614E-Ø2	-Ø.8852E+Ø1
52.	Ø.28Ø6E-Ø2	-Ø.1687E+Ø3	Ø.2713E-Ø2	-Ø.2Ø75E+Ø2	Ø.3Ø9ØE-Ø2	Ø.9598E+Ø2
53.	Ø.5125E-Ø2	-Ø.1621E+Ø3	Ø.6753E-Ø2	-Ø.8814E+Ø2	Ø.1753E-Ø2	Ø.159ØE+Ø3
54.	Ø.5554E-Ø2	Ø.1361E+Ø2	Ø.7433E-Ø2	-Ø.846ØE+Ø2	Ø.7Ø96E-Ø2	Ø.9322E+Ø2
55.	Ø.2224E-Ø2	Ø.5764E+Ø2	Ø.2967E-Ø2	-Ø.1786E+Ø2	Ø.4152E-Ø2	Ø.1782E+Ø2
56.	Ø.1435E-Ø1	-Ø.46Ø8E+Ø2	Ø.5771E-Ø2	-Ø.1Ø7ØE+Ø3	Ø.2Ø43E-Ø2	-Ø.7553E+Ø2
57.	Ø.4672E-Ø2	-Ø.1669E+Ø3	Ø.314ØE-Ø2	-Ø.52Ø6E+Ø2	Ø.71Ø9E-Ø2	-Ø.3271E+Ø2
58.	Ø.7787E-Ø2	Ø.1258E+Ø3	Ø.2313E-Ø2	-Ø.2648E+Ø2	Ø.6282E-Ø2	Ø.4845E+Ø2
59.	Ø.9775E-Ø2	Ø.7877E+Ø2	Ø.4ØØ1E-Ø2	-Ø.1571E+Ø3	Ø.4197E-Ø2	Ø.1732E+Ø3
6Ø.	Ø.7237E-Ø2	-Ø.52Ø2E+Ø2	Ø.593ØE-Ø2	-Ø.5384E+Ø1	Ø.1Ø46E-Ø1	-Ø.2667E+Ø2
61.	Ø.5474E-Ø2	Ø.1424E+Ø3	Ø.3512E-Ø2	Ø.1768E+Ø3	Ø.6179E-Ø2	Ø.1676E+Ø3
62.	Ø.7232E-Ø2	-Ø.12Ø9E+Ø3	Ø.2354E-Ø2	Ø.8714E+Ø2	Ø.29ØØE-Ø2	-Ø.5263E+Ø2
63.	Ø.465ØE-Ø2	Ø.1185E+Ø3	Ø.9971E-Ø2	Ø.5395E+Ø2	Ø.4848E-Ø2	Ø.6968E+Ø2
64.	Ø.3394E-Ø2	-Ø.5945E+Ø2	Ø.5Ø31E-Ø2	Ø.5383E+Ø2	Ø.5866E-Ø2	-Ø.689ØE+Ø2
65.	Ø.4ØØ9E-Ø2	-Ø.13Ø3E+Ø3	Ø.27Ø5E-Ø2	Ø.148ØE+Ø3	Ø.28Ø1E-Ø2	-Ø.1246E+Ø3
66.	Ø.8352E-Ø2	Ø.1273E+Ø3	Ø.2531E-Ø3	Ø.1Ø46E+Ø3	Ø.2454E-Ø2	Ø.1378E+Ø3
67.	Ø.6972E-Ø2	Ø.1973E+Ø2	Ø.659ØE-Ø2	-Ø.4Ø85E+Ø2	Ø.615ØE-Ø2	-Ø.5Ø7ØE+Ø2
68.	Ø.7668E-Ø2	-Ø.1Ø69E+Ø3	Ø.357ØE-Ø2	-Ø.1292E+Ø3	Ø.2593E-Ø2	Ø.1462E+Ø3
69.	Ø.1Ø51E-Ø1	-Ø.1Ø22E+Ø3	Ø.497ØE-Ø2	Ø.99Ø9E+Ø2	Ø.64Ø9E-Ø2	-Ø.2213E+Ø1
7Ø.	Ø.3849E-Ø2	-Ø.7481E+Ø1	Ø.1622E-Ø2	-Ø.7Ø31E+Ø2	Ø.1376E-Ø2	Ø.1Ø64E+Ø3
71.	Ø.6497E-Ø2	-Ø.1673E+Ø2	Ø.526ØE-Ø2	-Ø.1187E+Ø3	Ø.2812E-Ø2	-Ø.1121E+Ø3
72.	Ø.6673E-Ø2	-Ø.148ØE+Ø3	Ø.7223E-Ø2	-Ø.32Ø4E+Ø1	Ø.3128E-Ø2	-Ø.1618E+Ø2
73.	Ø.59Ø8E-Ø2	Ø.4599E+Ø2	Ø.6236E-Ø2	-Ø.4968E+Ø2	Ø.7199E-Ø2	-Ø.8268E+Ø2
74.	Ø.1Ø27E-Ø1	-Ø.5134E+Ø2	Ø.3667E-Ø2	-Ø.1543E+Ø3	Ø.22Ø6E-Ø2	Ø.3653E+Ø2
75.	Ø.7936E-Ø2	-Ø.2ØØ4E+Ø2	Ø.26Ø8E-Ø2	Ø.7631E+Ø2	Ø.2653E-Ø2	Ø.1364E+Ø3
76.	Ø.355ØE-Ø2	-Ø.1651E+Ø3	Ø.2435E-Ø2	Ø.122ØE+Ø3	Ø.5568E-Ø2	Ø.5169E+Ø2
77.	Ø.3815E-Ø2	Ø.1Ø19E+Ø3	Ø.8525E-Ø2	-Ø.168ØE+Ø3	Ø.7165E-Ø2	-Ø.1662E+Ø3
78.	Ø.6827E-Ø2	-Ø.2622E+Ø2	Ø.366ØE-Ø2	-Ø.2737E+Ø2	Ø.5948E-Ø2	Ø.11Ø2E+Ø3

ORIGINAL PAGE IS
OF POOR QUALITY

TABLE XXII.- CONTINUED

	TOP SURFACE					
	RADIUS= 0.970		RADIUS= 0.970		RADIUS= 0.970	
	CHORD= 0.150		CHORD= 0.250		CHORD= 0.350	
HARM	AMPLITUDE	PHASE	AMPLITUDE	PHASE	AMPLITUDE	PHASE
0.	0.1038E+02	0.0000E+00	0.1077E+02	0.0000E+00	0.1237E+02	0.0000E+00
1.	0.2156E+01	-0.1039E+03	0.2240E+01	-0.8881E+02	0.5835E+00	-0.7717E+02
2.	0.9261E+00	-0.3191E+02	0.1175E+01	-0.8497E+01	0.1438E+00	-0.2624E+02
3.	0.3857E+00	0.4380E+02	0.7563E+00	0.7666E+02	0.1328E+00	0.6347E+02
4.	0.1626E+00	0.3087E+02	0.4061E+00	0.1455E+03	0.1177E+00	0.1295E+03
5.	0.2391E+00	0.6111E+02	0.2463E+00	-0.1657E+03	0.1253E+00	-0.1378E+03
6.	0.1904E+00	0.1173E+03	0.2104E+00	-0.1185E+03	0.1270E+00	-0.4338E+02
7.	0.9894E-01	0.1561E+03	0.2052E+00	-0.5411E+02	0.1013E+00	0.3523E+02
8.	0.8554E-01	0.1427E+03	0.1710E+00	0.1231E+02	0.6488E-01	0.9920E+02
9.	0.1116E+00	-0.1664E+03	0.1015E+00	0.6094E+02	0.4758E-01	0.1549E+03
10.	0.8017E-01	-0.1003E+03	0.1053E+00	0.8863E+02	0.5124E-01	-0.1622E+03
11.	0.3225E-01	-0.8767E+02	0.1498E+00	0.1454E+03	0.4049E-01	-0.9499E+02
12.	0.6125E-01	-0.7947E+02	0.1453E+00	-0.1385E+03	0.4037E-01	-0.9005E+01
13.	0.6686E-01	-0.1581E+02	0.1069E+00	-0.5845E+02	0.2666E-01	0.4909E+02
14.	0.3877E-01	0.4726E+02	0.4583E-01	0.1033E+02	0.1499E-01	0.1215E+03
15.	0.2263E-01	0.1082E+02	0.3329E-01	-0.4544E+01	0.8907E-02	0.1452E+03
16.	0.4805E-01	0.6241E+02	0.5884E-01	0.5853E+02	0.1274E-01	-0.1738E+03
17.	0.4069E-01	0.1318E+03	0.6226E-01	0.1421E+03	0.1409E-01	-0.1234E+03
18.	0.1170E-01	0.1662E+03	0.3775E-01	-0.1355E+03	0.8933E-02	-0.5922E+02
19.	0.2534E-01	0.1420E+03	0.8637E-02	-0.9309E+02	0.9831E-02	0.2583E+02
20.	0.3616E-01	-0.1486E+03	0.3056E-01	-0.1033E+03	0.7561E-02	0.1270E+03
21.	0.1241E-01	-0.8285E+02	0.4059E-01	-0.1377E+01	0.6297E-02	0.1680E+03
22.	0.1312E-01	-0.1518E+03	0.3973E-01	0.9737E+02	0.3598E-02	-0.1075E+03
23.	0.2554E-01	-0.7307E+02	0.3138E-01	-0.1573E+03	0.3502E-02	-0.1087E+03
24.	0.1827E-01	0.1033E+02	0.1510E-01	-0.4587E+02	0.1701E-02	-0.4578E+02
25.	0.3103E-02	-0.7841E+02	0.7095E-02	0.1435E+03	0.2706E-02	0.3774E+02
26.	0.2533E-01	-0.4983E+01	0.1698E-01	-0.7928E+02	0.5175E-02	-0.1597E+03
27.	0.3068E-01	0.8414E+02	0.1957E-01	0.3674E+02	0.1541E-02	-0.1358E+03
28.	0.9000E-02	-0.1429E+03	0.1858E-01	0.1348E+03	0.6071E-02	-0.1707E+03
29.	0.1830E-01	0.2538E+02	0.9060E-02	-0.1659E+03	0.4420E-02	-0.6843E+02
30.	0.2403E-01	0.1396E+03	0.1004E-01	-0.1608E+03	0.5270E-02	0.4350E+02
31.	0.2128E-01	-0.1186E+03	0.2510E-01	-0.6467E+02	0.5497E-02	-0.2986E+01
32.	0.1331E-01	0.5211E+02	0.2363E-01	0.2025E+02	0.6712E-02	0.1332E+03
33.	0.2061E-01	0.1685E+03	0.1561E-01	0.8609E+02	0.5051E-02	-0.2932E+02
34.	0.2295E-01	-0.7500E+02	0.1232E-01	0.1629E+03	0.7795E-02	0.1457E+03
35.	0.1982E-01	0.5826E+02	0.9726E-02	0.1328E+03	0.6013E-02	-0.1548E+03
36.	0.1405E-01	-0.1593E+03	0.2170E-01	0.1765E+03	0.7627E-02	0.1472E+03
37.	0.2301E-01	-0.2598E+02	0.2249E-01	-0.9162E+02	0.2922E-02	0.1692E+03
38.	0.1309E-01	0.7630E+02	0.1871E-01	0.5208E+00	0.1078E-02	-0.4507E+02
39.	0.7391E-02	-0.1415E+03	0.8542E-02	0.5749E+02	0.3537E-02	0.9557E+02
40.	0.1479E-01	0.9109E+01	0.1201E-01	0.7917E+02	0.6203E-02	0.9754E+02
41.	0.1752E-01	0.1104E+03	0.1462E-01	0.1453E+03	0.8671E-04	0.1775E+03
42.	0.9513E-02	-0.1033E+03	0.1406E-01	-0.1488E+03	0.6680E-02	0.1677E+03
43.	0.1285E-01	0.9148E+02	0.5397E-02	-0.6734E+02	0.5558E-02	-0.9043E+02
44.	0.2019E-01	0.1777E+03	0.6772E-02	-0.1305E+03	0.3764E-02	-0.1680E+03
45.	0.7840E-02	-0.6218E+02	0.1170E-01	-0.1263E+02	0.2441E-02	-0.1537E+03
46.	0.6562E-02	0.1331E+03	0.9517E-02	0.7187E+02	0.5423E-02	-0.1365E+03
47.	0.1516E-01	-0.1105E+03	0.7495E-02	0.1543E+03	0.6914E-02	-0.3121E+01
48.	0.9195E-02	-0.2407E+02	0.1352E-01	-0.1329E+03	0.5204E-02	0.1720E+03
49.	0.3483E-02	-0.4483E+02	0.3746E-02	-0.7651E+02	0.3858E-03	-0.1813E+02
50.	0.4652E-02	-0.7537E+02	0.1189E-01	-0.8636E+02	0.4690E-02	-0.9679E+02
51.	0.6918E-02	0.4251E+02	0.1384E-01	-0.6687E+01	0.8278E-02	0.4139E+02
52.	0.1162E-01	0.1025E+03	0.6992E-02	0.4872E+02	0.4114E-02	-0.1554E+03
53.	0.4172E-02	0.6839E+02	0.1031E-01	0.1117E+03	0.6132E-02	0.1370E+03
54.	0.1347E-01	0.1083E+03	0.2978E-02	0.7520E+02	0.7804E-02	0.7299E+01
55.	0.4045E-02	-0.1481E+03	0.6682E-02	-0.5163E+02	0.1042E-01	0.2112E+02
56.	0.2804E-02	-0.7111E+02	0.1006E-01	-0.2268E+02	0.6524E-02	0.1202E+02
57.	0.8131E-02	-0.1173E+03	0.4113E-02	0.1453E+03	0.1016E-01	-0.1703E+03
58.	0.1144E-01	-0.3457E+02	0.5183E-02	-0.1541E+02	0.4705E-02	0.4008E+02
59.	0.4905E-02	0.3623E+02	0.4305E-02	0.5645E+02	0.6309E-02	-0.4670E+02
60.	0.1120E-01	-0.5553E+02	0.3603E-02	-0.1574E+03	0.9525E-03	0.1294E+03
61.	0.8035E-02	0.2626E+02	0.8029E-02	0.1586E+03	0.5407E-02	0.1409E+03
62.	0.1134E-02	0.2602E+02	0.5413E-02	-0.1046E+03	0.3072E-02	-0.9059E+02
63.	0.5426E-02	0.4379E+02	0.1124E-01	-0.5115E+02	0.9378E-02	-0.5155E+02
64.	0.6289E-02	0.4635E+02	0.4098E-02	-0.3801E+02	0.3146E-02	0.8041E+01
65.	0.1410E-01	0.1679E+03	0.3222E-02	-0.8710E+02	0.1070E-01	-0.1431E+03
66.	0.6161E-02	-0.1413E+03	0.9563E-02	0.1309E+03	0.7388E-02	0.1472E+03
67.	0.7556E-02	-0.4026E+02	0.7921E-02	0.1744E+03	0.7102E-02	0.1519E+03
68.	0.1244E-01	-0.1441E+03	0.1137E-02	0.9499E+02	0.6777E-02	0.8618E+01
69.	0.9779E-02	-0.4936E+02	0.1093E-02	0.1277E+03	0.4887E-02	0.1164E+03
70.	0.5132E-02	0.4143E+02	0.6801E-02	0.1472E+03	0.1141E-01	0.1479E+03
71.	0.4172E-02	-0.7661E+02	0.8159E-02	0.6610E+02	0.8141E-02	0.2171E+02
72.	0.9887E-02	0.2899E+02	0.8713E-02	-0.9475E+02	0.5996E-02	-0.4795E+02
73.	0.2967E-02	0.4346E+02	0.9822E-02	-0.8616E+02	0.1128E-01	-0.1031E+03
74.	0.1123E-02	-0.1410E+03	0.4946E-02	-0.1592E+03	0.4553E-02	-0.1344E+03
75.	0.1149E-01	0.6281E+02	0.9440E-02	-0.1090E+03	0.7199E-02	-0.9727E+02
76.	0.4482E-02	0.1042E+03	0.8677E-02	-0.8687E+02	0.1227E-01	-0.9183E+02
77.	0.1291E-01	0.1677E+03	0.5195E-02	0.1454E+03	0.6544E-02	-0.1566E+03
78.	0.7661E-02	0.8947E+02	0.3526E-02	-0.7868E+02	0.6750E-02	-0.8402E+02

ORIGINAL PAGE IS
OF POOR QUALITY

TABLE XXII.- CONTINUED

	RADIUS= 0.970 CHORD= 0.500		TOP SURFACE RADIUS= 0.970 CHORD= 0.550		RADIUS= 0.970 CHORD= 0.599	
HARM	AMPLITUDE	PHASE	AMPLITUDE	PHASE	AMPLITUDE	PHASE
0.	0.1268E+02	0.0000E+00	0.1306E+02	0.0000E+00	0.1295E+02	0.0000E+00
1.	0.2101E+00	0.1393E+02	0.2275E+00	0.1594E+02	0.2558E+00	0.1953E+02
2.	0.1033E+00	0.1774E+03	0.7923E-01	-0.1773E+03	0.6686E-01	-0.1719E+03
3.	0.4884E-01	-0.1168E+03	0.4206E-01	-0.1055E+03	0.3576E-01	-0.9997E+02
4.	0.6800E-01	-0.1838E+02	0.5217E-01	-0.1832E+02	0.4223E-01	-0.2433E+02
5.	0.4270E-01	0.5700E+02	0.3495E-01	0.6284E+02	0.2927E-01	0.6243E+02
6.	0.1347E-01	0.8597E+02	0.1204E-01	0.9625E+02	0.9222E-02	0.8757E+02
7.	0.1236E-01	0.1297E+03	0.7148E-02	0.1408E+03	0.4635E-02	0.1274E+03
8.	0.8138E-02	-0.1416E+03	0.5168E-02	-0.1345E+03	0.4096E-02	-0.1384E+03
9.	0.5955E-02	-0.5757E+02	0.4538E-04	-0.1596E+03	0.1914E-02	0.9320E+02
10.	0.2893E-02	-0.2727E+02	0.4196E-02	0.7413E+02	0.3895E-02	0.7031E+02
11.	0.1214E-02	0.1537E+03	0.4978E-02	0.1074E+03	0.3919E-02	0.1067E+03
12.	0.4340E-02	0.1373E+03	0.4587E-03	0.6194E+02	0.1581E-02	0.4499E+01
13.	0.2841E-02	0.1799E+03	0.1426E-02	-0.1710E+03	0.1495E-02	0.1493E+03
14.	0.1719E-02	0.1975E+02	0.2325E-02	-0.3013E+02	0.1889E-02	-0.3036E+02
15.	0.1669E-02	0.2910E+02	0.2187E-02	0.2513E+02	0.2579E-02	0.9109E+01
16.	0.3691E-02	0.7919E+02	0.2067E-02	-0.1681E+03	0.8384E-03	0.1266E+03
17.	0.3167E-02	0.1214E+03	0.1898E-02	-0.7262E+02	0.1330E-02	-0.8701E+02
18.	0.1892E-02	0.1619E+03	0.1288E-02	-0.6178E+02	0.1321E-02	-0.6929E+02
19.	0.1508E-02	0.7171E+02	0.1288E-02	-0.1015E+03	0.3481E-03	-0.1063E+03
20.	0.5028E-02	-0.8872E+02	0.2682E-02	-0.1323E+03	0.2687E-02	-0.1578E+03
21.	0.1322E-02	-0.1007E+03	0.2028E-02	0.1727E+03	0.1902E-02	0.1554E+03
22.	0.3116E-02	-0.9799E+02	0.6940E-03	0.1331E+03	0.4555E-03	0.1353E+03
23.	0.4029E-02	0.1029E+03	0.1534E-02	0.1341E+03	0.1480E-02	0.1180E+03
24.	0.8766E-03	0.7486E+02	0.1767E-02	-0.2701E+01	0.1080E-02	-0.2673E+01
25.	0.2412E-02	-0.1184E+03	0.2091E-02	-0.1009E+00	0.1582E-02	0.1912E+02
26.	0.1272E-03	-0.5532E+02	0.3100E-02	-0.2377E+02	0.1070E-02	-0.2753E+02
27.	0.8558E-03	0.1305E+03	0.1394E-02	-0.1218E+03	0.7296E-03	-0.1541E+03
28.	0.1226E-02	-0.1799E+03	0.3413E-02	-0.1299E+03	0.1204E-02	-0.1475E+03
29.	0.2164E-02	-0.7412E+02	0.2720E-02	-0.1002E+03	0.1868E-02	-0.9124E+02
30.	0.3276E-02	0.1082E+03	0.2291E-02	0.1594E+03	0.1487E-02	0.1116E+03
31.	0.5954E-02	0.1690E+02	0.1723E-02	0.1005E+03	0.7809E-03	0.1063E+03
32.	0.3353E-02	0.6489E+02	0.3574E-02	0.1248E+03	0.2070E-02	0.9993E+02
33.	0.2755E-02	-0.6892E+02	0.5694E-03	0.3090E+01	0.5612E-03	0.1521E+03
34.	0.3144E-02	-0.5408E+02	0.2031E-02	0.7283E+02	0.1060E-02	0.6556E+02
35.	0.5374E-02	-0.1301E+03	0.5975E-03	-0.1352E+03	0.1603E-02	0.6933E+02
36.	0.4033E-02	0.1165E+03	0.2682E-02	0.5586E+02	0.7764E-03	-0.6665E+01
37.	0.1711E-02	-0.1354E+03	0.2377E-02	-0.1286E+03	0.6781E-03	0.1585E+03
38.	0.4419E-02	0.1633E+03	0.2038E-02	-0.8246E+02	0.1480E-02	-0.1316E+03
39.	0.2266E-02	-0.4989E+02	0.1252E-02	0.2921E+02	0.1398E-02	-0.6059E+02
40.	0.2219E-02	-0.1063E+03			0.7109E-03	-0.1182E+03
41.	0.5159E-02	-0.8695E+02			0.8495E-03	0.1344E+03
42.	0.5299E-02	-0.8703E+01			0.1255E-02	0.1606E+03
43.	0.4329E-02	0.1415E+03			0.3338E-03	0.1466E+03
44.	0.2844E-02	0.1495E+03			0.8931E-03	0.4912E+02
45.	0.8119E-03	0.9942E+02			0.1433E-02	0.3161E+02
46.	0.1094E-02	-0.1223E+03			0.7959E-03	-0.2122E+02
47.	0.2230E-02	-0.8658E+02			0.9780E-03	-0.4219E+02
48.	0.3343E-02	-0.9976E+01			0.8699E-03	-0.1169E+03
49.	0.3659E-02	0.4949E+02			0.2301E-02	-0.1197E+03
50.	0.7391E-02	0.1082E+03			0.8001E-03	-0.1646E+03
51.	0.2793E-02	0.1268E+03			0.2073E-02	0.1588E+03
52.	0.4294E-02	0.6079E+02			0.2007E-02	0.1512E+03
53.	0.3267E-02	0.5769E+02			0.1778E-02	0.2061E+02
54.	0.1056E-02	-0.5500E+02			0.8813E-03	0.4749E+02
55.	0.5113E-02	-0.3323E+02			0.9792E-03	-0.2333E+02
56.	0.4175E-02	-0.7228E+02			0.7208E-03	-0.3739E+02
57.	0.4682E-02	-0.2588E+02			0.4360E-03	-0.9854E+02
58.	0.2724E-02	-0.1411E+03			0.3241E-02	-0.1300E+03
59.	0.7059E-02	-0.9561E+02			0.7262E-03	-0.1712E+03
60.	0.8132E-02	0.1733E+02			0.1355E-02	0.3947E+02
61.	0.1286E-02	0.1184E+02			0.9431E-03	-0.1622E+03
62.	0.3110E-02	-0.6514E+02			0.1537E-02	0.3531E+02
63.	0.8031E-02	-0.8325E+01			0.5649E-03	0.2511E+02
64.	0.2075E-02	0.4117E+02			0.1156E-02	-0.1129E+03
65.	0.2002E-02	-0.6224E+01			0.7333E-03	0.1405E+03
66.	0.4348E-02	-0.1506E+03			0.9242E-03	-0.1419E+02
67.	0.1818E-02	-0.1638E+03			0.2402E-02	0.1621E+03
68.	0.3411E-02	0.1686E+03			0.1341E-02	0.8005E+02
69.	0.6047E-02	0.1651E+03			0.8413E-03	0.1170E+03
70.	0.6744E-02	-0.1261E+03			0.1114E-02	0.2155E+02
71.	0.9472E-03	-0.1716E+03			0.1530E-02	0.5884E+02
72.	0.3260E-02	0.7821E+02			0.2605E-03	0.1220E+03
73.	0.1478E-02	0.4124E+02			0.7563E-03	-0.1685E+03
74.	0.3330E-02	0.1032E+03			0.1189E-02	-0.1016E+03
75.	0.4321E-02	0.7632E+02			0.1806E-02	-0.1378E+03
76.	0.7526E-02	-0.1603E+03			0.1382E-02	0.1263E+03
77.	0.7038E-02	-0.8160E+02			0.1407E-02	-0.1526E+03
78.	0.4895E-02	-0.1074E+03			0.2074E-02	0.1377E+03

ORIGINAL PAGE IS
OF POOR QUALITY

TABLE XXII.- CONTINUED

	RADIUS= 0.970		TOP SURFACE RADIUS= 0.970	
	CHORD= 0.699		CHORD= 0.919	
HARM	AMPLITUDE	PHASE	AMPLITUDE	PHASE
0.	0.1303E+02	0.0000E+00	0.1336E+02	0.0000E+00
1.	0.2439E+00	0.3380E+02	0.3337E+00	0.6985E+02
2.	0.3934E-01	-0.1790E+03	0.4294E-01	0.1535E+03
3.	0.2815E-01	-0.7818E+02	0.3227E-01	-0.7936E+02
4.	0.2697E-01	-0.3347E+02	0.2466E-02	-0.8489E+02
5.	0.1973E-01	0.7180E+02	0.8437E-02	0.5864E+02
6.	0.8245E-02	0.8571E+02	0.2570E-02	0.1026E+03
7.	0.2390E-02	0.1098E+03	0.3442E-02	0.5673E+02
8.	0.1453E-02	-0.1044E+03	0.1373E-02	-0.1036E+03
9.	0.2936E-02	0.1169E+03	0.2869E-02	0.1565E+03
10.	0.2534E-02	0.9979E+02	0.2074E-02	0.8263E+02
11.	0.2063E-02	0.1266E+03	0.2087E-02	0.5385E+01
12.	0.1330E-02	0.4062E+00	0.2788E-02	-0.6594E+02
13.	0.2052E-02	0.1293E+03	0.1686E-02	0.1279E+03
14.	0.1021E-02	0.1587E+03	0.1346E-02	0.6002E+02
15.	0.1215E-02	-0.1017E+02	0.1333E-02	-0.1791E+02
16.	0.4489E-03	0.1270E+03	0.1069E-02	-0.9746E+02
17.	0.9799E-03	-0.7062E+02	0.1117E-02	-0.9881E+02
18.	0.1070E-02	-0.1246E+03	0.5216E-03	0.1701E+03
19.	0.2461E-03	0.1098E+03	0.1151E-02	0.1856E+02
20.	0.1311E-02	-0.1713E+03	0.5920E-03	-0.6452E+02
21.	0.1324E-02	0.1415E+03	0.1230E-02	0.5296E+02
22.	0.8863E-03	-0.5332E+02	0.8865E-03	0.1312E+03
23.	0.2710E-03	0.1411E+03	0.1361E-02	-0.1775E+03
24.	0.4072E-03	0.1560E+03	0.1268E-02	-0.1005E+03
25.	0.1481E-03	0.8688E+02	0.1337E-02	-0.7311E+02
26.	0.1230E-02	-0.2727E+02	0.1394E-02	-0.1636E+03
27.	0.1657E-02	0.6387E+02	0.1230E-02	0.6959E+02
28.	0.1393E-02	0.1498E+03	0.7363E-03	0.7124E+02
29.	0.2567E-02	-0.6343E+02	0.2126E-02	-0.7403E+02
30.	0.6839E-03	-0.5577E+01	0.1484E-02	0.3854E+01
31.	0.1307E-02	-0.1178E+03	0.3489E-03	-0.1529E+03
32.	0.2139E-02	0.1283E+03	0.1673E-02	0.1070E+02
33.	0.2215E-02	0.1635E+03	0.1015E-02	0.1523E+03
34.	0.1956E-02	0.9033E+02	0.1034E-02	0.1156E+03
35.	0.1820E-02	0.8347E+02	0.1084E-02	0.1476E+03
36.	0.1935E-02	0.3566E+02	0.9611E-03	0.1733E+02
37.	0.1146E-02	0.2769E+02	0.1485E-02	-0.1692E+03
38.	0.1384E-02	-0.1028E+03	0.1781E-02	-0.1315E+03
39.	0.1278E-02	-0.5183E+02	0.6814E-03	-0.9919E+02
40.	0.1233E-02	-0.1150E+03	0.8782E-03	-0.1341E+03
41.	0.1071E-02	-0.1404E+03	0.1183E-02	0.1350E+03
42.	0.1075E-03	-0.4534E+02	0.3436E-03	0.1281E+03
43.	0.9973E-03	0.1107E+03	0.5121E-03	0.1725E+03
44.	0.1778E-03	0.1778E+03	0.8063E-03	-0.5655E+01
45.	0.6103E-03	0.1049E+03	0.4174E-03	0.1345E+03
46.	0.3700E-03	0.1665E+03	0.6460E-03	-0.1465E+03
47.	0.1257E-02	0.2254E+02	0.7223E-03	0.3093E+02
48.	0.1136E-02	0.3626E+02	0.1165E-02	0.8854E+02
49.	0.3247E-03	-0.3406E+02	0.4424E-03	-0.1992E+02
50.	0.3365E-03	-0.9810E+02	0.8474E-03	0.6672E+02
51.	0.1657E-02	-0.1178E+03	0.1294E-02	-0.1004E+02
52.	0.1774E-02	-0.1286E+03	0.3395E-03	-0.1376E+03
53.	0.1658E-03	-0.8223E+02	0.1946E-02	-0.4054E+02
54.	0.1323E-02	0.1459E+03	0.1148E-02	-0.1578E+03
55.	0.1312E-02	0.1343E+03	0.1097E-02	0.1626E+03
56.	0.1354E-02	0.8153E+02	0.4079E-03	-0.1153E+03
57.	0.1421E-02	0.5075E+02	0.1019E-02	0.4404E+02
58.	0.9369E-[illegible]	-0.5933E+02	0.6914E-03	-0.1382E+03
59.	0.3497E-03	-0.2301E+02	0.1340E-02	0.6314E+02
60.	0.1842E-02	-0.7877E+01	0.3126E-02	0.3005E+01
61.	0.1540E-02	-0.1458E+03	0.1711E-02	-0.1216E+03
62.	0.1100E-02	-0.1107E+03	0.9534E-03	-0.2671E+02
63.	0.1076E-02	-0.8570E+02	0.6168E-03	-0.5674E+02
64.	0.1480E-03	0.9500E+02	0.8199E-03	-0.1492E+03
65.	0.6961E-03	0.1534E+03	0.1384E-02	0.6211E+02
66.	0.1432E-03	0.1101E+03	0.1318E-02	0.1523E+03
67.	0.2951E-03	0.1910E+01	0.1188E-02	0.1731E+03
68.	0.1178E-02	0.3713E+02	0.1234E-02	0.3424E+02
69.	0.1768E-02	0.6774E+02	0.8195E-03	0.2254E+02
70.	0.6251E-03	0.3042E+02	0.1287E-02	0.1226E+03
71.	0.6197E-03	0.9833E+02	0.8314E-03	0.3874E+02
72.	0.1080E-02	-0.1039E+03	0.6870E-03	-0.1051E+03
73.	0.3922E-03	0.1180E+03	0.1043E-02	0.7023E+02
74.	0.1086E-02	-0.1580E+03	0.3468E-03	-0.3920E+02
75.	0.1787E-02	-0.1363E+03	0.1911E-02	-0.1257E+03
76.	0.1078E-02	0.1787E+03	0.1168E-02	0.1607E+03
77.	0.1130E-02	-0.3410E+02	0.2347E-02	-0.1047E+03
78.	0.1499E-02	0.9614E+02	0.1848E-02	-0.1662E+03

ORIGINAL PAGE IS
OF POOR QUALITY

TABLE XXII.- CONTINUED

BOTTOM SURFACE

	RADIUS= 0.990 CHORD= 0.010		RADIUS= 0.990 CHORD= 0.030		RADIUS= 0.990 CHORD= 0.150	
HARM	AMPLITUDE	PHASE	AMPLITUDE	PHASE	AMPLITUDE	PHASE
0.	0.1513E+02	0.0000E+00	0.1298E+02	0.0000E+00	0.1161E+02	0.0000E+00
1.	0.4606E+00	0.1875E+02	0.1808E+01	-0.7028E+02	0.2265E+01	-0.9149E+02
2.	0.2598E+00	0.1153E+03	0.1434E+00	0.7781E+02	0.6572E+00	-0.5240E+01
3.	0.3317E+00	-0.7596E+02	0.3775E+00	-0.7978E+02	0.2317E+00	0.5845E+02
4.	0.1191E+00	-0.4781E+02	0.1280E+00	-0.3000E+02	0.1487E+00	0.1373E+03
5.	0.1192E+00	-0.3217E+02	0.9705E-01	-0.2530E+02	0.8429E-01	-0.1649E+03
6.	0.4854E-01	0.9861E+01	0.5673E-01	0.1846E+02	0.8742E-01	-0.1281E+03
7.	0.3342E-01	0.3321E+01	0.2688E-01	0.1729E+02	0.1160E+00	-0.6026E+02
8.	0.1538E-01	0.1308E+02	0.1615E-01	0.6915E+01	0.1042E+00	0.1140E+02
9.	0.1725E-01	-0.4018E+01	0.1840E-01	0.1317E+02	0.7501E-01	0.8718E+02
10.	0.8079E-02	0.5503E+02	0.8476E-02	0.8982E+02	0.4445E-01	0.1604E+03
11.	0.1407E-01	0.7446E+02	0.1504E-01	0.7513E+02	0.1387E-01	0.1632E+03
12.	0.4009E-02	0.1289E+03	0.5412E-02	0.1393E+03	0.3414E-01	-0.1710E+03
13.	0.4962E-02	0.7748E+02	0.4407E-02	0.8006E+02	0.3837E-01	-0.9883E+02
14.	0.4176E-02	-0.4406E+02	0.2046E-02	-0.5864E+02	0.4591E-01	-0.3152E+02
15.	0.8150E-02	-0.5754E+02	0.7207E-02	-0.5701E+02	0.3700E-01	0.2711E+02
16.	0.1587E-02	0.2761E+02	0.3148E-02	0.3692E+02	0.3422E-01	0.9205E+02
17.	0.4634E-02	0.2201E+02	0.4258E-02	0.2127E+02	0.2690E-01	0.1425E+03
18.	0.5391E-02	0.1368E+03	0.4238E-02	0.1319E+03	0.2685E-01	-0.1567E+03
19.	0.6054E-02	0.7215E+02	0.4392E-02	0.7371E+02	0.1967E-01	-0.7110E+02
20.	0.3377E-03	-0.1652E+03	0.1005E-02	-0.4553E+02	0.1633E-01	-0.1460E+02
21.	0.2959E-02	0.9513E+02	0.4384E-02	0.9904E+02	0.1075E-01	0.4247E+02
22.	0.6183E-02	0.5360E+02	0.7570E-02	0.5298E+02	0.1754E-01	0.2264E+02
23.	0.7042E-02	0.5012E+02	0.7211E-02	0.5421E+02	0.1860E-01	0.7136E+02
24.	0.1935E-02	-0.1783E+03	0.3212E-03	-0.1366E+03	0.1511E-01	0.1515E+03
25.	0.3496E-02	-0.6140E+02	0.1761E-02	-0.6188E+02	0.1407E-01	-0.1607E+03
26.	0.4529E-02	0.1145E+03	0.3368E-02	0.9765E+02	0.1664E-01	-0.1294E+03
27.	0.3486E-02	0.5906E+02	0.3868E-02	0.7976E+02	0.2760E-01	-0.3241E+02
28.	0.4010E-02	-0.7405E+02	0.9309E-03	-0.1867E+02	0.2247E-01	0.4164E+02
29.	0.2921E-03	-0.6259E+02	0.1316E-02	0.1386E+03	0.1566E-01	0.1340E+03
30.	0.4213E-02	0.9951E+02	0.2502E-02	0.9767E+02	0.7875E-02	-0.1369E+03
31.	0.4761E-02	0.7834E+02	0.3497E-02	0.6674E+02	0.3930E-02	0.1112E+03
32.	0.5213E-03	0.1736E+03	0.1176E-02	0.1745E+03	0.4341E-02	-0.1027E+03
33.	0.7541E-03	-0.1508E+03	0.1729E-02	-0.1523E+03	0.7369E-02	-0.7801E+02
34.	0.1167E-02	0.1558E+03	0.1438E-02	-0.1661E+03	0.7998E-02	-0.2520E+02
35.	0.2332E-02	0.4671E+02	0.1786E-02	-0.2713E+01	0.9729E-02	-0.3548E+01
36.	0.1019E-02	0.1182E+03	0.9791E-03	-0.7788E+02	0.7744E-02	0.7165E+02
37.	0.2109E-02	-0.1739E+03	0.1821E-02	0.1442E+03	0.1355E-01	0.1618E+03
38.	0.2644E-02	-0.1011E+03	0.9959E-03	-0.4074E+02	0.1353E-01	-0.1338E+03
39.	0.3811E-02	0.1362E+03	0.2487E-02	0.1233E+03	0.1665E-01	-0.2286E+02
40.	0.9675E-03	0.9849E+02	0.1486E-02	-0.1656E+03	0.1298E-01	0.9767E+02
41.	0.1061E-02	-0.1582E+03	0.2849E-02	-0.1460E+03	0.5894E-02	-0.1045E+03
42.	0.1712E-02	0.1512E+03	0.2834E-03	0.1030E+03	0.4677E-02	0.2533E+02
43.	0.4543E-02	-0.1158E+03	0.3220E-02	-0.1081E+03	0.5430E-02	0.1504E+03
44.	0.1881E-02	0.2364E+02	0.8587E-03	0.1761E+03	0.5092E-02	-0.9477E+02
45.	0.8121E-03	0.1048E+03	0.8085E-03	0.1458E+03	0.2280E-02	-0.7978E+02
46.	0.2984E-02	0.4996E+02	0.1677E-02	-0.1716E+03	0.3024E-02	-0.5900E+02
47.	0.3848E-02	-0.6950E+02	0.4305E-02	-0.1156E+03	0.6149E-02	0.7660E+01
48.	0.2026E-02	0.7112E+02	0.3926E-02	0.4560E+02	0.4787E-02	-0.2059E+02
49.	0.9727E-03	-0.8734E+02	0.2311E-02	-0.7855E+02	0.9054E-02	0.4926E+02
50.	0.2256E-02	-0.8687E+01	0.1675E-02	-0.5152E+01	0.6797E-02	-0.1790E+03
51.	0.3449E-02	0.1291E+03	0.1278E-02	0.8436E+02	0.1021E-01	-0.3965E+01
52.	0.1049E-02	-0.6325E+02	0.2502E-02	-0.8591E+02	0.1132E-01	0.1653E+03
53.	0.2150E-02	0.6304E+02	0.4656E-03	0.3393E+02	0.1331E-01	-0.1142E+03
54.	0.2334E-02	0.1648E+03	0.2022E-02	-0.8515E+02	0.1298E-02	-0.7152E+02
55.	0.3618E-02	-0.2669E+02	0.2554E-02	0.9379E+01	0.3512E-02	0.2333E+02
56.	0.2355E-02	-0.8001E+01	0.2365E-02	0.8332E+02	0.3009E-02	-0.7383E+02
57.	0.1952E-02	0.1429E+03	0.2803E-02	0.4597E+02	0.4255E-02	0.1353E+03
58.	0.1158E-02	0.7082E+02	0.2769E-02	0.1033E+03	0.9411E-02	0.1758E+02
59.	0.2359E-02	0.9943E+02	0.5065E-02	0.6154E+02	0.6412E-02	0.5181E+02
60.	0.5670E-02	0.1280E+03	0.4820E-02	0.1162E+03	0.4707E-02	0.7624E+02
61.	0.3338E-02	-0.4532E+02	0.1991E-02	0.8527E+02	0.1746E-02	-0.5195E+02
62.	0.8448E-03	-0.8132E+02	0.2177E-02	-0.1648E+03	0.1113E-01	-0.7628E+02
63.	0.2702E-02	0.1547E+03	0.2671E-02	0.4799E+02	0.4498E-02	0.1147E+02
64.	0.1379E-02	-0.1571E+03	0.3915E-02	0.1011E+03	0.2967E-02	-0.8631E+02
65.	0.1991E-02	0.1466E+03	0.1680E-02	-0.1175E+03	0.7406E-02	0.8724E+02
66.	0.2060E-02	-0.2057E+01	0.2866E-02	0.1052E+03	0.1658E-02	0.1641E+03
67.	0.1655E-02	-0.2096E+02	0.4214E-02	-0.1695E+02	0.2333E-02	-0.8276E+02
68.	0.4659E-02	0.1219E+02	0.3406E-02	0.1730E+02	0.6343E-02	0.5281E+02
69.	0.4448E-02	0.1146E+03	0.2917E-02	0.1316E+03	0.5523E-03	0.7929E+02
70.	0.3243E-02	0.2637E+02	0.3668E-02	0.2449E+01	0.5143E-02	-0.2370E+02
71.	0.8863E-03	-0.2446E+02	0.2693E-02	0.5155E+02	0.4242E-02	0.1631E+03
72.	0.5521E-02	-0.1182E+03	0.3516E-02	-0.1040E+03	0.7117E-02	0.4199E+02
73.	0.6794E-02	0.1337E+03	0.2774E-02	0.9941E+02	0.7798E-02	-0.1165E+03
74.	0.4662E-03	-0.1664E+03	0.1758E-02	-0.7268E+02	0.1103E-02	-0.1155E+03
75.	0.6697E-02	0.8740E+01	0.5334E-02	0.4484E+02	0.7588E-03	0.1417E+03
76.	0.2787E-02	0.1495E+03	0.2956E-02	0.9169E+01	0.4319E-02	0.9407E+02
77.	0.2936E-02	0.1722E+03	0.2364E-02	0.1275E+03	0.1076E-01	-0.1213E+03
78.	0.2848E-02	0.7952E+01	0.1982E-02	0.3645E+01	0.2365E-02	0.2438E+02

ORIGINAL PAGE IS
OF POOR QUALITY

TABLE XXII.- CONTINUED

BOTTOM SURFACE

HARM	RADIUS= 0.990 CHORD= 0.200 AMPLITUDE	PHASE	RADIUS= 0.990 CHORD= 0.400 AMPLITUDE	PHASE	RADIUS= 0.990 CHORD= 0.450 AMPLITUDE	PHASE
0.	0.1167E+02	0.0000E+00	0.1303E+02	0.0000E+00	0.1303E+02	0.0000E+00
1.	0.1892E+01	-0.8840E+02	0.5366E+00	-0.7845E+02	0.4532E+00	-0.7411E+02
2.	0.4293E+00	0.2372E+02	0.1938E+00	0.9095E+02	0.2179E+00	0.9264E+02
3.	0.9444E-01	0.1651E+03	0.7341E-01	-0.7038E+02	0.7245E-01	-0.6394E+02
4.	0.6657E-01	-0.7589E+02	0.2705E-01	0.7808E+02	0.2922E-01	0.9307E+02
5.	0.6152E-01	0.4407E+02	0.1313E-01	0.1706E+03	0.1886E-01	0.1717E+03
6.	0.4490E-01	0.1524E+03	0.3233E-02	-0.1677E+03	0.6196E-02	0.1701E+03
7.	0.2082E-01	-0.8398E+02	0.2342E-02	-0.5087E+02	0.1897E-02	-0.1006E+03
8.	0.1113E-01	0.1410E+03	0.2320E-02	-0.1334E+03	0.3499E-02	-0.1445E+03
9.	0.3218E-01	-0.9557E+02	0.5723E-02	-0.1166E+02	0.3872E-02	-0.2719E+02
10.	0.3744E-01	0.2941E+01	0.3232E-02	0.1122E+03	0.4343E-02	0.1668E+03
11.	0.4765E-01	0.8845E+02	0.4739E-02	0.9402E+02	0.3517E-02	0.1047E+03
12.	0.4369E-01	0.1747E+03	0.5229E-02	-0.1789E+03	0.6888E-02	0.1799E+03
13.	0.2378E-01	-0.1064E+03	0.1016E-03	0.1107E+03	0.1869E-02	-0.9479E+02
14.	0.2285E-01	-0.6135E+02	0.1198E-02	0.6166E+01	0.1762E-02	0.1452E+02
15.	0.3166E-01	-0.1293E+02	0.3798E-02	-0.6618E+02	0.4087E-02	-0.1074E+03
16.	0.3894E-01	0.7534E+02	0.1739E-02	0.5645E+02	0.1272E-02	-0.4743E+02
17.	0.3623E-01	0.1626E+03	0.8998E-03	0.1020E+03	0.1217E-02	0.5490E+02
18.	0.2815E-01	-0.1067E+03	0.1325E-02	0.7845E+02	0.1265E-02	0.1430E+03
19.	0.2322E-01	-0.3369E+01	0.1875E-02	0.8686E+02	0.1472E-02	0.3966E+02
20.	0.1103E-01	0.6725E+02	0.2548E-02	-0.1002E+03	0.1829E-02	-0.1212E+03
21.	0.1082E-01	0.7794E+02	0.1872E-02	0.8247E+02	0.9848E-03	0.4537E+02
22.	0.1091E-01	0.9807E+02	0.5601E-03	0.8543E+02	0.1088E-02	0.9297E+02
23.	0.6466E-02	-0.1498E+03	0.3435E-02	0.8643E+01	0.2929E-02	-0.1724E+02
24.	0.1089E-01	-0.4203E+02	0.7187E-03	0.1429E+03	0.7022E-03	0.2154E+02
25.	0.8078E-02	0.6592E+02	0.2117E-02	-0.7236E+02	0.1253E-02	-0.5273E+02
26.	0.9619E-02	0.1767E+03	0.2005E-02	0.6620E+02	0.1202E-02	0.9682E+02
27.	0.9423E-02	-0.1720E+02	0.1179E-02	0.9960E+02	0.1957E-02	0.3993E+02
28.	0.4145E-02	0.1153E+03	0.1600E-02	0.1234E+02	0.1541E-02	0.6023E+02
29.	0.4294E-02	-0.6786E+02	0.1482E-02	0.7577E+02	0.8329E-03	0.5815E+02
30.	0.1067E-01	0.9005E+02	0.8681E-03	-0.1655E+03	0.5311E-03	0.1072E+03
31.	0.1415E-01	-0.1723E+03	0.1978E-02	0.6649E+02	0.1324E-02	0.1059E+03
32.	0.1329E-01	-0.5409E+02	0.9513E-03	0.3894E+02	0.1336E-02	0.3401E+02
33.	0.1312E-01	0.4391E+02	0.6562E-03	-0.1386E+03	0.1396E-02	-0.1680E+03
34.	0.2918E-02	0.1498E+03	0.5664E-03	0.5911E+02	0.2271E-03	0.6012E+02
35.	0.4275E-02	0.1129E+03	0.1771E-02	0.1587E+03	0.1304E-02	0.1341E+03
36.	0.1368E-01	-0.1584E+03	0.1725E-02	0.3742E+02	0.1163E-02	0.1042E+02
37.	0.1442E-01	-0.6853E+02	0.9562E-03	-0.4983E+02	0.3312E-03	-0.3727E+02
38.	0.8226E-02	0.3008E+02	0.5497E-03	0.5187E+02	0.6592E-03	-0.6378E+02
39.	0.1318E-02	0.7296E+02	0.5382E-03	0.1664E+03	0.5877E-03	0.8151E+02
40.	0.4741E-02	0.6359E+02	0.1704E-02	0.1150E+03	0.1462E-02	0.1419E+03
41.	0.3962E-02	0.1445E+03	0.6547E-03	-0.1638E+03	0.2563E-03	0.6941E+02
42.	0.1086E-01	-0.9005E+02	0.1124E-02	-0.1696E+03	0.1189E-02	0.1691E+03
43.	0.4781E-02	0.3088E+02	0.9385E-03	-0.6192E+01	0.7645E-03	-0.2153E+02
44.	0.4526E-02	-0.6807E+02	0.1761E-02	0.1347E+03	0.1150E-02	0.1406E+03
45.	0.1772E-02	0.1547E+03	0.6687E-03	-0.8736E+02	0.3207E-03	0.7615E+02
46.	0.3640E-02	-0.7651E+02	0.9000E-03	-0.4354E+02	0.1006E-02	-0.1094E+03
47.	0.7475E-02	0.2107E+02	0.7594E-03	-0.2100E+01	0.1144E-02	0.3671E+02
48.	0.1626E-02	0.4588E+02	0.2717E-03	0.1212E+03	0.5546E-03	0.1188E+03
49.	0.6123E-02	0.9625E+02	0.4594E-03	0.3629E+02	0.6328E-03	-0.1011E+03
50.	0.8329E-02	-0.1649E+03	0.6618E-03	0.5009E+02	0.6332E-03	-0.1401E+02
51.	0.1606E-01	-0.4287E+02	0.8272E-03	-0.5231E+02	0.8059E-03	-0.2755E+01
52.	0.9453E-02	0.1120E+03	0.2482E-03	0.3192E+02	0.6738E-03	0.1477E+03
53.	0.4793E-02	-0.1196E+03	0.4008E-03	0.5556E+02	0.8326E-03	-0.4813E+02
54.	0.2166E-02	-0.1372E+02	0.2831E-03	-0.1560E+03	0.9514E-03	-0.1071E+03
55.	0.4500E-02	-0.1587E+03	0.7745E-03	-0.2327E+02	0.1349E-02	-0.5603E+02
56.	0.8442E-02	-0.5742E+02	0.8234E-03	-0.9768E+01	0.9965E-03	0.6033E+02
57.	0.7379E-02	0.7823E+02	0.1253E-03	0.3851E+02	0.5525E-03	-0.4215E+02
58.	0.1076E-02	0.3592E+02	0.9384E-03	0.1138E+03	0.6951E-03	-0.1444E+03
59.	0.2253E-02	0.1104E+03	0.5861E-03	-0.5022E+01	0.4510E-03	0.7990E+02
60.	0.3137E-02	0.8417E+02	0.2853E-03	0.1189E+03	0.1314E-02	0.1054E+03
61.	0.5233E-02	-0.1878E+02	0.1585E-02	-0.8718E+02	0.8745E-03	-0.1134E+03
62.	0.3867E-02	-0.1462E+03	0.1202E-02	-0.1549E+03	0.1048E-02	0.1197E+03
63.	0.5338E-02	0.1246E+02	0.9889E-03	0.5267E+02	0.8952E-03	-0.5722E+02
64.	0.4411E-02	-0.3824E+02	0.3225E-03	0.1477E+03	0.2823E-03	0.8982E+02
65.	0.4614E-02	0.1963E+02	0.5512E-03	0.1558E+03	0.6880E-03	0.1271E+03
66.	0.3324E-02	0.1798E+03	0.4391E-03	0.1040E+03	0.1144E-02	0.7706E+02
67.	0.6232E-02	-0.1566E+03	0.1128E-02	-0.6655E+02	0.1631E-02	-0.1149E+03
68.	0.2043E-02	-0.5003E+02	0.1907E-02	-0.4843E+01	0.1944E-02	-0.5194E+01
69.	0.2902E-02	-0.1666E+03	0.2840E-03	0.8351E+02	0.2720E-03	0.2701E+02
70.	0.1293E-02	0.3682E+02	0.1865E-02	-0.7324E+02	0.7332E-03	-0.4435E+02
71.	0.2483E-02	0.9097E+02	0.2160E-02	-0.3776E+02	0.1996E-02	-0.5202E+02
72.	0.4641E-02	0.3895E+02	0.1171E-02	-0.1094E+02	0.1185E-02	-0.1465E+02
73.	0.9217E-02	-0.1132E+03	0.1595E-02	-0.7522E+02	0.1531E-02	-0.2059E+02
74.	0.5128E-02	0.1144E+02	0.1002E-02	-0.6796E+02	0.4953E-03	0.1728E+02
75.	0.6964E-02	-0.9793E+02	0.1344E-02	-0.8796E+01	0.1306E-02	0.9989E+00
76.	0.4665E-02	0.9738E+02	0.4989E-03	-0.9067E+02	0.1260E-02	-0.1167E+03
77.	0.4498E-02	-0.6215E+02	0.7891E-03	-0.1565E+02	0.1078E-02	-0.3083E+02
78.	0.2496E-02	-0.5052E+02	0.7990E-03	0.5988E+02	0.8390E-03	0.6046E+02

TABLE XXII.- CONTINUED

	BOTTOM SURFACE					
	RADIUS= 0.990 CHORD= 0.500		RADIUS= 0.990 CHORD= 0.550		RADIUS= 0.990 CHORD= 0.599	
HARM	AMPLITUDE	PHASE	AMPLITUDE	PHASE	AMPLITUDE	PHASE
0.	0.1316E+02	0.0000E+00	0.1327E+02	0.0000E+00	0.1342E+02	0.0000E+00
1.	0.3317E+00	-0.7349E+02	0.2668E+00	-0.7224E+02	0.2189E+00	-0.7033E+02
2.	0.2078E+00	0.9090E+02	0.2203E+00	0.9023E+02	0.2187E+00	0.8969E+02
3.	0.5900E-01	-0.6302E+02	0.4532E-01	-0.6043E+02	0.3482E-01	-0.7477E+02
4.	0.3030E-01	0.1004E+03	0.3013E-01	0.1088E+03	0.2611E-01	0.1227E+03
5.	0.2466E-01	0.1688E+03	0.3110E-01	-0.1791E+03	0.3469E-01	-0.1727E+03
6.	0.7349E-02	-0.1760E+03	0.9702E-02	-0.1506E+03	0.1289E-01	-0.1184E+03
7.	0.2635E-02	-0.1504E+03	0.5416E-02	-0.1475E+03	0.6148E-02	-0.1242E+03
8.	0.4617E-02	-0.1632E+03	0.4739E-02	-0.1649E+03	0.3503E-02	-0.1485E+03
9.	0.3302E-02	-0.8750E+02	0.5998E-02	-0.9567E+02	0.7299E-02	-0.8172E+02
10.	0.3383E-02	-0.1761E+03	0.2904E-02	-0.1239E+03	0.3120E-02	-0.8278E+02
11.	0.2136E-02	0.1649E+03	0.2390E-02	-0.1555E+03	0.2008E-02	-0.7957E+02
12.	0.3883E-02	-0.1711E+03	0.2973E-02	-0.1650E+03	0.1773E-02	-0.1680E+03
13.	0.6045E-03	-0.1207E+03	0.1924E-02	-0.5393E+02	0.2412E-02	-0.2427E+02
14.	0.2171E-02	-0.8014E+02	0.1920E-02	-0.4831E+02	0.2648E-02	-0.2433E+02
15.	0.2897E-02	-0.1175E+03	0.3369E-02	-0.1096E+03	0.2467E-02	-0.1041E+03
16.	0.5174E-03	-0.1038E+03	0.1469E-02	-0.3993E+02	0.1093E-02	-0.1057E+02
17.	0.6954E-03	-0.2503E+02	0.1348E-02	-0.1471E+00	0.1475E-02	0.2765E+02
18.	0.1795E-02	0.2651E+02	0.1498E-02	0.2872E+02	0.1334E-02	0.3957E+02
19.	0.6891E-03	0.7187E+02	0.1042E-02	0.3233E+02	0.1939E-02	0.3910E+02
20.	0.1956E-02	-0.1212E+03	0.9564E-03	-0.1287E+03	0.7083E-03	0.1784E+03
21.	0.1530E-02	0.1856E+02	0.5692E-03	0.1878E+02	0.1682E-02	0.5787E+02
22.	0.1054E-02	0.1236E+03	0.9374E-03	0.7848E+02	0.1892E-02	0.9360E+02
23.	0.2611E-02	-0.7358E+02	0.1094E-02	-0.4893E+02	0.1078E-02	-0.9204E+02
24.	0.1245E-02	0.1856E+02	0.4745E-03	0.1591E+02	0.2481E-03	0.3629E+02
25.	0.1684E-02	-0.1511E+03	0.8144E-03	-0.1533E+03	0.4944E-03	-0.1564E+03
26.	0.6475E-03	-0.6363E+02	0.8759E-03	0.4251E+02	0.5043E-03	0.8303E+02
27.	0.2140E-02	0.1891E+02	0.1154E-02	0.2107E+02	0.1006E-02	0.5671E+02
28.	0.3538E-03	-0.1137E+03	0.6640E-03	-0.9682E+02	0.6938E-03	-0.7559E+02
29.	0.1421E-02	-0.2304E+02	0.6915E-03	0.5031E+01	0.1380E-02	-0.1148E+02
30.	0.1297E-02	0.7395E+02	0.7115E-03	0.7267E+02	0.1002E-02	0.3412E+02
31.	0.8839E-03	0.1130E+03	0.7629E-03	0.1084E+03	0.4932E-03	0.2432E+02
32.	0.9404E-03	-0.4136E+02	0.1604E-03	0.1784E+03	0.9465E-03	-0.3271E+02
33.	0.7336E-03	0.1224E+03	0.1295E-02	0.1552E+03	0.1064E-02	0.1498E+03
34.	0.5316E-03	-0.6595E+02	0.5073E-03	-0.2886E+02	0.8415E-03	-0.8966E+02
35.	0.5640E-03	0.1038E+02	0.8057E-03	0.4610E+02	0.6549E-03	-0.1102E+02
36.	0.5671E-03	0.2513E+01	0.3745E-03	0.1531E+03	0.7710E-03	0.1862E+02
37.	0.4888E-03	-0.1469E+03	0.4581E-03	-0.7854E+02	0.5228E-03	-0.1644E+03
38.	0.6431E-03	-0.8454E+01	0.6644E-03	0.8753E+02	0.4521E-03	-0.1691E+01
39.	0.3366E-03	0.4086E+02	0.4297E-03	0.1696E+03	0.2908E-03	0.1222E+03
40.	0.6096E-03	0.1167E+03	0.7998E-03	0.8471E+02	0.1494E-02	0.9249E+02
41.	0.3365E-03	0.1094E+03	0.8796E-03	0.1591E+03	0.1008E-02	0.1654E+03
42.	0.1266E-02	0.8699E+02	0.4315E-03	0.1264E+03	0.7183E-03	0.8671E+02
43.	0.7265E-03	-0.1516E+03	0.4186E-03	0.1547E+03	0.4053E-03	0.1793E+03
44.	0.4909E-03	-0.6620E+01	0.3671E-03	0.8567E+02	0.7681E-04	-0.1786E+03
45.	0.3267E-04	-0.1263E+02	0.7781E-03	0.1372E+03	0.7317E-03	0.1720E+03
46.	0.5232E-03	-0.1690E+03	0.5078E-03	0.1404E+03	0.5317E-03	0.1704E+03
47.	0.7419E-03	0.6986E+02	0.1010E-02	0.1109E+03	0.1297E-02	0.1053E+03
48.	0.6124E-03	0.6844E+02	0.5218E-03	0.9084E+02	0.6060E-03	0.9208E+02
49.	0.3601E-03	0.1153E+03	0.8016E-03	0.9945E+02	0.6852E-03	0.1299E+03
50.	0.3224E-03	-0.1139E+03	0.1151E-02	0.1687E+03	0.6757E-03	0.1563E+03
51.	0.5020E-03	-0.7587E+02	0.8352E-03	-0.1257E+03	0.6498E-03	-0.1308E+03
52.	0.3721E-03	-0.1030E+03	0.5172E-03	0.1330E+03	0.2240E-03	-0.1086E+03
53.	0.4703E-03	-0.1416E+03	0.4578E-03	0.1735E+03	0.5932E-03	0.1235E+03
54.	0.3126E-03	0.1485E+03	0.6374E-03	-0.1617E+03	0.3025E-03	0.1088E+03
55.	0.9204E-03	-0.7374E+02	0.6653E-03	-0.8517E+02	0.6609E-03	-0.1242E+03
56.	0.8102E-03	-0.1428E+03	0.4126E-03	0.3142E+02	0.3690E-03	-0.1050E+03
57.	0.3930E-03	-0.1160E+03	0.2440E-03	0.4430E+02	0.2668E-03	-0.4355E+02
58.	0.1004E-02	-0.1053E+03	0.7121E-03	-0.6665E+02	0.6425E-03	-0.1185E+03
59.	0.7071E-03	-0.9149E+02	0.1376E-03	-0.1016E+03	0.2627E-03	-0.1079E+03
60.	0.5215E-03	-0.3536E+02	0.1166E-03	0.5842E+02	0.4857E-03	0.7007E+02
61.	0.5030E-03	0.1514E+03	0.7344E-03	-0.1517E+03	0.9161E-03	0.1355E+03
62.	0.6990E-03	0.7708E+02	0.6763E-03	0.4120E+02	0.1052E-02	0.1006E+03
63.	0.6204E-03	-0.7240E+02	0.3059E-03	-0.1088E+03	0.7293E-03	-0.1057E+03
64.	0.2208E-03	-0.4704E+02	0.8971E-04	0.3517E+01	0.4500E-03	0.1512E+03
65.	0.2224E-03	0.1687E+03	0.9376E-04	0.1101E+03	0.4909E-03	-0.1503E+03
66.	0.4751E-03	-0.7390E+02	0.2723E-03	0.1749E+03	0.4403E-03	-0.1152E+03
67.	0.2555E-03	-0.3846E+02	0.5095E-03	-0.1212E+03	0.5460E-03	-0.1049E+03
68.	0.5694E-03	-0.1539E+03	0.5975E-03	-0.6991E+02	0.1035E-02	-0.1869E+02
69.	0.7176E-03	-0.1023E+03	0.6377E-03	-0.5199E+02	0.2040E-03	-0.8081E+02
70.	0.2182E-03	-0.1635E+03	0.5154E-03	0.1720E+03	0.4294E-03	0.1682E+03
71.	0.1385E-02	-0.1590E+03	0.7728E-03	-0.1172E+03	0.1217E-02	-0.1594E+03
72.	0.1093E-02	0.1669E+03	0.7378E-03	0.1420E+03	0.5315E-03	-0.1526E+03
73.	0.9544E-03	-0.1715E+03	0.2118E-03	-0.1668E+03	0.2747E-03	0.1792E+03
74.	0.7325E-03	0.1319E+03	0.4463E-03	0.1586E+03	0.2183E-03	0.8832E+02
75.	0.6253E-03	-0.1436E+03	0.3001E-03	-0.1135E+03	0.2703E-03	0.5775E+02
76.	0.7174E-03	-0.1467E+03	0.6558E-03	0.1780E+03	0.4862E-03	-0.1382E+03
77.	0.5303E-03	-0.9348E+02	0.6723E-03	-0.1356E+03	0.3452E-03	-0.8765E+02
78.	0.8266E-03	-0.1577E+03	0.1096E-02	-0.1712E+03	0.1519E-02	-0.1736E+03

ORIGINAL PAGE IS
OF POOR QUALITY

TABLE XXII.- CONTINUED

	RADIUS= 0.990 CHORD= 0.699		BOTTOM SURFACE RADIUS= 0.990 CHORD= 0.919	
HARM	AMPLITUDE	PHASE	AMPLITUDE	PHASE
0.	0.1359E+02	0.0000E+00	0.1342E+02	0.0000E+00
1.	0.9948E-01	-0.8032E+02	0.2336E+00	0.2968E+02
2.	0.2040E+00	0.8974E+02	0.2814E+00	0.1266E+03
3.	0.1981E-01	-0.1306E+03	0.1727E+00	-0.5771E+02
4.	0.1054E-01	0.1769E+03	0.1266E+00	0.1037E+03
5.	0.3113E-01	-0.1669E+03	0.1005E+00	-0.1064E+03
6.	0.1584E-01	-0.7080E+02	0.6941E-01	0.4724E+02
7.	0.1035E-02	0.5902E+02	0.3899E-01	-0.1679E+03
8.	0.1616E-02	0.7472E+02	0.1760E-01	-0.1705E+01
9.	0.3717E-02	-0.5547E+02	0.1433E-01	0.1623E+03
10.	0.3075E-02	0.1466E+02	0.9229E-02	-0.7116E+02
11.	0.1945E-02	0.4208E+02	0.3231E-02	0.8221E+02
12.	0.2570E-02	0.1338E+03	0.4489E-02	-0.1396E+03
13.	0.2058E-03	-0.1753E+02	0.2313E-02	0.6315E+02
14.	0.2609E-02	0.2391E+02	0.1876E-02	-0.9564E+02
15.	0.2056E-02	-0.1426E+03	0.9829E-03	-0.3624E+02
16.	0.1493E-02	0.4581E+02	0.1477E-02	-0.1528E+03
17.	0.5974E-03	-0.7118E+02	0.2965E-02	-0.2581E+02
18.	0.2132E-02	0.7578E+02	0.2055E-02	0.4757E+02
19.	0.1043E-02	0.6313E+02	0.1426E-02	0.6994E+02
20.	0.6673E-03	0.1448E+03	0.1256E-02	0.7167E+02
21.	0.1431E-02	0.5661E+02	0.2589E-03	0.4839E+01
22.	0.2971E-02	0.1266E+03	0.1918E-02	0.8463E+02
23.	0.2286E-02	-0.6210E+02	0.1010E-02	-0.1571E+03
24.	0.1081E-02	0.5609E+02	0.1330E-02	0.2623E+02
25.	0.5422E-03	-0.1249E+03	0.2818E-02	-0.1001E+03
26.	0.4696E-03	0.1610E+03	0.3254E-02	0.8062E+02
27.	0.1983E-02	0.1472E+02	0.1699E-02	-0.9077E+02
28.	0.5592E-03	-0.7580E+02	0.2034E-02	0.3311E+02
29.	0.1320E-02	-0.4232E+02	0.2928E-02	-0.1217E+03
30.	0.3914E-03	-0.2541E+02	0.2487E-02	0.6479E+02
31.	0.1533E-02	0.9518E+02	0.2677E-02	-0.1536E+03
32.	0.7311E-03	-0.6470E+02	0.1007E-02	-0.1310E+02
33.	0.6747E-03	0.1670E+03	0.1379E-02	-0.1656E+03
34.	0.2353E-03	0.1646E+03	0.1898E-02	0.7795E+02
35.	0.4412E-03	0.8627E+02	0.2360E-02	-0.1250E+03
36.	0.1638E-02	-0.8663E+02	0.9177E-03	0.7045E+02
37.	0.7515E-03	0.8922E+02	0.3048E-02	-0.1508E+03
38.	0.9624E-03	0.1593E+03	0.1043E-02	-0.1097E+02
39.	0.8325E-03	0.7595E+02	0.2010E-02	0.1678E+03
40.	0.8685E-03	0.1146E+03	0.1262E-02	-0.8287E+01
41.	0.4502E-03	-0.1617E+03	0.8800E-03	0.1279E+03
42.	0.5917E-03	0.5312E+02	0.1505E-02	-0.7562E+01
43.	0.5969E-03	-0.1046E+03	0.1467E-02	0.1541E+03
44.	0.1115E-02	0.4093E+02	0.8444E-03	-0.4946E+02
45.	0.1134E-02	-0.1388E+03	0.8053E-03	0.1127E+03
46.	0.8280E-03	0.8640E+02	0.6840E-03	-0.1452E+03
47.	0.9122E-03	0.1203E+03	0.7983E-03	0.8538E+02
48.	0.1256E-02	0.1395E+03	0.1171E-02	0.1019E+03
49.	0.5450E-03	-0.1231E+03	0.5781E-03	-0.1411E+03
50.	0.9724E-03	0.1556E+03	0.1283E-02	0.1077E+03
51.	0.6270E-03	-0.4421E+02	0.1734E-02	-0.9940E+02
52.	0.1045E-02	-0.1796E+03	0.1150E-02	0.7124E+02
53.	0.9466E-03	-0.4284E+02	0.2163E-02	-0.1318E+03
54.	0.8270E-03	0.1549E+03	0.7037E-03	0.4598E+02
55.	0.2629E-03	-0.1020E+03	0.1524E-02	-0.8455E+02
56.	0.6529E-03	0.1033E+03	0.2595E-02	0.6588E+02
57.	0.1116E-02	0.4440E+02	0.1762E-02	-0.1184E+03
58.	0.4071E-03	-0.1070E+03	0.2121E-02	0.6021E+02
59.	0.1432E-02	0.5289E+02	0.1373E-02	-0.1408E+03
60.	0.4722E-03	0.4165E+02	0.8262E-03	0.5108E+02
61.	0.1052E-02	0.1311E+03	0.4421E-03	-0.1421E+03
62.	0.9767E-03	-0.1287E+03	0.1261E-02	0.4721E+02
63.	0.1377E-02	0.1915E+02	0.4791E-03	-0.6868E+02
64.	0.8762E-04	0.1664E+03	0.1528E-02	0.7000E+02
65.	0.1204E-02	0.1160E+03	0.4252E-03	-0.1544E+03
66.	0.9716E-03	-0.1049E+03	0.7220E-03	-0.1534E+02
67.	0.1143E-02	0.2240E+02	0.8207E-03	0.8227E+02
68.	0.6617E-03	0.6768E+01	0.3574E-03	-0.1116E+02
69.	0.1209E-02	0.5870E+02	0.1516E-02	0.5151E+02
70.	0.6149E-03	-0.4446E+02	0.8191E-03	-0.4354E+02
71.	0.7529E-03	-0.1610E+03	0.7505E-03	0.1634E+03
72.	0.6871E-03	-0.1329E+03	0.4727E-03	-0.1636E+03
73.	0.4397E-03	-0.1098E+03	0.1845E-02	-0.6411E+02
74.	0.5614E-03	0.5953E+02	0.2182E-02	0.6360E+02
75.	0.6394E-03	0.7122E+02	0.1293E-02	-0.1197E+03
76.	0.1393E-02	-0.8102E+02	0.8964E-03	0.2904E+02
77.	0.1063E-02	0.5380E+01	0.1421E-02	-0.1369E+03
78.	0.3087E-03	-0.1027E+03	0.1871E-02	0.2624E+02

TABLE XXII.- CONTINUED

TOP SURFACE

HARM	RADIUS= 0.990 CHORD= 0.010 AMPLITUDE	PHASE	RADIUS= 0.990 CHORD= 0.030 AMPLITUDE	PHASE	RADIUS= 0.990 CHORD= 0.080 AMPLITUDE	PHASE
0.	0.1174E+02	0.0000E+00	0.9874E+01	0.0000E+00	0.9806E+01	0.0000E+00
1.	0.3958E+01	0.1249E+03	0.1951E+01	0.1620E+03	0.2106E+01	-0.1196E+03
2.	0.5715E+00	0.1422E+03	0.5825E+00	-0.1752E+03	0.7319E+00	-0.6150E+02
3.	0.5077E+00	0.9142E+02	0.3730E+00	0.1328E+03	0.1860E+00	-0.1438E+02
4.	0.2427E+00	0.8420E+02	0.2345E+00	0.1257E+03	0.2302E+00	-0.2886E+01
5.	0.1252E+00	0.1177E+03	0.2510E+00	0.1358E+03	0.1421E+00	0.4933E+02
6.	0.5664E-01	0.1359E+03	0.1854E+00	0.1389E+03	0.7948E-01	0.3640E+02
7.	0.4963E-01	0.1335E+03	0.1579E+00	0.1262E+03	0.1260E+00	0.6138E+02
8.	0.2946E-01	0.1127E+03	0.1244E+00	0.1117E+03	0.9942E-01	0.9904E+02
9.	0.2327E-01	0.1797E+03	0.8590E-01	0.1110E+03	0.5159E-01	0.1090E+03
10.	0.2039E-01	-0.1403E+03	0.6941E-01	0.9883E+02	0.7556E-01	0.1173E+03
11.	0.1943E-01	-0.1418E+03	0.5479E-01	0.9488E+02	0.7379E-01	0.1590E+03
12.	0.1260E-01	-0.1421E+03	0.3371E-01	0.7424E+02	0.3681E-01	0.1763E+03
13.	0.4081E-02	0.1739E+03	0.1801E-01	0.5041E+02	0.5019E-01	0.1711E+03
14.	0.3369E-02	0.1139E+03	0.1372E-01	0.2138E+02	0.5413E-01	-0.1499E+03
15.	0.5524E-02	0.1766E+03	0.6860E-02	-0.1164E+02	0.4105E-01	-0.1201E+03
16.	0.1159E-01	-0.1671E+03	0.1334E-01	-0.1318E+03	0.4071E-01	-0.1168E+03
17.	0.7585E-02	-0.1529E+03	0.2283E-01	-0.1242E+03	0.4134E-01	-0.8965E+02
18.	0.4220E-03	0.1684E+03	0.2334E-01	-0.1277E+03	0.3507E-01	-0.7037E+02
19.	0.2977E-04	-0.7217E+02	0.2427E-01	-0.1294E+03	0.4269E-01	-0.4815E+02
20.	0.4278E-02	-0.1126E+03	0.2291E-01	-0.1346E+03	0.3896E-01	-0.1343E+02
21.	0.5893E-02	-0.1790E+03	0.2322E-01	-0.1581E+03	0.2047E-01	0.1006E+02
22.	0.5386E-02	-0.1751E+03	0.2623E-01	-0.1599E+03	0.2735E-01	-0.1545E+01
23.	0.6295E-02	0.1606E+03	0.2425E-01	-0.1710E+03	0.3358E-01	0.4320E+02
24.	0.4285E-02	-0.1583E+03	0.1936E-01	-0.1643E+03	0.2423E-01	0.7619E+02
25.	0.2083E-02	0.1716E+03	0.9504E-02	-0.1749E+03	0.2175E-01	0.7561E+02
26.	0.4938E-02	0.1427E+03	0.1209E-01	0.1635E+03	0.2737E-01	0.1009E+03
27.	0.2999E-02	-0.1757E+03	0.1045E-01	0.1676E+03	0.2418E-01	0.1274E+03
28.	0.3086E-02	-0.1620E+03	0.7406E-02	0.1587E+03	0.2130E-01	0.1406E+03
29.	0.4949E-02	-0.1028E+03	0.3910E-02	-0.1135E+03	0.1954E-01	0.1782E+03
30.	0.2347E-02	0.1624E+03	0.2156E-02	0.6007E+02	0.1702E-01	-0.1783E+03
31.	0.1126E-02	-0.1068E+03	0.2974E-02	0.1113E+02	0.1736E-01	-0.1526E+03
32.	0.4031E-02	-0.1433E+03	0.2692E-02	0.2136E+02	0.2117E-01	-0.1387E+03
33.	0.2428E-02	-0.1659E+03	0.4326E-02	0.1275E+01	0.1708E-01	-0.1158E+03
34.	0.2046E-02	-0.1204E+03	0.7331E-02	-0.4479E+02	0.1578E-01	-0.8706E+02
35.	0.7465E-02	-0.1652E+03	0.3668E-02	-0.8926E+02	0.1303E-01	-0.8312E+02
36.	0.6347E-03	0.6670E+01	0.6519E-02	-0.3842E+02	0.1486E-01	-0.4621E+02
37.	0.1001E-02	-0.1518E+03	0.4366E-02	-0.5661E+02	0.1410E-01	-0.2140E+02
38.	0.4019E-02	-0.1091E+03	0.7070E-02	-0.8680E+02	0.1255E-01	-0.1175E+02
39.	0.3337E-02	-0.7511E+02	0.7981E-02	-0.8865E+02	0.1471E-01	0.3809E+01
40.	0.3426E-02	-0.9739E+02	0.7922E-02	-0.9939E+02	0.1227E-01	0.3495E+02
41.	0.2342E-02	-0.2308E+02	0.3544E-02	-0.7808E+02	0.1215E-01	0.6107E+02
42.	0.2165E-02	-0.4544E+02	0.4886E-02	-0.1776E+03	0.1262E-01	0.9138E+02
43.	0.3596E-02	-0.8663E+02	0.5082E-02	-0.1553E+03	0.9605E-02	0.1059E+03
44.	0.5716E-03	0.1007E+03	0.6551E-02	0.1682E+03	0.1340E-01	0.1318E+03
45.	0.1326E-02	-0.4609E+02	0.4095E-02	0.1631E+03	0.1104E-01	0.1559E+03
46.	0.1094E-02	0.5247E+01	0.3524E-02	0.1180E+03	0.1157E-01	0.1502E+03
47.	0.5561E-02	-0.1536E+02	0.5043E-02	0.1993E+02	0.8326E-02	-0.1659E+03
48.	0.2120E-02	-0.1325E+03	0.3395E-02	0.1245E+03	0.1338E-01	-0.1512E+03
49.	0.3504E-02	-0.3731E+02	0.1642E-02	0.7569E+01	0.9866E-02	-0.1169E+03
50.	0.2662E-02	-0.9107E+00	0.4857E-03	-0.4816E+02	0.1030E-01	-0.1119E+03
51.	0.1678E-02	-0.9653E+02	0.2731E-02	-0.1809E+01	0.1243E-01	-0.8524E+02
52.	0.3696E-02	-0.1365E+03	0.1636E-02	-0.1762E+03	0.1012E-01	-0.7609E+02
53.	0.2630E-02	-0.5215E+01	0.1662E-02	-0.3263E+02	0.1056E-01	-0.4679E+02
54.	0.2313E-02	-0.2019E+02	0.6396E-03	-0.7013E+01	0.1142E-01	-0.2597E+02
55.	0.2012E-02	0.1711E+03	0.1174E-02	-0.1667E+03	0.6377E-02	0.1153E+02
56.	0.7527E-03	0.6209E+02	0.4923E-02	-0.7934E+02	0.9347E-02	0.9082E+01
57.	0.4793E-02	-0.1756E+03	0.5661E-02	-0.1161E+03	0.4907E-02	0.8815E+01
58.	0.2536E-02	-0.1546E+03	0.7281E-02	-0.1334E+03	0.4782E-02	0.6020E+02
59.	0.1311E-02	-0.1154E+03	0.5379E-02	-0.1141E+03	0.3180E-02	0.6123E+02
60.	0.1510E-02	0.1074E+02	0.2877E-02	-0.1183E+03	0.6414E-02	0.7614E+02
61.	0.3912E-02	-0.1458E+03	0.6414E-02	-0.1655E+03	0.9557E-02	0.1538E+03
62.	0.2644E-02	-0.7988E+02	0.3517E-02	-0.1483E+03	0.5197E-02	-0.1693E+03
63.	0.7505E-03	-0.5283E+02	0.2682E-02	-0.1676E+03	0.6521E-02	0.1410E+03
64.	0.1290E-02	-0.9758E+02	0.1828E-02	-0.1566E+03	0.3202E-02	-0.1711E+03
65.	0.1539E-02	0.9089E+02	0.2287E-02	0.1311E+03	0.3424E-02	-0.1520E+03
66.	0.3416E-02	-0.1298E+03	0.4623E-02	-0.1074E+03	0.7527E-02	-0.1269E+03
67.	0.1662E-02	-0.9885E+02	0.7673E-03	-0.4309E+02	0.6456E-02	-0.8071E+02
68.	0.5425E-03	0.1472E+03	0.1062E-02	0.1157E+03	0.6181E-02	-0.1023E+03
69.	0.2656E-02	-0.1381E+03	0.3100E-02	-0.8849E+02	0.5354E-02	-0.1005E+03
70.	0.2637E-02	-0.5646E+01	0.4613E-02	-0.3866E+02	0.5397E-02	-0.6240E+02
71.	0.1521E-02	0.5652E+02	0.5865E-03	0.1030E+03	0.3896E-02	0.6257E+02
72.	0.3614E-02	-0.1507E+03	0.3027E-02	-0.9774E+02	0.4200E-02	0.1196E+03
73.	0.2688E-02	-0.7703E+02	0.4157E-02	-0.5180E+02	0.3037E-02	-0.1751E+02
74.	0.1421E-02	-0.1355E+03	0.3444E-02	-0.8434E+01	0.6159E-02	0.5507E+02
75.	0.3600E-02	-0.1513E+03	0.3730E-02	-0.1567E+03	0.4495E-02	0.8774E+02
76.	0.3157E-02	-0.6735E+02	0.7141E-02	-0.7350E+02	0.8984E-03	0.3014E+02
77.	0.1672E-02	0.4058E+02	0.2436E-02	-0.1671E+02	0.2608E-02	0.5208E+02
78.	0.2095E-02	-0.3222E+02	0.3413E-02	-0.6074E+02	0.1204E-02	-0.1792E+03

ORIGINAL PAGE IS
OF POOR QUALITY

TABLE XXII.- CONTINUED

TOP SURFACE

	RADIUS= 0.990 CHORD= 0.150		RADIUS= 0.990 CHORD= 0.200		RADIUS= 0.990 CHORD= 0.250	
HARM	AMPLITUDE	PHASE	AMPLITUDE	PHASE	AMPLITUDE	PHASE
0.	0.1046E+02	0.0000E+00	0.1140E+02	0.0000E+00	0.1139E+02	0.0000E+00
1.	0.2104E+01	-0.1062E+03	0.1479E+01	-0.9405E+02	0.1393E+01	-0.8506E+02
2.	0.1226E+01	-0.3755E+02	0.7068E+00	-0.2037E+02	0.6864E+00	0.1149E+01
3.	0.7548E+00	0.3677E+02	0.4487E+00	0.6656E+02	0.5379E+00	0.9917E+02
4.	0.4635E+00	0.8559E+02	0.2487E+00	0.1186E+03	0.3143E+00	-0.1751E+03
5.	0.3162E+00	0.1287E+03	0.2016E+00	0.1651E+03	0.1799E+00	-0.9409E+02
6.	0.2227E+00	0.1706E+03	0.1769E+00	-0.1352E+03	0.9873E-01	-0.2694E+02
7.	0.1684E+00	-0.1487E+03	0.1547E+00	-0.7232E+02	0.6956E-01	0.5103E+01
8.	0.1100E+00	-0.1101E+03	0.1407E+00	-0.7164E+01	0.9958E-01	0.5064E+02
9.	0.9680E-01	-0.8361E+02	0.1014E+00	0.4977E+02	0.1092E+00	0.1233E+03
10.	0.1177E+00	-0.4881E+02	0.7508E-01	0.9635E+02	0.9694E-01	-0.1538E+03
11.	0.1249E+00	0.9290E+00	0.7211E-01	0.1407E+03	0.6972E-01	-0.6973E+02
12.	0.1254E+00	0.5463E+02	0.6338E-01	-0.1584E+03	0.4463E-01	0.1989E+02
13.	0.9888E-01	0.1107E+03	0.5054E-01	-0.8787E+02	0.2068E-01	0.1125E+03
14.	0.5969E-01	0.1604E+03	0.3427E-01	-0.1026E+02	0.4560E-02	0.5165E+02
15.	0.3093E-01	-0.1759E+03	0.1070E-01	0.2749E+02	0.1123E-01	0.1265E+03
16.	0.4256E-01	-0.1656E+03	0.8857E-02	0.2944E+02	0.2294E-01	-0.1355E+03
17.	0.5974E-01	-0.1179E+03	0.1581E-01	0.1149E+03	0.2884E-01	-0.5097E+02
18.	0.5547E-01	-0.5575E+02	0.1944E-01	-0.1641E+03	0.3251E-01	0.5310E+02
19.	0.4595E-01	-0.3865E+01	0.1799E-01	-0.6412E+02	0.2979E-01	0.1477E+03
20.	0.3369E-01	0.3951E+02	0.1088E-01	0.7612E+01	0.2712E-01	-0.1159E+03
21.	0.3409E-01	0.9037E+02	0.7237E-02	0.1019E+03	0.1138E-01	0.3810E+01
22.	0.3079E-01	0.1559E+03	0.2779E-02	0.1249E+03	0.7649E-02	0.1726E+03
23.	0.2051E-01	-0.1556E+03	0.1096E-01	0.1209E+03	0.1494E-01	-0.4250E+02
24.	0.1351E-01	-0.1173E+03	0.1206E-01	-0.1547E+03	0.2122E-01	0.6131E+02
25.	0.1747E-01	-0.1012E+03	0.1126E-01	-0.6229E+02	0.2306E-01	0.1673E+03
26.	0.2064E-01	-0.5245E+02	0.3504E-02	0.1733E+02	0.1967E-01	-0.8839E+02
27.	0.2161E-01	0.5072E+01	0.4977E-02	-0.6752E+02	0.1227E-01	0.2276E+02
28.	0.2329E-01	0.5503E+02	0.1081E-01	0.2830E+02	0.9104E-02	0.1538E+03
29.	0.2195E-01	0.1209E+03	0.1052E-01	0.1372E+03	0.9723E-02	-0.7196E+02
30.	0.2066E-01	0.1729E+03	0.9005E-02	-0.1393E+03	0.1248E-01	0.6673E+02
31.	0.1496E-01	-0.1324E+03	0.4990E-02	-0.2385E+02	0.1334E-01	0.1689E+03
32.	0.9310E-02	-0.9473E+02	0.6644E-03	0.8810E+02	0.1373E-01	-0.7334E+02
33.	0.1190E-01	-0.7055E+02	0.5313E-02	-0.5400E+02	0.1307E-01	0.2112E+02
34.	0.1648E-01	-0.5148E+02	0.2377E-02	0.6785E+02	0.9590E-02	0.1716E+03
35.	0.2243E-01	0.1289E+02	0.1016E-02	0.1239E+03	0.9898E-02	-0.5966E+02
36.	0.2096E-01	0.7469E+02	0.6609E-03	0.1048E+03	0.9180E-02	0.6749E+02
37.	0.1944E-01	0.1148E+03	0.3325E-02	0.6315E+02	0.6778E-02	0.1760E+03
38.	0.1392E-01	0.1759E+03	0.2224E-02	-0.1277E+03	0.6818E-02	-0.6716E+02
39.	0.1231E-01	-0.1426E+03	0.1400E-02	-0.1716E+03	0.6881E-02	0.6860E+02
40.	0.7067E-02	-0.1195E+03	0.2818E-02	-0.1616E+03	0.6845E-02	-0.1728E+03
41.	0.7028E-02	-0.1127E+03	0.2074E-02	0.1234E+03	0.2622E-02	-0.9413E+02
42.	0.1350E-01	-0.5785E+02	0.2349E-02	0.1274E+03	0.4446E-02	0.7398E+02
43.	0.1613E-01	0.1027E+02	0.2238E-02	0.1760E+03	0.2922E-02	0.1641E+03
44.	0.1420E-01	0.7401E+02	0.4879E-02	-0.1789E+02	0.4237E-02	-0.1358E+02
45.	0.8290E-02	0.1326E+03	0.4778E-02	0.4500E+02	0.7008E-02	0.6483E+02
46.	0.6684E-02	0.1747E+03	0.6886E-03	-0.1696E+03	0.5211E-02	-0.1629E+03
47.	0.5660E-02	-0.1671E+03	0.1858E-02	0.2980E+02	0.5603E-02	-0.5584E+02
48.	0.9804E-02	-0.1335E+03	0.2142E-02	-0.1772E+03	0.4082E-02	0.1206E+03
49.	0.7445E-02	-0.9149E+02	0.3071E-03	-0.1398E+03	0.5651E-02	-0.1572E+03
50.	0.1260E-01	-0.4565E+02	0.1656E-02	-0.1292E+02	0.6010E-02	-0.1363E+02
51.	0.9747E-02	0.1280E+02	0.4081E-02	-0.3051E+02	0.3192E-02	0.6008E+02
52.	0.4162E-02	0.1228E+03	0.2701E-02	-0.1636E+03	0.7674E-02	-0.1637E+03
53.	0.2240E-02	0.1583E+03	0.3324E-02	-0.1628E+03	0.6801E-02	-0.7280E+02
54.	0.7732E-02	0.1433E+03	0.1248E-02	0.1776E+03	0.4835E-02	0.9662E+02
55.	0.8698E-02	-0.1651E+03	0.7958E-03	-0.4671E+02	0.4669E-02	-0.1503E+03
56.	0.5682E-02	-0.1141E+03	0.1695E-02	-0.1554E+03	0.1089E-02	-0.7499E+02
57.	0.4684E-02	-0.8452E+02	0.2955E-02	-0.1038E+02	0.2406E-02	0.5442E+02
58.	0.4377E-02	-0.6109E+02	0.1513E-02	-0.1199E+02	0.2932E-02	-0.1123E+03
59.	0.5784E-02	-0.4343E+02	0.3857E-02	-0.1421E+03	0.3019E-02	-0.7540E+02
60.	0.3159E-02	0.3343E+02	0.6898E-02	-0.1077E+03	0.3300E-02	-0.1346E+03
61.	0.8991E-02	0.9765E+02	0.4445E-02	0.5502E+02	0.1227E-02	-0.1615E+03
62.	0.4900E-02	0.1466E+03	0.1595E-02	0.1685E+03	0.1648E-02	0.7070E+02
63.	0.4647E-02	-0.1773E+03	0.7502E-03	-0.7802E+02	0.2409E-03	0.7077E+02
64.	0.3378E-02	-0.1167E+03	0.3207E-02	0.6301E+02	0.1391E-02	-0.2888E+02
65.	0.6651E-02	-0.9368E+02	0.5527E-02	-0.1284E+03	0.2913E-02	-0.6148E+02
66.	0.9368E-02	-0.4359E+02	0.4771E-02	-0.3322E+02	0.3552E-02	-0.1426E+02
67.	0.6166E-02	0.6126E+01	0.1672E-02	0.9960E+02	0.2378E-02	-0.1547E+03
68.	0.7476E-02	0.5656E+02	0.1096E-02	0.8302E+02	0.4990E-02	0.2640E+02
69.	0.6213E-02	0.8501E+02	0.3741E-02	0.4582E+02	0.3655E-02	0.8623E+02
70.	0.3253E-02	0.1002E+03	0.1458E-02	0.1002E+03	0.9240E-03	0.1418E+03
71.	0.8986E-03	0.1890E+02	0.2491E-02	0.7910E+01	0.3286E-02	0.3510E+02
72.	0.3263E-02	-0.1313E+03	0.1731E-02	-0.1338E+02	0.1284E-02	-0.1941E+02
73.	0.3725E-02	-0.9802E+02	0.2771E-02	0.1796E+03	0.3602E-02	-0.1629E+03
74.	0.7184E-02	-0.2593E+02	0.7180E-02	-0.2584E+02	0.5539E-02	-0.6309E+01
75.	0.2279E-02	-0.8250E+01	0.4337E-02	0.7780E+02	0.2737E-02	0.1052E+03
76.	0.1644E-02	0.8006E+02	0.1509E-02	-0.1497E+03	0.2106E-02	-0.1333E+03
77.	0.1094E-02	0.5972E+02	0.1745E-02	-0.3390E+02	0.2689E-02	0.7649E+01
78.	0.2458E-02	0.4365E+02	0.3605E-02	0.2180E+02	0.1723E-02	0.4481E+02

TABLE XXII.- CONTINUED

TOP SURFACE

HARM	RADIUS= 0.990 CHORD= 0.350 AMPLITUDE	PHASE	RADIUS= 0.990 CHORD= 0.400 AMPLITUDE	PHASE	RADIUS= 0.990 CHORD= 0.500 AMPLITUDE	PHASE
0.	0.1220E+02	0.0000E+00	0.1234E+02	0.0000E+00	0.1275E+02	0.0000E+00
1.	0.4232E+00	-0.3758E+02	0.3519E+00	-0.3889E+01	0.4585E+00	0.3411E+02
2.	0.4050E-01	-0.1691E+02	0.4959E-01	-0.9442E+02	0.1301E+00	-0.5947E+02
3.	0.1180E+00	0.1523E+03	0.9814E-01	0.1585E+03	0.1502E+00	-0.1715E+03
4.	0.2266E-01	-0.4123E+02	0.4113E-01	0.1666E+02	0.9212E-01	0.5738E+02
5.	0.2376E-01	-0.1916E+02	0.1015E-01	0.2658E+02	0.6204E-01	-0.3399E+02
6.	0.2132E-01	0.4400E+02	0.1273E-01	0.9929E+01	0.3070E-01	-0.1621E+03
7.	0.1833E-01	0.1226E+03	0.1211E-01	0.1236E+03	0.3183E-01	0.8623E+02
8.	0.2829E-02	0.1267E+03	0.6258E-02	0.1270E+03	0.1665E-01	-0.2471E+02
9.	0.9782E-02	0.1694E+03	0.9093E-02	-0.1793E+03	0.1353E-01	-0.1454E+03
10.	0.8334E-02	-0.1616E+03	0.5035E-02	-0.1036E+03	0.5353E-02	0.8879E+02
11.	0.5962E-02	-0.6266E+02	0.4577E-02	-0.1057E+02	0.7452E-02	-0.1261E+02
12.	0.1014E-01	-0.1175E+02	0.1084E-01	0.1838E+02	0.6248E-02	0.4261E+02
13.	0.1983E-02	0.1419E+02	0.4874E-02	-0.9144E+02	0.1292E-02	0.9845E+02
14.	0.1074E-02	0.4923E+02	0.1511E-02	0.6309E+02	0.5357E-03	0.1653E+03
15.	0.2150E-02	-0.3343E+01	0.3993E-02	0.3288E+02	0.3967E-02	0.2047E+02
16.	0.1990E-02	-0.1625E+03	0.1760E-02	-0.1768E+03	0.2444E-02	-0.1307E+03
17.	0.9530E-03	-0.1161E+03	0.1397E-02	-0.1004E+03	0.1532E-02	0.1350E+03
18.	0.3931E-02	-0.9048E+02	0.1884E-02	-0.8251E+02	0.1637E-02	0.3420E+02
19.	0.2264E-02	0.1862E+02	0.1041E-02	-0.1285E+03	0.6052E-04	0.1471E+03
20.	0.3062E-02	-0.8108E+02	0.2674E-02	-0.5553E+02	0.8364E-03	-0.1457E+03
21.	0.1877E-02	-0.1099E+02	0.2280E-02	-0.7963E+02	0.1393E-03	0.5680E+02
22.	0.2218E-02	-0.1449E+03	0.3684E-02	-0.1310E+03	0.3856E-02	0.1537E+03
23.	0.2895E-02	-0.1451E+03	0.3231E-02	-0.1715E+03	0.3275E-02	0.6555E+02
24.	0.3208E-02	-0.1301E+02	0.3721E-02	-0.4257E+02	0.2764E-02	-0.3437E+02
25.	0.1096E-02	-0.1777E+02	0.2934E-02	0.1395E+03	0.1317E-02	-0.1263E+03
26.	0.1453E-02	0.4740E+02	0.4504E-03	0.4233E+02	0.1803E-02	-0.2628E+01
27.	0.3780E-02	0.1536E+03	0.1362E-02	0.1612E+03	0.1960E-02	0.1716E+03
28.	0.4434E-02	0.9557E+02	0.3379E-02	0.2703E+02	0.8502E-03	-0.1413E+03
29.	0.3102E-02	-0.1270E+03	0.2716E-02	-0.9476E+02	0.2015E-02	-0.2165E+02
30.	0.8422E-03	-0.1212E+03	0.1052E-02	-0.1730E+03	0.6094E-03	-0.5010E+02
31.	0.1912E-02	0.8845E+02	0.1930E-02	0.1005E+03	0.1563E-02	0.1514E+02
32.	0.2921E-02	-0.1421E+03	0.2057E-02	0.1383E+03	0.1358E-02	0.4585E+02
33.	0.3568E-02	-0.1353E+02	0.2786E-02	-0.1587E+02	0.1038E-02	-0.7784E+02
34.	0.1952E-02	-0.1224E+03	0.1534E-02	0.1799E+03	0.1552E-02	-0.2627E+02
35.	0.5420E-03	-0.4633E+02	0.1099E-02	-0.1720E+03	0.4651E-02	0.1766E+03
36.	0.4372E-02	0.1253E+03	0.2947E-02	0.1161E+03	0.3273E-02	-0.2232E+02
37.	0.2101E-03	-0.1038E+03	0.1362E-02	0.3366E+02	0.3072E-02	0.3993E+02
38.	0.2831E-02	-0.1243E+03	0.2638E-02	0.1100E+03	0.1584E-02	-0.1420E+03
39.	0.1540E-02	-0.4169E+02	0.1243E-02	-0.8469E+02	0.2694E-02	0.1475E+03
40.	0.2939E-02	-0.3538E+02	0.4878E-02	-0.1784E+01	0.1645E-02	0.1158E+03
41.	0.3644E-02	0.1378E+03	0.2762E-02	0.1401E+03	0.9189E-03	0.9885E+02
42.	0.5720E-03	-0.1328E+03	0.3241E-02	-0.9675E+02	0.1070E-02	-0.1503E+03
43.	0.2455E-02	0.1664E+03	0.2915E-02	-0.1562E+03	0.2238E-02	0.1250E+02
44.	0.2044E-02	-0.8918E+02	0.5177E-03	0.8401E+01	0.9468E-03	0.1411E+03
45.	0.7555E-03	0.2126E+01	0.1183E-02	-0.2558E+02	0.2264E-02	0.6719E+02
46.	0.3894E-02	-0.9829E+02	0.5512E-02	-0.1100E+03	0.2541E-02	-0.1332E+03
47.	0.1100E-02	0.8138E+00	0.1602E-02	-0.2610E+02	0.2064E-02	-0.1454E+03
48.	0.1671E-02	-0.1638E+03	0.2015E-02	-0.1663E+03	0.1239E-02	-0.4436E+02
49.	0.4950E-02	0.1743E+03	0.5239E-02	0.1621E+03	0.2241E-02	-0.1264E+03
50.	0.2131E-02	0.1449E+03	0.1319E-02	0.1550E+03	0.1565E-02	0.5847E+02
51.	0.5080E-03	-0.1021E+03	0.3133E-02	-0.8882E+02	0.2762E-02	-0.5954E+02
52.	0.5510E-02	-0.4490E+02	0.4350E-02	0.3812E+01	0.2651E-02	-0.1692E+03
53.	0.3700E-02	-0.4927E+02	0.1993E-02	-0.6819E+02	0.2824E-02	-0.1519E+02
54.	0.3130E-02	-0.1463E+03	0.3029E-02	-0.4846E+02	0.9252E-03	0.1177E+03
55.	0.6181E-02	0.8988E+01	0.5293E-02	-0.1777E+02	0.3040E-02	-0.1428E+03
56.	0.5453E-02	-0.1242E+03	0.1167E-02	-0.5935E+02	0.1047E-02	-0.1241E+03
57.	0.3397E-02	0.1260E+03	0.1586E-02	0.1244E+03	0.1171E-02	0.3700E+02
58.	0.2426E-02	0.2604E+02	0.2566E-02	-0.6248E+02	0.1678E-02	0.6980E+02
59.	0.8801E-03	-0.1765E+03	0.6281E-02	-0.1217E+03	0.1382E-02	0.9110E+02
60.	0.3288E-02	-0.1225E+03	0.3177E-02	-0.1271E+03	0.2980E-03	-0.7093E+02
61.	0.1720E-02	-0.1255E+02	0.5152E-02	-0.5917E+02	0.2840E-02	0.1770E+03
62.	0.4779E-02	0.2873E+02	0.4212E-02	0.9957E+02	0.1551E-02	0.1485E+02
63.	0.4483E-02	0.1471E+03	0.9000E-03	-0.1101E+03	0.3706E-02	-0.1326E+03
64.	0.3825E-02	-0.1412E+03	0.7861E-02	-0.1247E+03	0.1266E-02	-0.1891E+02
65.	0.2790E-02	-0.5597E+02	0.1139E-02	-0.1030E+03	0.3140E-02	0.3071E+02
66.	0.3360E-02	0.9831E+02	0.2372E-02	0.5534E+02	0.2870E-02	-0.6846E+02
67.	0.2449E-02	0.1522E+03	0.6374E-02	-0.1633E+03	0.1710E-02	0.1373E+03
68.	0.5643E-02	-0.1734E+03	0.6557E-02	-0.1546E+03	0.2142E-02	0.1366E+03
69.	0.3568E-02	-0.4753E+01	0.5965E-02	-0.1629E+02	0.3827E-02	0.1323E+03
70.	0.3692E-02	-0.2828E+01	0.2753E-02	-0.4433E+02	0.4469E-02	0.1665E+03
71.	0.2714E-02	-0.7133E+02	0.7897E-03	-0.6974E+02	0.9732E-03	0.1333E+03
72.	0.1761E-02	0.3078E+02	0.2633E-02	0.3358E+02	0.7392E-03	-0.3810E+02
73.	0.1974E-02	0.1295E+03	0.7605E-02	0.1115E+03	0.3040E-02	-0.3818E+02
74.	0.2234E-02	-0.9609E+02	0.2392E-02	0.3247E+02	0.1793E-02	0.1021E+03
75.	0.8594E-02	0.8776E+02	0.8300E-02	0.8692E+02	0.2654E-02	-0.1532E+03
76.	0.3712E-02	0.7200E+01	0.4929E-02	0.2233E+02	0.3898E-03	-0.9351E+02
77.	0.6936E-02	0.1327E+03	0.7559E-02	0.1181E+03	0.2862E-02	-0.1605E+03
78.	0.2200E-02	0.2337E+02	0.2130E-02	-0.3987E+02	0.3596E-02	0.8044E+02

TABLE XXII.- CONCLUDED

HARM	RADIUS= 0.990 CHORD= 0.599 AMPLITUDE	PHASE	TOP SURFACE RADIUS= 0.990 CHORD= 0.919 AMPLITUDE	PHASE
0.	0.1248E+02	0.0000E+00	0.1267E+02	0.0000E+00
1.	0.9471E+00	0.4499E+02	0.1180E+01	0.4071E+02
2.	0.5076E+00	-0.6721E+02	0.2543E+00	-0.1261E+03
3.	0.3851E+00	0.1693E+03	0.1767E+00	-0.3748E+02
4.	0.2512E+00	0.3226E+02	0.2200E+00	0.1643E+03
5.	0.1096E+00	-0.8639E+02	0.7139E-01	0.3141E+02
6.	0.5062E-01	0.1336E+03	0.5487E-01	0.4571E+02
7.	0.2614E-01	0.5487E+02	0.7794E-01	-0.7675E+02
8.	0.1769E-01	-0.3476E+02	0.5176E-01	0.1580E+03
9.	0.1861E-01	-0.1670E+03	0.3010E-01	0.4231E+02
10.	0.1436E-01	0.7084E+02	0.1537E-01	-0.9364E+02
11.	0.8589E-02	-0.4332E+02	0.5362E-02	0.3132E+02
12.	0.7033E-02	0.1311E+03	0.1229E-01	0.1552E+03
13.	0.3436E-02	0.8091E+02	0.1213E-01	0.1080E+02
14.	0.2903E-02	0.1282E+03	0.1045E-01	-0.1245E+03
15.	0.5809E-02	0.1134E+02	0.6846E-02	0.9050E+02
16.	0.1000E-01	-0.1157E+03	0.3878E-02	-0.9762E+02
17.	0.6795E-02	0.1570E+03	0.1541E-02	0.5180E+02
18.	0.4689E-02	0.2281E+02	0.4185E-02	-0.1431E+03
19.	0.1901E-02	-0.7019E+02	0.6671E-02	0.4732E+02
20.	0.2202E-02	-0.1259E+03	0.9083E-02	-0.7548E+02
21.	0.1711E-02	-0.1730E+03	0.8854E-02	0.1587E+03
22.	0.3818E-02	0.1263E+03	0.8099E-02	0.5720E+02
23.	0.4075E-02	0.5195E+02	0.4419E-02	-0.5313E+02
24.	0.3817E-02	-0.6171E+02	0.4625E-02	-0.7919E+02
25.	0.3153E-02	0.1768E+03	0.8165E-02	0.1463E+03
26.	0.1676E-02	0.6782E+02	0.4375E-02	0.9127E+00
27.	0.2514E-02	0.9479E+02	0.4191E-02	0.1612E+03
28.	0.1470E-02	-0.5512E+02	0.4465E-02	-0.1089E+02
29.	0.1960E-02	-0.8074E+02	0.2308E-02	-0.4232E+02
30.	0.1274E-02	0.7826E+02	0.8920E-03	-0.5680E+02
31.	0.8869E-03	0.1705E+03	0.3269E-02	0.1168E+03
32.	0.2902E-02	0.7015E+02	0.2348E-02	0.1792E+01
33.	0.1848E-02	-0.8093E+02	0.5034E-02	-0.1127E+03
34.	0.8725E-03	0.1087E+03	0.6392E-03	-0.1585E+03
35.	0.4136E-02	0.1323E+03	0.3181E-02	-0.4207E+02
36.	0.3084E-02	-0.1301E+02	0.4499E-03	0.6223E+02
37.	0.2246E-02	-0.4539E+02	0.6000E-02	-0.1222E+03
38.	0.2082E-02	-0.1777E+03	0.5517E-02	0.1286E+03
39.	0.3460E-02	-0.1540E+03	0.3370E-02	-0.2461E+02
40.	0.2929E-02	0.1062E+03	0.5200E-02	0.7794E+02
41.	0.1462E-02	-0.1051E+03	0.1697E-02	0.4854E+02
42.	0.3329E-02	0.1182E+03	0.2737E-02	0.1636E+03
43.	0.2345E-02	-0.1306E+02	0.1426E-02	-0.1159E+03
44.	0.1739E-02	0.9095E+02	0.3804E-02	0.1674E+03
45.	0.1124E-02	-0.5772E+02	0.3151E-02	0.6248E+02
46.	0.1525E-02	-0.1648E+03	0.1693E-02	-0.8577E+01
47.	0.3966E-02	-0.1315E+03	0.3486E-02	-0.1048E+03
48.	0.3427E-02	0.1685E+03	0.2513E-02	0.5621E+02
49.	0.1439E-02	-0.1633E+03	0.1174E-02	-0.2775E+02
50.	0.1131E-02	-0.1615E+03	0.5512E-02	-0.1361E+03
51.	0.1140E-02	0.9544E+02	0.1516E-02	0.8451E+02
52.	0.2842E-02	-0.7683E+02	0.1777E-02	-0.1310E+03
53.	0.2555E-03	-0.6933E+02	0.1312E-02	-0.7736E+01
54.	0.9840E-03	0.1671E+03	0.1714E-02	-0.7580E+02
55.	0.2865E-02	-0.8910E+02	0.3643E-02	0.1161E+01
56.	0.9382E-03	-0.4334E+02	0.4015E-02	-0.1173E+03
57.	0.4386E-02	0.9761E+02	0.3902E-02	0.7375E+02
58.	0.2713E-02	-0.3787E+02	0.5291E-02	-0.1673E+03
59.	0.6579E-03	0.1725E+03	0.5430E-02	0.4058E+02
60.	0.1361E-02	0.9393E+02	0.5401E-02	-0.8210E+02
61.	0.4224E-02	-0.1256E+03	0.5859E-02	0.9905E+02
62.	0.1554E-02	0.6513E+02	0.3328E-02	0.1130E+03
63.	0.2332E-02	-0.9437E+02	0.4659E-02	-0.5561E+02
64.	0.2561E-02	0.1159E+03	0.3289E-02	-0.1277E+03
65.	0.2279E-02	0.8621E+01	0.2888E-02	0.5818E+02
66.	0.2394E-02	-0.7149E+02	0.3895E-02	0.1552E+03
67.	0.1938E-02	0.6203E+02	0.3727E-02	0.4630E+02
68.	0.2989E-02	0.1756E+03	0.4983E-02	-0.1300E+03
69.	0.4077E-02	0.1169E+03	0.2843E-02	-0.1509E+03
70.	0.4607E-02	0.1722E+03	0.3280E-02	0.2085E+02
71.	0.3730E-02	-0.6362E+02	0.3525E-02	-0.2359E+01
72.	0.4294E-02	0.1560E+03	0.5680E-02	-0.1044E+03
73.	0.3353E-02	-0.3186E+02	0.4055E-02	0.2474E+02
74.	0.1235E-02	0.1557E+03	0.6381E-02	-0.5830E+02
75.	0.1682E-02	-0.8556E+02	0.2331E-02	0.2000E+02
76.	0.2968E-02	0.1401E+03	0.2984E-02	-0.1296E+03
77.	0.3129E-02	-0.1708E+03	0.1176E-02	0.4415E+02
78.	0.2555E-02	0.9014E+01	0.3559E-02	-0.8769E+02

TABLE XXIII.- HARMONICS OF BLADE BEAMWISE STRAIN GAGES AT 159 KTAS

BLADE BEAMWISE BENDING

HARM	RADIUS= 0.500 AMPLITUDE IN-LB	RADIUS= 0.500 PHASE DEGREES	RADIUS= 0.700 AMPLITUDE IN-LB	RADIUS= 0.700 PHASE DEGREES	RADIUS= 0.804 AMPLITUDE IN-LB	RADIUS= 0.804 PHASE DEGREES
0.	-2651.32	0.00	-3157.32	0.00	-3271.21	0.00
1.	9383.42	-62.17	6958.23	-72.04	4413.35	-88.96
2.	3497.91	123.07	2655.48	129.57	2064.10	132.28
3.	3955.96	75.70	6202.54	78.85	5399.96	75.60
4.	725.89	13.02	827.05	64.27	911.58	82.07
5.	148.09	4.16	1038.68	177.07	1329.41	174.12
6.	84.16	-42.82	143.84	168.19	236.54	168.68
7.	1000.76	-10.69	934.33	-179.48	1665.30	-178.57
8.	503.14	1.51	312.21	-157.43	777.44	-165.08
9.	308.44	107.71	140.50	-34.42	542.61	-56.78

BLADE BEAMWISE BENDING

HARM	RADIUS= 0.902 AMPLITUDE IN-LB	RADIUS= 0.902 PHASE DEGREES
0.	594.79	0.00
1.	1631.38	-122.92
2.	1121.51	133.00
3.	2550.57	72.15
4.	567.65	88.59
5.	766.41	171.53
6.	175.21	-173.98
7.	1011.88	-179.01
8.	493.99	-166.75
9.	331.68	-56.87

TABLE XXIII.- CONCLUDED

BLADE BEAMWISE BENDING

HARM	RADIUS= 0.227 AMPLITUDE IN-LB	RADIUS= 0.227 PHASE DEGREES	RADIUS= 0.309 AMPLITUDE IN-LB	RADIUS= 0.309 PHASE DEGREES	RADIUS= 0.390 AMPLITUDE IN-LB	RADIUS= 0.390 PHASE DEGREES
0.	7916.18	0.00	4954.16	0.00	1636.74	0.00
1.	18462.80	-62.15	12798.00	-63.12	10701.60	-61.14
2.	6547.38	172.12	4392.31	146.21	4141.21	132.65
3.	1565.11	-109.67	727.31	88.39	2367.61	75.35
4.	654.14	146.58	401.25	31.65	699.27	11.58
5.	119.78	-0.07	328.42	-26.46	401.59	-21.06
6.	288.21	110.67	99.25	-79.36	204.28	-77.49
7.	986.56	166.57	365.82	0.20	1148.59	-13.83
8.	1084.10	-175.84	345.33	154.51	250.38	12.03
9.	530.92	-43.93	220.88	-94.17	120.98	159.20
10.			107.01	-1.45	62.52	-106.33
11.			212.07	30.72	144.86	3.05
12.			150.14	100.10	223.65	89.68
13.			18.83	-41.79	87.16	-10.15
14.			63.48	92.56	53.61	-106.75
15.			117.31	74.92	150.99	-132.55
16.			18.65	170.01	71.39	-39.19
17.			87.00	-132.68	36.87	55.12
18.			153.30	-146.58	112.34	-156.44
19.			28.96	-144.05	67.19	-133.91
20.			25.02	-0.31	53.32	88.24
21.			49.17	169.94	50.14	100.61
22.			29.79	-137.27	41.99	-140.56
23.			41.91	47.84	48.43	-62.05
24.			40.23	-178.35	27.25	34.61
25.			45.32	-148.10	42.39	-140.77
26.			23.63	-112.27	42.75	-126.17
27.			28.38	115.78	19.92	153.66
28.			28.21	-153.54	45.14	-66.47
29.			9.06	160.58	29.64	1.84
30.			52.81	138.41	10.11	-43.38
31.			12.23	177.73	10.41	-89.08
32.			18.57	146.23	26.68	-146.17
33.			29.38	130.79	20.33	-156.27
34.			43.75	32.02	20.64	176.84
35.			34.07	-74.63	30.06	-57.25
36.			39.09	-37.70	33.03	55.75
37.			30.06	89.51	23.11	141.06
38.			15.73	-8.22	10.09	134.24
39.			35.12	35.79	49.04	37.80

TABLE XXIV.- HARMONICS OF BLADE CHORDWISE STRAIN GAGES AT 159 KTAS

	BLADE CHORDWISE BENDING					
	RADIUS= 0.227		RADIUS= 0.309		RADIUS= 0.390	
HARM	AMPLITUDE IN-LB	PHASE DEGREES	AMPLITUDE IN-LB	PHASE DEGREES	AMPLITUDE IN-LB	PHASE DEGREES
0.	132194.00	0.00	125047.00	0.00	117020.00	0.00
1.	47145.70	-63.17	38582.70	-63.96	30313.80	-64.48
2.	4262.64	95.26	2639.23	109.07	1625.66	127.78
3.	46789.70	-90.87	40015.80	-95.92	33706.10	-96.68
4.	6609.53	26.00	7214.00	19.03	7432.88	16.95
5.	2202.48	178.36	1761.84	-178.09	1401.47	-166.51
6.	872.27	103.36	637.47	110.04	769.50	122.31
7.	941.32	171.68	763.75	146.66	743.03	146.44
8.	3538.87	-56.55	3989.62	-80.68	4266.14	-80.02
9.	473.13	33.76	630.95	3.07	668.97	17.62
10.			244.22	-177.13	442.79	-174.60
11.			2323.67	7.03	3820.47	6.65
12.			595.57	-78.11	723.27	-64.75
13.			199.43	-53.28	119.13	-177.41
14.			245.62	47.96	383.89	-139.97
15.			125.88	-114.50	291.32	-162.64
16.			467.11	-123.28	126.91	23.45
17.			637.14	47.38	207.04	64.83
18.			399.85	-161.76	151.15	179.36
19.			277.97	-112.88	166.56	-98.35
20.			467.86	94.41	180.54	69.85
21.			611.18	133.13	349.28	129.70
22.			175.49	-132.23	134.71	-137.29
23.			579.56	18.83	401.30	29.49
24.			179.22	-168.81	135.81	-178.78
25.			996.38	-59.08	731.14	-59.08
26.			306.37	-76.60	269.74	-83.91
27.			487.27	-133.29	490.89	-127.18
28.			87.11	103.92	49.94	58.90
29.			202.29	2.75	235.35	-0.82
30.			490.23	-106.51	675.49	-115.56
31.			228.12	141.23	316.29	146.94
32.			252.98	-78.99	309.74	-61.57
33.			116.67	178.14	114.38	38.61
34.			196.19	-131.60	154.86	-115.01
35.			85.13	-100.70	19.99	-42.41
36.			15.38	-127.25	103.31	54.74
37.			155.14	110.13	126.58	-18.80
38.			41.12	-119.69	137.44	-86.57
39.			127.18	22.01	26.75	-89.83

TABLE XXIV. CONCLUDED

BLADE CHORDWISE BENDING

BL,

HARM	RADIUS= 0.500 AMPLITUDE IN-LB	RADIUS= 0.500 PHASE DEGREES
0.	91427.10	0.00
1.	19997.70	-65.05
2.	1039.05	-169.94
3.	25754.40	-96.64
4.	6930.38	19.15
5.	1332.12	-143.17
6.	449.33	129.76
7.	480.26	134.42
8.	3867.96	-81.17
9.	664.93	15.94
10.	371.15	-178.78
11.	4501.07	9.18
12.	899.49	-65.68
13.	269.12	165.39
14.	880.56	-140.92
15.	590.92	-172.79
16.	567.09	25.77
17.	117.44	-176.98
18.	208.25	111.66
19.	188.91	-20.14
20.	197.82	-53.51
21.	248.12	-175.16
22.	207.30	-154.24
23.	242.35	-9.62
24.	106.49	128.28
25.	208.92	-103.76
26.	259.00	-38.24
27.	225.30	-179.71
28.	74.45	-171.02
29.	217.36	-8.16
30.	358.33	-105.08
31.	226.09	135.96
32.	192.51	-77.28
33.	100.88	139.16
34.	182.11	-136.03
35.	54.87	84.17
36.	112.13	73.06
37.	230.86	-8.49
38.	203.68	-114.58
39.	45.69	-40.86

HARM	RADIUS= 0.700 AMPLITUDE IN-LB	RADIUS= 0.700 PHASE DEGREES	RADIUS= 0.804 AMPLITUDE IN-LB	RADIUS= 0.804 PHASE DEGREES	RADIUS= 0.902 AMPLITUDE IN-LB	RADIUS= 0.902 PHASE DEGREES
0.	29356.70	0.00	-45847.10	0.00	-52509.00	0.00
1.	7994.35	-63.70	4168.24	-69.03	956.40	-37.69
2.	995.33	-142.37	786.64	-119.90	685.25	-82.26
3.	11232.10	-91.99	5270.61	-91.28	1925.02	-68.15
4.	4420.93	18.72	2507.23	21.17	558.14	52.72
5.	656.04	-96.15	466.24	-97.19	346.76	-91.91
6.	526.54	153.35	124.94	125.41	370.23	63.54
7.	111.60	4.99	209.87	39.76	173.92	19.53
8.	2515.72	-46.61	1331.21	-51.38	233.13	-82.30
9.	501.39	83.75	246.33	55.95	139.11	68.66

TABLE XXV.- HARMONICS OF BLADE TORSION AT 159 KTAS

BL.

BLADE TORSION

HARM	RADIUS= 0.309 AMPLITUDE IN-LB	RADIUS= 0.309 PHASE DEGREES	RADIUS= 0.500 AMPLITUDE IN-LB	RADIUS= 0.500 PHASE DEGREES	RADIUS= 0.700 AMPLITUDE IN-LB	RADIUS= 0.700 PHASE DEGREES	RADIUS= 0.902 AMPLITUDE IN-LB	RADIUS= 0.902 PHASE DEGREES
0.	-8478.80	0.00	-3703.10	0.00	-2480.68	0.00	945.47	0.00
1.	4481.01	25.58	4486.72	28.31	4139.06	41.00	2599.09	36.88
2.	5010.30	-177.69	3699.33	-167.87	2484.19	-154.32	957.21	-124.43
3.	1375.18	61.44	688.78	44.72	334.58	-62.25	566.70	-117.09
4.	699.86	167.85	691.89	-178.08	506.68	-171.98	223.71	-121.50
5.	402.36	-14.28	241.74	21.27	184.86	15.88	253.22	-1.67
6.	487.58	-73.15	428.53	-58.82	313.80	-57.56	151.66	-30.97
7.	986.32	-18.27	437.66	-8.25	166.59	-21.34	253.39	-5.26
8.	275.21	-11.29	109.72	-54.15	192.33	-121.29	93.62	-54.02
9.	151.27	169.52	42.57	-28.55	209.24	-11.19	80.44	36.85
10.	106.46	-81.74	58.52	110.02				
11.	92.72	-87.27	39.71	-168.92				
12.	251.63	117.57	64.26	-48.58				
13.	107.52	-124.43	24.30	-55.43				
14.	83.33	-171.61	21.46	-149.67				
15.	72.22	-150.10	6.83	163.27				
16.	22.34	78.37	2.91	38.01				
17.	54.42	109.14	5.99	84.19				
18.	83.38	169.59	4.53	45.01				
19.	74.12	79.83	2.35	-39.77				
20.	117.31	106.15	2.61	11.96				
21.	60.55	60.09	2.17	118.52				
22.	40.16	-88.35	1.83	99.66				
23.	47.48	-89.31	2.28	64.50				
24.	12.32	-10.86	1.95	89.52				
25.	16.82	124.21	2.89	93.96				
26.	87.03	-8.48	2.00	110.33				
27.	26.22	45.57	1.31	59.24				
28.	25.74	-79.75	2.10	69.71				
29.	28.81	-14.44	2.55	73.17				
30.	15.94	91.86	1.28	89.82				
31.	2.83	-39.22	1.23	38.79				
32.	0.97	174.78	1.74	82.69				
33.	22.08	-112.12	2.05	78.67				
34.	33.59	-120.14	1.26	62.40				
35.	24.68	-40.68	1.11	142.37				
36.	14.52	-58.16	2.26	73.88				
37.	3.84	86.15	1.14	98.50				
38.	16.63	149.86	2.98	50.18				
39.	9.81	25.81	1.19	30.22				

TABLE XXVI.- AERODYNAMIC PHENOMENON BY TEST CONDITION

	V_h	0.9	0.8	0.7	0.6	0.5	Hover
Shock	X	X	X	X			
BVI			X	X	X	X	
Tip effects	X	X	X	X	X	X	X
Stall	X	X	X				
Hub wake	X	X	X	X	X	X	

TABLE XXVII.- BLADE-ACCELERATION BIAS OFFSETS

r/R	Az	Ay	Ar
1.00	29	3.6	615
.90	26	3.7	554
.70	20	3.6	430
.60	17	3.4	369
.50	14	3.1	307

Figure 1.- NASA 736 White Cobra.

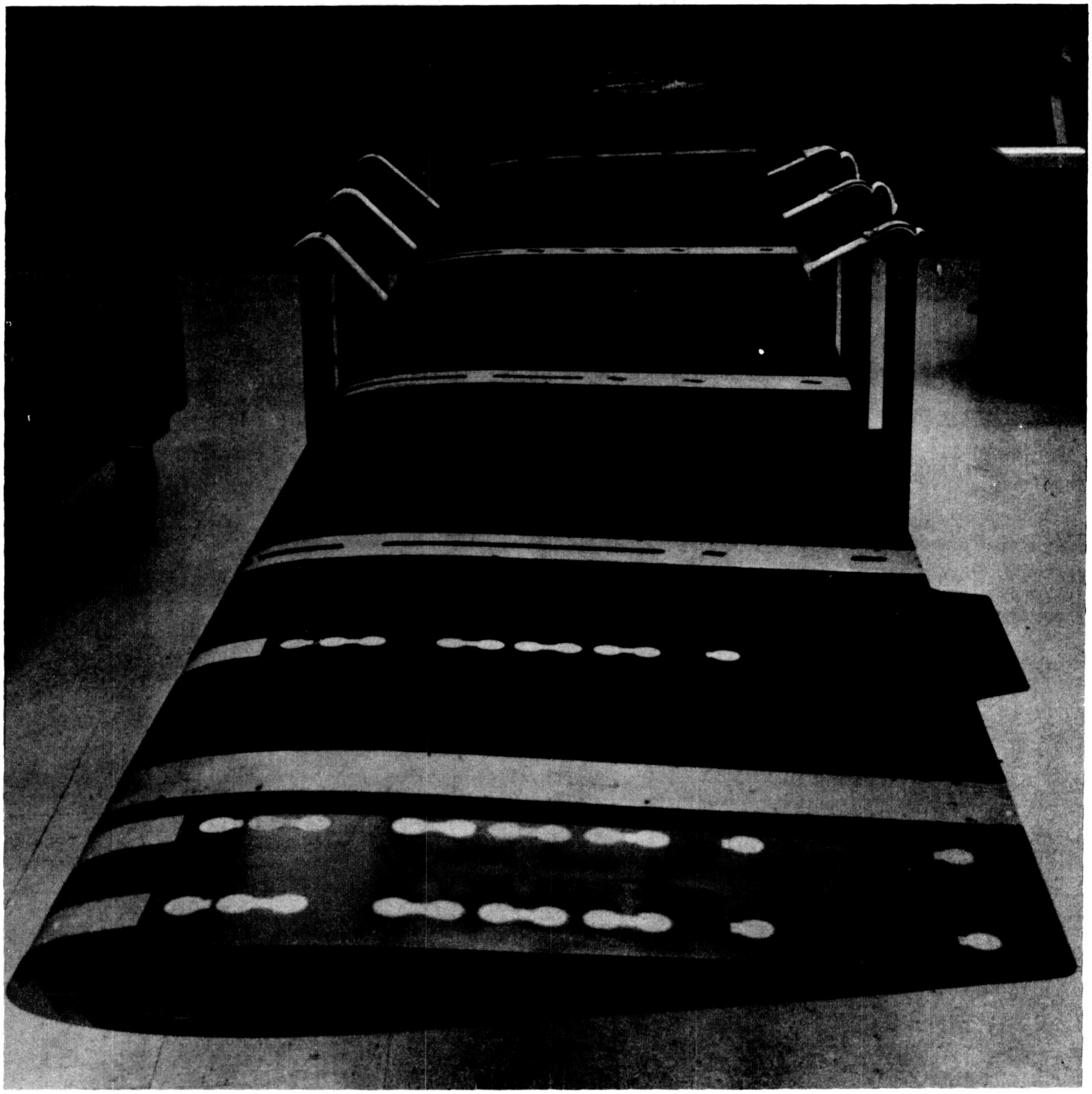

Figure 2.- The OLS White blade with five radial pressure array.

ORIGINAL PAGE IS
OF POOR QUALITY

Figure 3.- The OLS Red blade with miscellaneous instrumentation.

ORIGINAL PAGE IS
OF POOR QUALITY

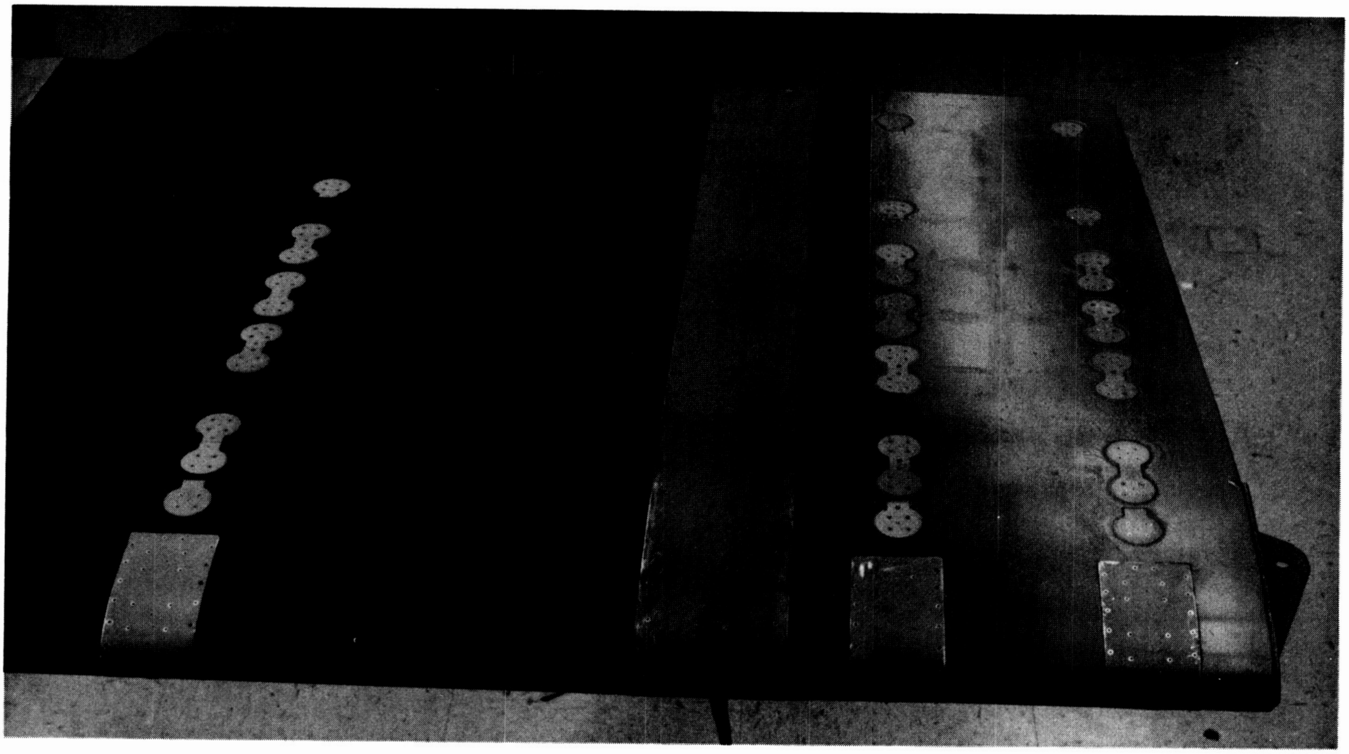

Figure 4.- Extra three radial array installation.

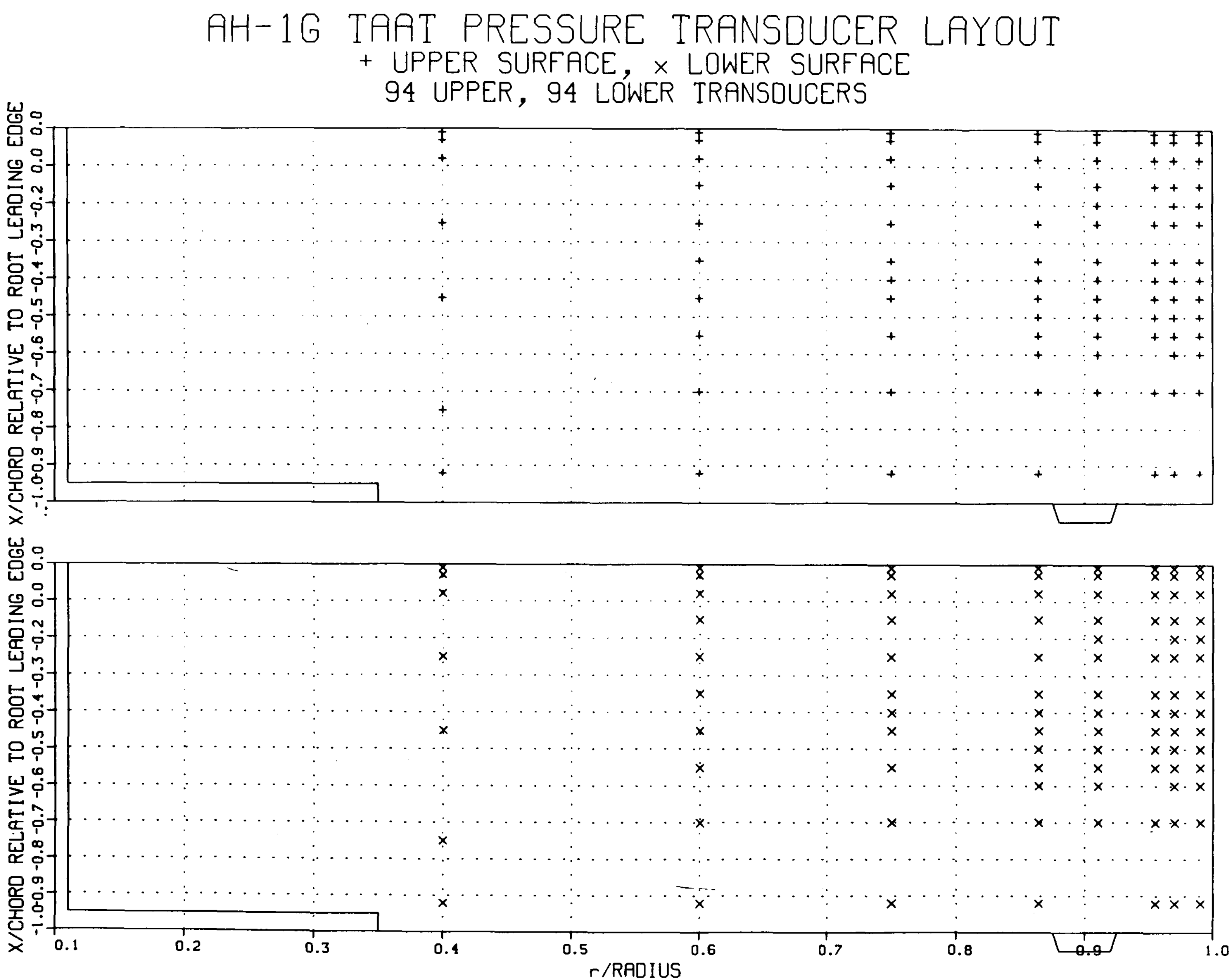

Figure 5.- The TAAT blade-pressure instrumentation locations.

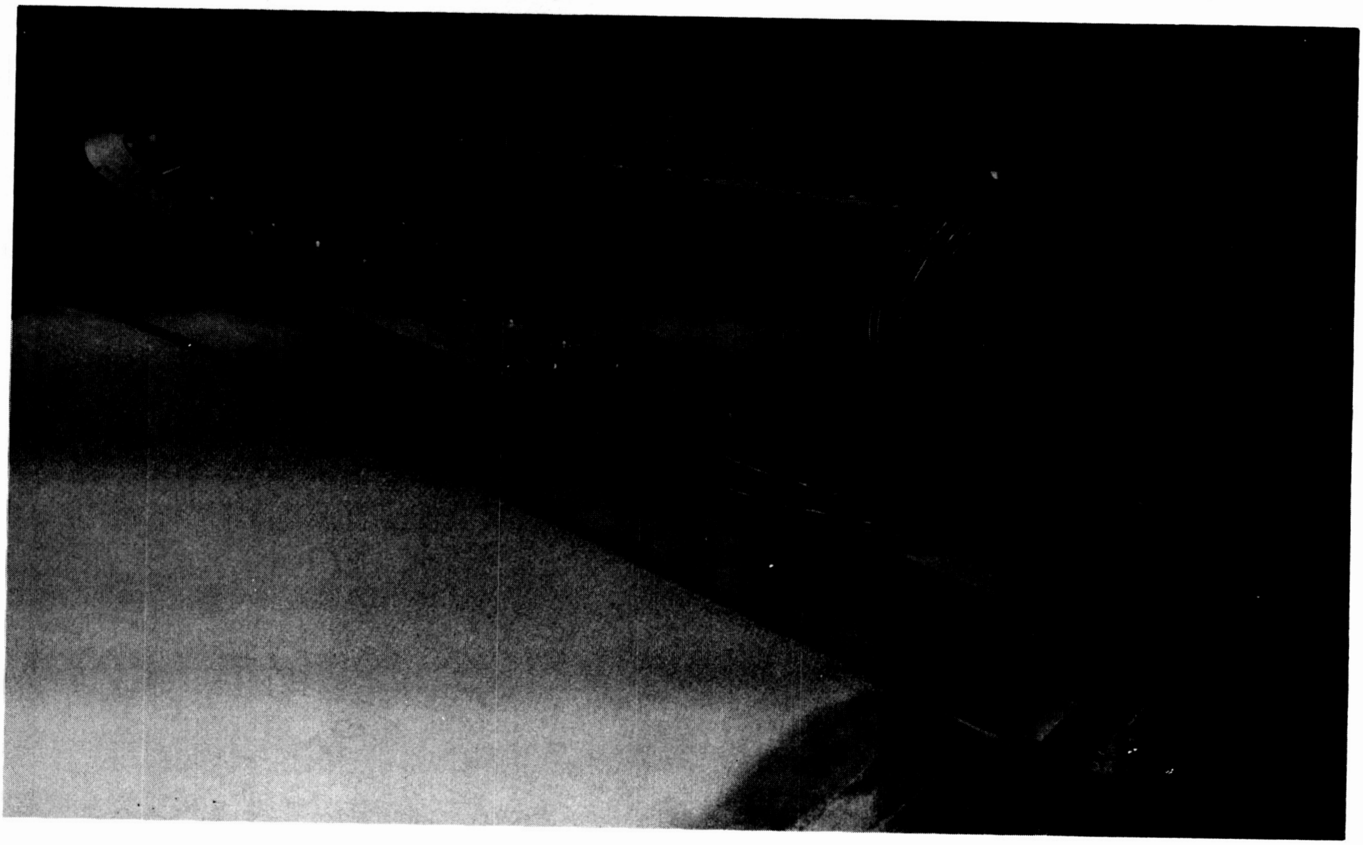

Figure 6.- The OLS channel installation.

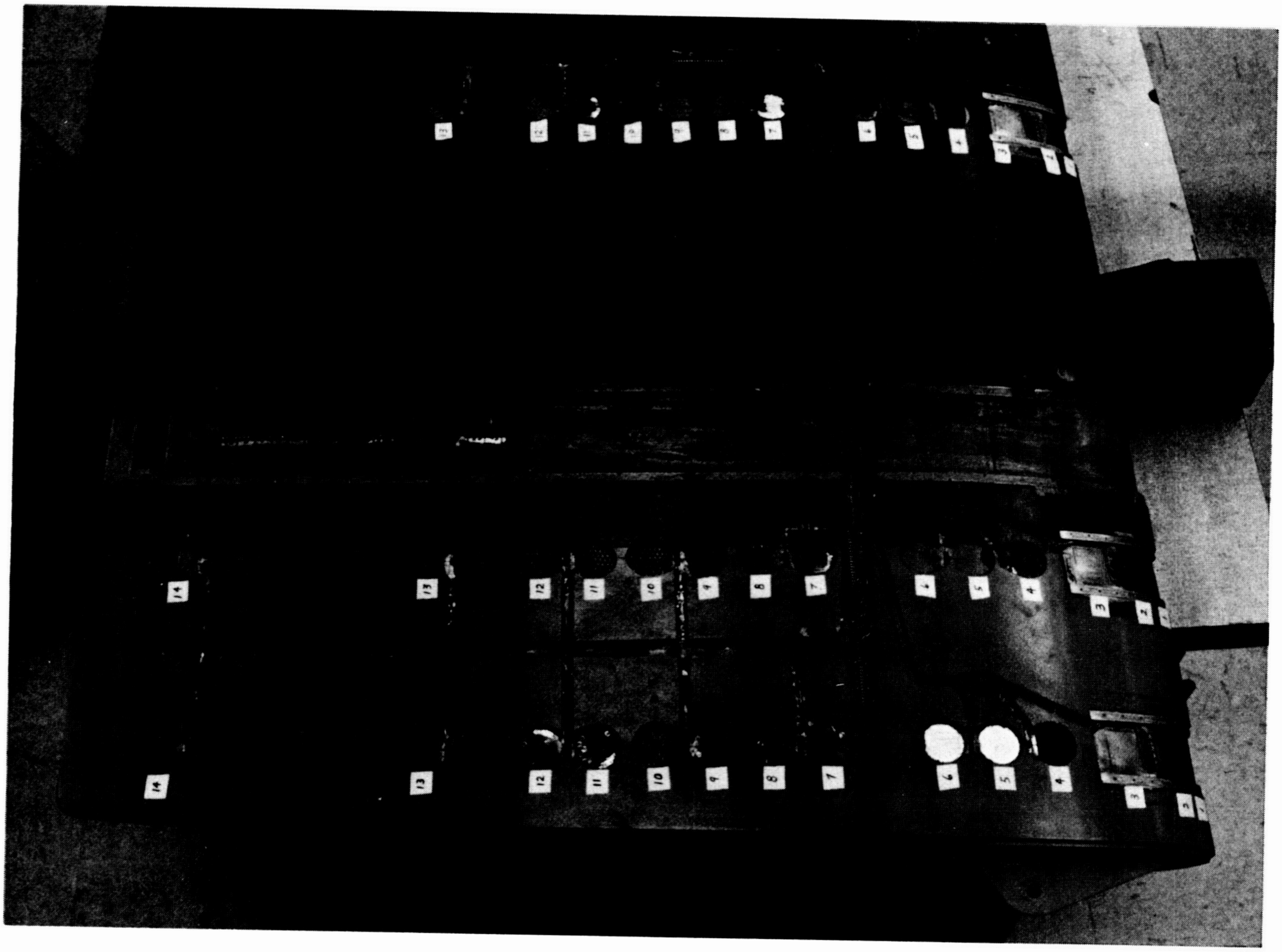

Figure 7.- Routed out Nomex transducer locations.

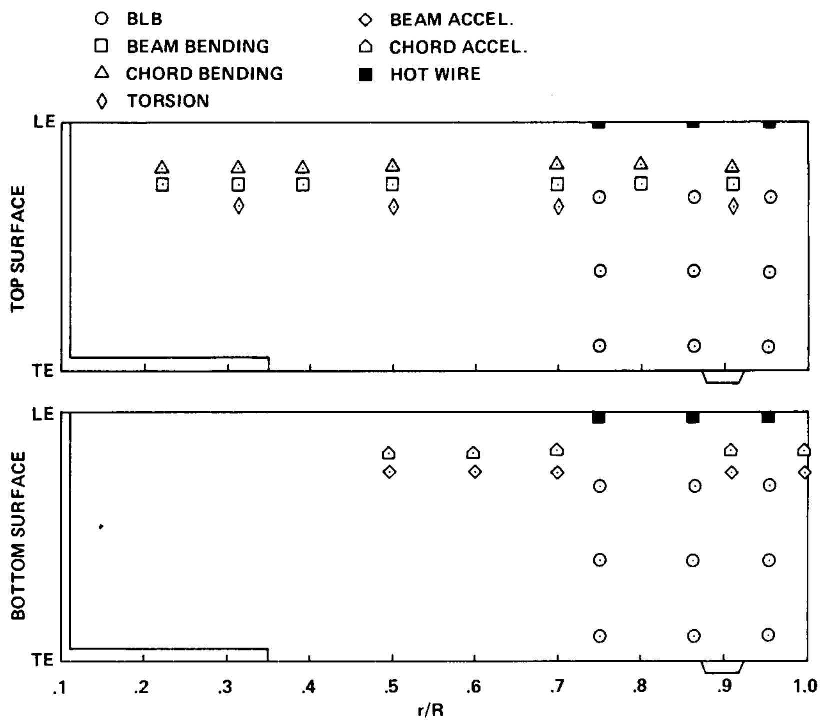

Figure 8.- The TAAT blade strain gage, hot-wire, and accelerometer locations.

ORIGINAL PAGE IS
OF POOR QUALITY

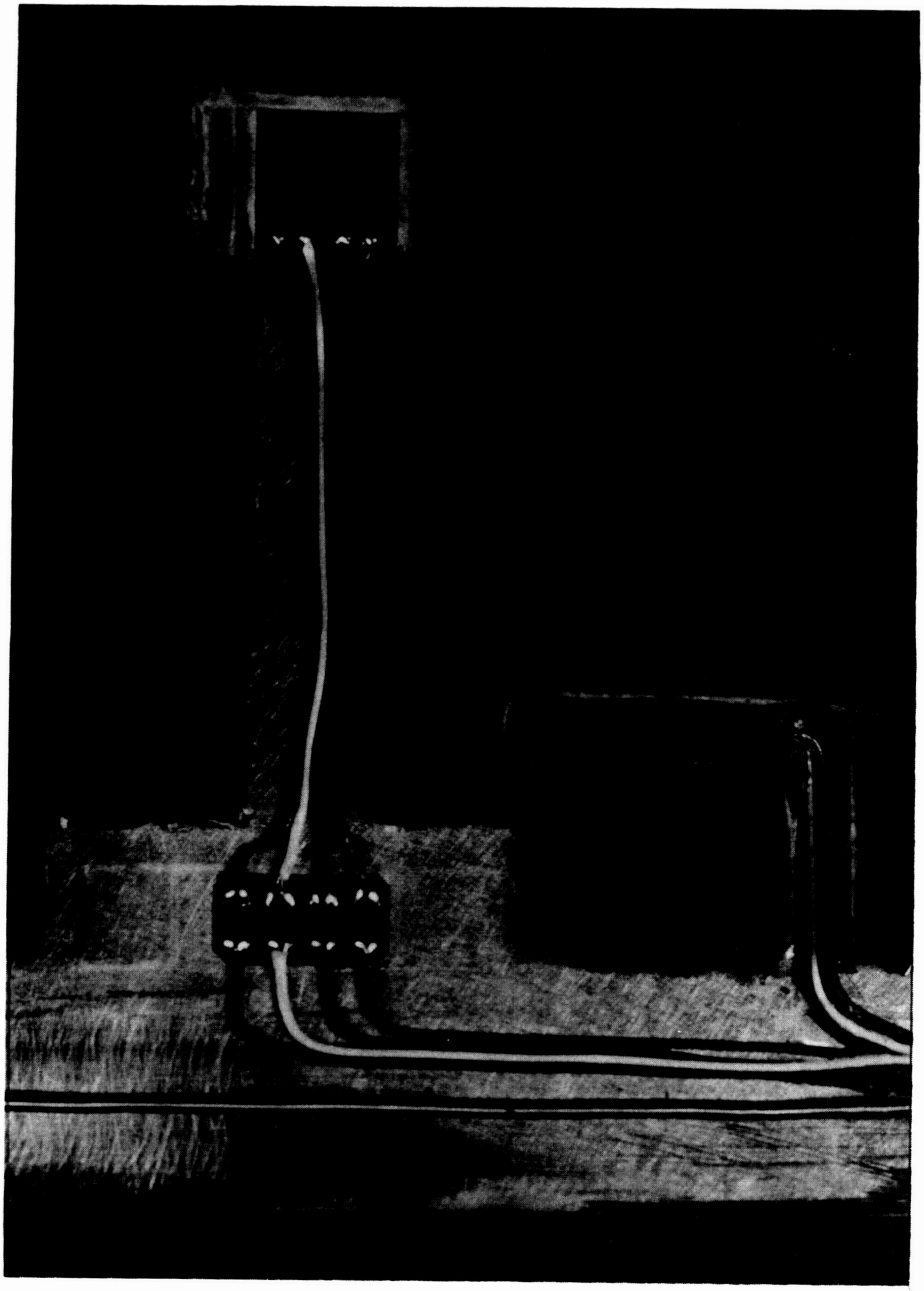

Figure 9.- Strain gage and accelerometer installation.

ORIGINAL PAGE IS
OF POOR QUALITY

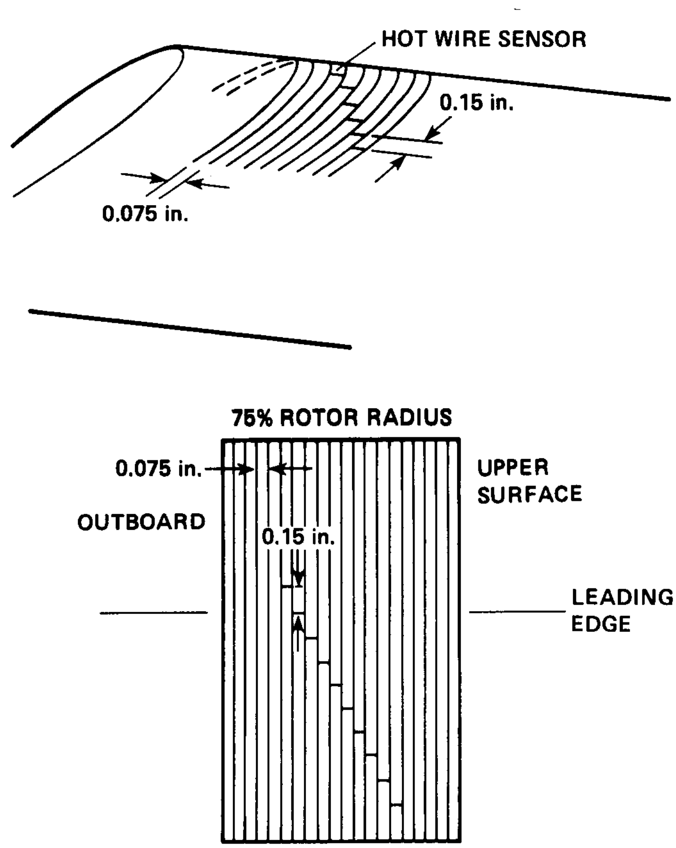

Figure 10.- Hot-wire anemometer installation.

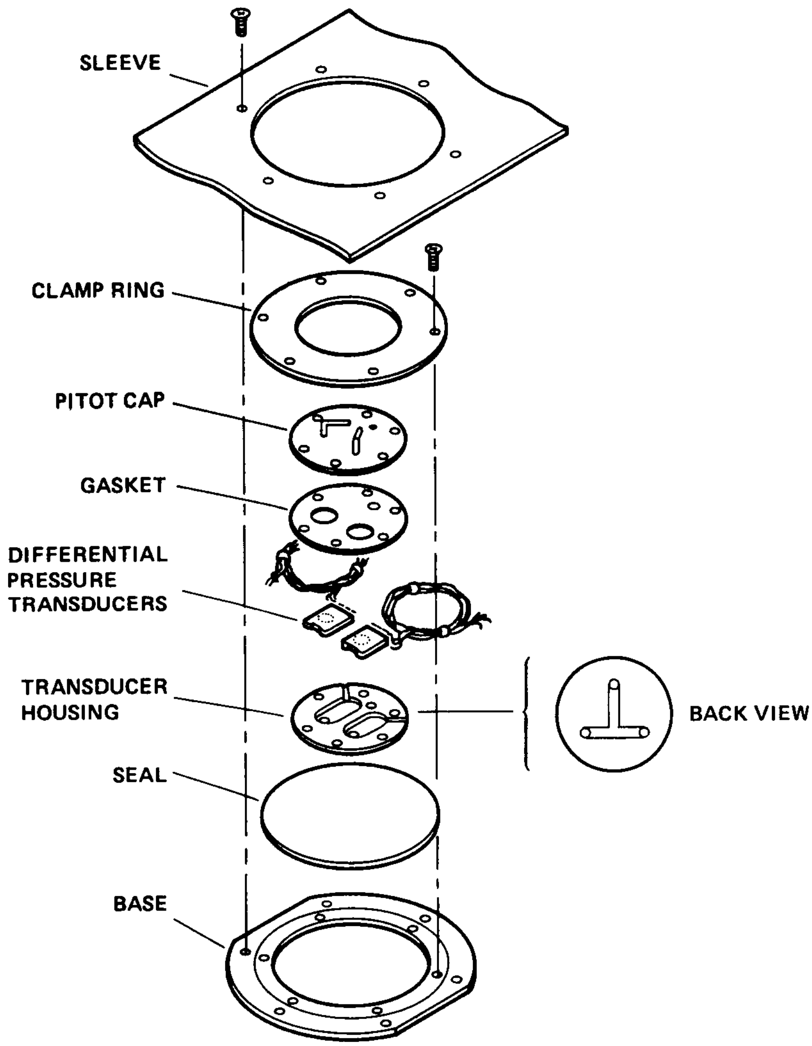

Figure 11.- The BLB installation.

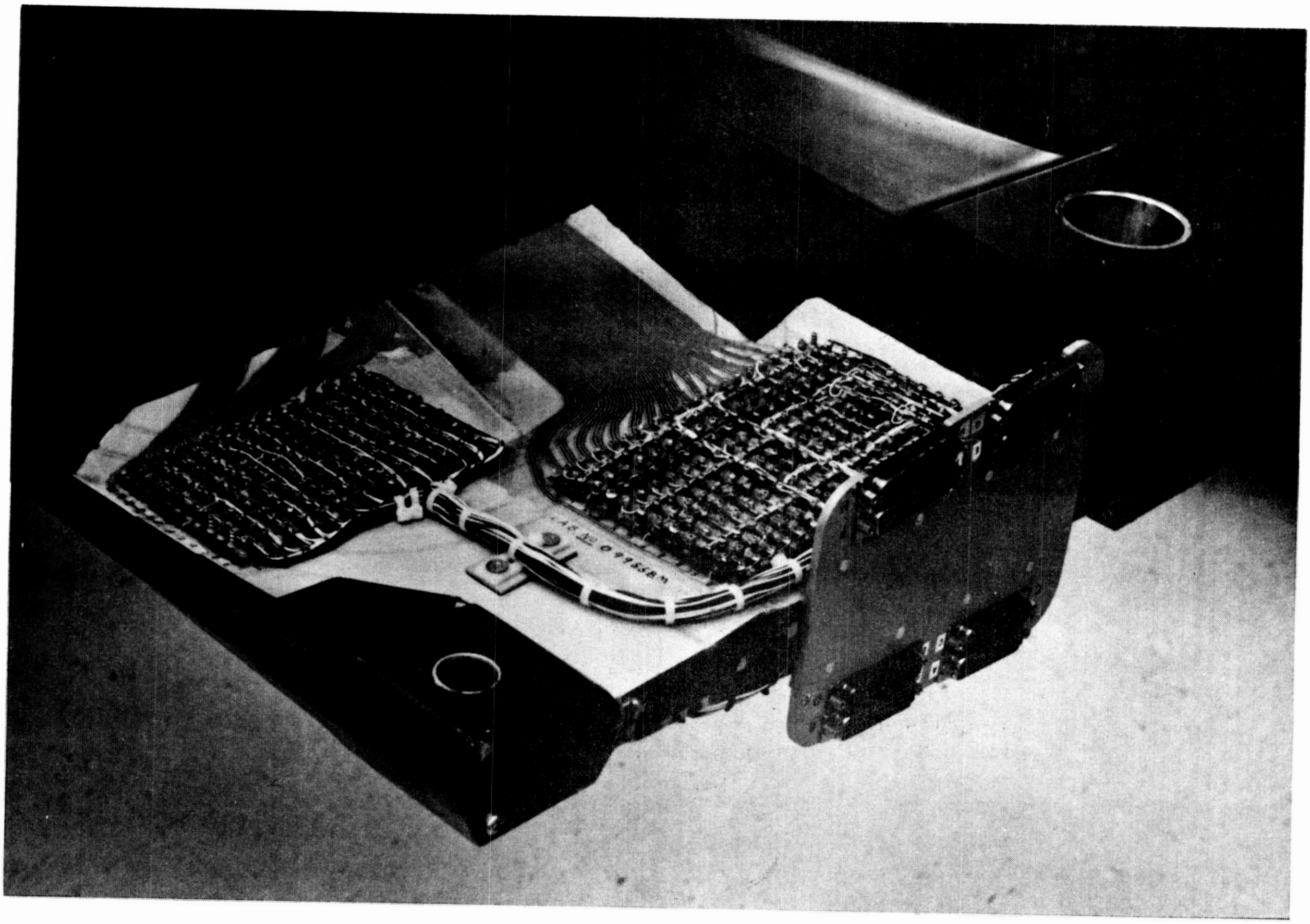

Figure 12.- Root end multiprong pin connectors.

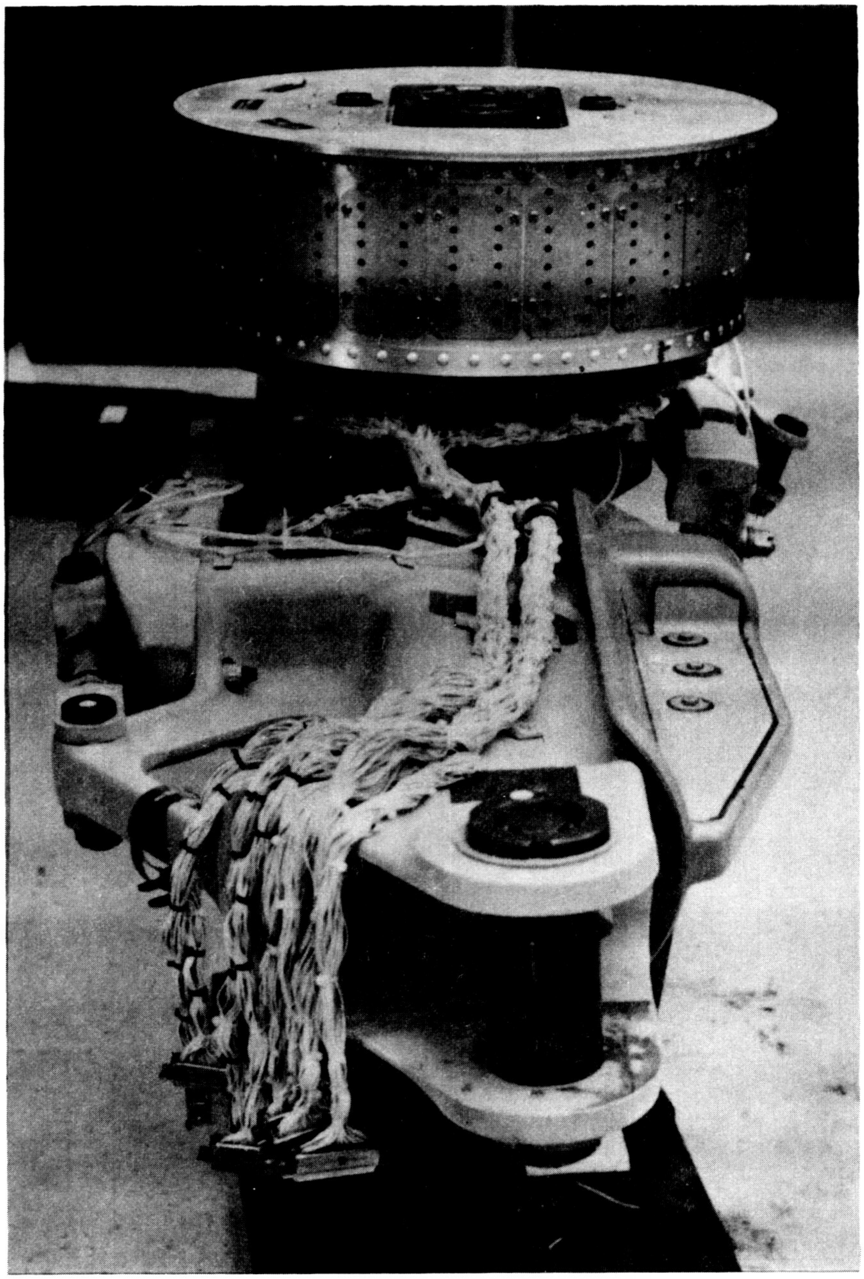

Figure 13.- Mux-bucket/hub/wiring assemblage.

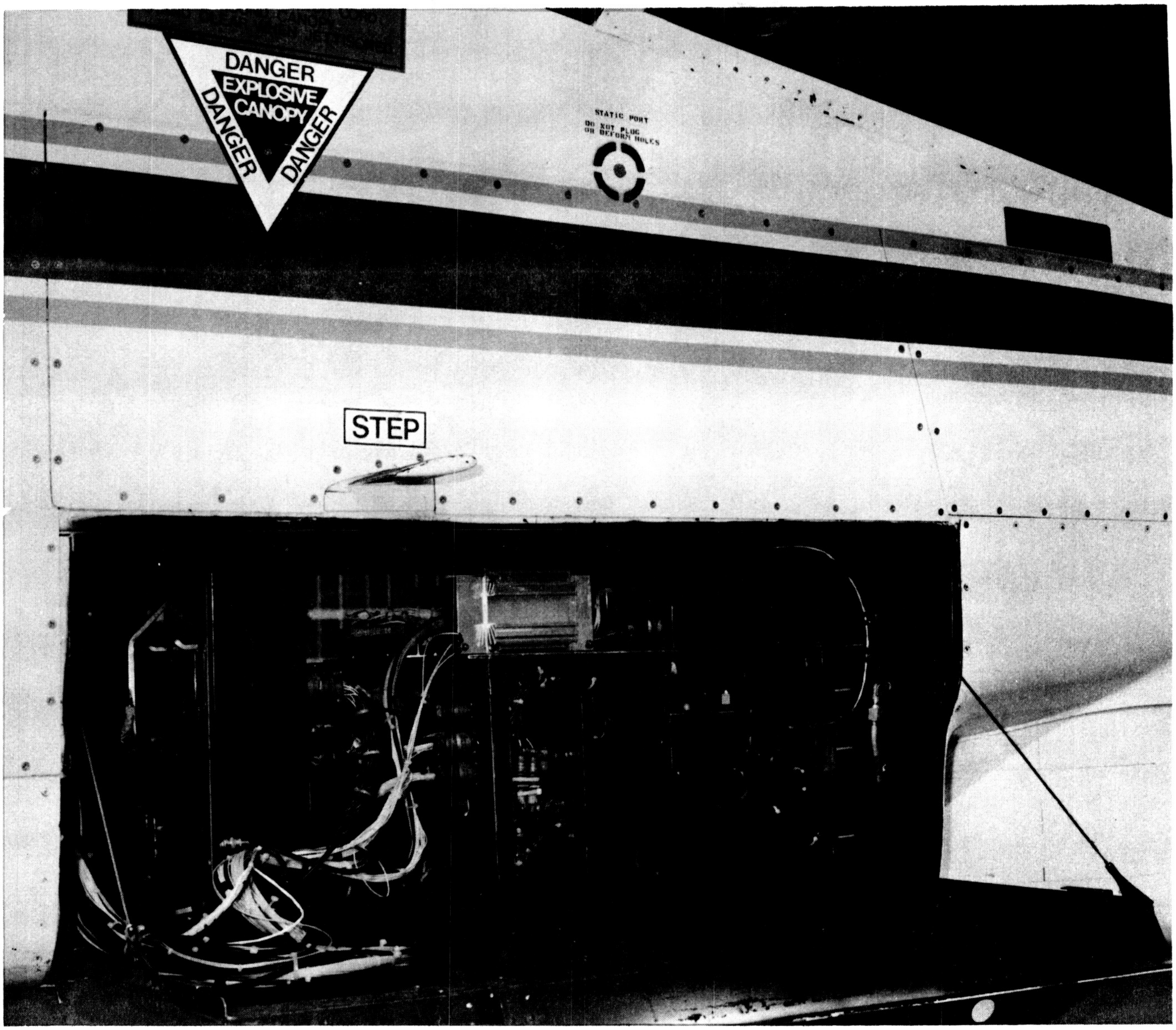

Figure 14.- Instrument package in ammo bay.

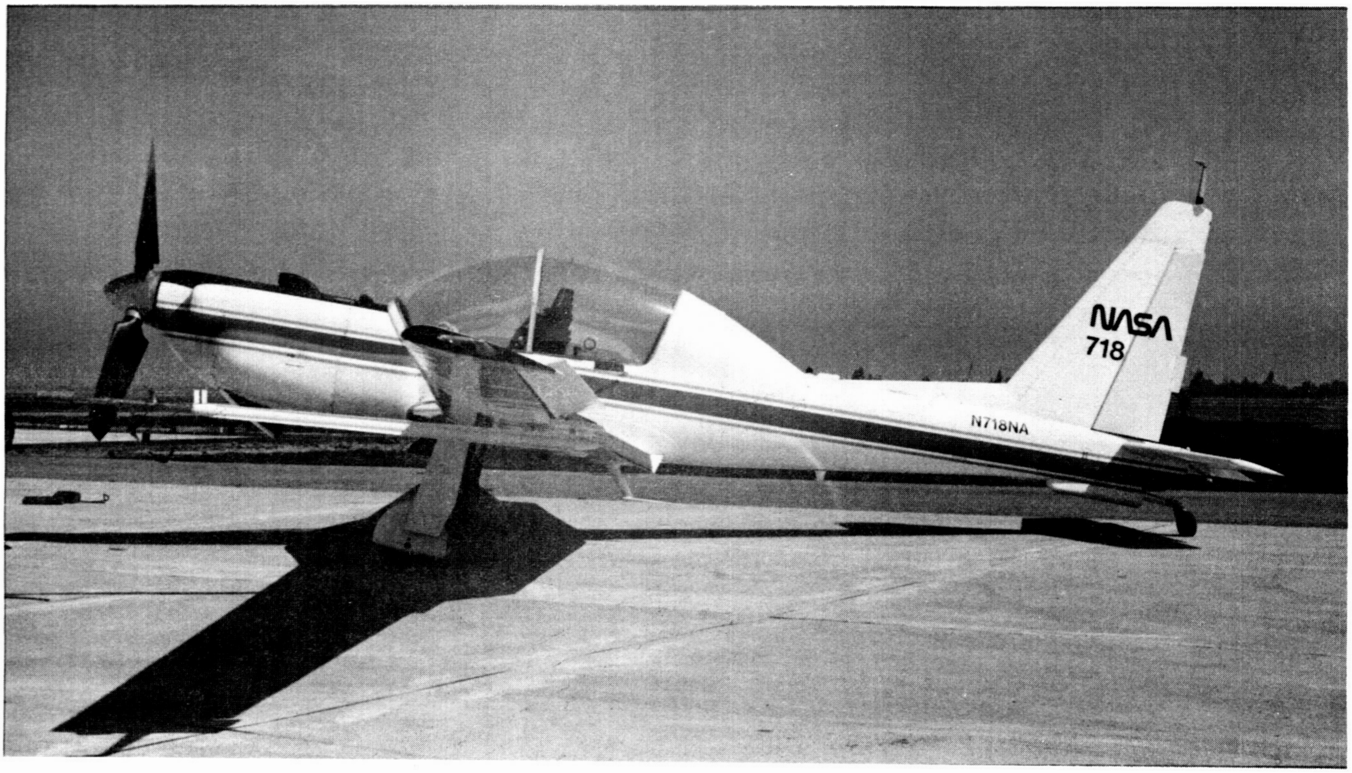

Figure 15.- The YO-3A Acoustic Research Aircraft.

ORIGINAL PAGE IS
OF POOR QUALITY

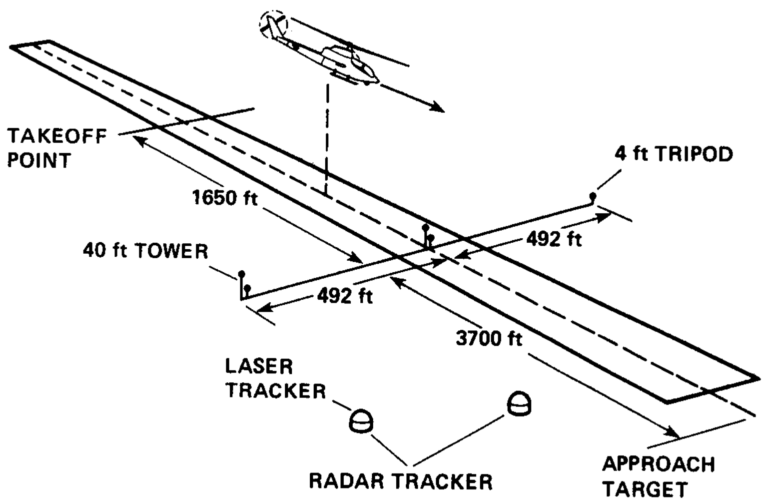

Figure 16.- Ground-array microphone layout.

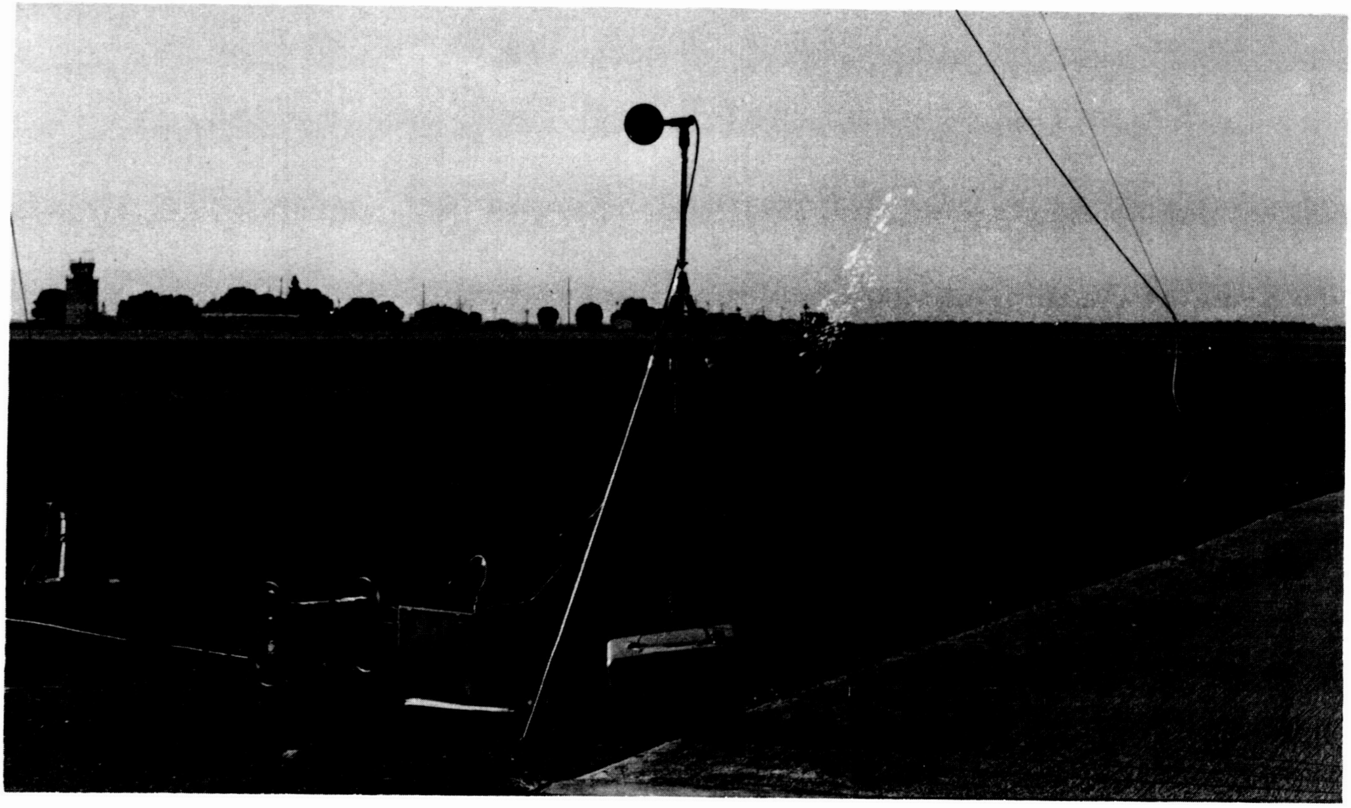

Figure 17.- Tripod microphone stands.

ORIGINAL PAGE IS
OF POOR QUALITY

ORIGINAL PAGE IS
OF POOR QUALITY

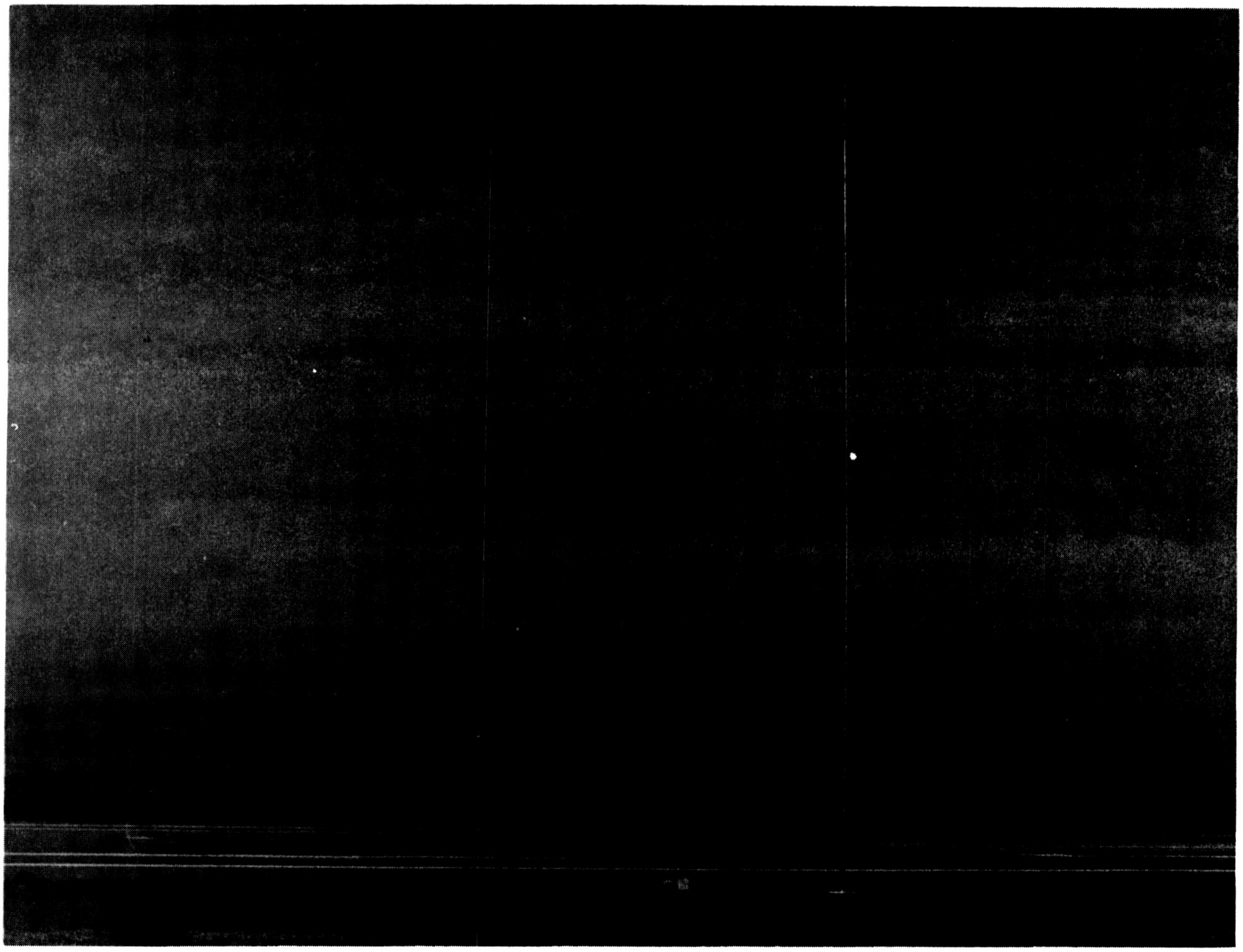

Figure 18.- Forty-foot microphone towers.

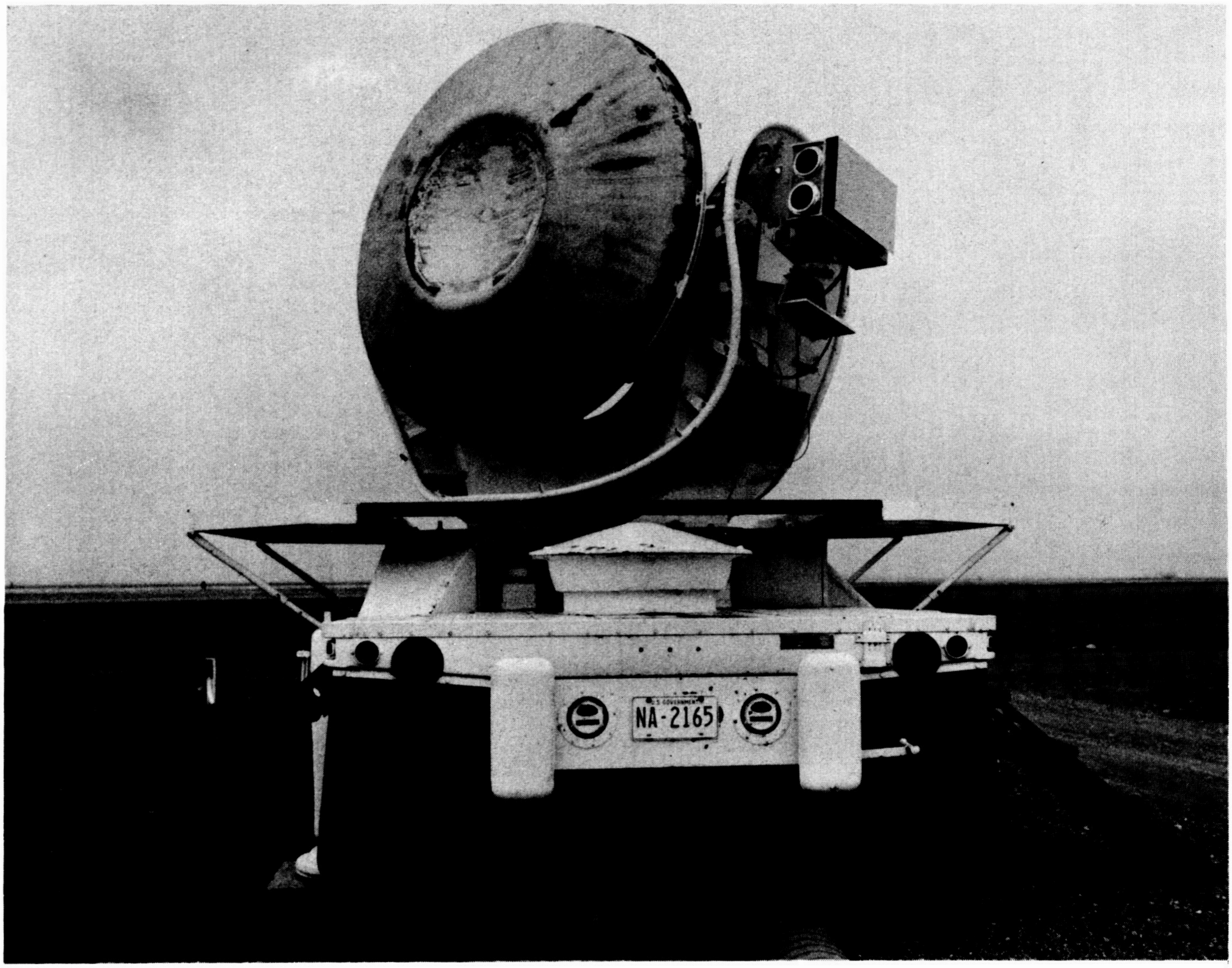

Figure 19.- Radar and laser tracker.

ORIGINAL PAGE IS
OF POOR QUALITY

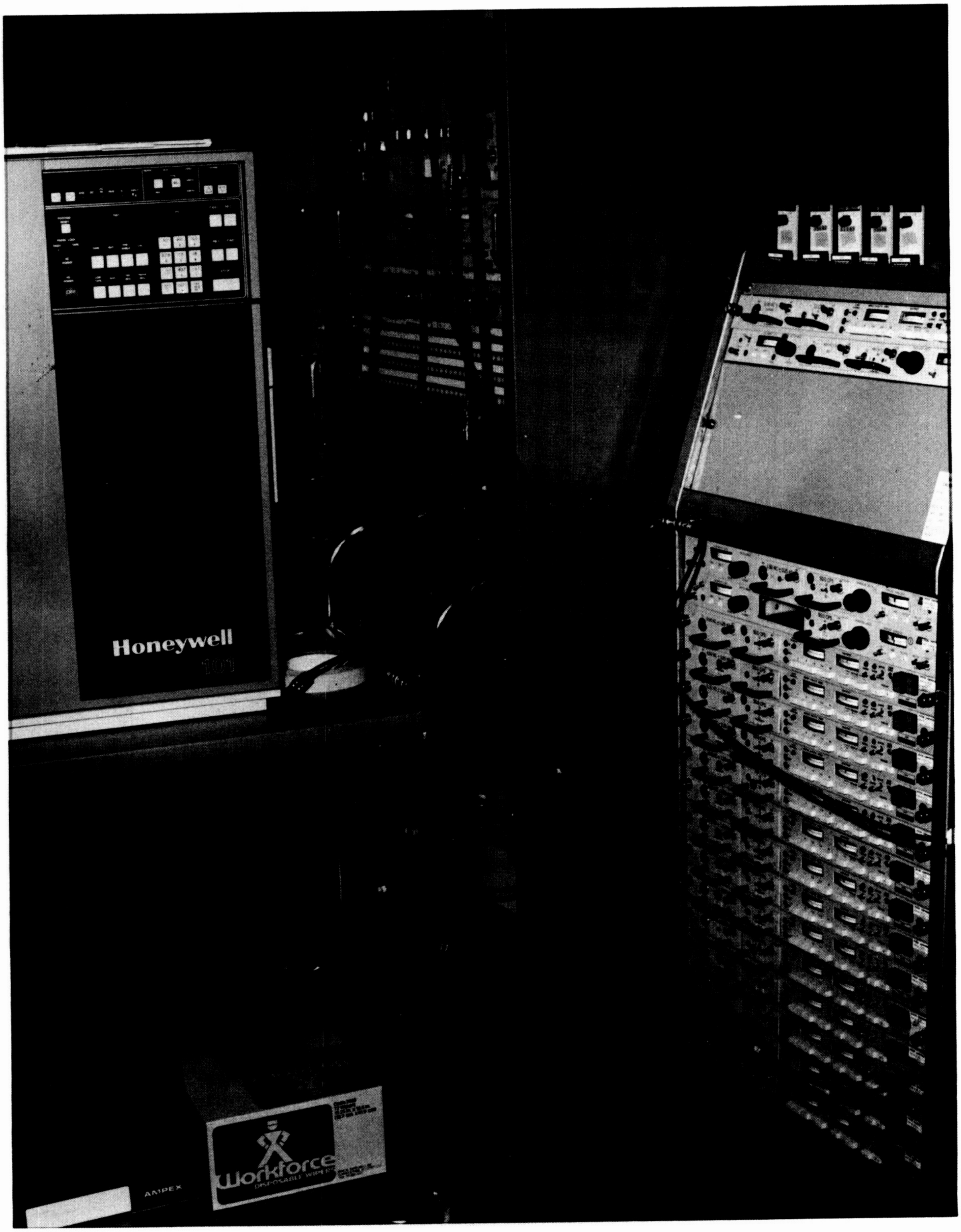

Figure 20.- Ground-station discriminator rack.

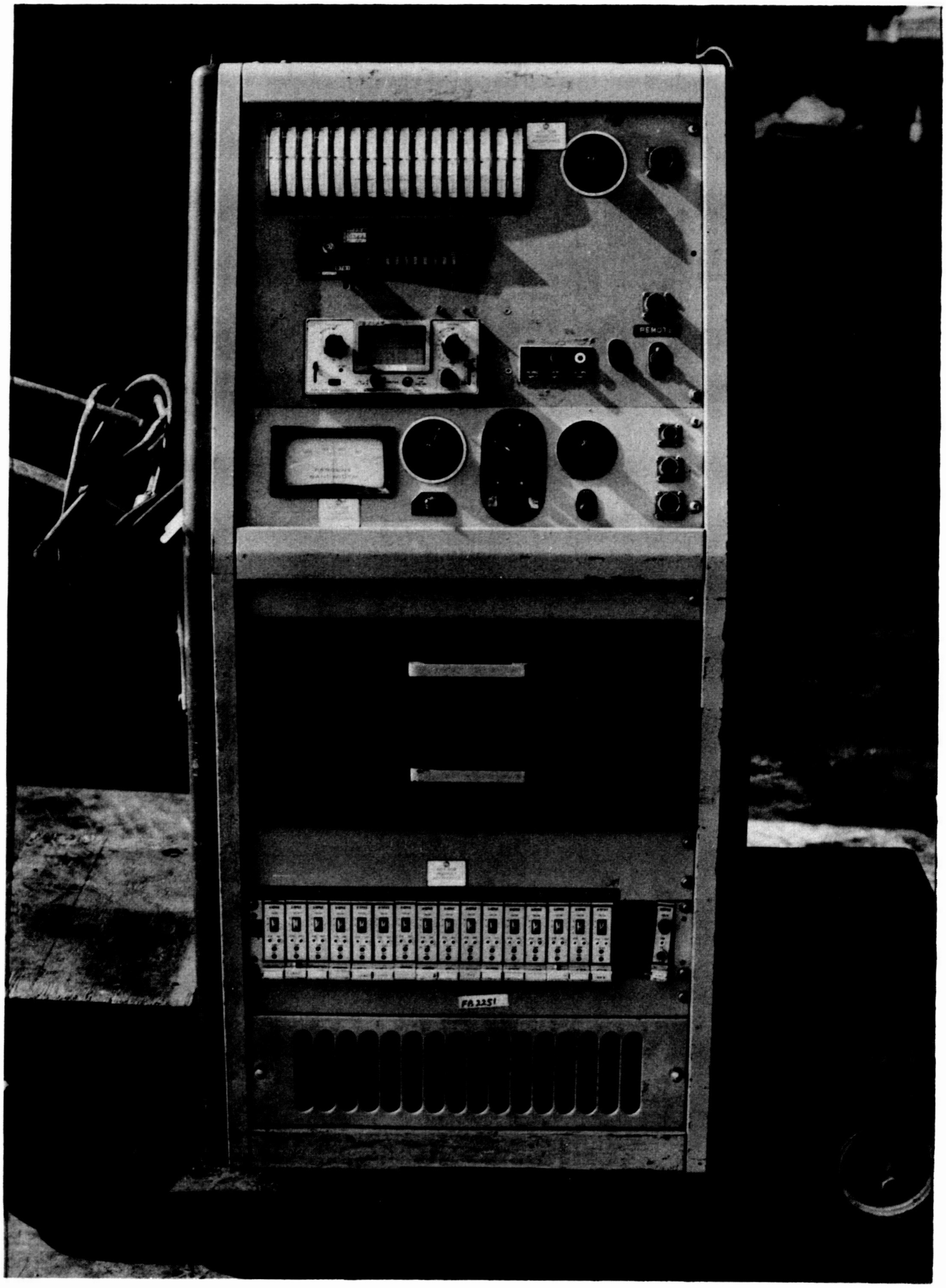

Figure 21.- Preflight calibration hardware.

ORIGINAL PAGE IS
OF POOR QUALITY

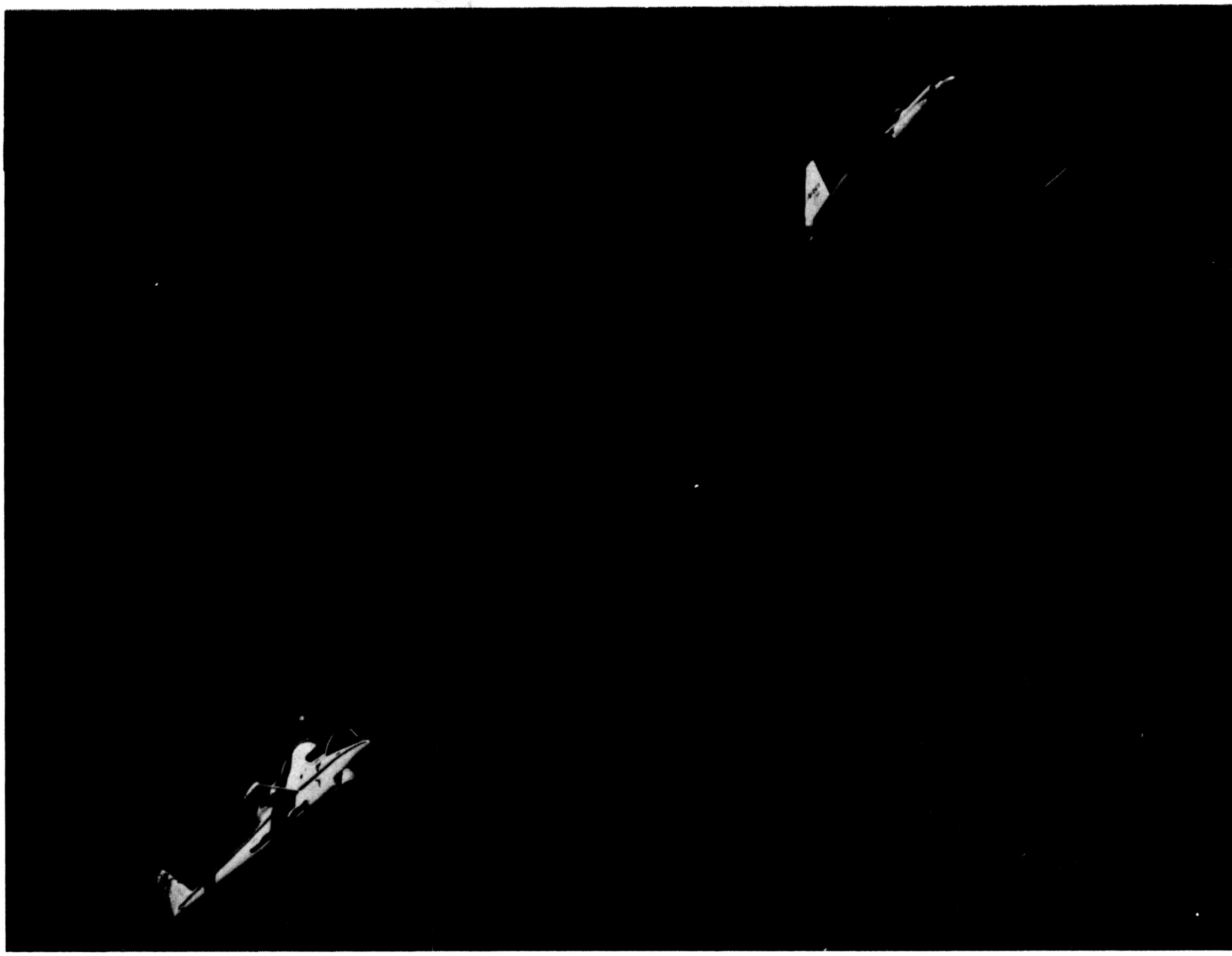

Figure 22.- The YO-3A and Cobra flying information.

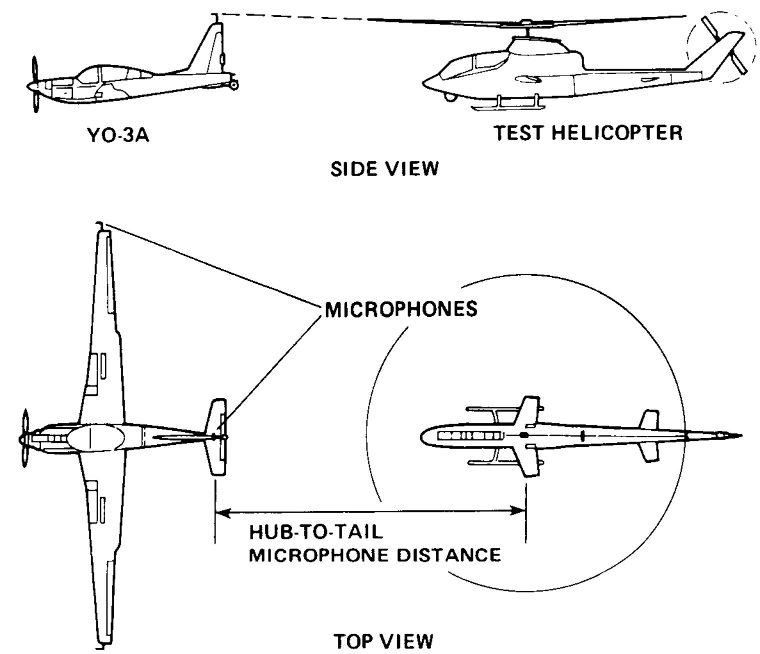

Figure 23.- The YO-3A/Cobra trail formation.

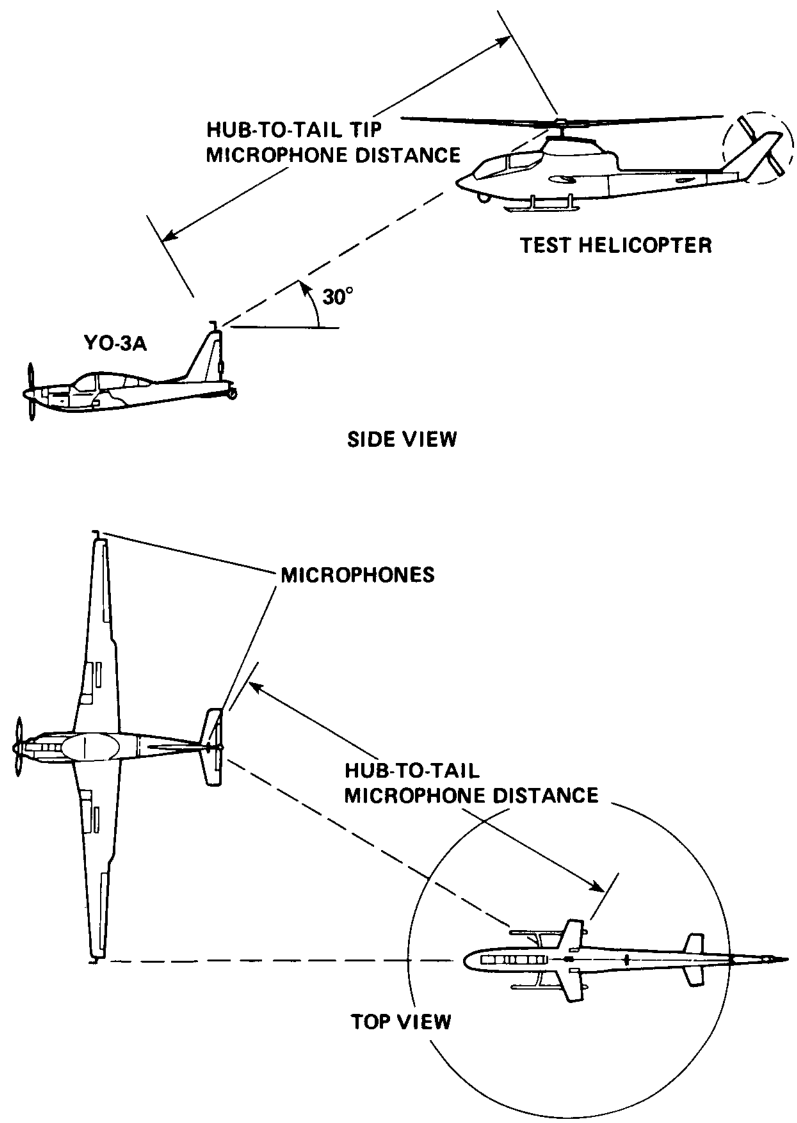

(a) Left position.

Figure 24.- The YO-3A/Cobra left and right formation.

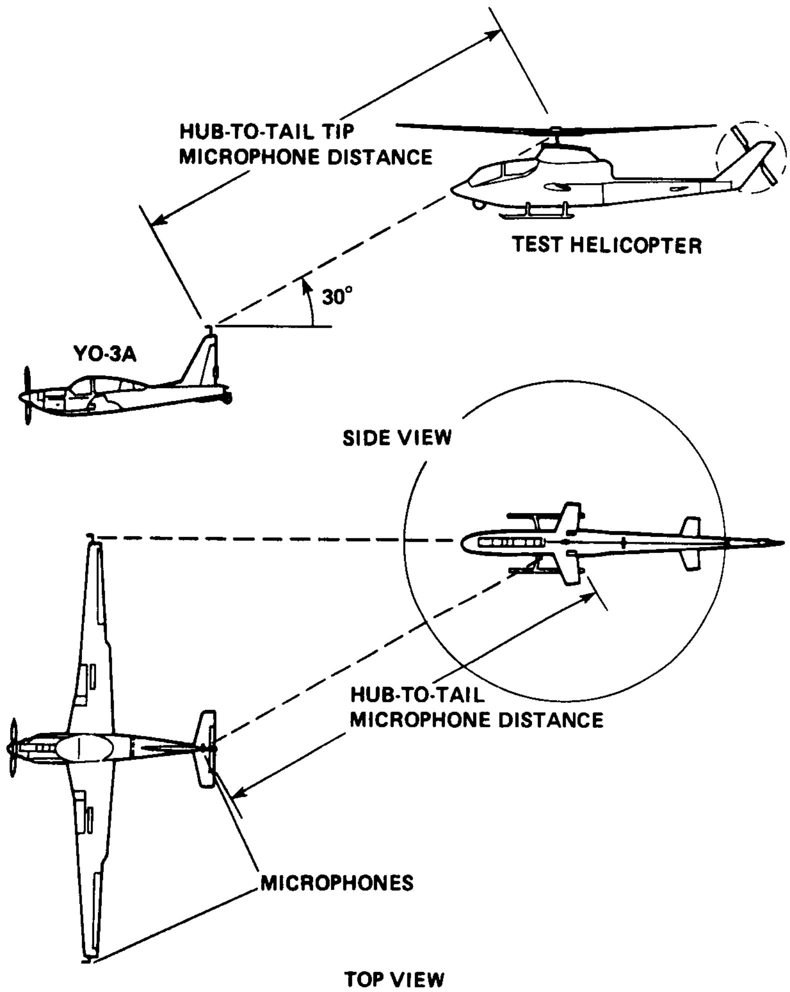

(b) Right position.

Figure 24.- Concluded.

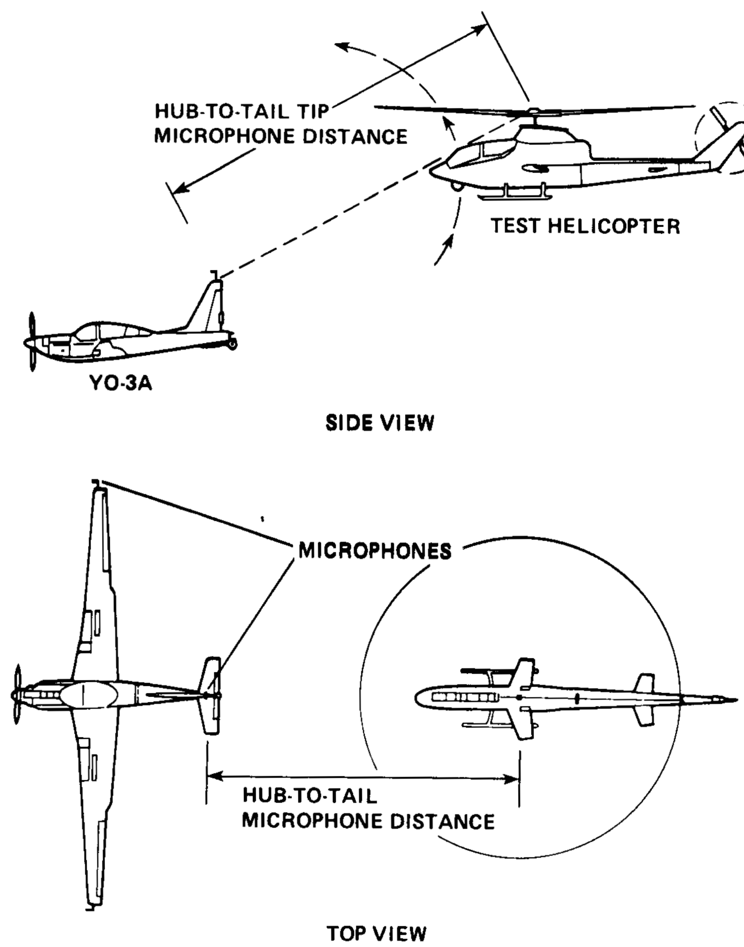

Figure 25.- The YO-3A/Cobra experimental formation.

Figure 26.- Supplementary calibration-test setup.

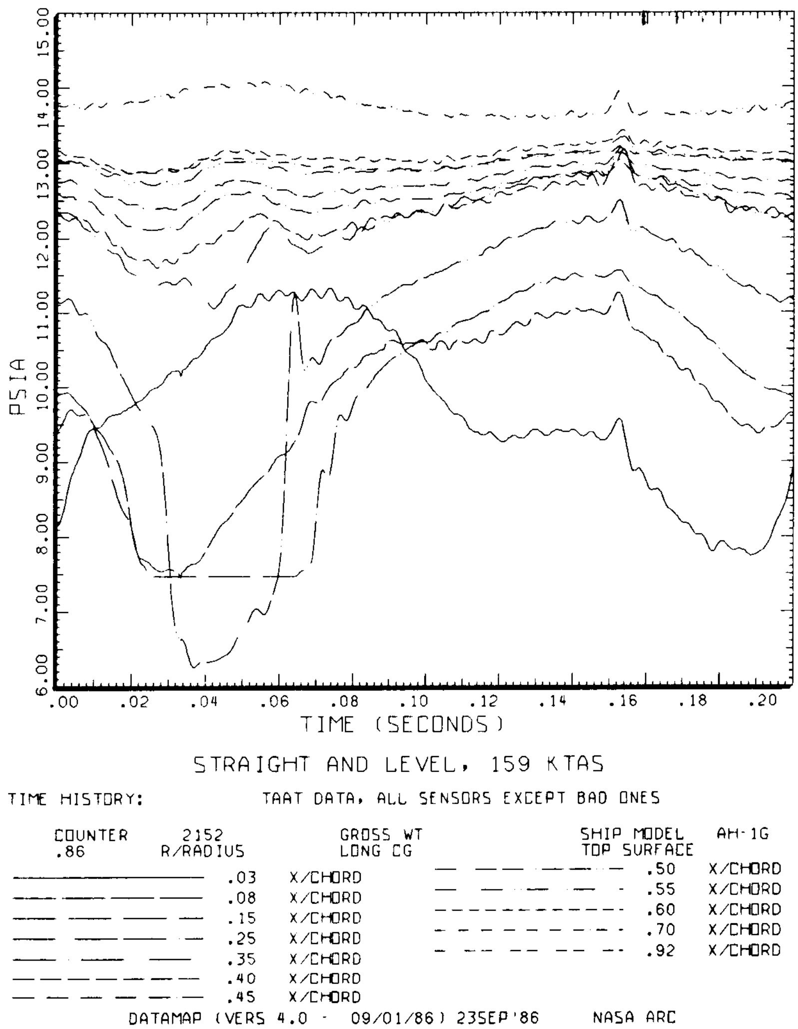

Figure 27.- Sample data spike, upper-surface variety.

ORIGINAL PAGE IS
OF POOR QUALITY

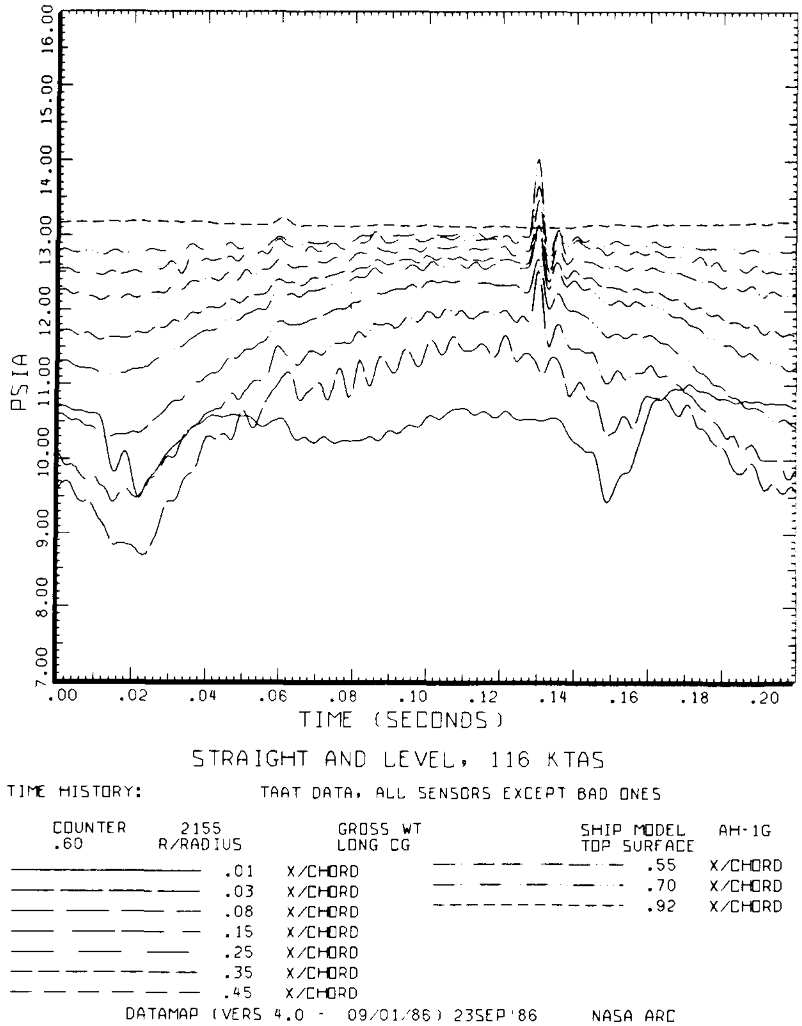

Figure 28.- Sample data spike, track variety.

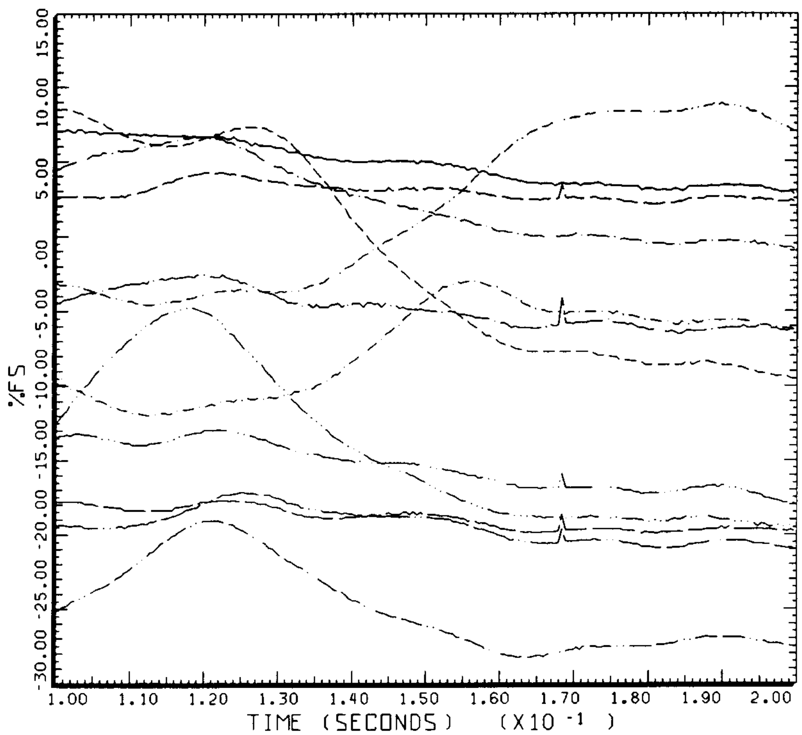

SAMPLE OF DIGITIZING SPIKES

TIME HISTORY: HOT-WIRE ATTENUATION SENSORS, TAAT, BOTTOM SURFACE

COUNTER .95 2153 R/RADIUS GROSS WT LONG CG SHIP MODEL SHIP ID AH-1G 20004

-1.56 INCHES
-1.44 INCHES
-1.32 INCHES
-1.20 INCHES
-1.08 INCHES
-.96 INCHES
-.84 INCHES
-.72 INCHES
-.60 INCHES
-.48 INCHES
-.12 INCHES
-.06 INCHES

DATAMAP (VERS 4.0 - 09/01/86) 29SEP'86 NASA ARC

Figure 29.- Sample data spike, digitizing variety.

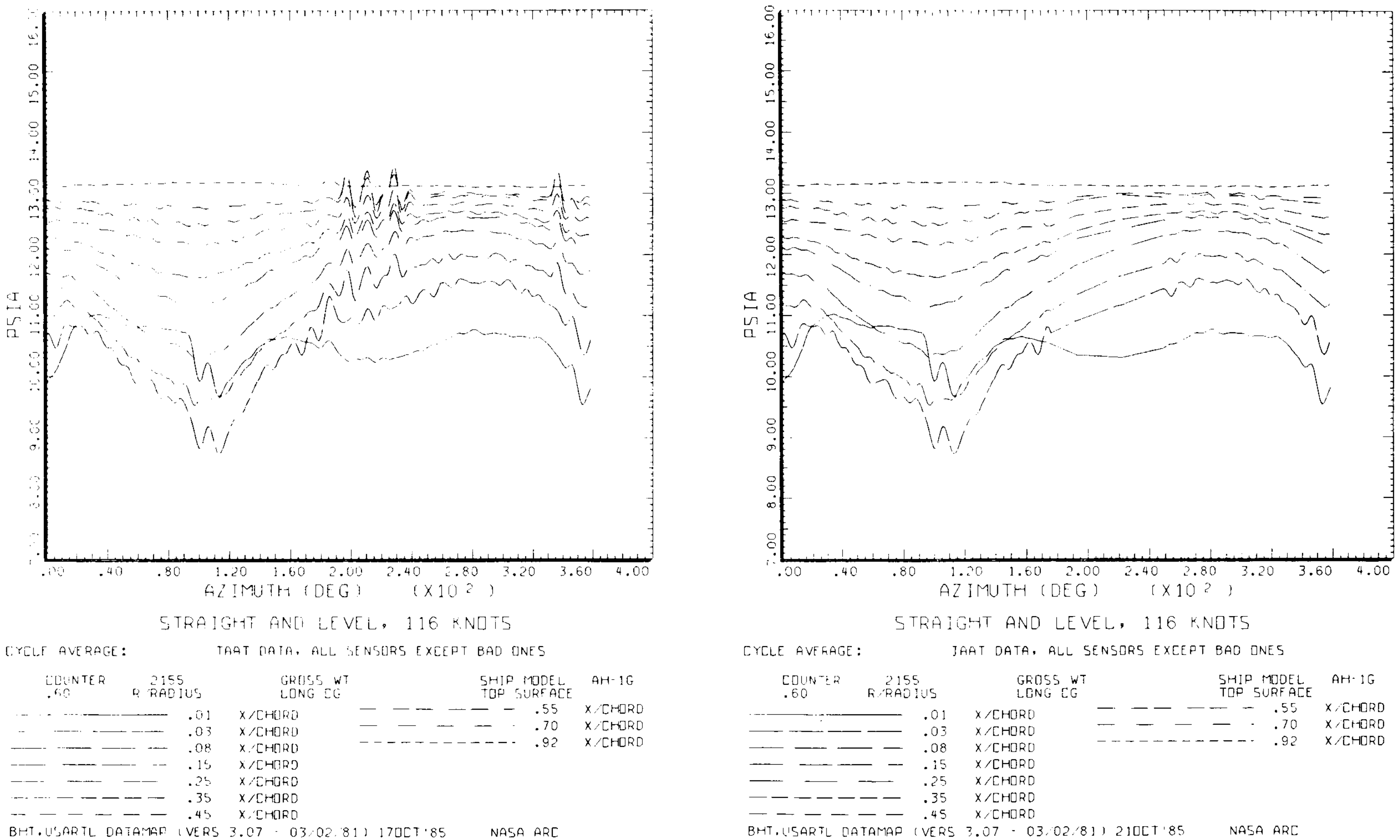

Figure 30.- Pressure versus azimuth, with and without spikes.

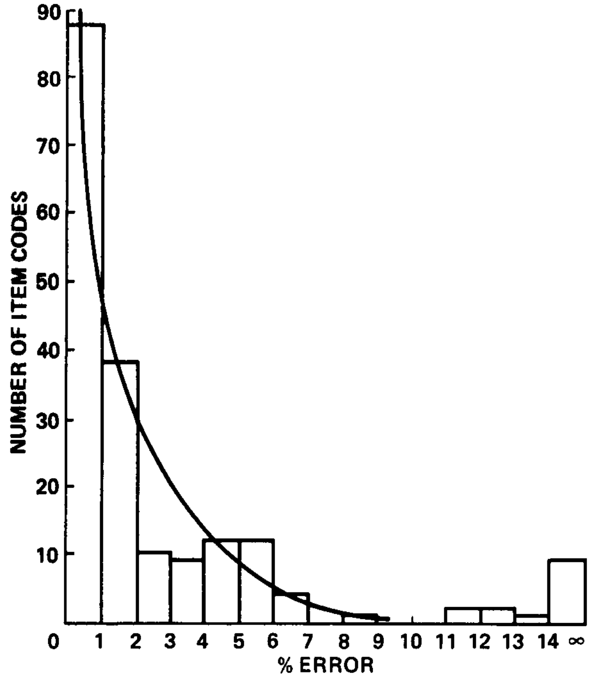

Figure 31.- Summary of slope changes.

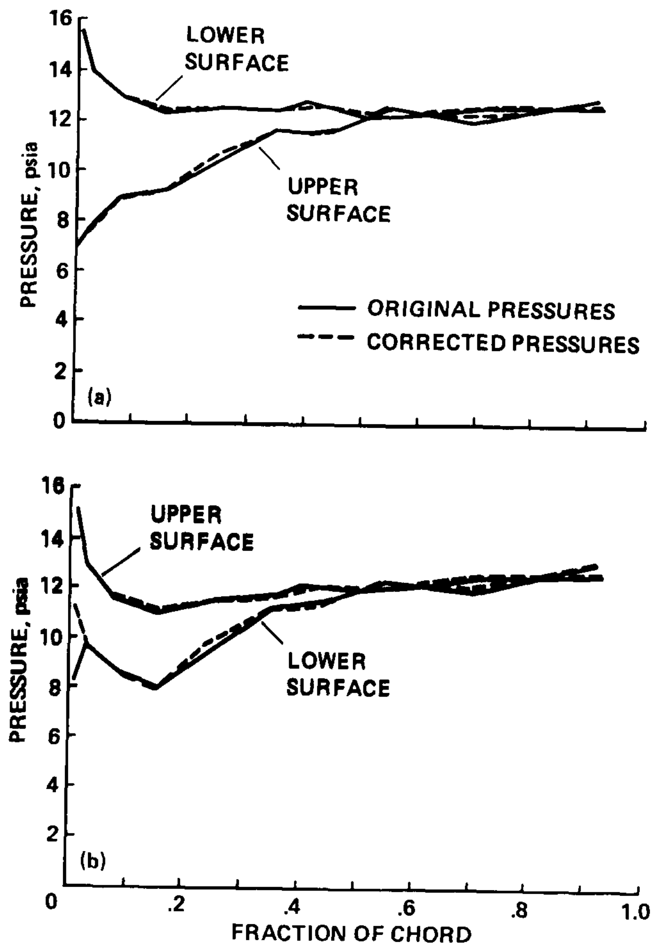

Figure 32.- Example of slope adjustment. (a) 0° azimuth; (b) 90° azimuth.

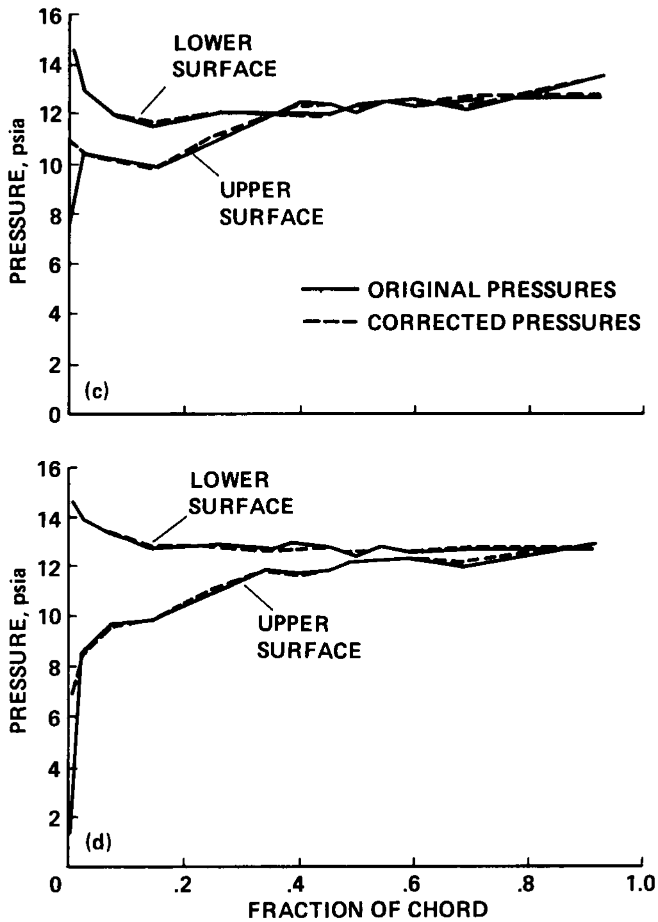

Figure 32.- Concluded. (c) 180° azimuth; (d) 270° azimuth.

ORIGINAL PAGE IS
OF POOR QUALITY

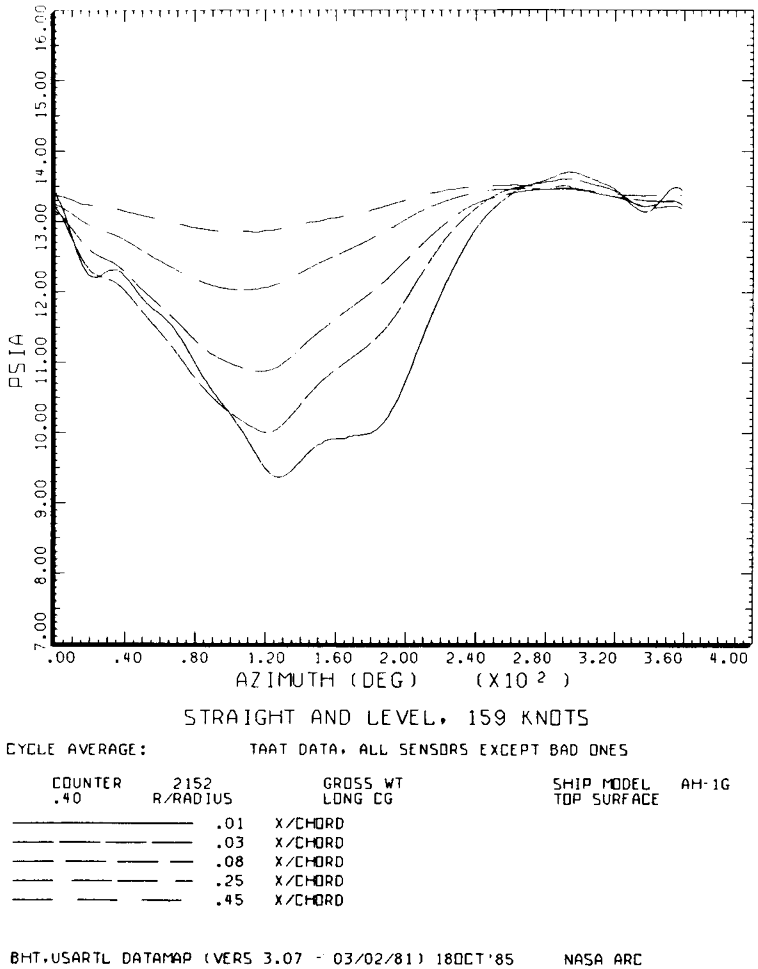

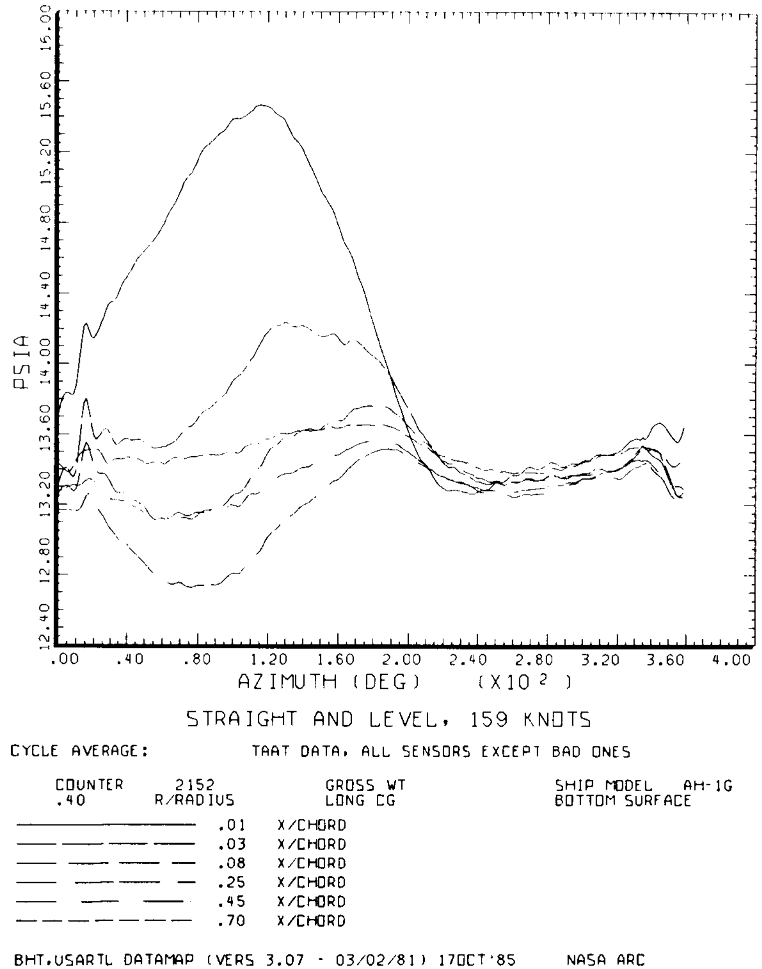

(a) At 40% radius pressure data.

Figure 33.- Blade pressure versus azimuth at 159 KTAS.

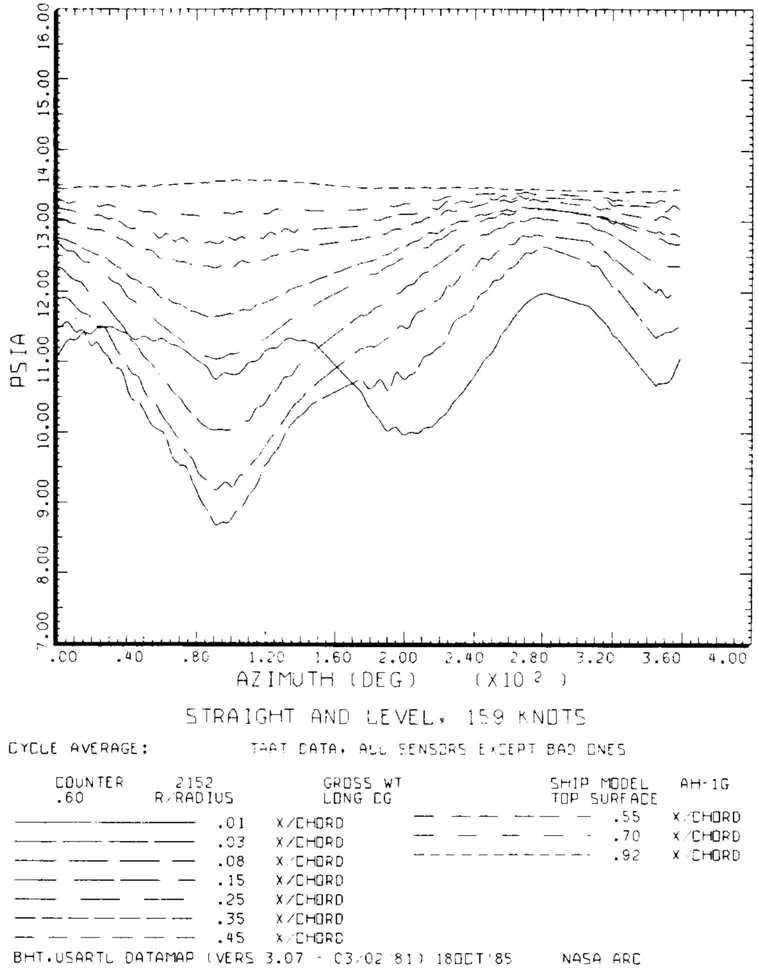

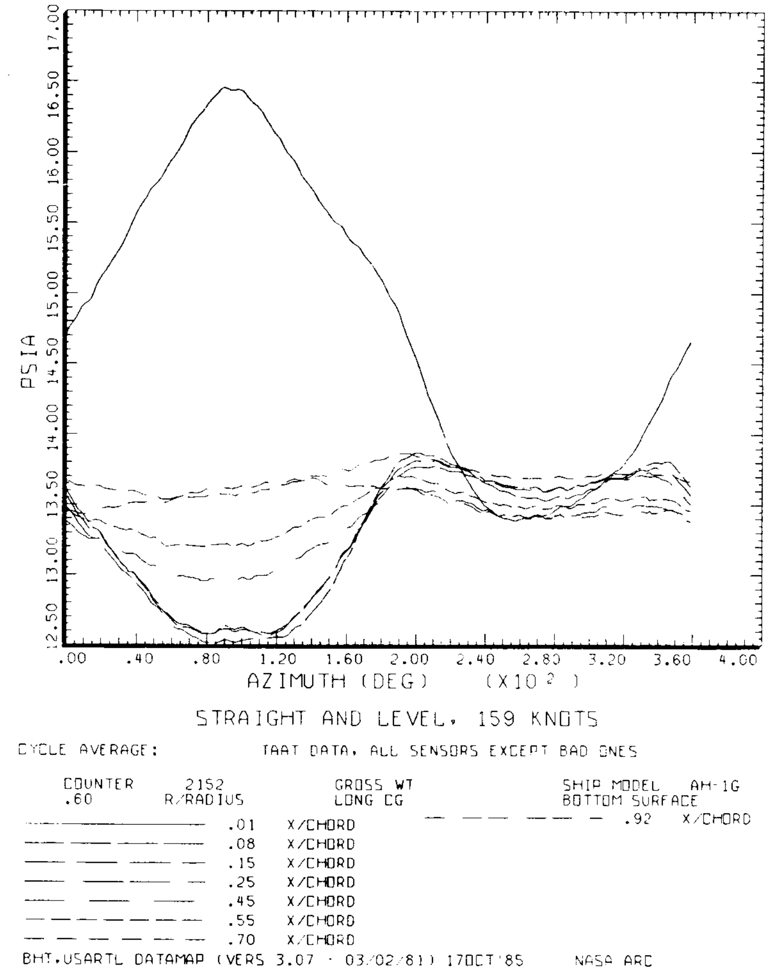

(b) At 60% radius pressure data.

Figure 33.- Continued.

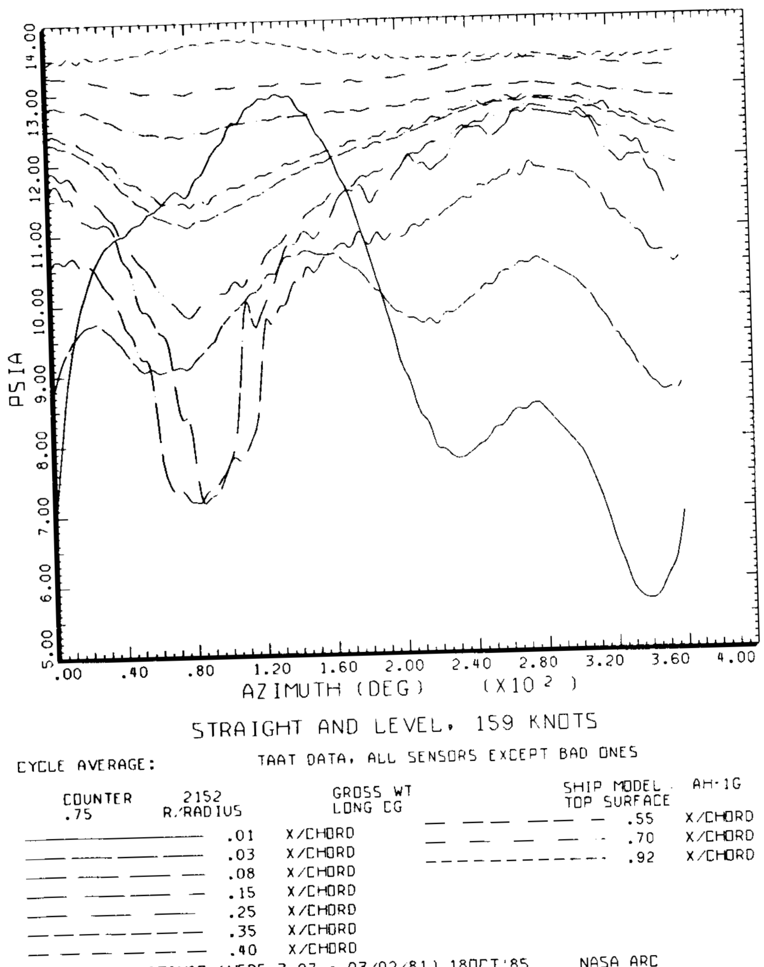

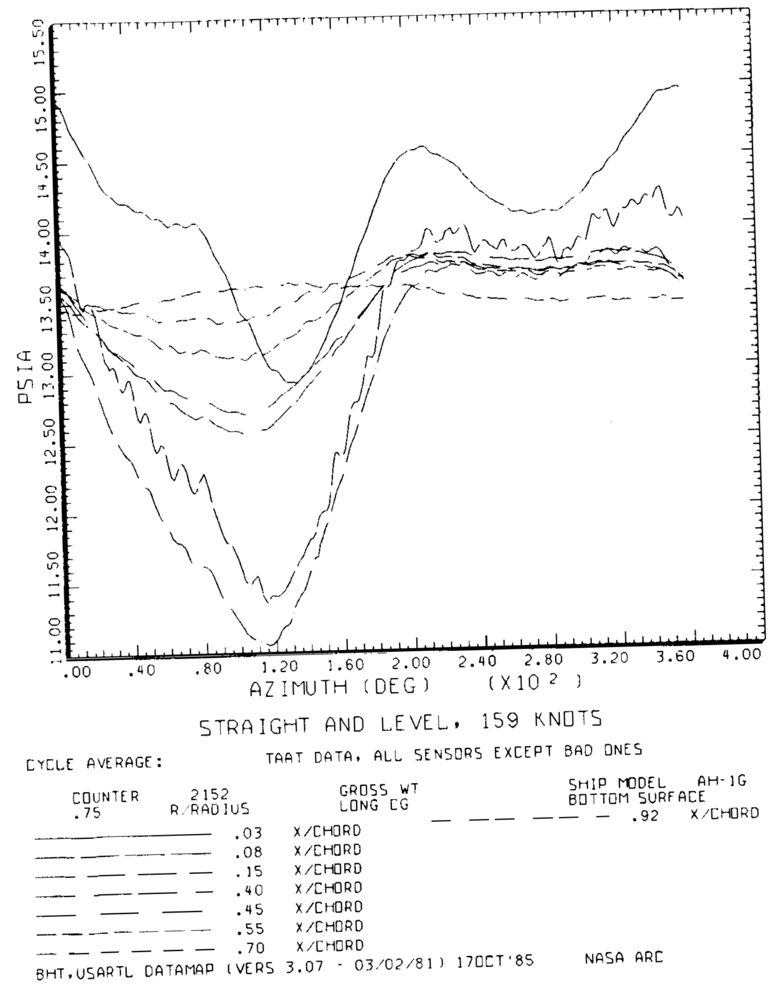

(c) At 75% radius pressure data.

Figure 33.- Continued.

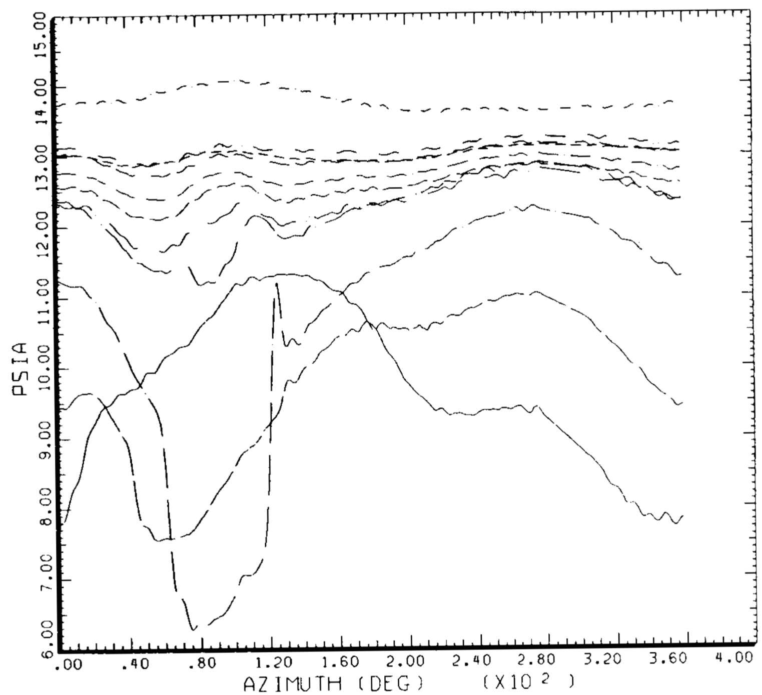

STRAIGHT AND LEVEL, 159 KNOTS

CYCLE AVERAGE: TAAT DATA, ALL SENSORS EXCEPT BAD ONES

COUNTER .86 2152 R/RADIUS GROSS WT LONG CG SHIP MODEL AH-1G TOP SURFACE

.03 X/CHORD
.08 X/CHORD
.25 X/CHORD
.35 X/CHORD
.40 X/CHORD
.45 X/CHORD
.50 X/CHORD
.55 X/CHORD
.60 X/CHORD
.70 X/CHORD
.92 X/CHORD

BHT.USARTL DATAMAP (VERS 3.07 - 03/02/81) 18OCT'85 NASA ARC

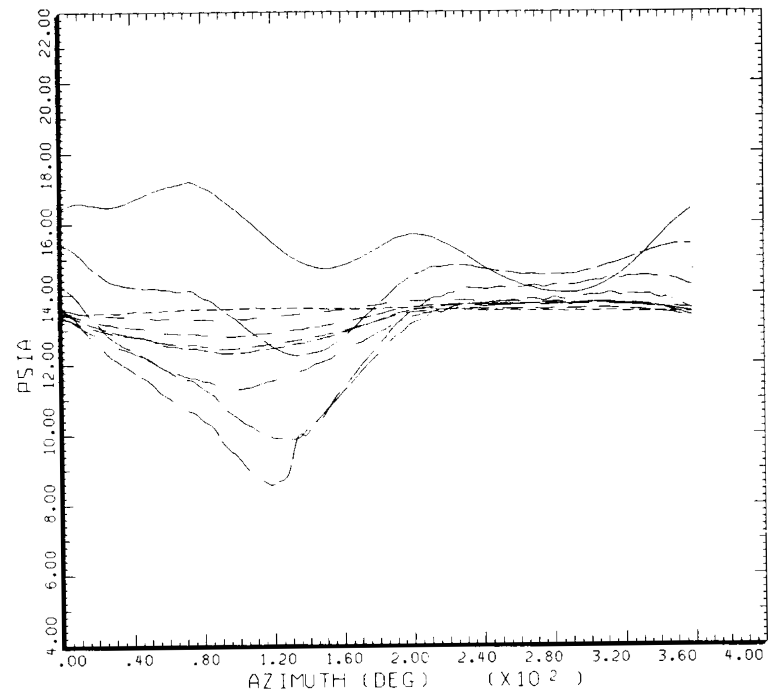

STRAIGHT AND LEVEL, 159 KNOTS

CYCLE AVERAGE: TAAT DATA, ALL SENSORS EXCEPT BAD ONES

COUNTER .86 2152 R/RADIUS GROSS WT LONG CG SHIP MODEL AH-1G BOTTOM SURFACE

.01 X/CHORD
.03 X/CHORD
.08 X/CHORD
.15 X/CHORD
.35 X/CHORD
.45 X/CHORD
.50 X/CHORD
.55 X/CHORD
.70 X/CHORD
.92 X/CHORD

BHT.USARTL DATAMAP (VERS 3.07 - 03/02/81) 17OCT'85 NASA ARC

(d) At 86% radius pressure data.

Figure 33.- Continued.

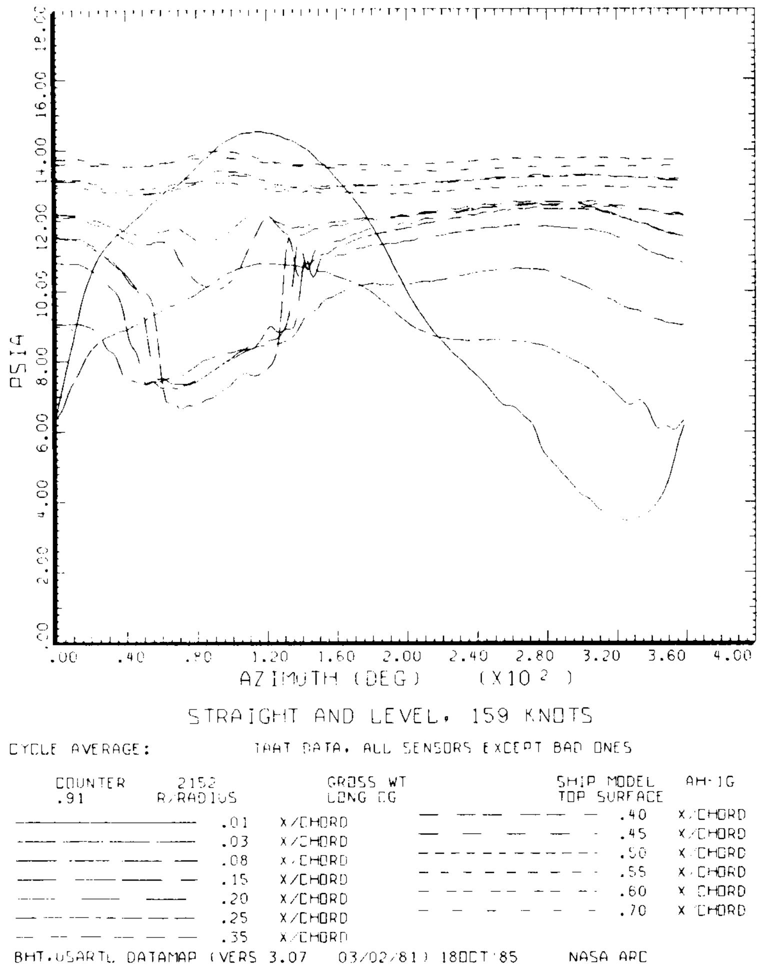

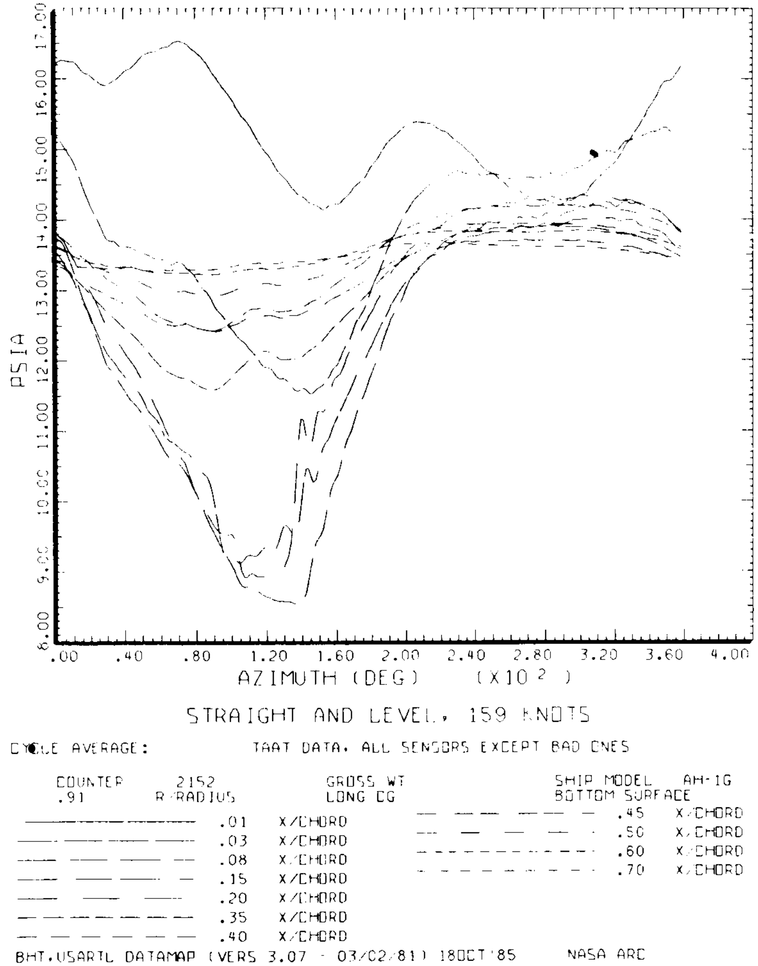

(e) At 91% radius pressure data.

Figure 33.- Continued.

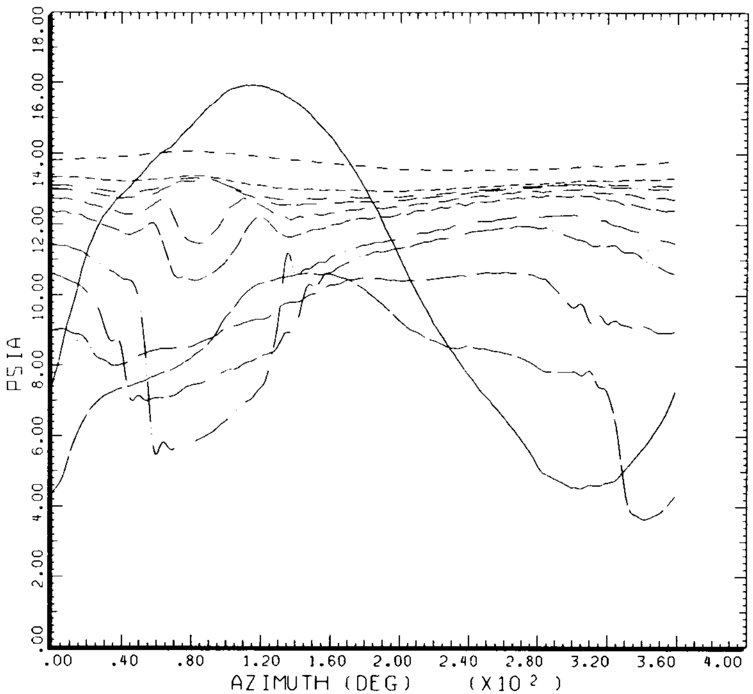

STRAIGHT AND LEVEL, 159 KNOTS

CYCLE AVERAGE: TAAT DATA, ALL SENSORS EXCEPT BAD ONES

COUNTER .96 — 2152 R/RADIUS — GROSS WT LONG CG — SHIP MODEL AH-1G TOP SURFACE

.01 X/CHORD
.03 X/CHORD
.08 X/CHORD
.15 X/CHORD
.25 X/CHORD
.35 X/CHORD
.40 X/CHORD
.50 X/CHORD
.55 X/CHORD
.70 X/CHORD
.92 X/CHORD

BHT.USARTL DATAMAP (VERS 3.07 - 03/02/81) 18OCT'85 NASA ARC

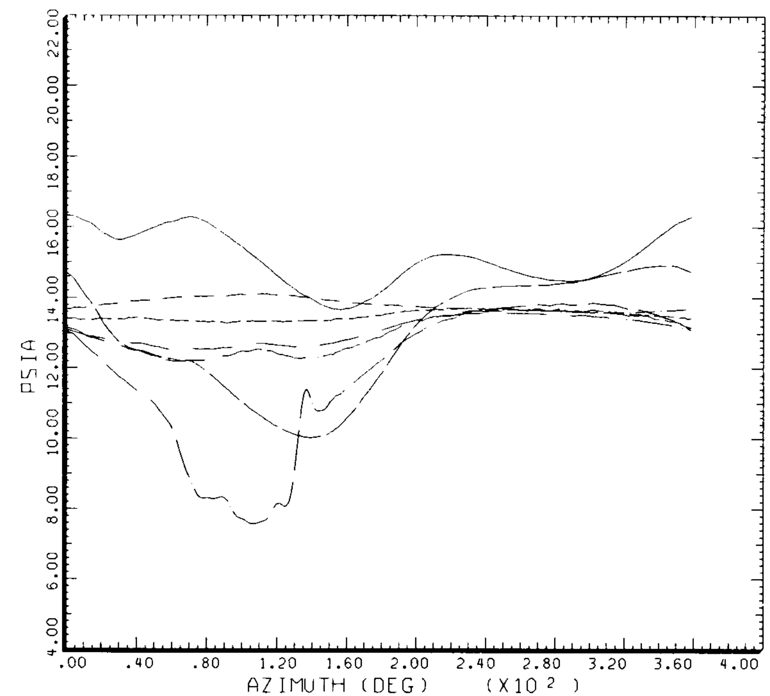

STRAIGHT AND LEVEL, 159 KNOTS

CYCLE AVERAGE: TAAT DATA, ALL SENSORS EXCEPT BAD ONES

COUNTER .96 — 2152 R/RADIUS — GROSS WT LONG CG — SHIP MODEL AH-1G BOTTOM SURFACE

.01 X/CHORD
.03 X/CHORD
.25 X/CHORD
.40 X/CHORD
.50 X/CHORD
.70 X/CHORD
.92 X/CHORD

BHT.USARTL DATAMAP (VERS 3.07 - 03/02/81) 17OCT'85 NASA ARC

(f) At 96% radius pressure data.

Figure 33.- Continued.

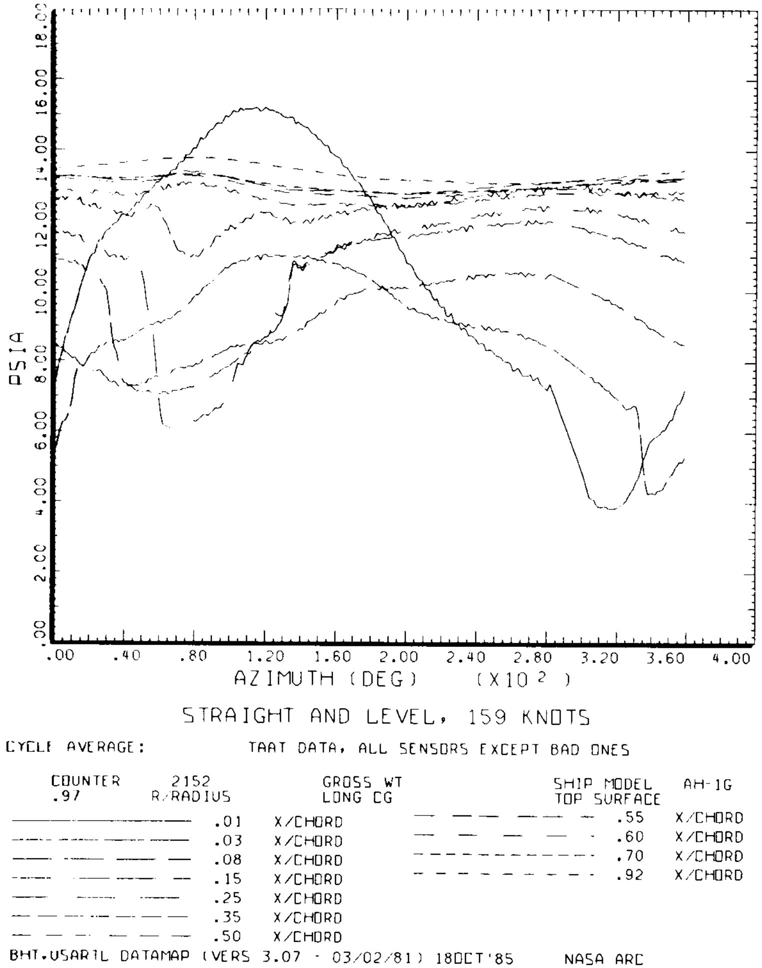

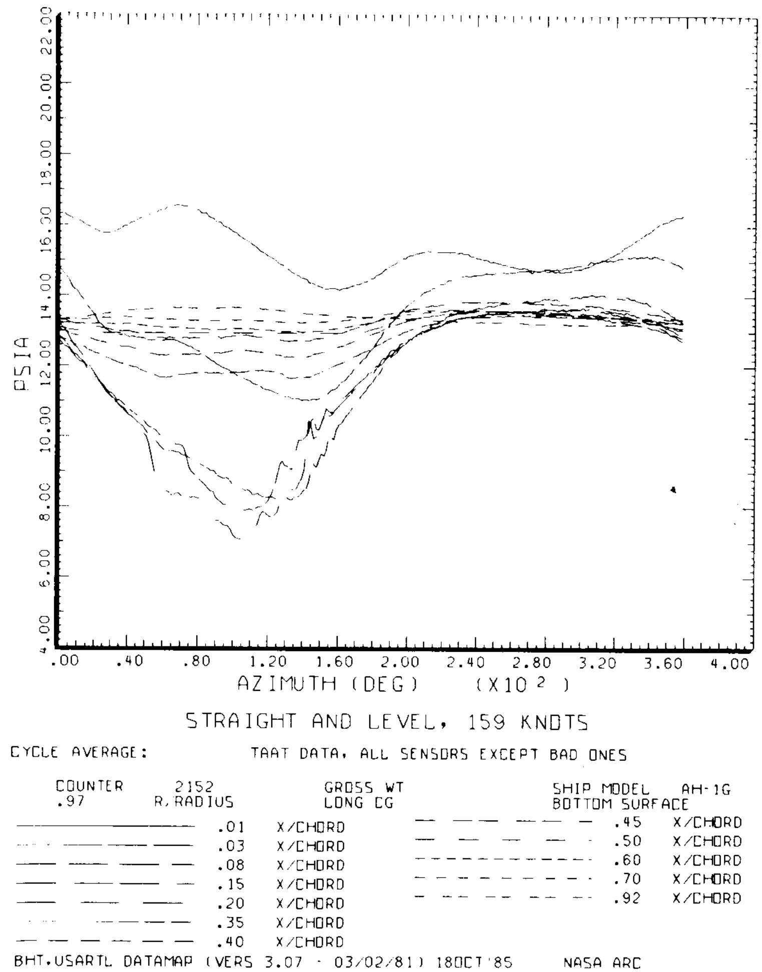

(g) At 97% radius pressure data.

Figure 33.- Continued.

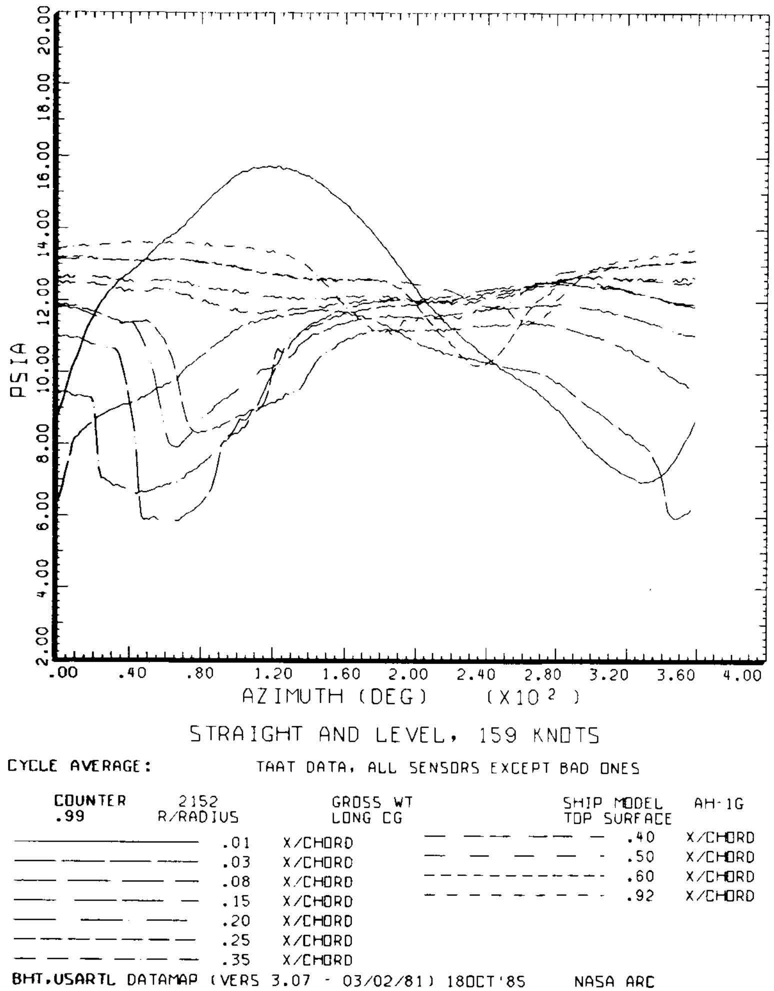

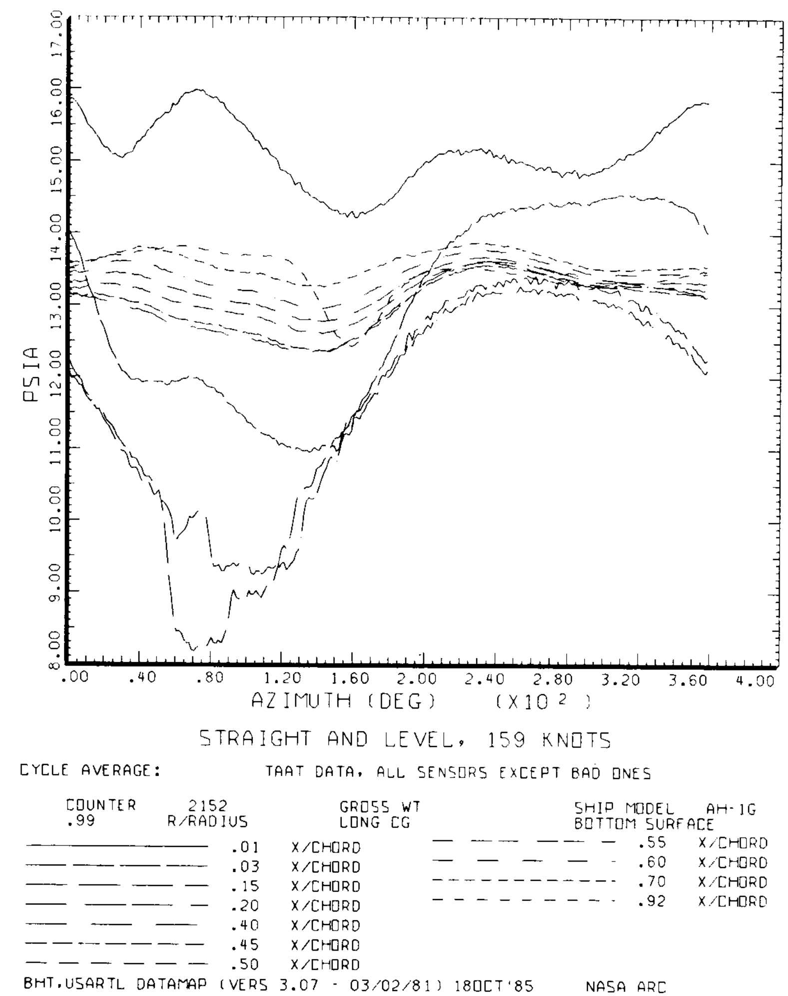

(h) At 99% radius pressure data.

Figure 33.- Concluded.

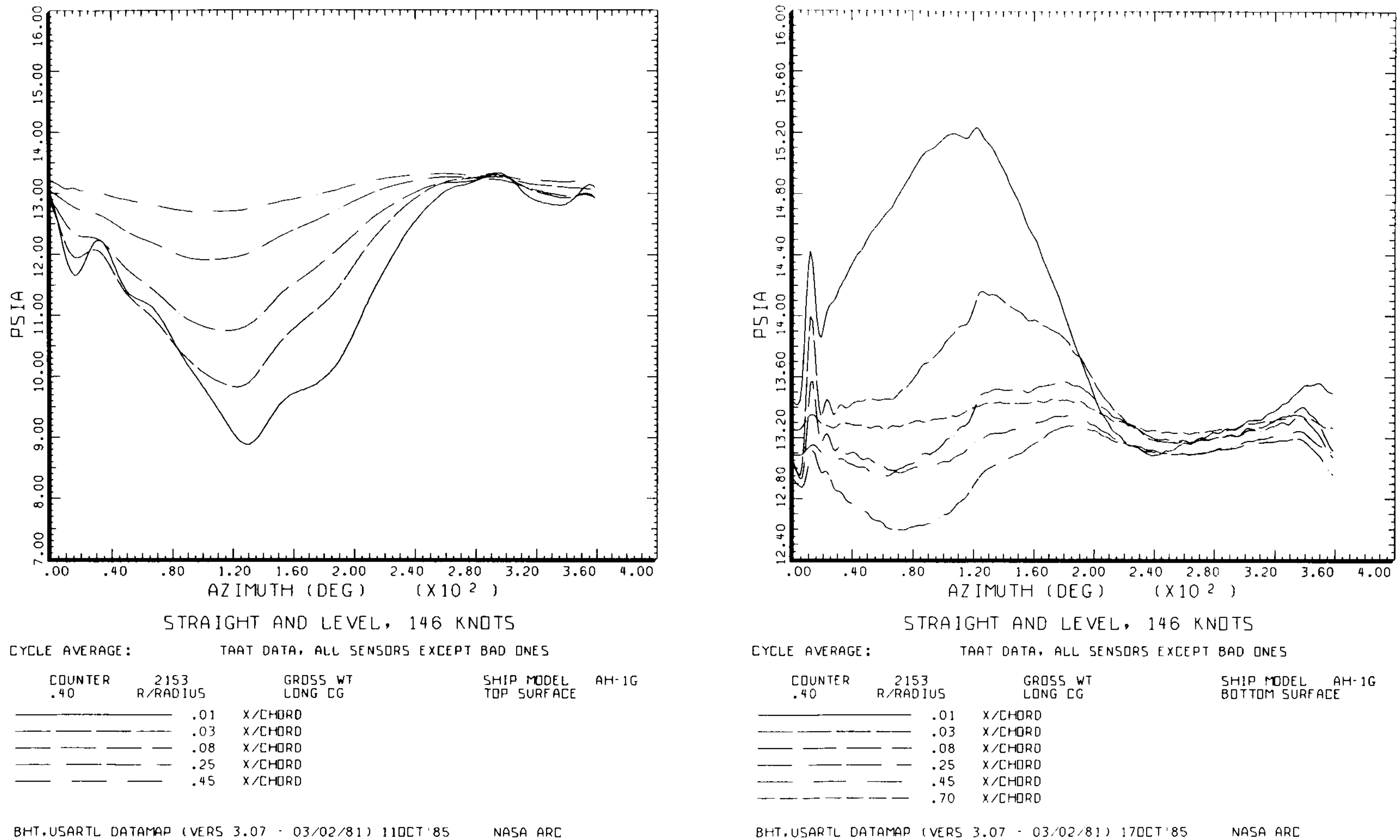

(a) At 40% radius pressure data.

Figure 34.- Blade pressure versus azimuth at 146 KTAS.

ORIGINAL PAGE IS
OF POOR QUALITY

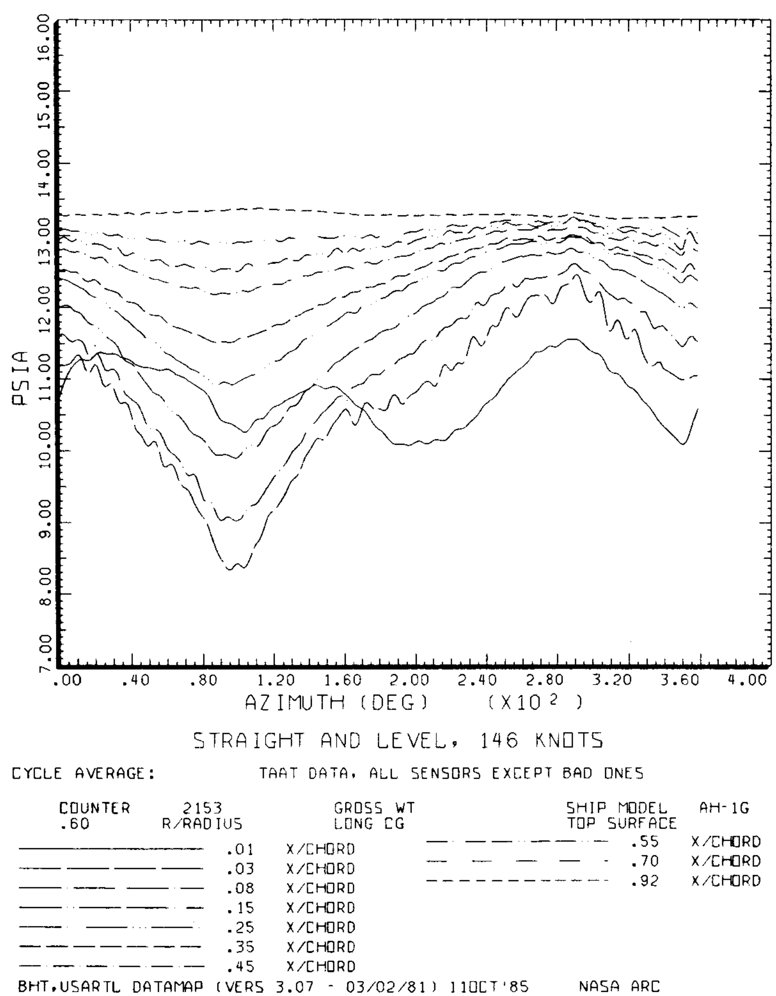

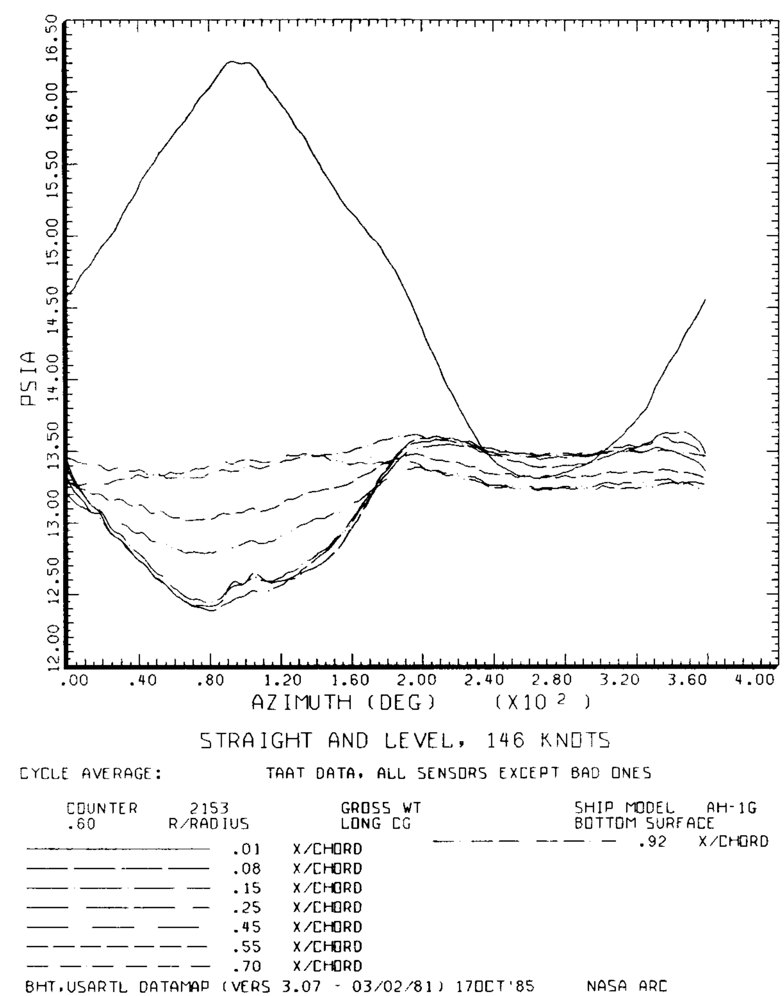

(b) At 60% radius pressure data.

Figure 34.- Continued.

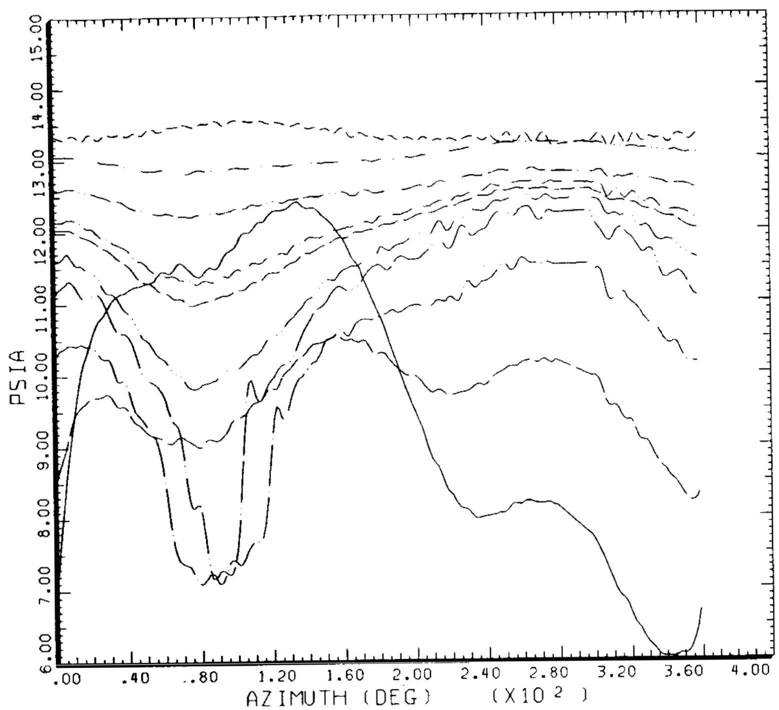

STRAIGHT AND LEVEL, 146 KNOTS

CYCLE AVERAGE: TAAT DATA, ALL SENSORS EXCEPT BAD ONES

COUNTER .75 2153 R/RADIUS GROSS WT LONG CG SHIP MODEL TOP SURFACE AH-1G

.01 X/CHORD
.03 X/CHORD
.08 X/CHORD
.15 X/CHORD
.25 X/CHORD
.35 X/CHORD
.40 X/CHORD
.55 X/CHORD
.70 X/CHORD
.92 X/CHORD

BHT,USARTL DATAMAP (VERS 3.07 - 03/02/81) 11OCT'85 NASA ARC

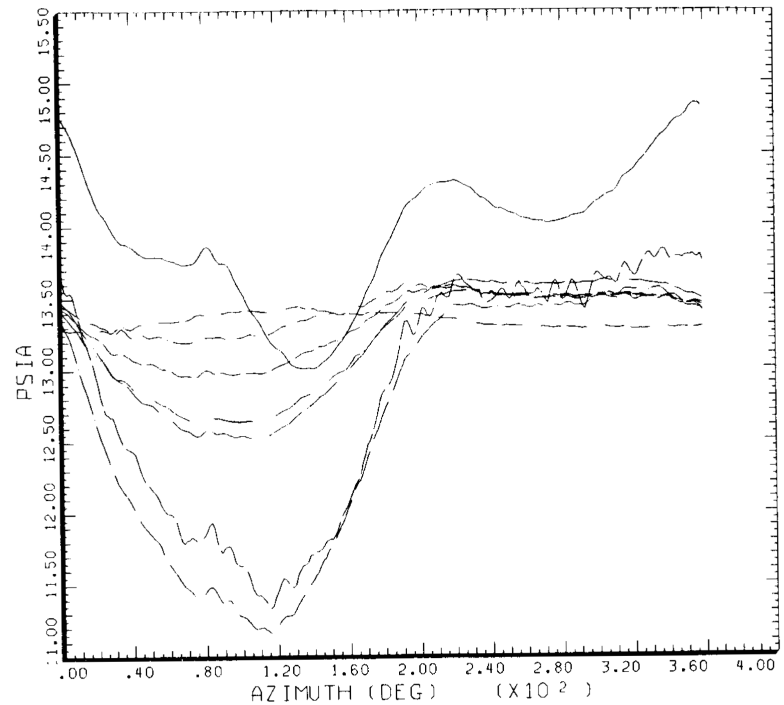

STRAIGHT AND LEVEL, 146 KNOTS

CYCLE AVERAGE: TAAT DATA, ALL SENSORS EXCEPT BAD ONES

COUNTER .75 2153 R/RADIUS GROSS WT LONG CG SHIP MODEL BOTTOM SURFACE AH-1G

.03 X/CHORD
.08 X/CHORD
.15 X/CHORD
.40 X/CHORD
.45 X/CHORD
.55 X/CHORD
.70 X/CHORD
.92 X/CHORD

BHT,USARTL DATAMAP (VERS 3.07 - 03/02/81) 17OCT'85 NASA ARC

(c) At 75% radius pressure data.

Figure 34.- Continued.

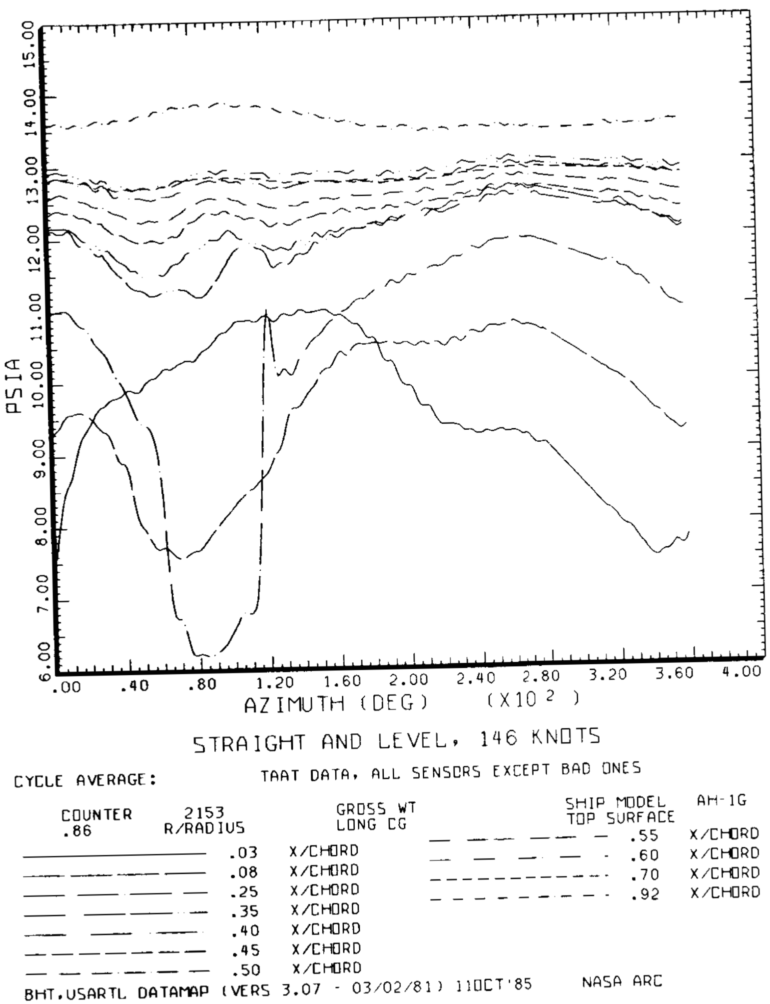

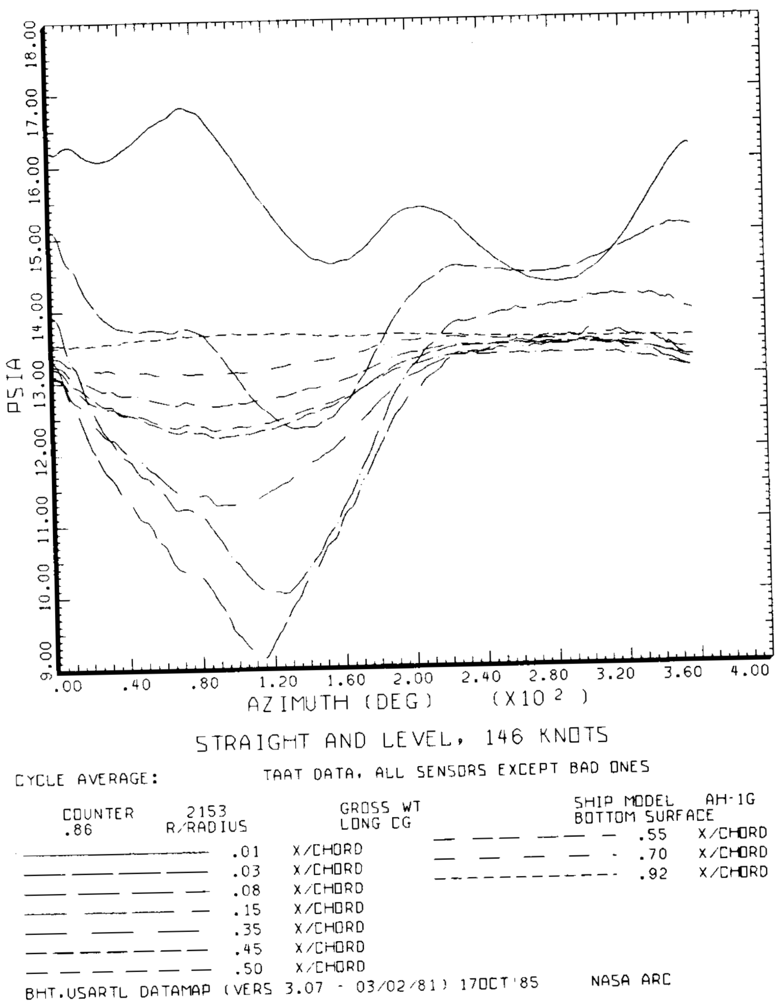

(d) At 86% radius pressure data.

Figure 34.- Continued.

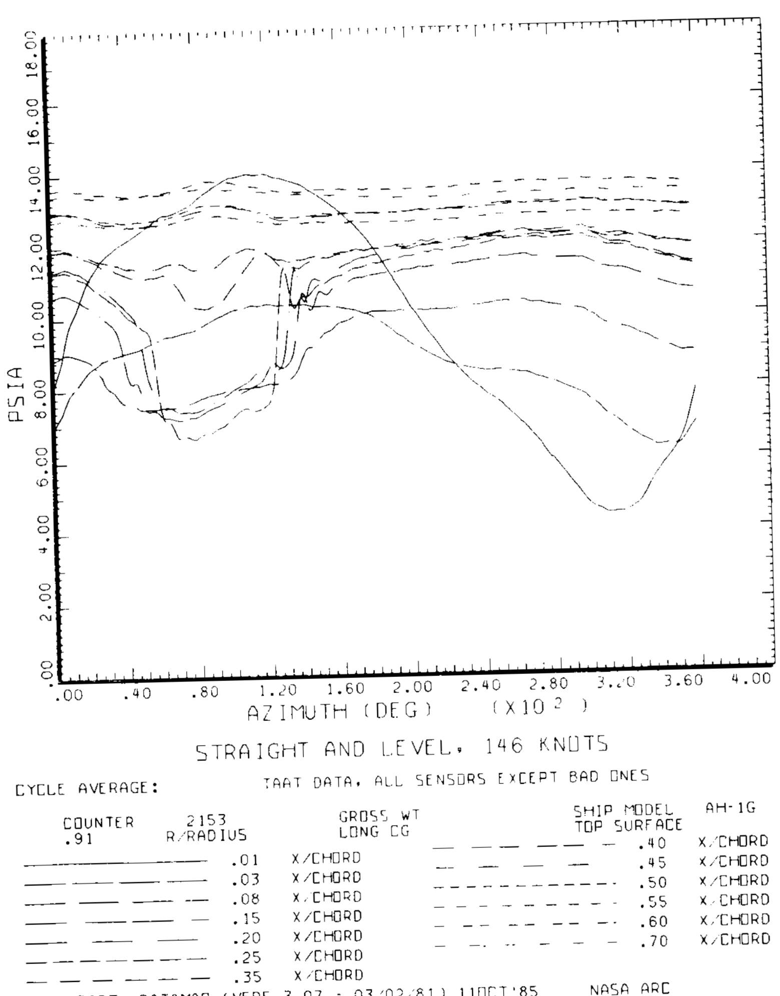

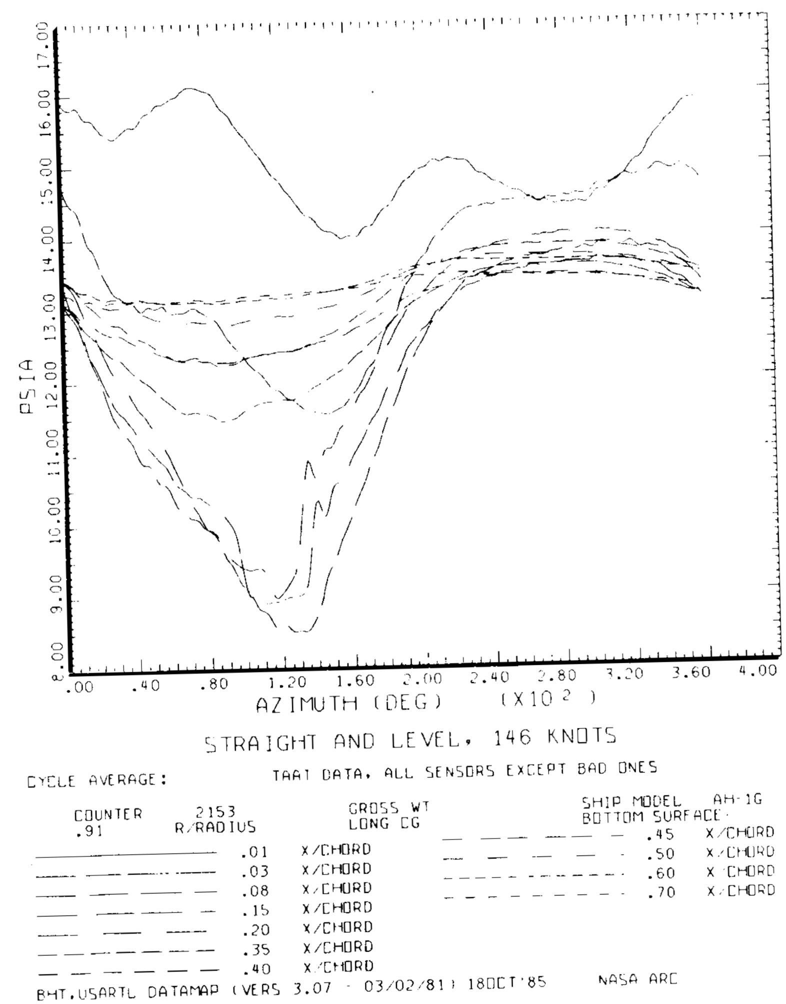

(e) At 91% radius pressure data.

Figure 34.- Continued.

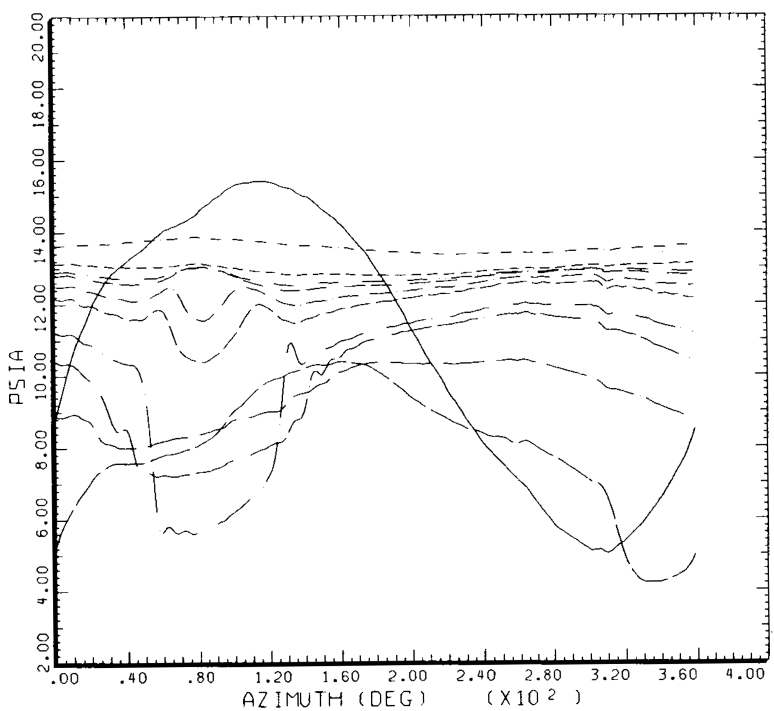

STRAIGHT AND LEVEL, 146 KNOTS

CYCLE AVERAGE: TAAT DATA, ALL SENSORS EXCEPT BAD ONES

COUNTER .96 2153 R/RADIUS GROSS WT LONG CG SHIP MODEL AH-1G TOP SURFACE

.01 X/CHORD
.03 X/CHORD
.08 X/CHORD
.15 X/CHORD
.25 X/CHORD
.35 X/CHORD
.40 X/CHORD
.50 X/CHORD
.55 X/CHORD
.70 X/CHORD
.92 X/CHORD

BHT.USARTL DATAMAP (VERS 3.07 - 03/02/81) 11OCT'85 NASA ARC

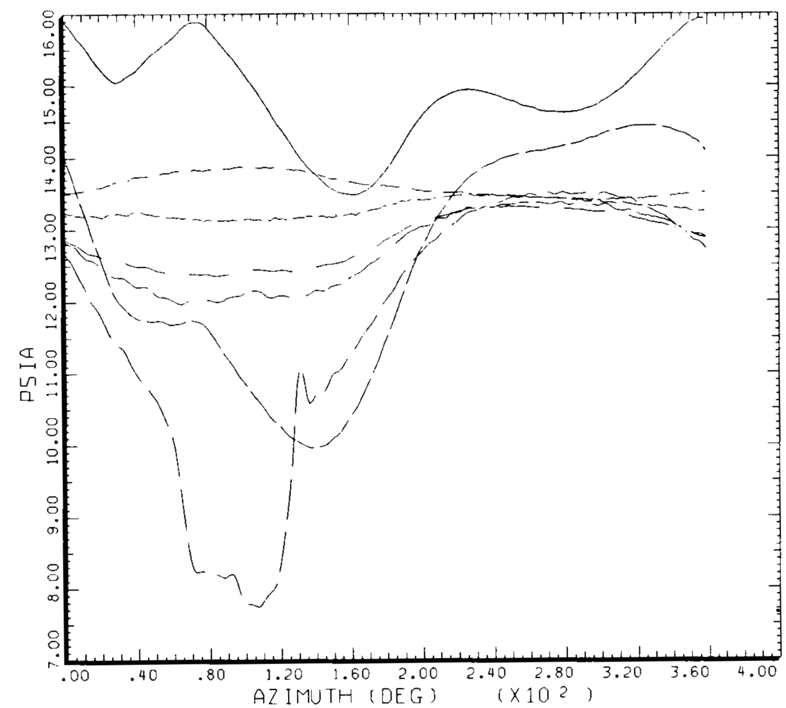

STRAIGHT AND LEVEL, 146 KNOTS

CYCLE AVERAGE: TAAT DATA, ALL SENSORS EXCEPT BAD ONES

COUNTER .96 2153 R/RADIUS GROSS WT LONG CG SHIP MODEL AH-1G BOTTOM SURFACE

.01 X/CHORD
.03 X/CHORD
.25 X/CHORD
.40 X/CHORD
.50 X/CHORD
.70 X/CHORD
.92 X/CHORD

BHT.USARTL DATAMAP (VERS 3.07 - 03/02/81) 17OCT'85 NASA ARC

(f) At 96% radius pressure data.

Figure 34.- Continued.

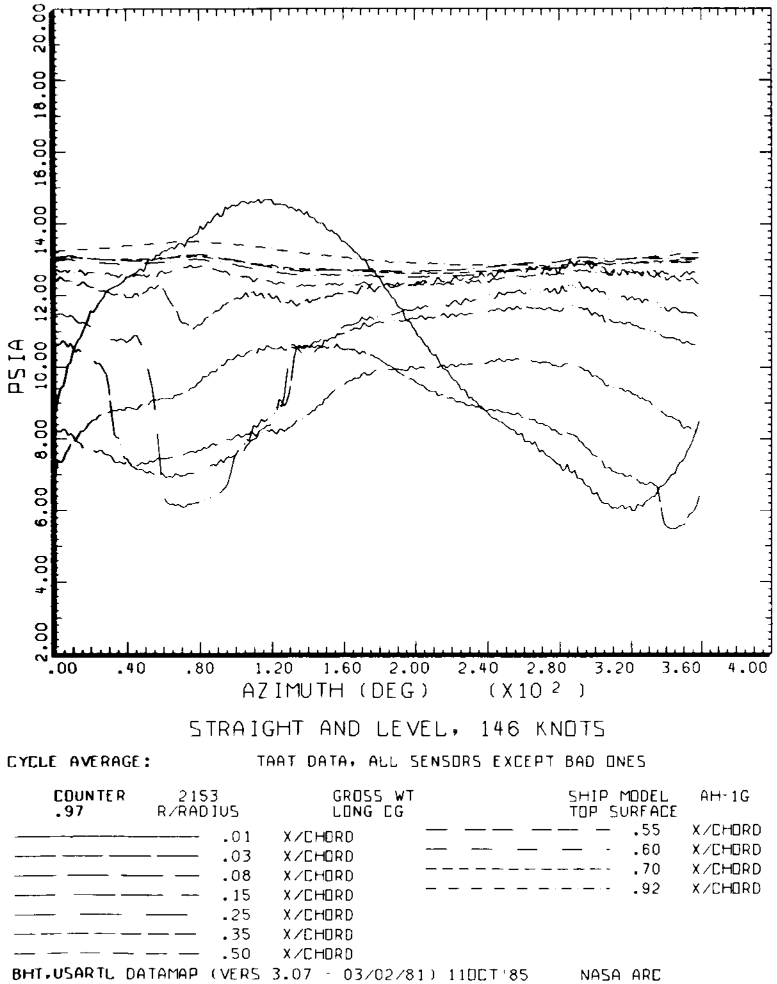

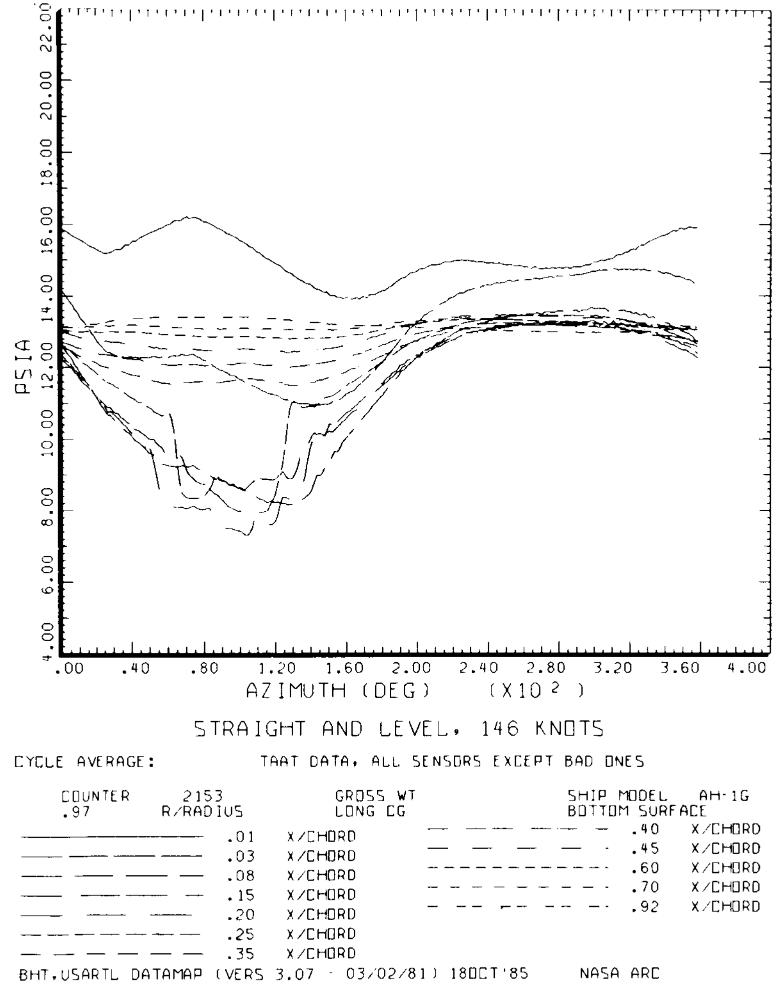

(g) At 97% radius pressure data.

Figure 34.- Continued.

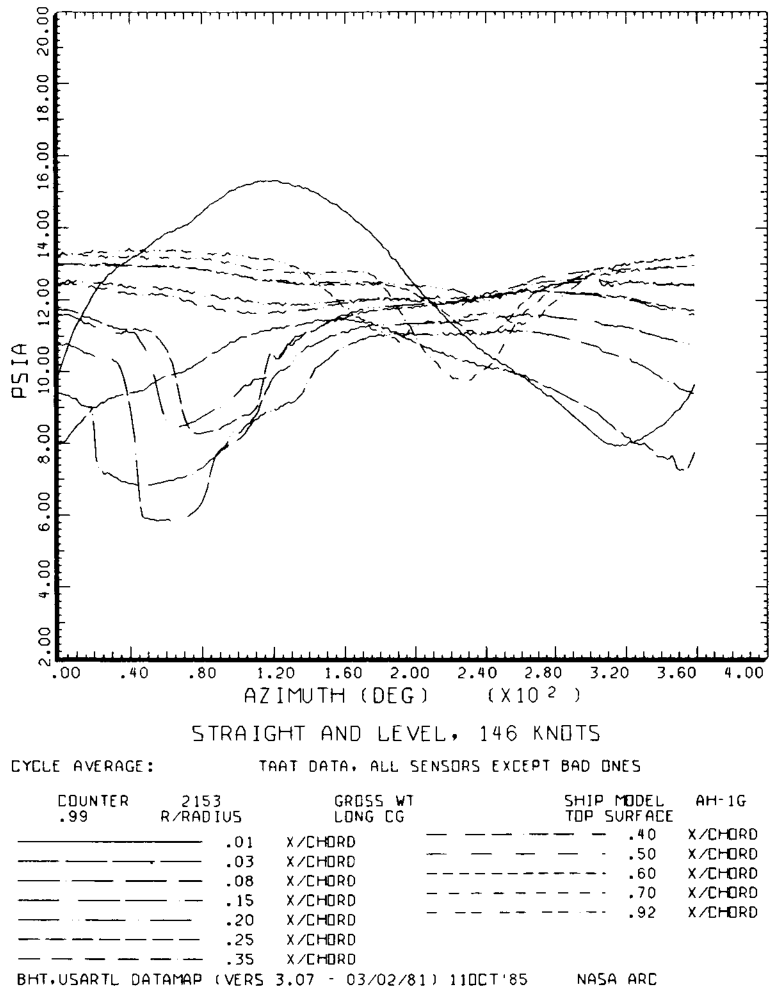

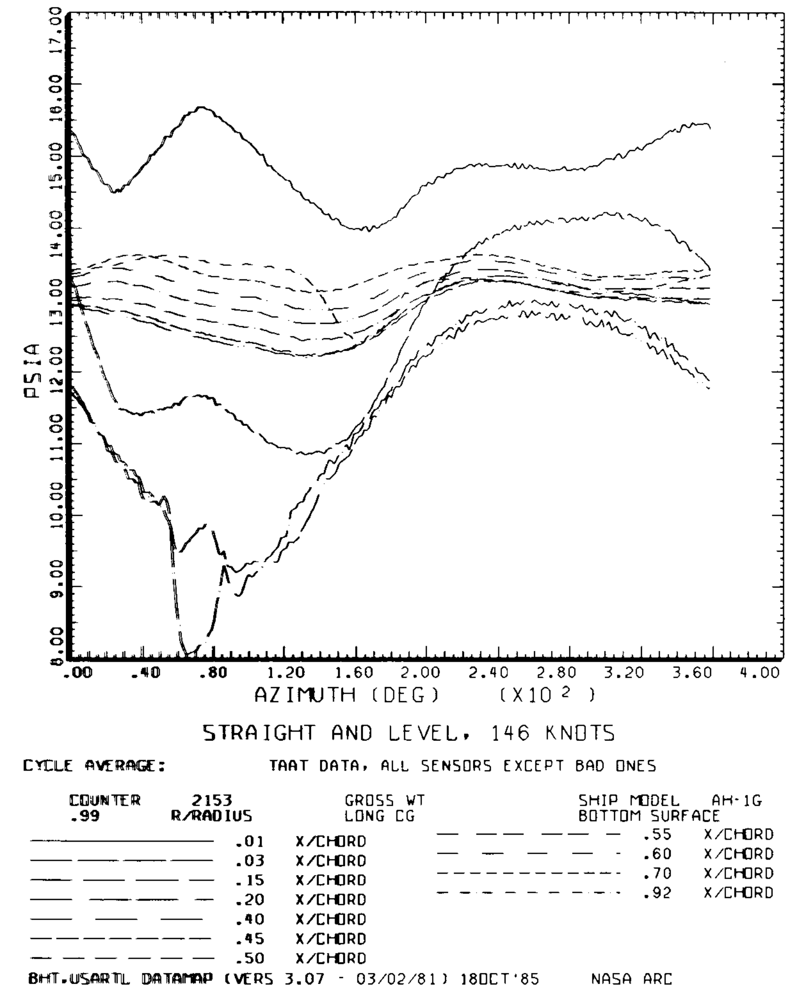

(h) At 99% radius pressure data.

Figure 34.- Concluded.

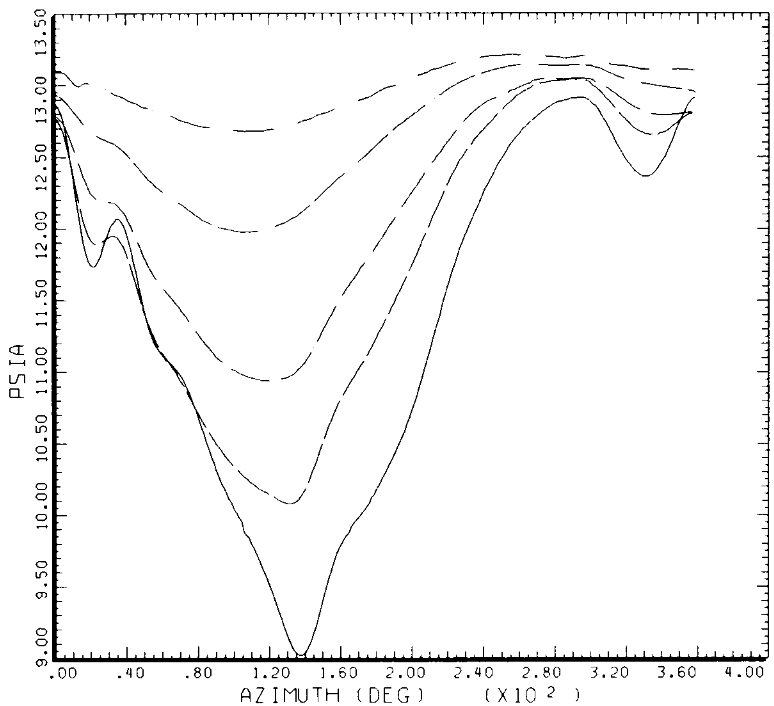

STRAIGHT AND LEVEL, 129 KNOTS

CYCLE AVERAGE: TAAT DATA, ALL SENSORS EXCEPT BAD ONES

COUNTER .40 2154 R/RADIUS GROSS WT LONG CG SHIP MODEL AH-1G TOP SURFACE

.01 X/CHORD
.03 X/CHORD
.08 X/CHORD
.25 X/CHORD
.45 X/CHORD

BHT.USARTL DATAMAP (VERS 3.07 - 03/02/81) 21OCT'85 NASA ARC

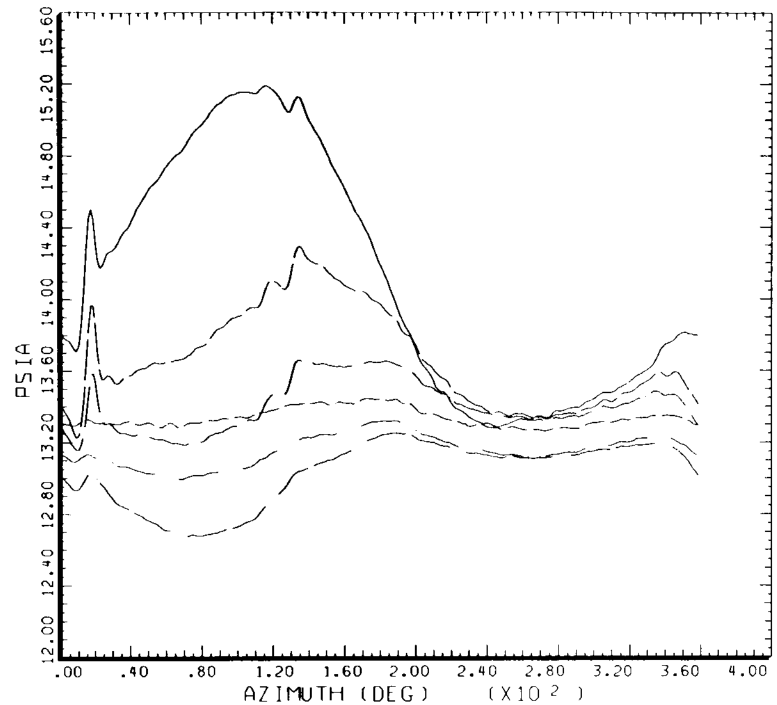

STRAIGHT AND LEVEL, 129 KNOTS

CYCLE AVERAGE: TAAT DATA, ALL SENSORS EXCEPT BAD ONES

COUNTER .40 2154 R/RADIUS GROSS WT LONG CG SHIP MODEL AH-1G BOTTOM SURFACE

.01 X/CHORD
.03 X/CHORD
.08 X/CHORD
.25 X/CHORD
.45 X/CHORD
.70 X/CHORD

BHT.USARTL DATAMAP (VERS 3.07 - 03/02/81) 17OCT'85 NASA ARC

(a) At 40% radius pressure data.

Figure 35.- Blade pressure versus azimuth at 129 KTAS.

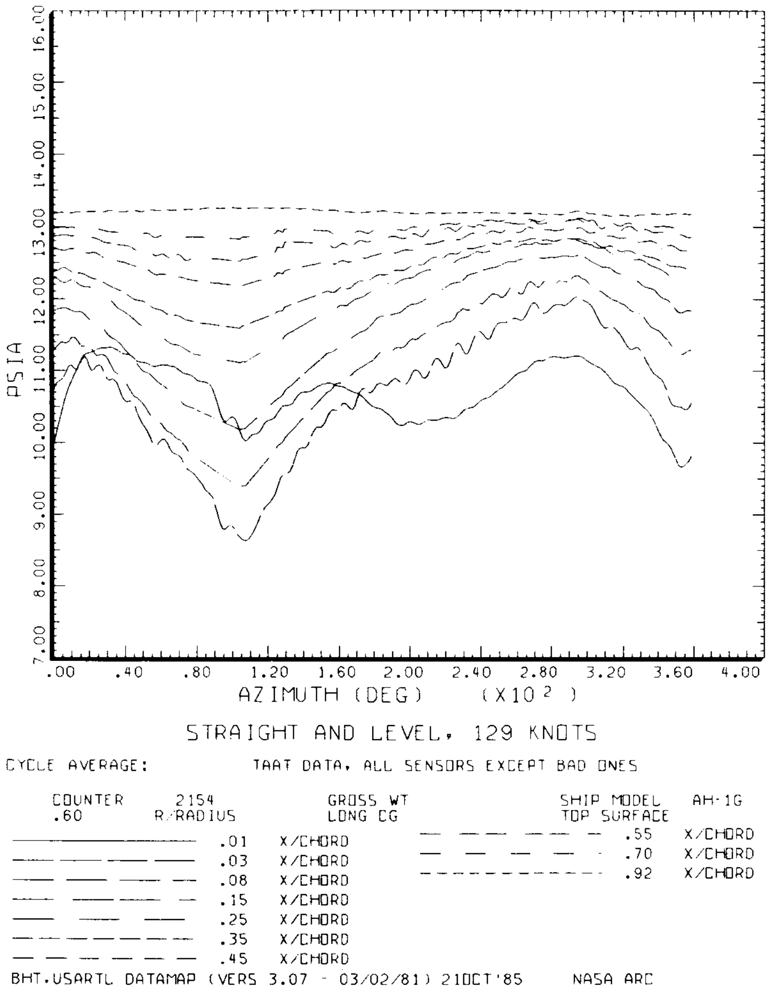

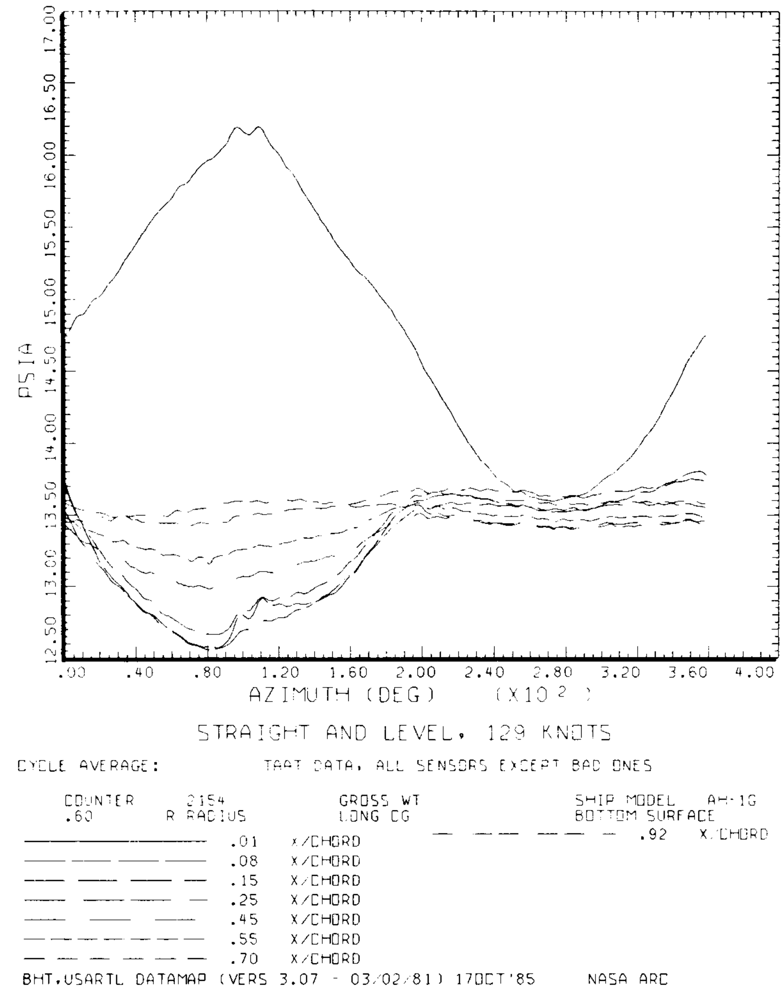

(b) At 60% radius pressure data.

Figure 35.- Continued.

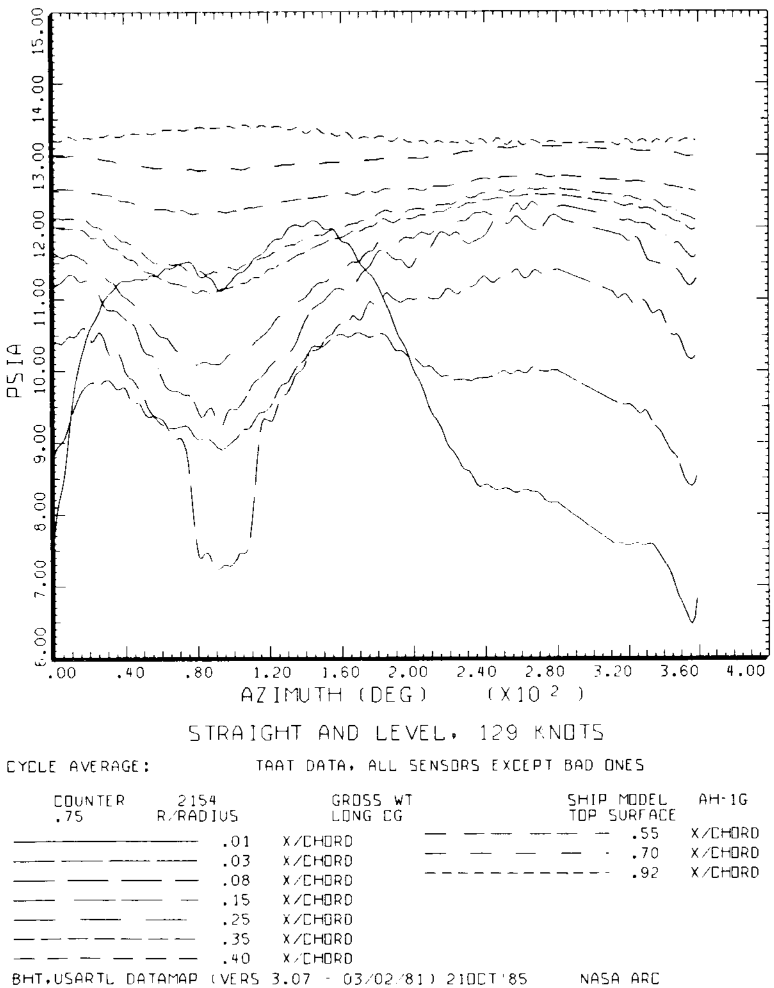

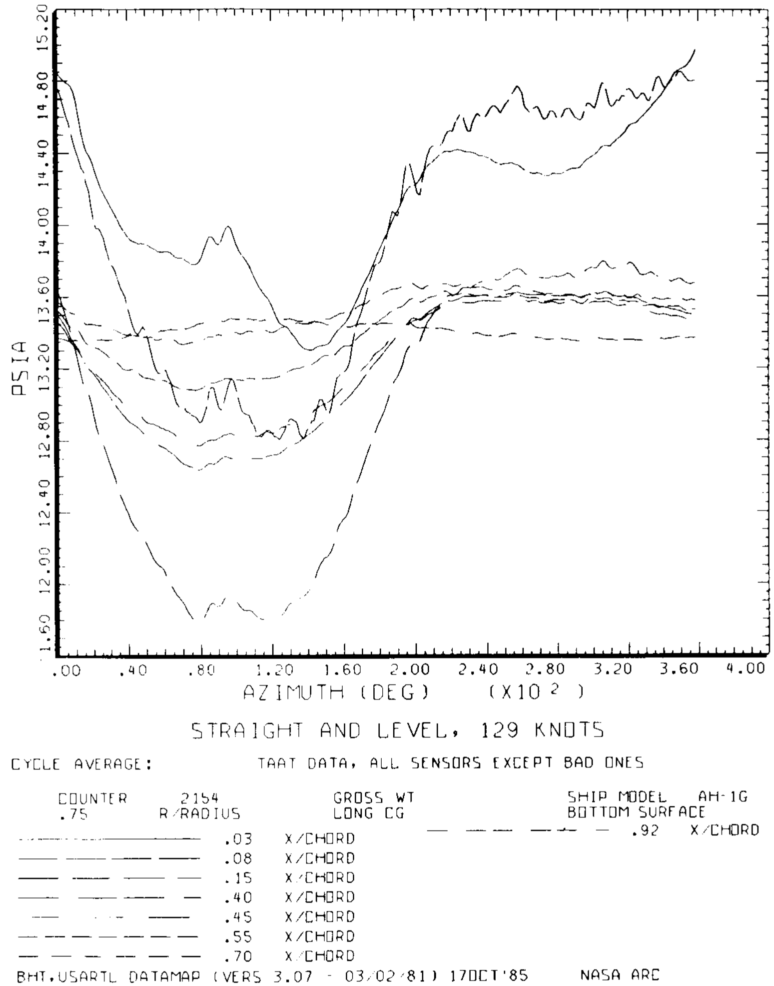

(c) At 75% radius pressure data.

Figure 35.- Continued.

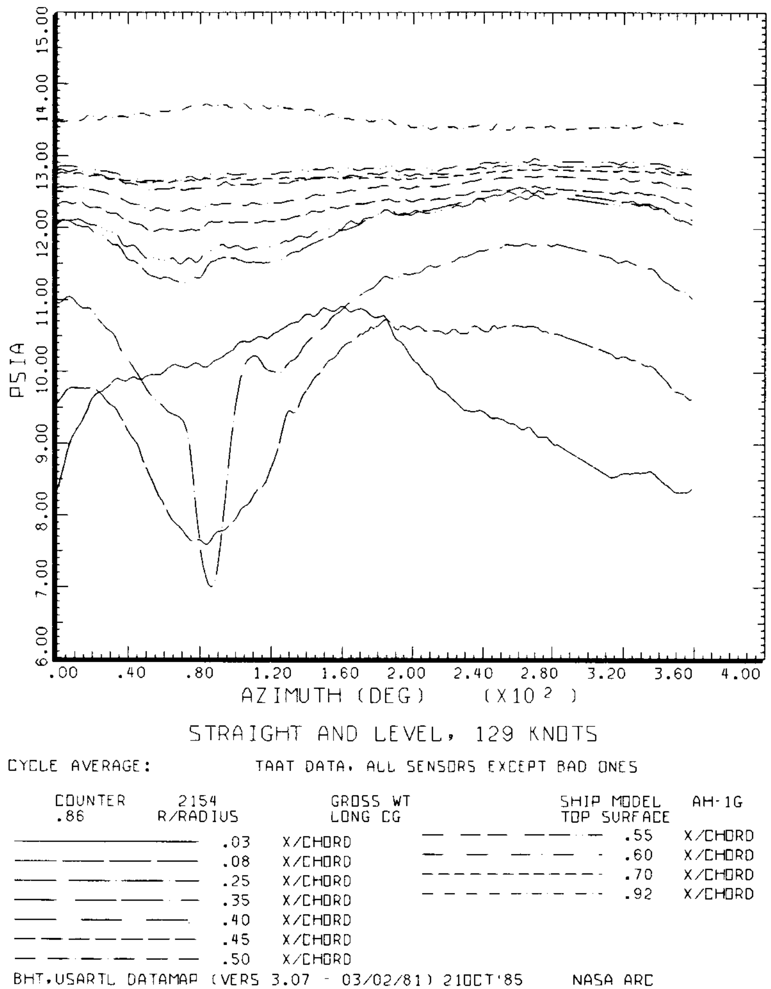

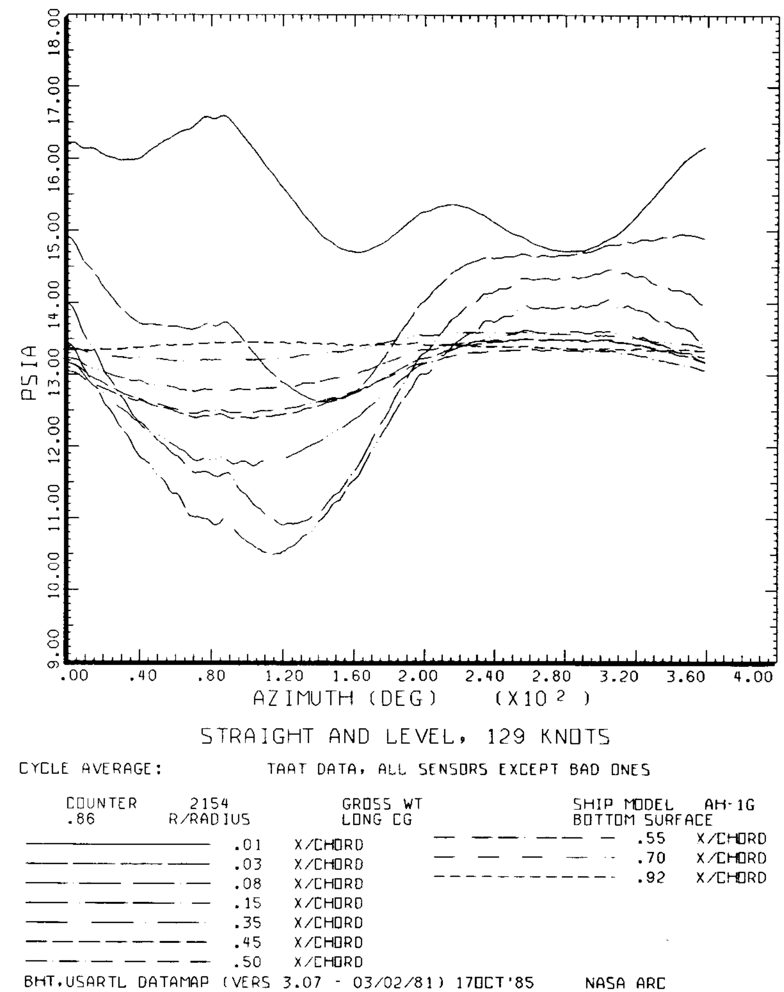

(d) At 86% radius pressure data.

Figure 35.- Continued.

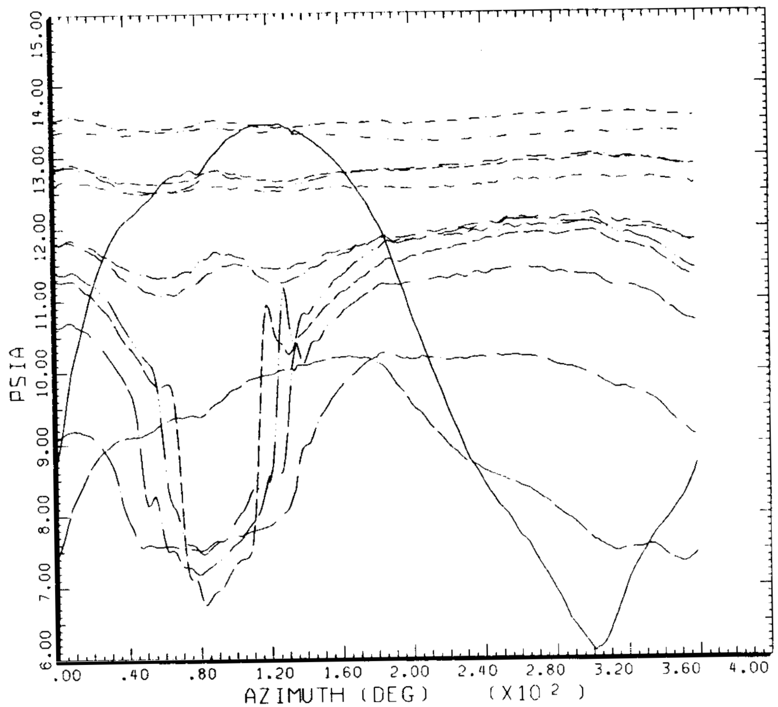

STRAIGHT AND LEVEL, 129 KNOTS

CYCLE AVERAGE: TAAT DATA, ALL SENSORS EXCEPT BAD ONES

COUNTER .91 | 2154 R/RADIUS | GROSS WT LONG CG | SHIP MODEL TOP SURFACE | AH-1G
.01 X/CHORD | .40 X/CHORD
.03 X/CHORD | .45 X/CHORD
.08 X/CHORD | .50 X/CHORD
.15 X/CHORD | .55 X/CHORD
.20 X/CHORD | .60 X/CHORD
.25 X/CHORD | .70 X/CHORD
.35 X/CHORD

BHT.USARTL DATAMAP (VERS 3.07 - 03/02/81) 21OCT'85 NASA ARC

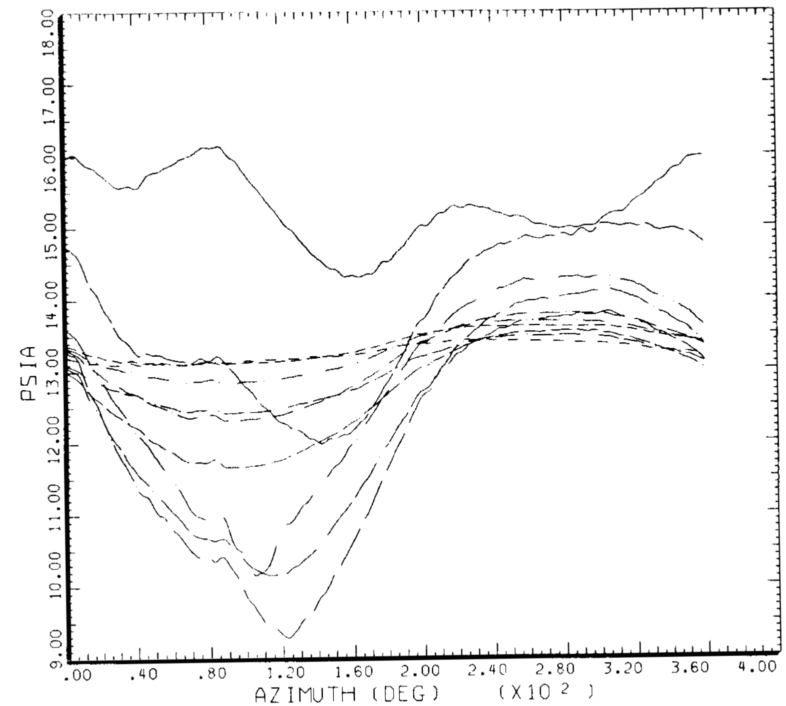

STRAIGHT AND LEVEL, 129 KNOTS

CYCLE AVERAGE: TAAT DATA, ALL SENSORS EXCEPT BAD ONES

COUNTER .91 | 2154 R/RADIUS | GROSS WT LONG CG | SHIP MODEL BOTTOM SURFACE | AH-1G
.01 X/CHORD | .45 X/CHORD
.03 X/CHORD | .50 X/CHORD
.08 X/CHORD | .60 X/CHORD
.15 X/CHORD | .70 X/CHORD
.20 X/CHORD
.35 X/CHORD
.40 X/CHORD

BHT.USARTL DATAMAP (VERS 3.07 - 03/02/81) 18OCT'85 NASA ARC

(e) At 91% radius pressure data.

Figure 35.- Continued.

ORIGINAL PAGE IS
OF POOR QUALITY

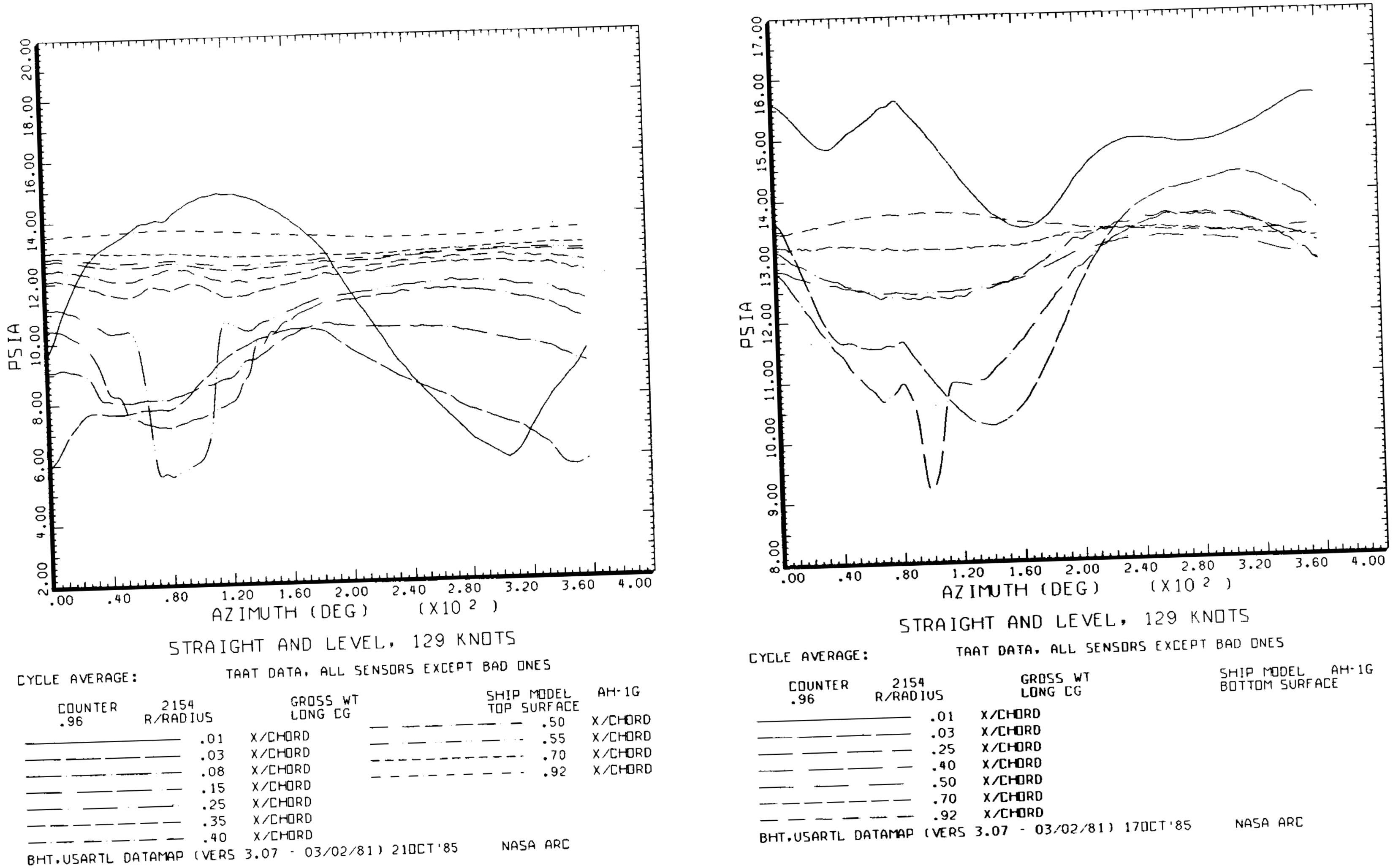

(f) At 96% radius pressure data.

Figure 35.- Continued.

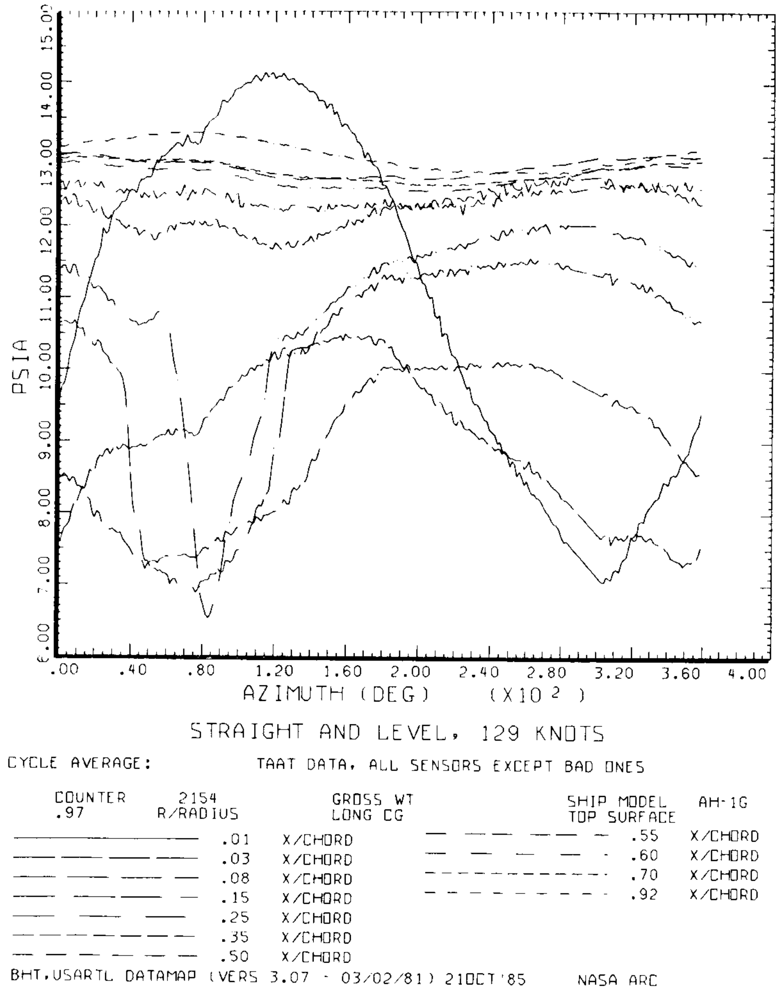

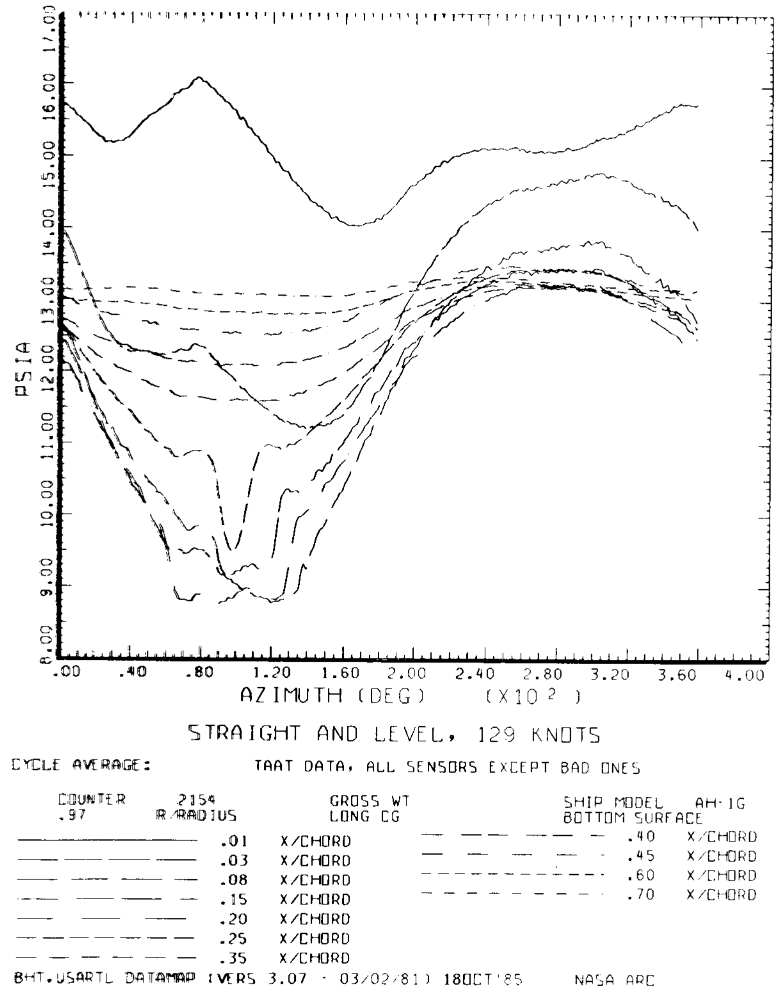

(g) At 97% radius pressure data.

Figure 35.- Continued.

ORIGINAL PAGE IS
OF POOR QUALITY

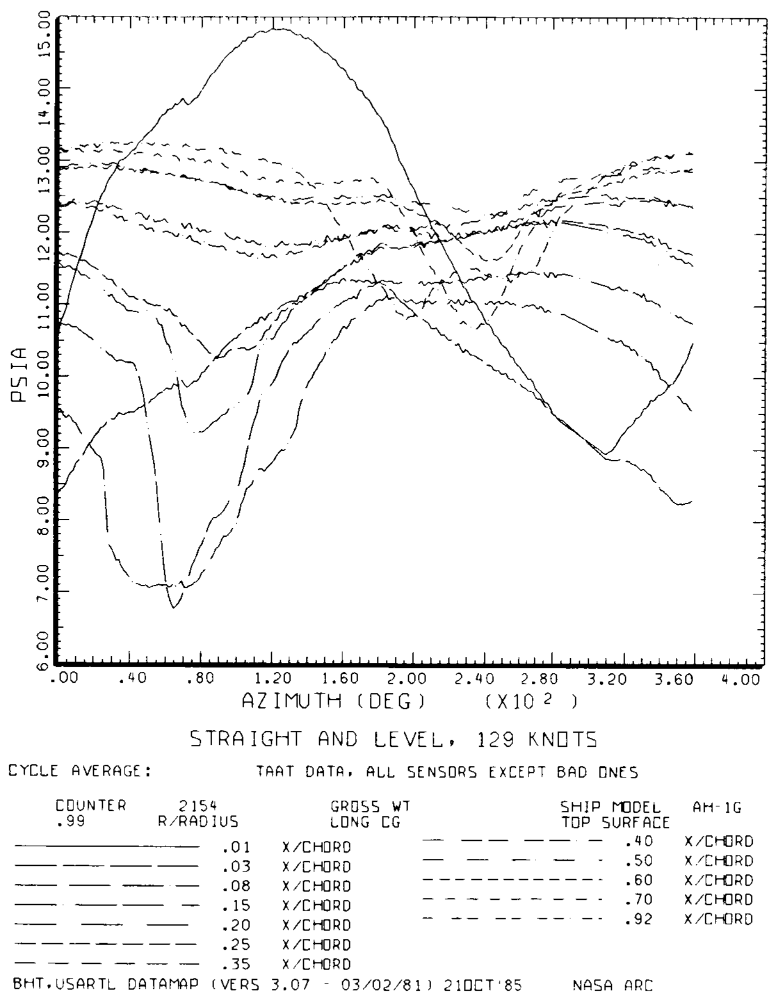

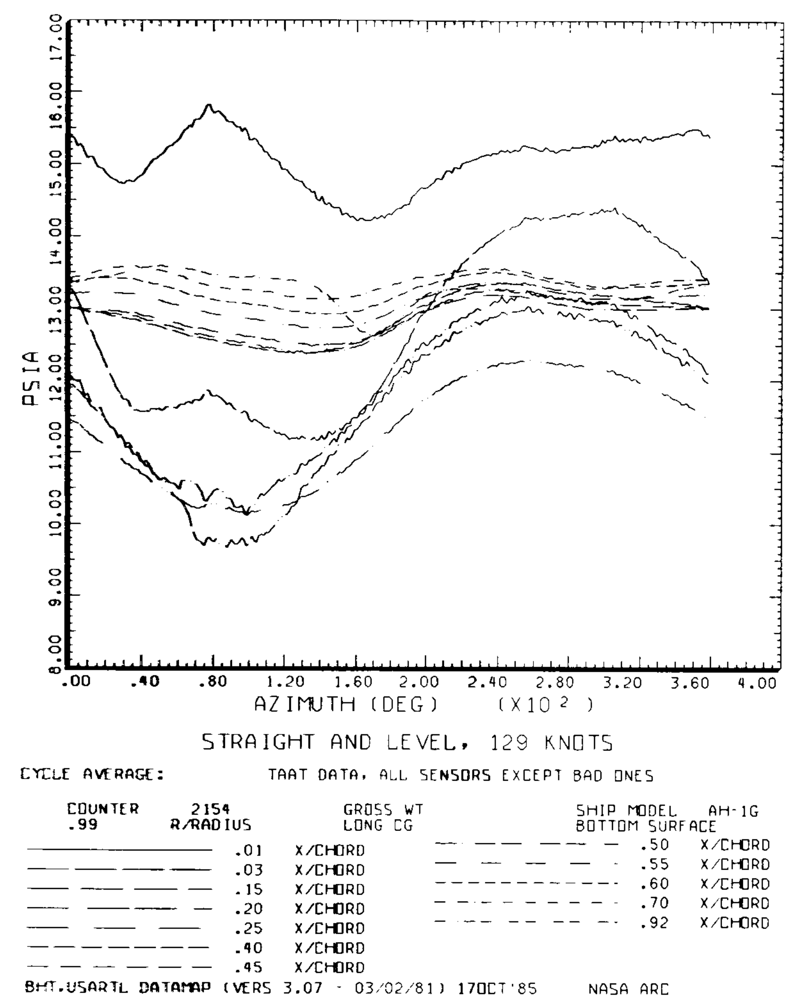

(h) At 99% radius pressure data.

Figure 35.- Concluded.

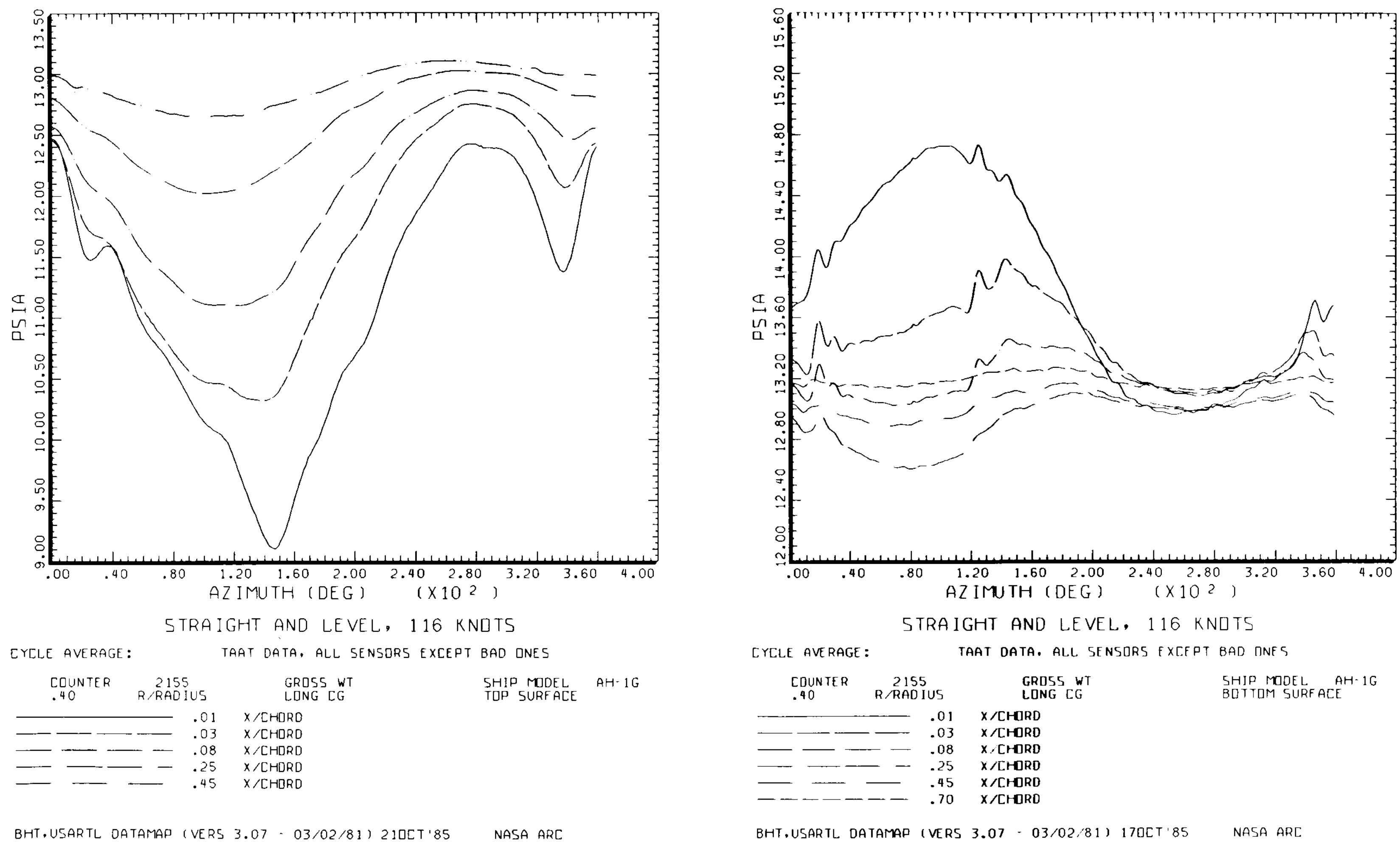

(a) At 40% radius pressure data.

Figure 36.- Blade pressure versus rotor azimuth at 116 KTAS.

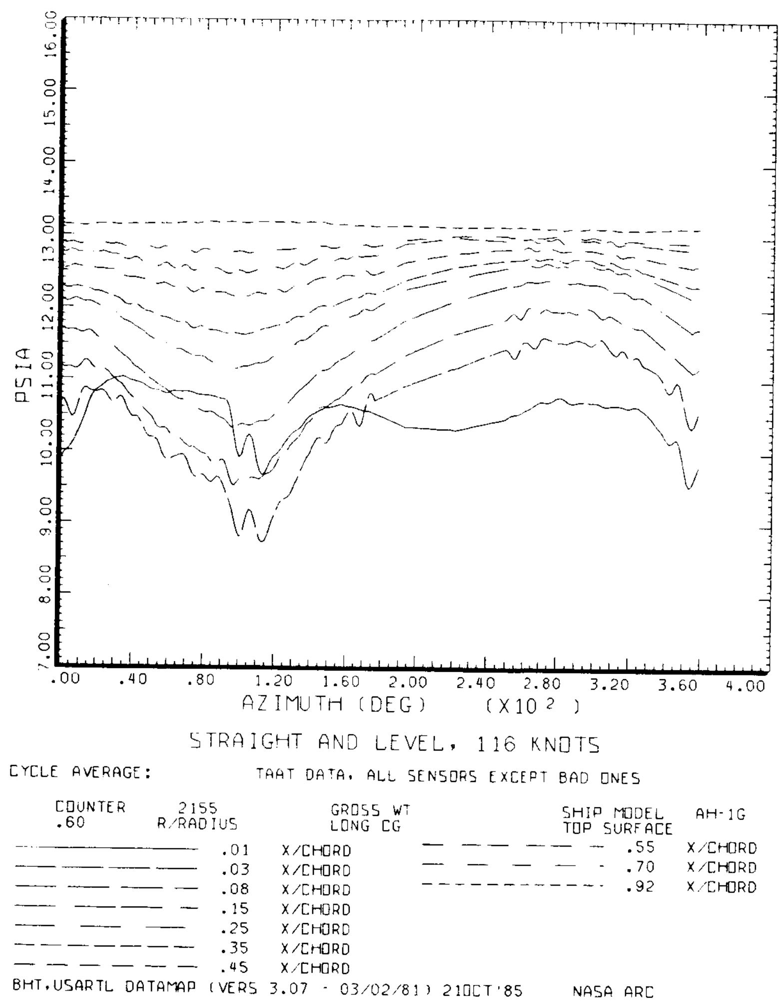

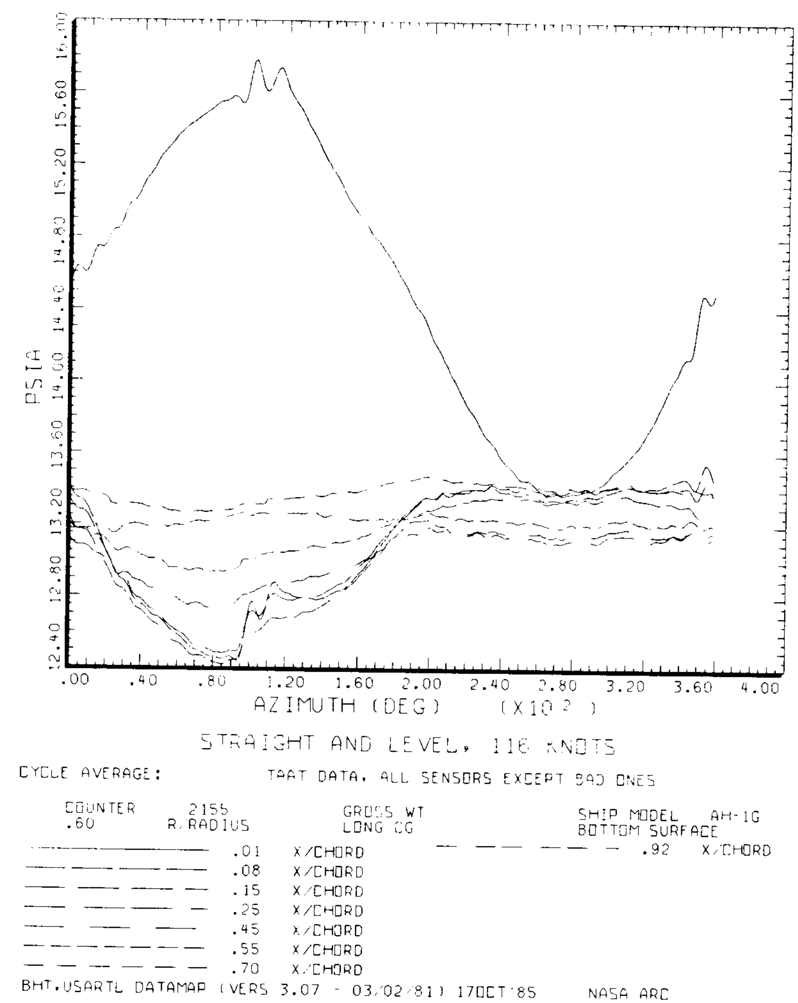

(b) 60% radius pressure data.

Figure 36.- Continued.

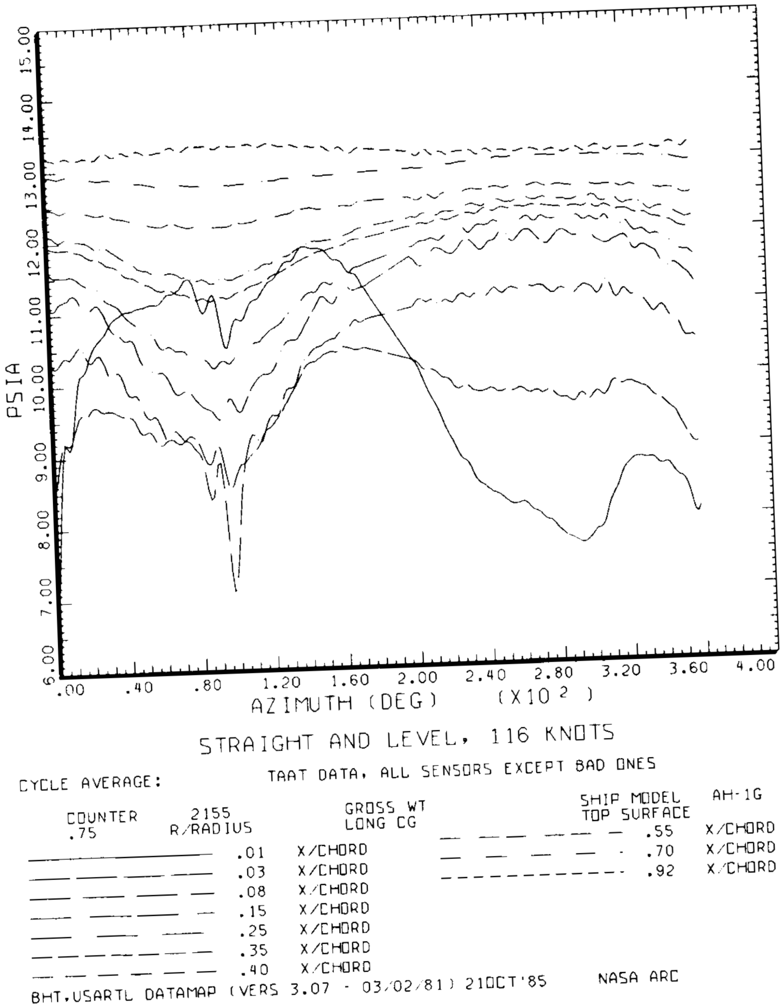

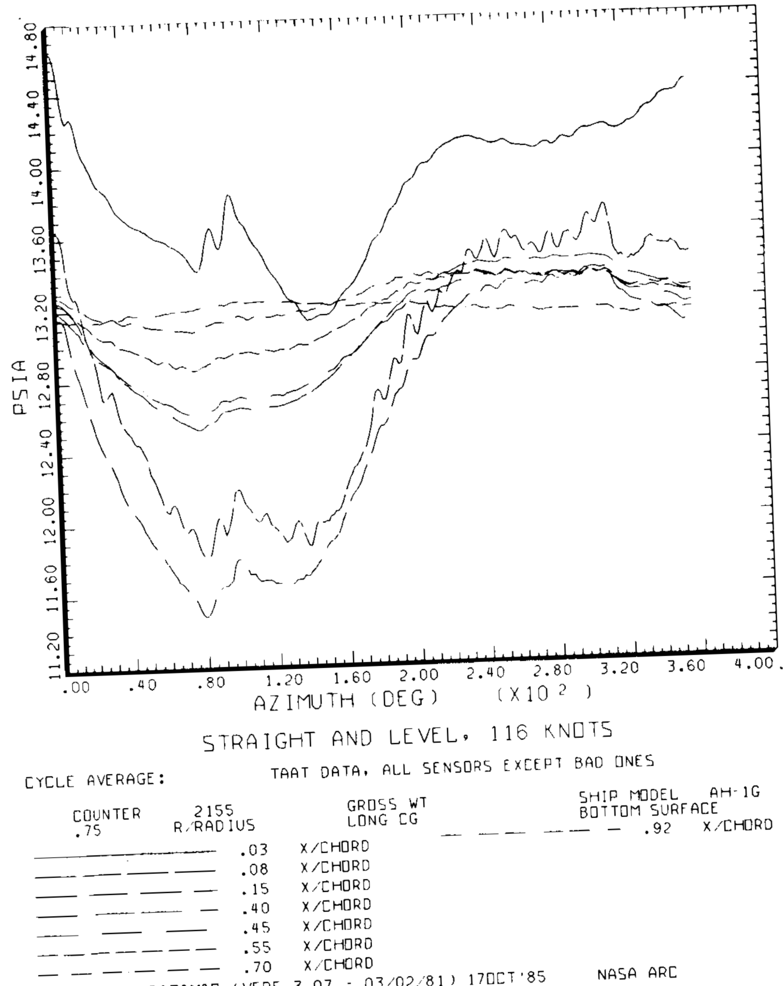

(c) At 75% radius pressure data.

Figure 36.- Continued.

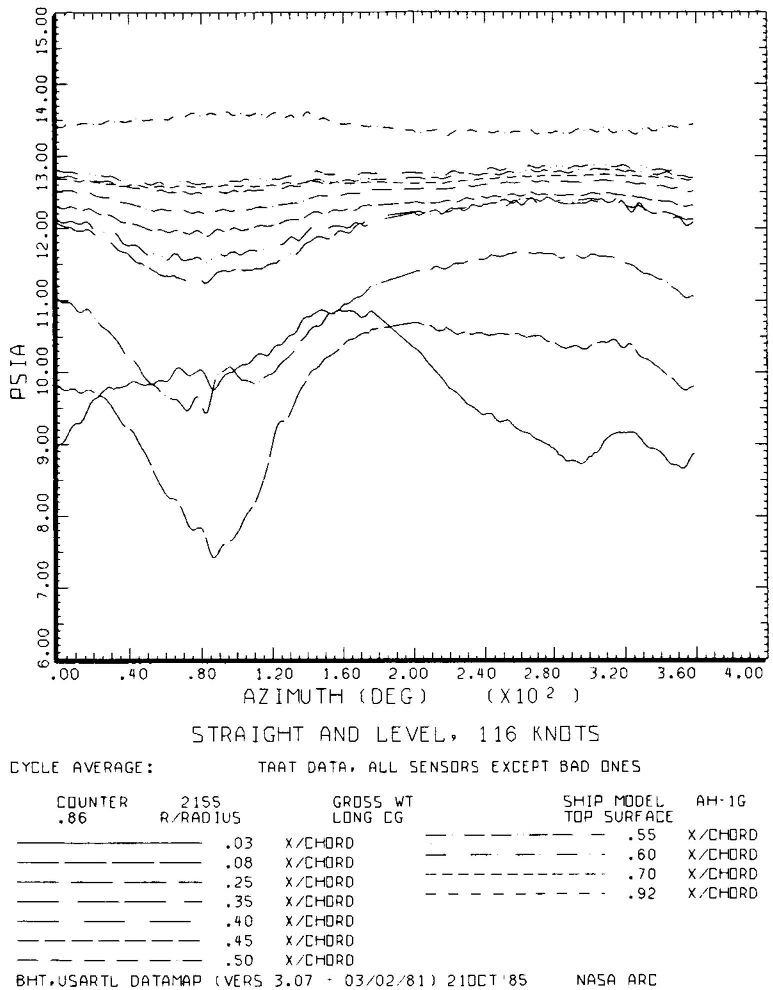

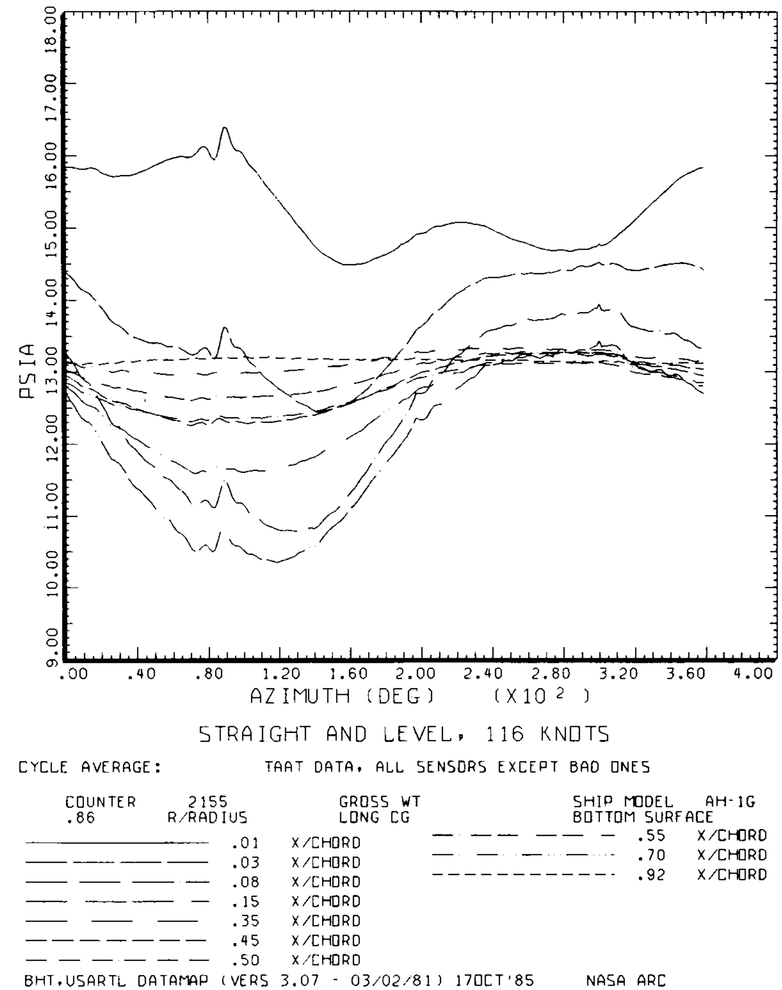

ORIGINAL PAGE IS OF POOR QUALITY

(d) At 86% radius pressure data.

Figure 36.- Continued.

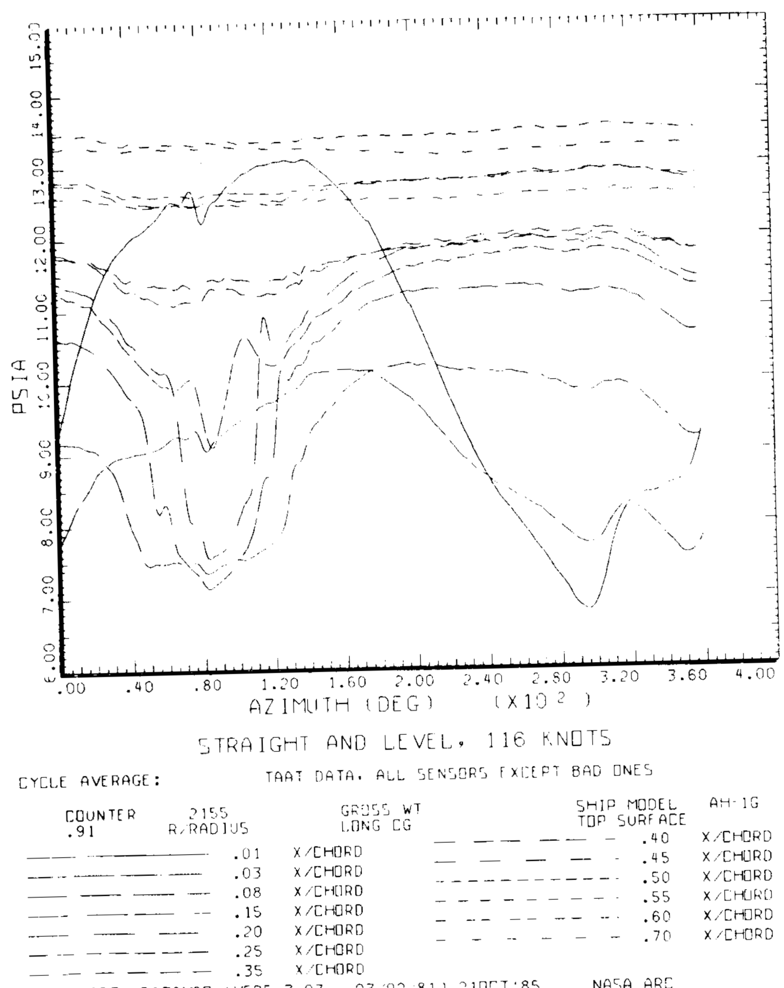

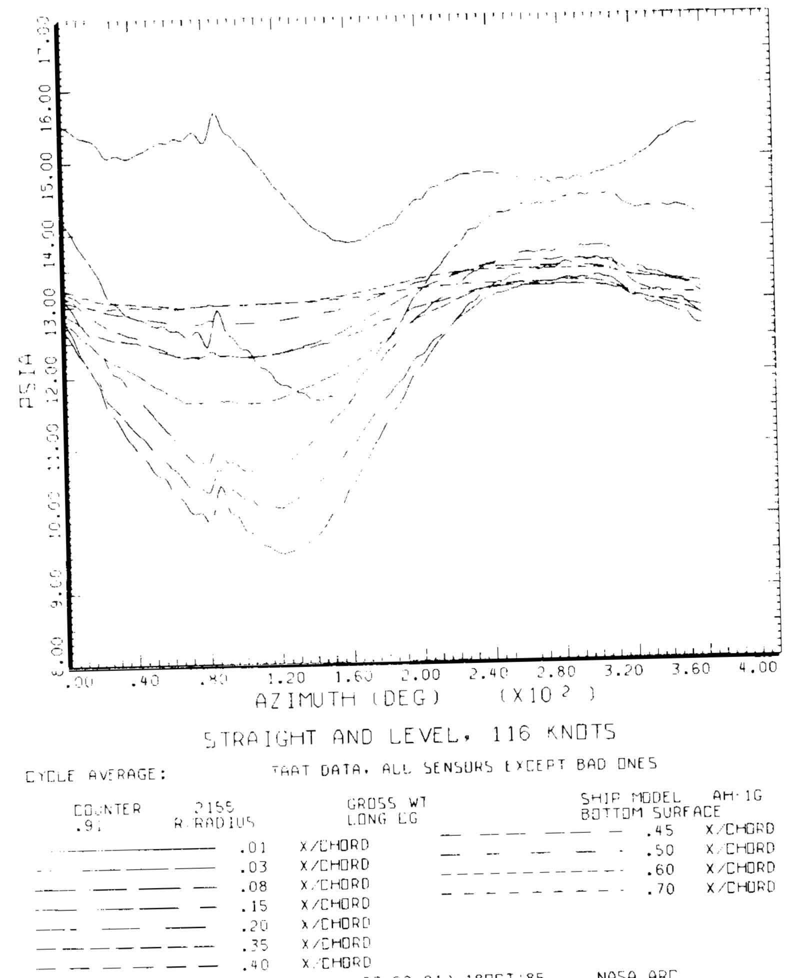

(e) At 91% radius pressure data.

Figure 36.- Continued.

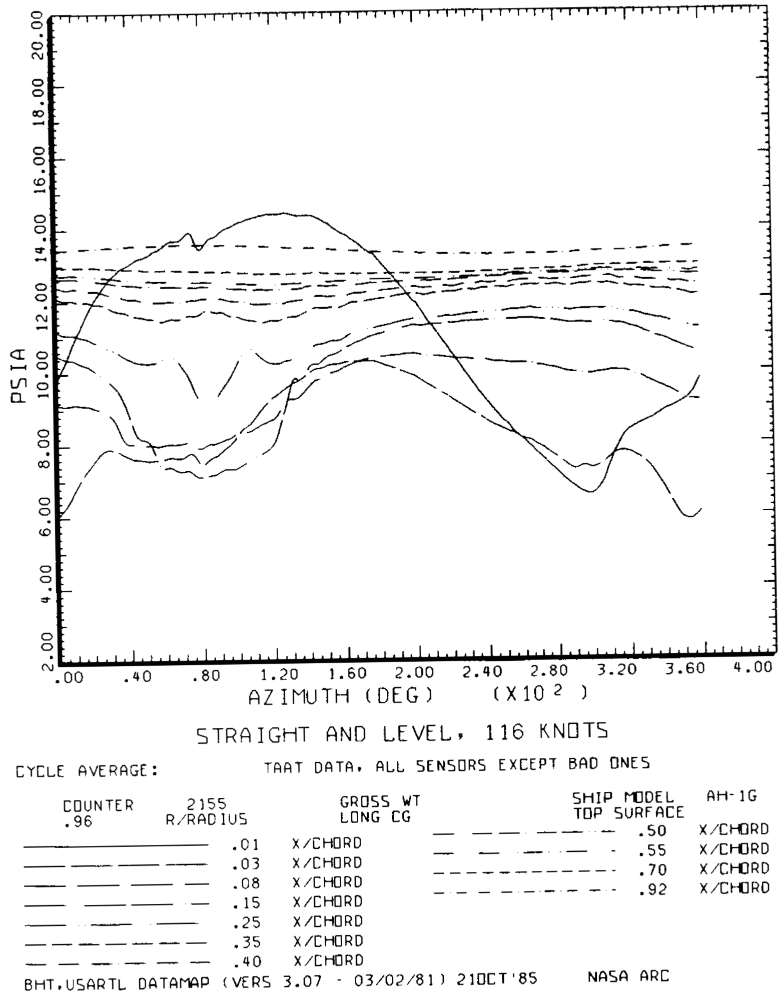

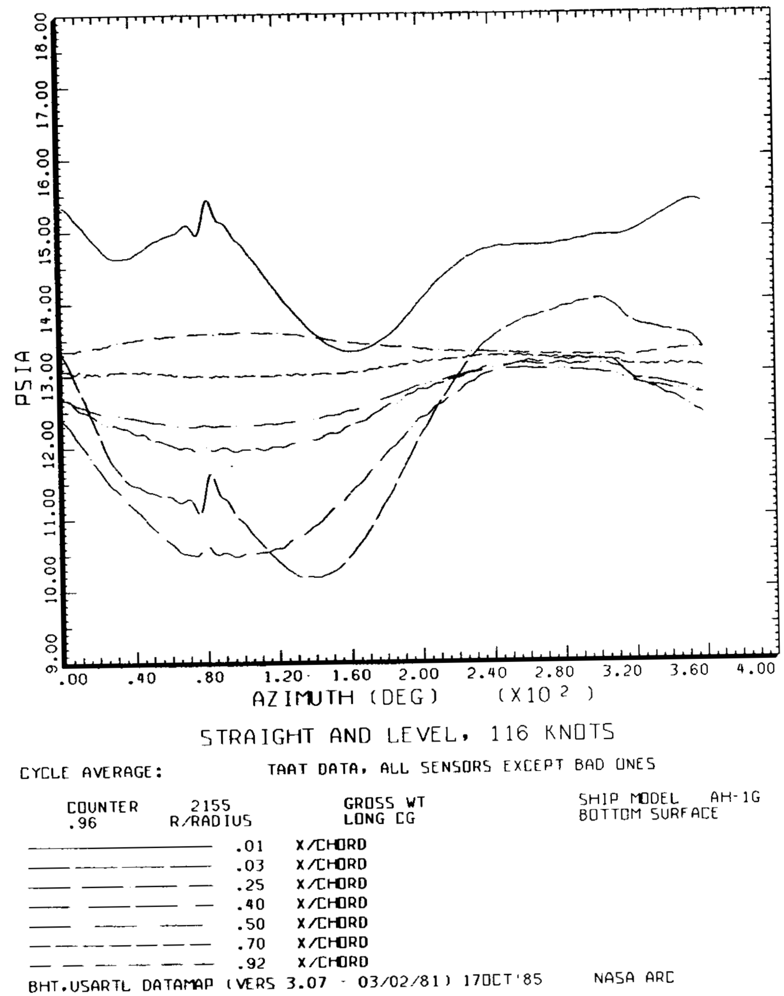

(f) At 96% radius pressure data.

Figure 36.- Continued.

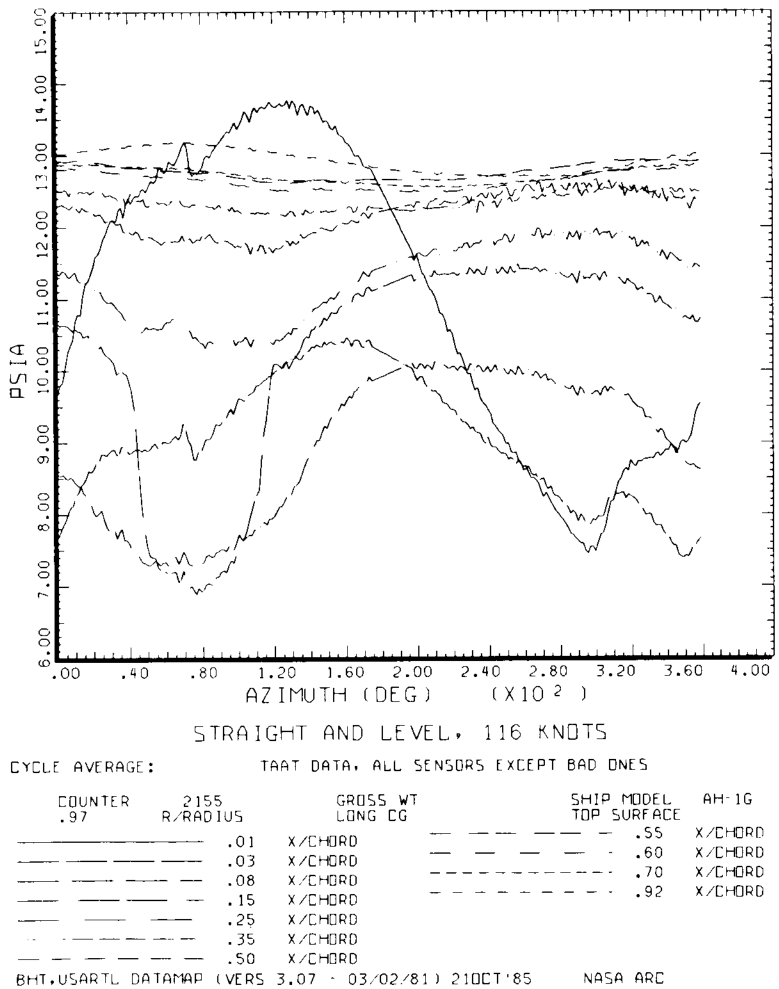

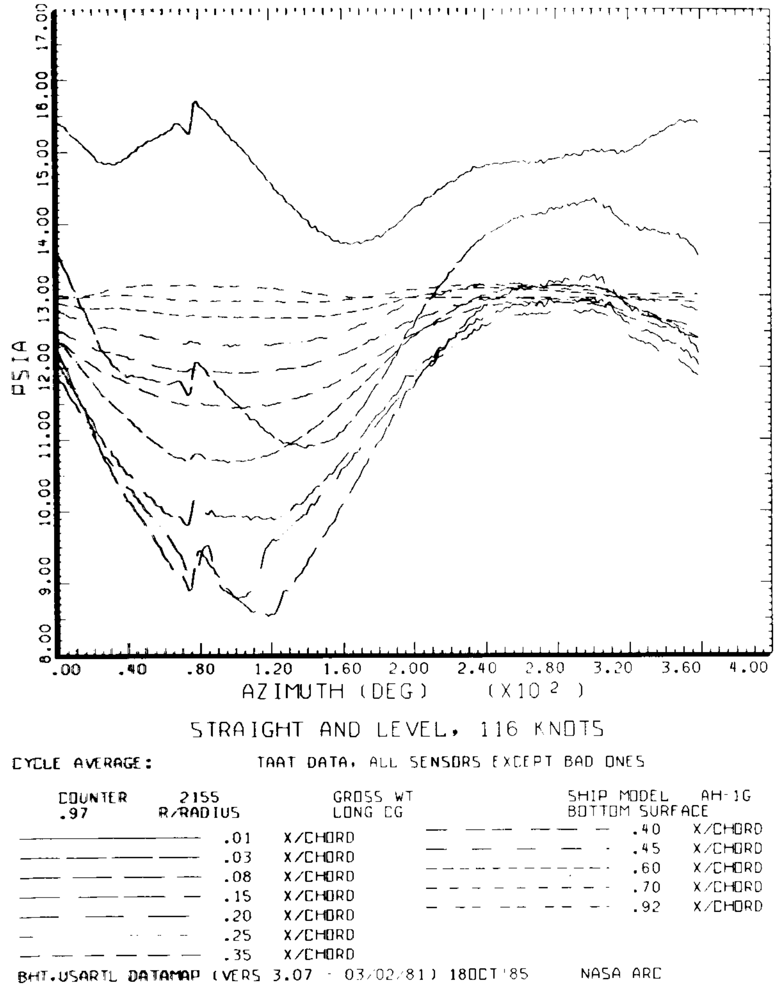

(g) At 97% radius pressure data.

Figure 36.- Continued.

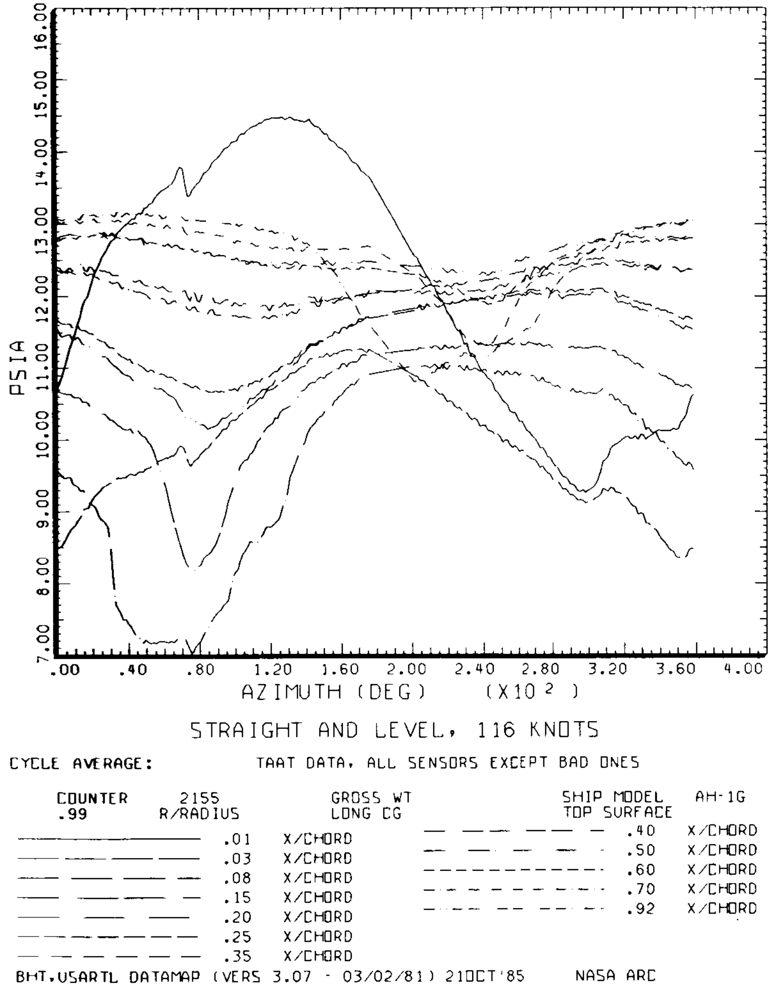

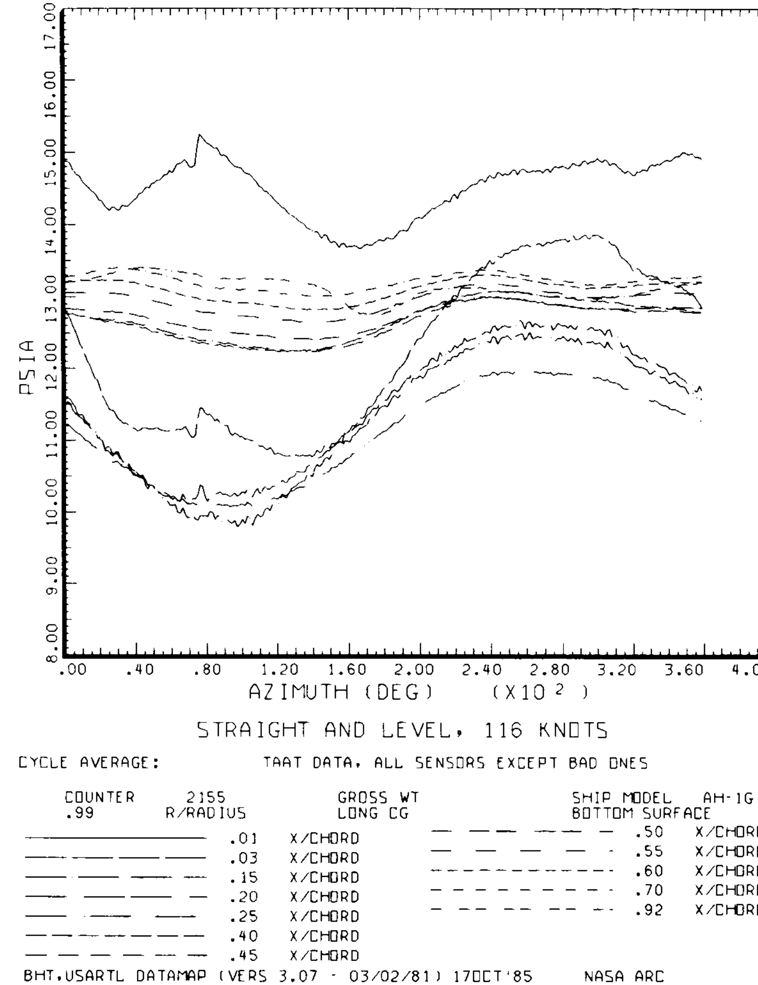

(h) At 99% radius pressure data.

Figure 36.- Concluded.

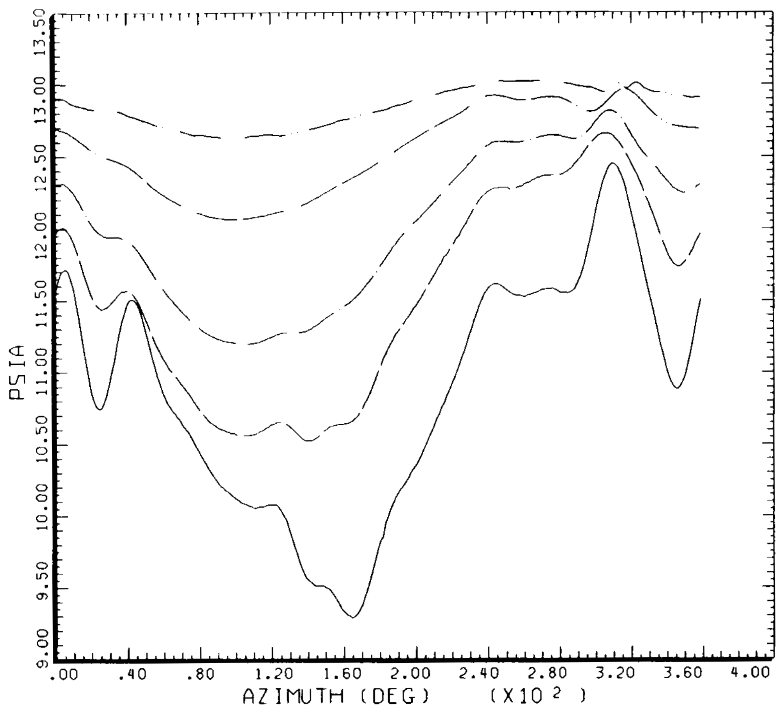

STRAIGHT AND LEVEL, 98 KNOTS

CYCLE AVERAGE: TAAT DATA, ALL SENSORS EXCEPT BAD ONES

COUNTER .40 | 2156 R/RADIUS | GROSS WT LONG CG | SHIP MODEL AH-1G TOP SURFACE

.01 X/CHORD
.03 X/CHORD
.08 X/CHORD
.25 X/CHORD
.45 X/CHORD

BHT.USARTL DATAMAP (VERS 3.07 - 03/02/81) 21OCT'85 NASA ARC

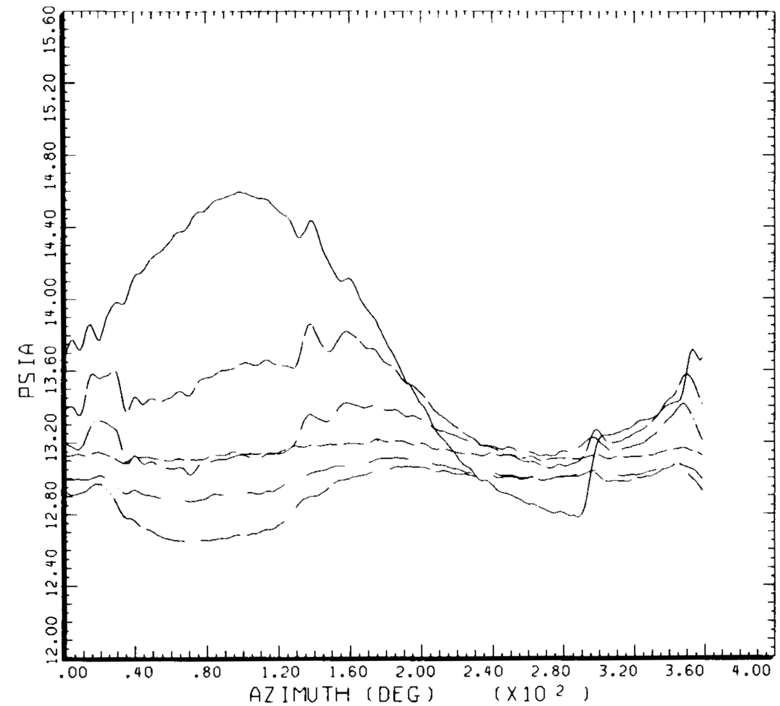

STRAIGHT AND LEVEL, 98 KNOTS

CYCLE AVERAGE: TAAT DATA, ALL SENSORS EXCEPT BAD ONES

COUNTER .40 | 2156 R/RADIUS | GROSS WT LONG CG | SHIP MODEL AH-1G BOTTOM SURFACE

.01 X/CHORD
.03 X/CHORD
.08 X/CHORD
.25 X/CHORD
.45 X/CHORD
.70 X/CHORD

BHT.USARTL DATAMAP (VERS 3.07 - 03/02/81) 17OCT'85 NASA ARC

(a) At 40% radius pressure data.

Figure 37.- Blade pressure versus rotor azimuth at 98 KTAS.

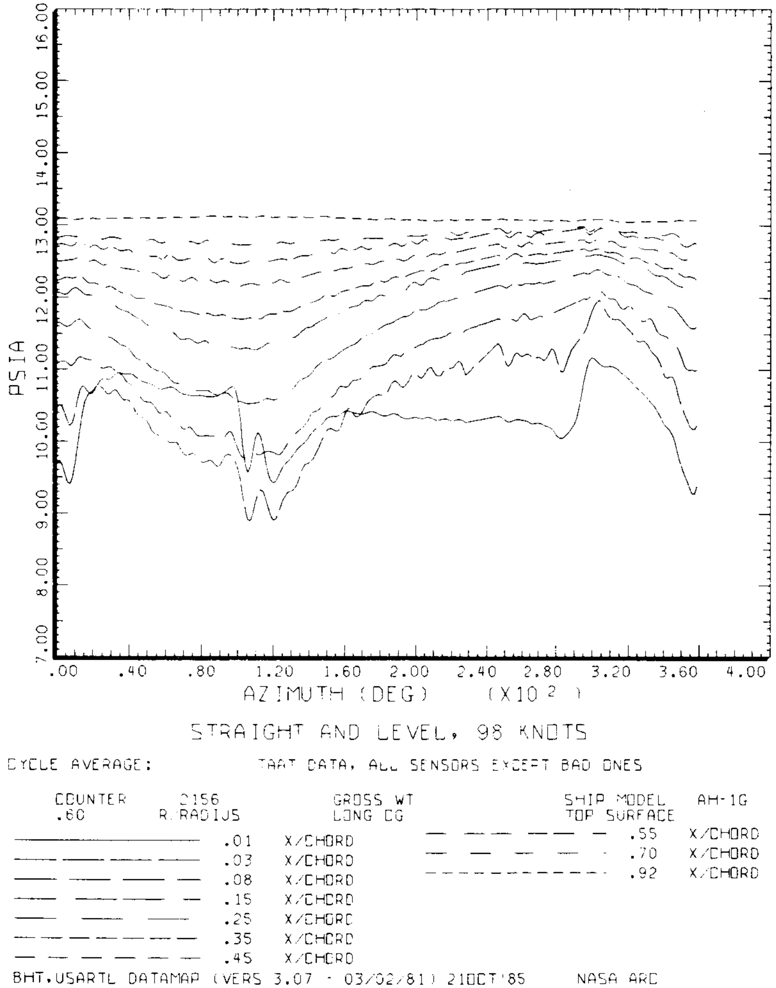

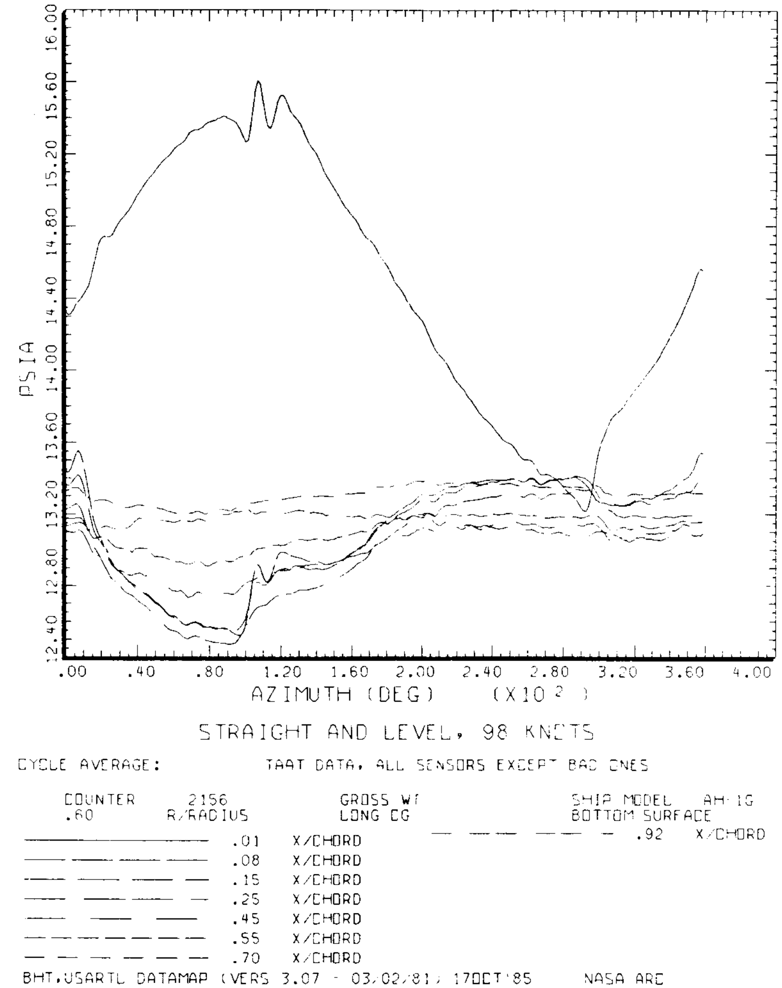

(b) At 60% radius pressure data.

Figure 37.- Continued.

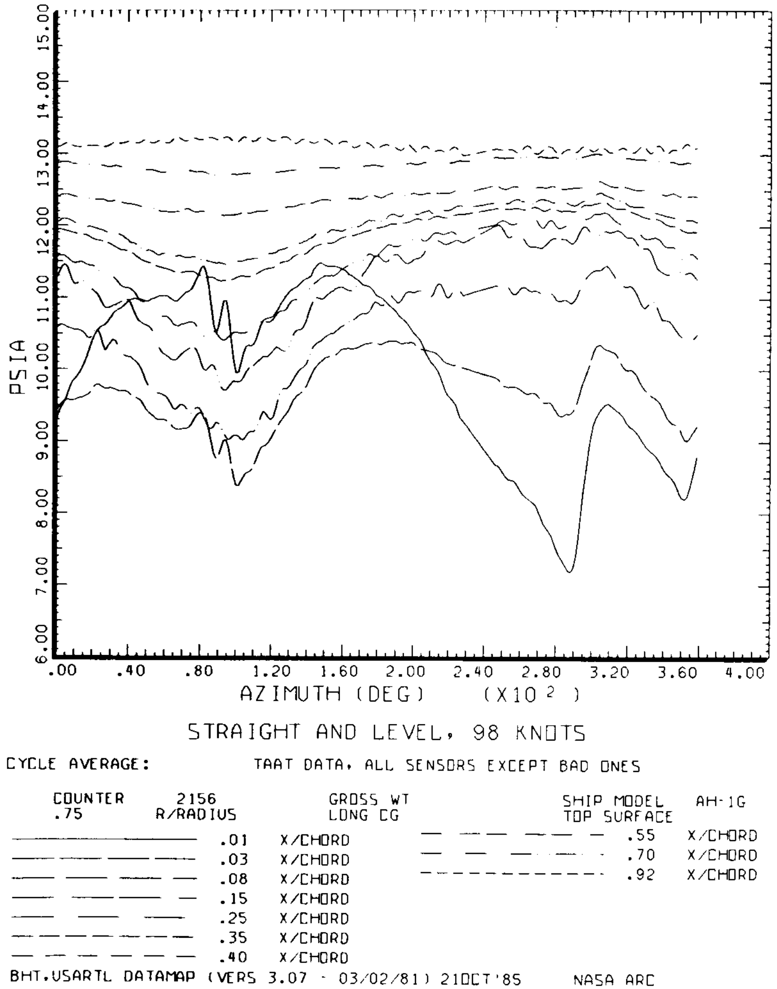

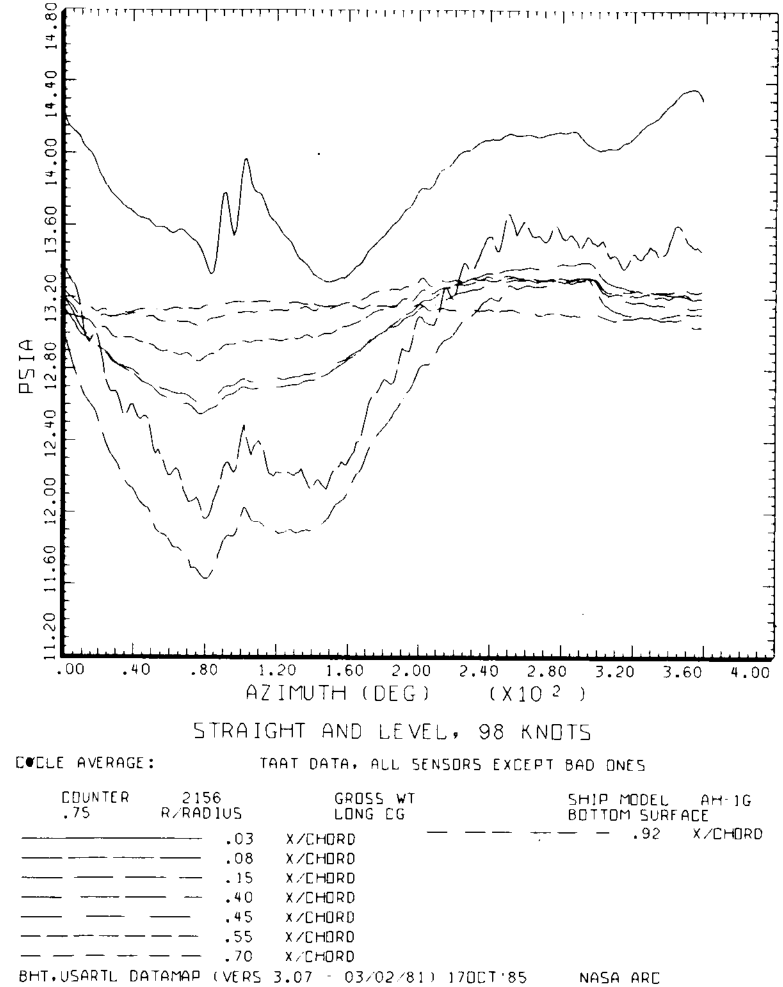

(c) At 75% radius pressure data.

Figure 37.- Continued.

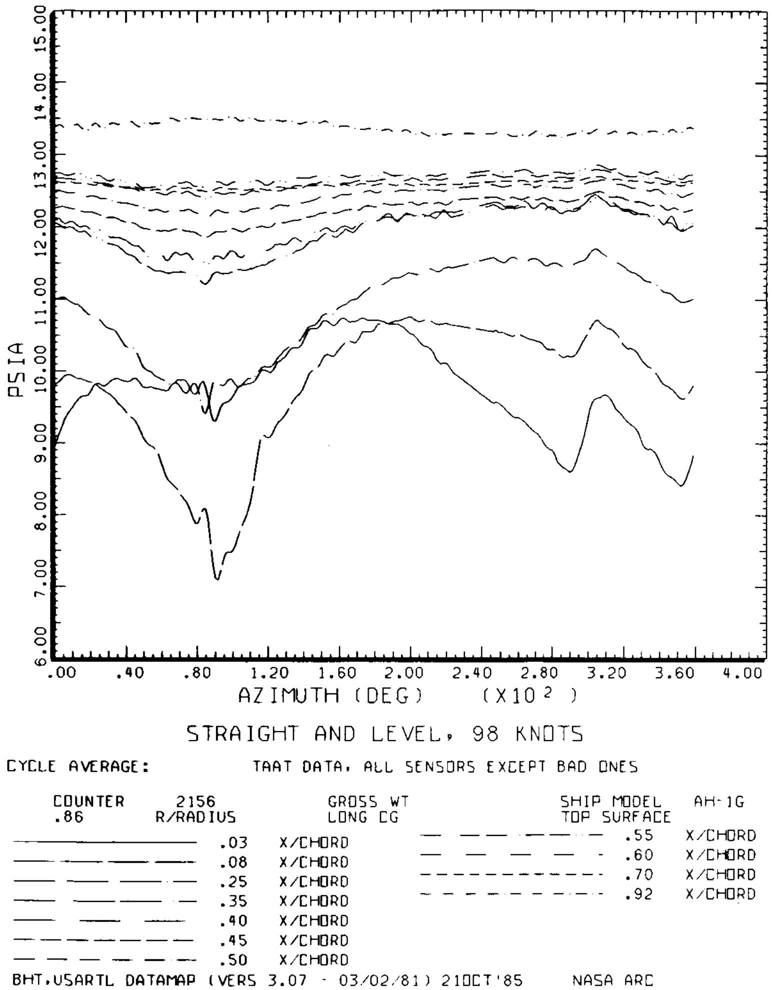

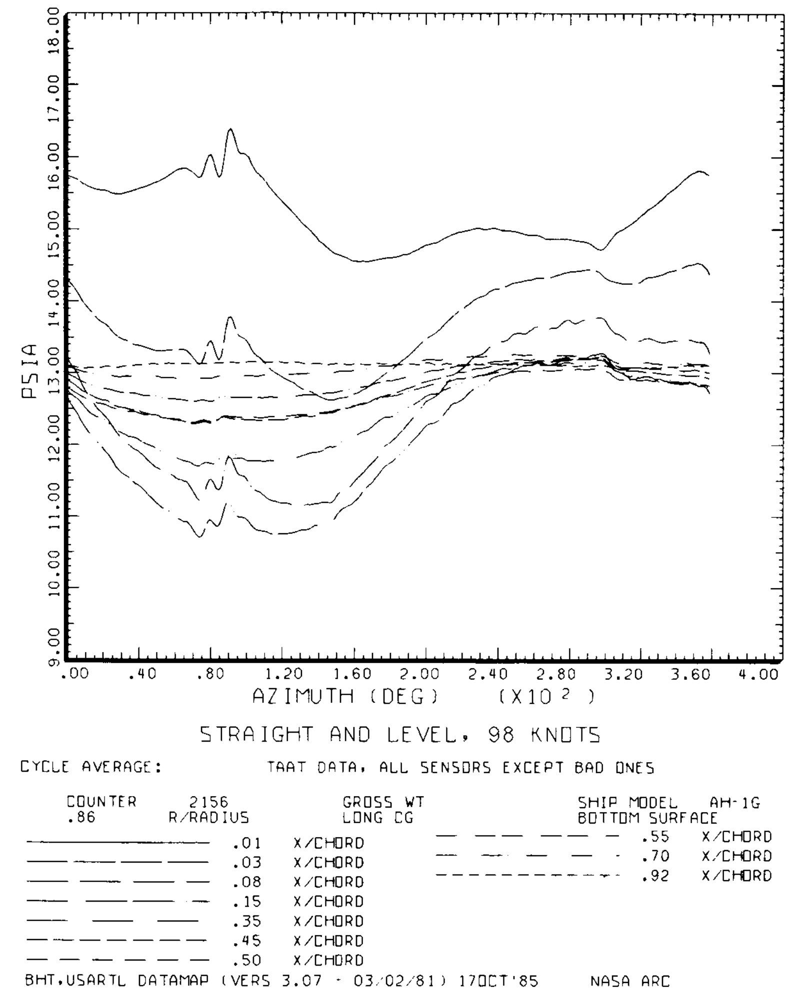

(d) At 86% radius pressure data.

Figure 37.- Continued.

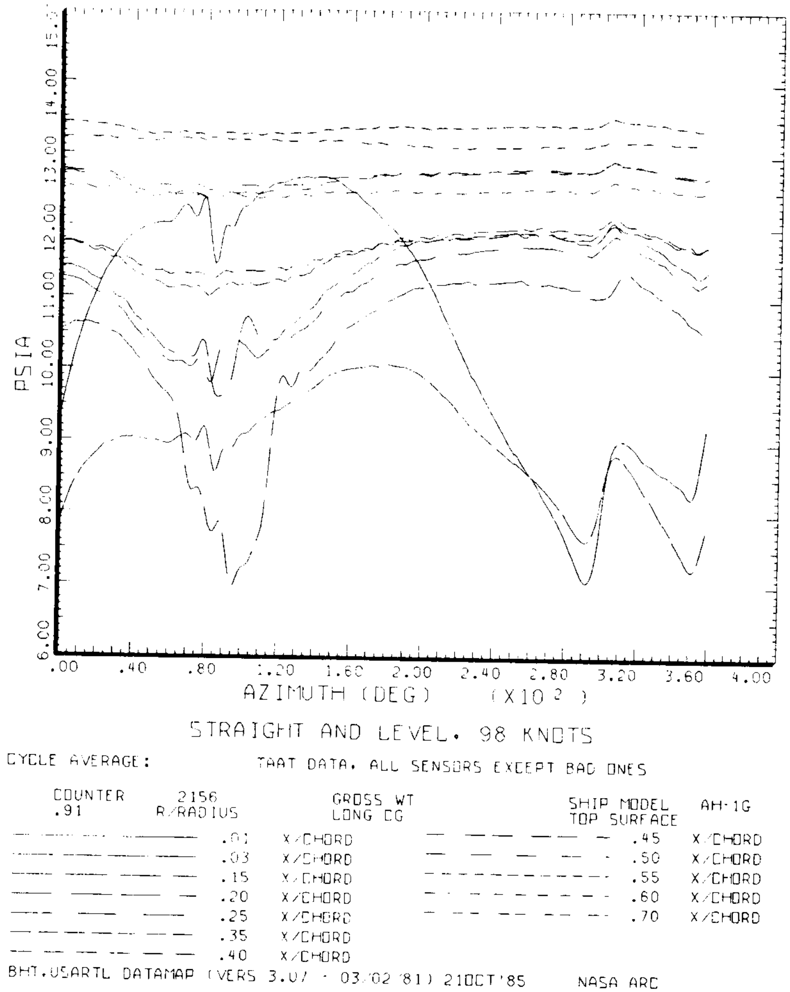

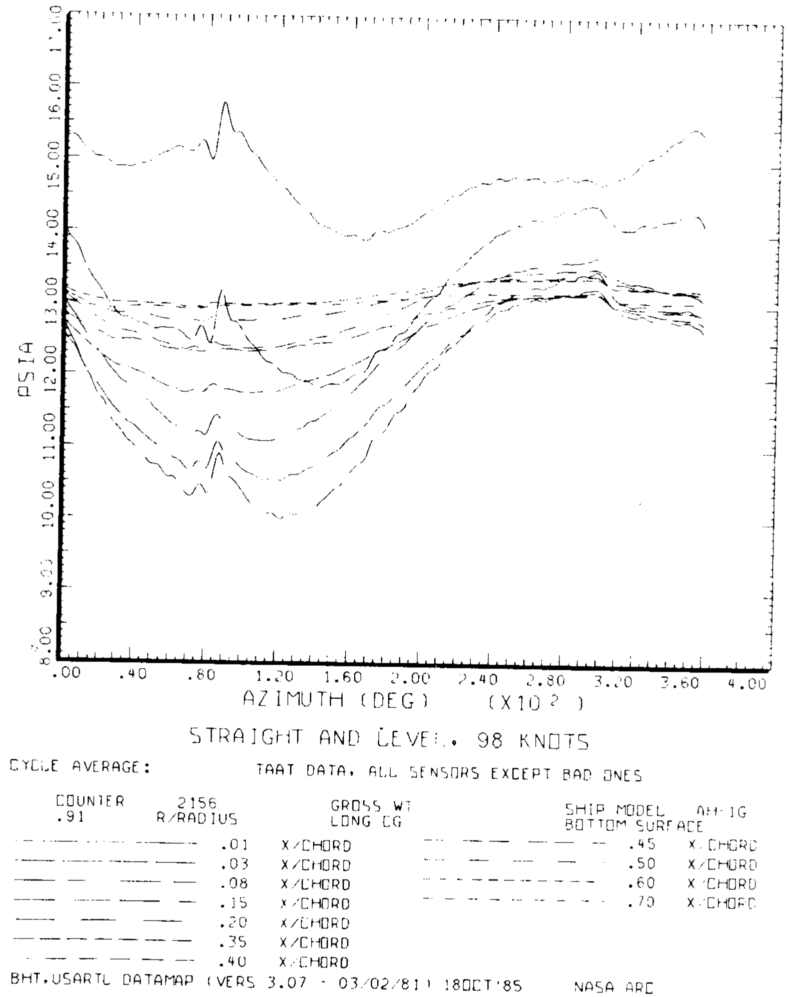

(e) At 91% radius pressure data.

Figure 37.- Continued.

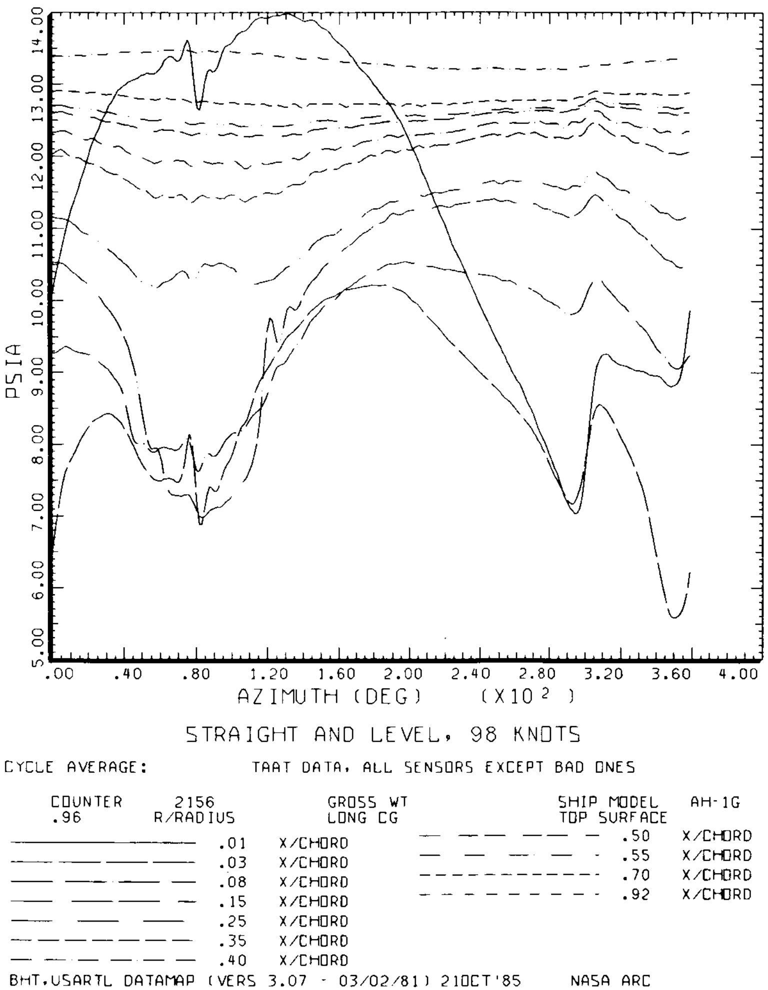

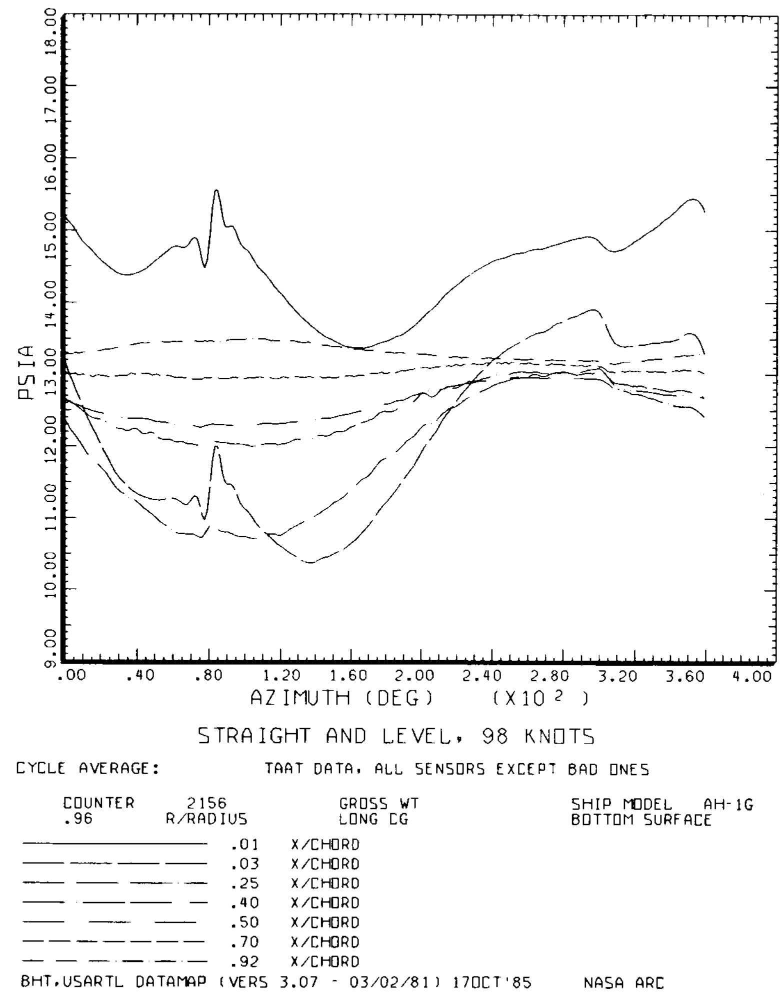

(f) At 96% radius pressure data.

Figure 37.- Continued.

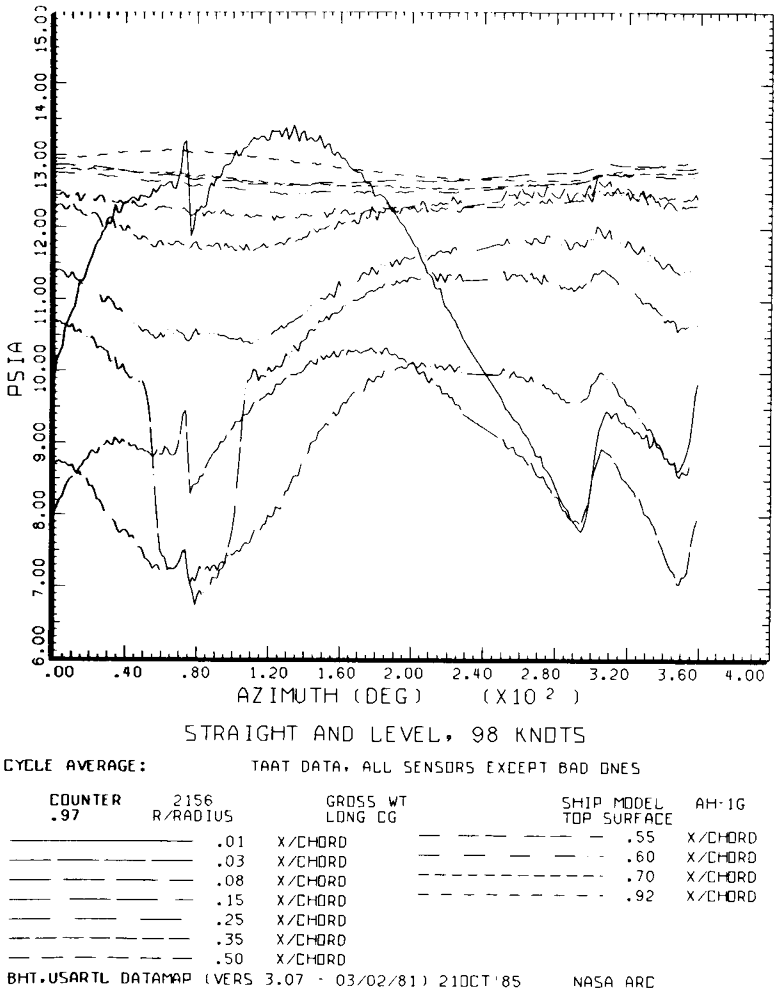

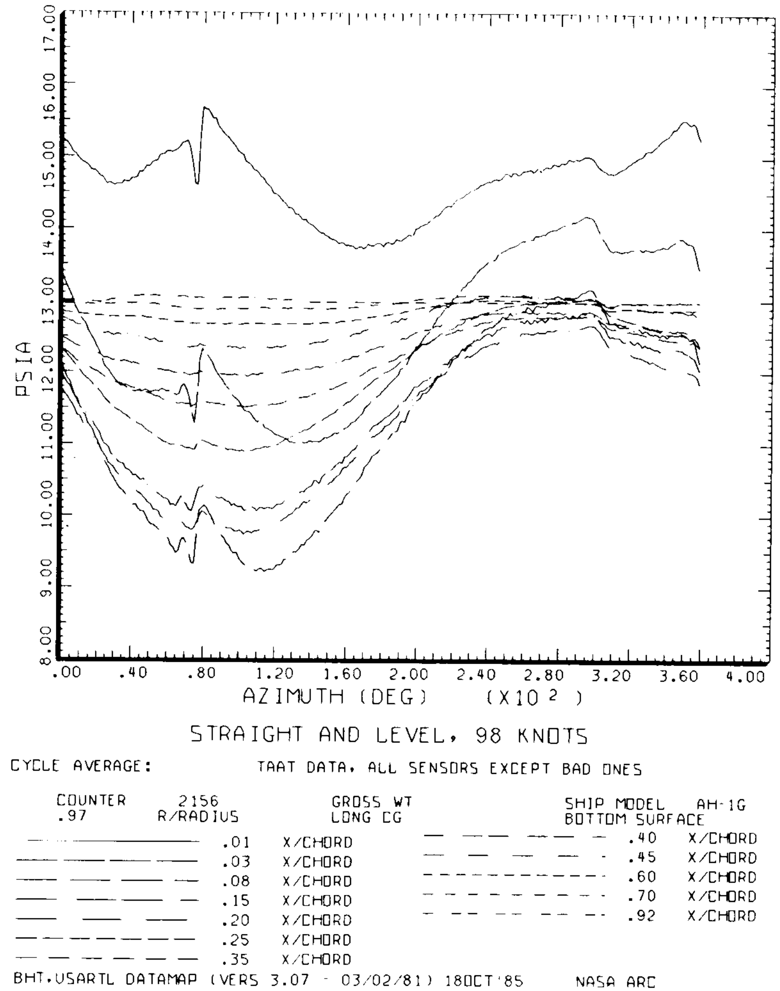

(g) At 97% radius pressure data.

Figure 37.- Continued.

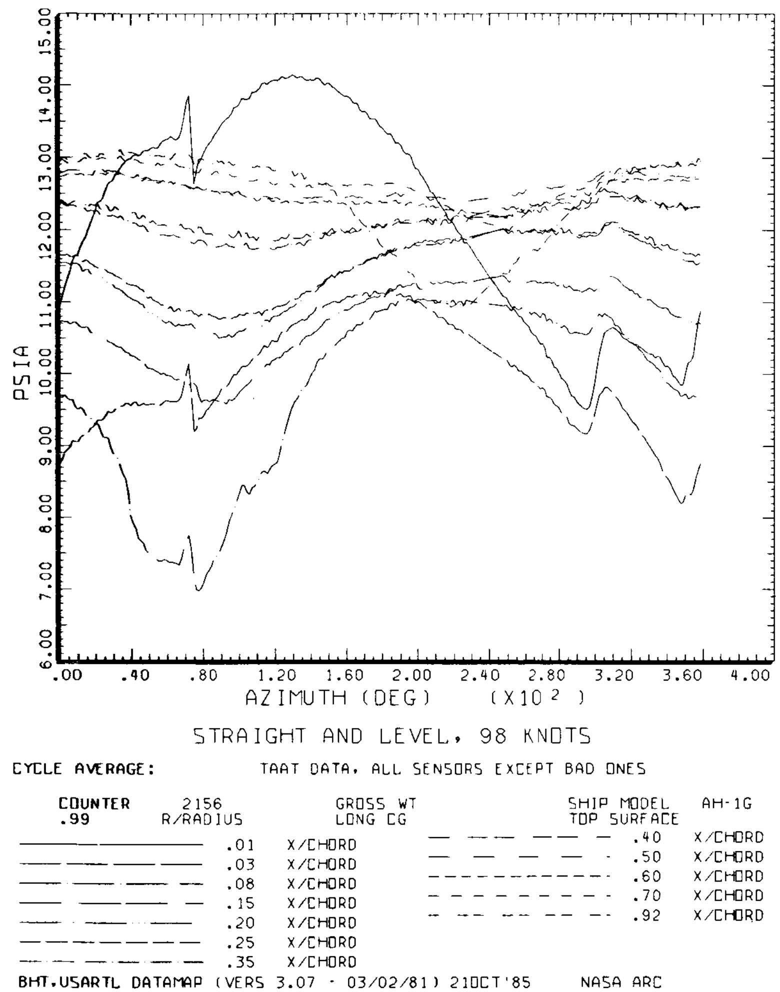

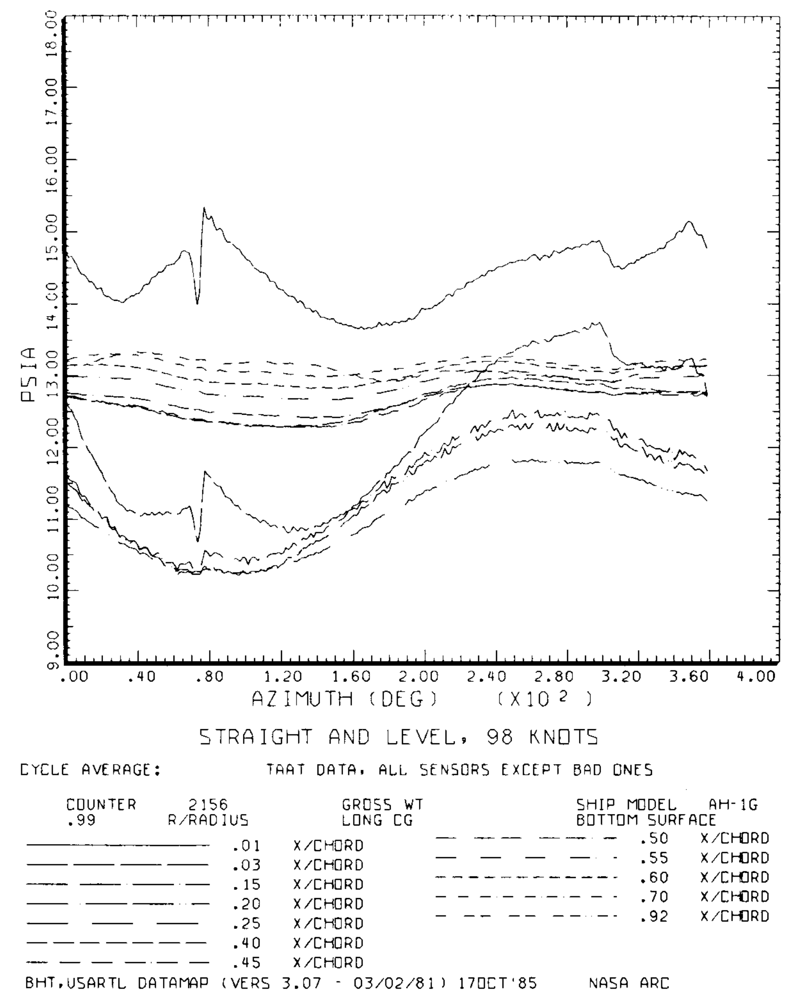

(h) At 99% radius pressure data.

Figure 37.- Concluded.

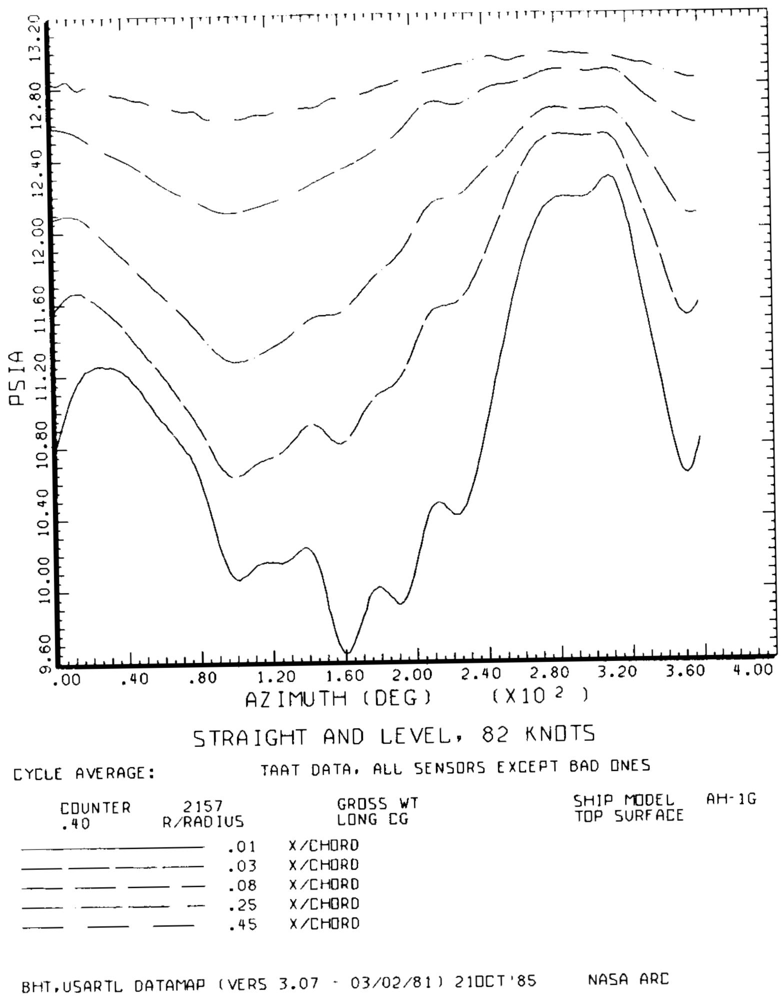

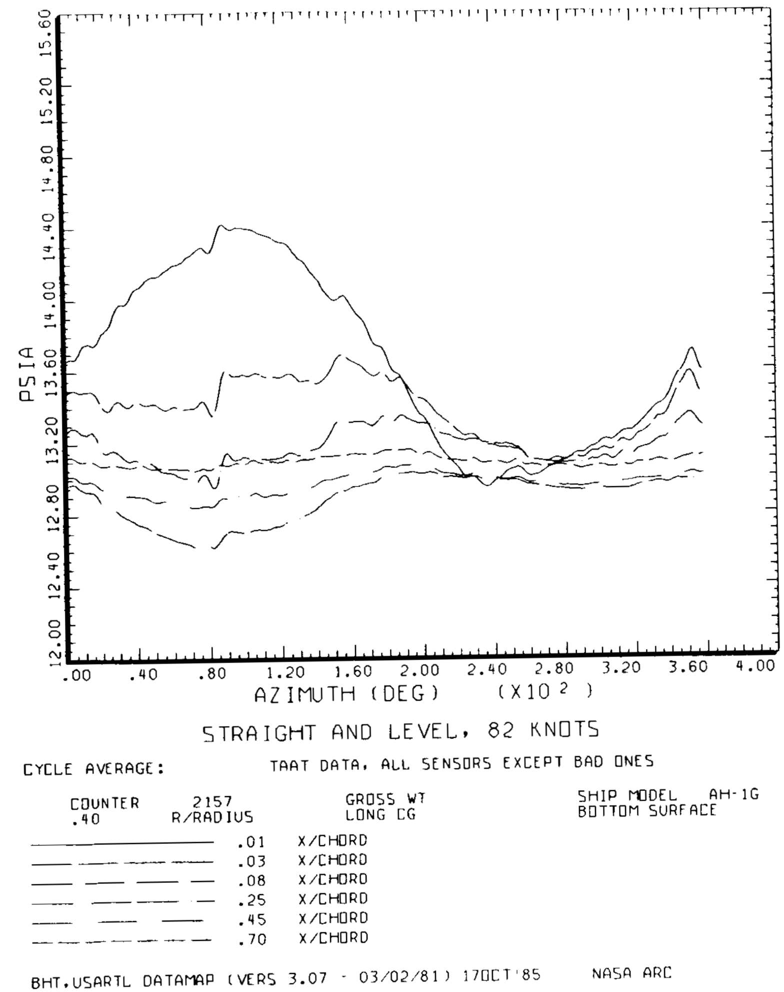

(a) At 40% radius pressure data.

Figure 38.- Blade pressure versus rotor azimuth at 82 KTAS.

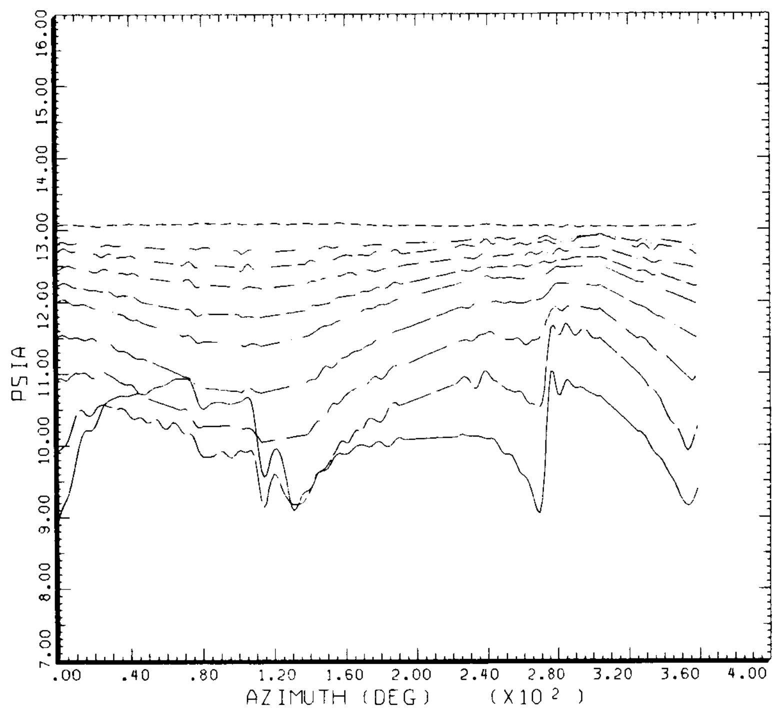

STRAIGHT AND LEVEL, 82 KNOTS

CYCLE AVERAGE: TAAT DATA, ALL SENSORS EXCEPT BAD ONES

COUNTER 2157 .60 R/RADIUS
.01 X/CHORD
.03 X/CHORD
.08 X/CHORD
.15 X/CHORD
.25 X/CHORD
.35 X/CHORD
.45 X/CHORD

GROSS WT LONG CG

SHIP MODEL AH-1G TOP SURFACE
.55 X/CHORD
.70 X/CHORD
.92 X/CHORD

BHT.USARTL DATAMAP (VERS 3.07 - 03/02/81) 21OCT'85 NASA ARC

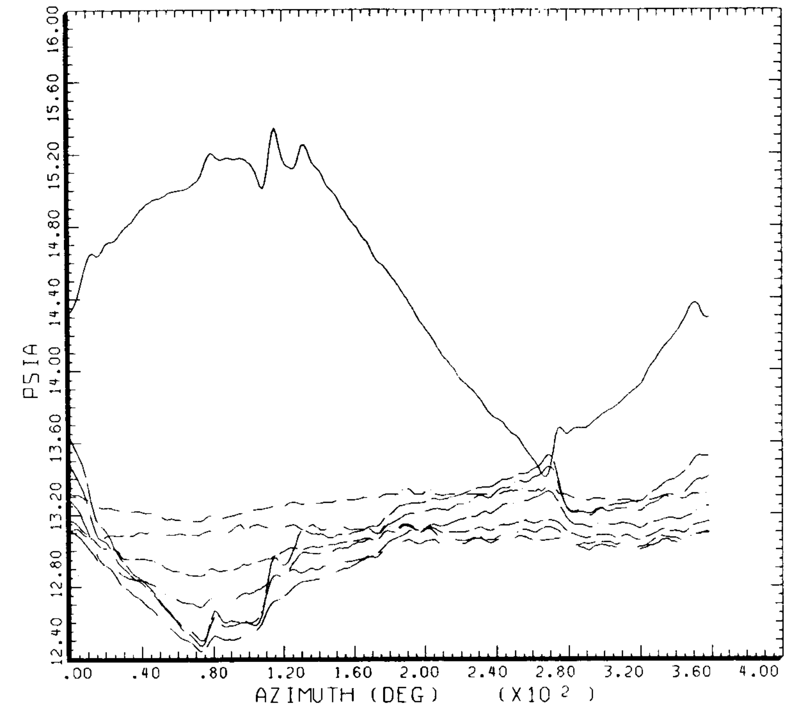

STRAIGHT AND LEVEL, 82 KNOTS

CYCLE AVERAGE: TAAT DATA, ALL SENSORS EXCEPT BAD ONES

COUNTER 2157 .60 R/RADIUS
.01 X/CHORD
.08 X/CHORD
.15 X/CHORD
.25 X/CHORD
.45 X/CHORD
.55 X/CHORD
.70 X/CHORD

GROSS WT LONG CG

SHIP MODEL AH-1G BOTTOM SURFACE
.92 X/CHORD

BHT.USARTL DATAMAP (VERS 3.07 - 03/02/81) 17OCT'85 NASA ARC

(b) At 60% radius pressure data.

Figure 38.- Continued.

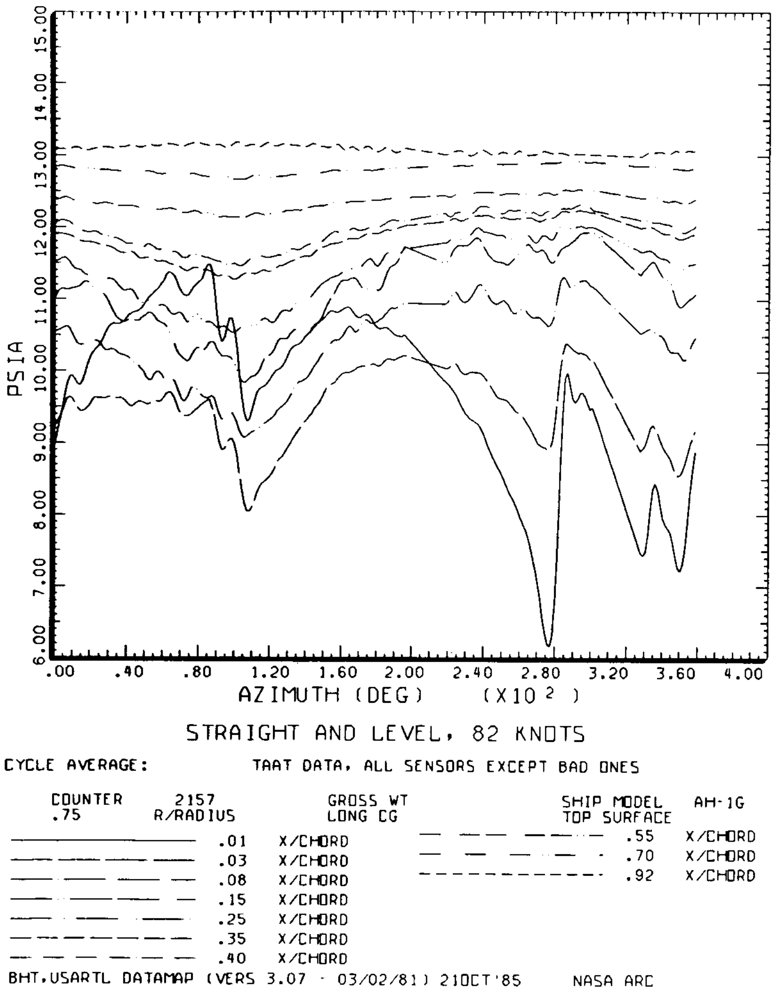

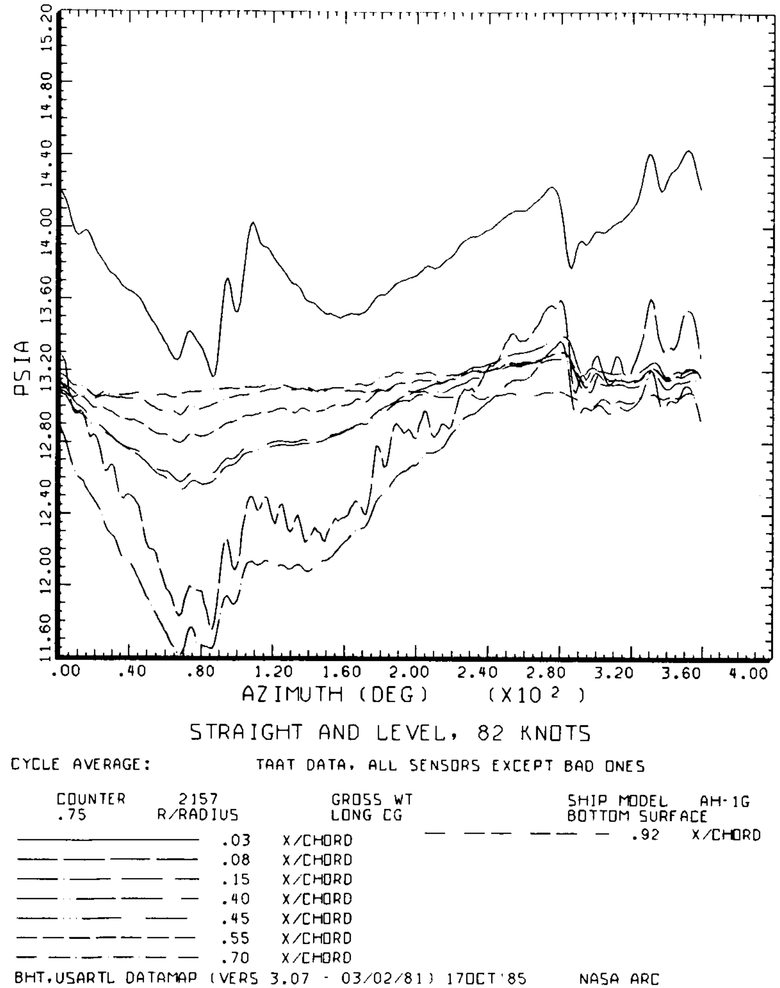

(c) At 75% radius pressure data.

Figure 38.- Continued.

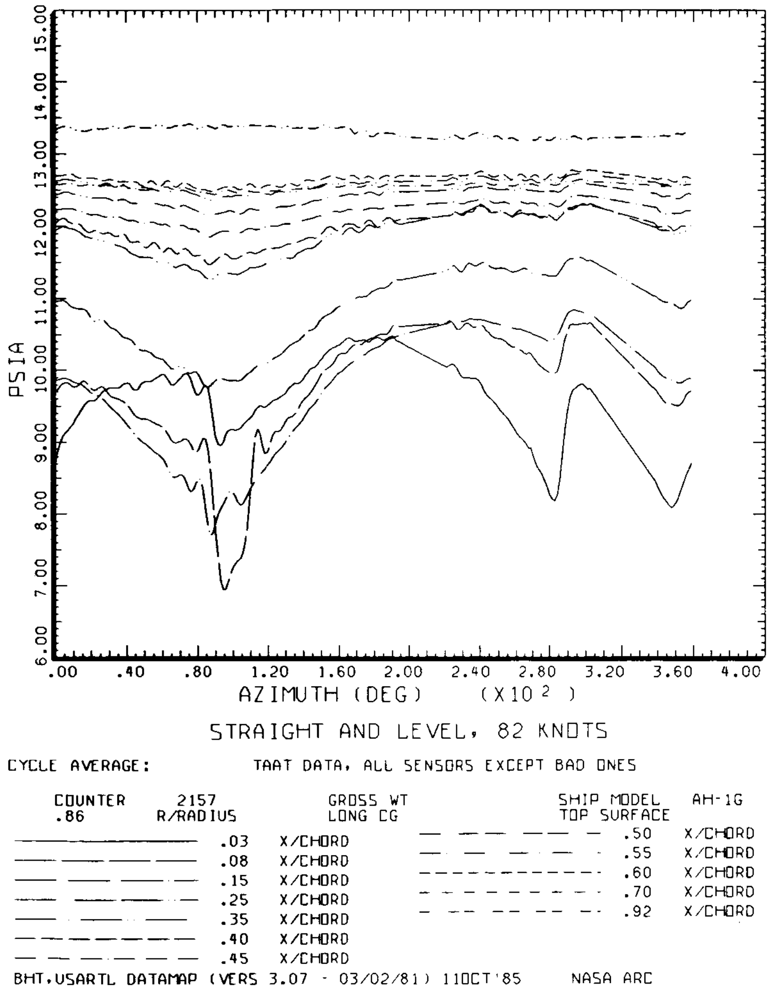

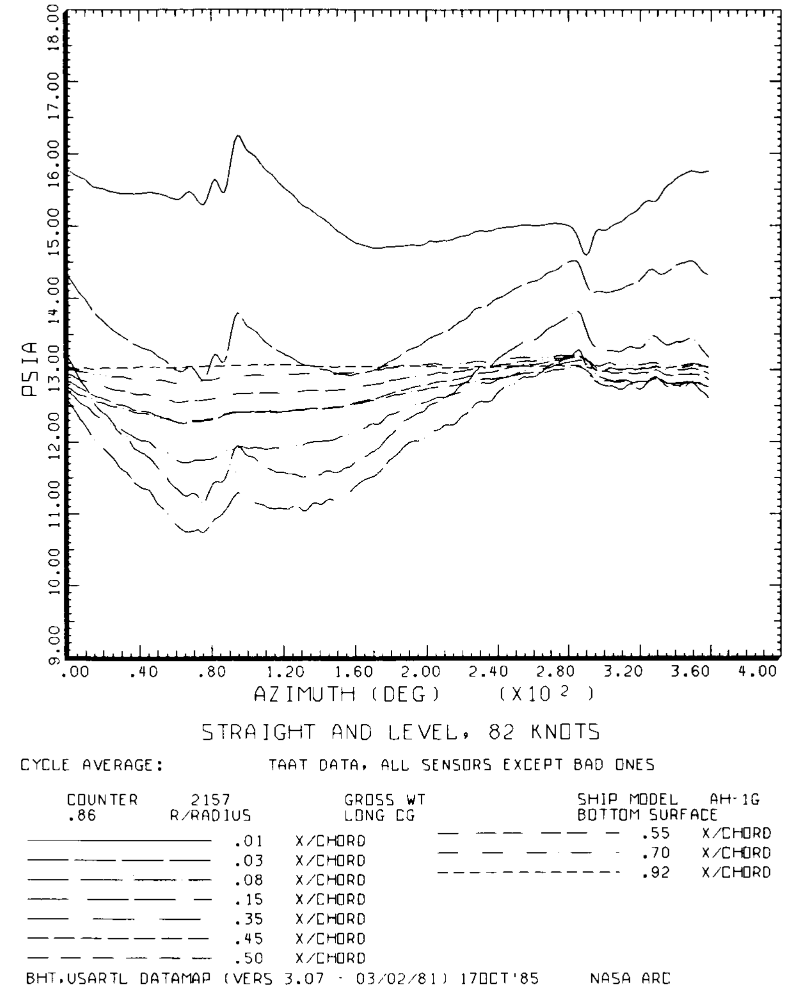

(d) At 86% radius pressure data.

Figure 38.- Continued.

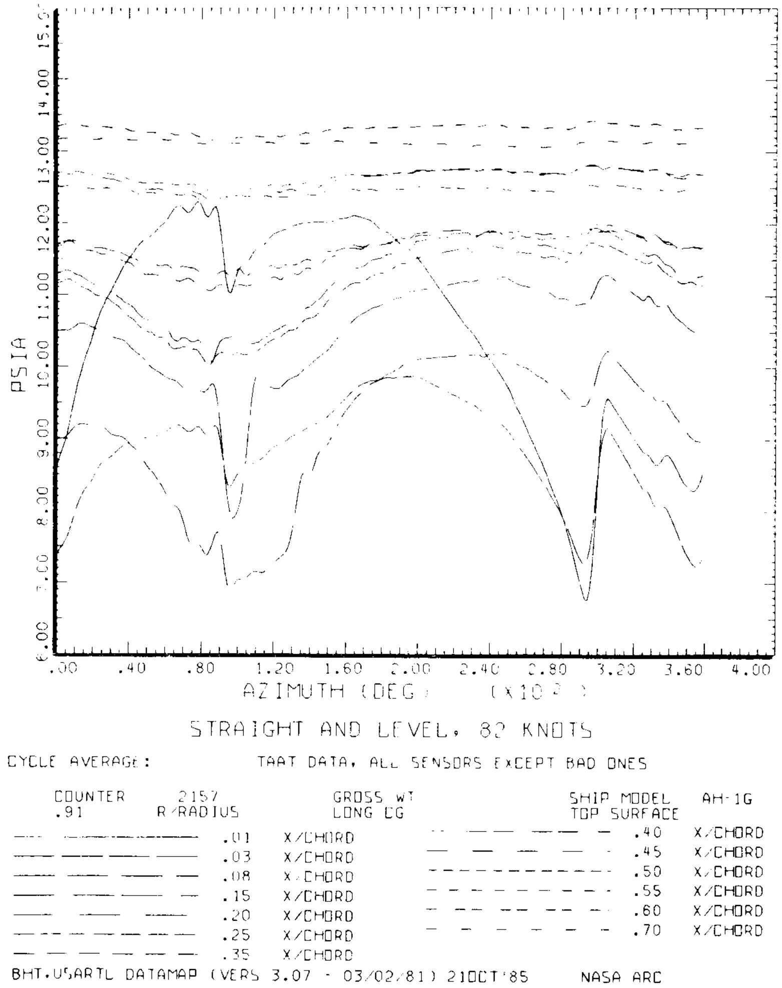

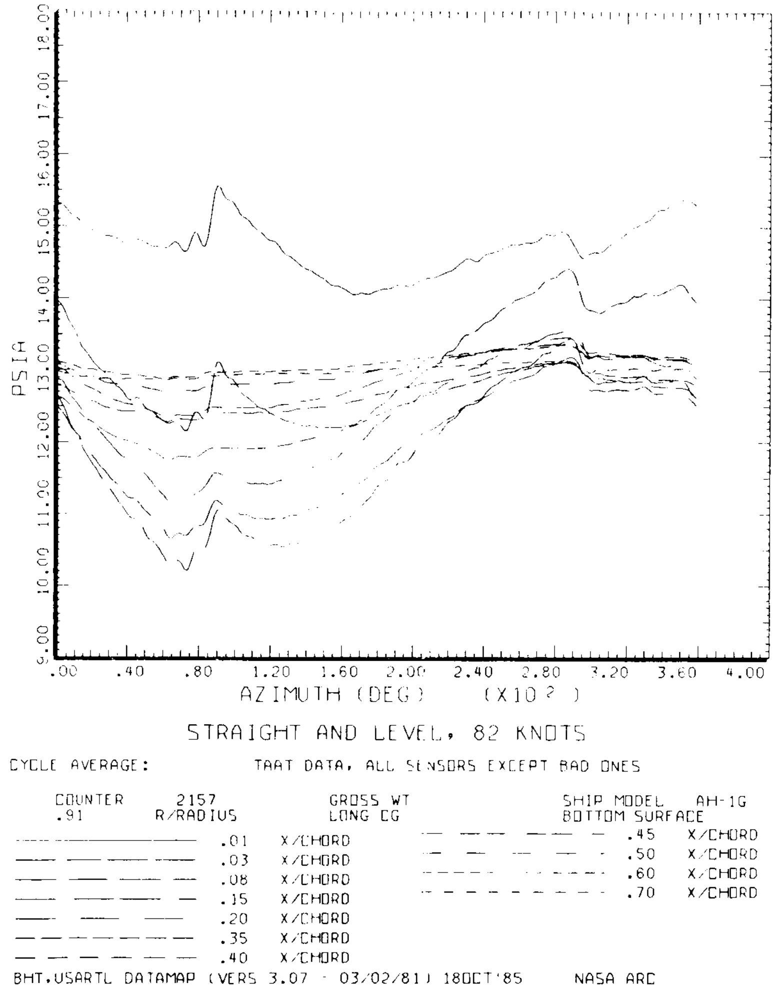

(e) At 91% radius pressure data.

Figure 38.- Continued.

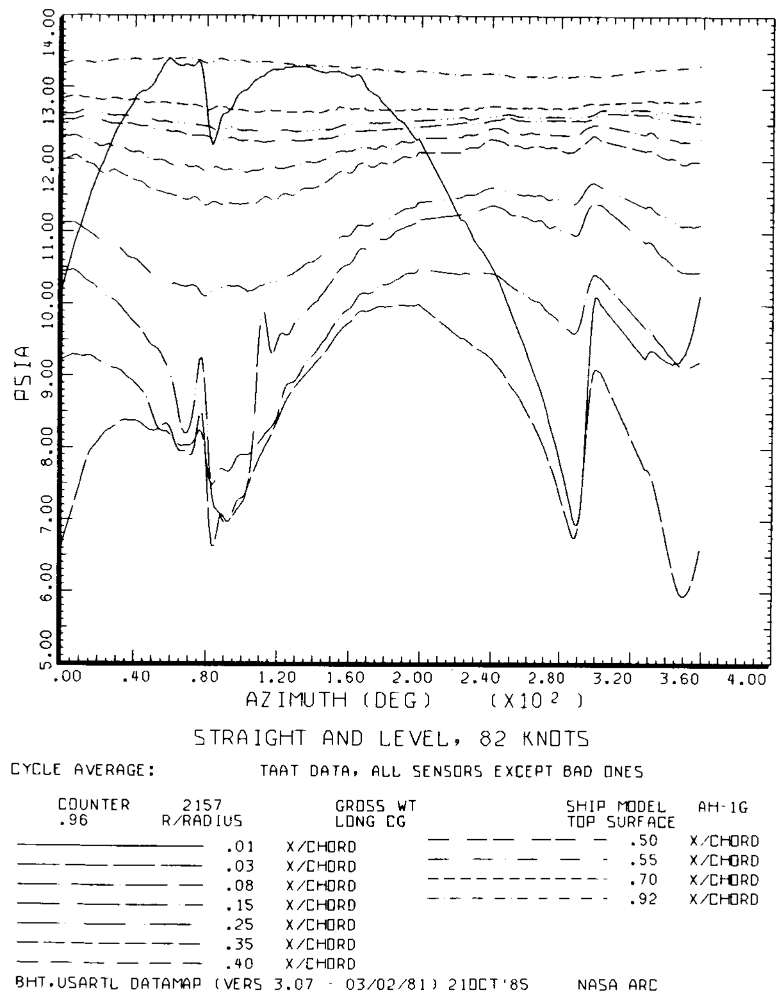

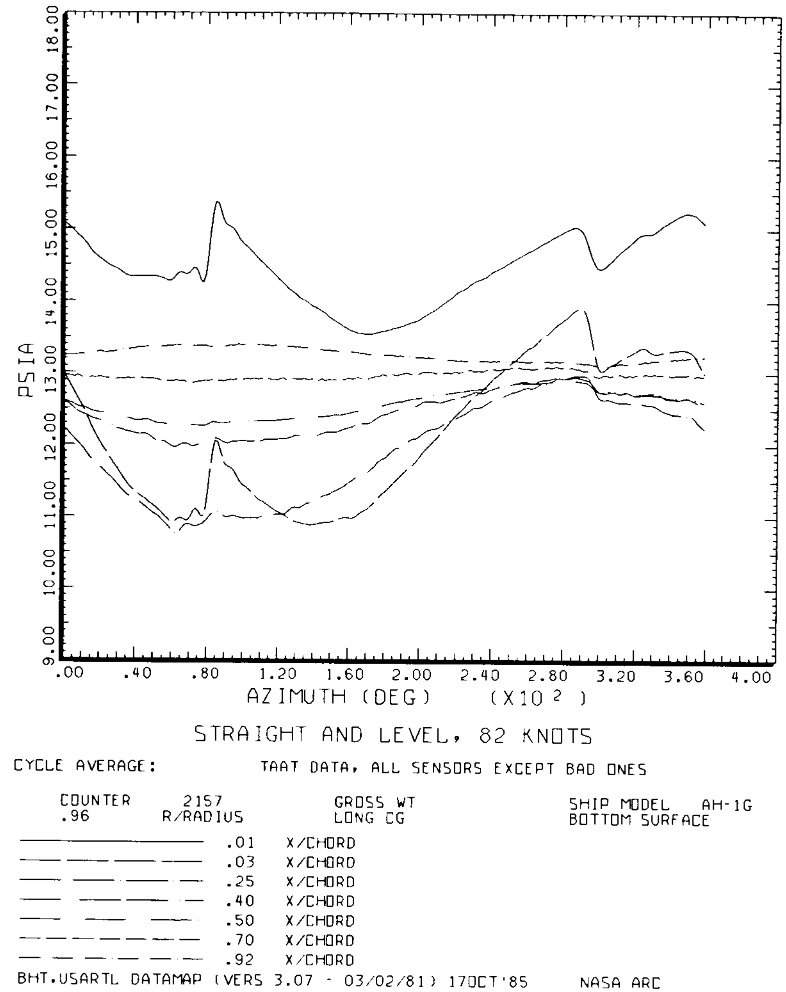

(f) At 96% radius pressure data.

Figure 38.- Continued.

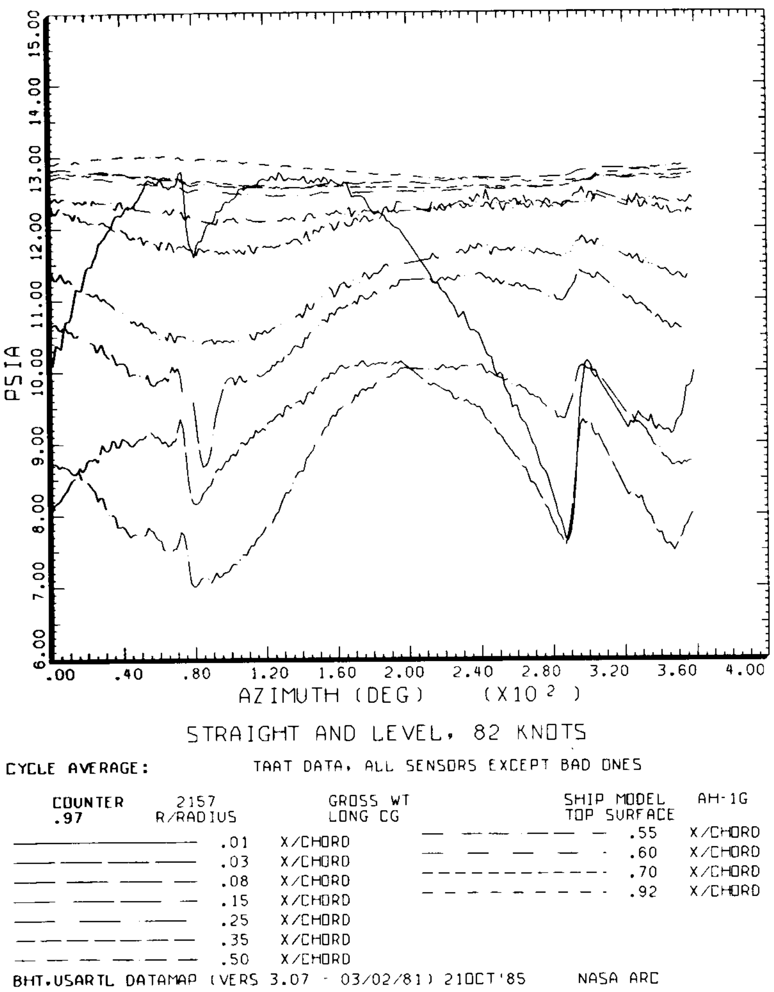

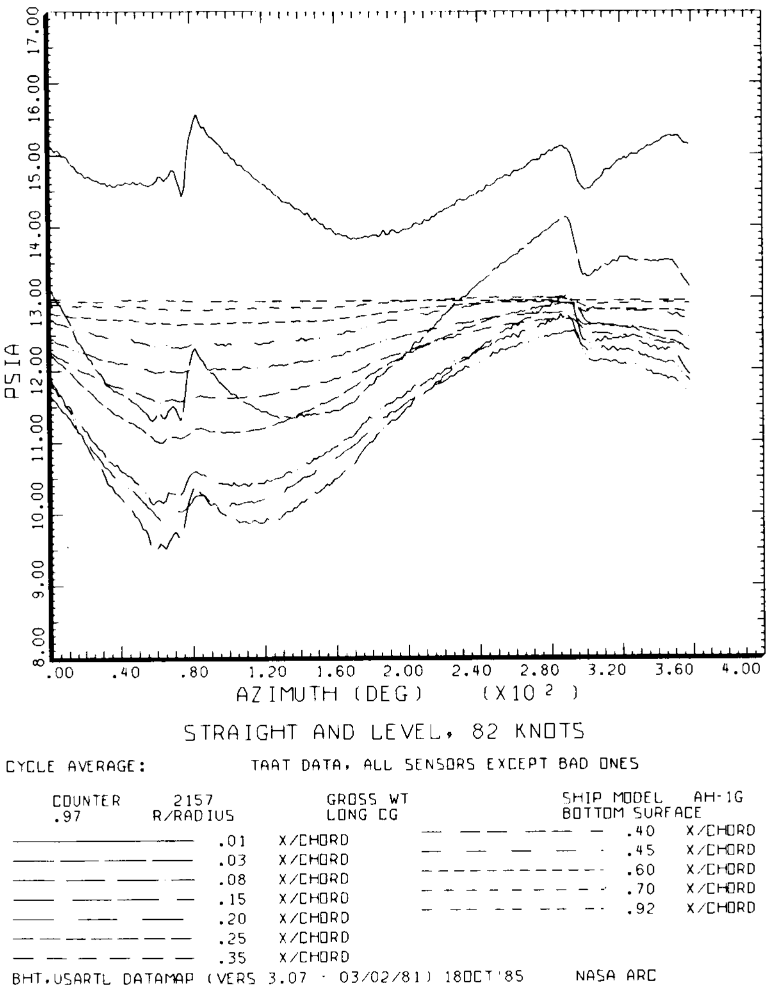

(g) At 97% radius pressure data.

Figure 38.- Continued.

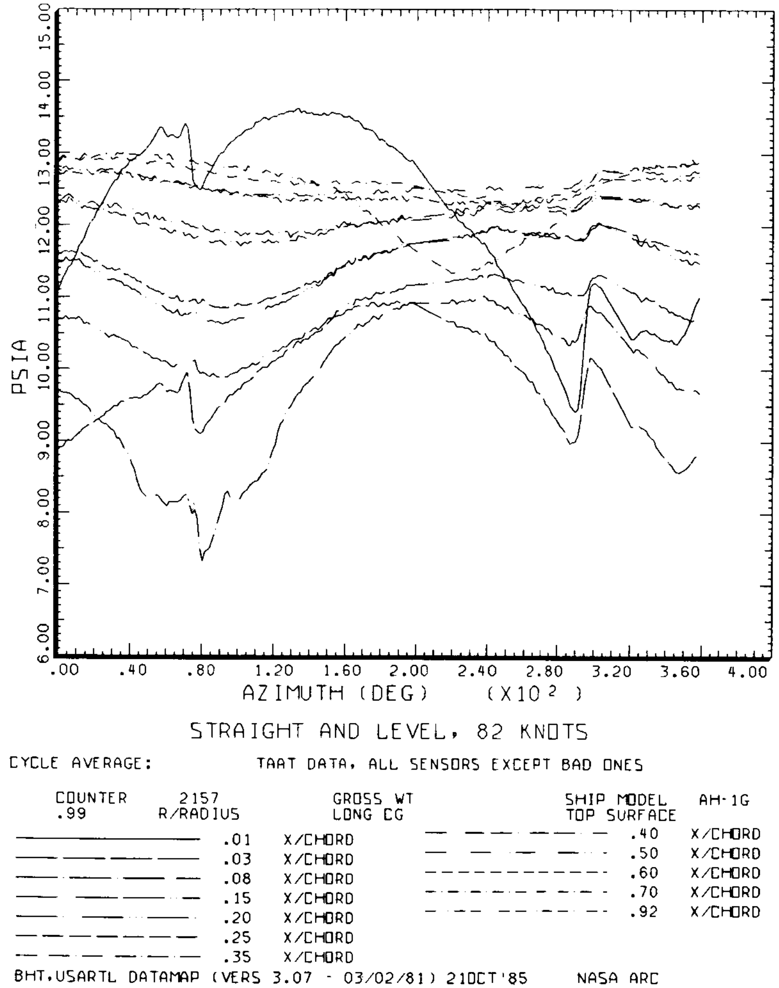

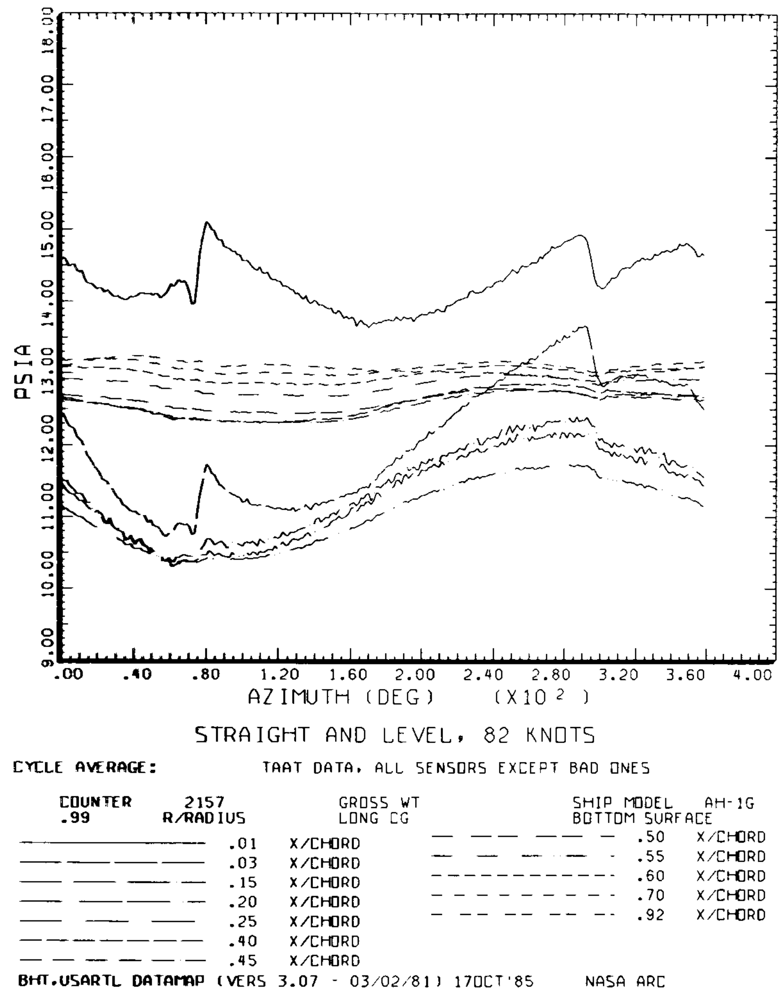

(h) At 99% radius pressure data.

Figure 38.- Concluded.

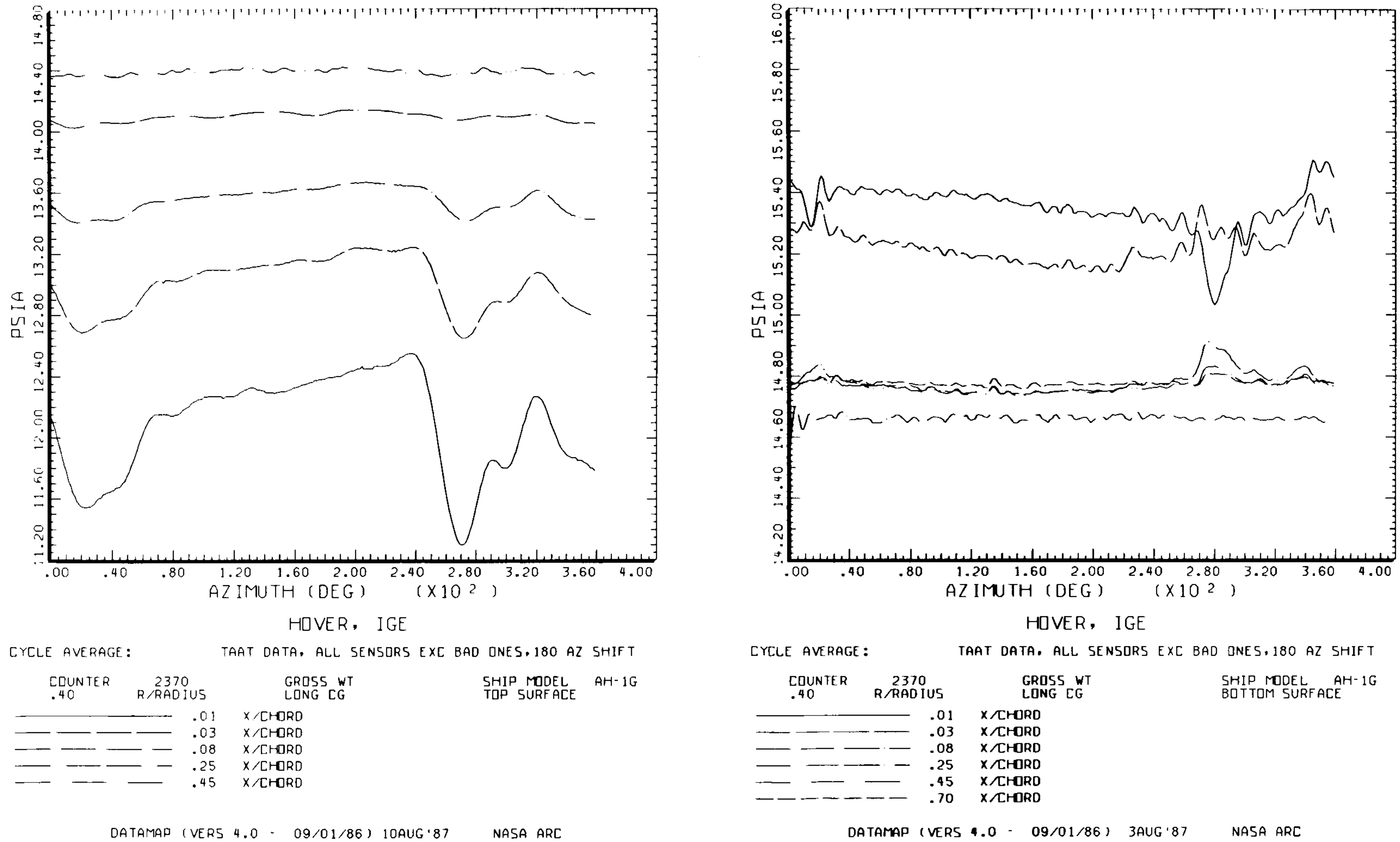

(a) At 40% radius Pressure data.

Figure 39.- Blade pressure versus rotor azimuth in hover.

ORIGINAL PAGE IS
OF POOR QUALITY

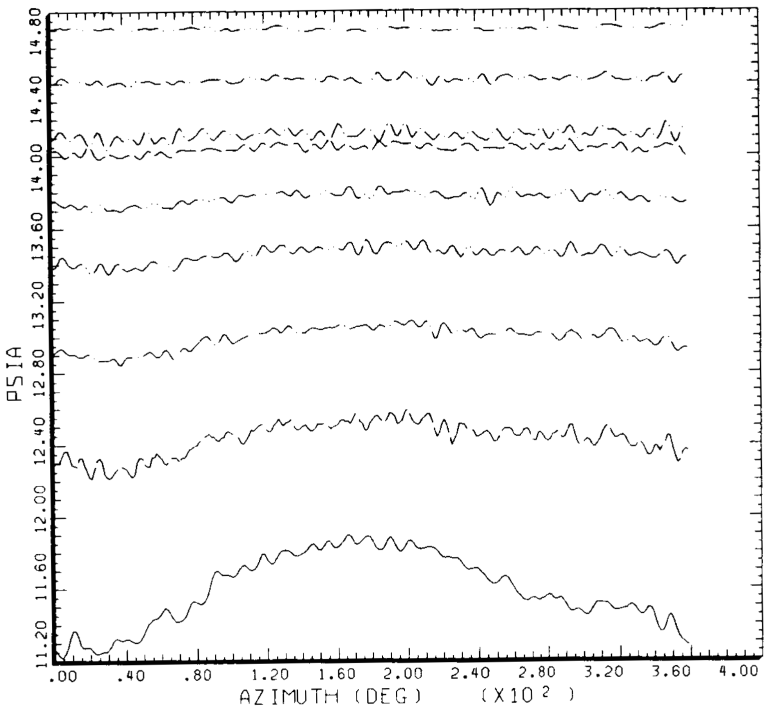

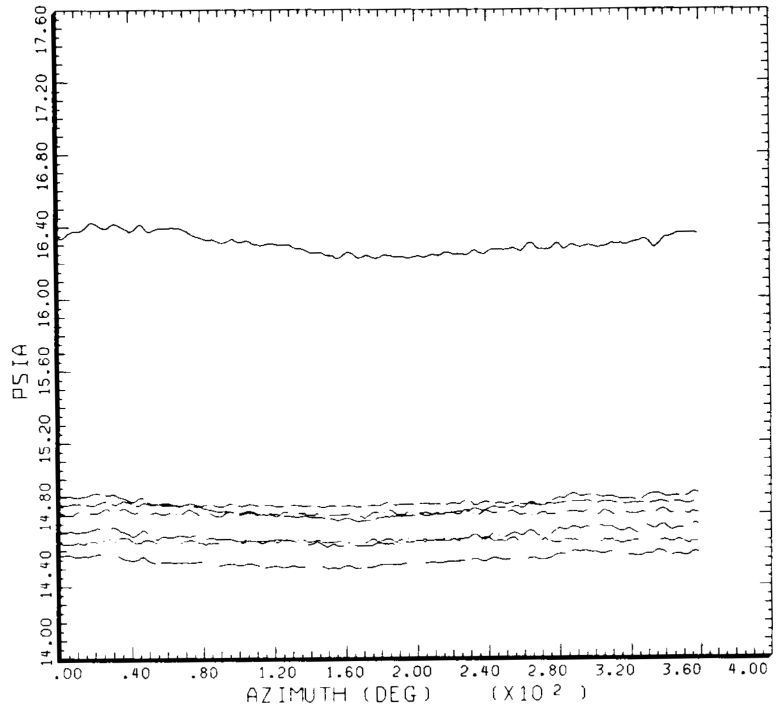

(b) At 60% radius pressure data.

Figure 39.- Continued.

ORIGINAL PAGE IS OF POOR QUALITY

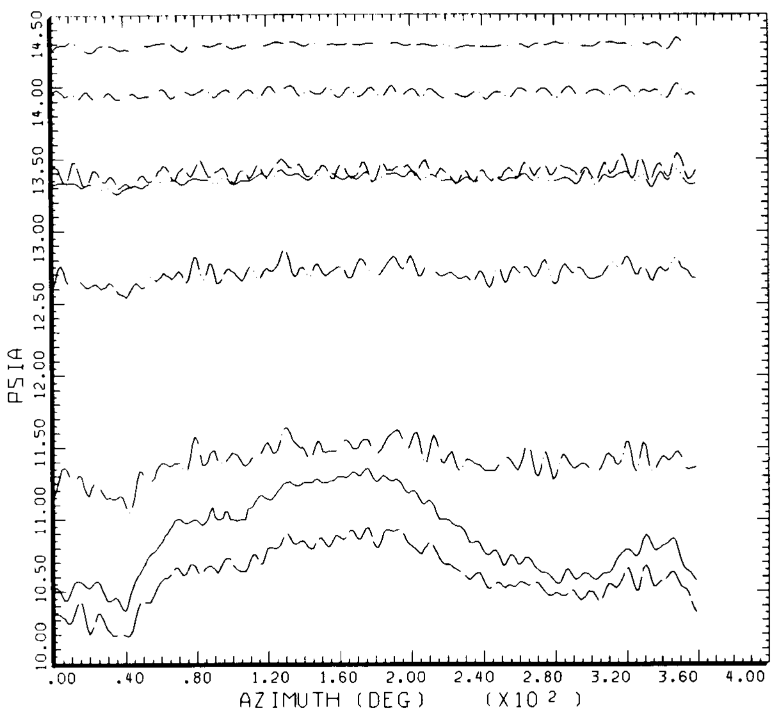

HOVER, IGE

CYCLE AVERAGE: TAAT DATA. ALL SENSORS EXC BAD ONES.180 AZ SHIFT

COUNTER .75 | 2370 R/RADIUS | GROSS WT LONG CG | SHIP MODEL TOP SURFACE AH-1G

.01 X/CHORD
.03 X/CHORD
.08 X/CHORD
.25 X/CHORD
.35 X/CHORD
.40 X/CHORD
.55 X/CHORD
.70 X/CHORD

DATAMAP (VERS 4.0 - 09/01/86) 10AUG'87 NASA ARC

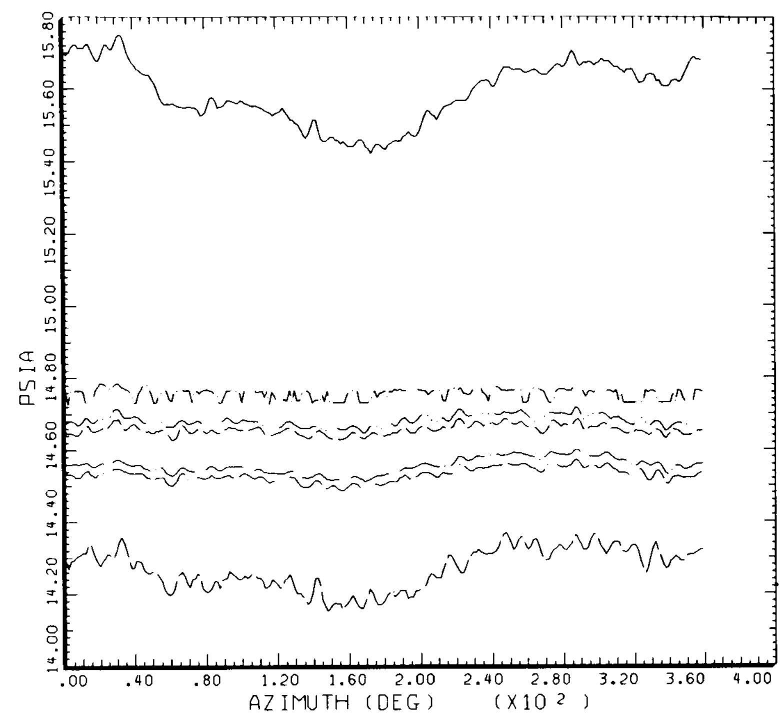

HOVER, IGE

CYCLE AVERAGE: TAAT DATA. ALL SENSORS EXC BAD ONES.180 AZ SHIFT

COUNTER .75 | 2370 R/RADIUS | GROSS WT LONG CG | SHIP MODEL BOTTOM SURFACE AH-1G

.03 X/CHORD
.15 X/CHORD
.40 X/CHORD
.45 X/CHORD
.55 X/CHORD
.70 X/CHORD
.92 X/CHORD

DATAMAP (VERS 4.0 - 09/01/86) 3AUG'87 NASA ARC

(c) At 75% radius pressure data.

Figure 39.- Continued.

ORIGINAL PAGE IS OF POOR QUALITY

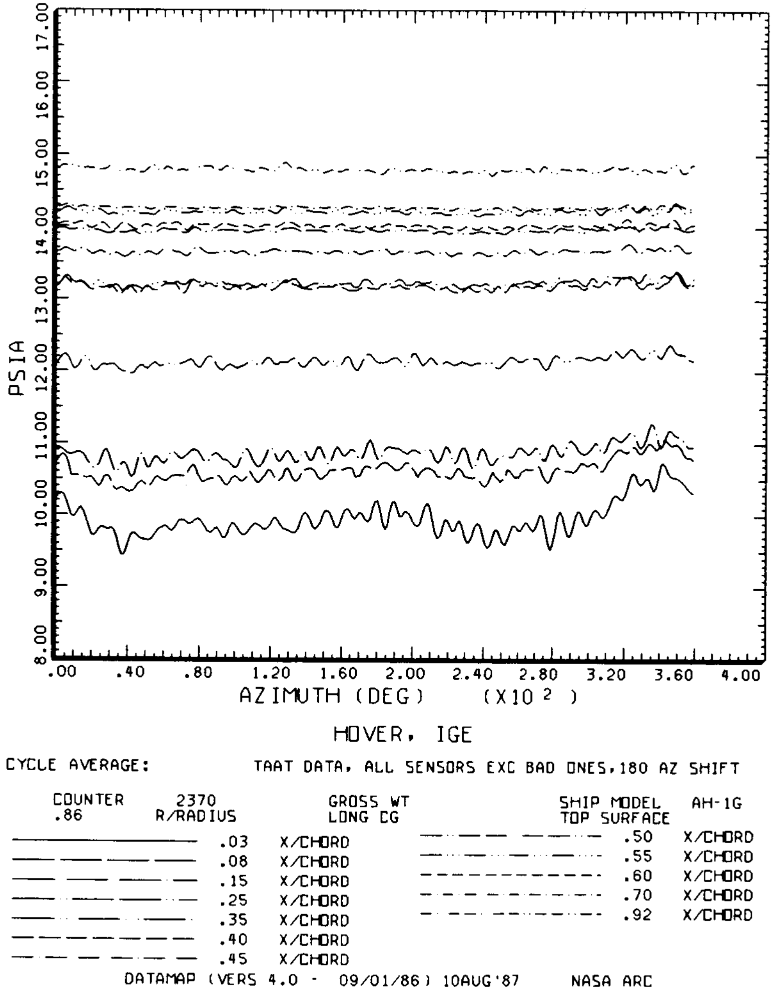

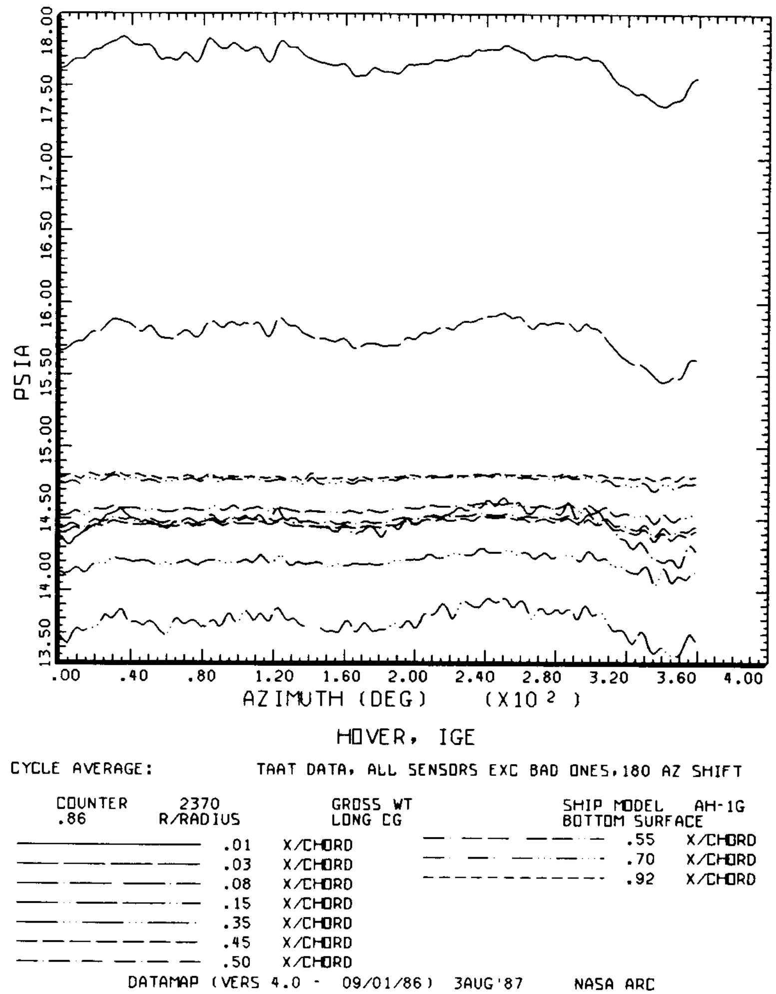

ORIGINAL PAGE IS OF POOR QUALITY

(d) At 86% radius pressure data.

Figure 39.- Continued.

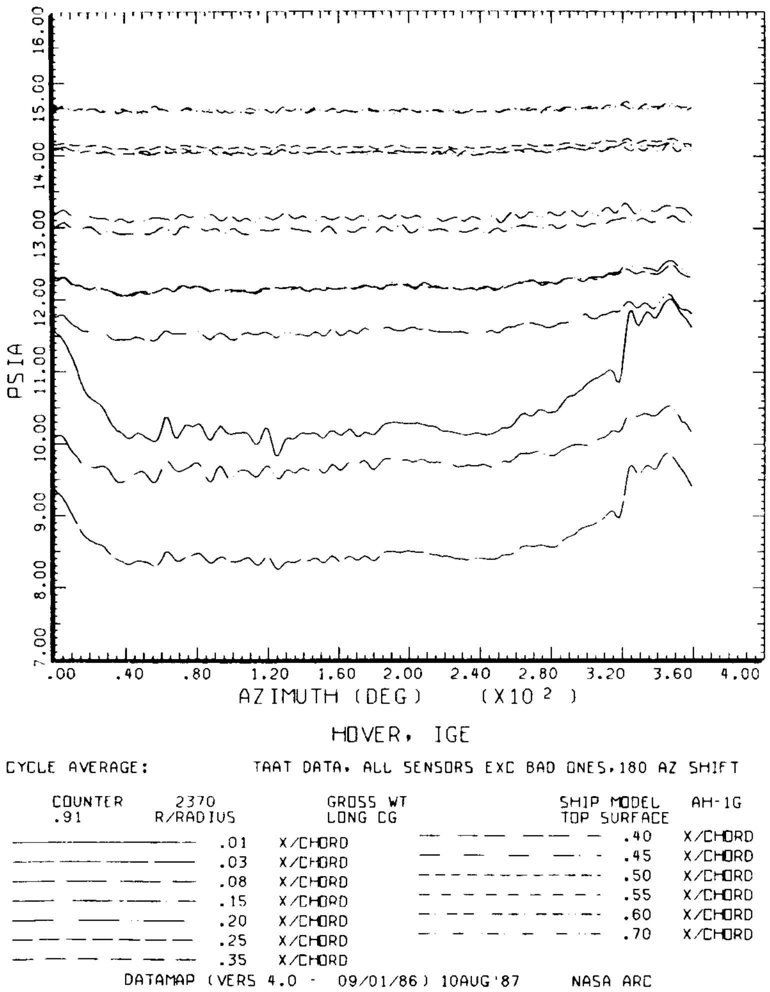

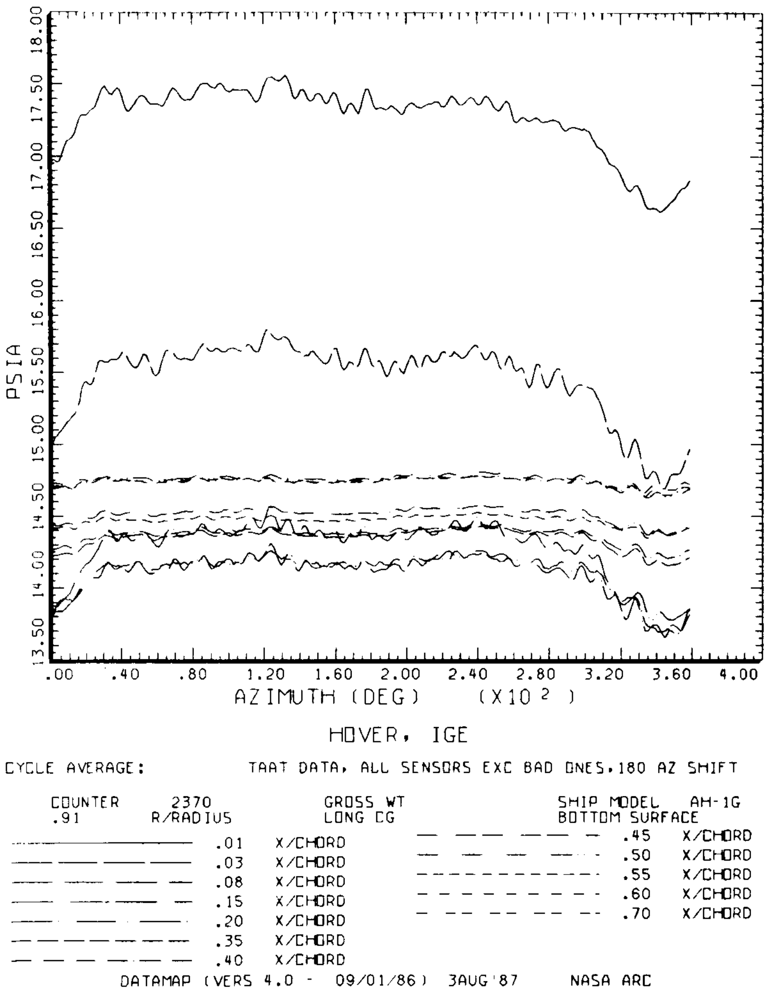

(e) At 91% radius pressure data.

Figure 39.- Continued.

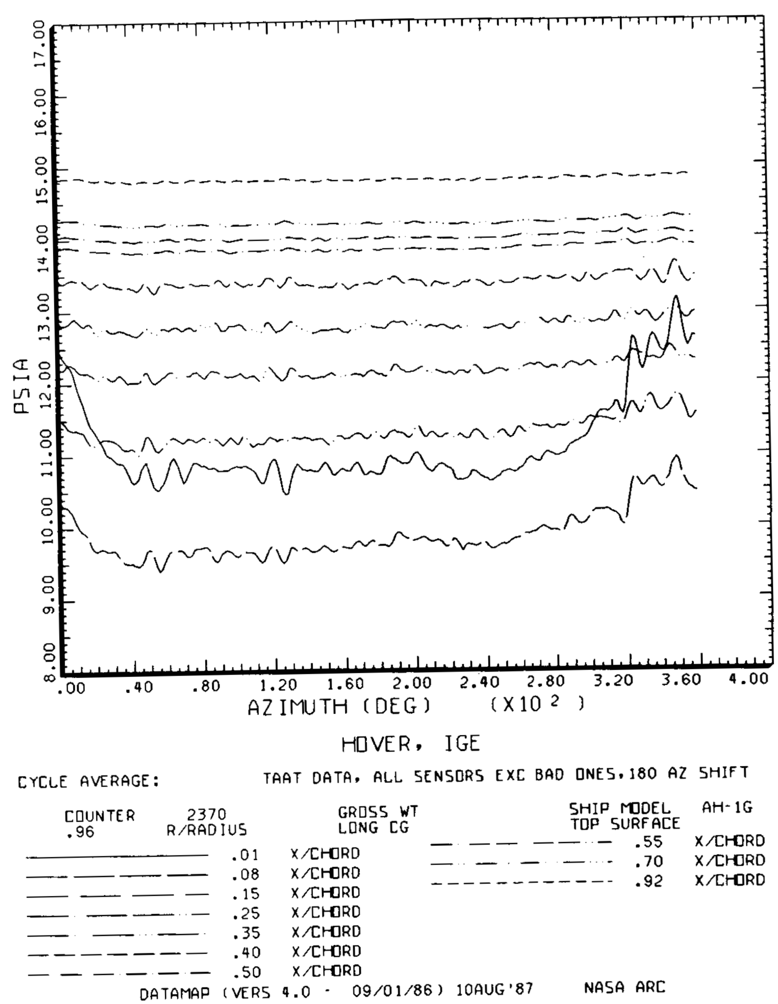

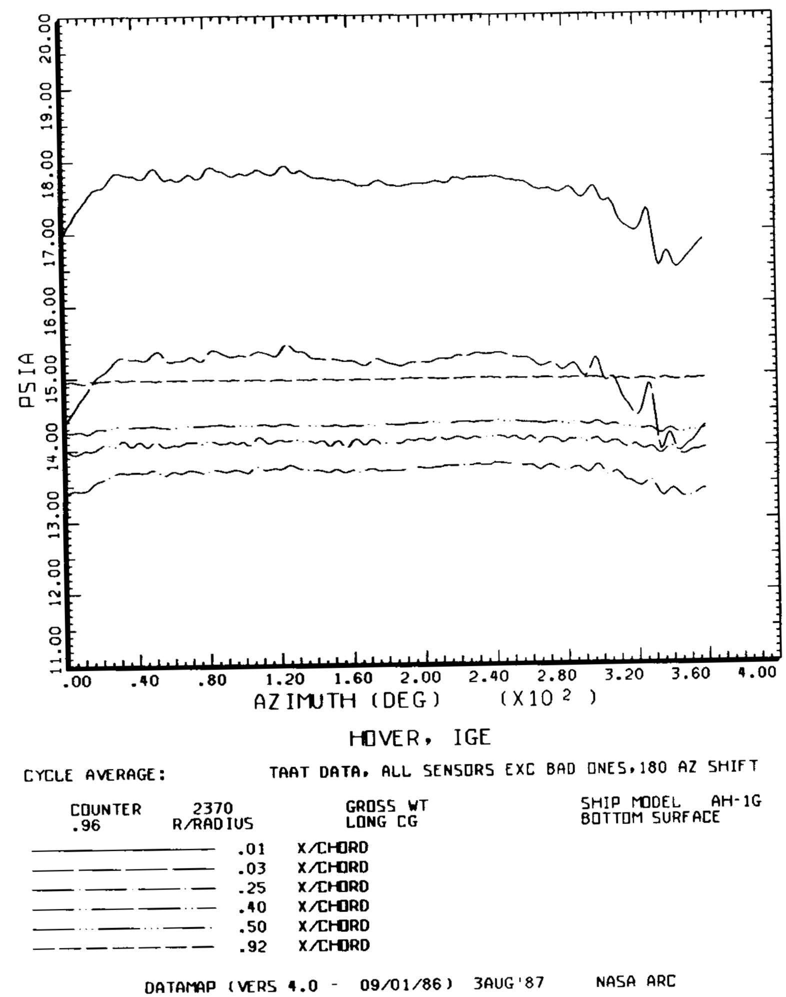

(f) At 96% radius pressure data.

Figure 39.- Continued.

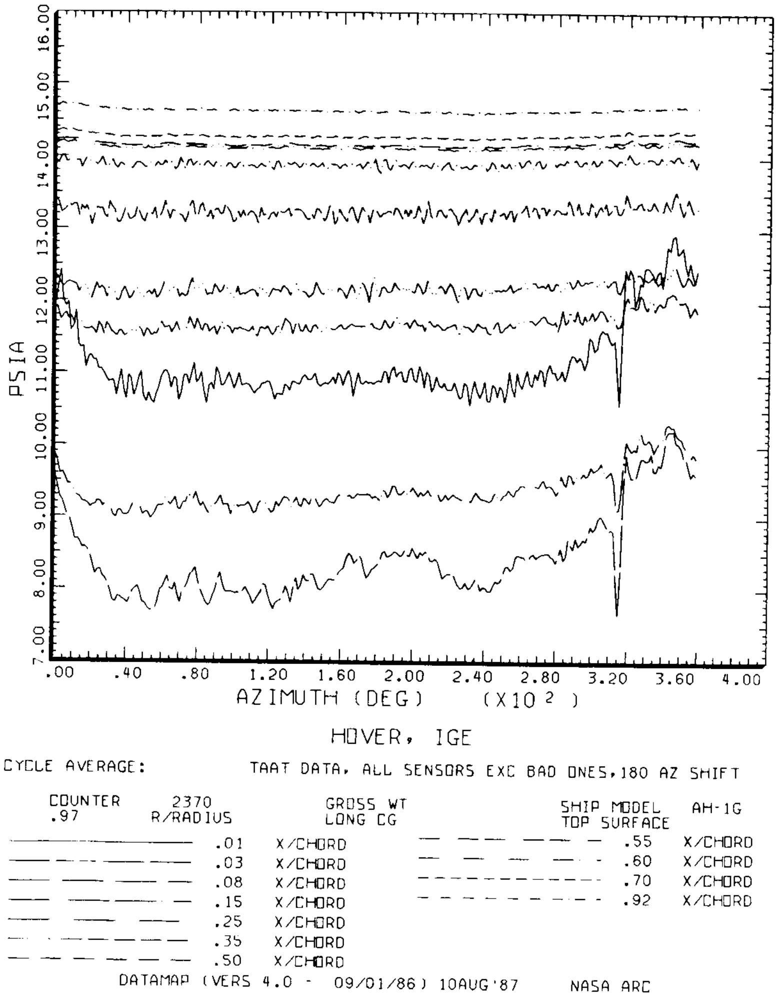

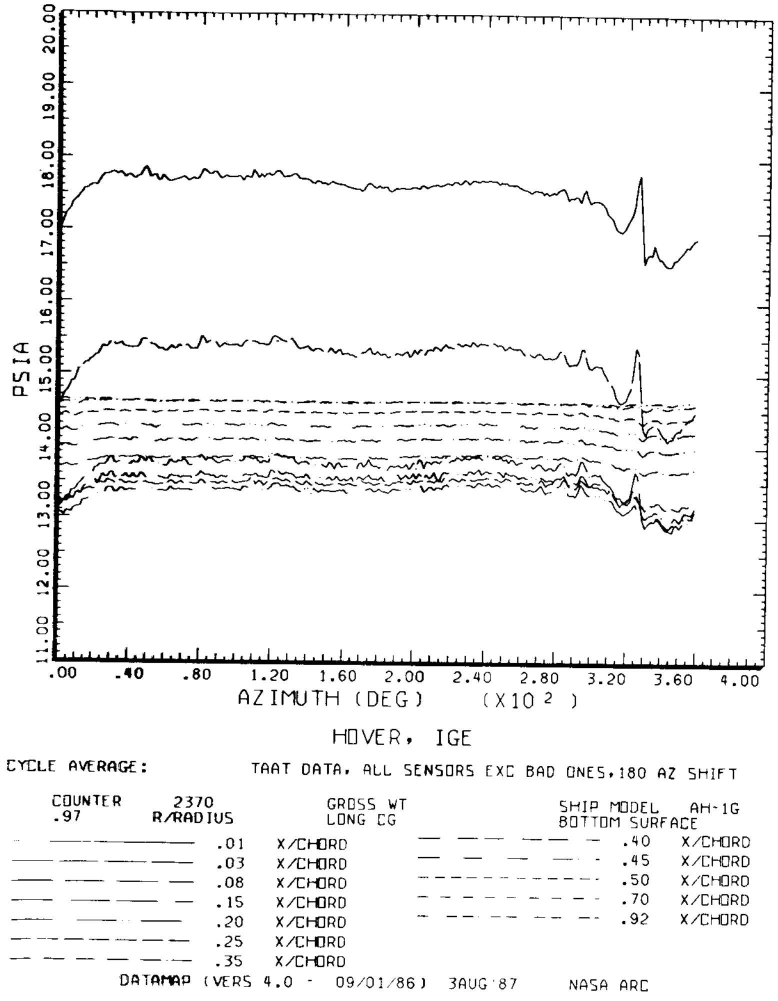

(g) At 97% radius pressure data.

Figure 39.- Continued.

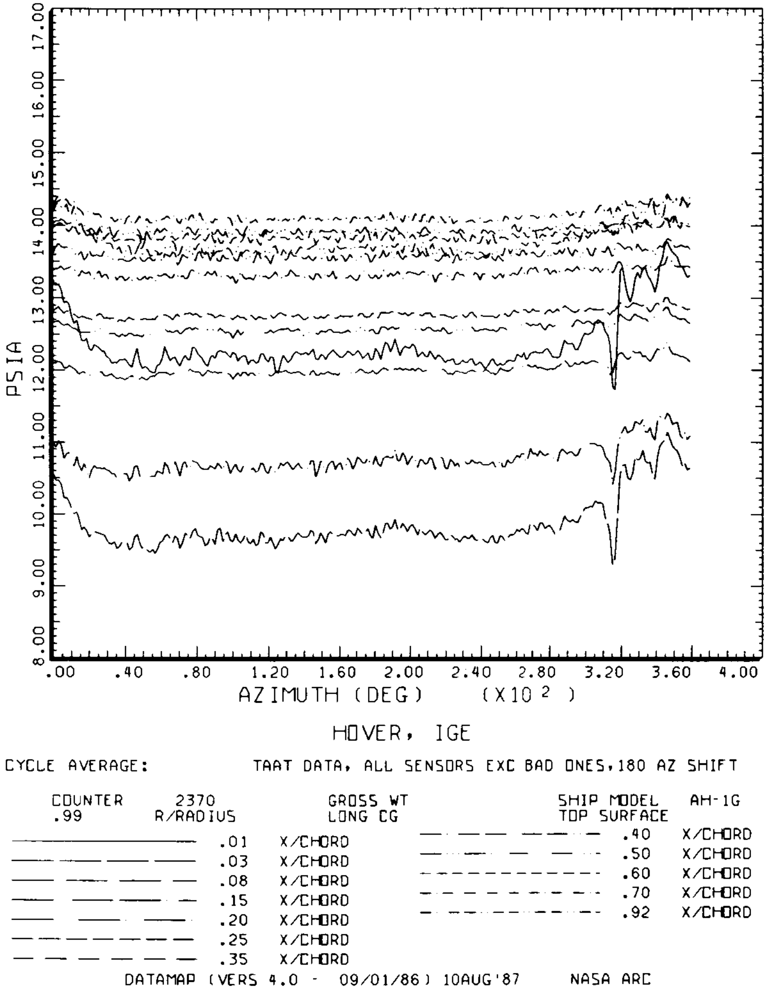

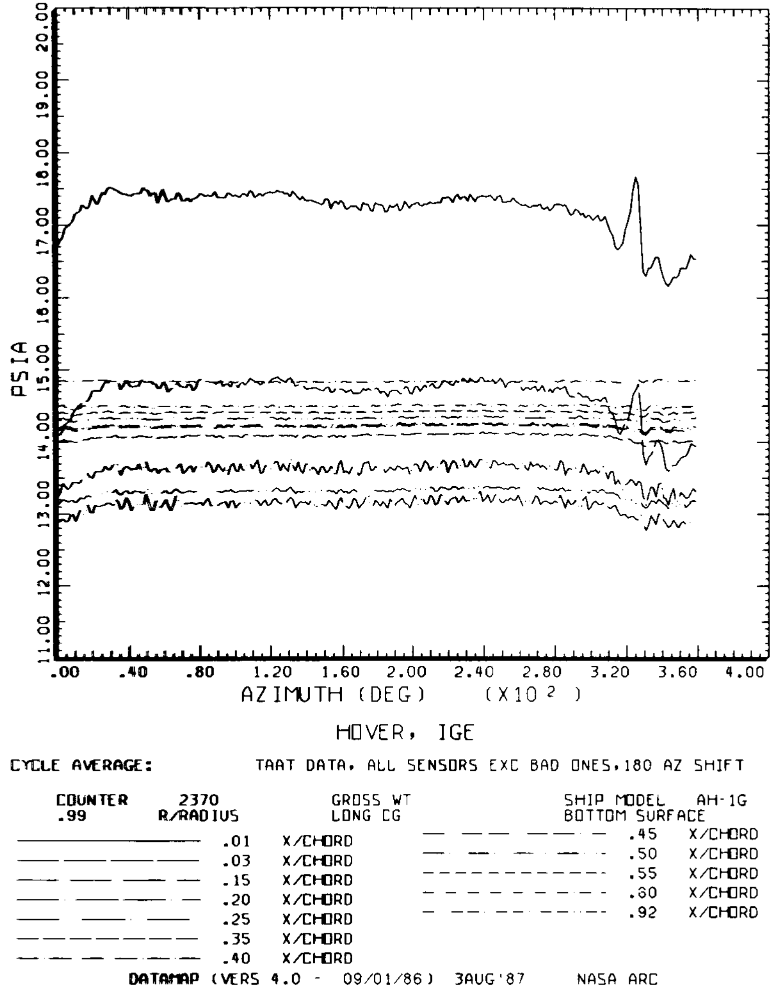

(h) At 99% radius pressure data.

Figure 39.- Concluded.

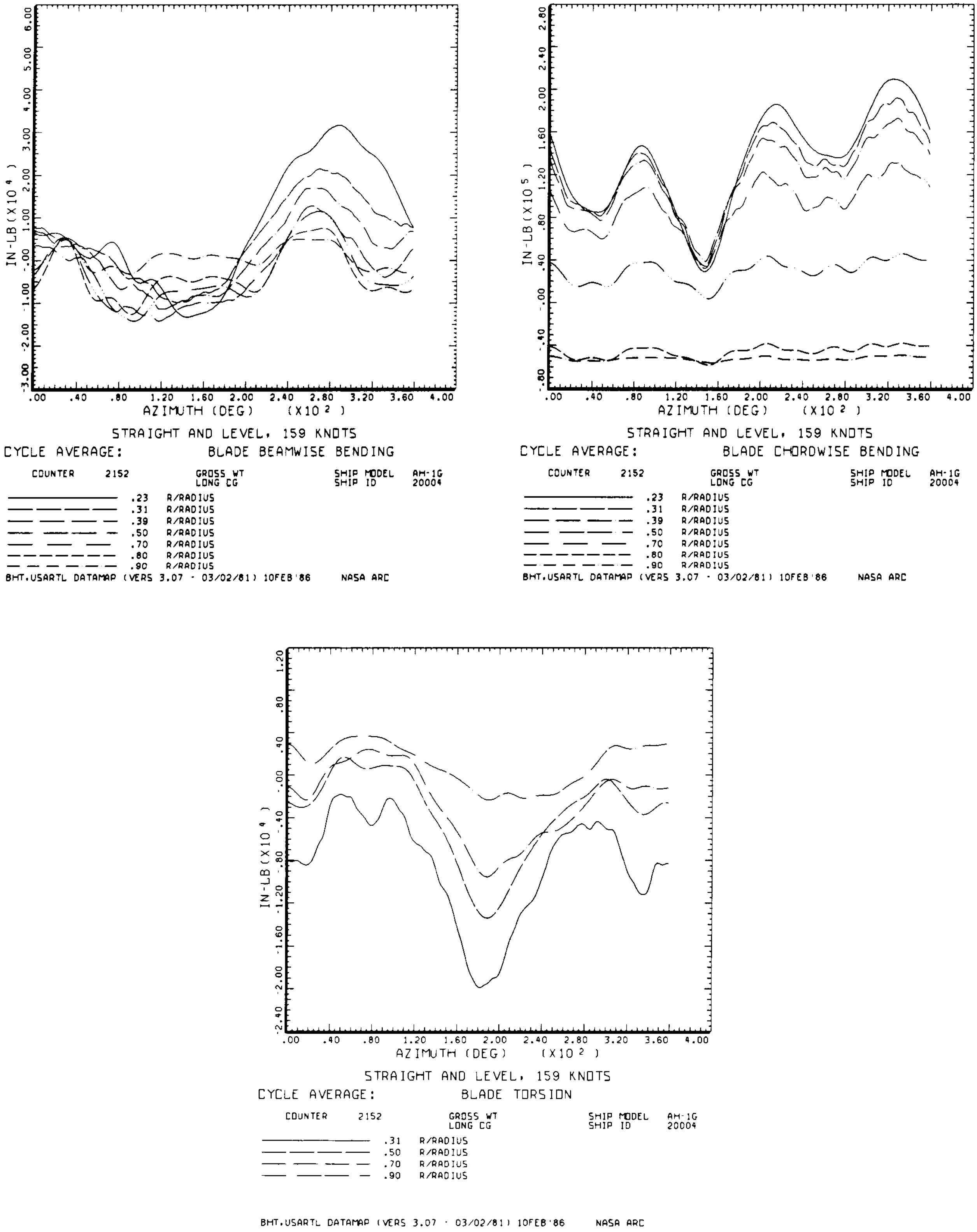

Figure 40.- Blade loads versus azimuth at 159 KTAS. (a) Beamwise strain-gage data; (b) chordwise strain-gage data; (c) torsion strain-gage data.

ORIGINAL PAGE IS
OF POOR QUALITY

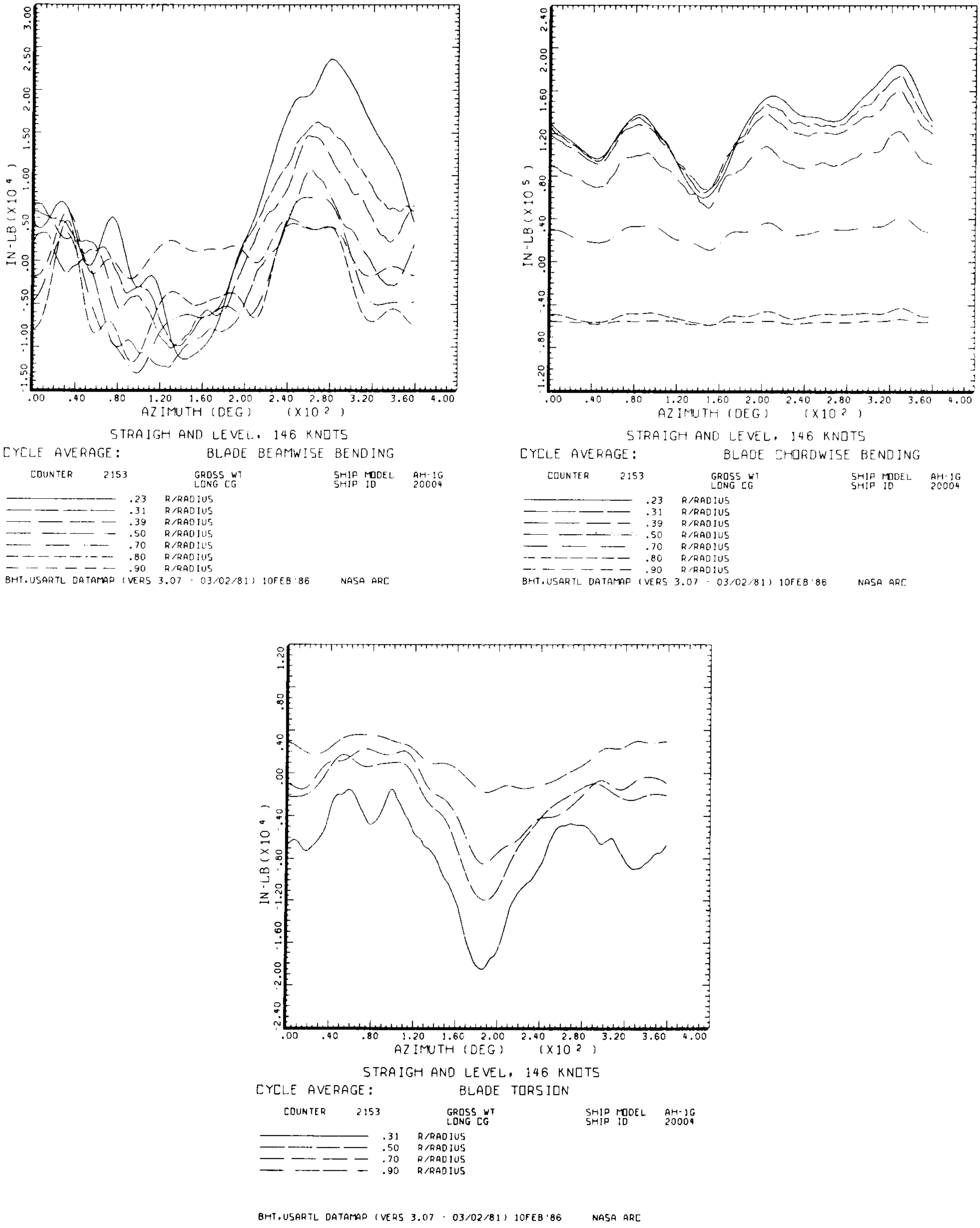

Figure 41.- Blade loads versus azimuth at 146 KTAS. (a) Beamwise strain-gage data; (b) chordwise strain-gage data; (c) torsion strain-gage data.

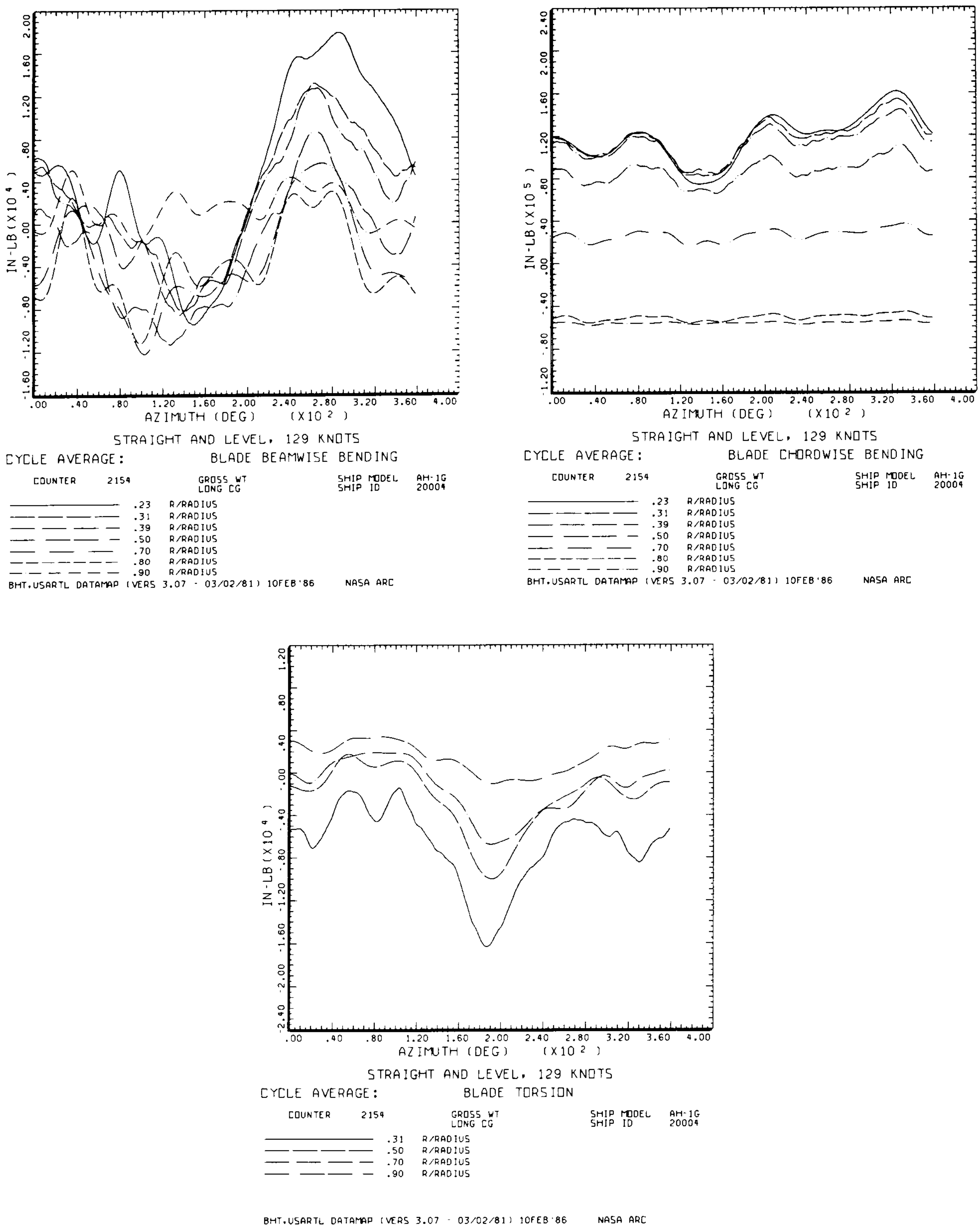

Figure 42.- Blade loads versus azimuth at 129 KTAS. (a) Beamwise strain-gage data; (b) chordwise strain-gage data; (c) torsion strain-gage data.

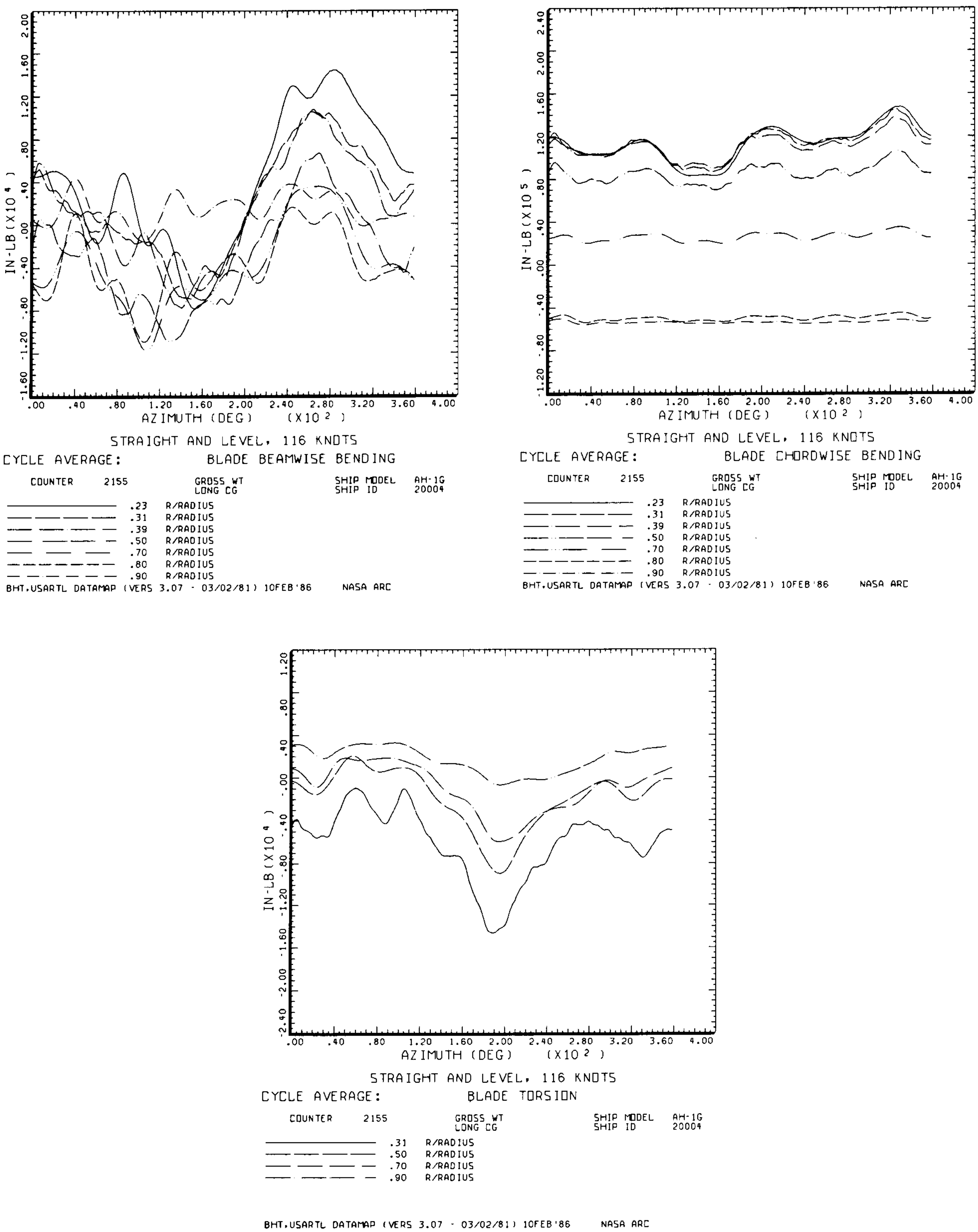

Figure 43.- Blade load versus azimuth at 116 KTAS. (a) Beamwise strain-gage data; (b) chordwise strain-gage data; (c) torsion strain-gage data.

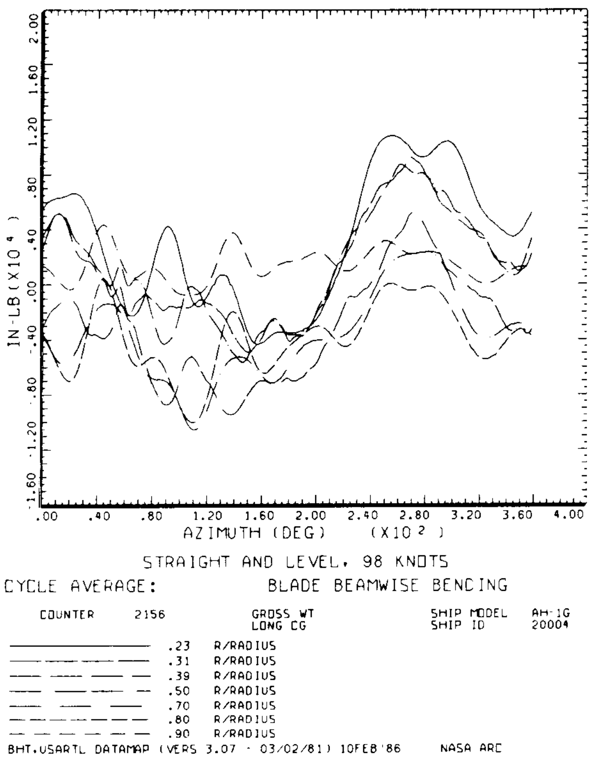

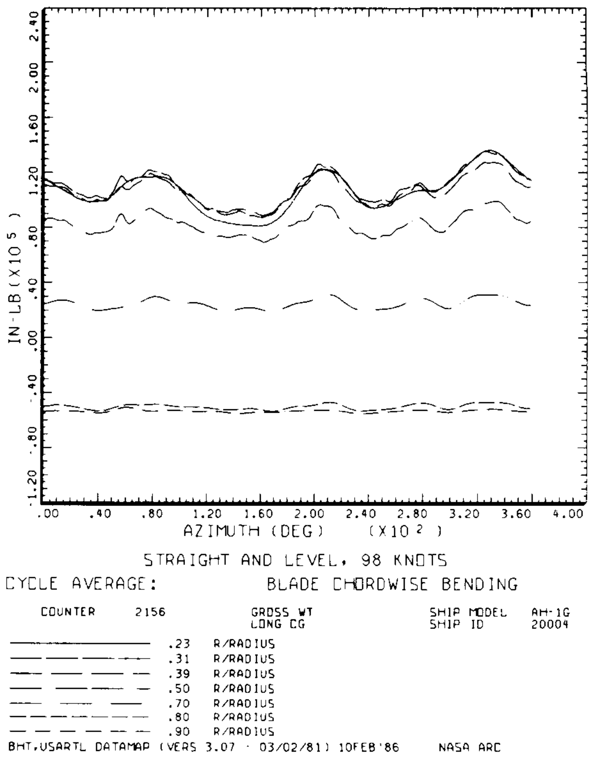

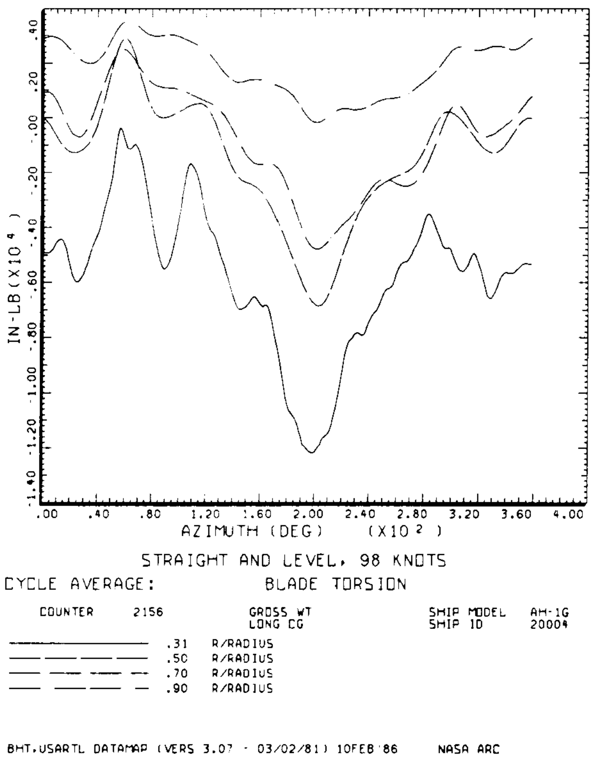

Figure 44.- Blade load versus azimuth at 98 KTAS. (a) Beamwise strain-gage data; (b) chordwise strain-gage data; (c) torsion strain-gage data.

ORIGINAL PAGE IS
OF POOR QUALITY

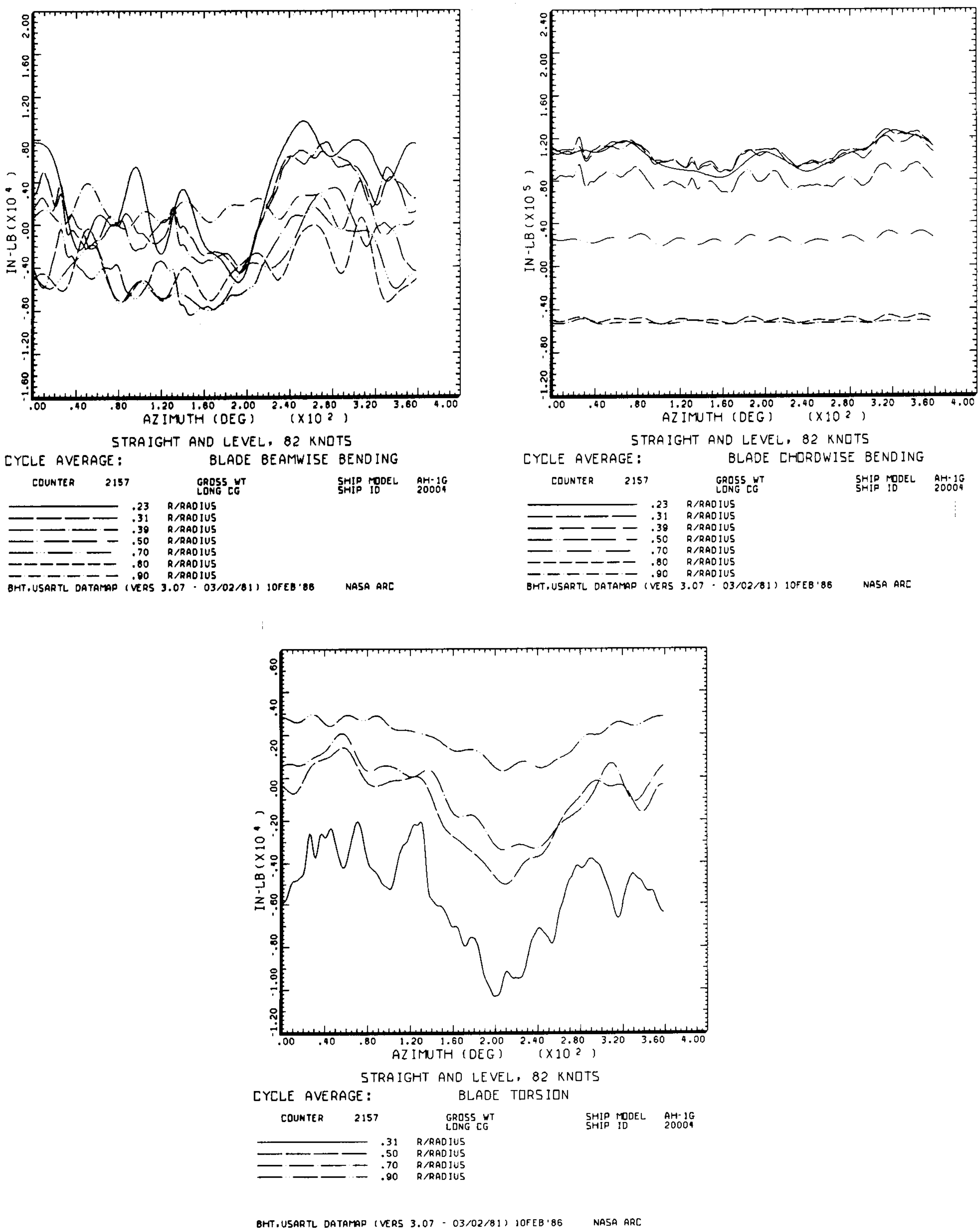

Figure 45.- Blade load versus azimuth at 82 KTAS. (a) Beamwise strain-gage data; (b) chordwise strain-gage data; (c) torsion strain-gage data.

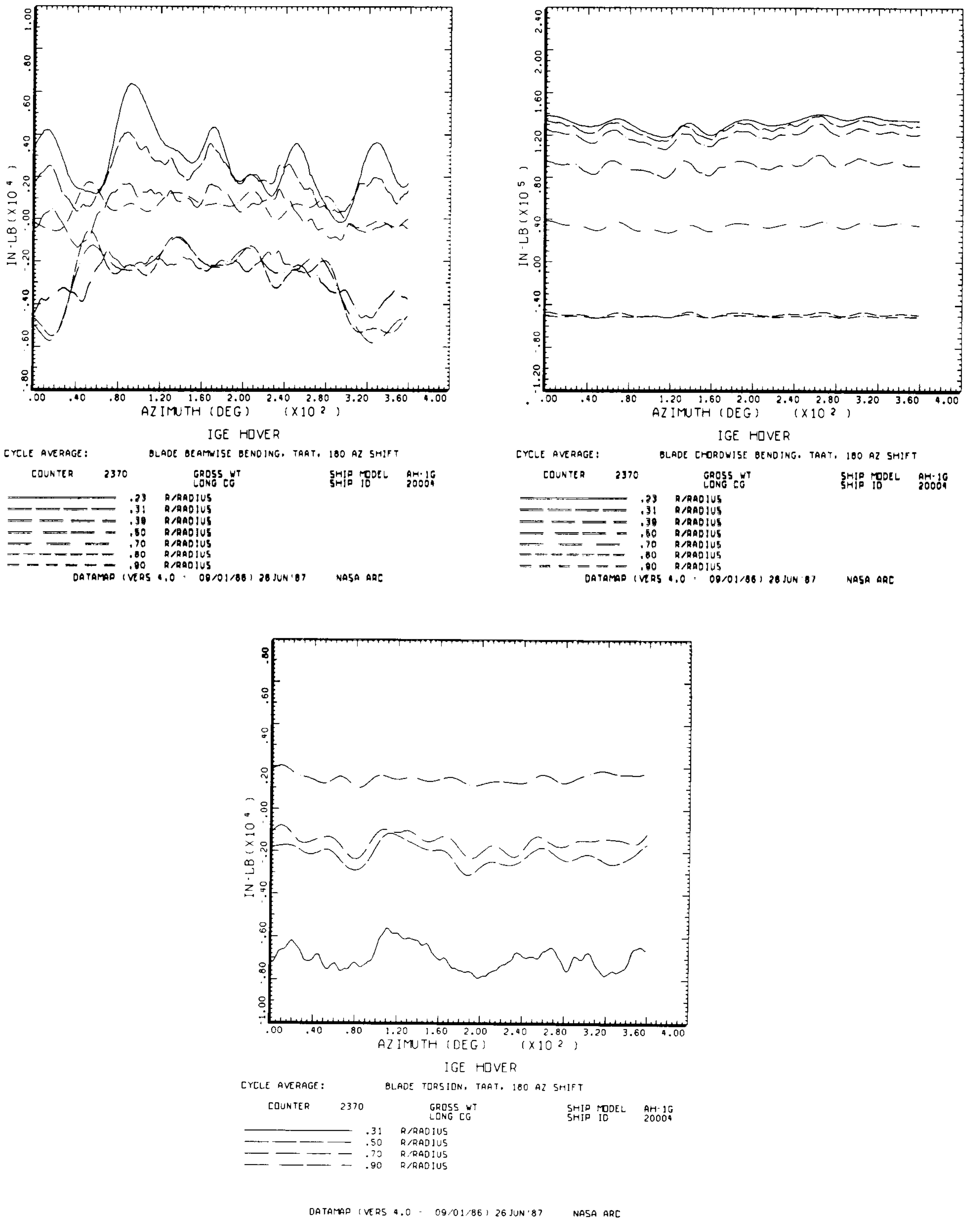

Figure 46.- Blade load versus azimuth in hover. (a) Beamwise strain-gage data; (b) chordwise strain-gage data; (c) torsion strain-gage data.

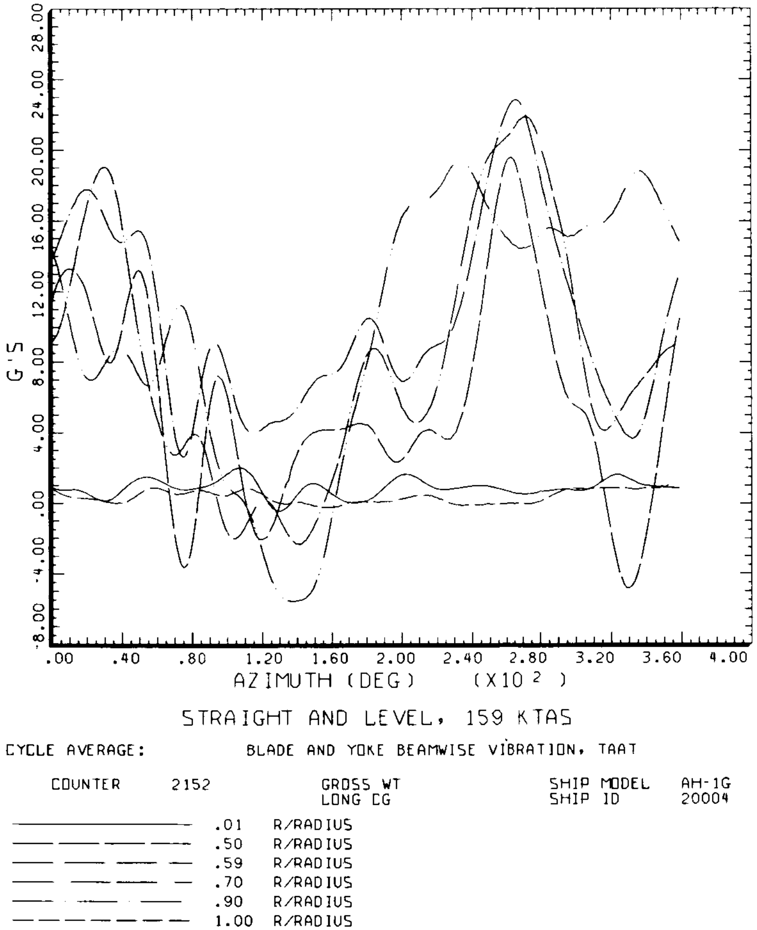

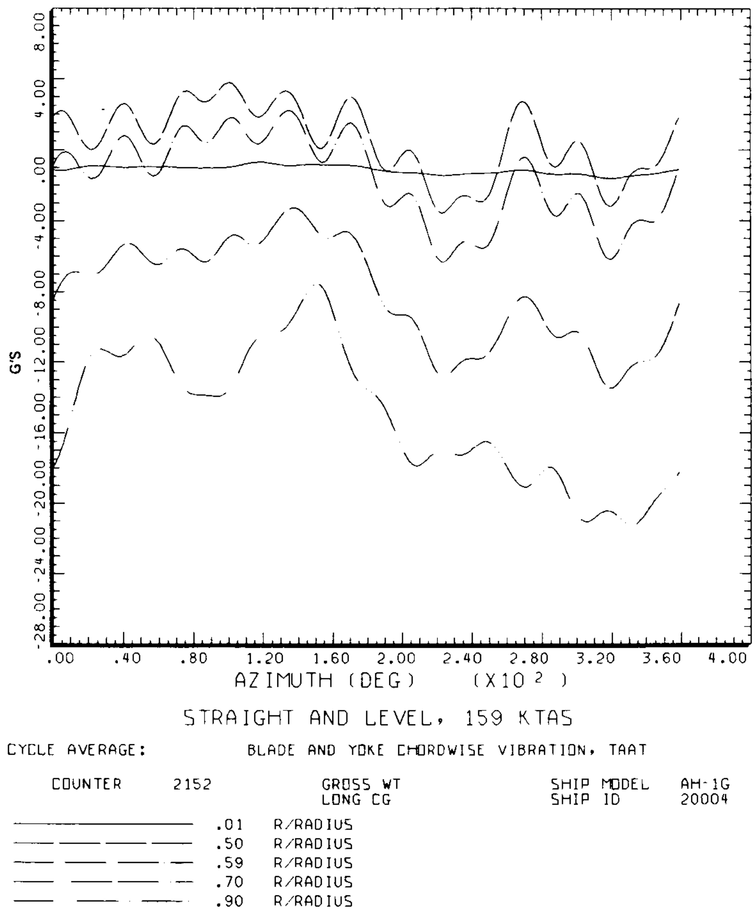

Figure 47.- Blade vibration versus azimuth at 159 KTAS. (a) Beamwise accelerometer data; (b) chordwise accelerometer data.

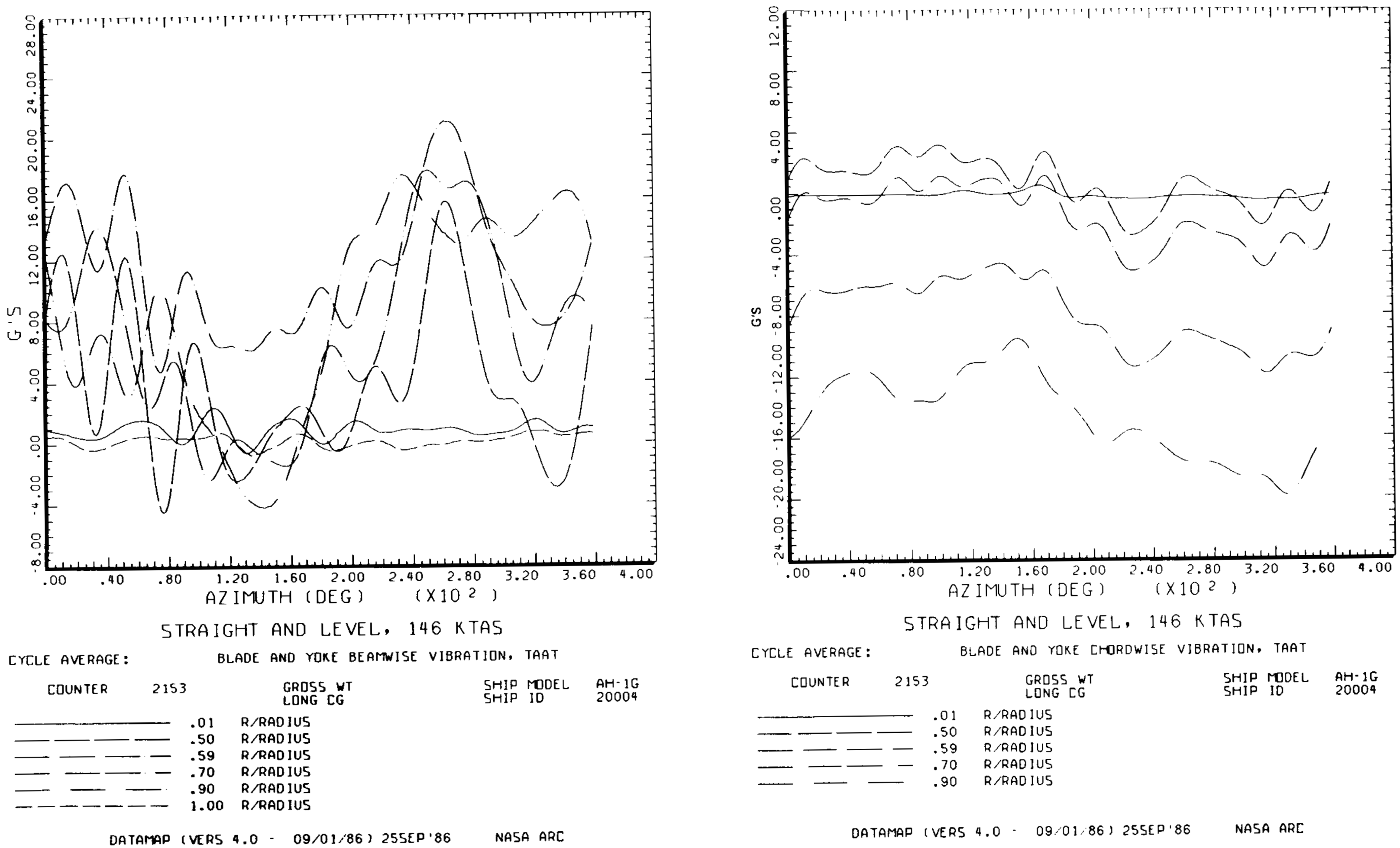

Figure 48.- Blade vibration versus azimuth at 146 KTAS. (a) Beamwise accelerometer data; (b) chordwise accelerometer data.

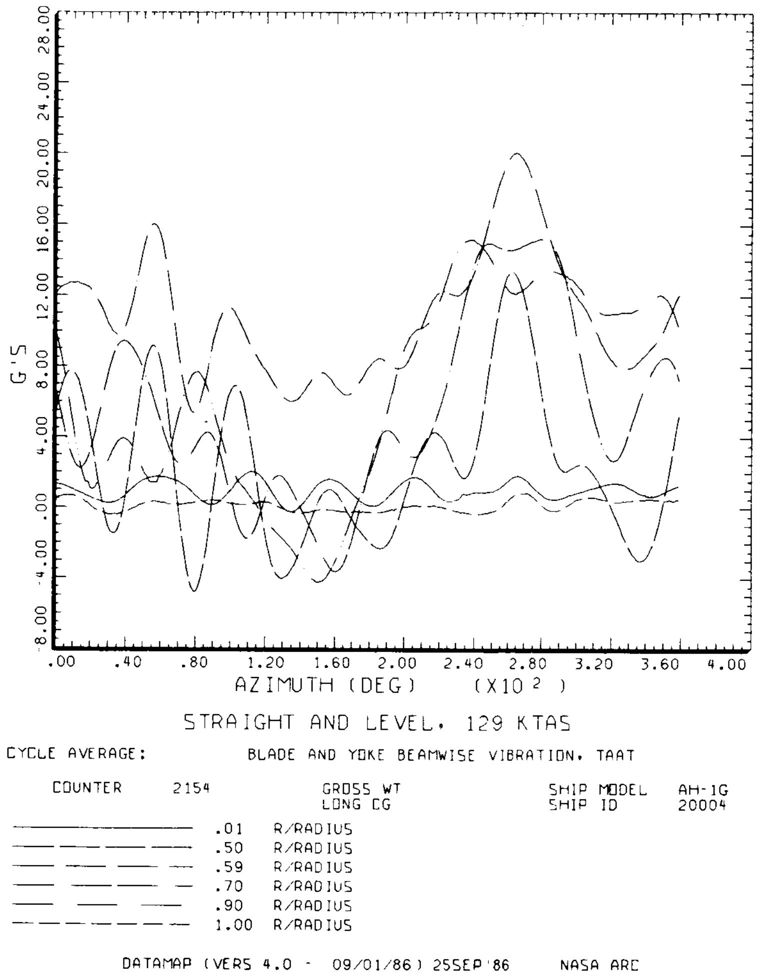

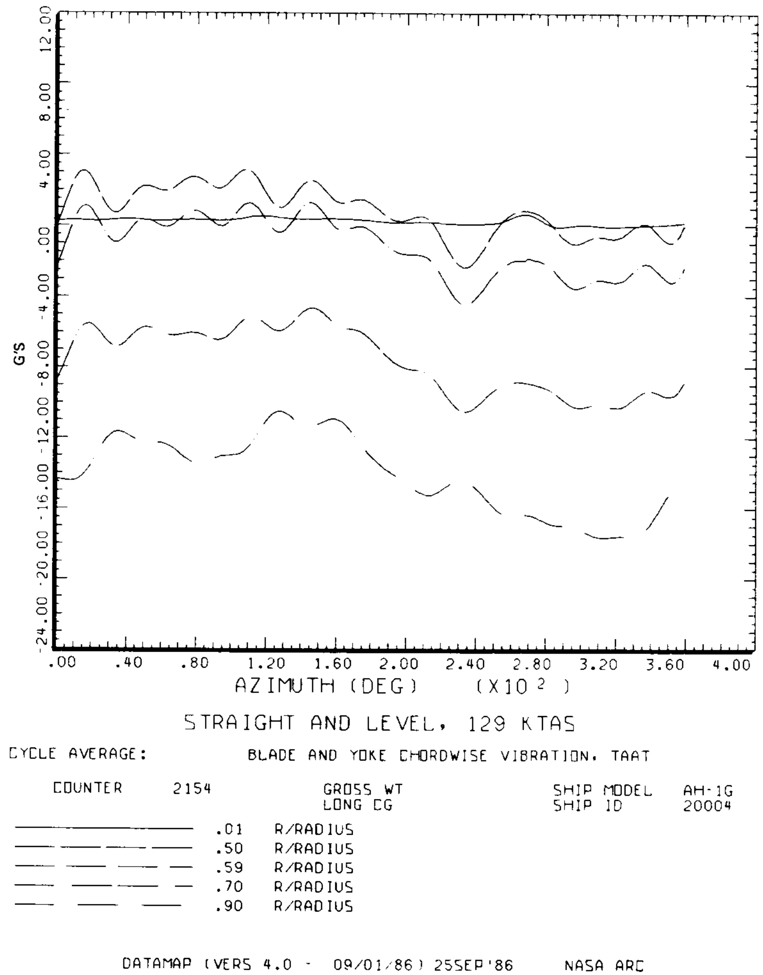

Figure 49.- Blade vibration versus azimuth at 129 KTAS. (a) Beamwise accelerometer data; (b) chordwise accelerometer data.

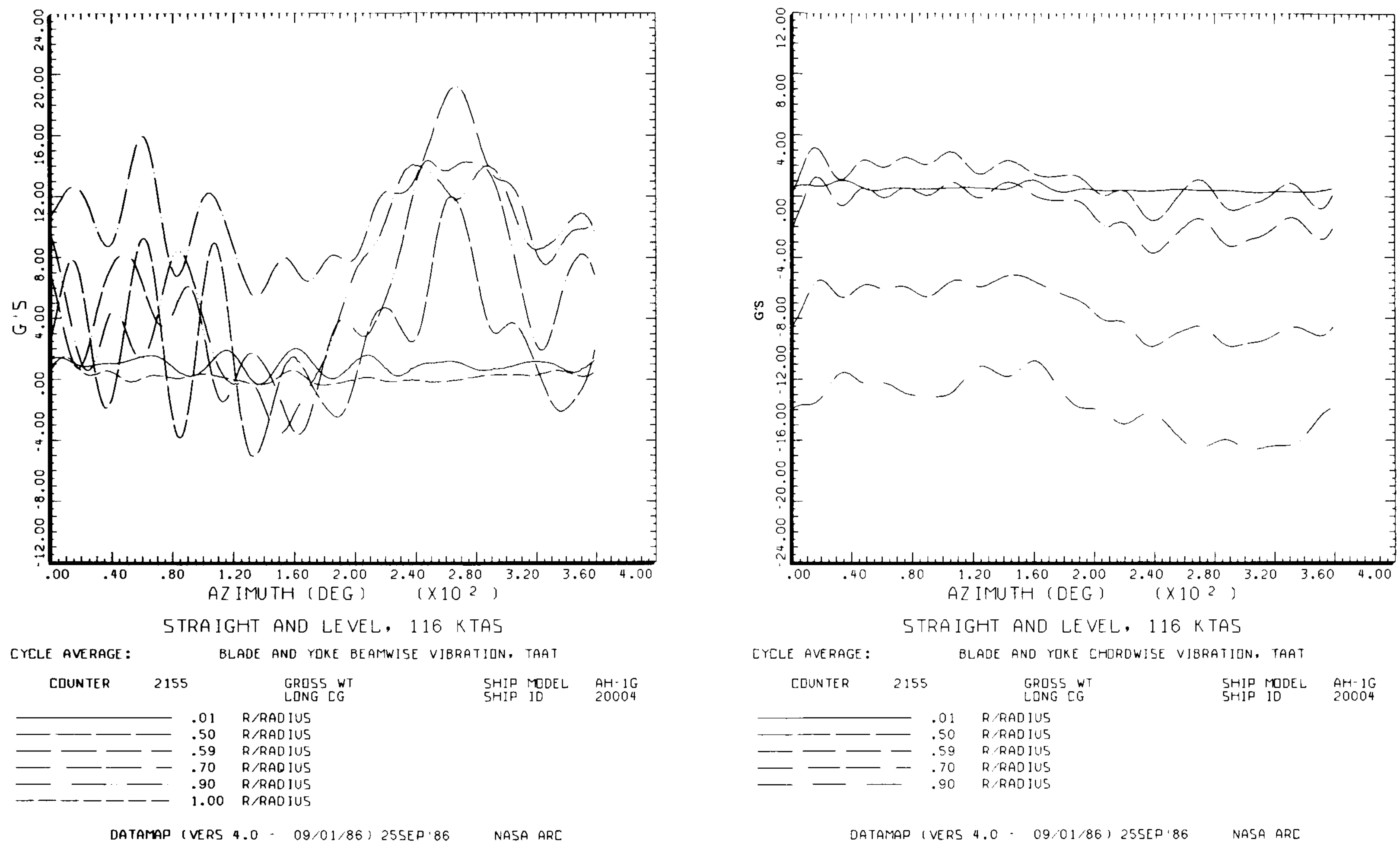

Figure 50.- Blade vibration versus azimuth at 116 KTAS. (a) Beamwise accelerometer data; (b) chordwise accelerometer data.

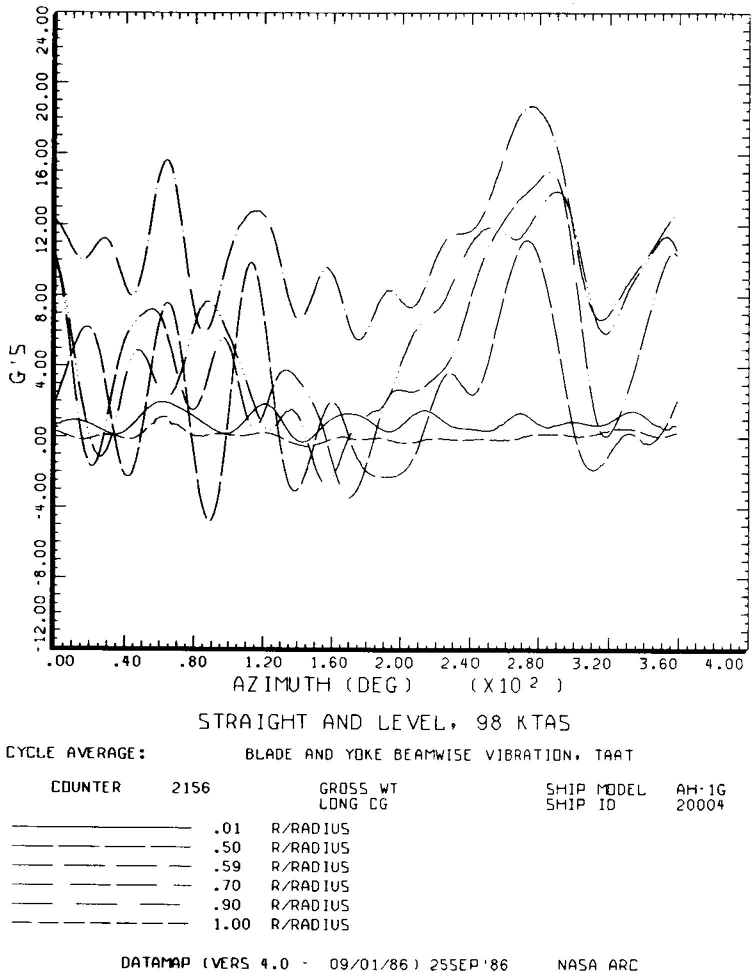

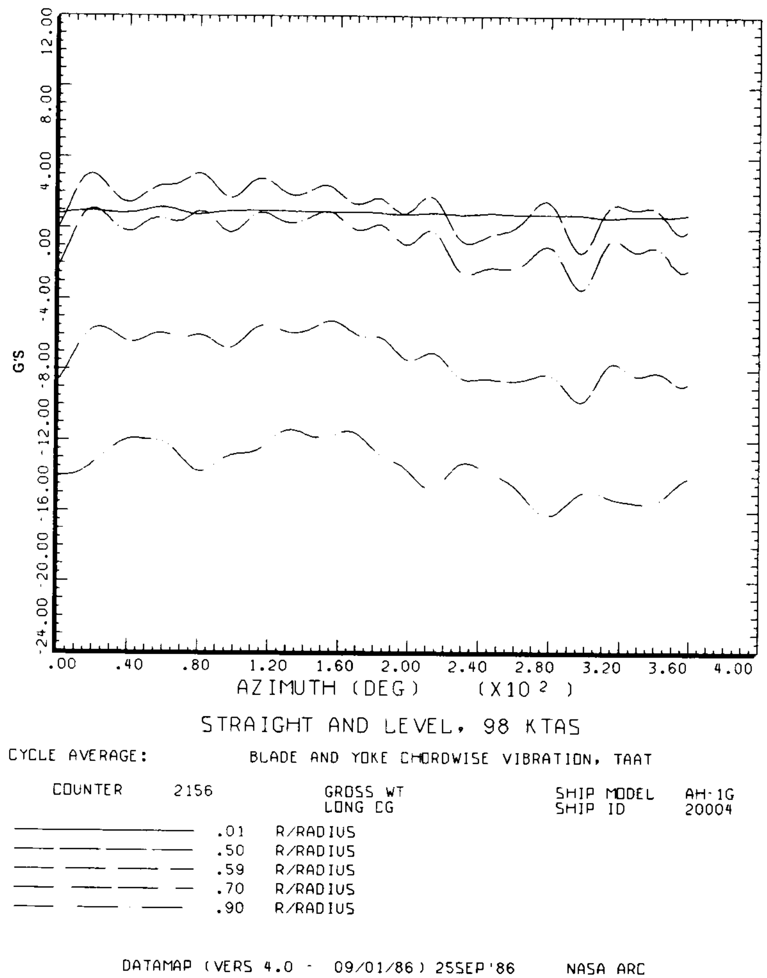

Figure 51.- Blade vibration versus azimuth at 98 KTAS. (a) Beamwise accelerometer data; (b) chordwise accelerometer data.

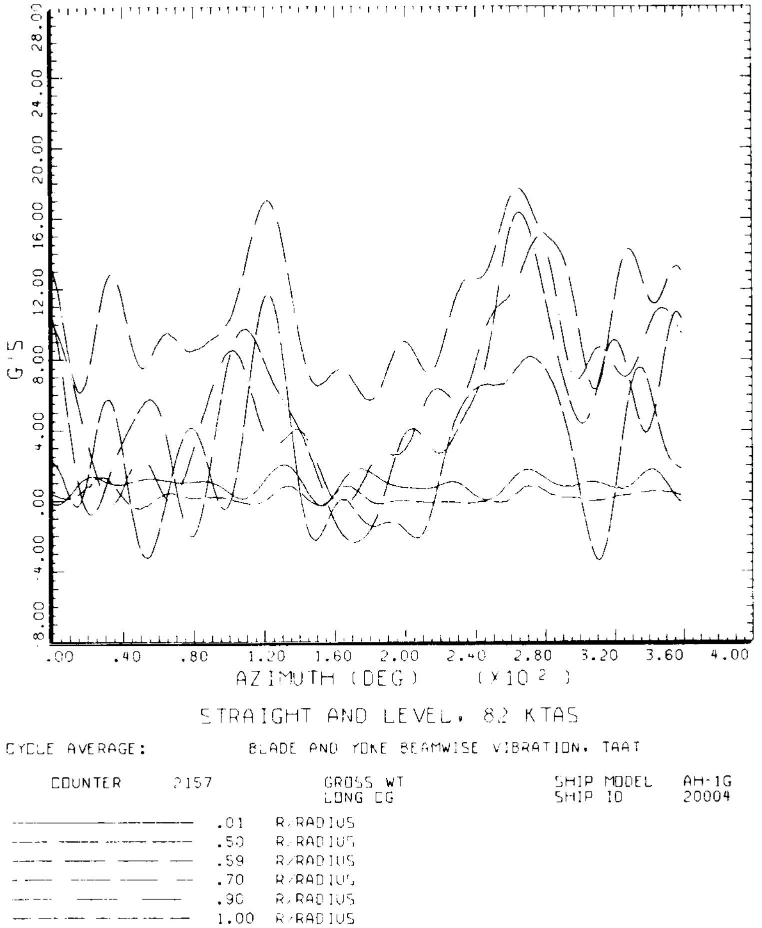

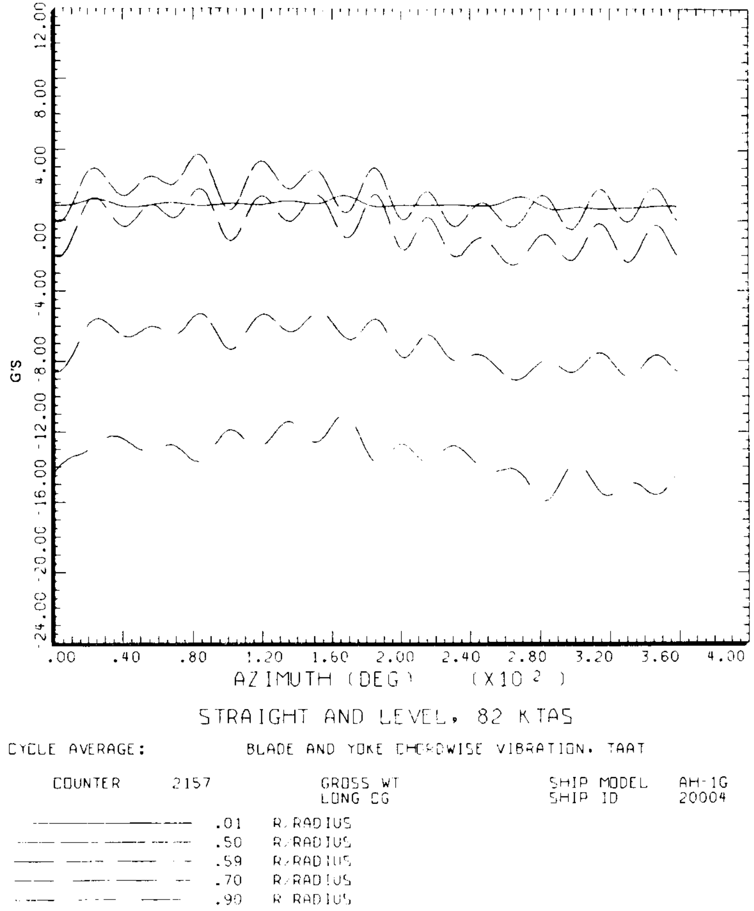

Figure 52.- Blade vibration versus azimuth at 82 KTAS. (a) Beamwise accelerometer data; (b) chordwise accelerometer data.

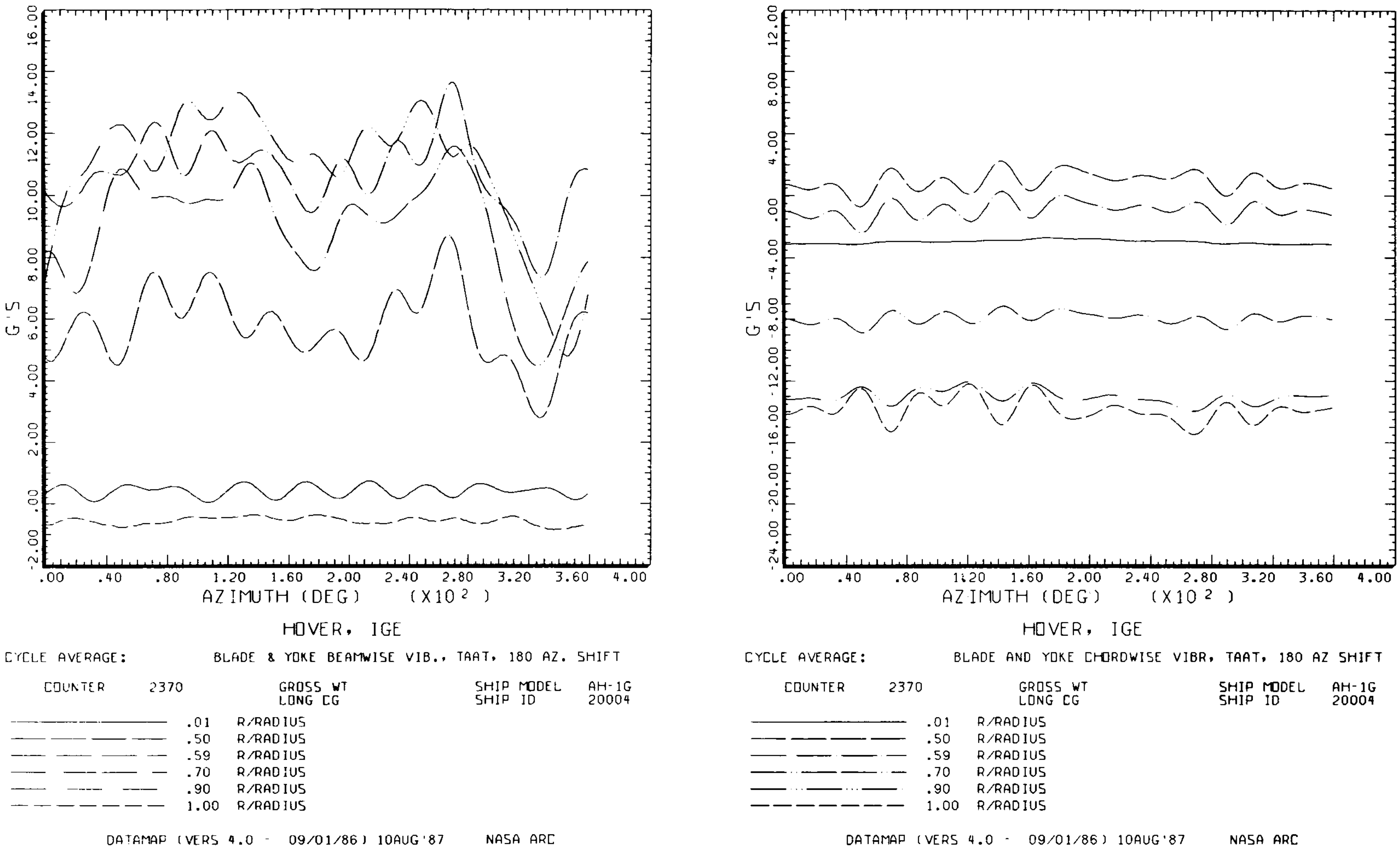

Figure 53.- Blade vibration versus azimuth in hover. (a) Beamwise accelerometer data; (b) chordwise accelerometer data.

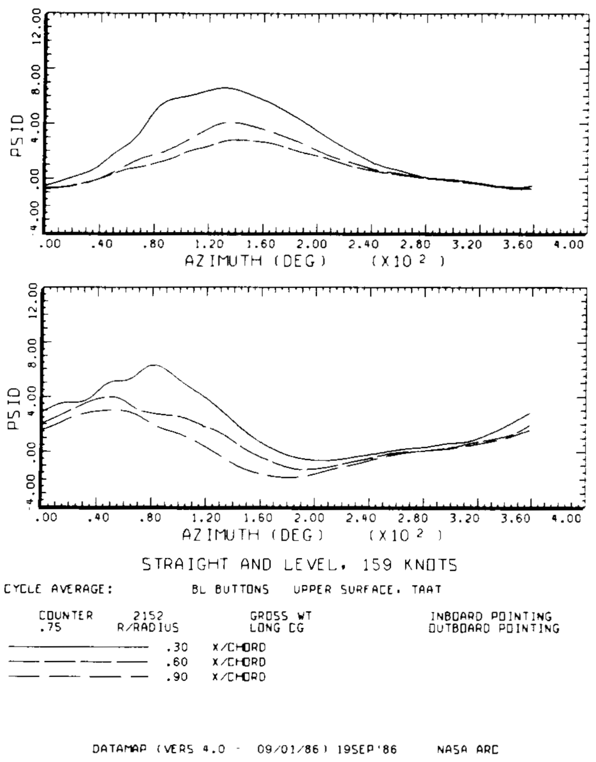

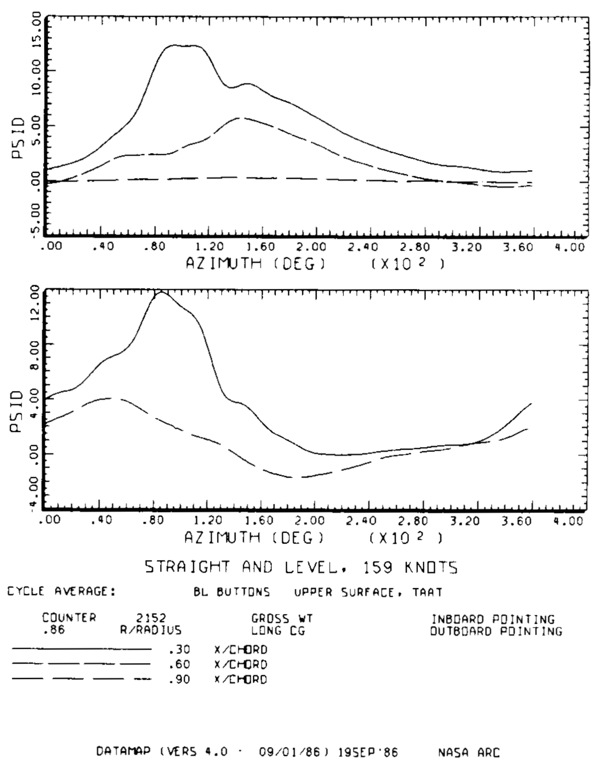

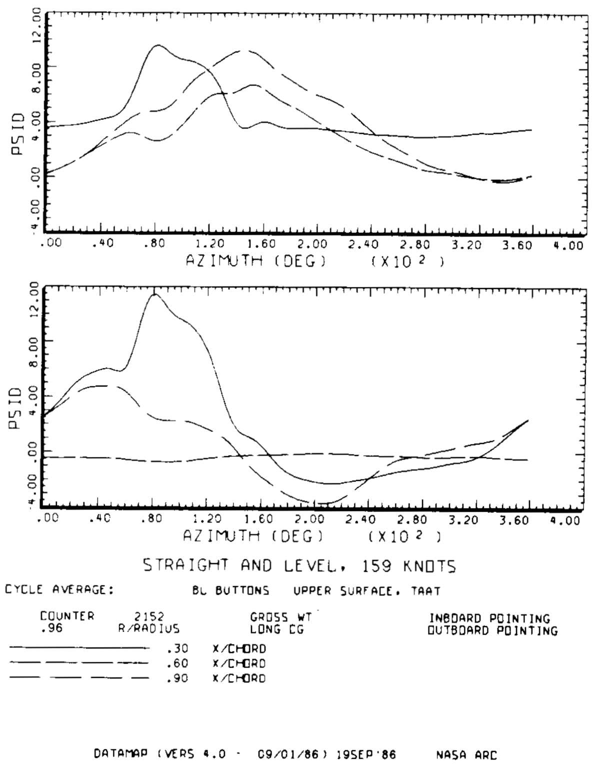

Figure 54.- The BLB versus azimuth at 159 Ktas. (a) Upper surface, 75% radius; (b) upper surface, 86% radius; (c) upper surface, 95% radius.

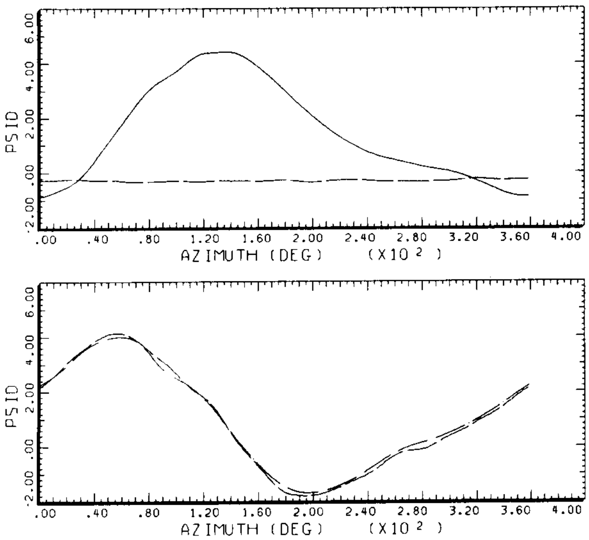

STRAIGHT AND LEVEL, 159 KNOTS

CYCLE AVERAGE: BL BUTTONS LOWER SURFACE, TAAT

COUNTER .75 2152 R/RADIUS GROSS WT LONG CG INBOARD POINTING OUTBOARD POINTING

.30 X/CHORD
.60 X/CHORD
.90 X/CHORD

DATAMAP (VERS 4.0 - 09/01/86) 19SEP'86 NASA ARC

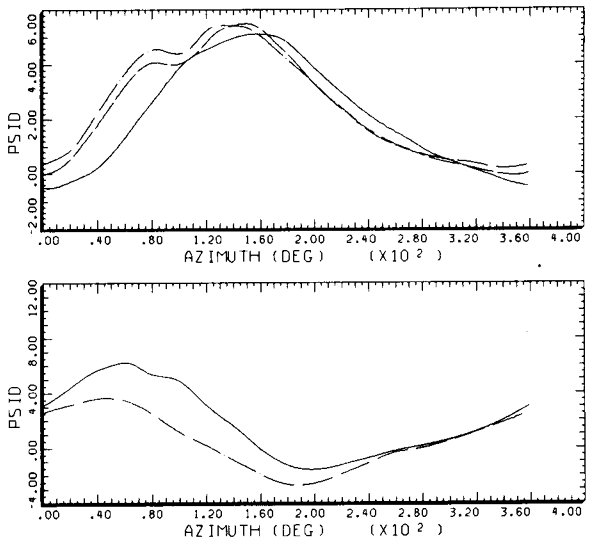

STRAIGHT AND LEVEL, 159 KNOTS

CYCLE AVERAGE: BL BUTTONS LOWER SURFACE, TAAT

COUNTER .86 2152 R/RADIUS GROSS WT LONG CG INBOARD POINTING OUTBOARD POINTING

.30 X/CHORD
.60 X/CHORD
.90 X/CHORD

DATAMAP (VERS 4.0 - 09/01/86) 19SEP'86 NASA ARC

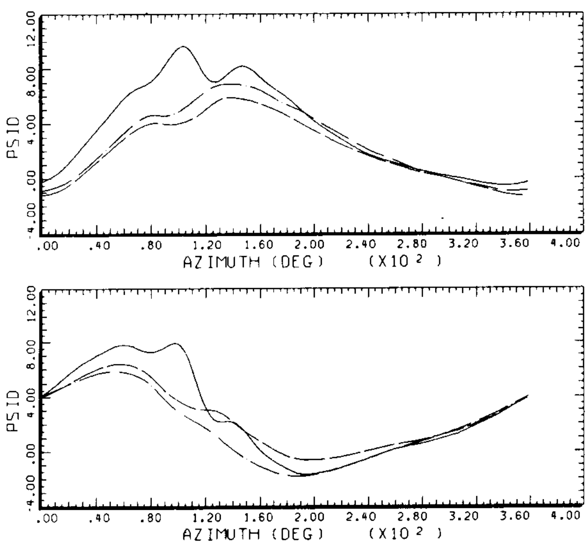

STRAIGHT AND LEVEL, 159 KNOTS

CYCLE AVERAGE: BL BUTTONS LOWER SURFACE, TAAT

COUNTER .96 2152 R/RADIUS GROSS WT LONG CG INBOARD POINTING OUTBOARD POINTING

.30 X/CHORD
.60 X/CHORD
.90 X/CHORD

DATAMAP (VERS 4.0 - 09/01/86) 19SEP'86 NASA ARC

Figure 54.- Concluded. (d) Lower surface, 75% radius; (e) lower surface, 86% radius; (f) lower surface, 95% radius.

ORIGINAL PAGE IS OF POOR QUALITY

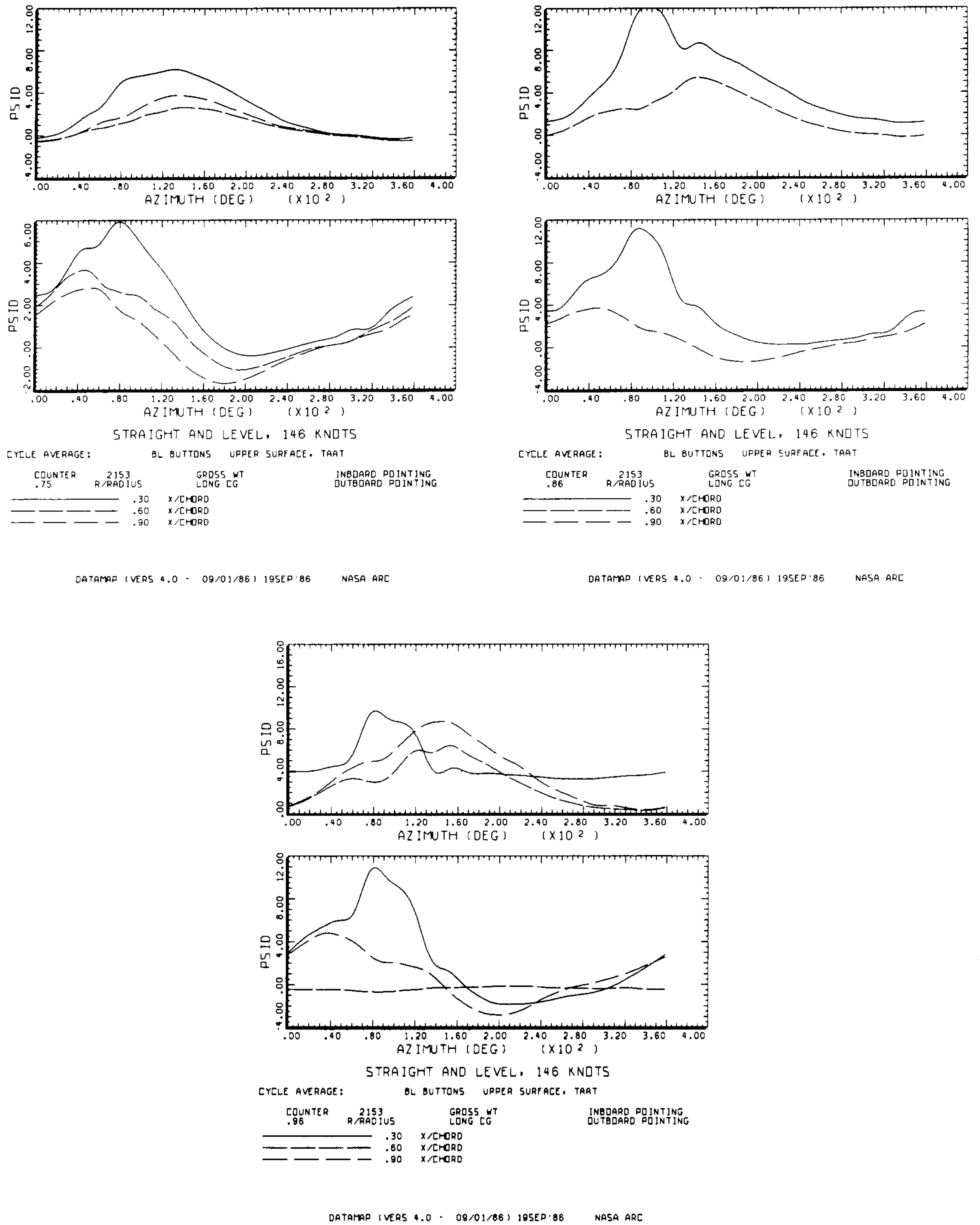

Figure 55.- The BLB versus azimuth at 146 KTAS. (a) Upper surface, 75% radius; (b) upper surface, 86% radius; (c) upper surface, 95% radius.

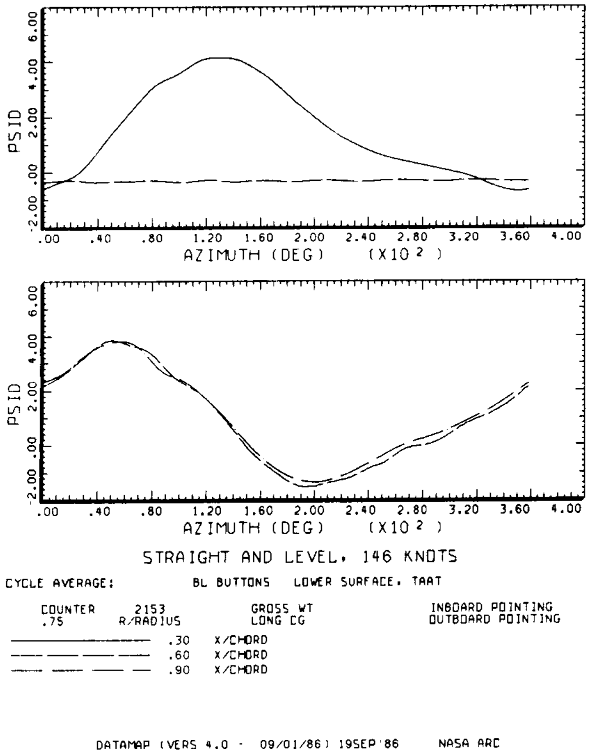

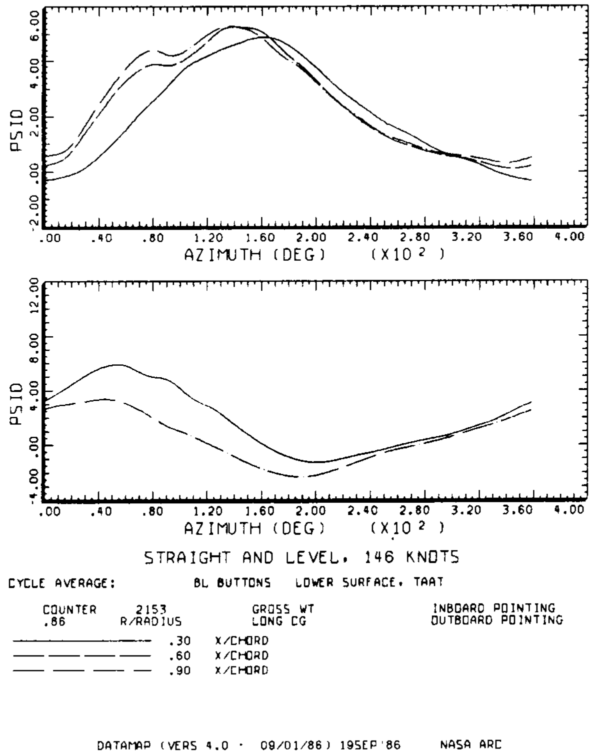

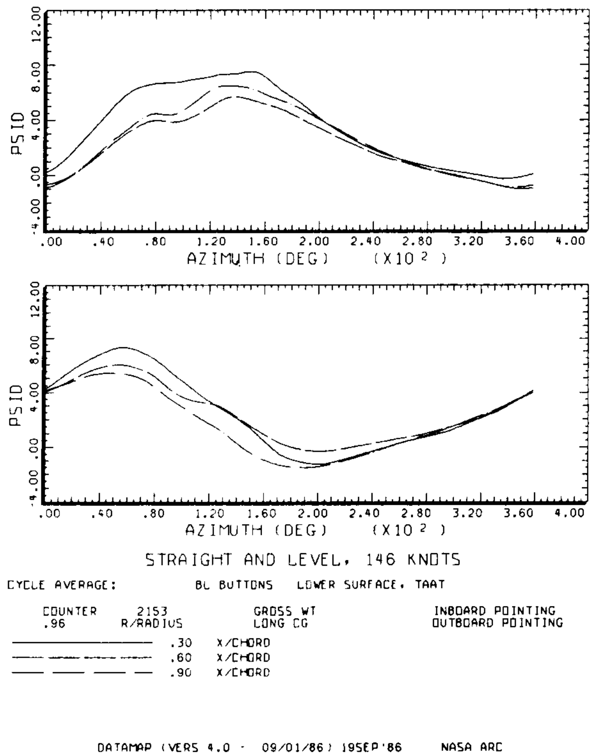

Figure 55.- Concluded. (d) Lower surface, 75% radius; (e) lower surface, 86% radius; (f) lower surface, 95% radius.

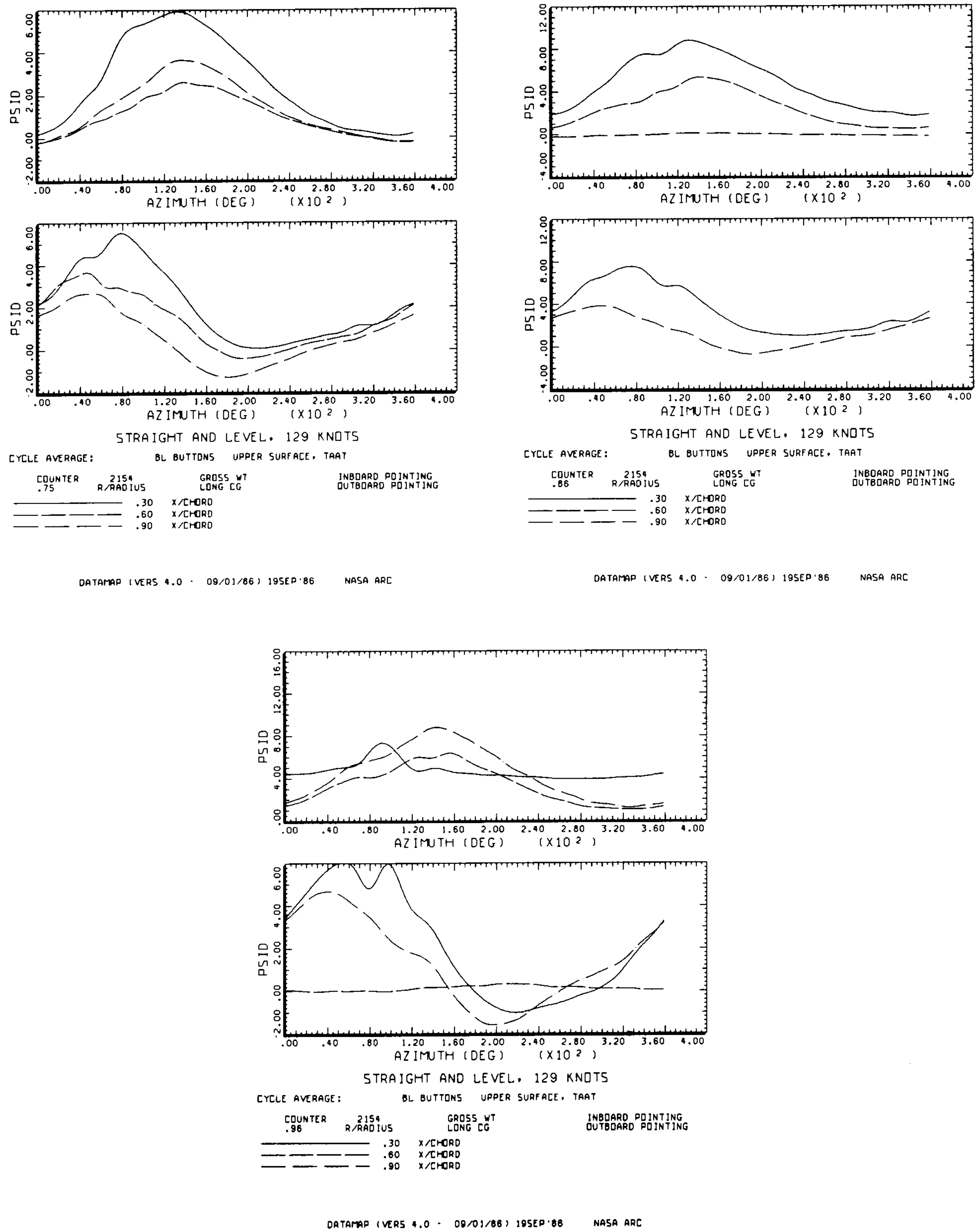

Figure 56.- The BLB versus azimuth at 129 KTAS. (a) Upper surface, 75% radius; (b) upper surface, 86% radius; (c) upper surface, 95% radius.

ORIGINAL PAGE IS
OF POOR QUALITY

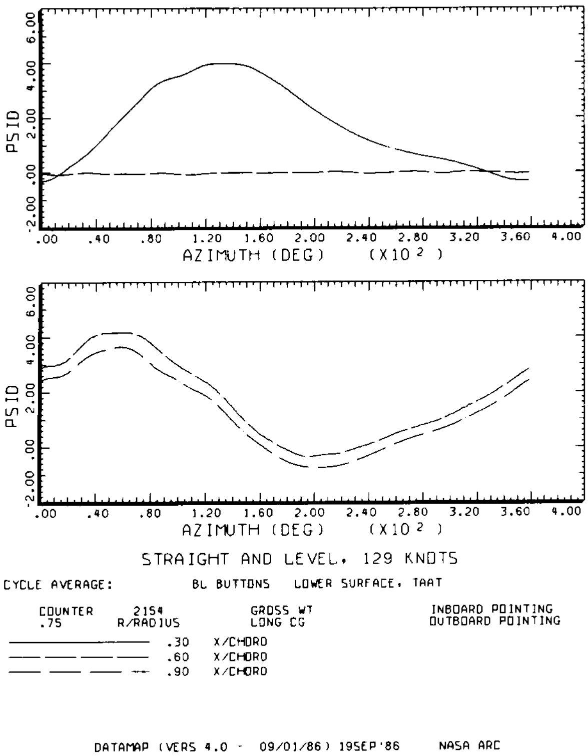

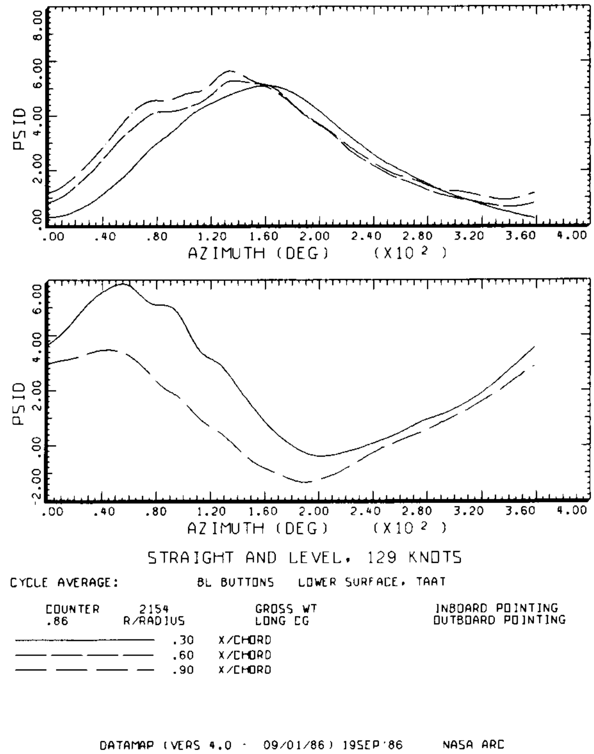

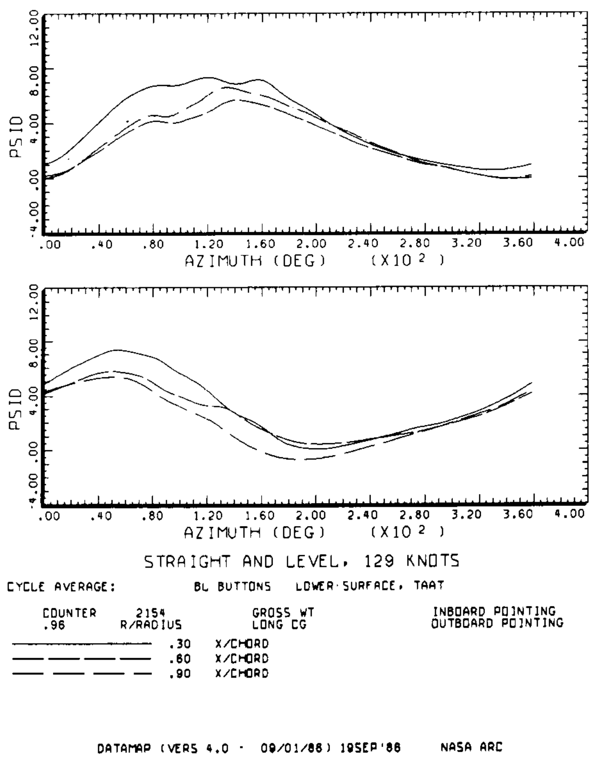

Figure 56.- Concluded. (d) Lower surface, 75% radius; (e) lower surface, 86% radius; (f) lower surface, 95% radius.

ORIGINAL PAGE IS OF POOR QUALITY

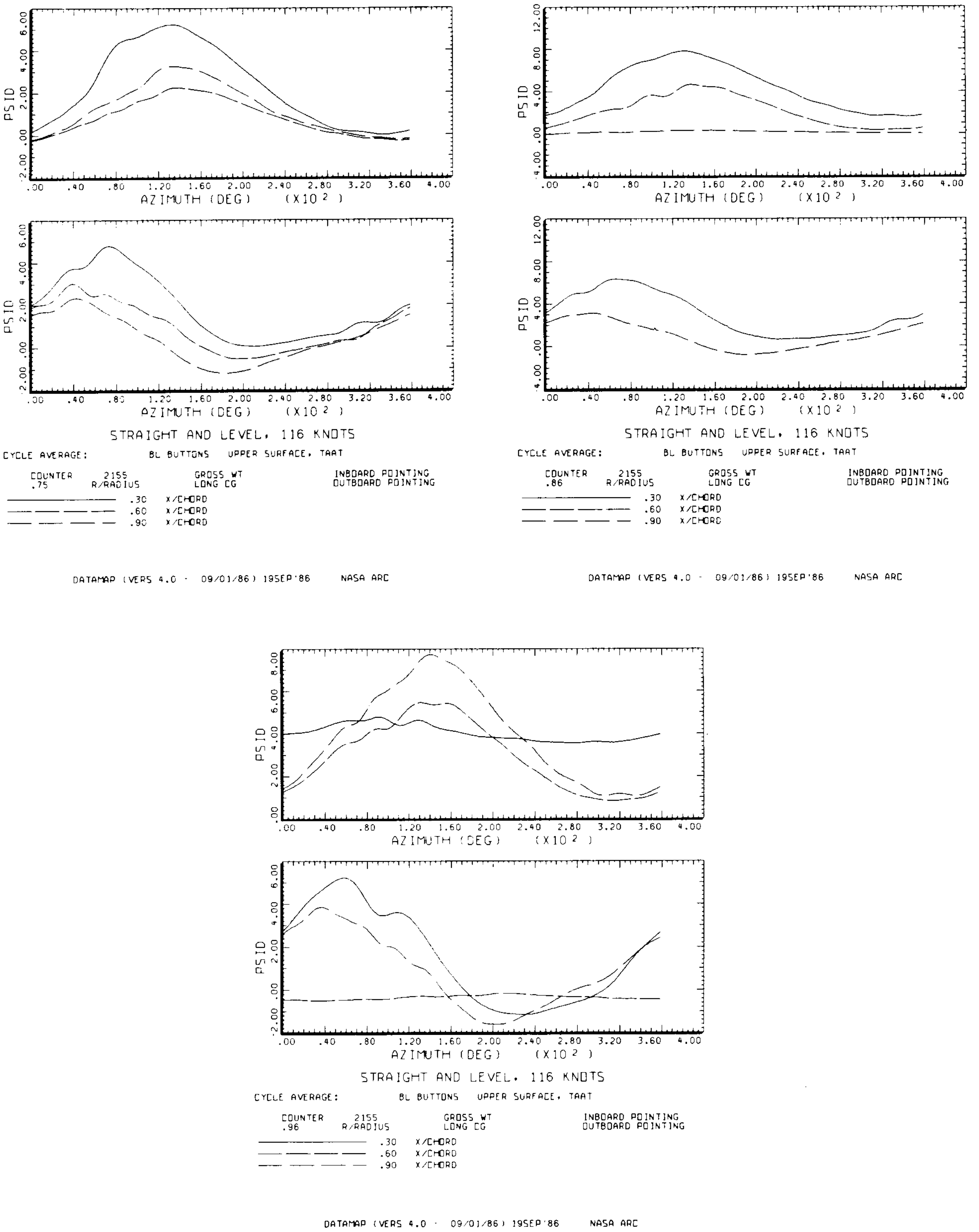

Figure 57.- The BLB versus azimuth at 116 KTAS. (a) Upper surface, 75% radius; (b) upper surface 86% radius; (c) upper surface, 95% radius.

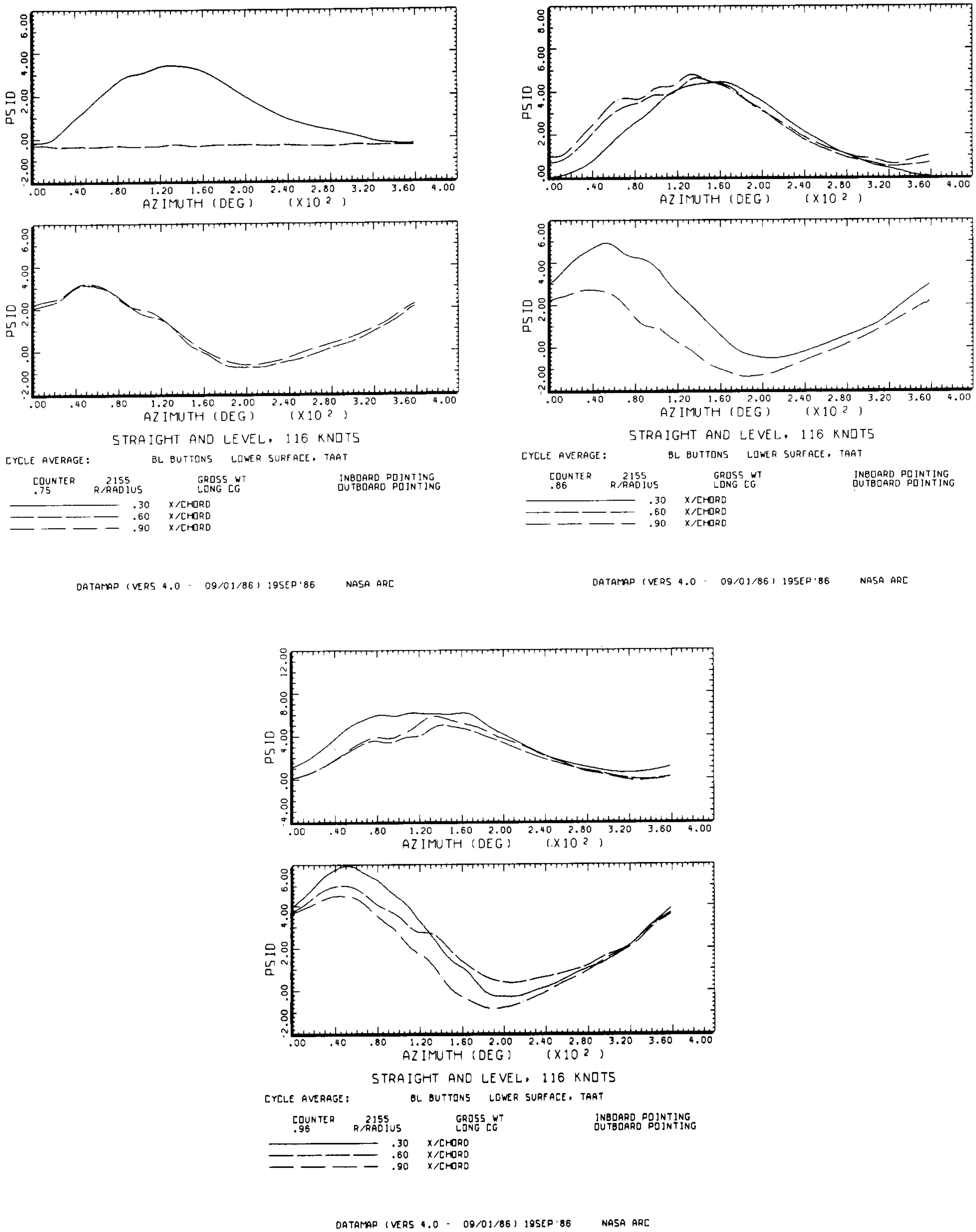

Figure 57.- Concluded. (d) Lower surface, 75% radius; (e) lower surface, 86% radius; (f) lower surface, 95% radius.

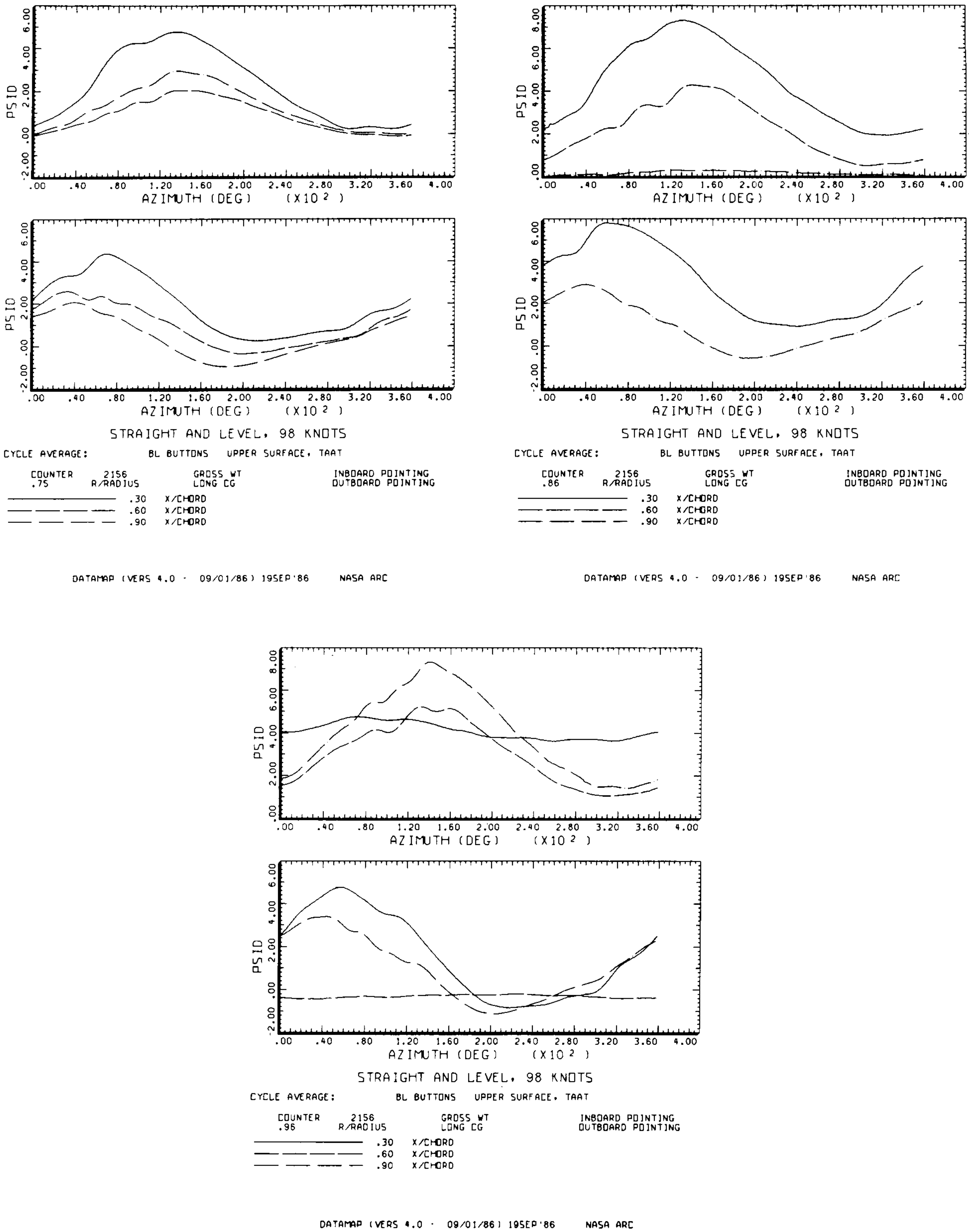

Figure 58.- The BLB versus azimuth at 98 KTAS. (a) Upper surface, 75% radius; (b) upper surface, 86% radius; (c) upper surface, 95% radius.

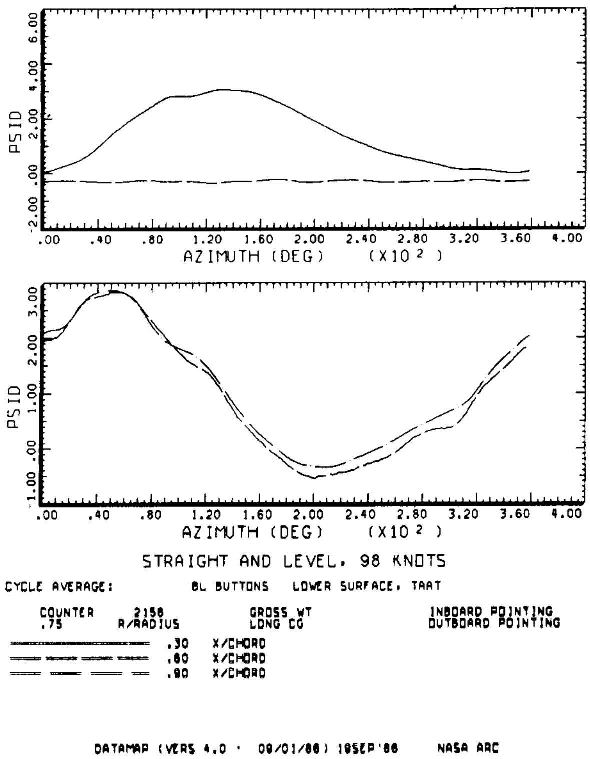

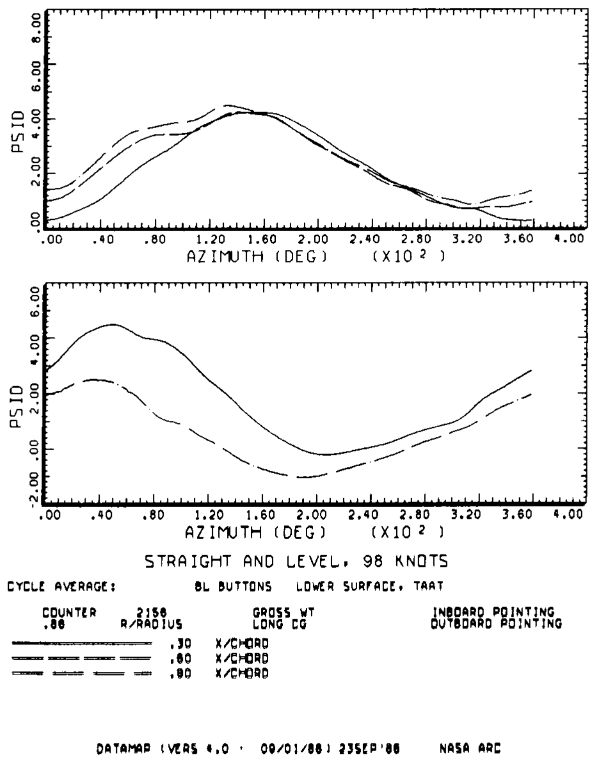

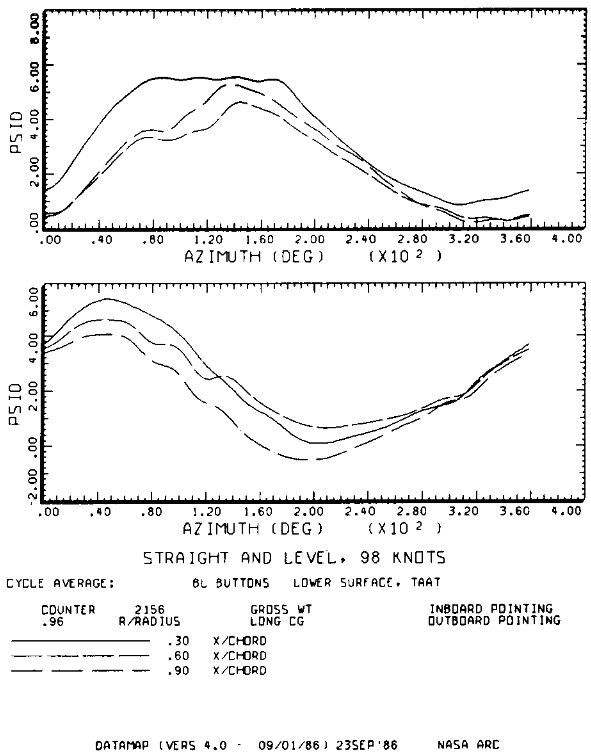

Figure 58.- Concluded. (d) Lower surface, 75% radius; (e) lower surface, 86% radius; (f) lower surface, 95% radius.

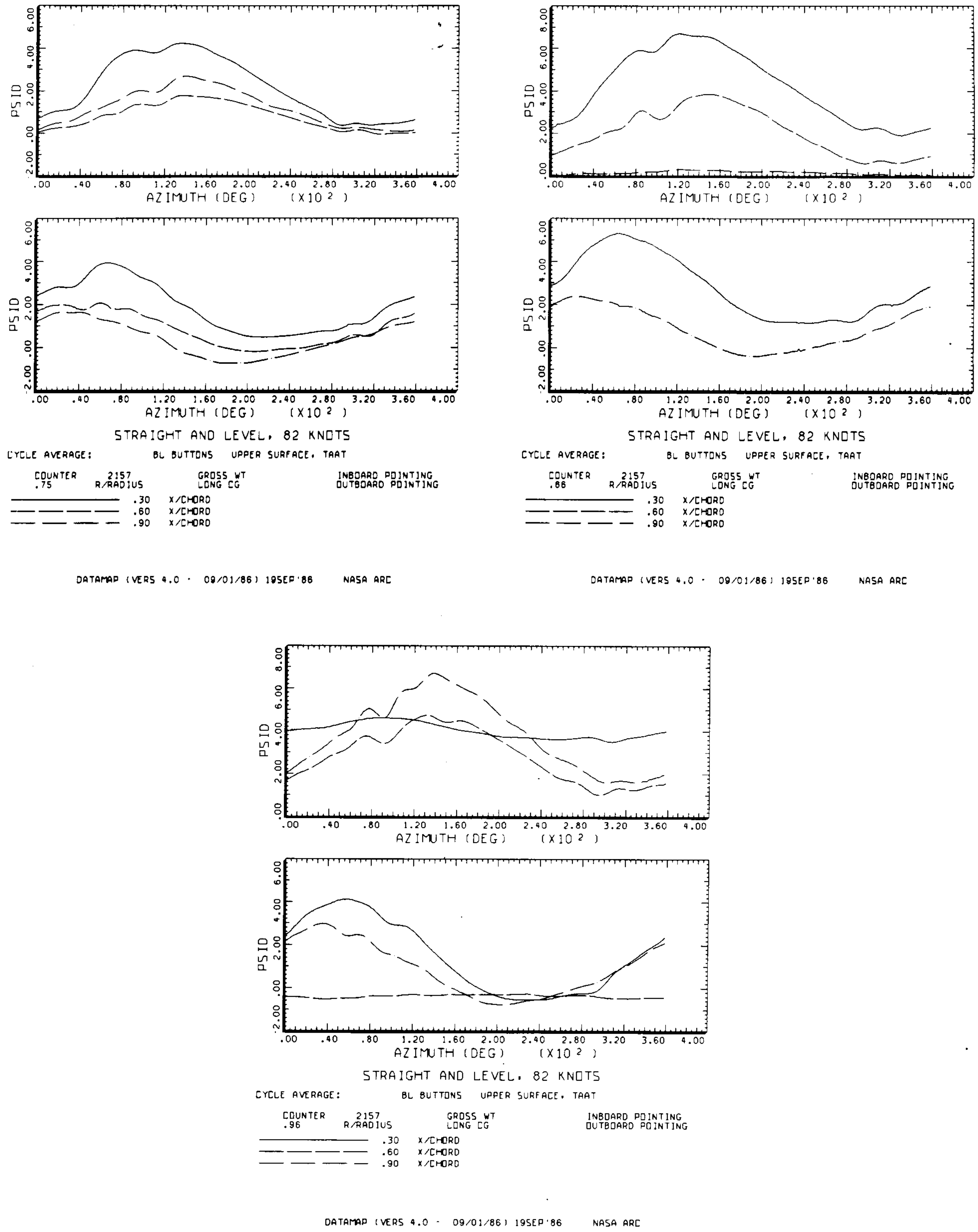

Figure 59.- The BLB versus azimuth at 82 KTAS. (a) Upper surface, 75% radius; (b) upper surface, 86% radius; (c) upper surface, 95% radius.

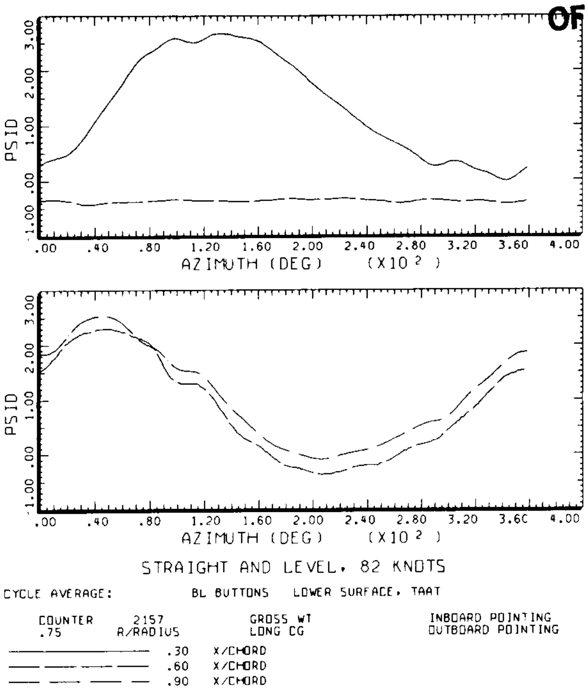

DATAMAP (VERS 4.0 - 09/01/86) 19SEP'86 NASA ARC

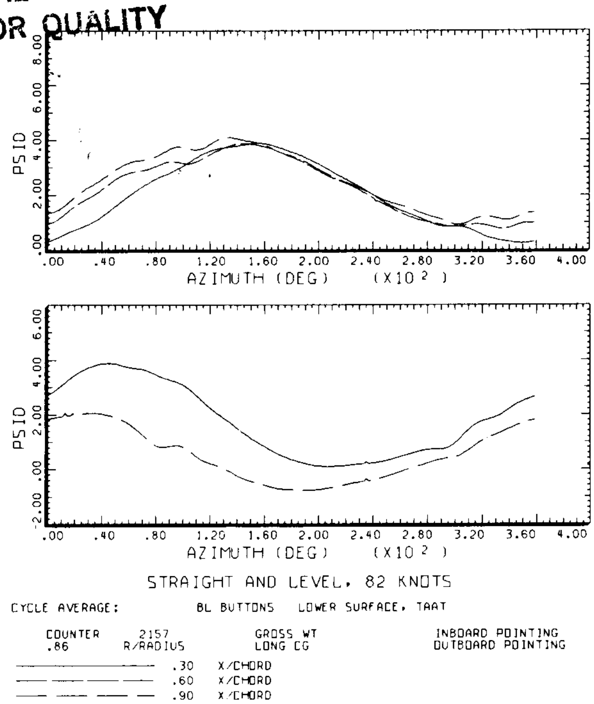

DATAMAP (VERS 4.0 - 09/01/86) 19SEP'86 NASA ARC

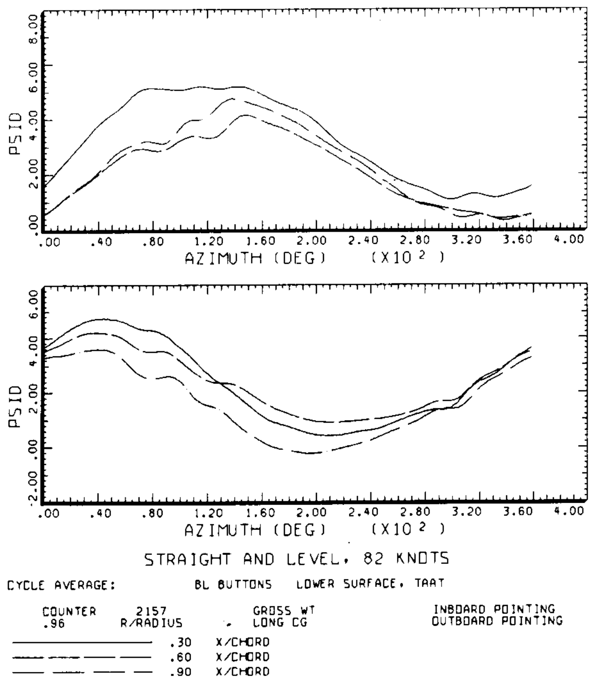

DATAMAP (VERS 4.0 - 09/01/86) 19SEP'86 NASA ARC

Figure 59.- Concluded. (d) Lower surface, 75% radius; (e) lower surface, 86% radius; (f) lower surface, 95% radius.

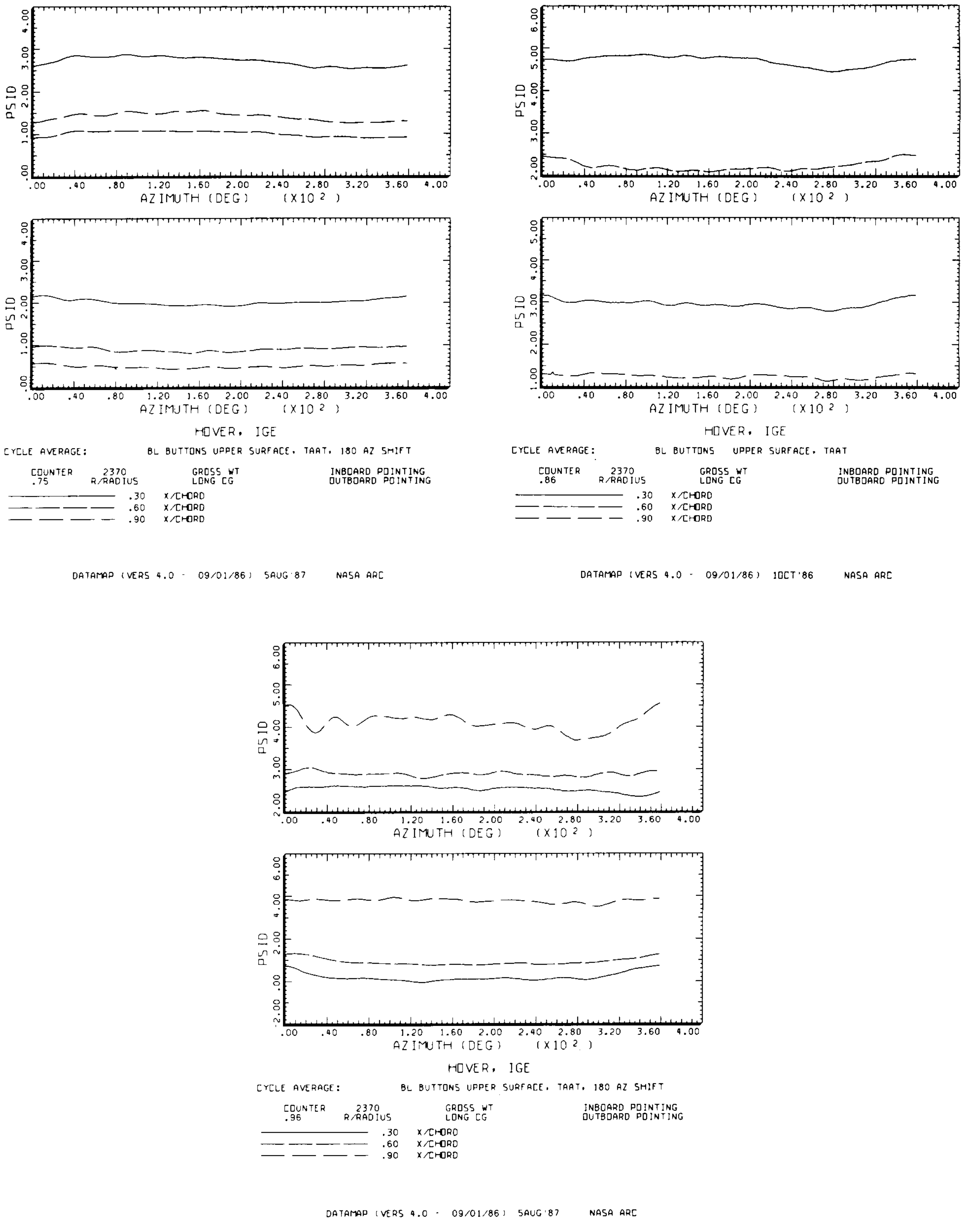

Figure 60.- The BLB versus azimuth in hover. (a) Upper surface, 75% radius; (b) upper surface, 86% radius; (c) upper surface, 95% radius.

ORIGINAL PAGE IS
OF POOR QUALITY

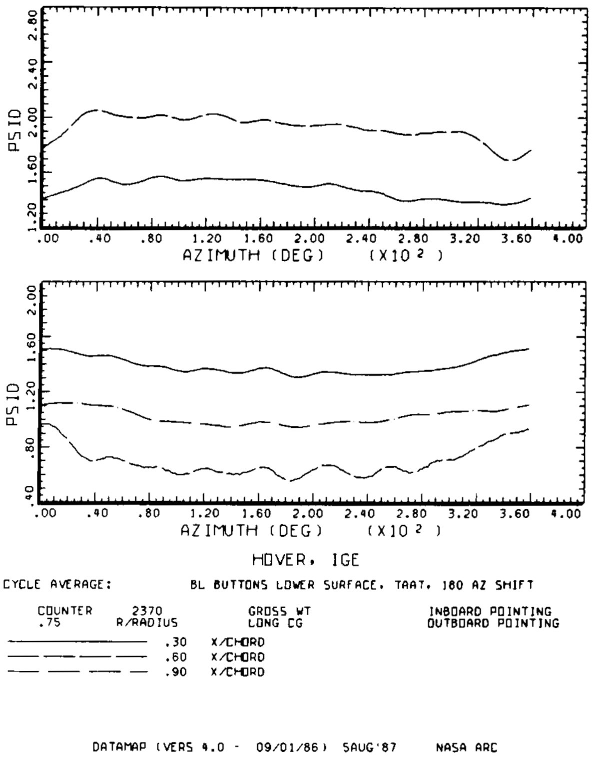

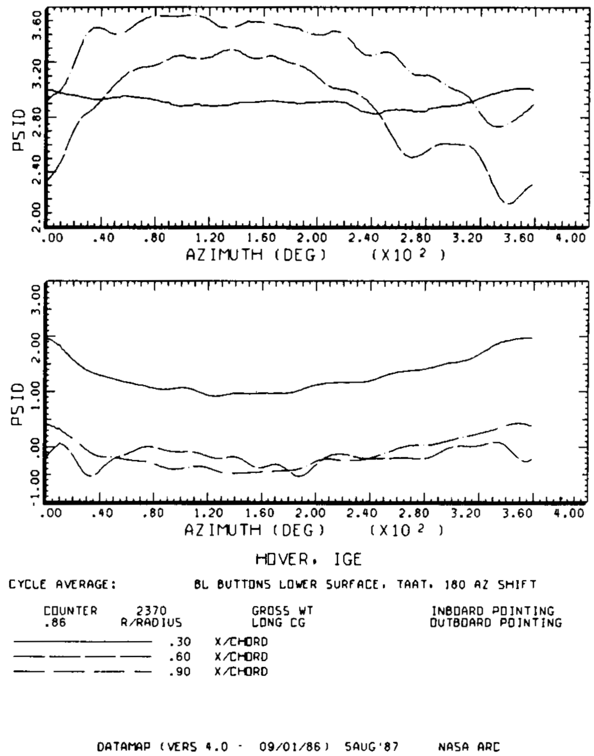

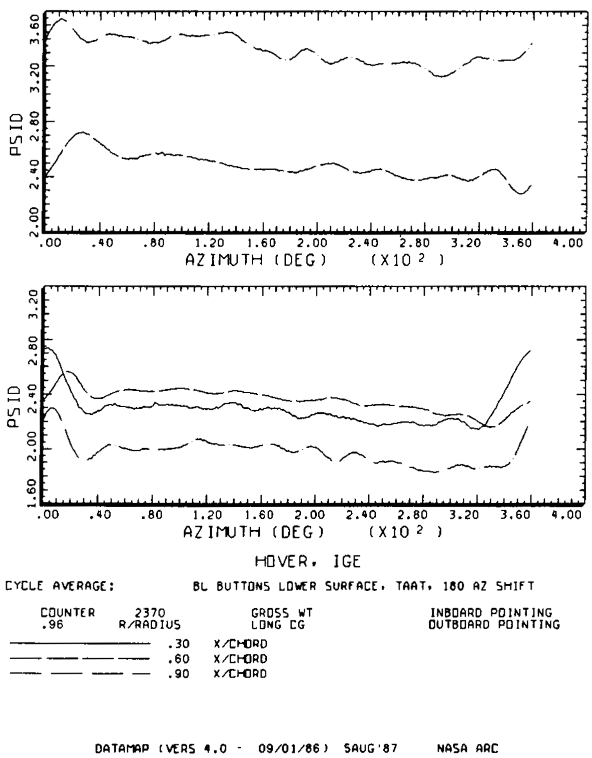

Figure 60.- Concluded. (d) Lower surface, 75% radius; (e) lower surface, 86% radius; (f) lower surface, 95% radius.

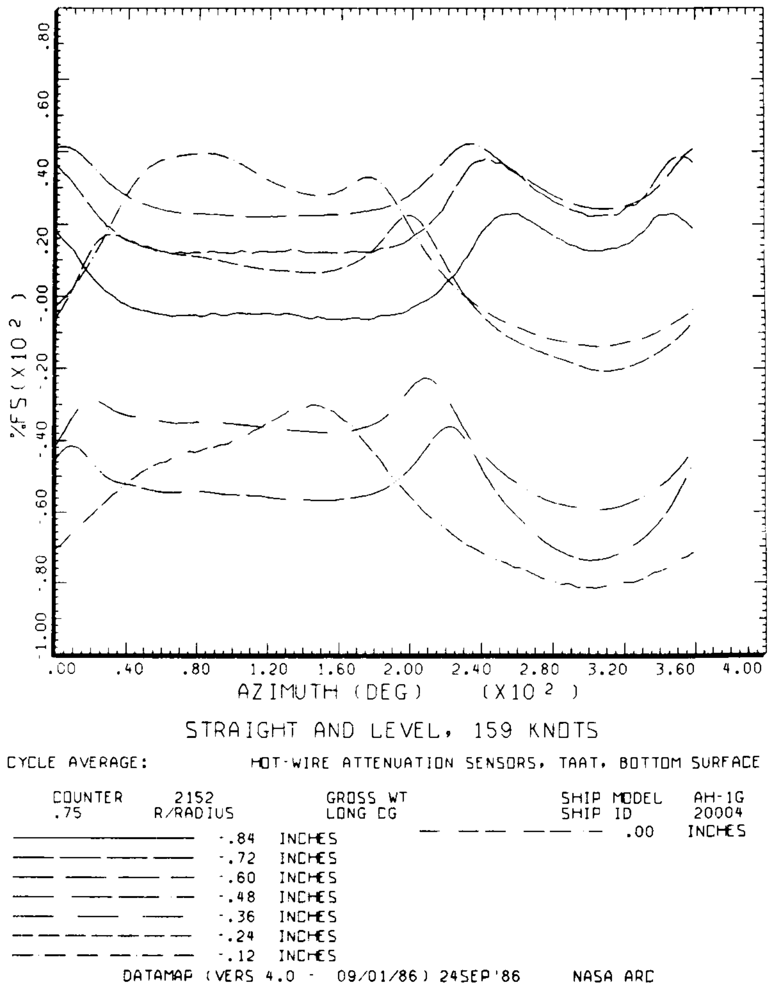

Figure 61.- Hot-wire anemometer versus azimuth at 159 KTAS. (a) 75% radius.

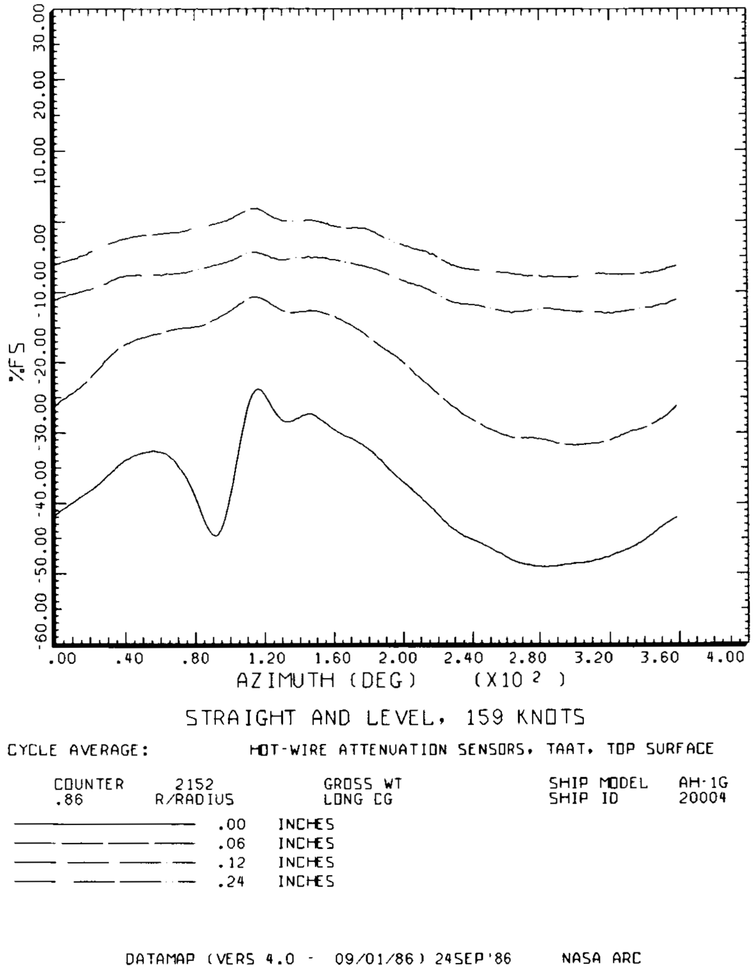

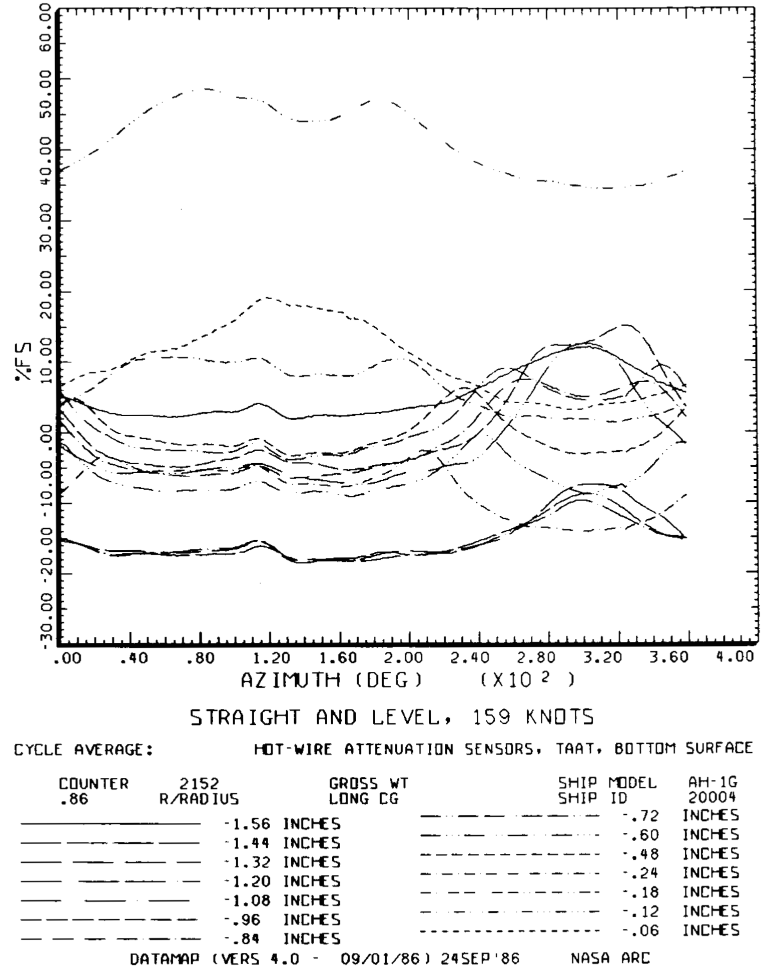

Figure 61.- Continued. (b) 86% radius, upper surface; (c) 86% radius, lower surface.

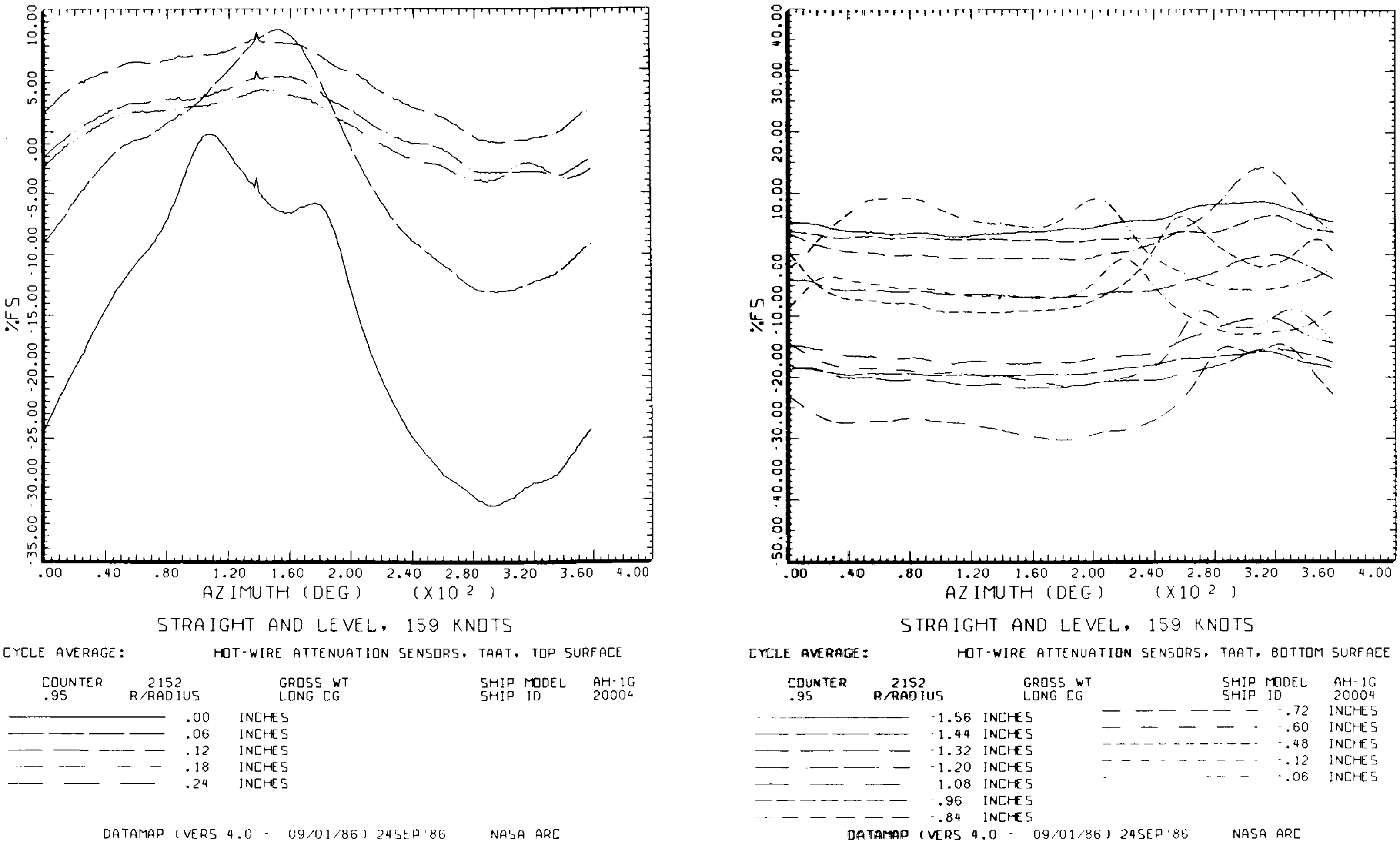

Figure 61.- Concluded. (d) 95% radius, upper surface; (e) 95% radius, lower surface.

ORIGINAL PAGE IS
OF POOR QUALITY

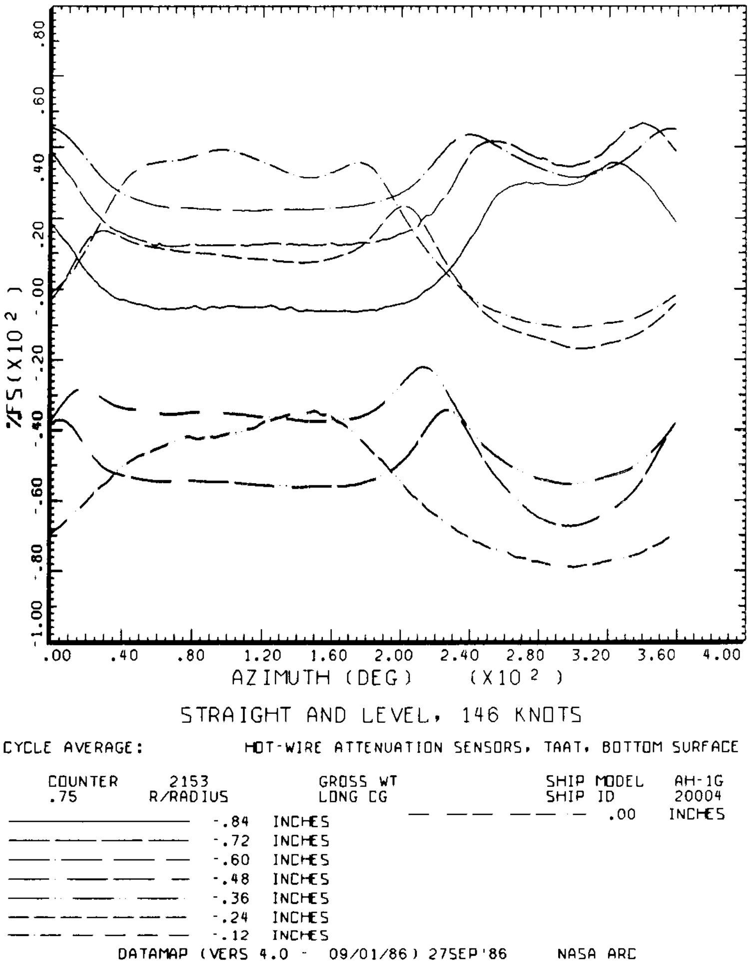

Figure 62.- Hot-wire anemometer versus azimuth at 146 KTAS. (a) 75% radius.

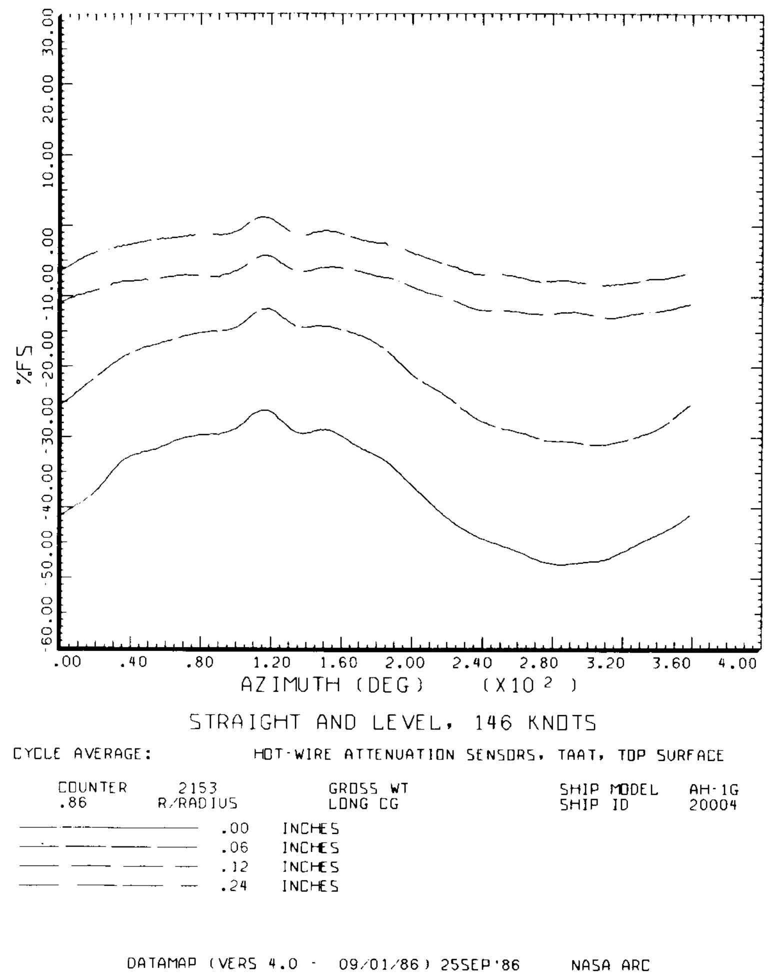

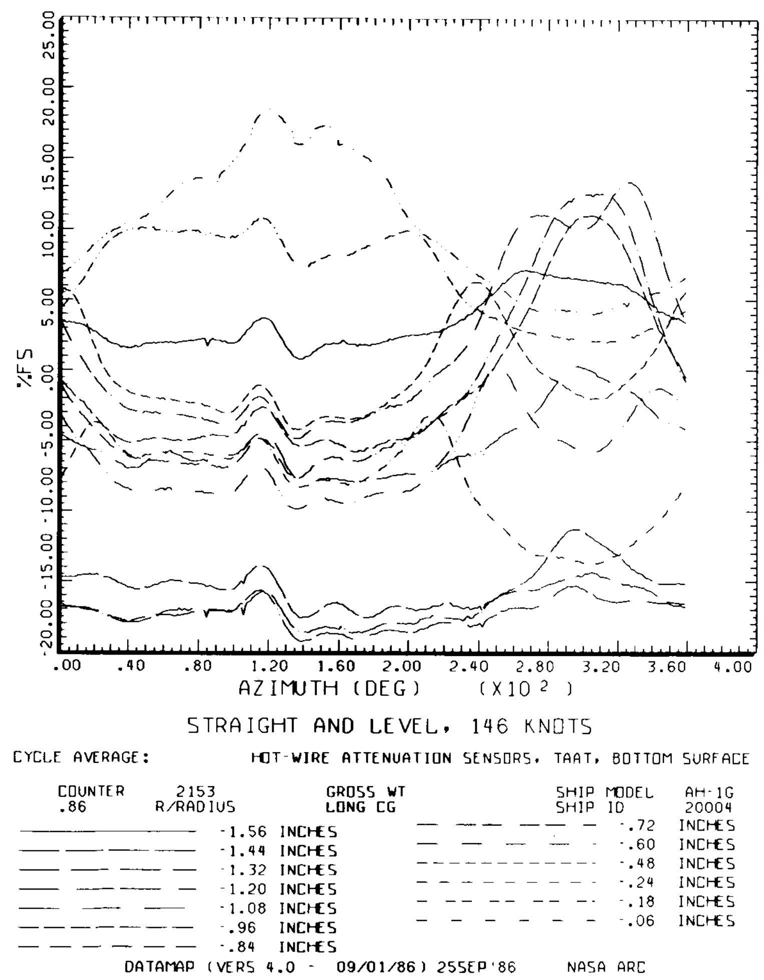

Figure 62.- Continued. (b) 86% radius, upper surface; (c) 86% radius, lower surface.

ORIGINAL PAGE IS
OF POOR QUALITY

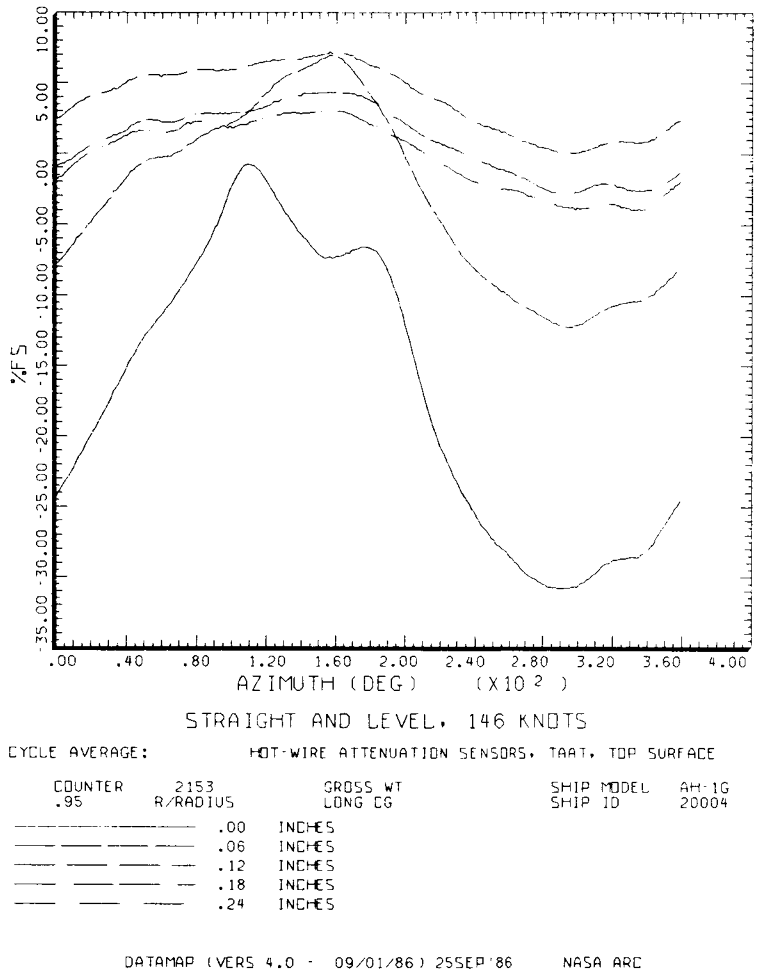

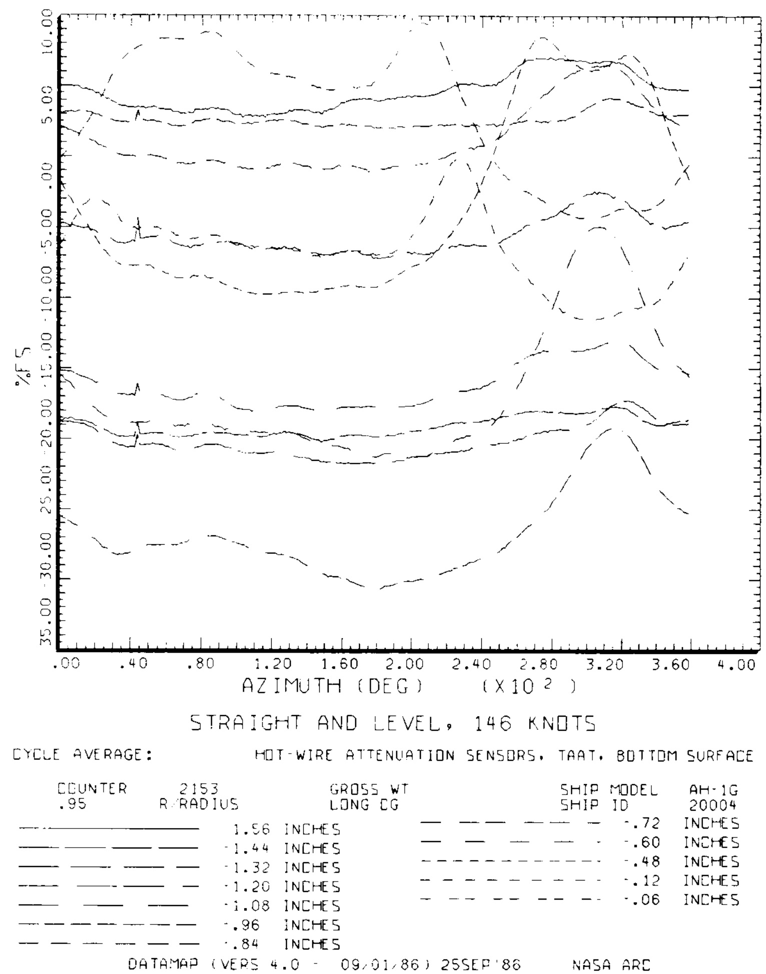

Figure 62.- Concluded. (d) 95% radius, upper surface; (e) 95% radius, lower surface.

ORIGINAL PAGE IS
OF POOR QUALITY

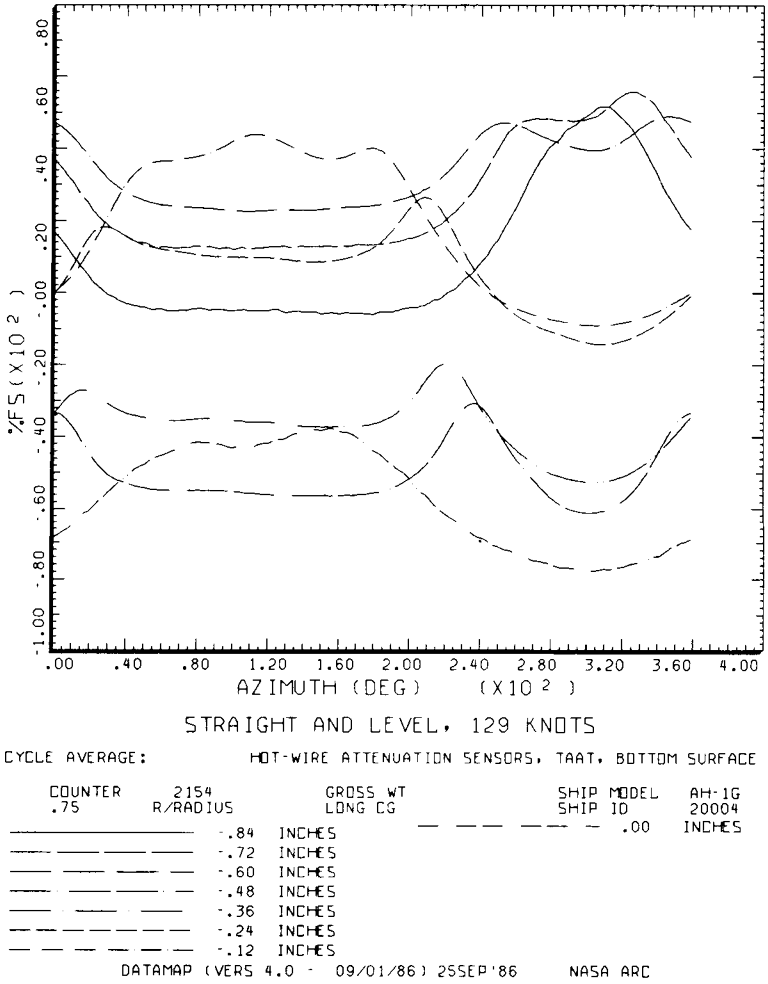

Figure 63.- Hot-wire anemometer versus azimuth at 129 KTAS. (a) 75% radius.

ORIGINAL PAGE IS OF POOR QUALITY

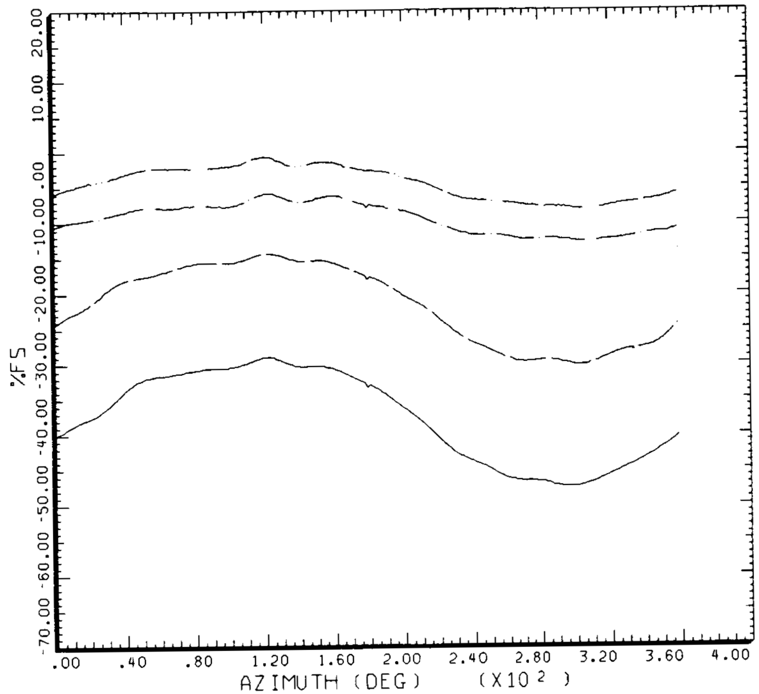

STRAIGHT AND LEVEL, 129 KNOTS

CYCLE AVERAGE: HOT-WIRE ATTENUATION SENSORS, TAAT, TOP SURFACE

COUNTER .86	2154 R/RADIUS	GROSS WT LONG CG	SHIP MODEL SHIP ID	AH-1G 20004
	.00 INCHES			
	.06 INCHES			
	.12 INCHES			
	.24 INCHES			

DATAMAP (VERS 4.0 - 09/01/86) 25SEP'86 NASA ARC

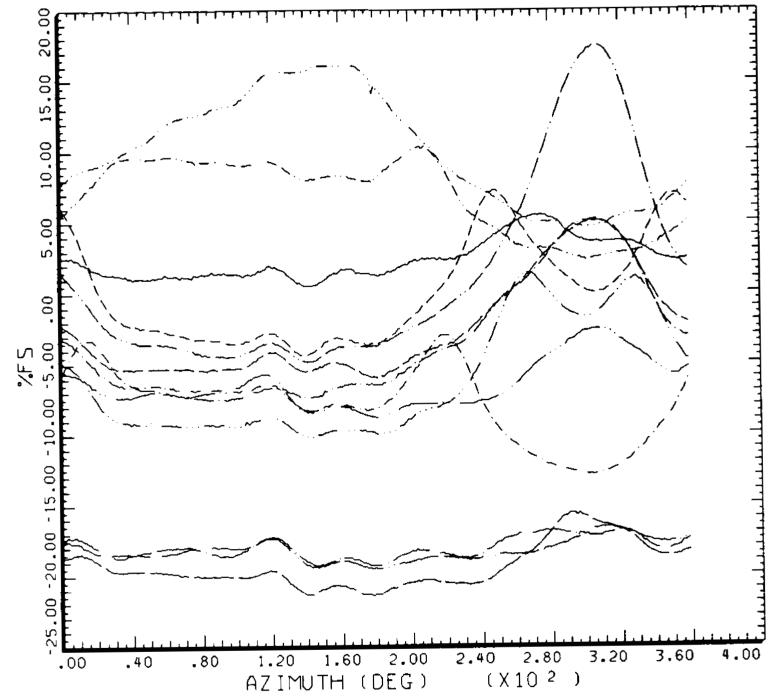

STRAIGHT AND LEVEL, 129 KNOTS

CYCLE AVERAGE: HOT-WIRE ATTENUATION SENSORS, TAAT, BOTTOM SURFACE

COUNTER .86	2154 R/RADIUS	GROSS WT LONG CG	SHIP MODEL SHIP ID	AH-1G 20004
	-1.56 INCHES		-.72	INCHES
	-1.44 INCHES		-.60	INCHES
	-1.32 INCHES		-.48	INCHES
	-1.20 INCHES		-.24	INCHES
	-1.08 INCHES		-.18	INCHES
	-.96 INCHES		-.06	INCHES
	-.84 INCHES			

DATAMAP (VERS 4.0 - 09/01/86) 25SEP'86 NASA ARC

Figure 63.- Continued. (b) 86% radius, upper surface; (c) 86% radius, lower surface.

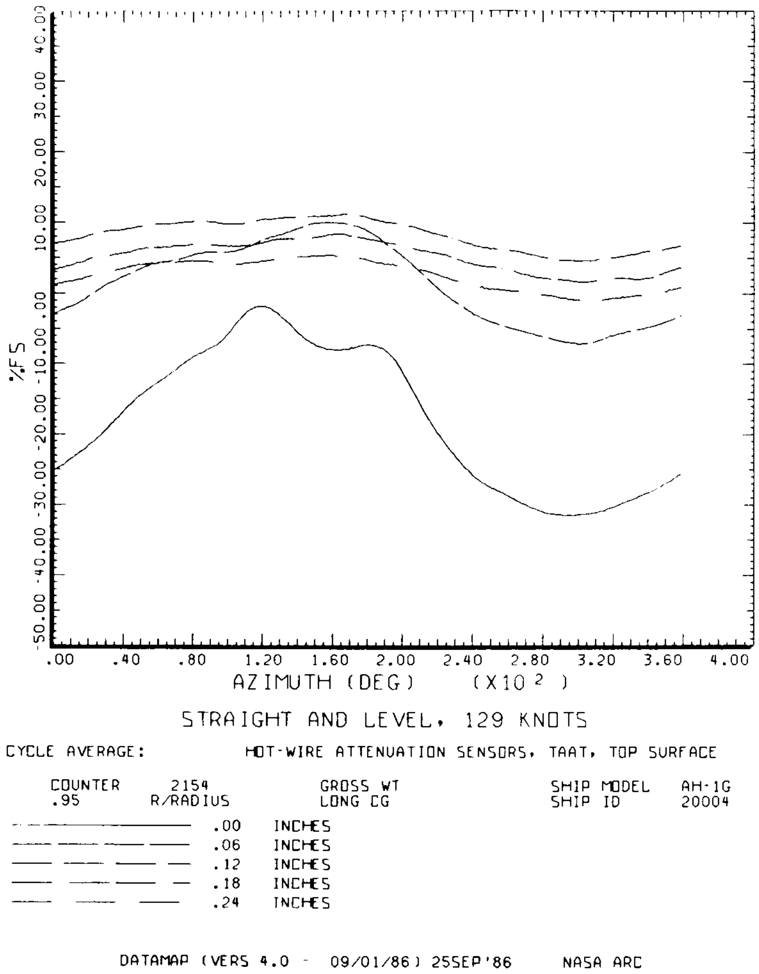

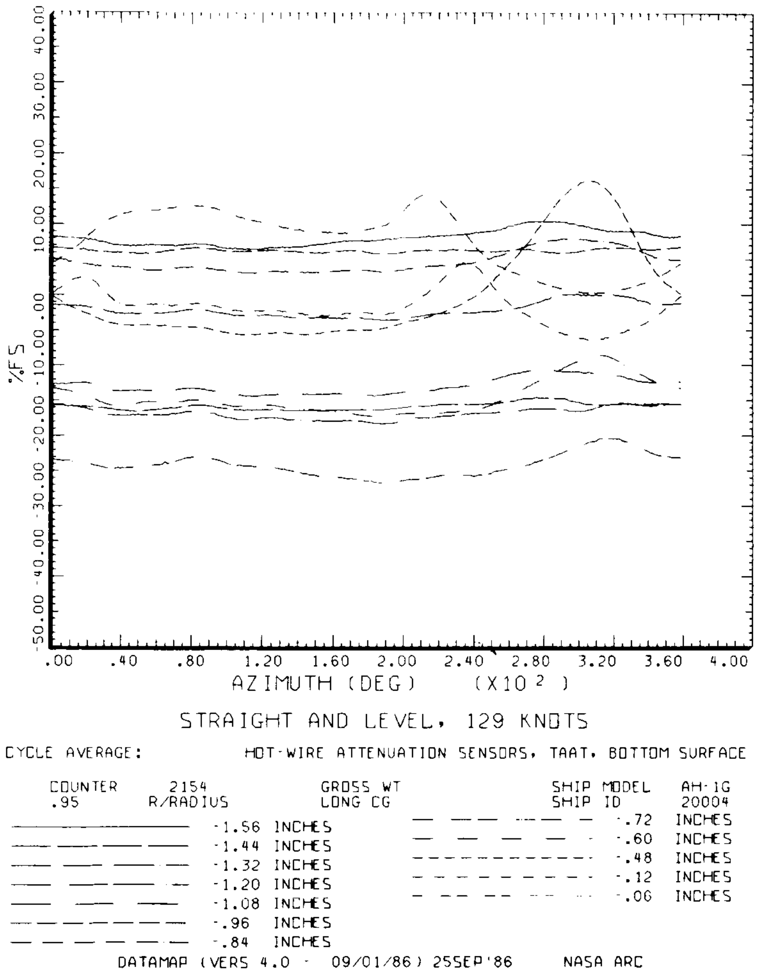

Figure 63.- Concluded. (d) 95% radius, upper surface; (e) 95% radius, lower surface.

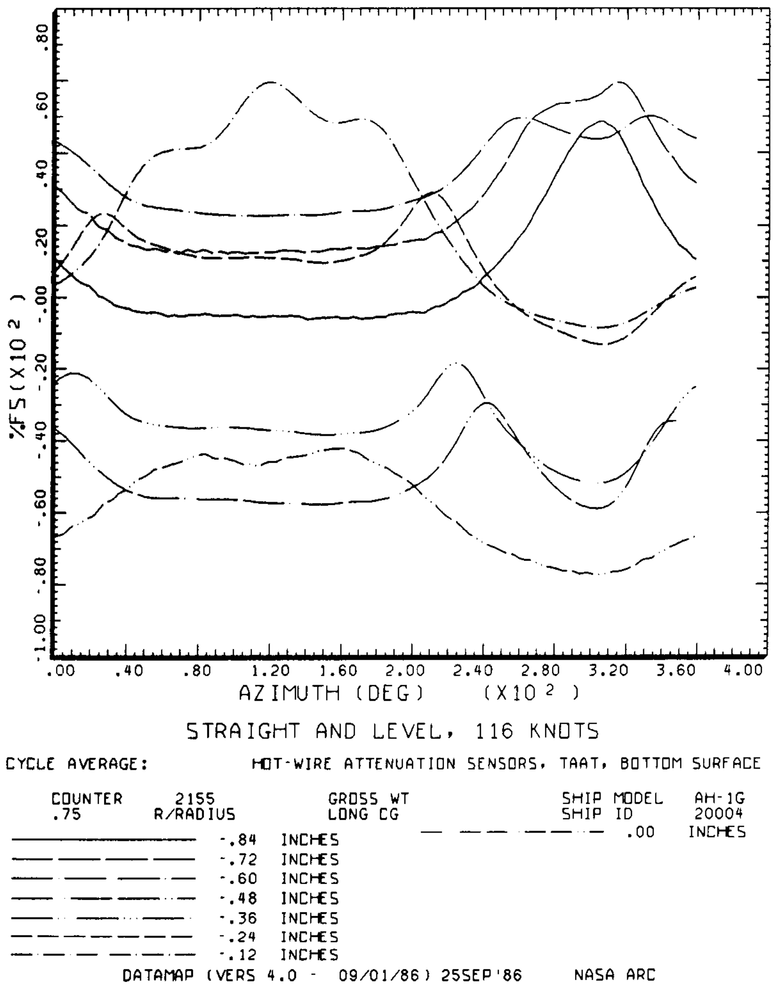

Figure 64.- Hot-wire anemometer versus azimuth at 116 KTAS. (a) 75% radius.

C-3

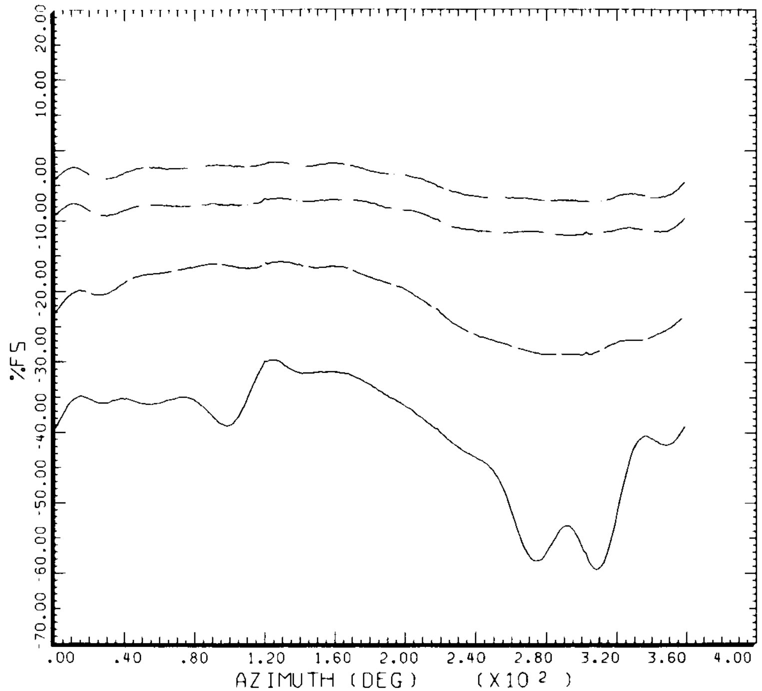

STRAIGHT AND LEVEL, 116 KNOTS

CYCLE AVERAGE: HOT-WIRE ATTENUATION SENSORS, TAAT, TOP SURFACE

COUNTER .86	2155 R/RADIUS		GROSS WT LONG CG	SHIP MODEL SHIP ID	AH-1G 20004
	.00	INCHES			
	.06	INCHES			
	.12	INCHES			
	.24	INCHES			

DATAMAP (VERS 4.0 - 09/01/86) 25SEP'86 NASA ARC

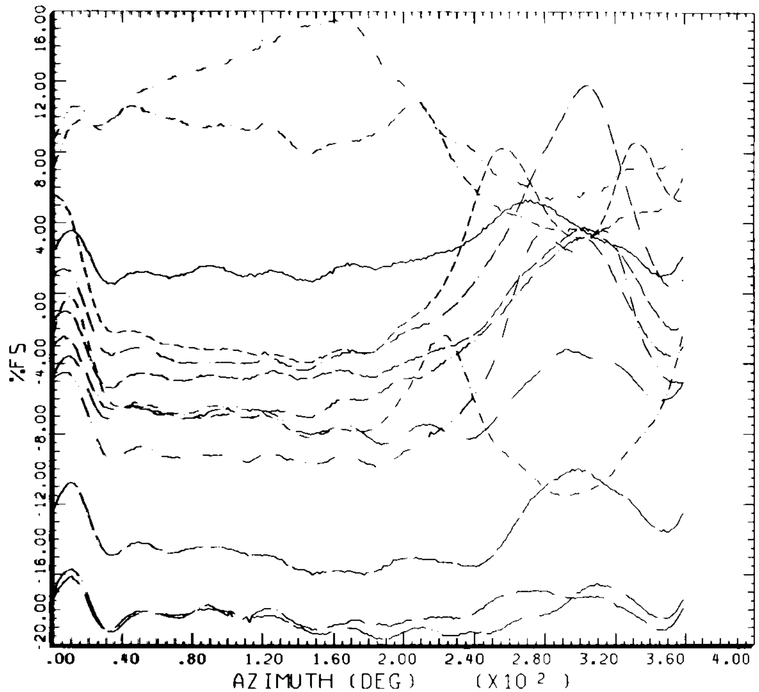

STRAIGHT AND LEVEL, 116 KNOTS

CYCLE AVERAGE: HOT-WIRE ATTENUATION SENSORS, TAAT, BOTTOM SURFACE

COUNTER .86	2155 R/RADIUS		GROSS WT LONG CG	SHIP MODEL SHIP ID	AH-1G 20004
	-1.56	INCHES		-.72	INCHES
	-1.44	INCHES		-.60	INCHES
	-1.32	INCHES		-.48	INCHES
	-1.20	INCHES		-.24	INCHES
	-1.08	INCHES		-.18	INCHES
	-.96	INCHES		-.06	INCHES
	-.84	INCHES			

DATAMAP (VERS 4.0 - 09/01/86) 25SEP'86 NASA ARC

Figure 64.- Continued. (b) 86% radius, upper surface; (c) 86% radius, lower surface.

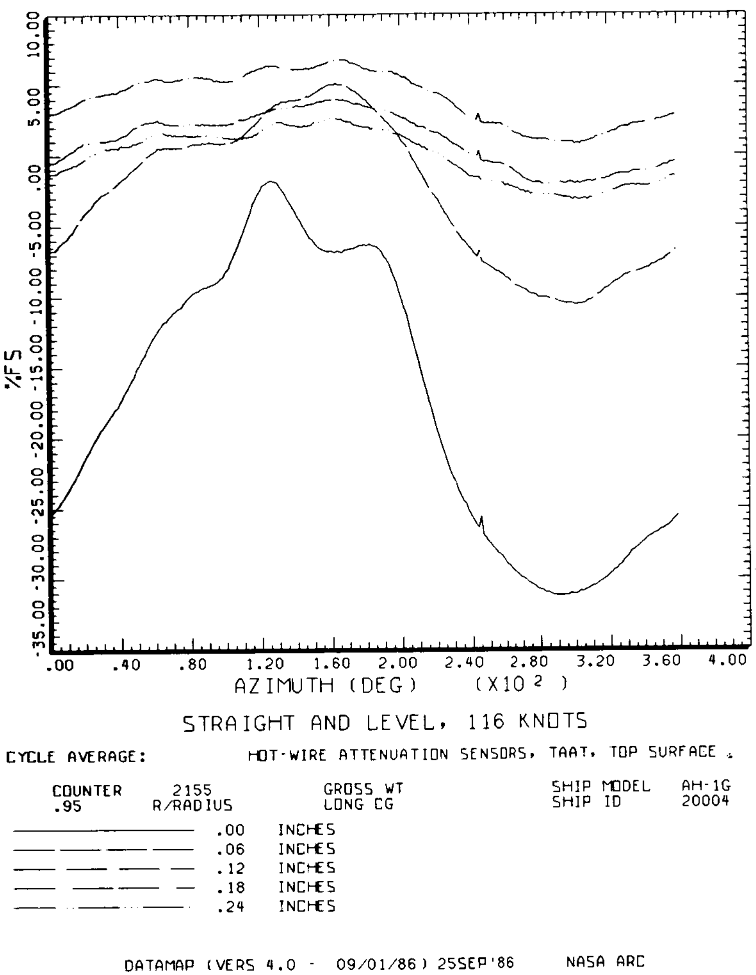

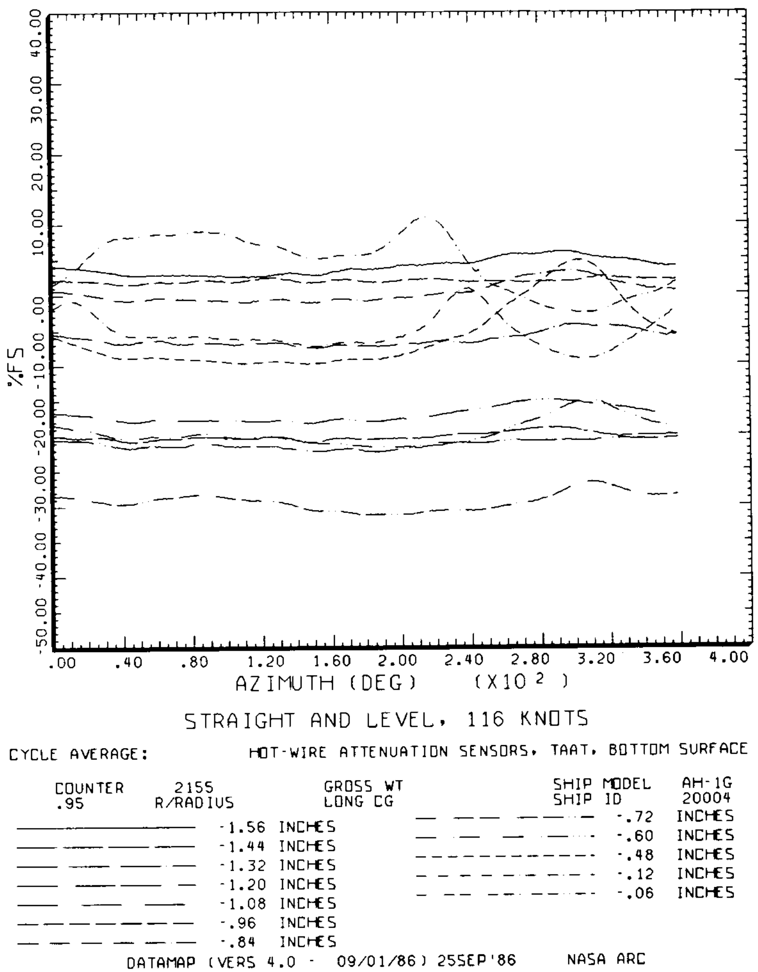

Figure 64.- Concluded. (d) 95% radius, upper surface; (e) 95% radius, lower surface.

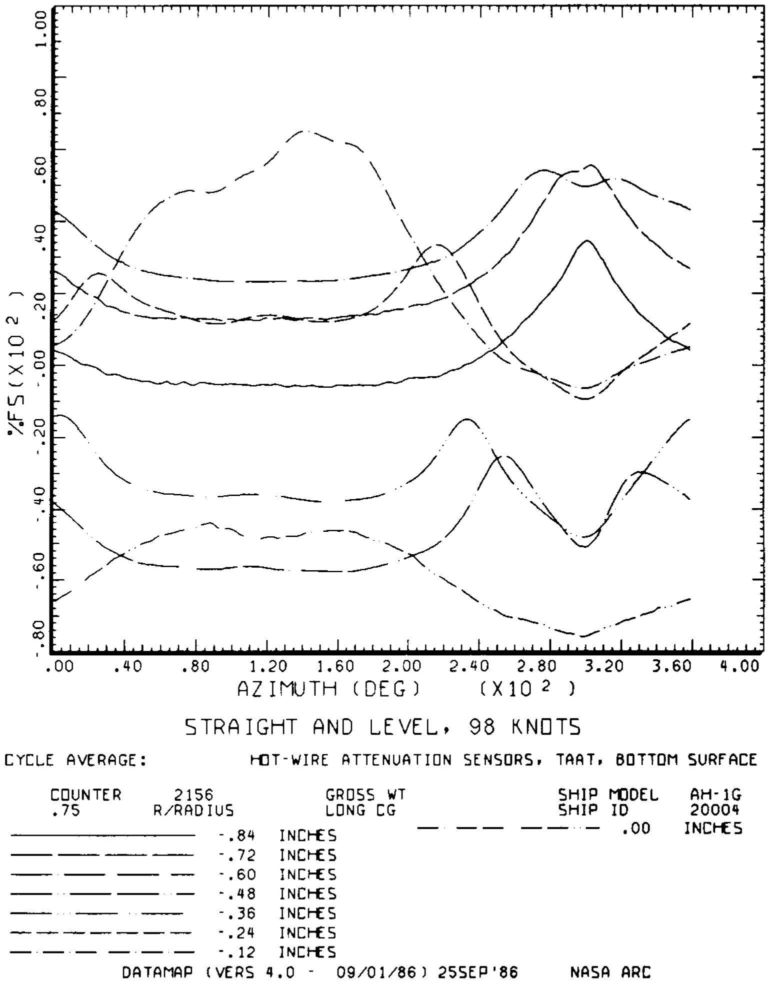

Figure 65.- Hot-wire anemometer versus azimuth at 116 KTAS. (a) 75% radius.

ORIGINAL PAGE IS
OF POOR QUALITY

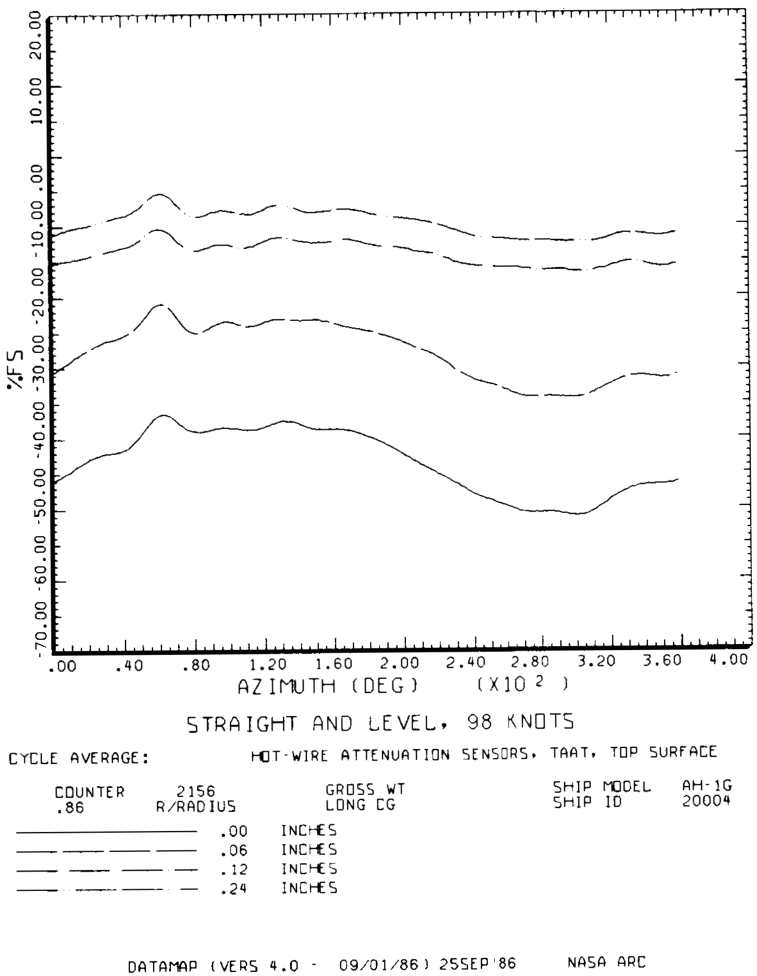

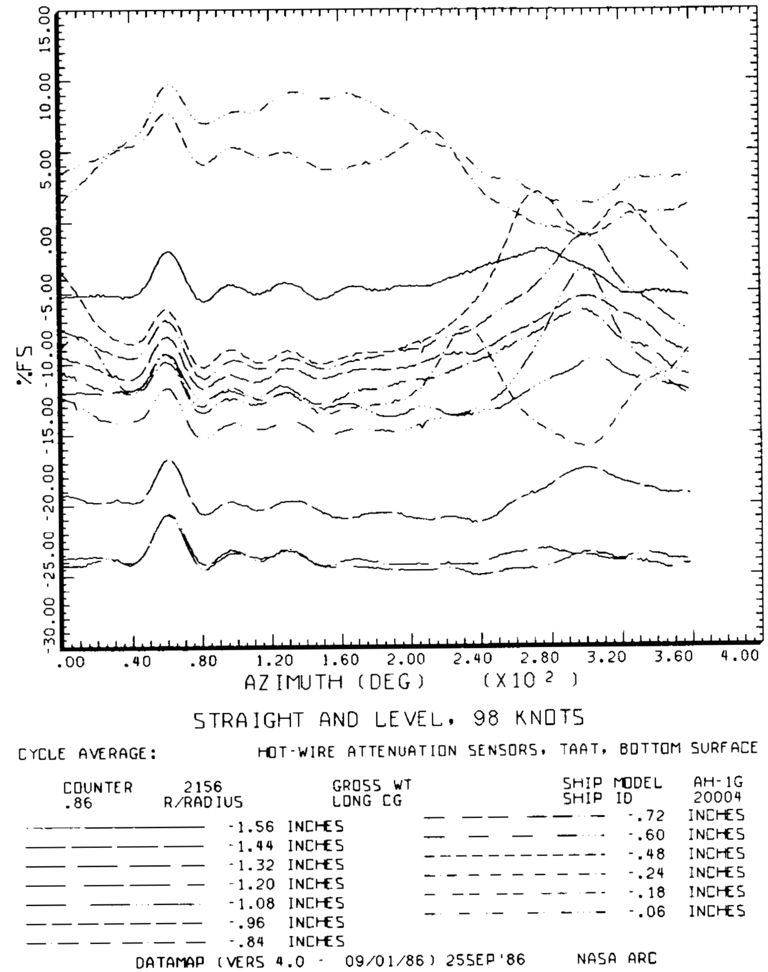

Figure 65.- Continued. (b) 86% radius, upper surface; (c) 86% radius, lower surface.

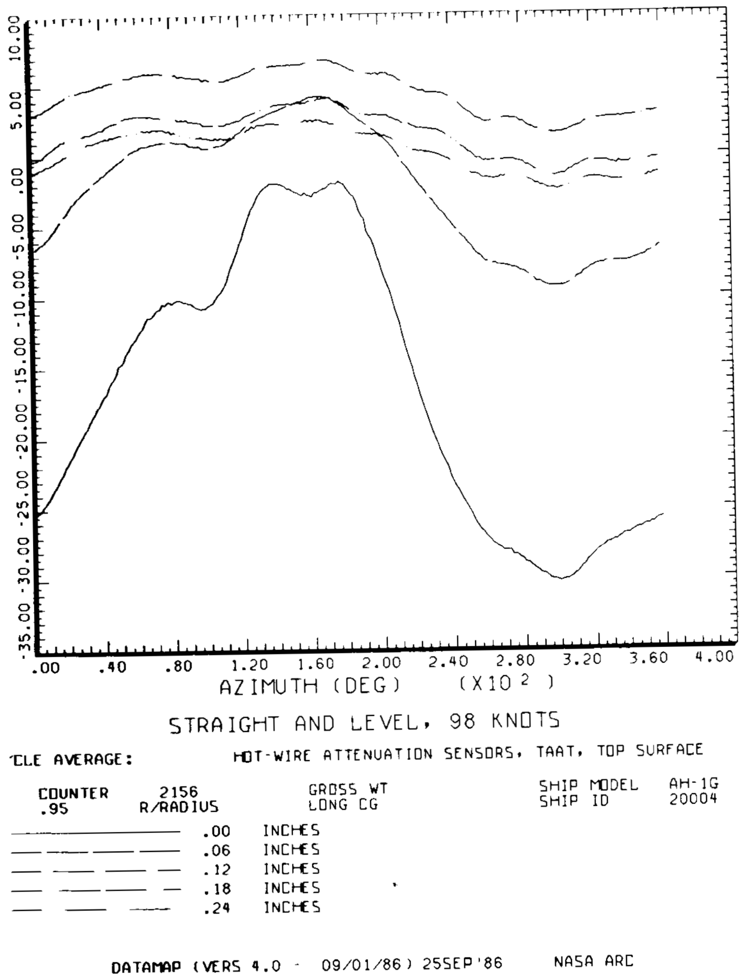

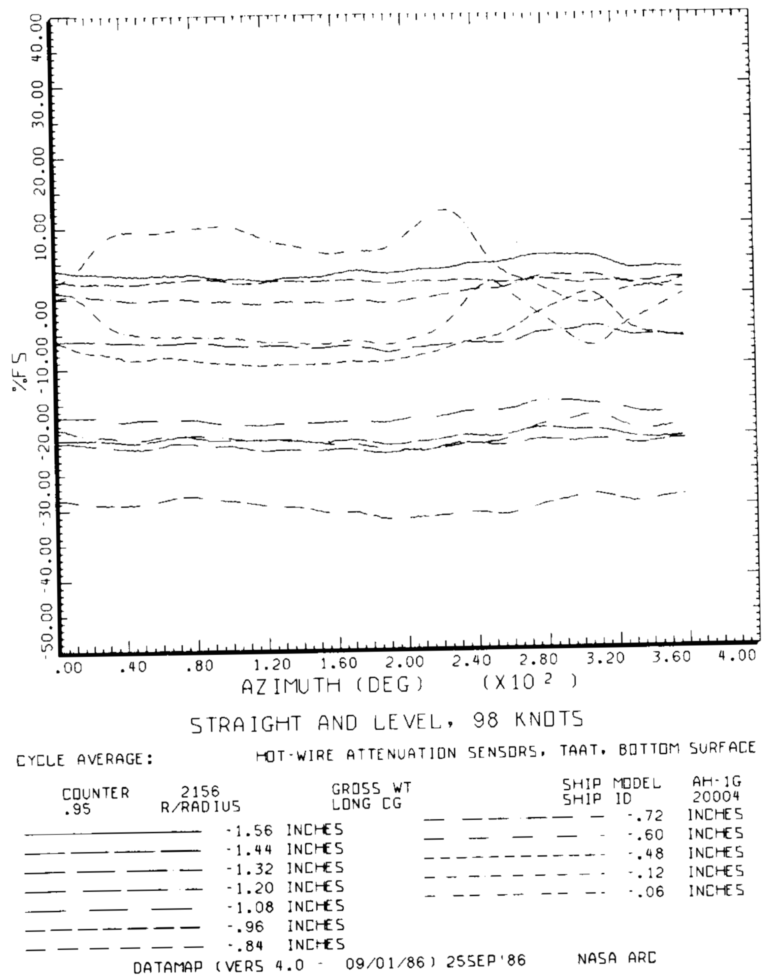

Figure 65.- Concluded. (d) 95% radius, upper surface; (e) 95% radius, lower surface.

ORIGINAL PAGE IS
OF POOR QUALITY

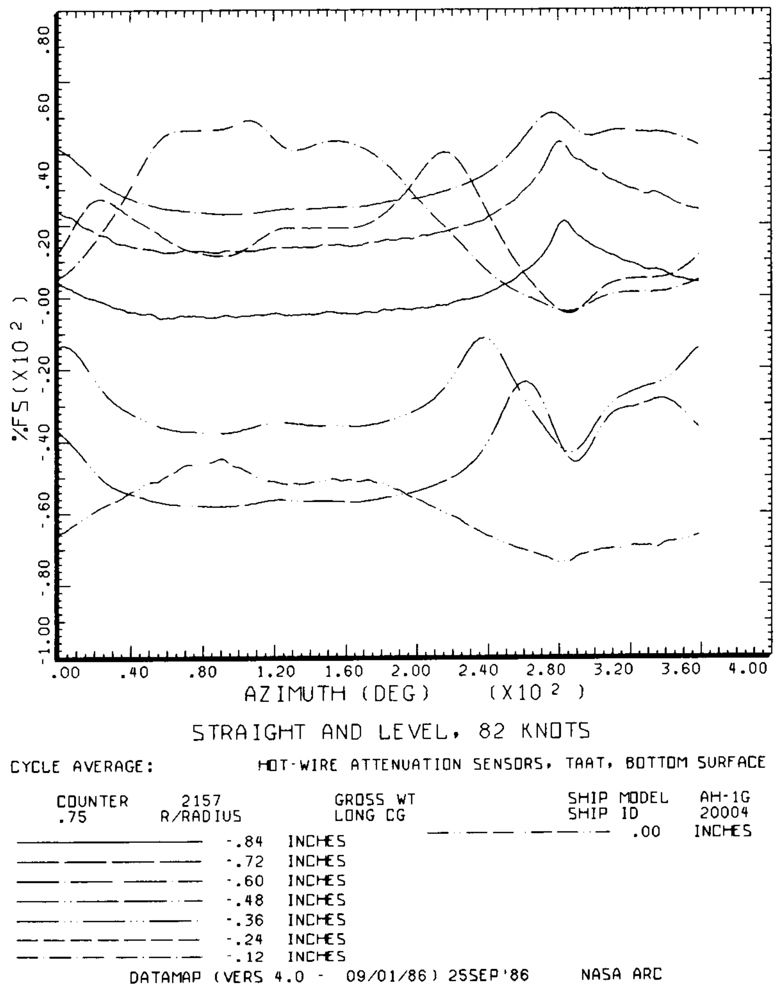

Figure 66.- Hot-wire anemometer versus azimuth at 82 KTAS. (a) 75% radius.

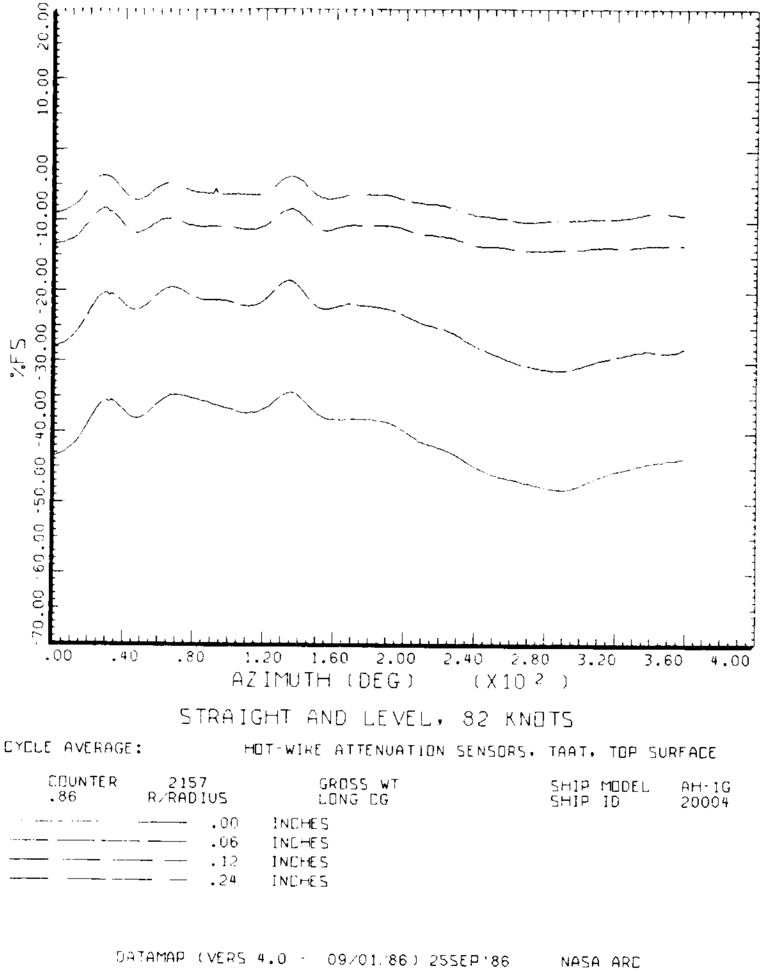

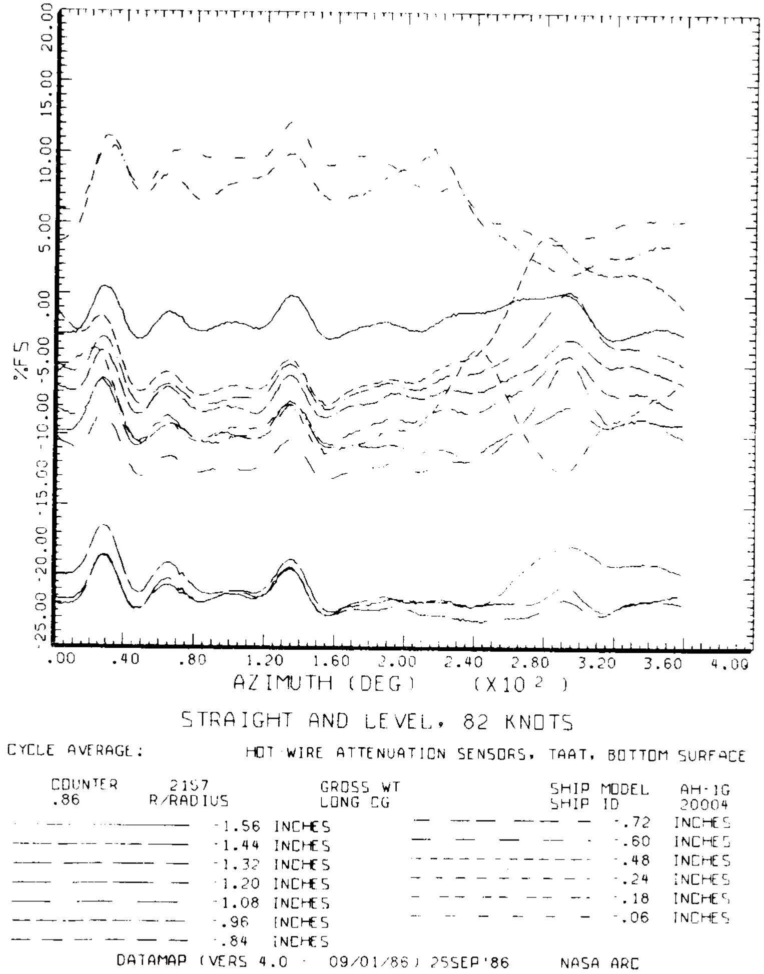

Figure 66.- Continued. (b) 86% radius, upper surface; (c) 86% radius, lower surface.

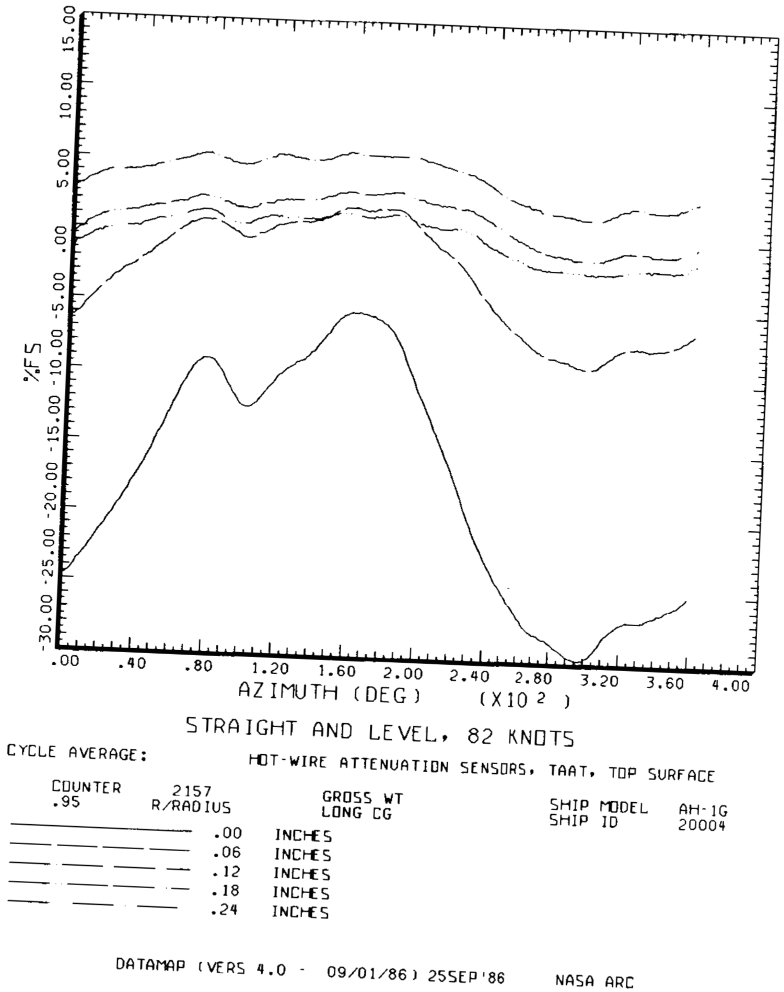

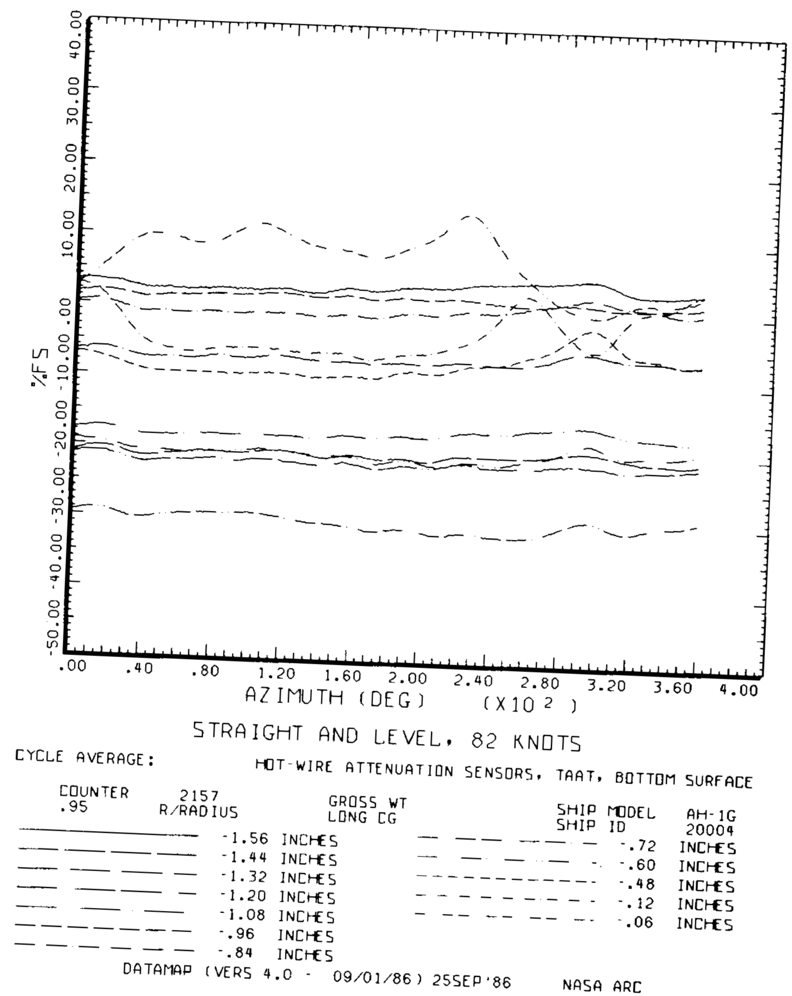

Figure 66.- Concluded. (d) 95% radius, upper surface; (e) 95% radius, lower surface.

ORIGINAL PAGE IS
OF POOR QUALITY

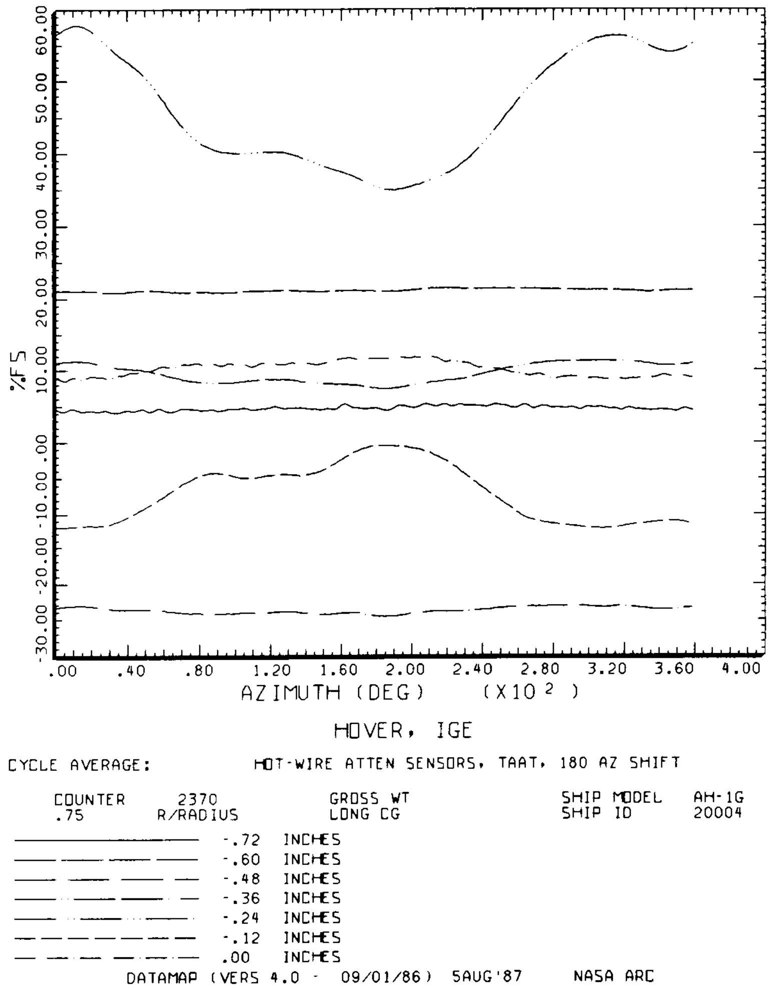

Figure 67.- Hot-wire anemometer versus azimuth in hover. (a) 75% radius.

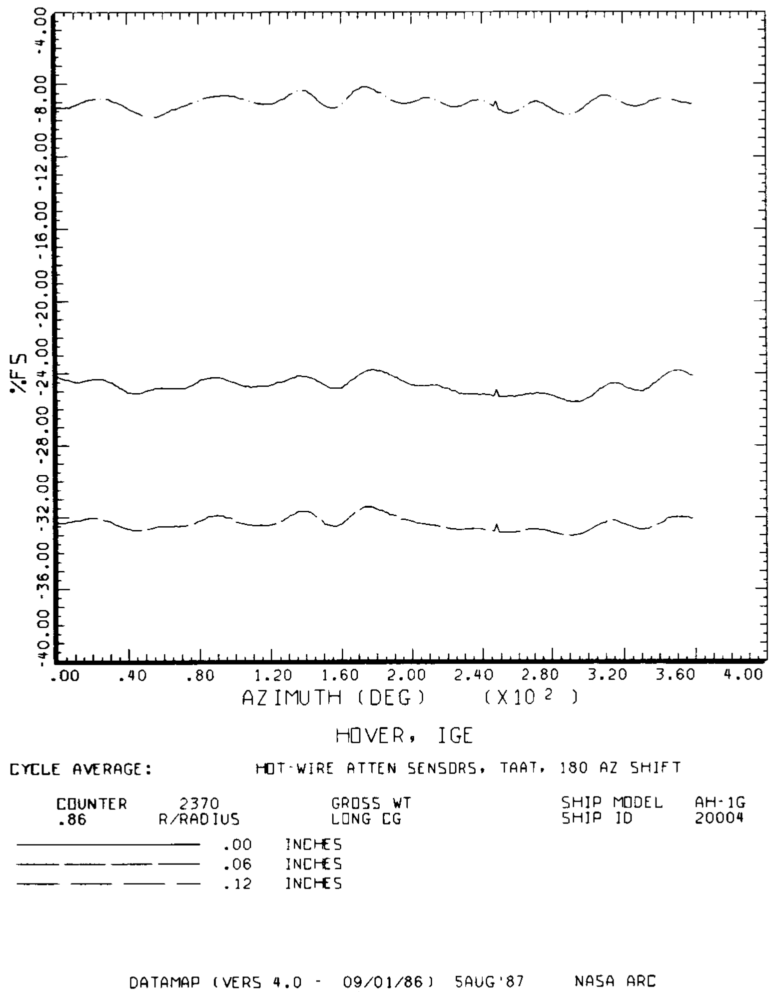

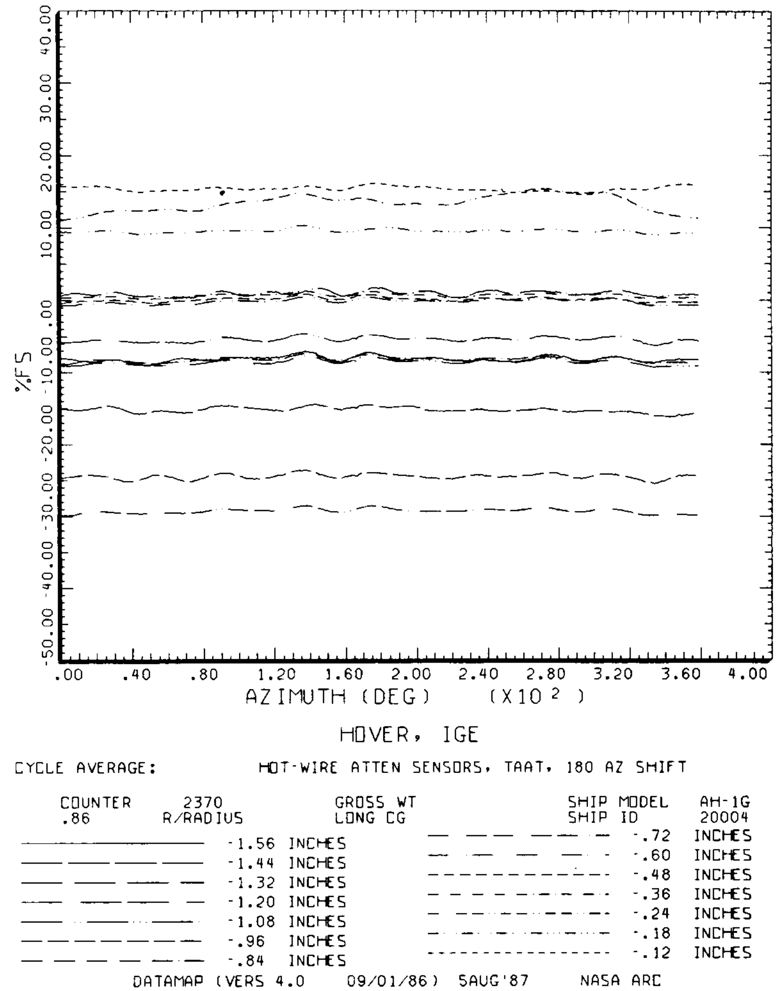

Figure 67.- Continued. (b) 86% radius, upper surface; (c) 86% radius, lower surface.

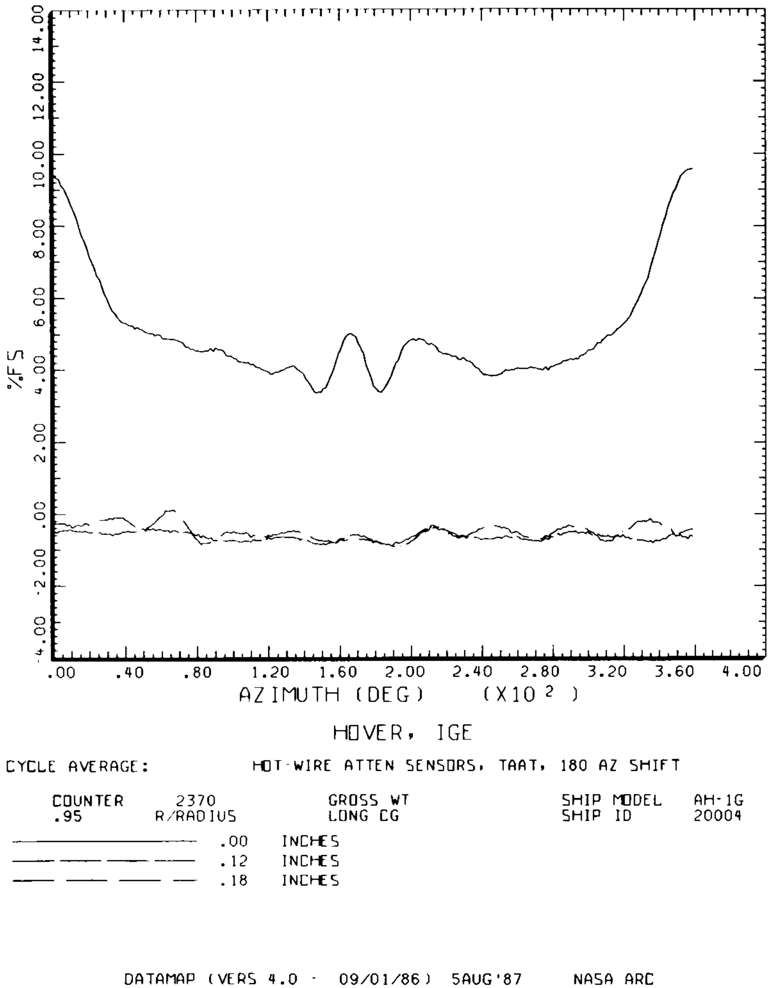

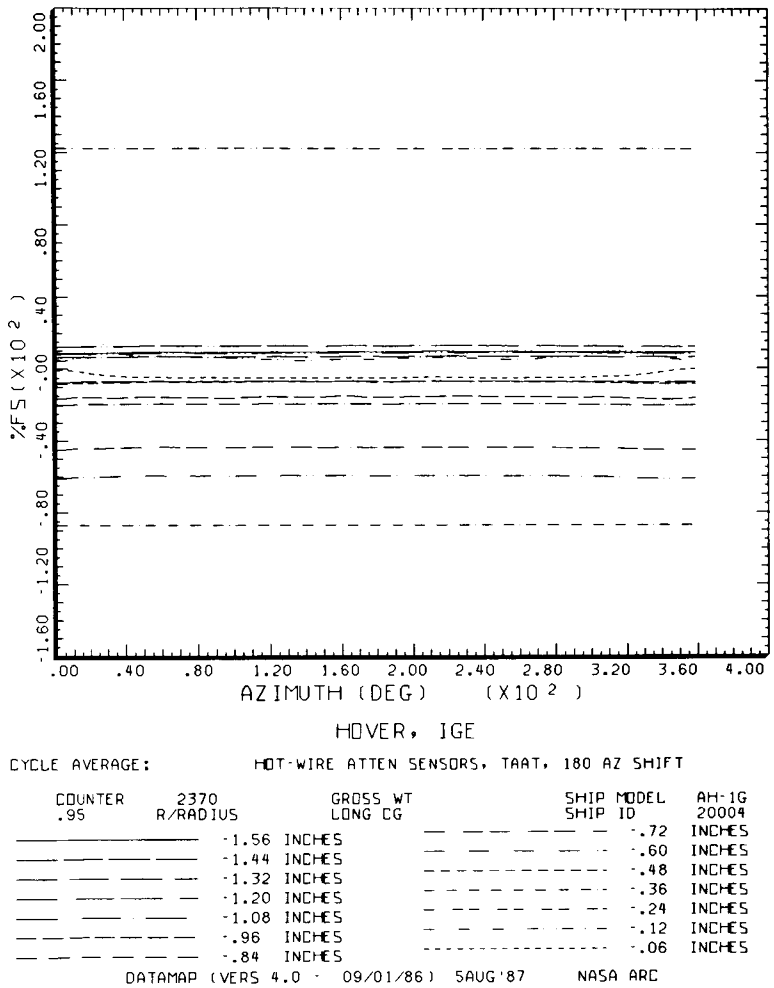

Figure 67.- Concluded. (d) 95% radius, upper surface; (e) 95% radius, lower surface.

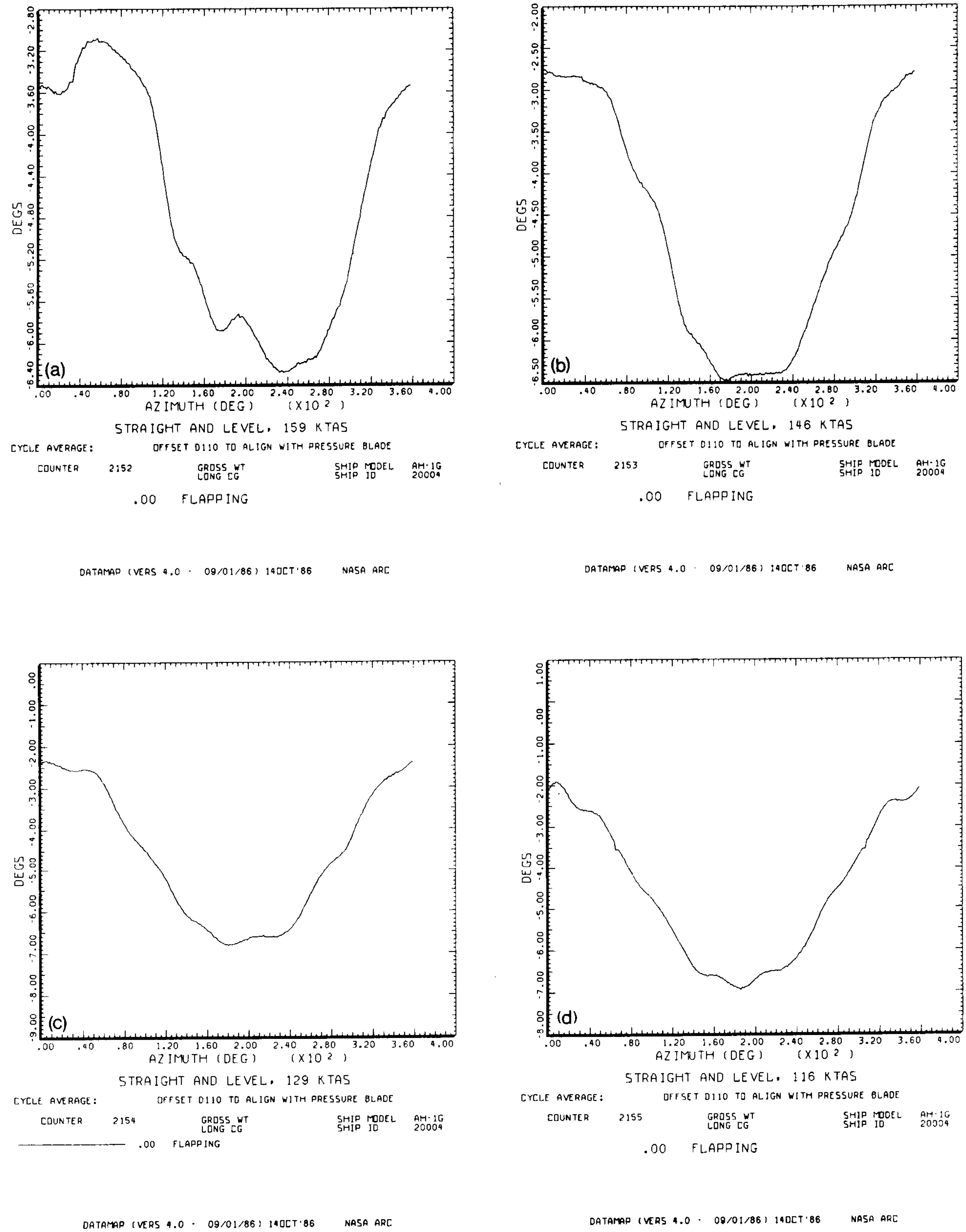

Figure 68.- Blade flapping versus azimuth. (a) At 159 KTAS; (b) at 146 KTAS; (c) at 129 KTAS; (d) at 116 KTAS.

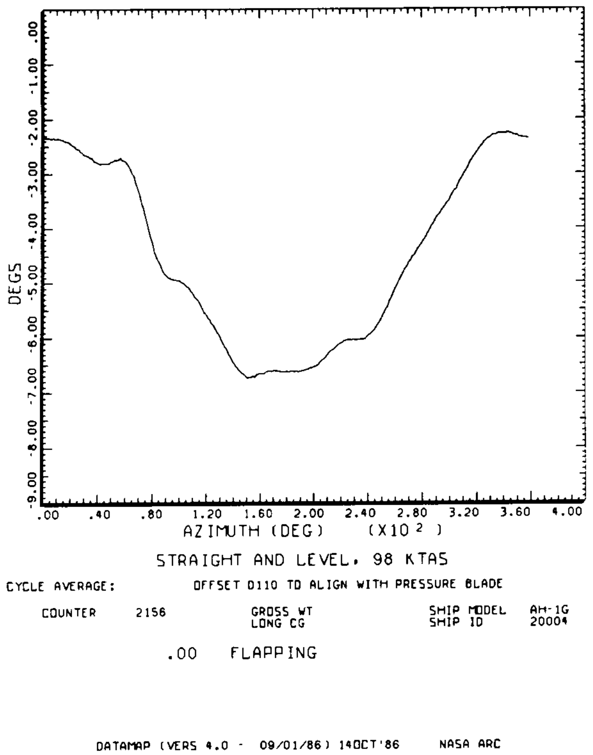

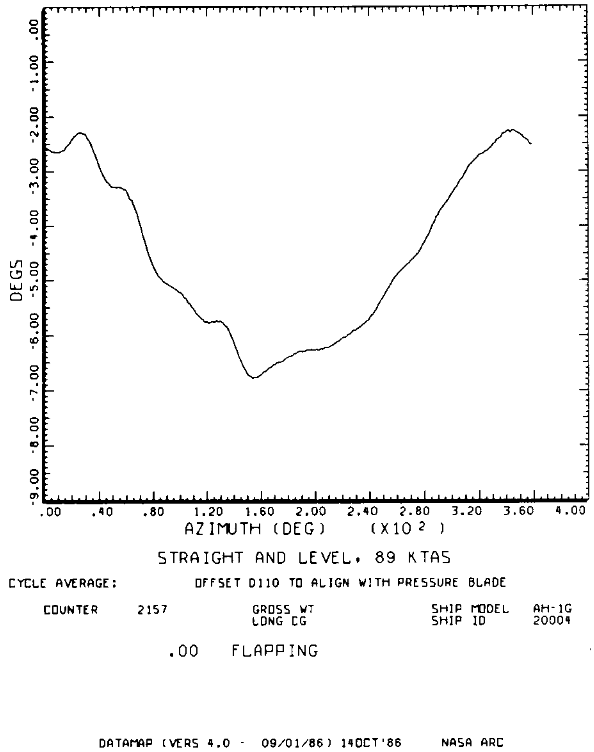

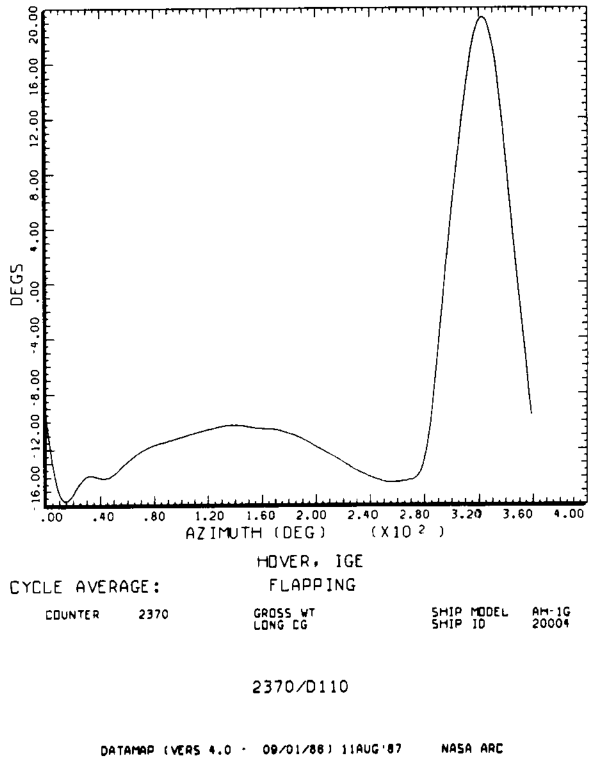

Figure 68.- Concluded. (e) At 98 KTAS; (f) at 82 KTAS; (g) at hover.

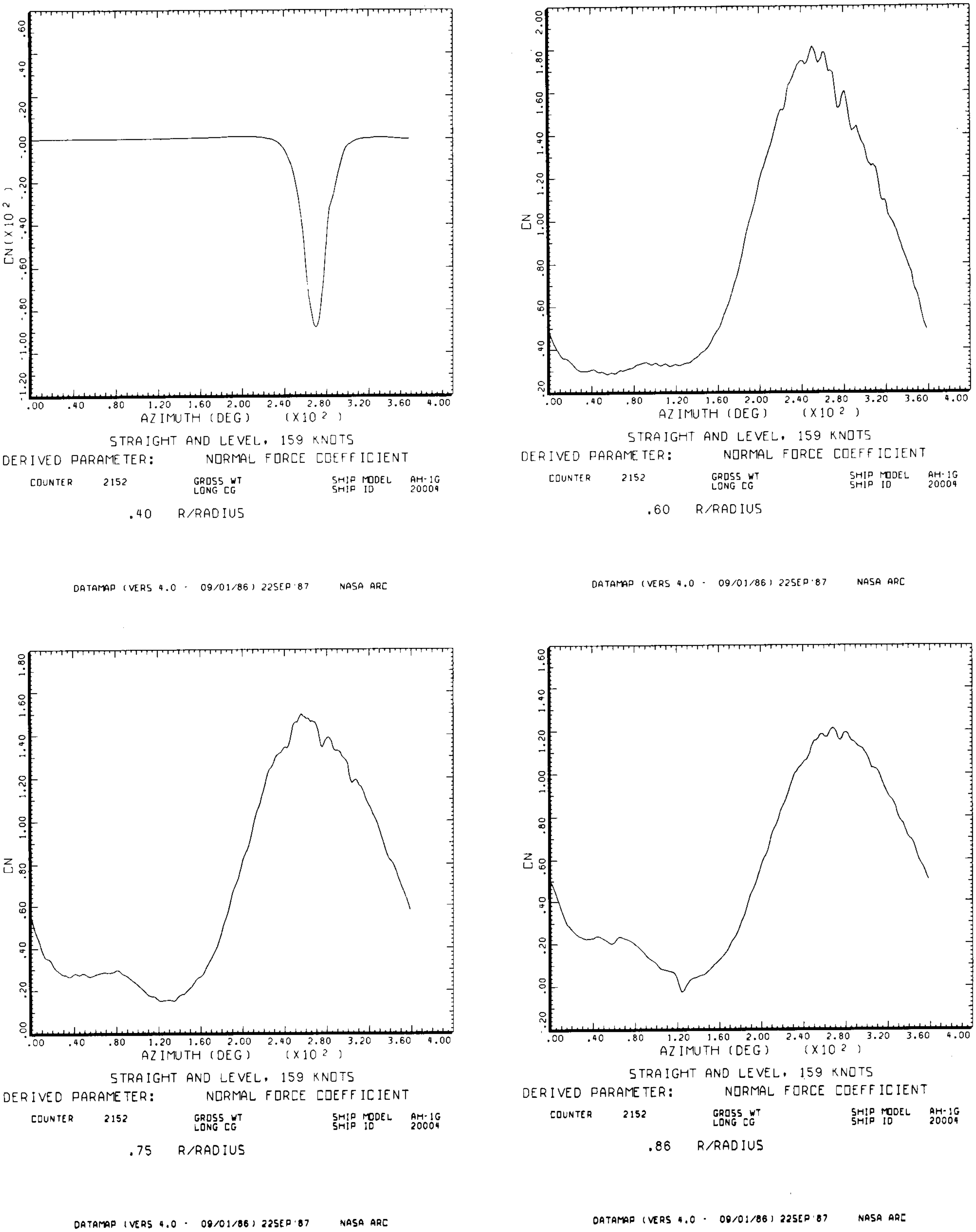

Figure 69.- C_n versus azimuth at 159 KTAS. (a) At 40% radius; (b) at 60% radius; (c) at 75% radius; (d) at 86% radius.

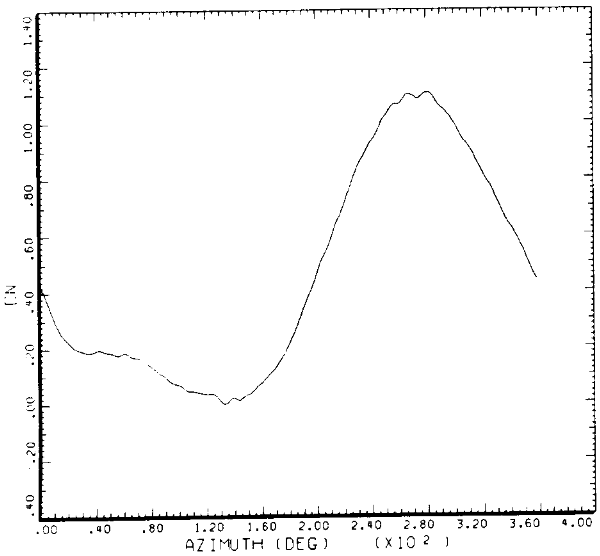

STRAIGHT AND LEVEL, 159 KNOTS
DERIVED PARAMETER: NORMAL FORCE COEFFICIENT
COUNTER 2152 GROSS WT LONG CG SHIP MODEL AH-1G SHIP ID 20004
.91 R/RADIUS

DATAMAP (VERS 4.0 - 09/01/86) 22SEP 87 NASA ARC

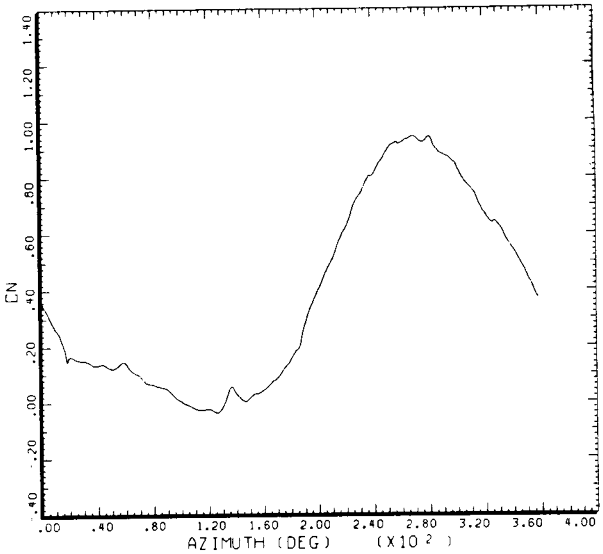

STRAIGHT AND LEVEL, 159 KNOTS
DERIVED PARAMETER: NORMAL FORCE COEFFICIENT
COUNTER 2152 GROSS WT LONG CG SHIP MODEL AH-1G SHIP ID 20004
.96 R/RADIUS

DATAMAP (VERS 4.0 - 09/01/86) 22SEP 87 NASA ARC

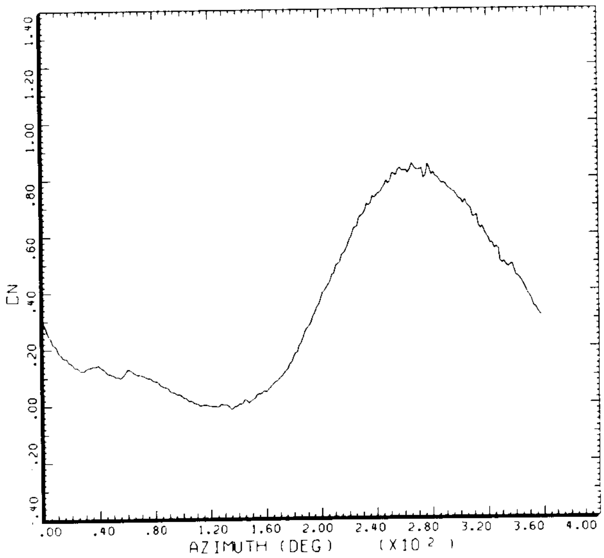

STRAIGHT AND LEVEL, 159 KNOTS
DERIVED PARAMETER: NORMAL FORCE COEFFICIENT
COUNTER 2152 GROSS WT LONG CG SHIP MODEL AH-1G SHIP ID 20004
.97 R/RADIUS

DATAMAP (VERS 4.0 - 09/01/86) 22SEP 87 NASA ARC

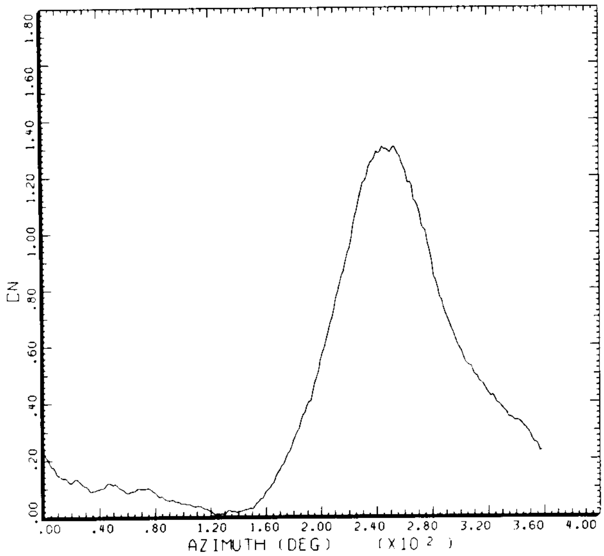

STRAIGHT AND LEVEL, 159 KNOTS
DERIVED PARAMETER: NORMAL FORCE COEFFICIENT
COUNTER 2152 GROSS WT LONG CG SHIP MODEL AH-1G SHIP ID 20004
.99 R/RADIUS

DATAMAP (VERS 4.0 - 09/01/86) 22SEP 87 NASA ARC

Figure 69.- Concluded. (e) At 91% radius; (f) at 96% radius; (g) 97% radius; (h) 99% radius.

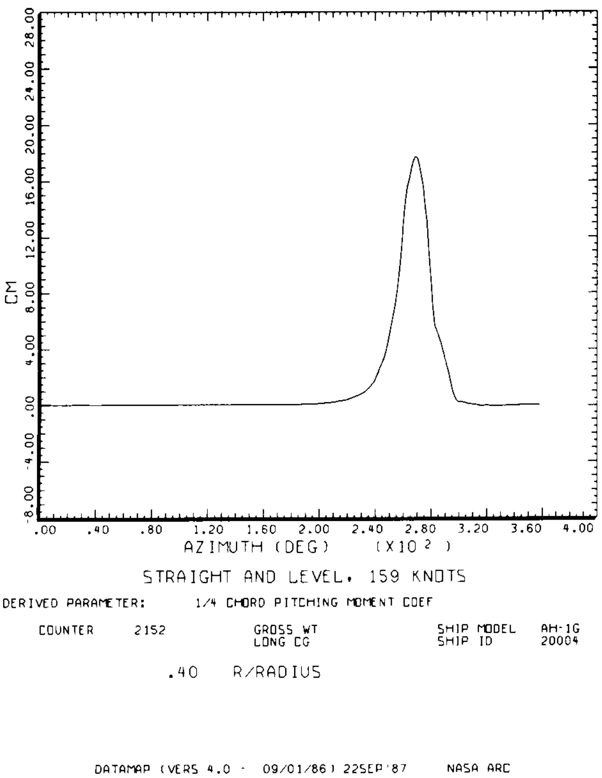

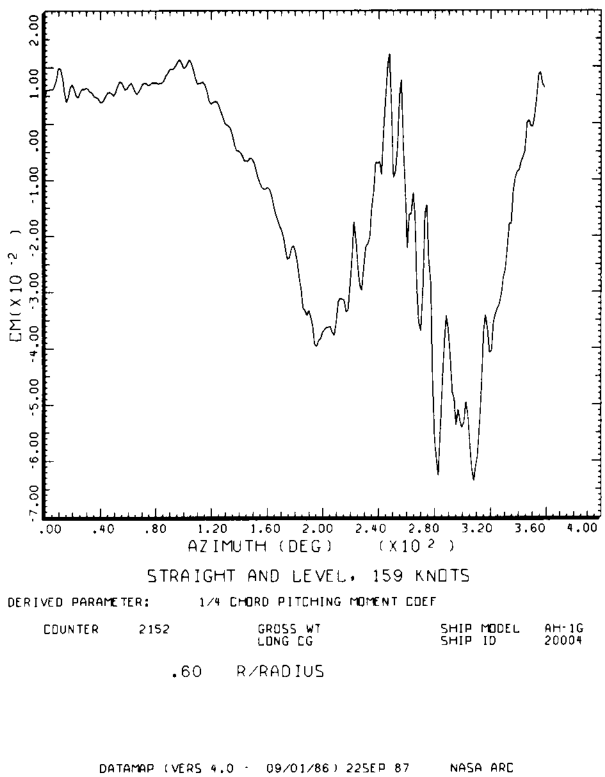

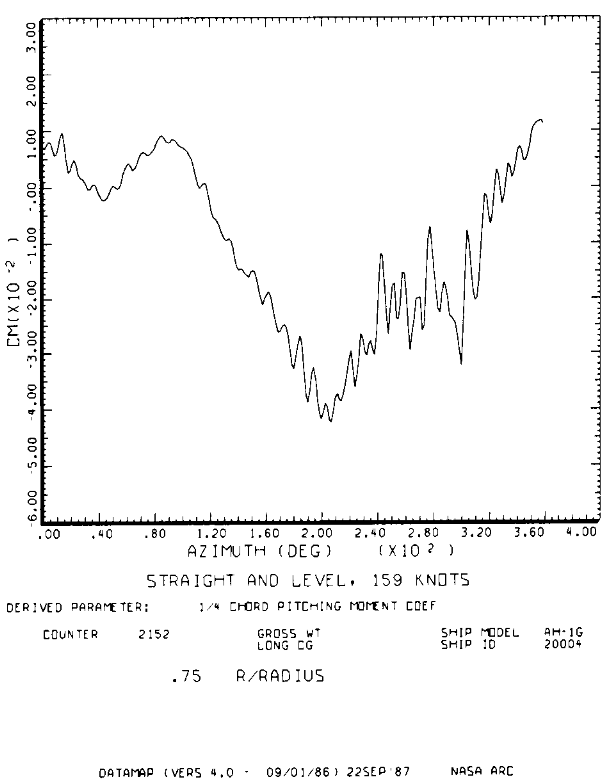

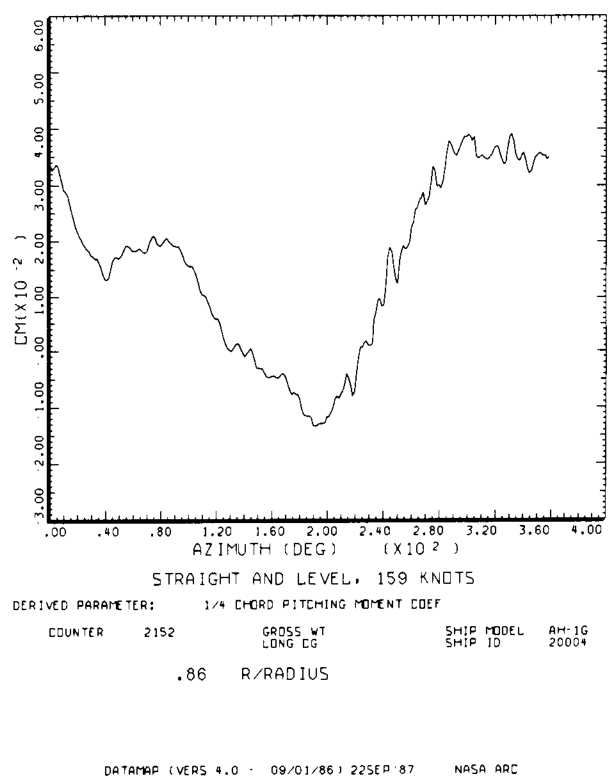

Figure 70.- C_m versus azimuth at 159 KTAS. (a) At 40% radius; (b) at 60% radius; (c) at 75% radius; (d) at 86% radius.

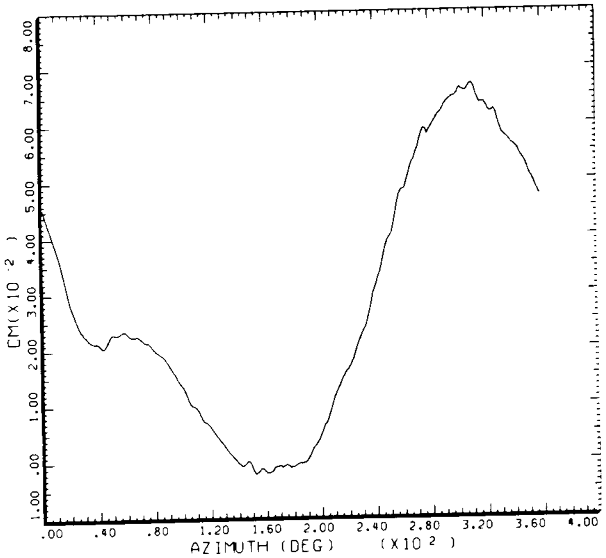

STRAIGHT AND LEVEL, 159 KNOTS

DERIVED PARAMETER: 1/4 CHORD PITCHING MOMENT COEF

COUNTER 2152 GROSS WT LONG CG SHIP MODEL AH-1G SHIP ID 20004

.91 R/RADIUS

DATAMAP (VERS 4.0 - 09/01/86) 22SEP'87 NASA ARC

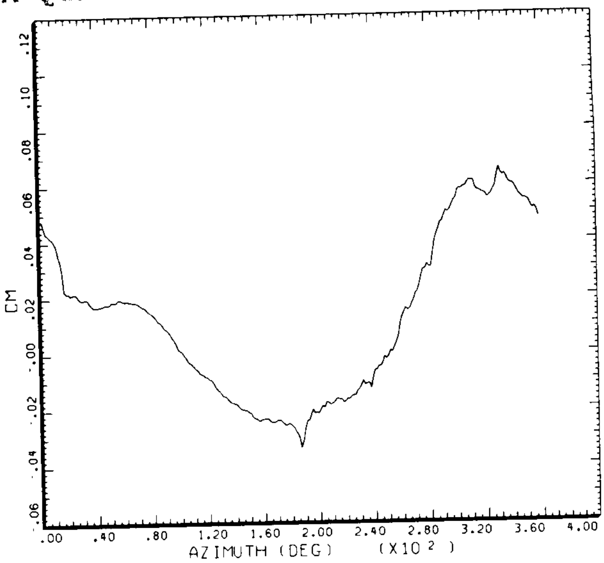

STRAIGHT AND LEVEL, 159 KNOTS

DERIVED PARAMETER: 1/4 CHORD PITCHING MOMENT COEF

COUNTER 2152 GROSS WT LONG CG SHIP MODEL AH-1G SHIP ID 20004

.96 R/RADIUS

DATAMAP (VERS 4.0 - 09/01/86) 22SEP'87 NASA ARC

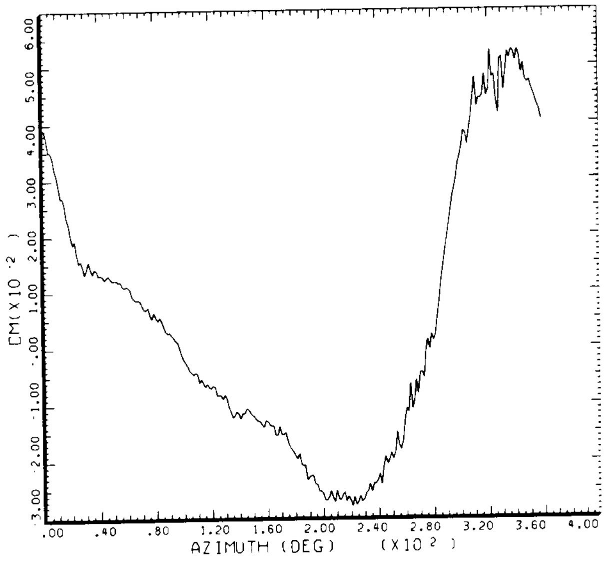

STRAIGHT AND LEVEL, 159 KNOTS

DERIVED PARAMETER: 1/4 CHORD PITCHING MOMENT COEF

COUNTER 2152 GROSS WT LONG CG SHIP MODEL AH-1G SHIP ID 20004

.97 R/RADIUS

DATAMAP (VERS 4.0 - 09/01/86) 22SEP'87 NASA ARC

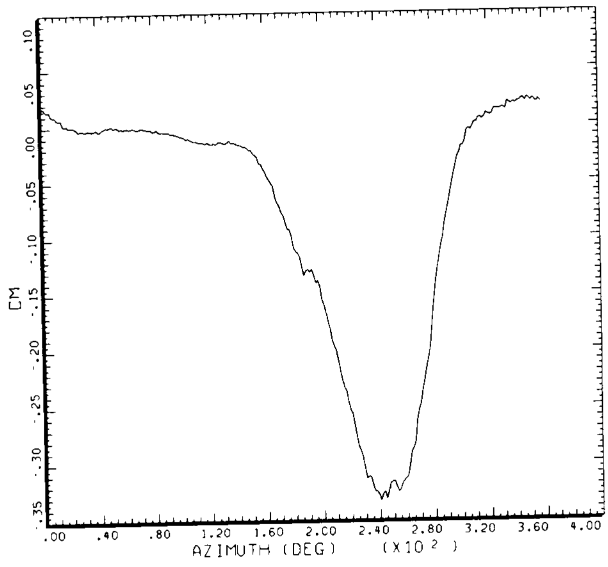

STRAIGHT AND LEVEL, 159 KNOTS

DERIVED PARAMETER: 1/4 CHORD PITCHING MOMENT COEF

COUNTER 2152 GROSS WT LONG CG SHIP MODEL AH-1G SHIP ID 20004

.99 R/RADIUS

DATAMAP (VERS 4.0 - 09/01/86) 22SEP'87 NASA ARC

Figure 70.- Concluded. (e) At 91% radius; (f) at 96% radius; (g) 97% radius; (h) 99% radius.

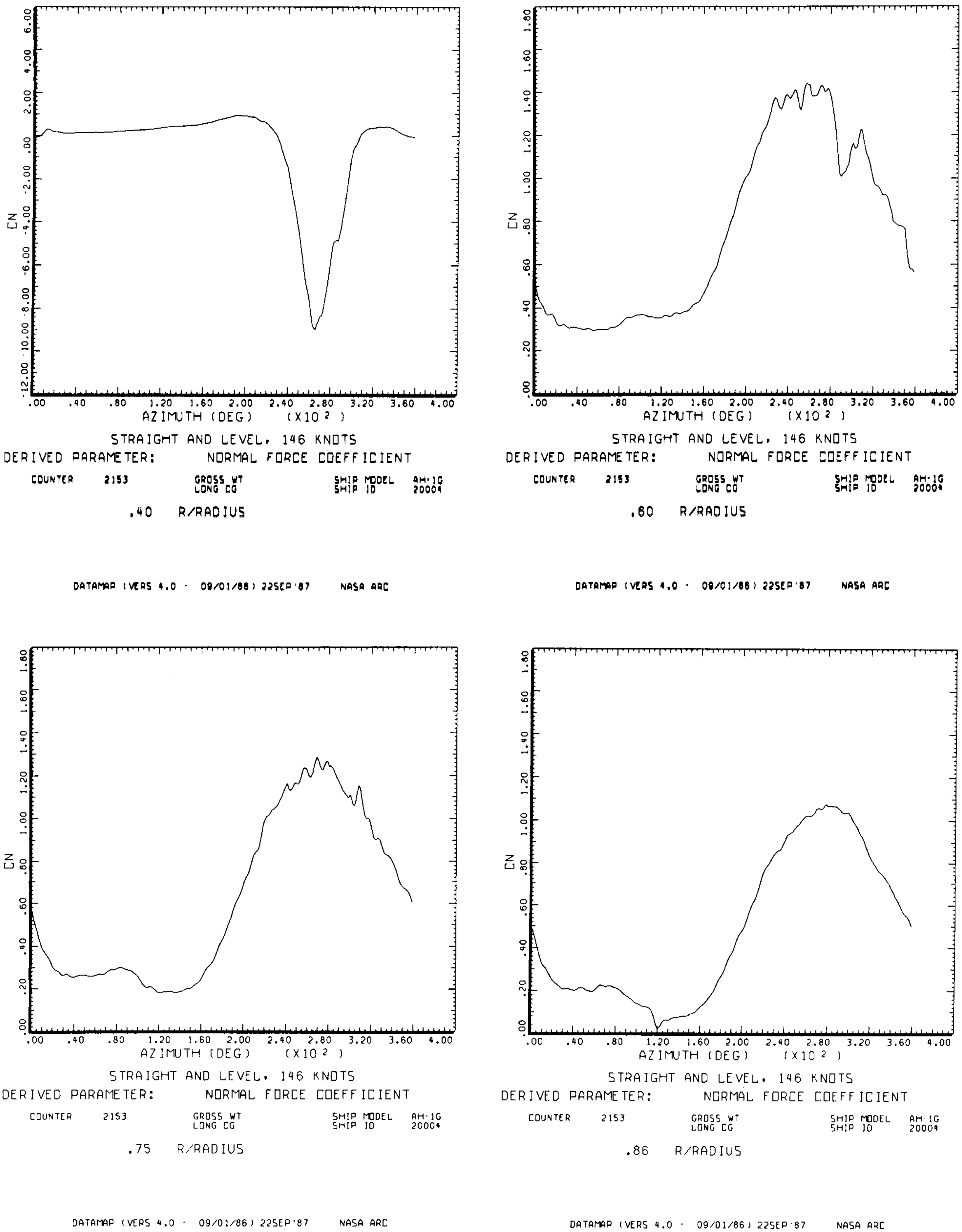

Figure 71.- C_n versus azimuth at 146 KTAS. (a) At 40% radius; (b) at 60% radius; (c) at 75% radius; (d) at 86% radius.

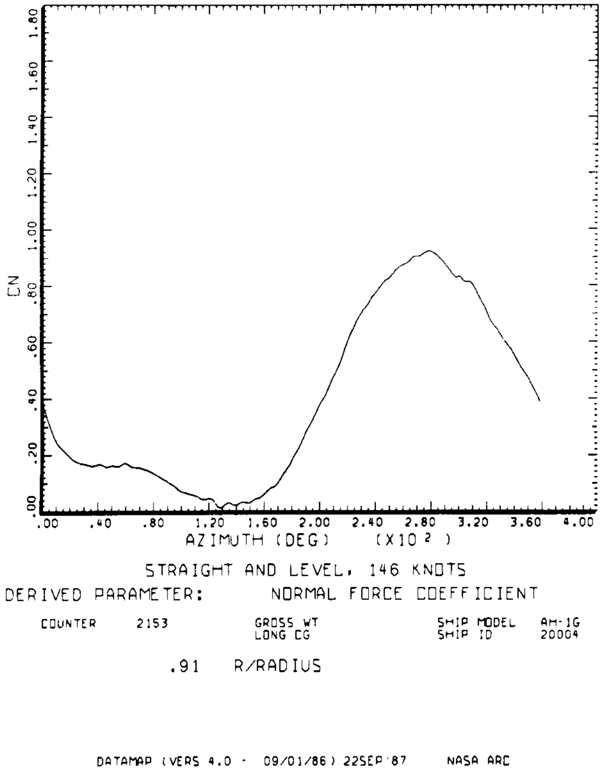

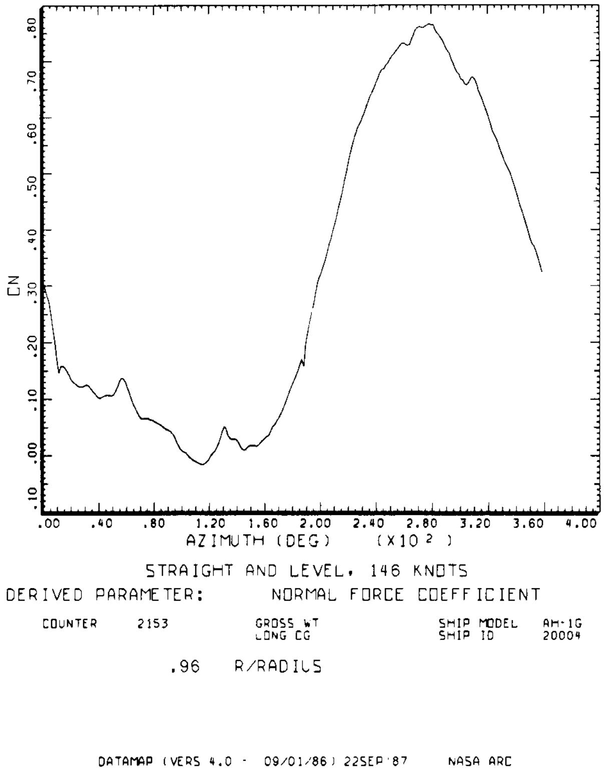

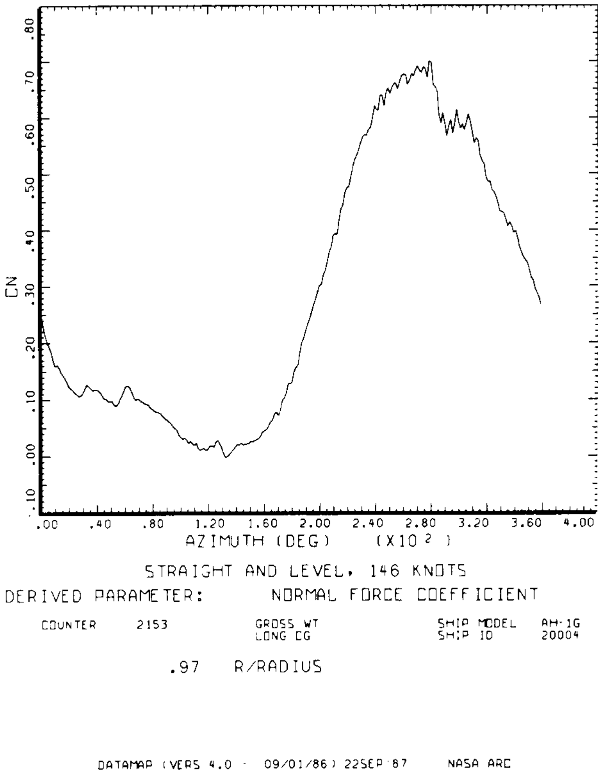

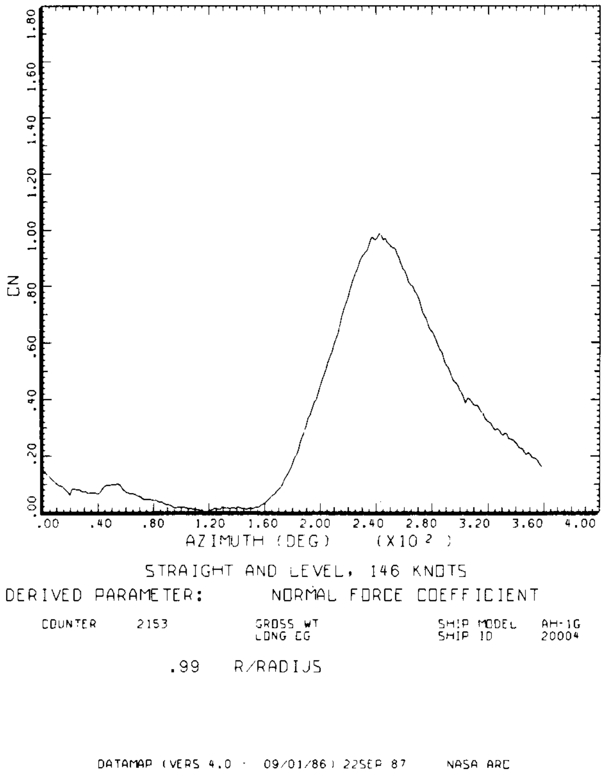

Figure 71.- Concluded. (e) At 91% radius; (f) at 96% radius; (g) 97% radius; (h) 99% radius.

ORIGINAL PAGE IS
OF POOR QUALITY

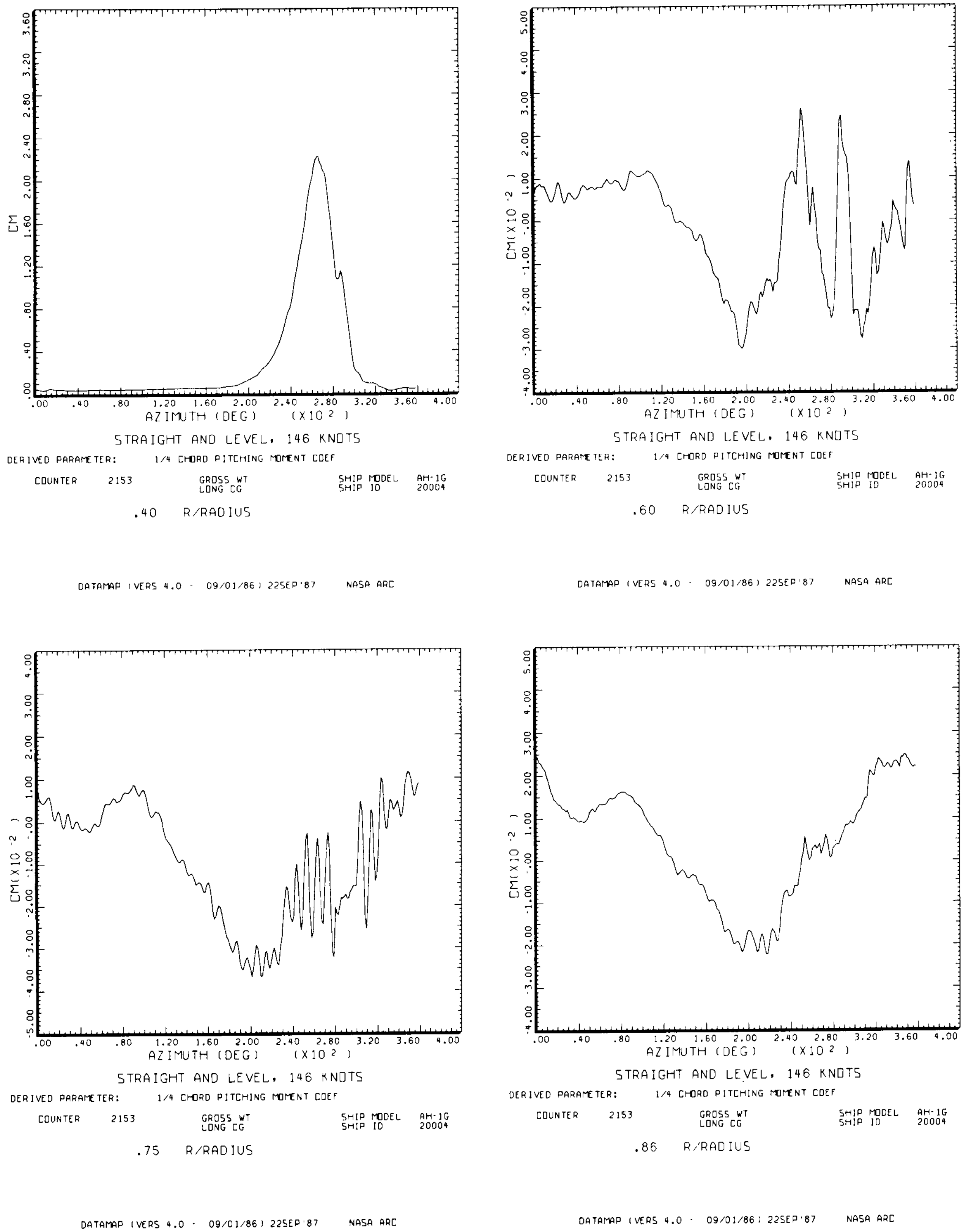

Figure 72.- C_m versus azimuth at 146 KTAS. (a) At 40% radius; (b) at 60% radius; (c) at 75% radius; (d) at 86% radius.

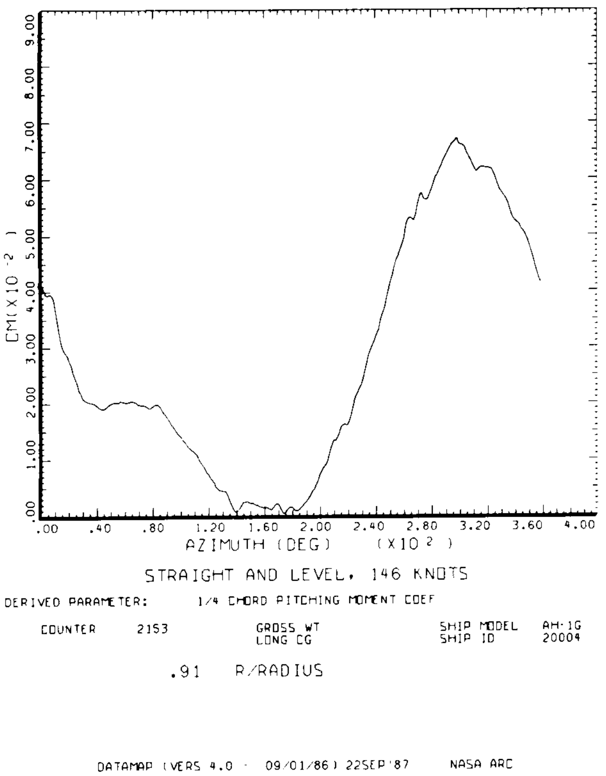

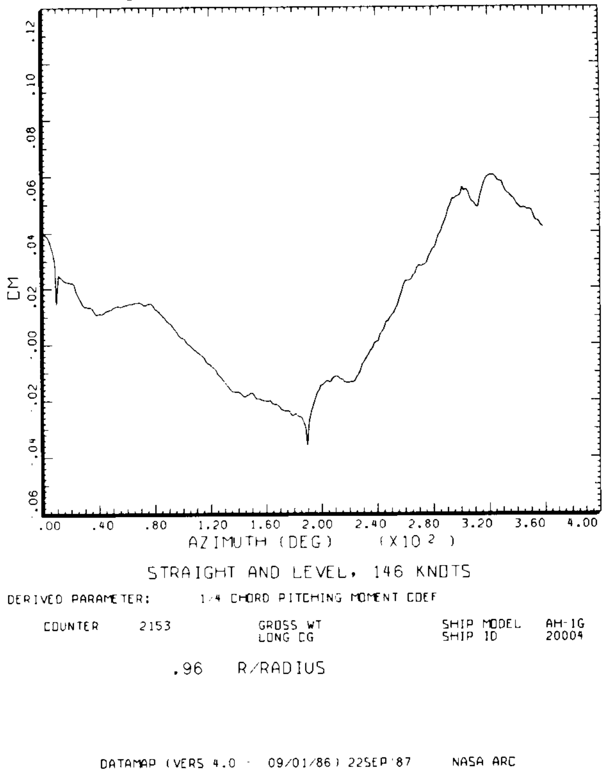

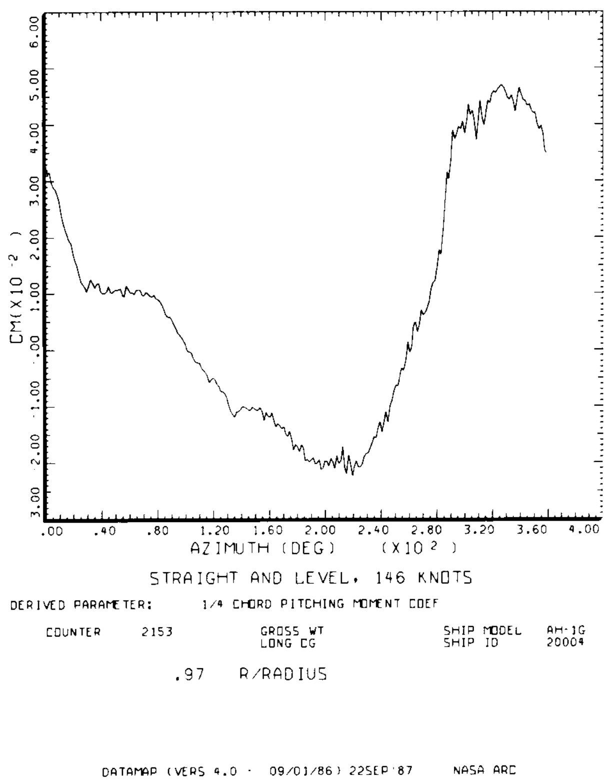

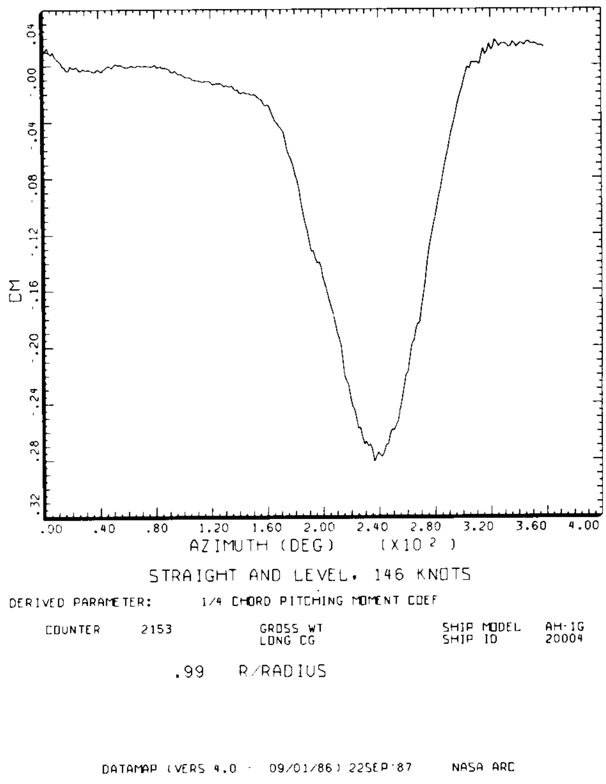

Figure 72.- Concluded. (e) At 91% radius; (f) at 96% radius; (g) 97% radius; (h) 99% radius.

ORIGINAL PAGE IS
OF POOR QUALITY

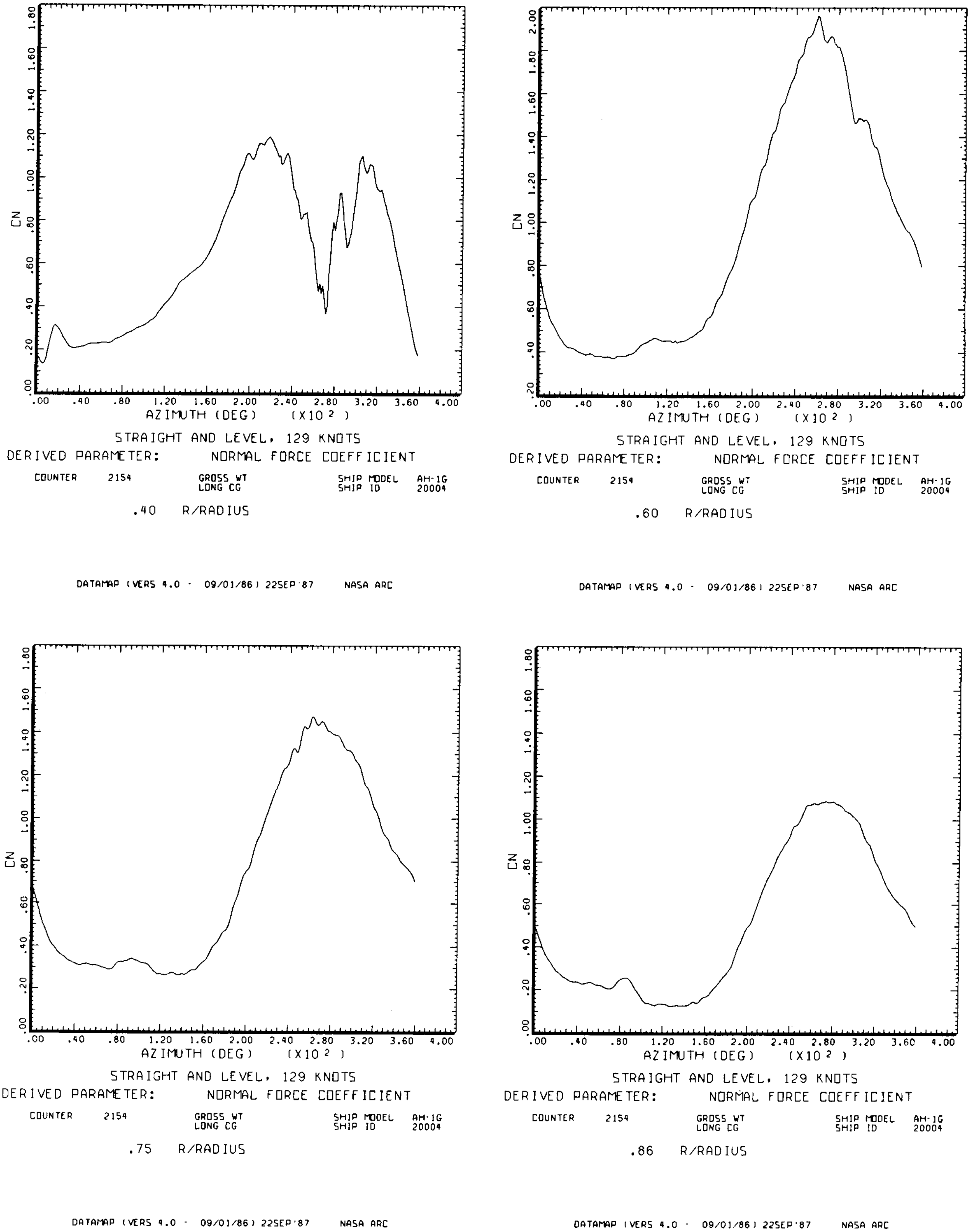

Figure 73.- C_n versus azimuth at 129 KTAS. (a) At 40% radius; (b) at 60% radius; (c) at 75% radius; (d) at 86% radius.

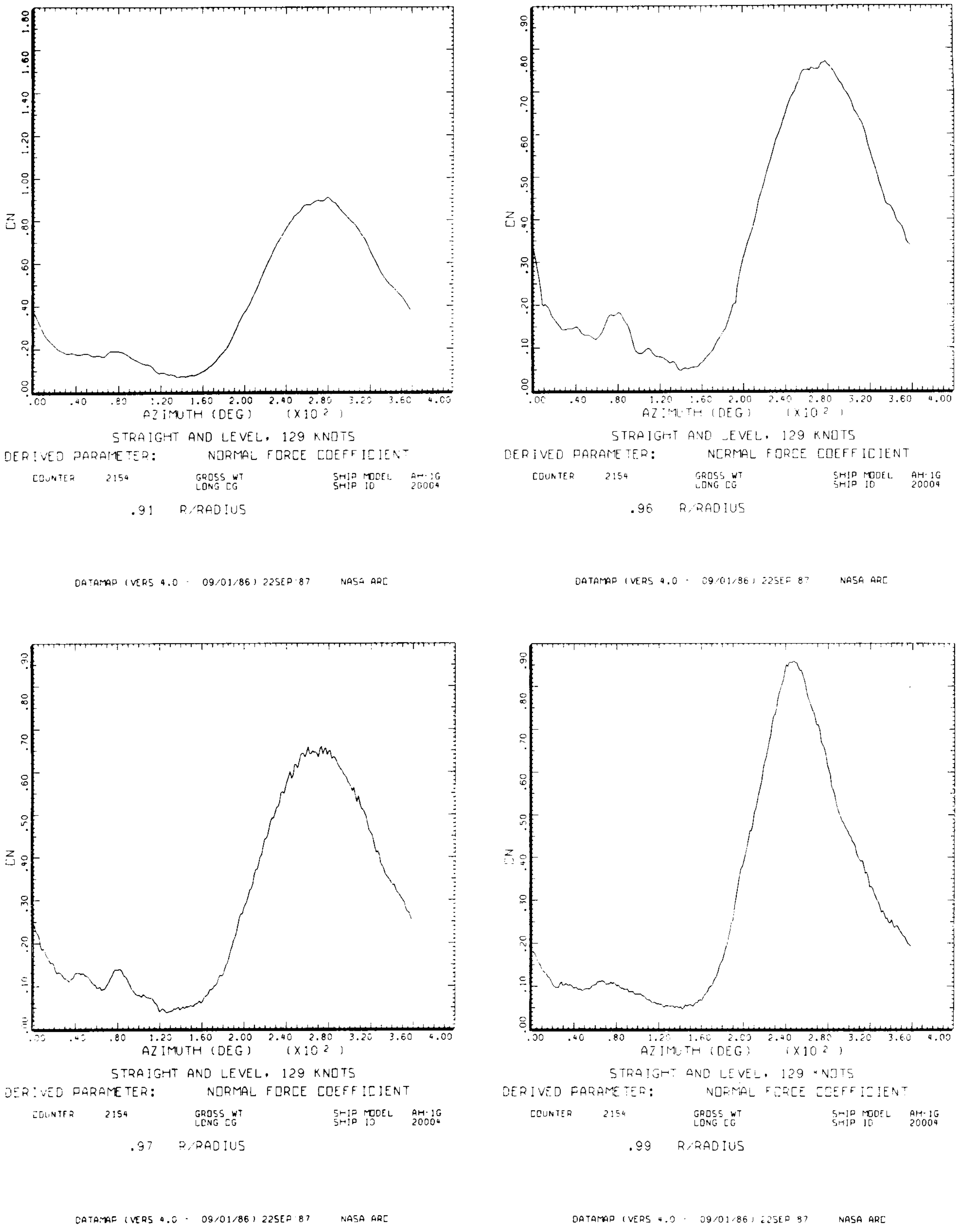

Figure 73.- Concluded. (e) At 91% radius; (f) at 96% radius; (g) 97% radius; (h) 99% radius.

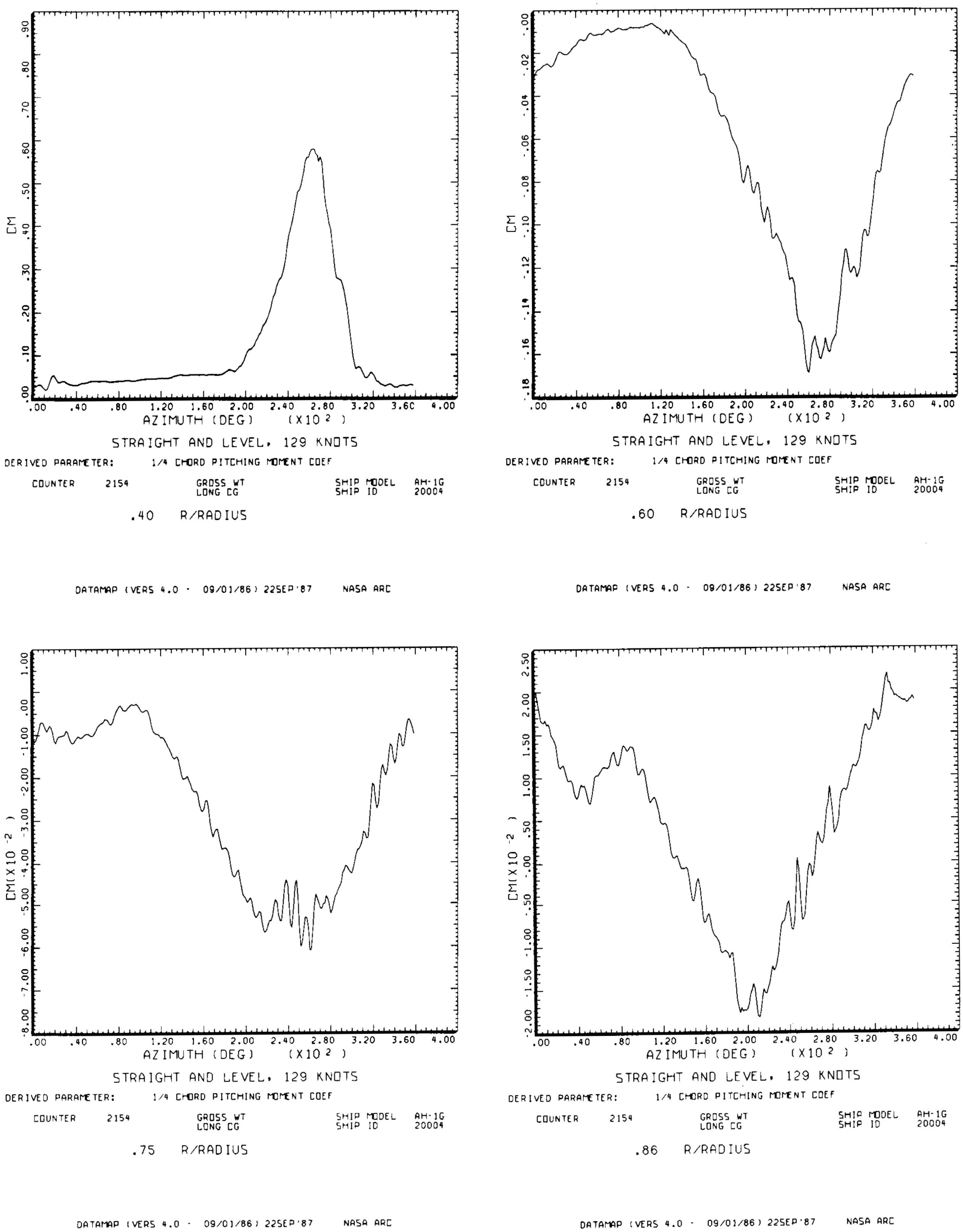

Figure 74.- C_m versus azimuth at 129 KTAS. (a) At 40% radius; (b) at 60% radius; (c) at 75% radius; (d) at 86% radius.

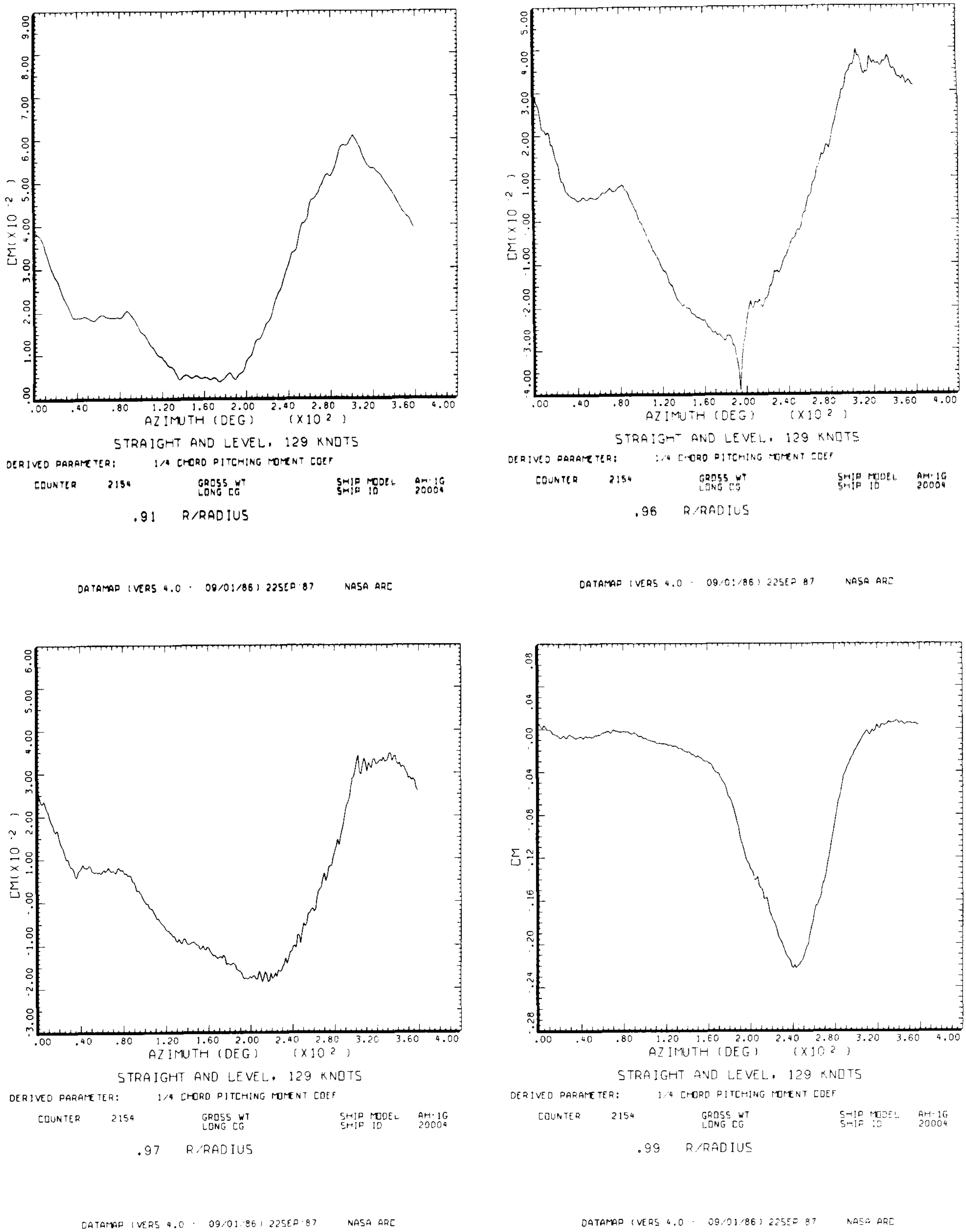

Figure 74.- Concluded. (e) At 91% radius; (f) at 96% radius; (g) 97% radius; (h) 99% radius.

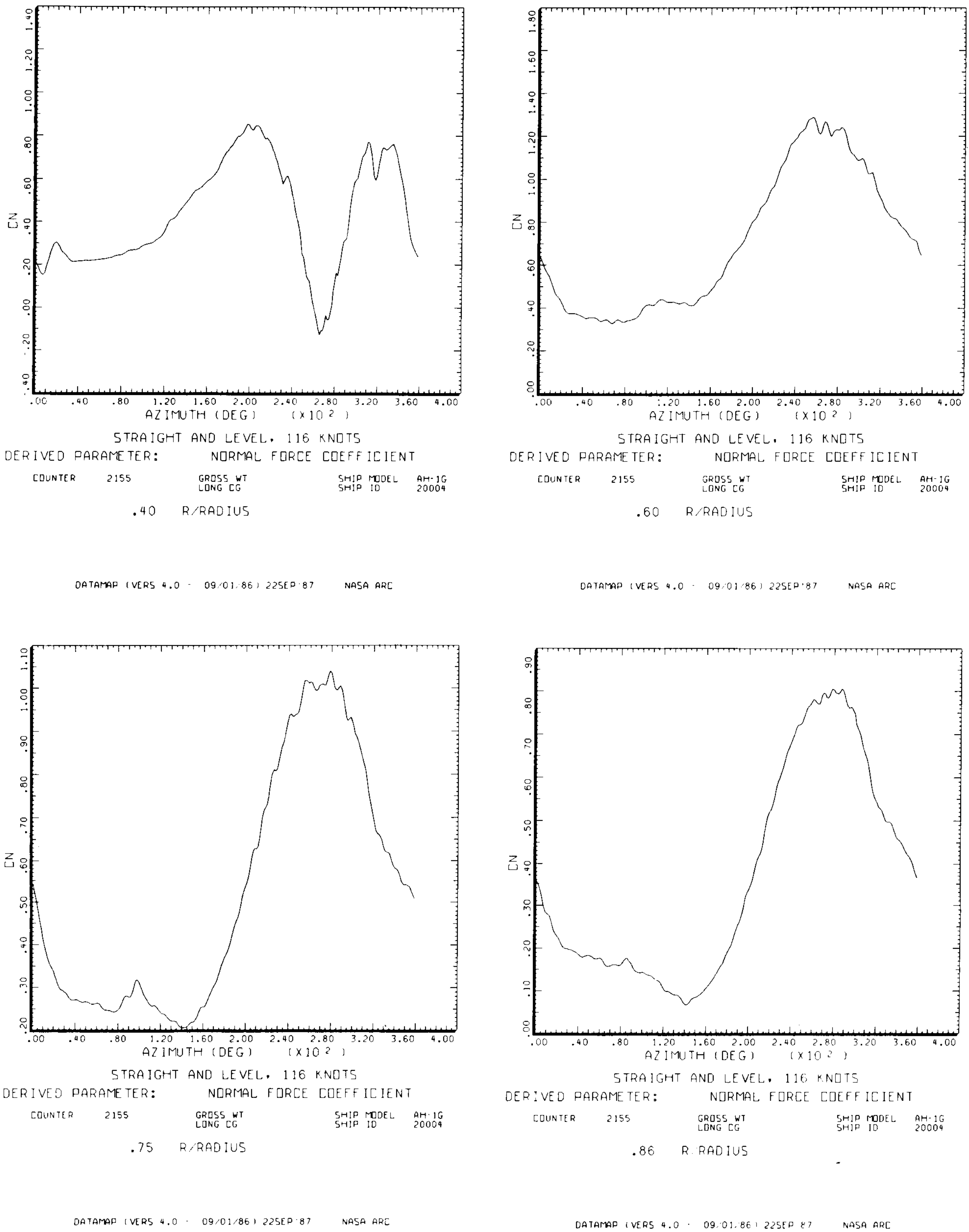

Figure 75.- C_n versus azimuth at 116 KTAS. (a) At 40% radius; (b) at 60% radius; (c) at 75% radius; (d) at 86% radius.

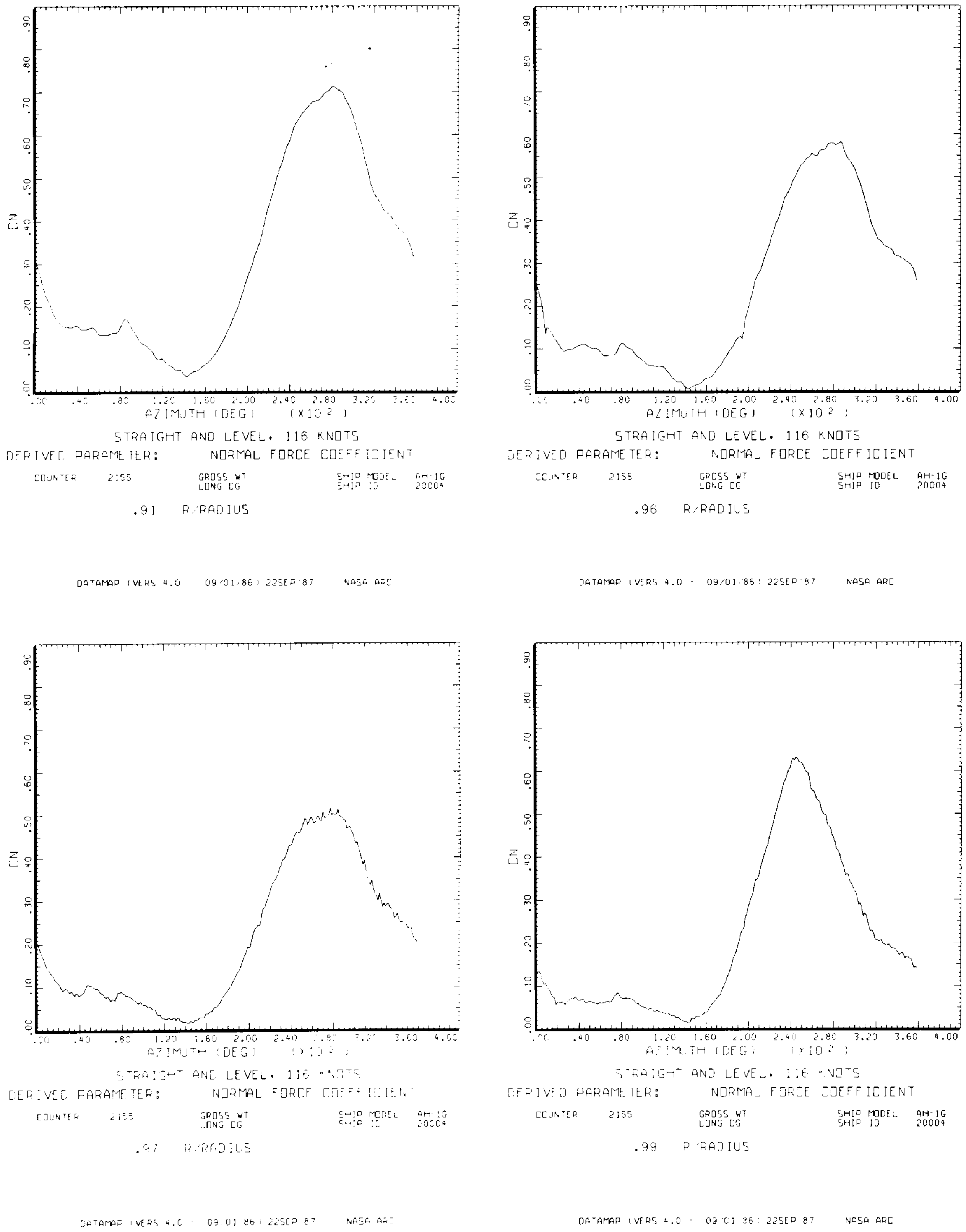

Figure 75.- Concluded. (e) At 91% radius; (f) at 96% radius; (g) 97% radius; (h) 99% radius.

ORIGINAL PAGE IS OF POOR QUALITY

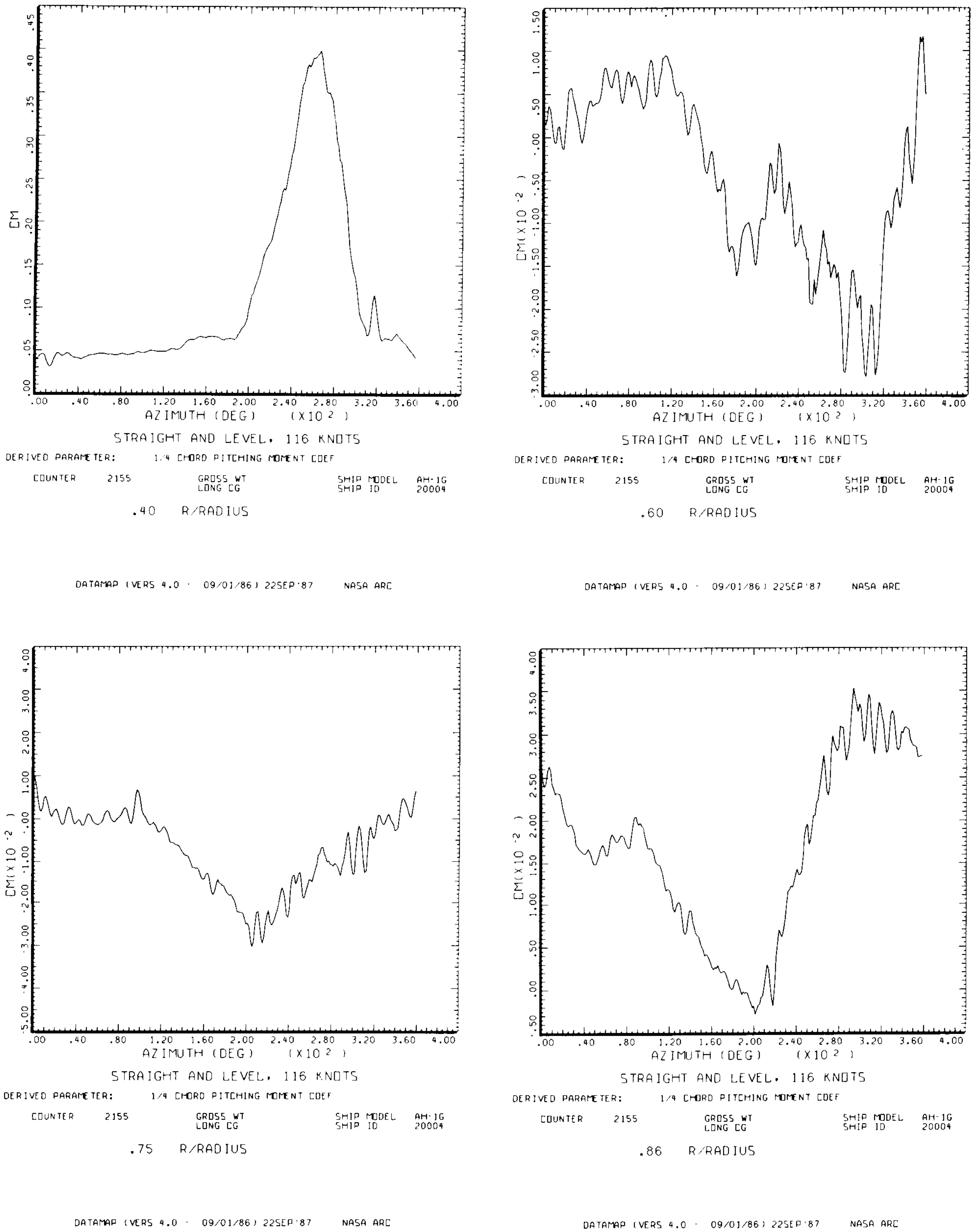

Figure 76.- C_m versus azimuth at 116 KTAS. (a) At 40% radius; (b) at 60% radius; (c) at 75% radius; (d) at 86% radius.

ORIGINAL PAGE IS OF POOR QUALITY

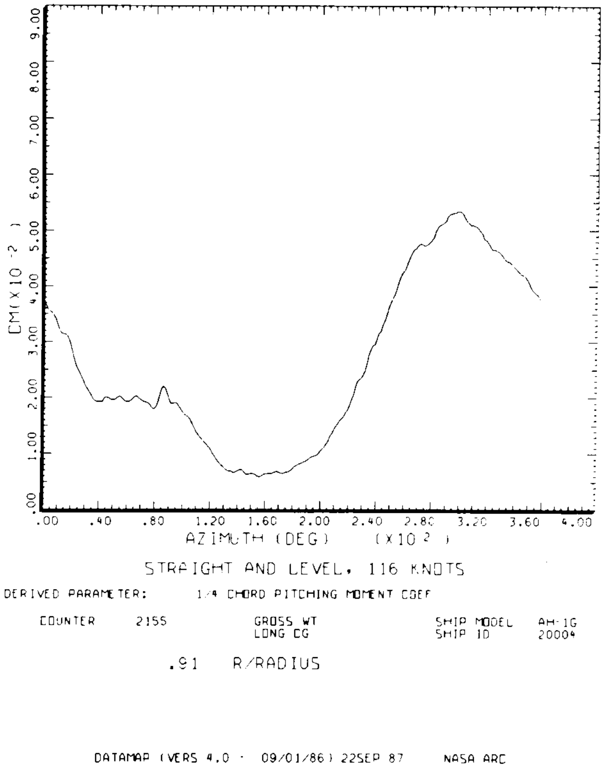

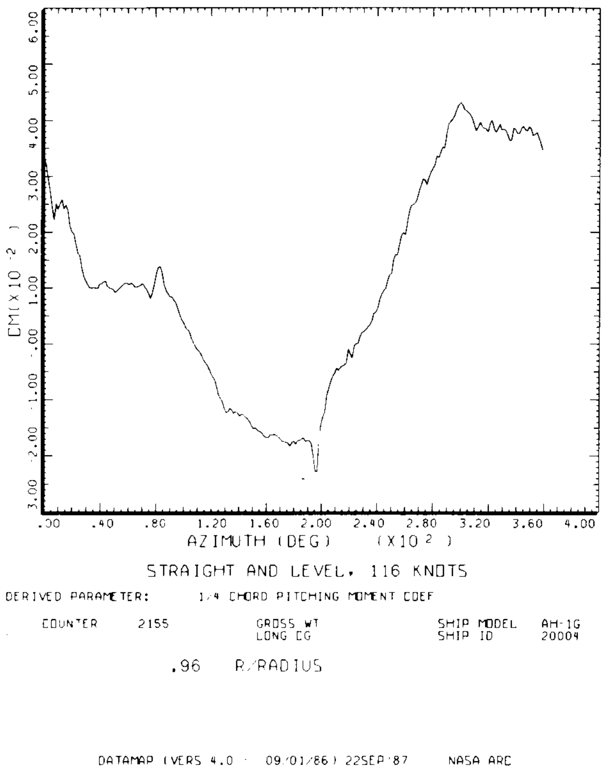

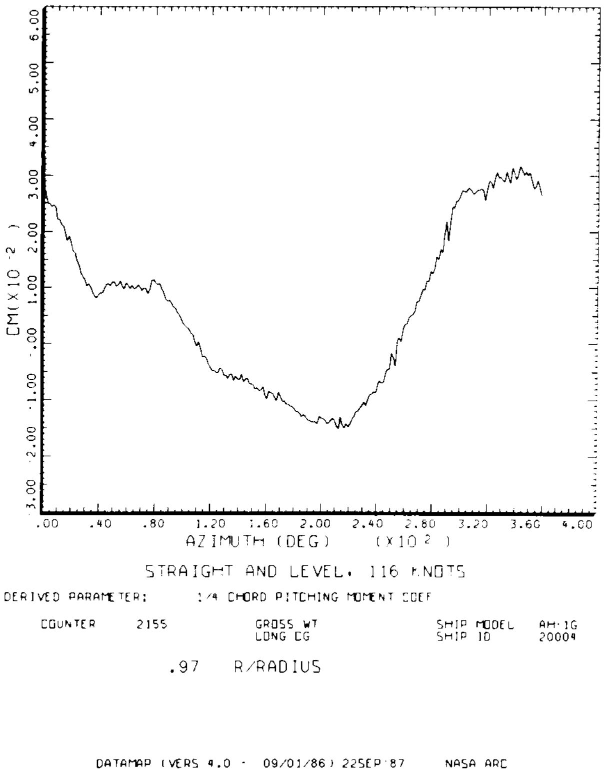

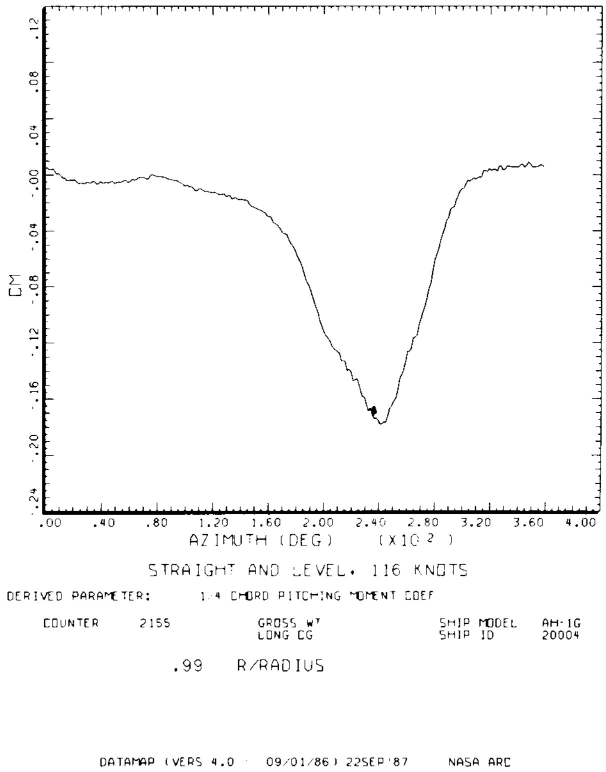

Figure 76.- Concluded. (e) At 91% radius; (f) at 96% radius; (g) 97% radius; (h) 99% radius.

ORIGINAL PAGE IS
OF POOR QUALITY

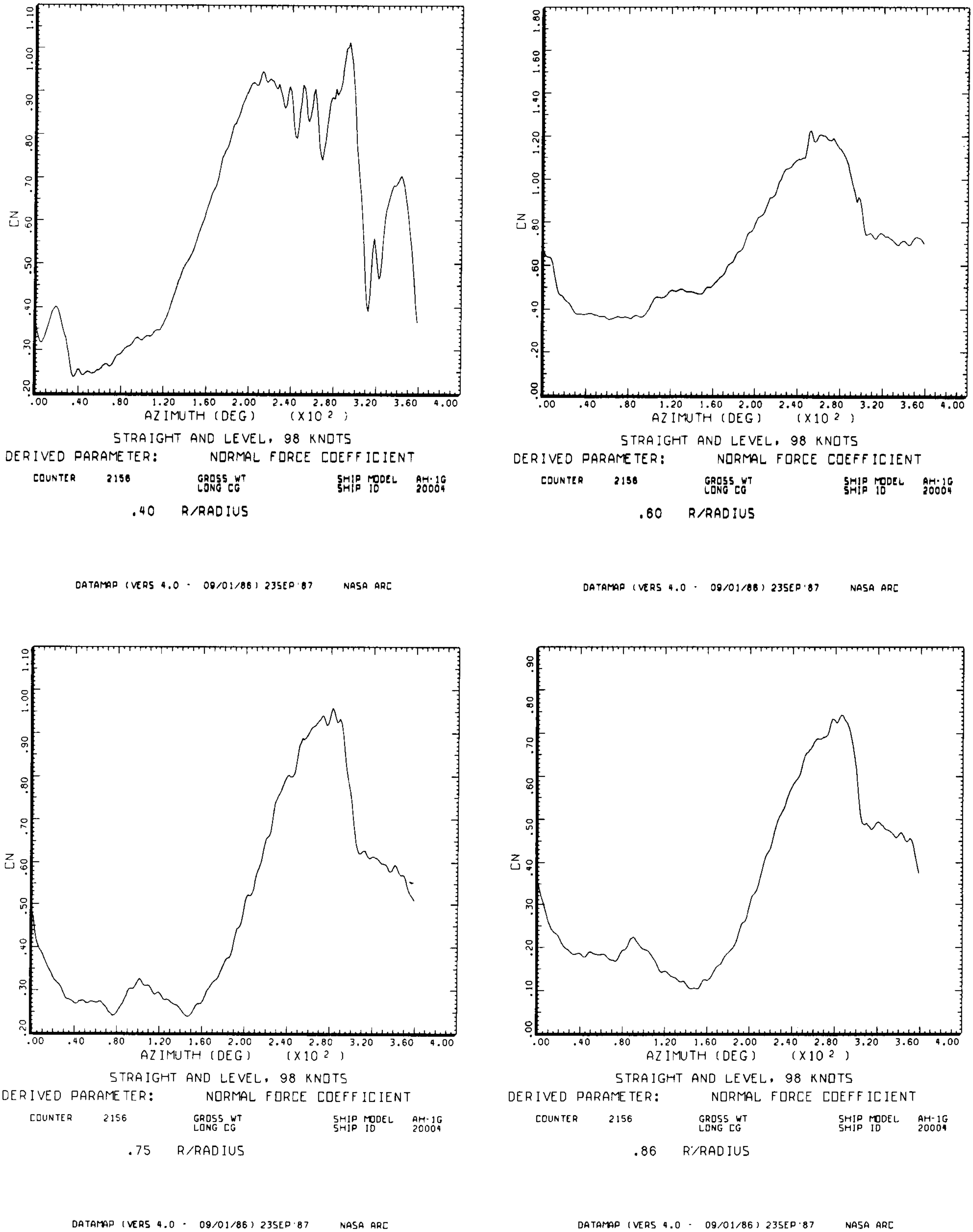

Figure 77.- C_n versus azimuth at 98 KTAS. (a) At 40% radius; (b) at 60% radius; (c) at 75% radius; (d) at 86% radius.

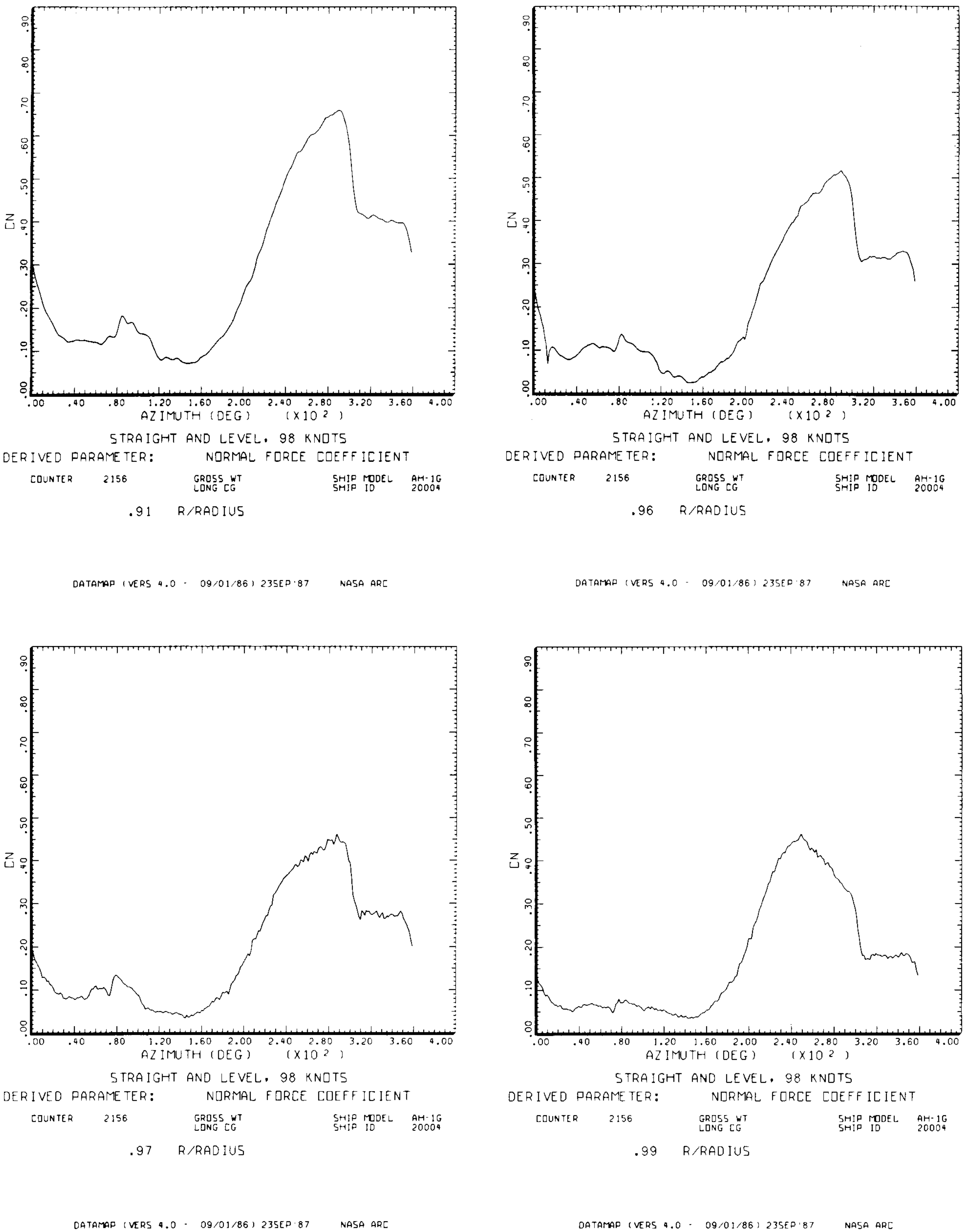

Figure 77.- Concluded. (e) At 91% radius; (f) at 96% radius; (g) 97% radius; (h) 99% radius.

ORIGINAL PAGE IS OF POOR QUALITY

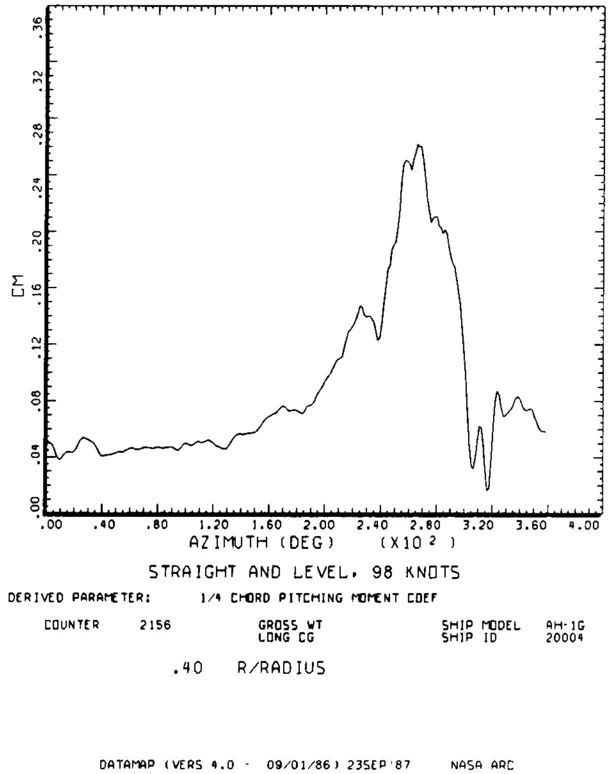

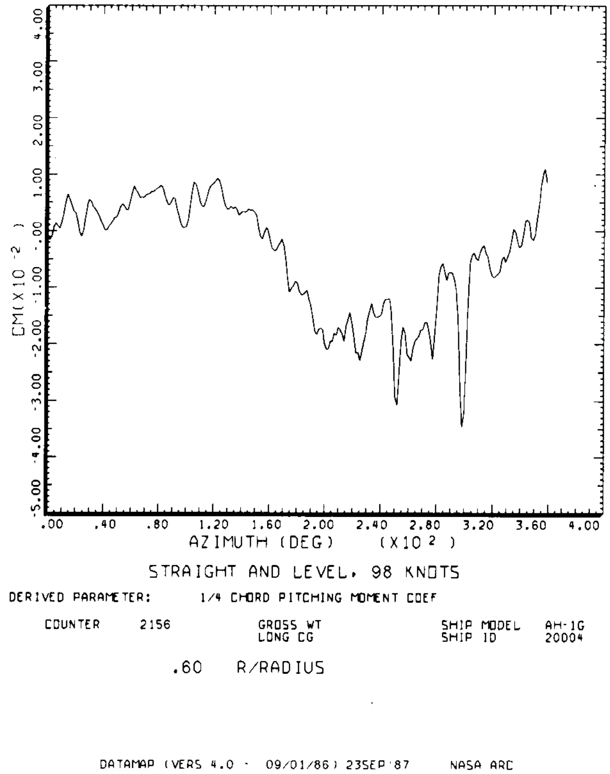

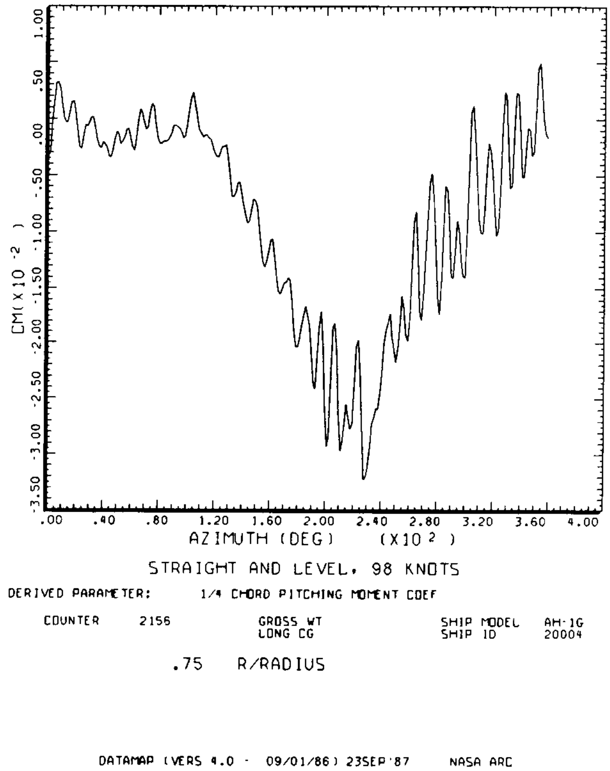

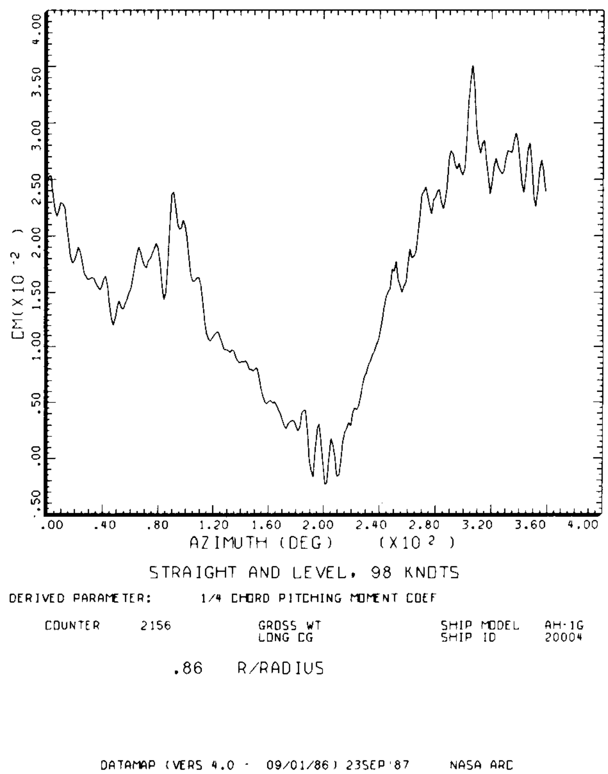

Figure 78.- C_m versus azimuth at 98 KTAS. (a) At 40% radius; (b) at 60% radius; (c) at 75% radius; (d) at 86% radius.

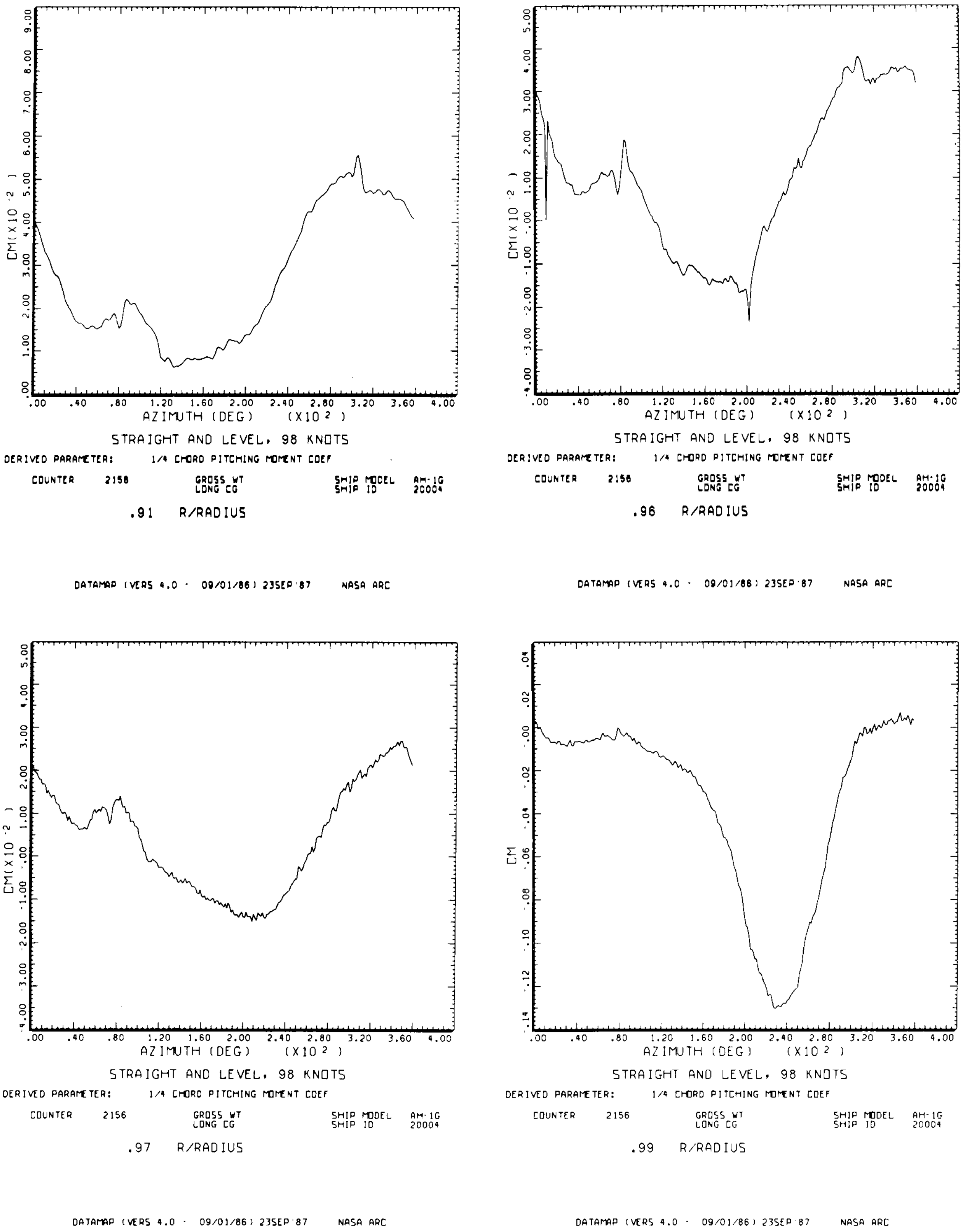

Figure 78.- Concluded. (e) At 91% radius; (f) at 96% radius; (g) 97% radius; (h) 99% radius.

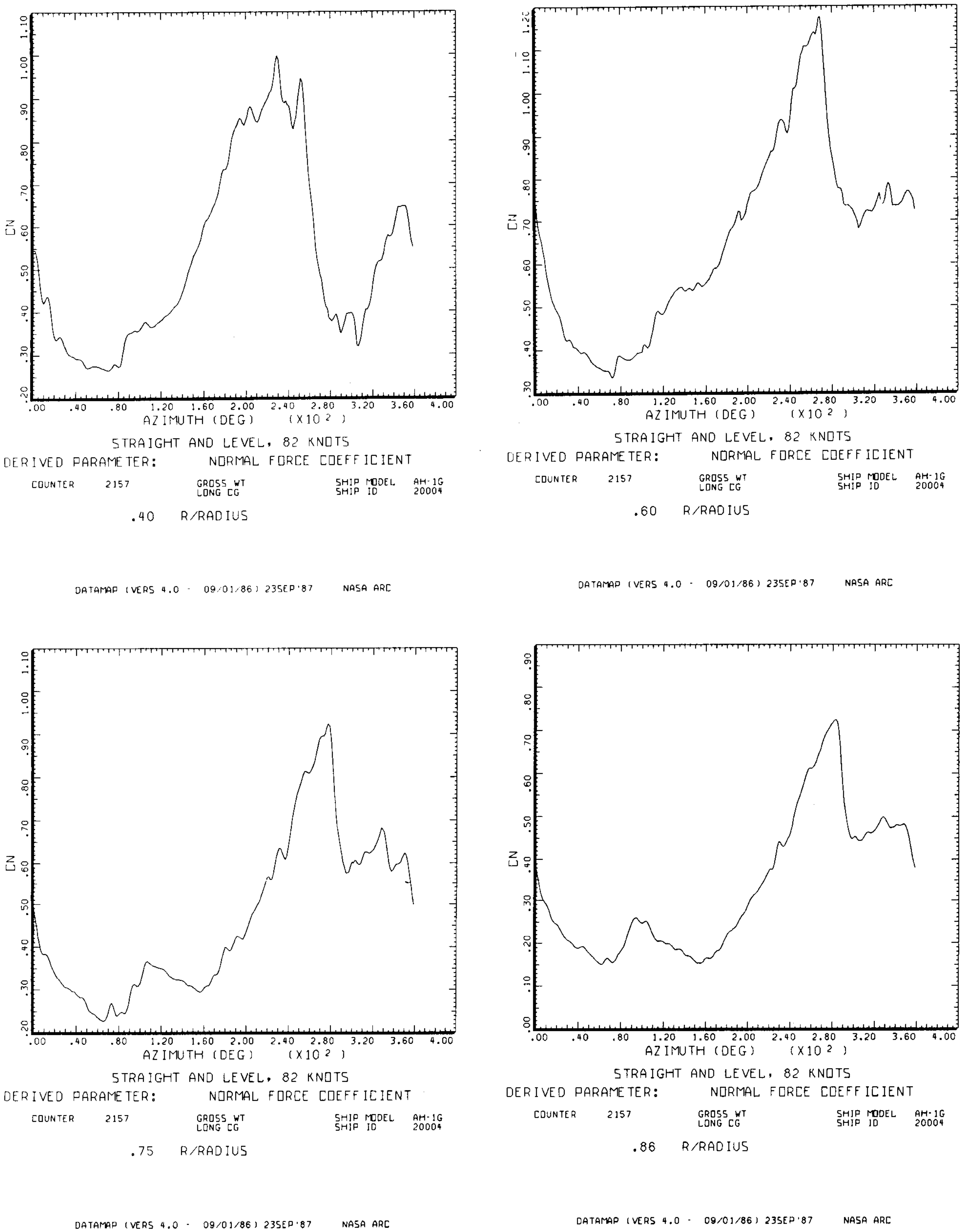

Figure 79.- C_n versus azimuth at 82 KTAS. (a) At 40% radius; (b) at 60% radius; (c) at 75% radius; (d) at 86% radius.

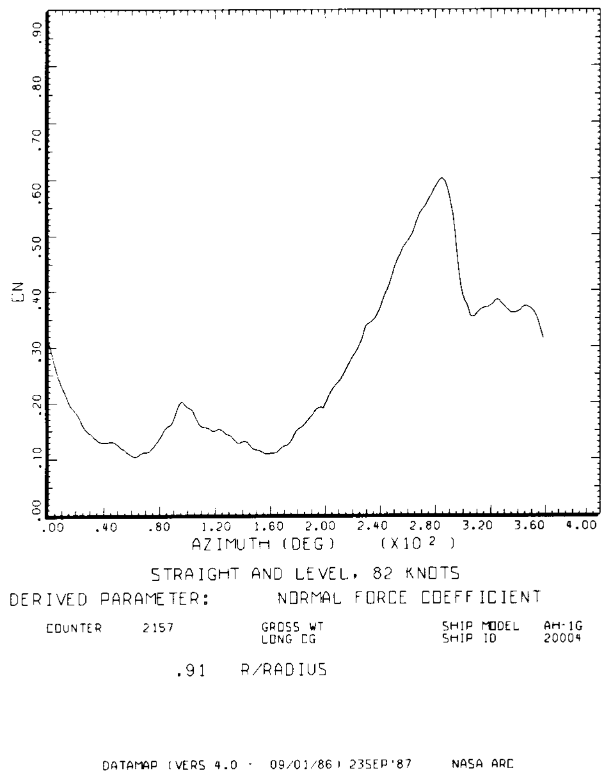

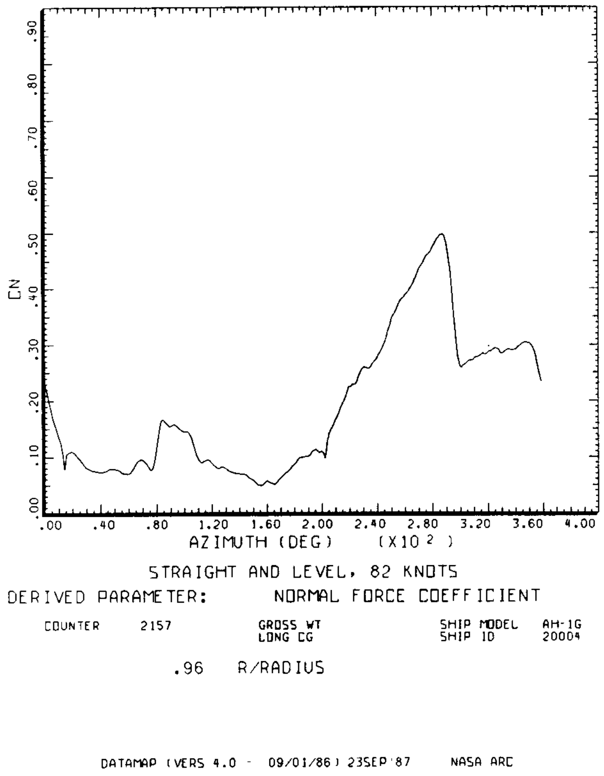

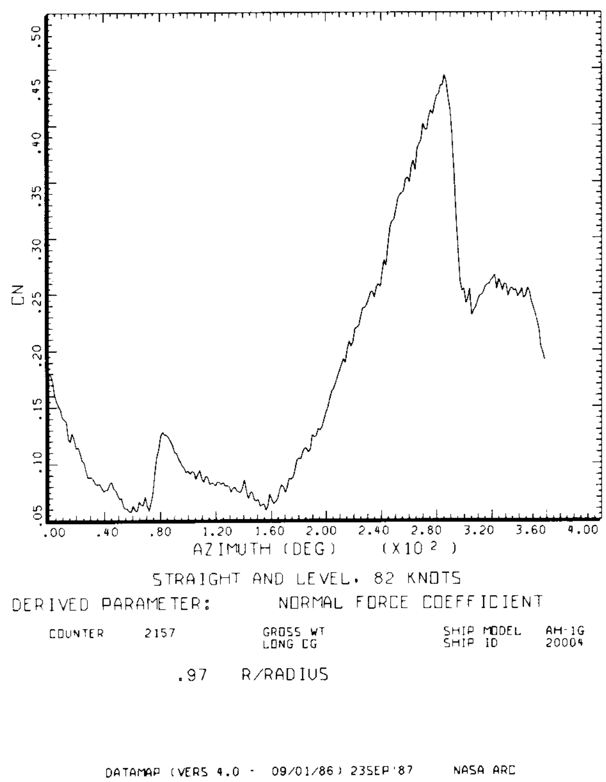

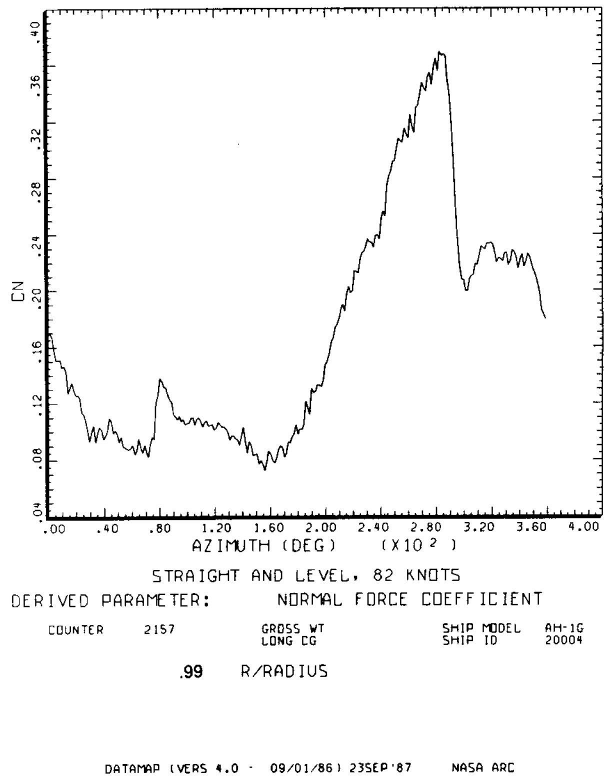

Figure 79.- Concluded. (e) At 91% radius; (f) at 96% radius; (g) 97% radius; (h) 99% radius.

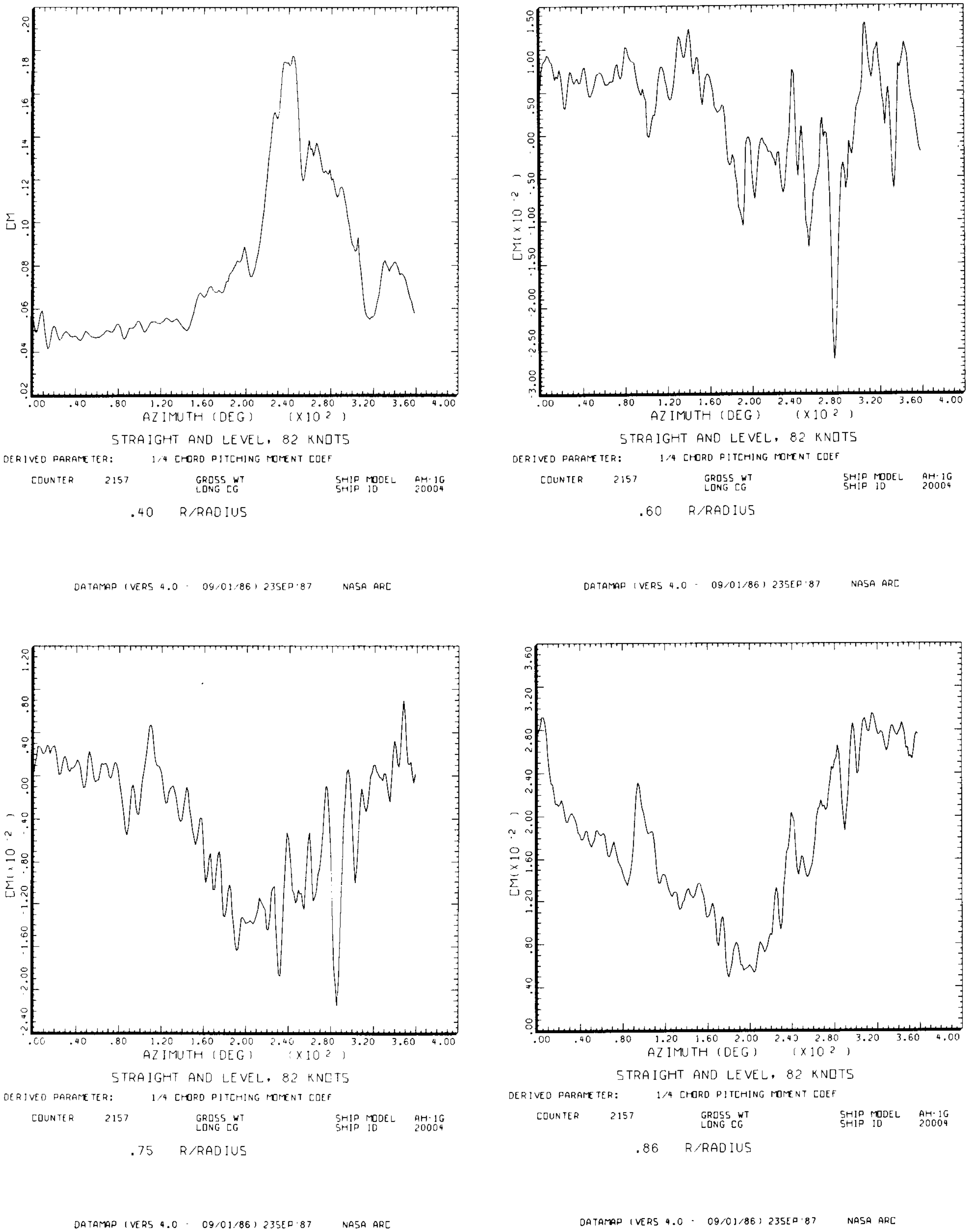

Figure 80.- C_m versus azimuth at 82 KTAS. (a) At 40% radius; (b) at 60% radius; (c) at 75% radius; (d) at 86% radius.

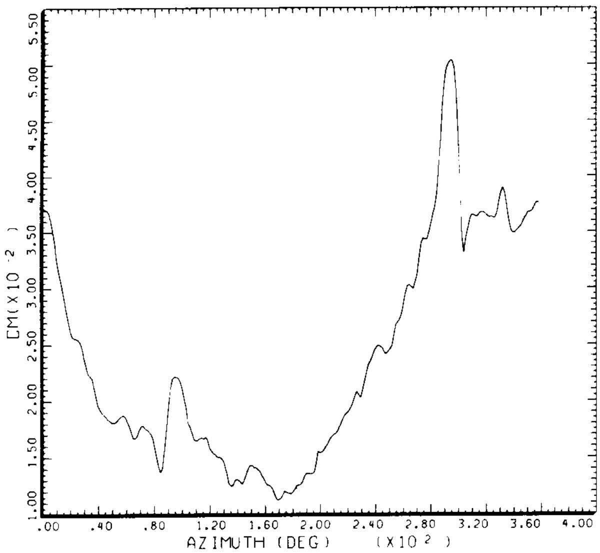

STRAIGHT AND LEVEL, 82 KNOTS

DERIVED PARAMETER: 1/4 CHORD PITCHING MOMENT COEF

COUNTER 2157 GROSS WT LONG CG SHIP MODEL AH-1G SHIP ID 20004

.91 R/RADIUS

DATAMAP (VERS 4.0 - 09/01/86) 23SEP'87 NASA ARC

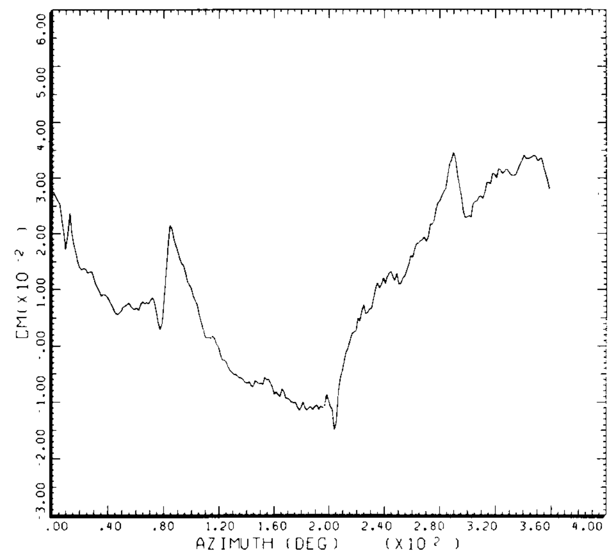

STRAIGHT AND LEVEL, 82 KNOTS

DERIVED PARAMETER: 1/4 CHORD PITCHING MOMENT COEF

COUNTER 2157 GROSS WT LONG CG SHIP MODEL AH-1G SHIP ID 20004

.96 R/RADIUS

DATAMAP (VERS 4.0 - 09/01/86) 23SEP'87 NASA ARC

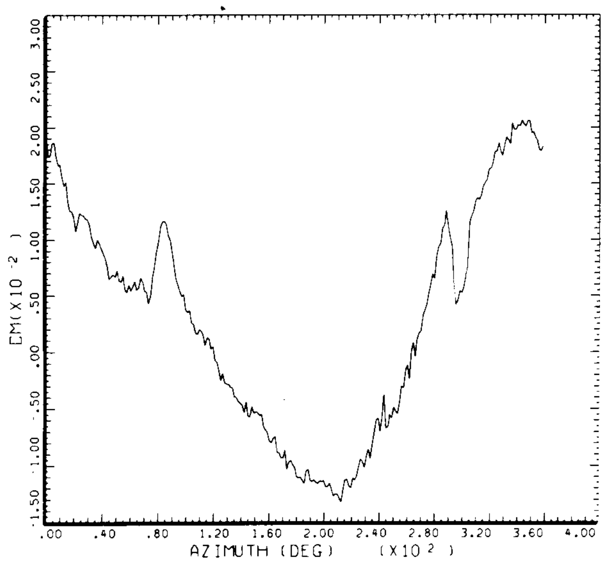

STRAIGHT AND LEVEL, 82 KNOTS

DERIVED PARAMETER: 1/4 CHORD PITCHING MOMENT COEF

COUNTER 2157 GROSS WT LONG CG SHIP MODEL AH-1G SHIP ID 20004

.97 R/RADIUS

DATAMAP (VERS 4.0 - 09/01/86) 23SEP'87 NASA ARC

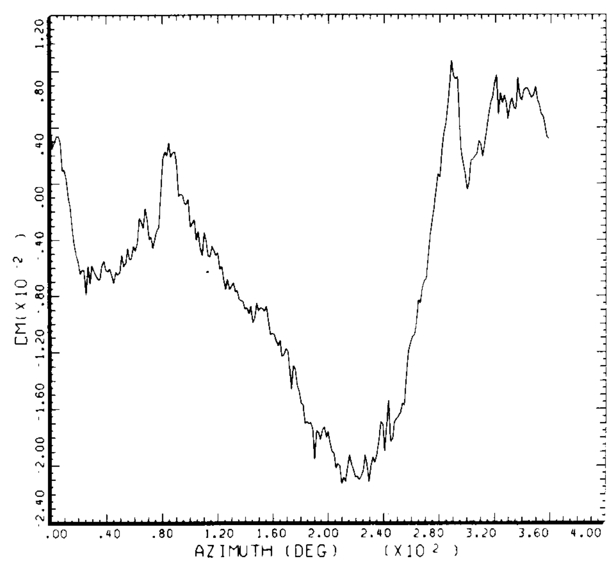

STRAIGHT AND LEVEL, 82 KNOTS

DERIVED PARAMETER: 1/4 CHORD PITCHING MOMENT COEF

COUNTER 2157 GROSS WT LONG CG SHIP MODEL AH-1G SHIP ID 20004

.99 R/RADIUS

DATAMAP (VERS 4.0 - 09/01/86) 23SEP'87 NASA ARC

Figure 80.- Concluded. (e) At 91% radius; (f) at 96% radius; (g) 97% radius; (h) 99% radius.

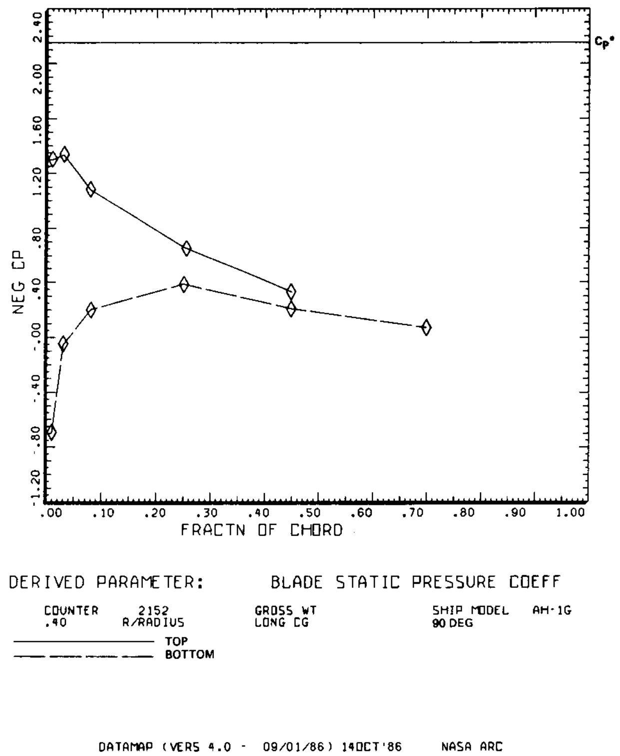

Figure 81.- At 159 KTAS, C_p versus chord, 40% radius, 90° azimuth.

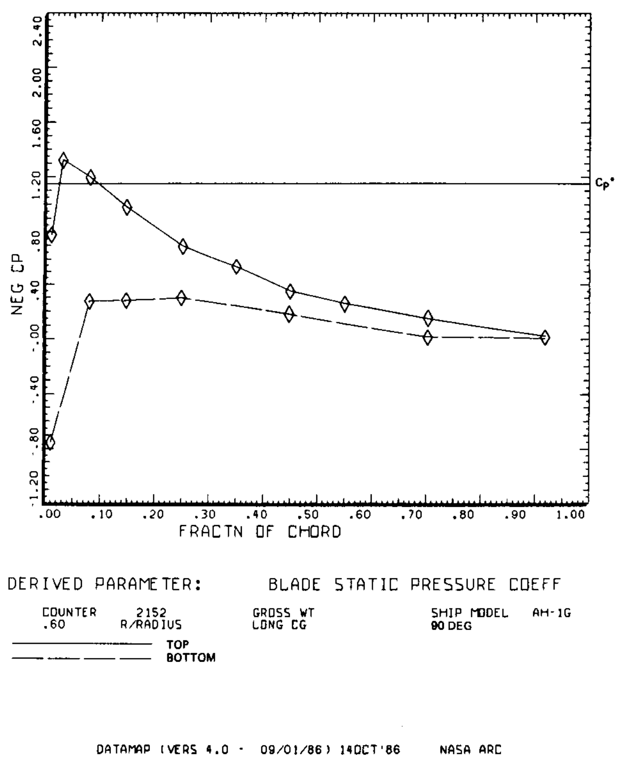

Figure 82.- At 159 KTAS, C_p versus chord, 60% radius, 90° azimuth.

ORIGINAL PAGE IS
OF POOR QUALITY

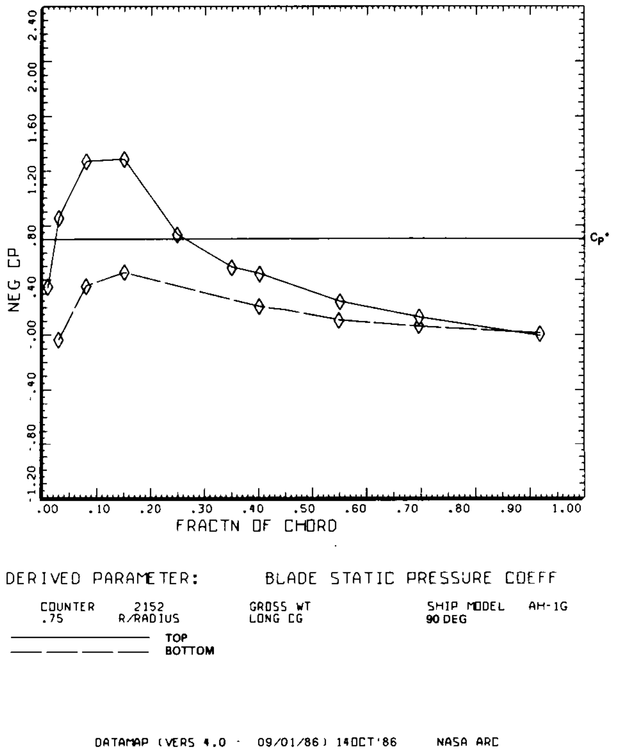

Figure 83.- At 159 KTAS, C_p versus chord, 75% radius, 90° azimuth.

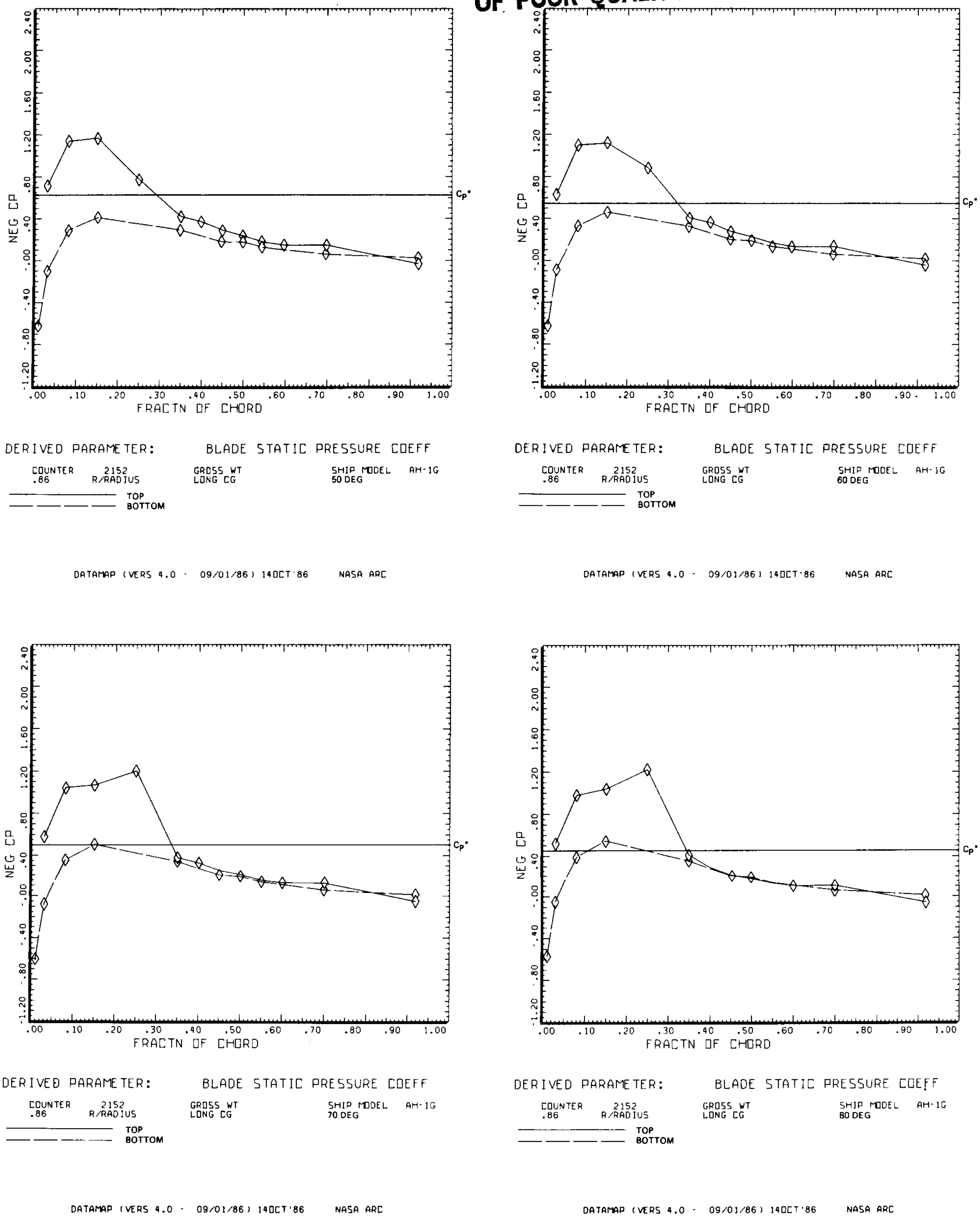

Figure 84.- At 159 KTAS, C_p versus chord at 86% radius. (a) 50° azimuth; (b) 60° azimuth; (c) 70° azimuth; (d) 80° azimuth.

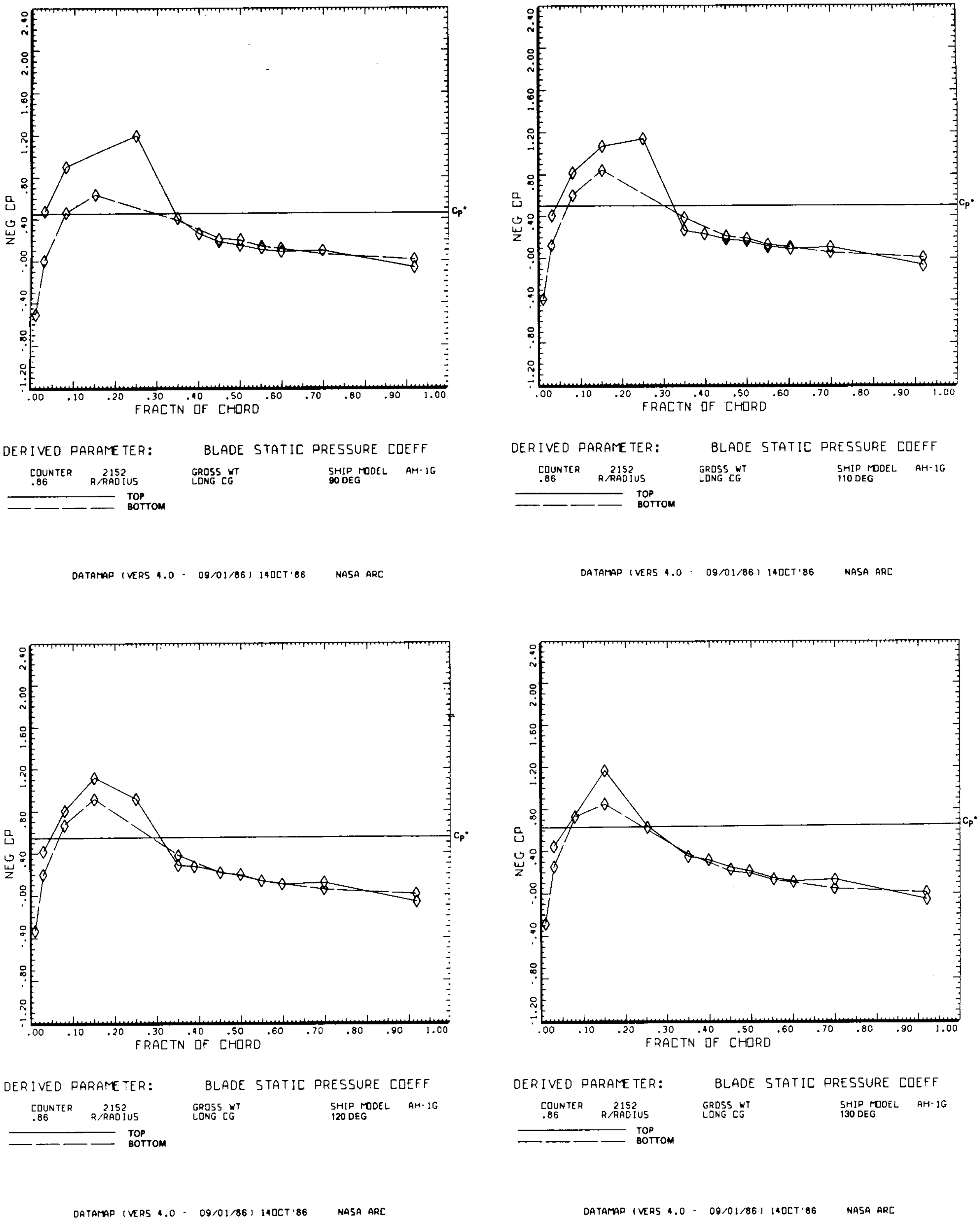

Figure 84.- Concluded. (e) 90° azimuth; (f) 110° azimuth; (g) 120° azimuth; (h) 130° azimuth.

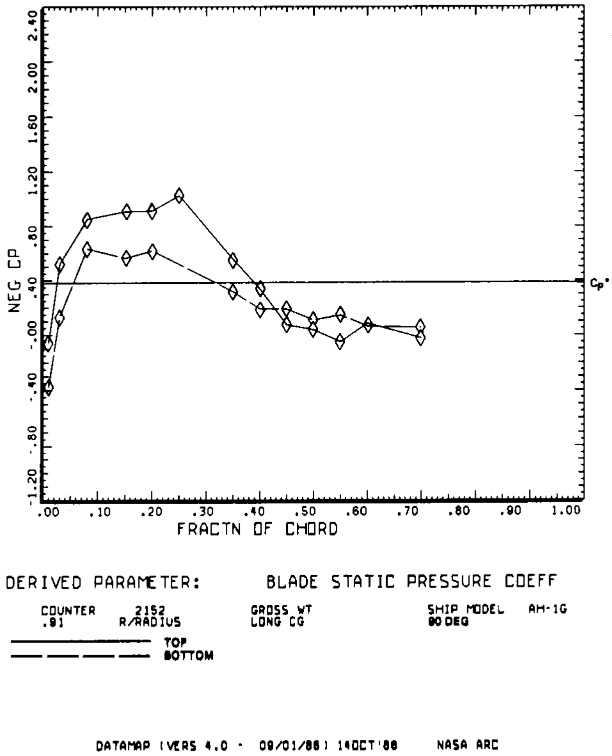

Figure 85.- At 159 KTAS, C_p versus chord at 91% radius, 90° azimuth.

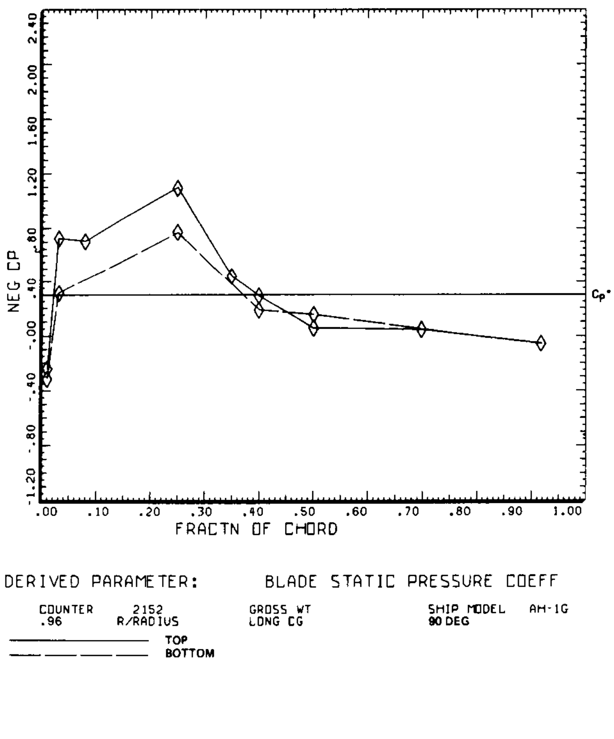

Figure 86.- At 159 KTAS, C_p versus chord at 96% radius, 90° azimuth.

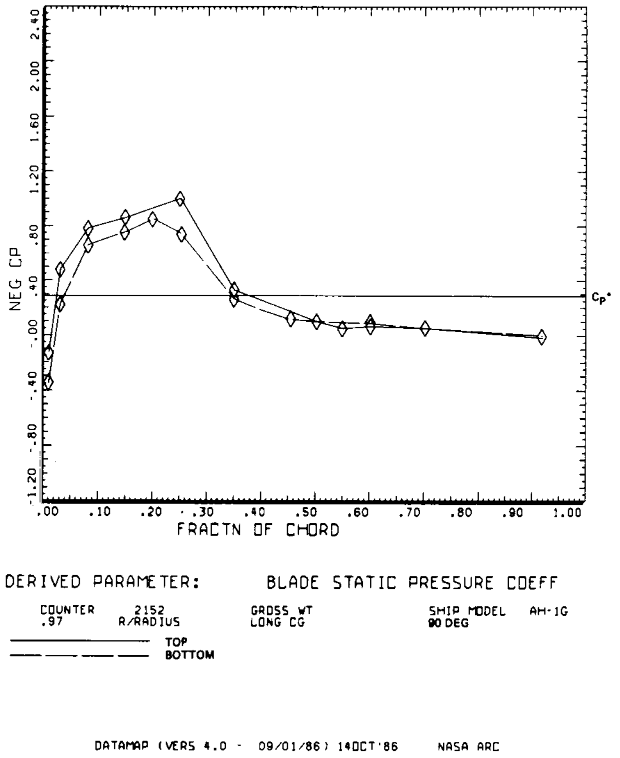

Figure 87.- At 159 KTAS, C_p versus chord at 97% radius, 90° azimuth.

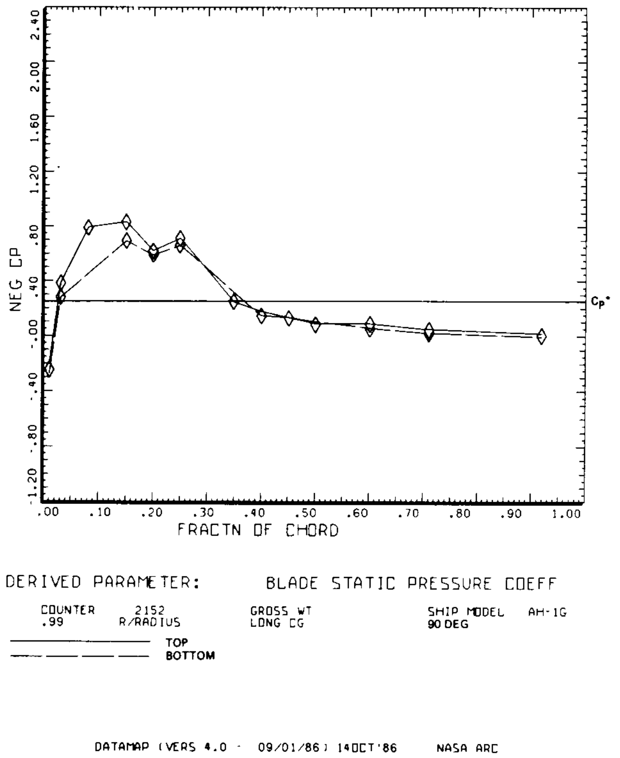

Figure 88.- At 159 KTAS, C_p versus chord at 99% radius, 90° azimuth.

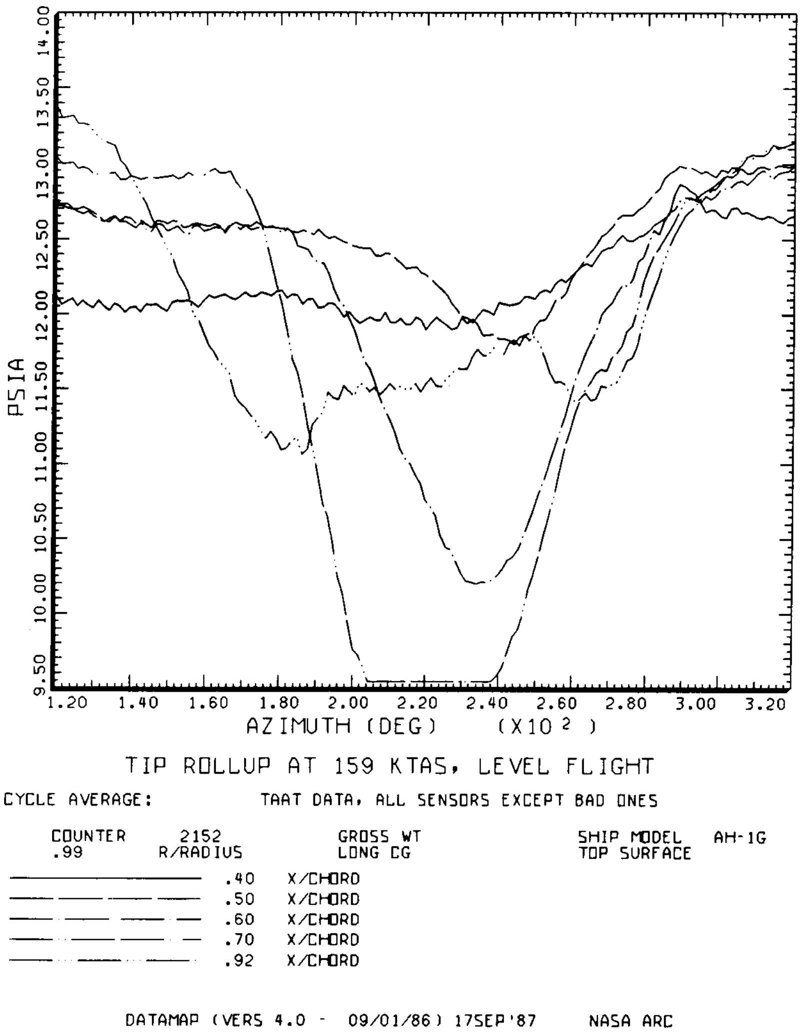

Figure 89.- At 159 KTAS, 99% radius with 70% chord included.

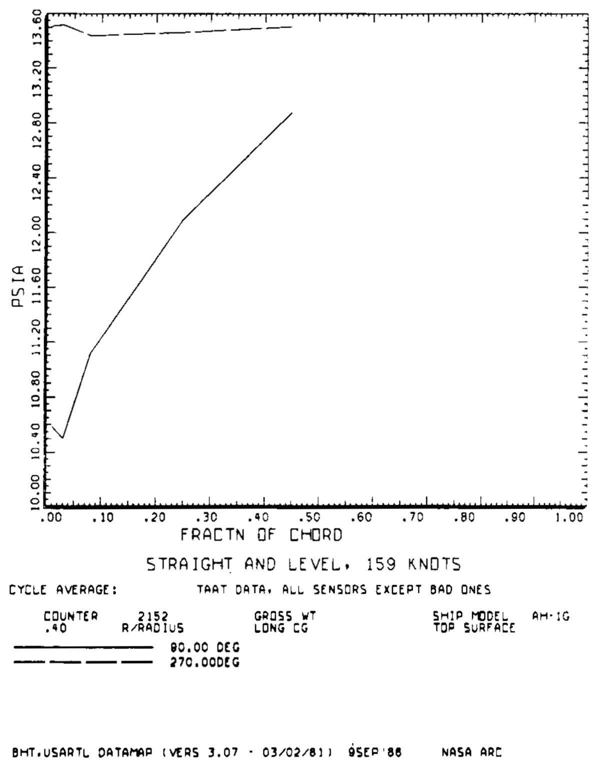

Figure 90.- At 159 KTAS, 40% radius, 90° versus 270°, upper surface pressure.

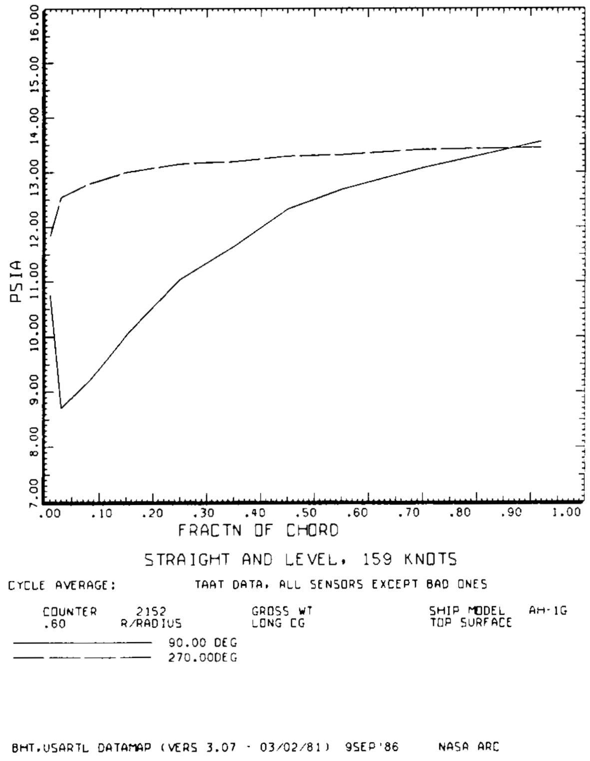

Figure 91.- At 159 KTAS, 60% radius, 90° versus 270°, upper surface pressure.

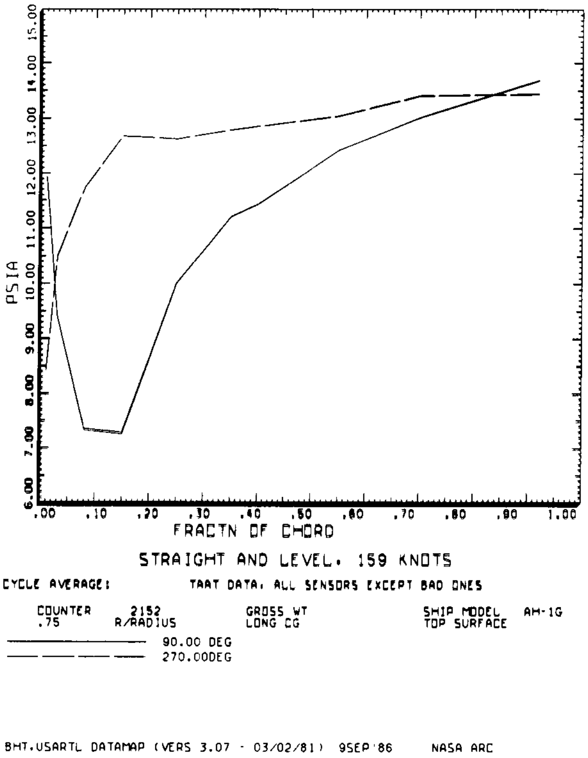

Figure 92.- At 159 KTAS, 75% radius, 90° versus 270°, upper surface pressure.

ORIGINAL PAGE IS
OF POOR QUALITY

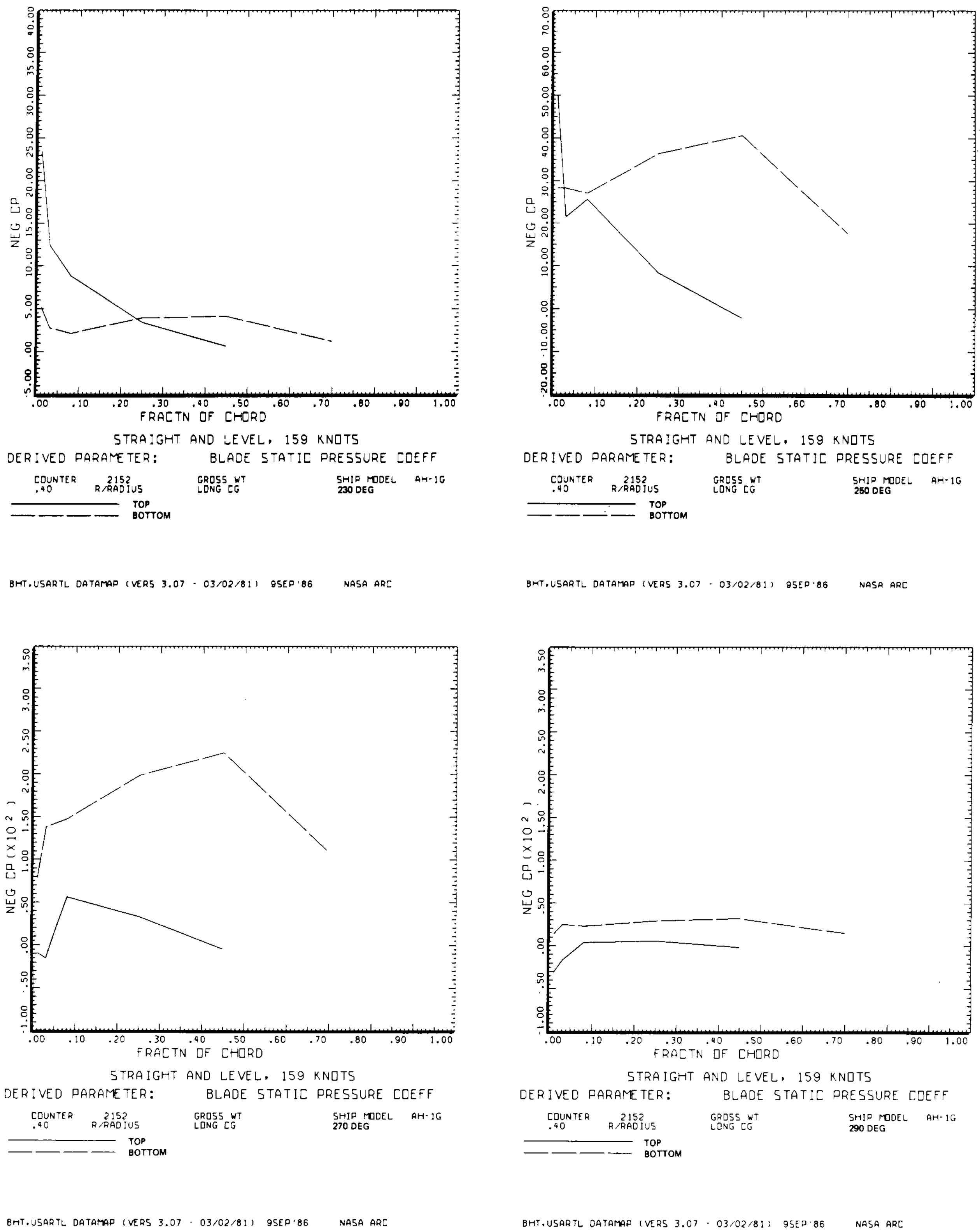

Figure 93.- At 159 KTAS, 40% radius, C_p chordwise distribution. (a) 230° azimuth; (b) 250° azimuth; (c) 270° azimuth; (d) 290° azimuth.

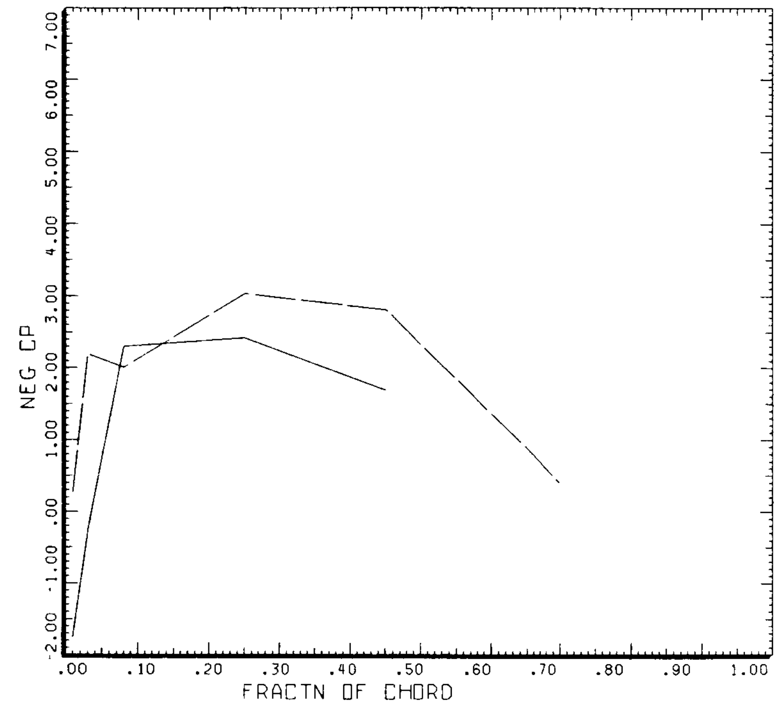

STRAIGHT AND LEVEL, 159 KNOTS

DERIVED PARAMETER: BLADE STATIC PRESSURE COEFF

COUNTER .40 | 2152 R/RADIUS | GROSS WT LONG CG | SHIP MODEL 310 DEG | AH-1G

——— TOP

— — — BOTTOM

BHT,USARTL DATAMAP (VERS 3.07 - 03/02/81) 9SEP'86 NASA ARC

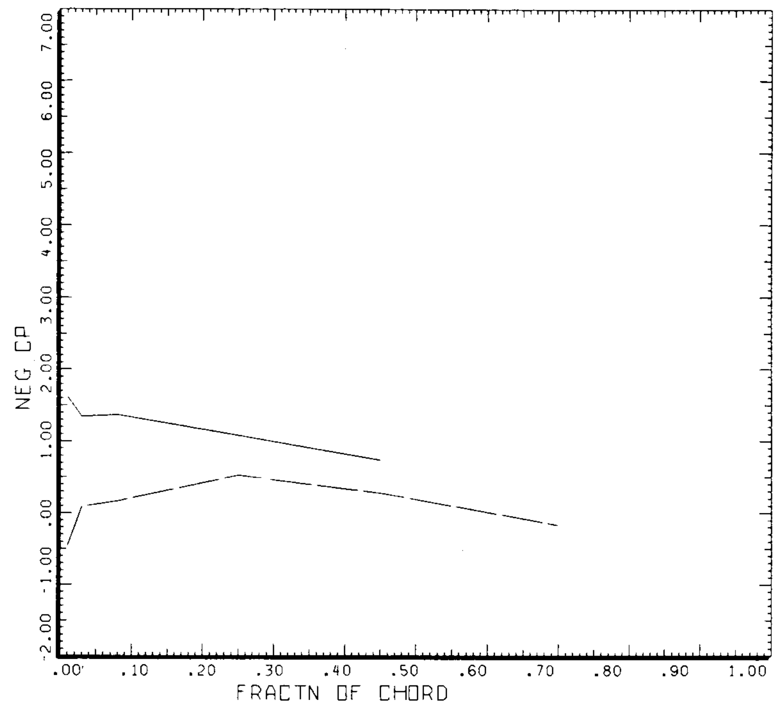

STRAIGHT AND LEVEL, 159 KNOTS

DERIVED PARAMETER: BLADE STATIC PRESSURE COEFF

COUNTER .40 | 2152 R/RADIUS | GROSS WT LONG CG | SHIP MODEL 330 DEG | AH-1G

——— TOP

— — — BOTTOM

BHT,USARTL DATAMAP (VERS 3.07 - 03/02/81) 9SEP'86 NASA ARC

Figure 93.- Concluded. (e) 310° azimuth; (f) 330° azimuth.

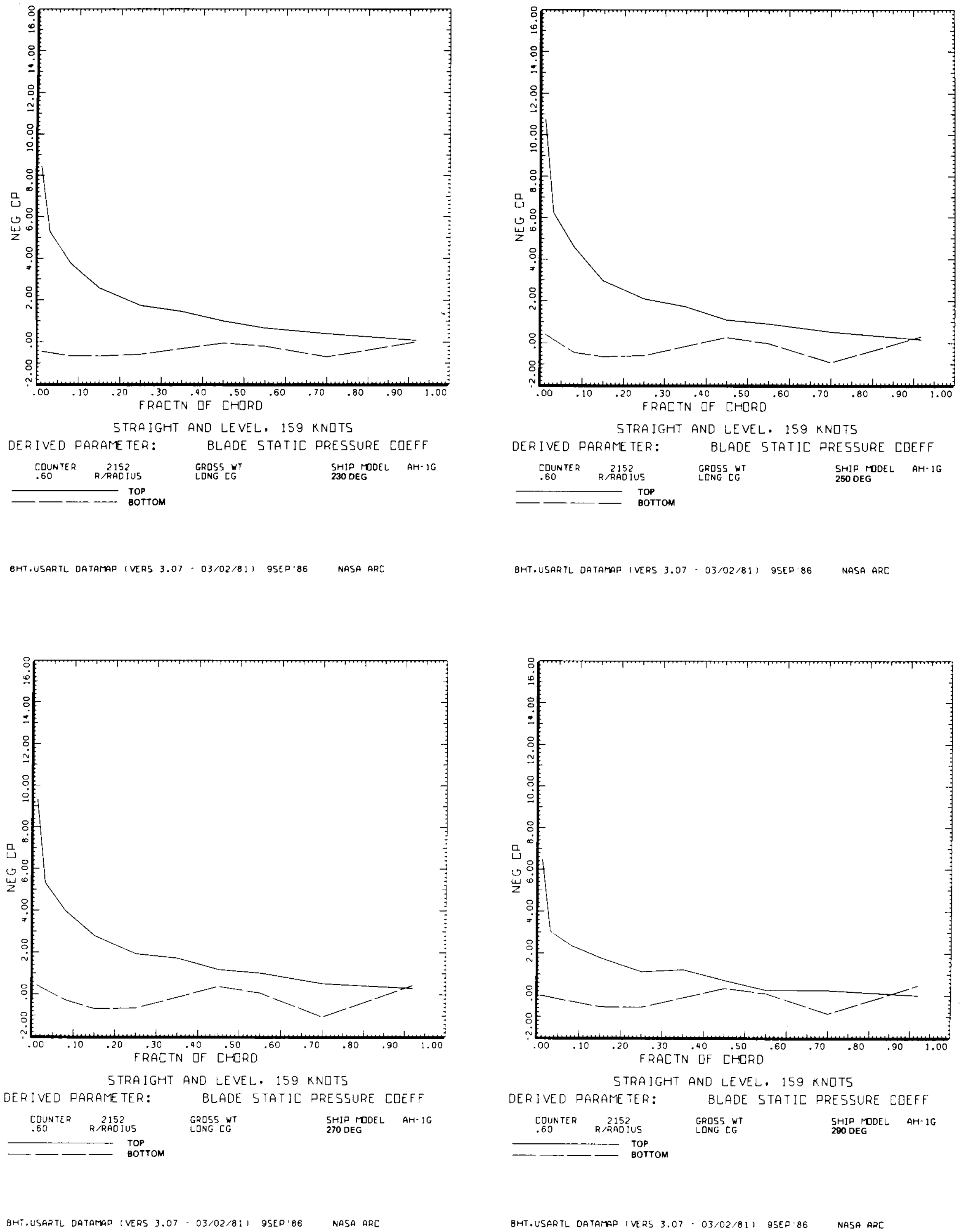

Figure 94.- At 159 KTAS, 60% radius, C_p chordwise distribution. (a) 230° azimuth; (b) 250° azimuth; (c) 270° azimuth; (d) 290° azimuth.

ORIGINAL PAGE IS
OF POOR QUALITY

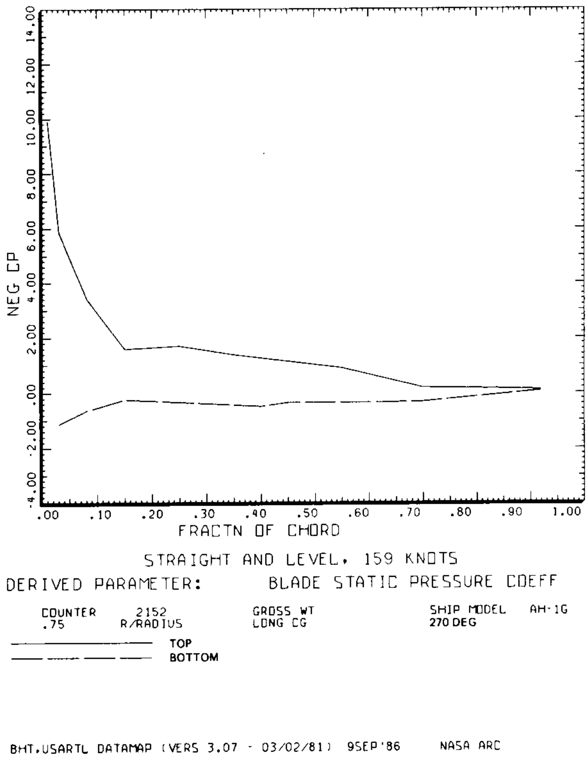

Figure 95.- At 159 KTAS, 75% radius, 270° azimuth, C_p chordwise distribution.

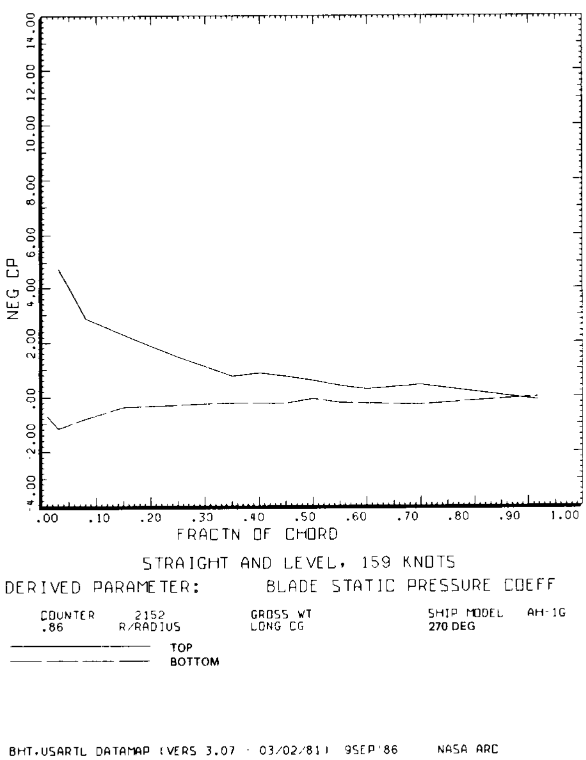

Figure 96.- At 159 KTAS, 86% radius, 270° azimuth, C_p chordwise distribution.

ORIGINAL PAGE IS
OF POOR QUALITY

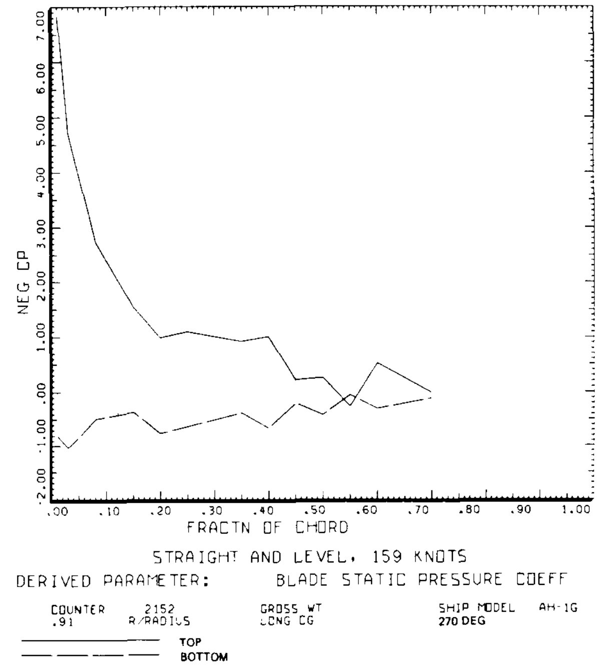

Figure 97.- At 159 KTAS, 91% radius, 270° azimuth, C_p chordwise distribution.

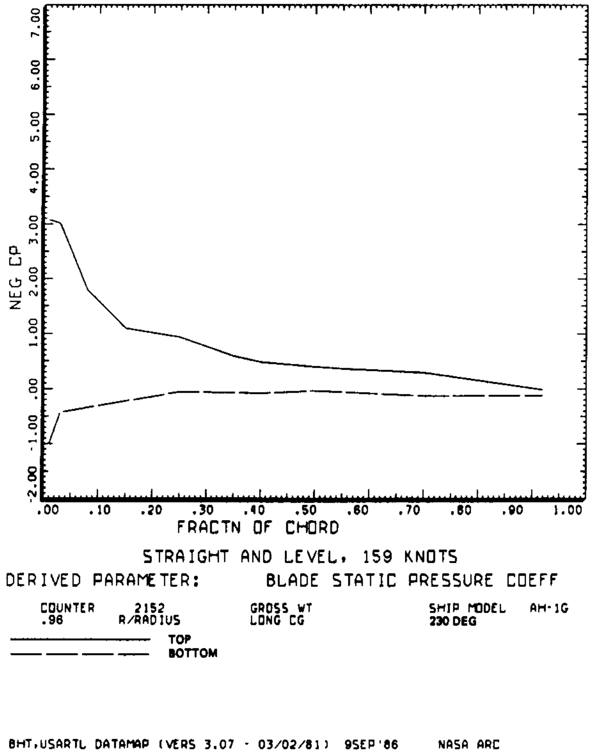

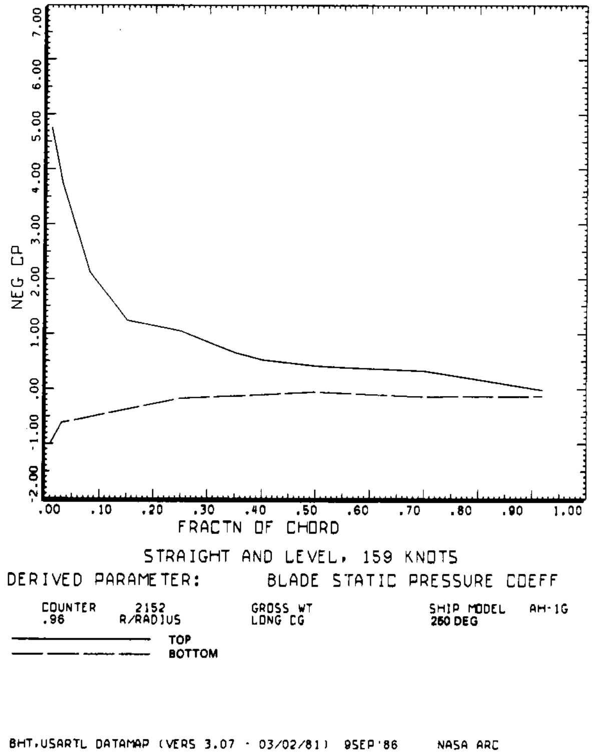

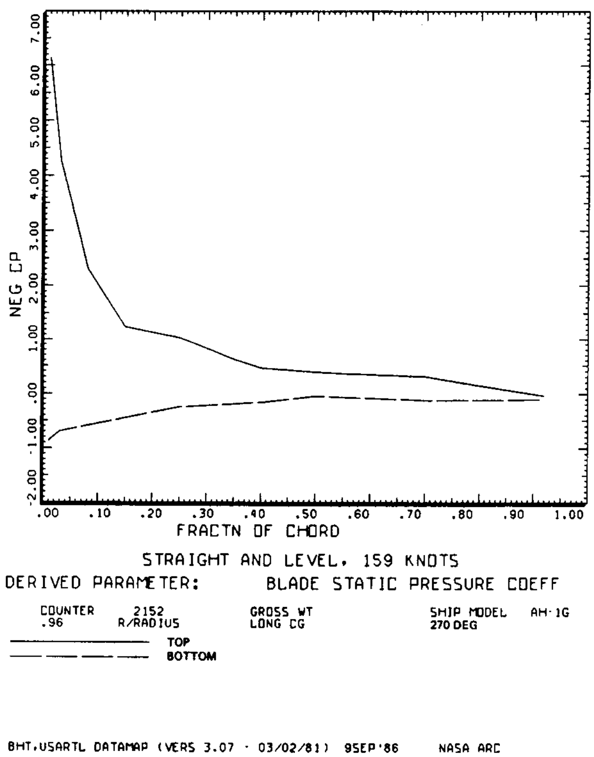

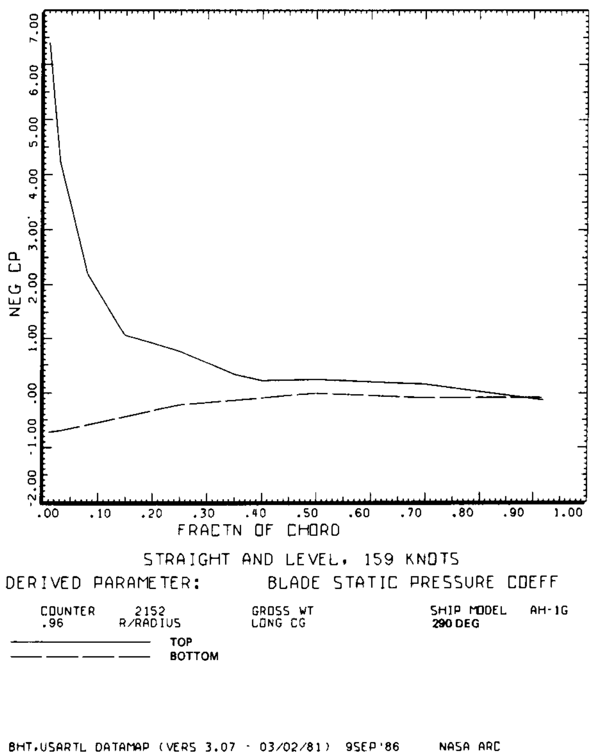

Figure 98.- At 159 KTAS, 96% radius, C_p chordwise distribution. (a) 230° azimuth; (b) 250° azimuth; (c) 270° azimuth; (d) 290° azimuth.

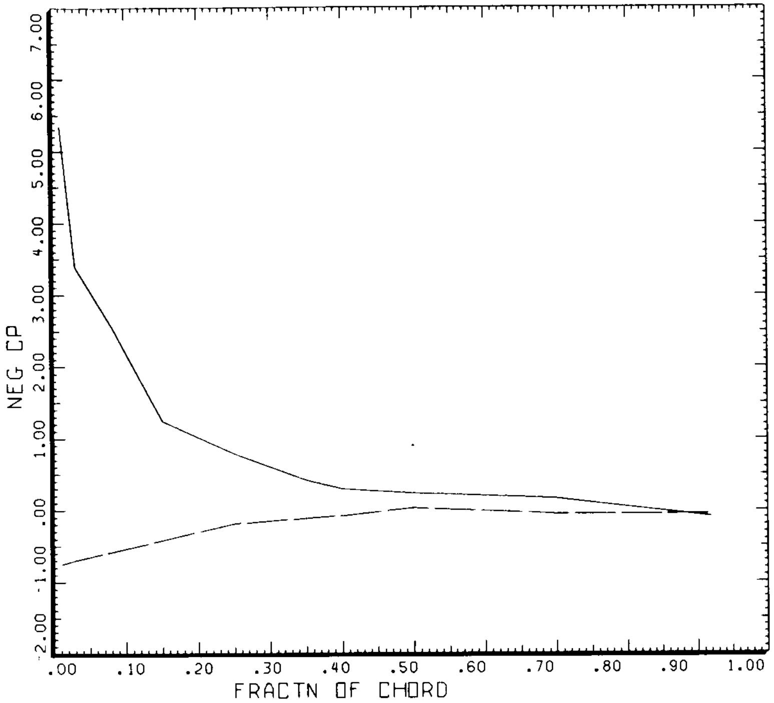

STRAIGHT AND LEVEL, 159 KNOTS

DERIVED PARAMETER: BLADE STATIC PRESSURE COEFF

COUNTER 2152 GROSS WT SHIP MODEL AH-1G
.96 R/RADIUS LONG CG 310 DEG

TOP
BOTTOM

BHT.USARTL DATAMAP (VERS 3.07 - 03/02/81) 9SEP'86 NASA ARC

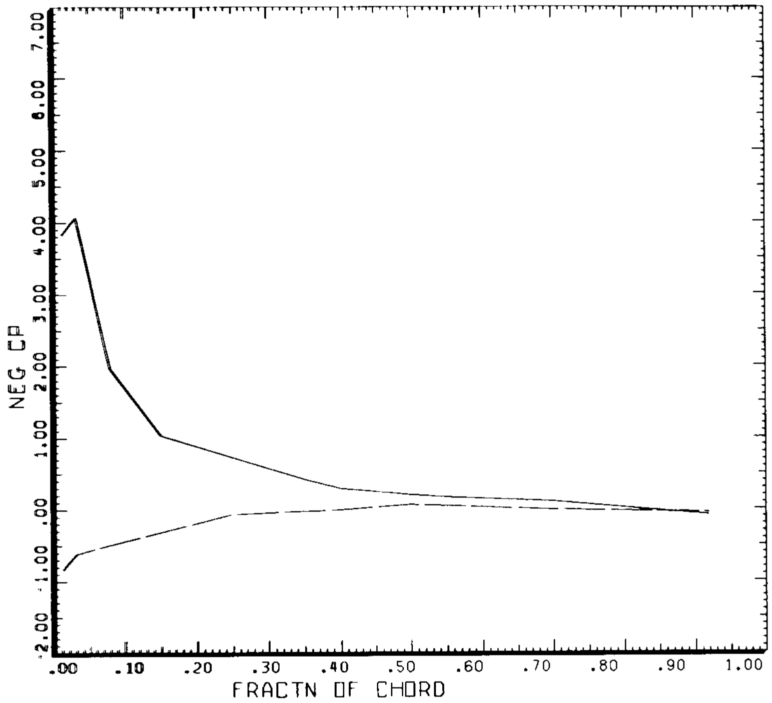

STRAIGHT AND LEVEL, 159 KNOTS

DERIVED PARAMETER: BLADE STATIC PRESSURE COEFF

COUNTER 2152 GROSS WT SHIP MODEL AH-1G
.96 R/RADIUS LONG CG 330 DEG

TOP
BOTTOM

BHT.USARTL DATAMAP (VERS 3.07 - 03/02/81) 9SEP'86 NASA ARC

Figure 98.- Concluded. (e) 310° azimuth; (f) 330° azimuth.

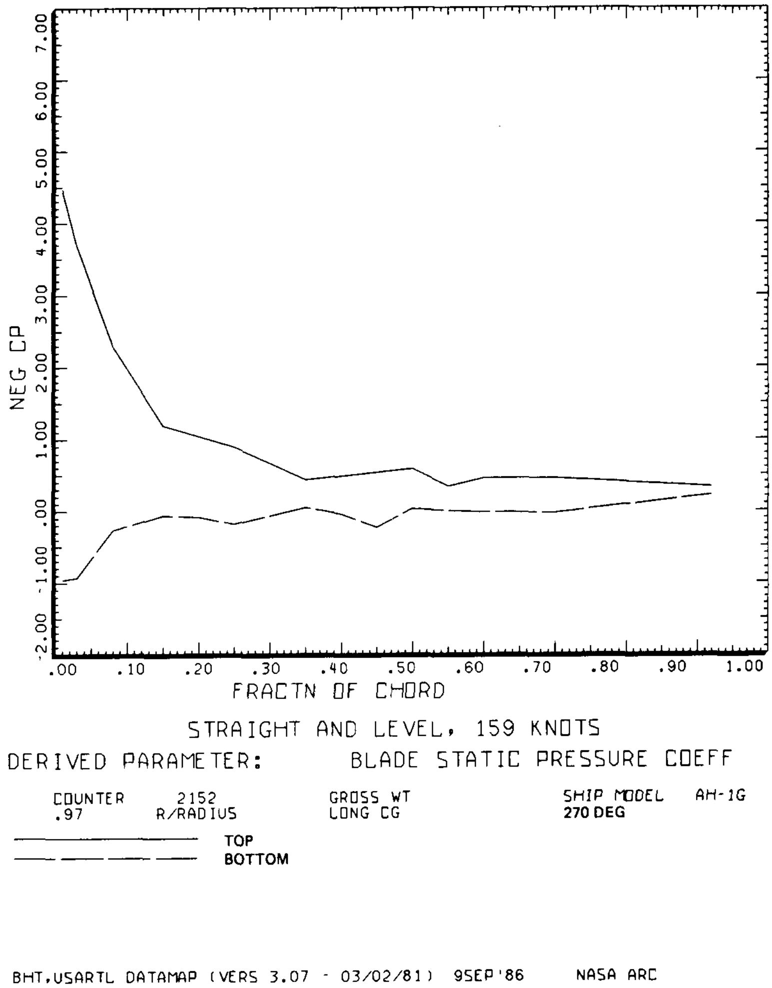

Figure 99.- At 159 KTAS, 97% radius, 270° azimuth, C_p chordwise distribution.

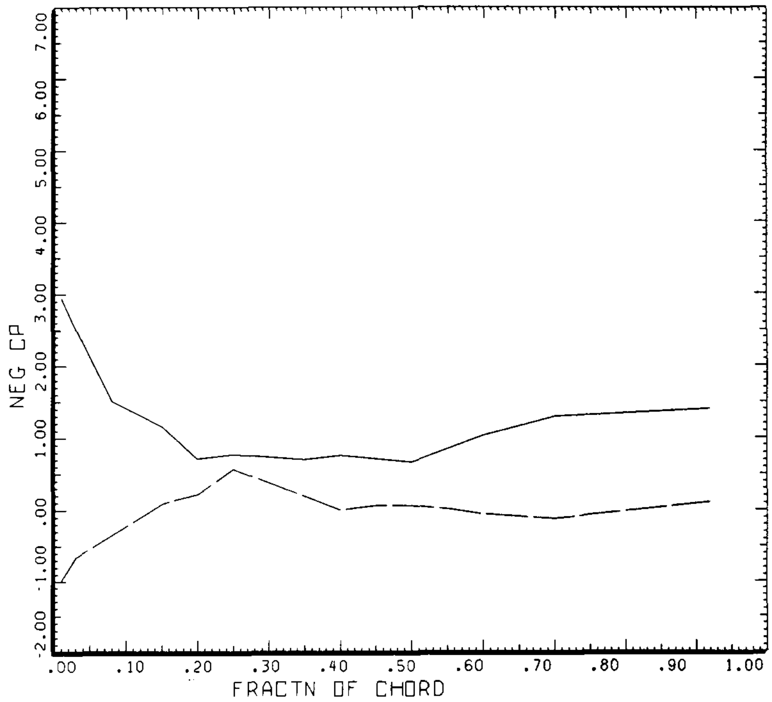

STRAIGHT AND LEVEL, 159 KNOTS

DERIVED PARAMETER: BLADE STATIC PRESSURE COEFF

COUNTER 2152 GROSS WT SHIP MODEL AH-1G
.99 R/RADIUS LONG CG 270 DEG

TOP
BOTTOM

BHT.USARTL DATAMAP (VERS 3.07 - 03/02/81) 9SEP'86 NASA ARC

Figure 100.- At 159 KTAS, 99% radius, 270° azimuth, C_p chordwise distribution.

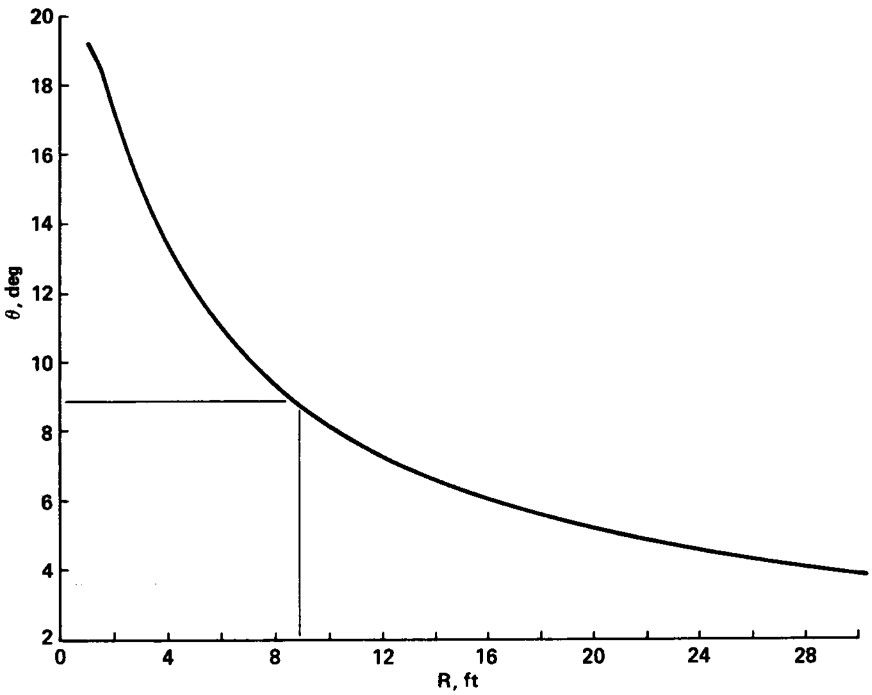

Figure 101.- Hub wake path at 159 KTAS.

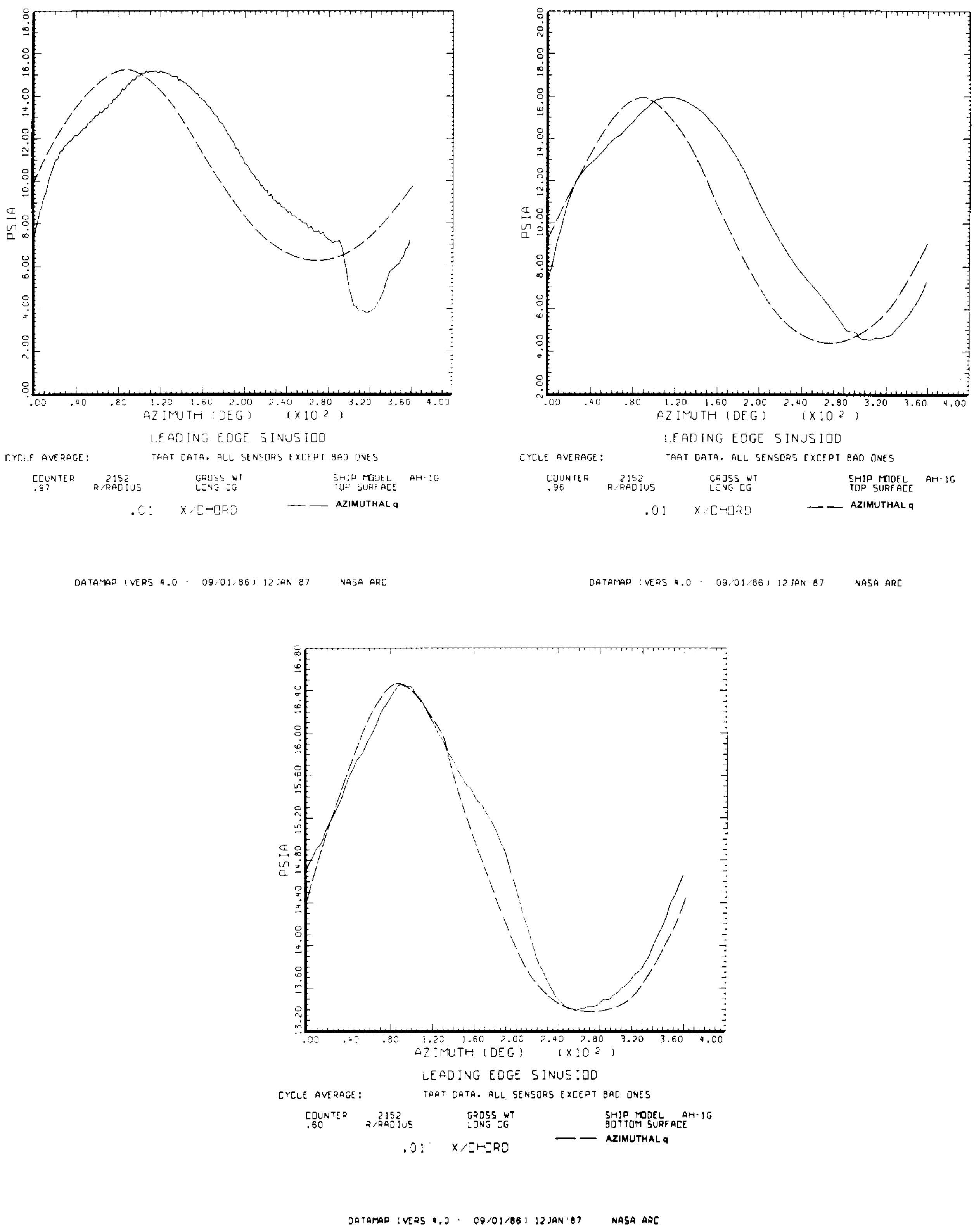

Figure 102.- Sinusoidal leading-edge pressure, 159 KTAS. (a) 60% radius; (b) 96% radius; (c) 97% radius.

ORIGINAL PAGE IS OF POOR QUALITY

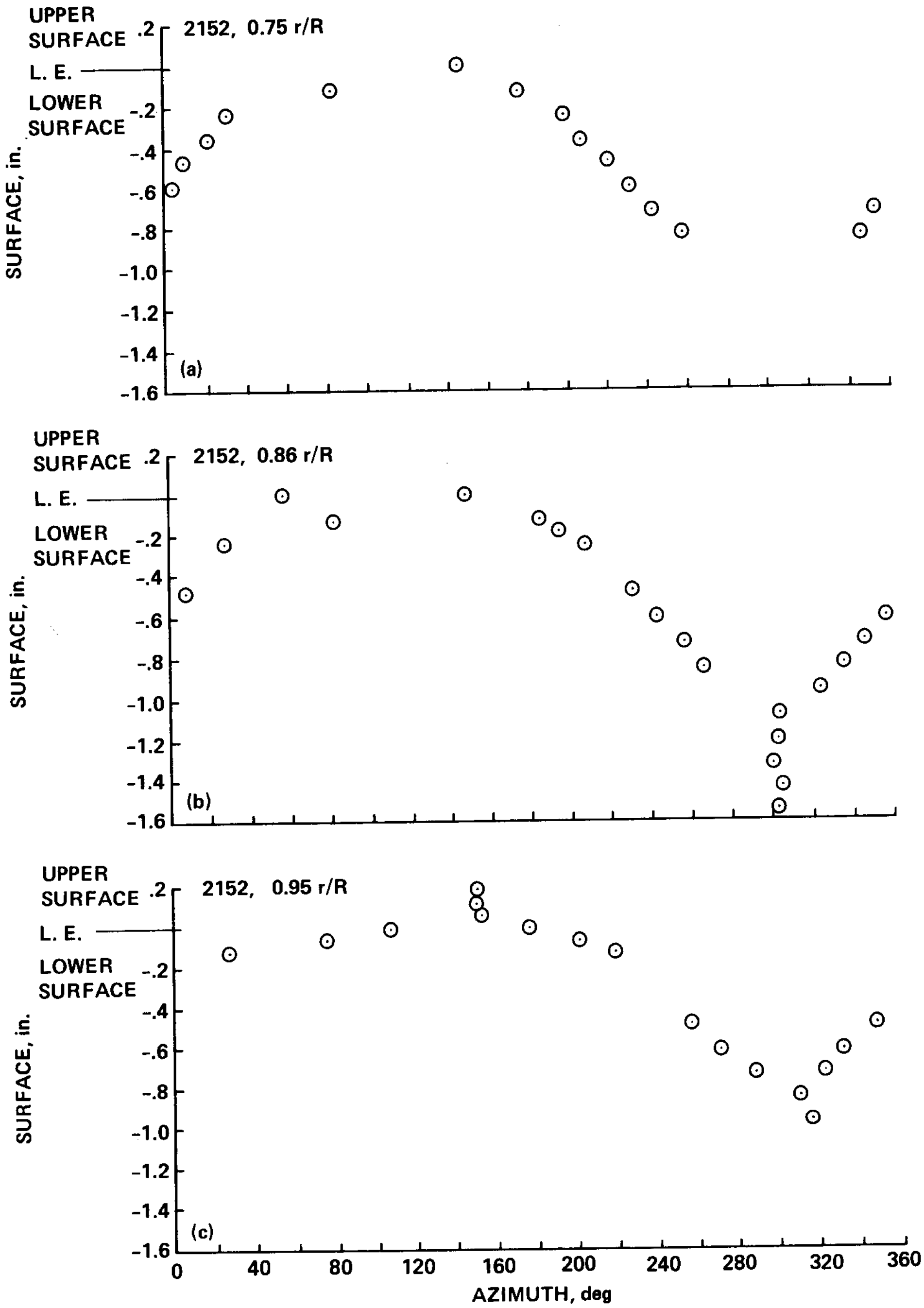

Figure 103.- Hot-wire stagnation point versus azimuth at 159 KTAS. (a) 75% radius; (b) 86% radius; (c) 96% radius.

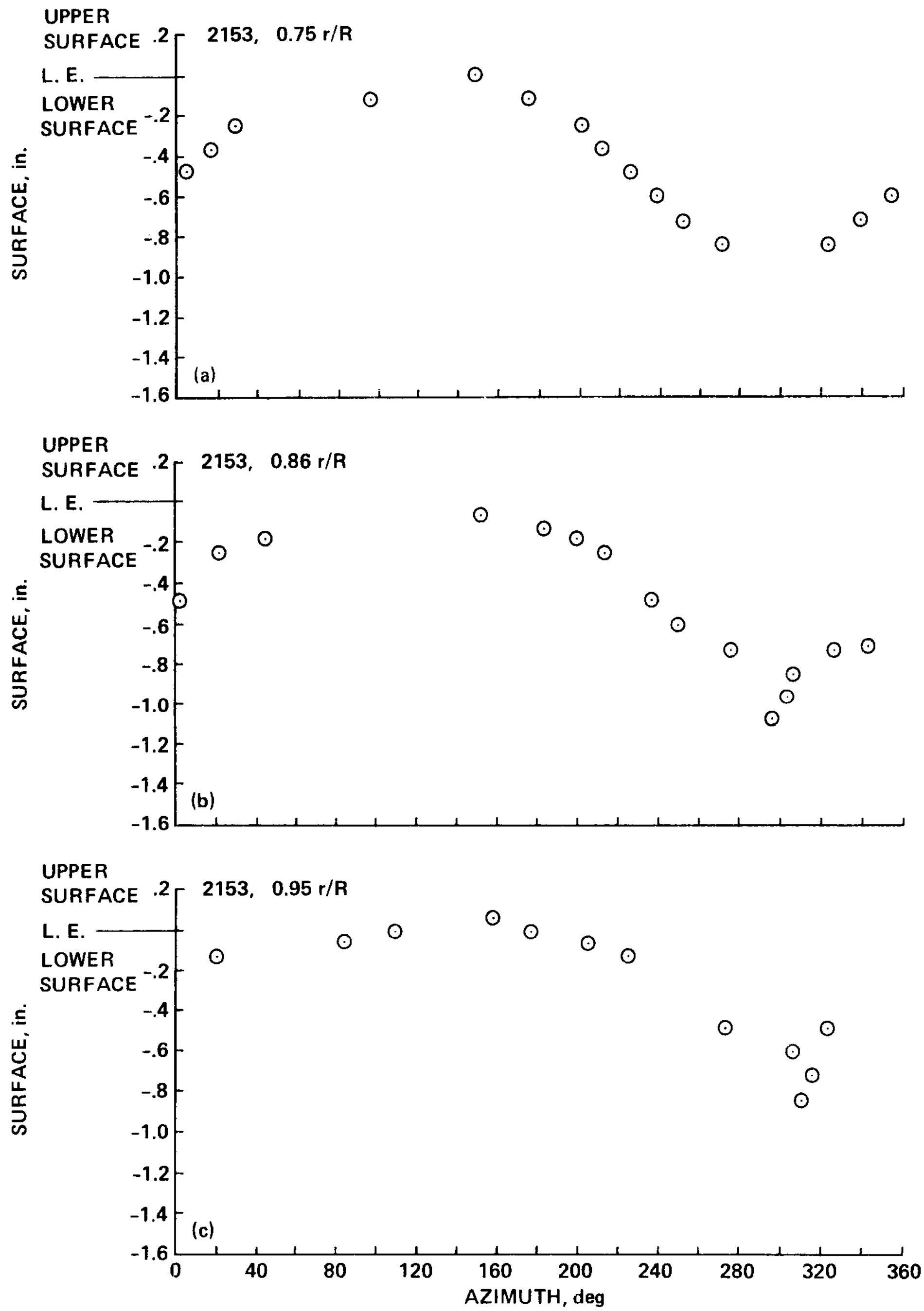

Figure 104.- Hot-wire stagnation point versus azimuth at 146 KTAS. (a) 75% radius; (b) 86% radius; (c) 96% radius.

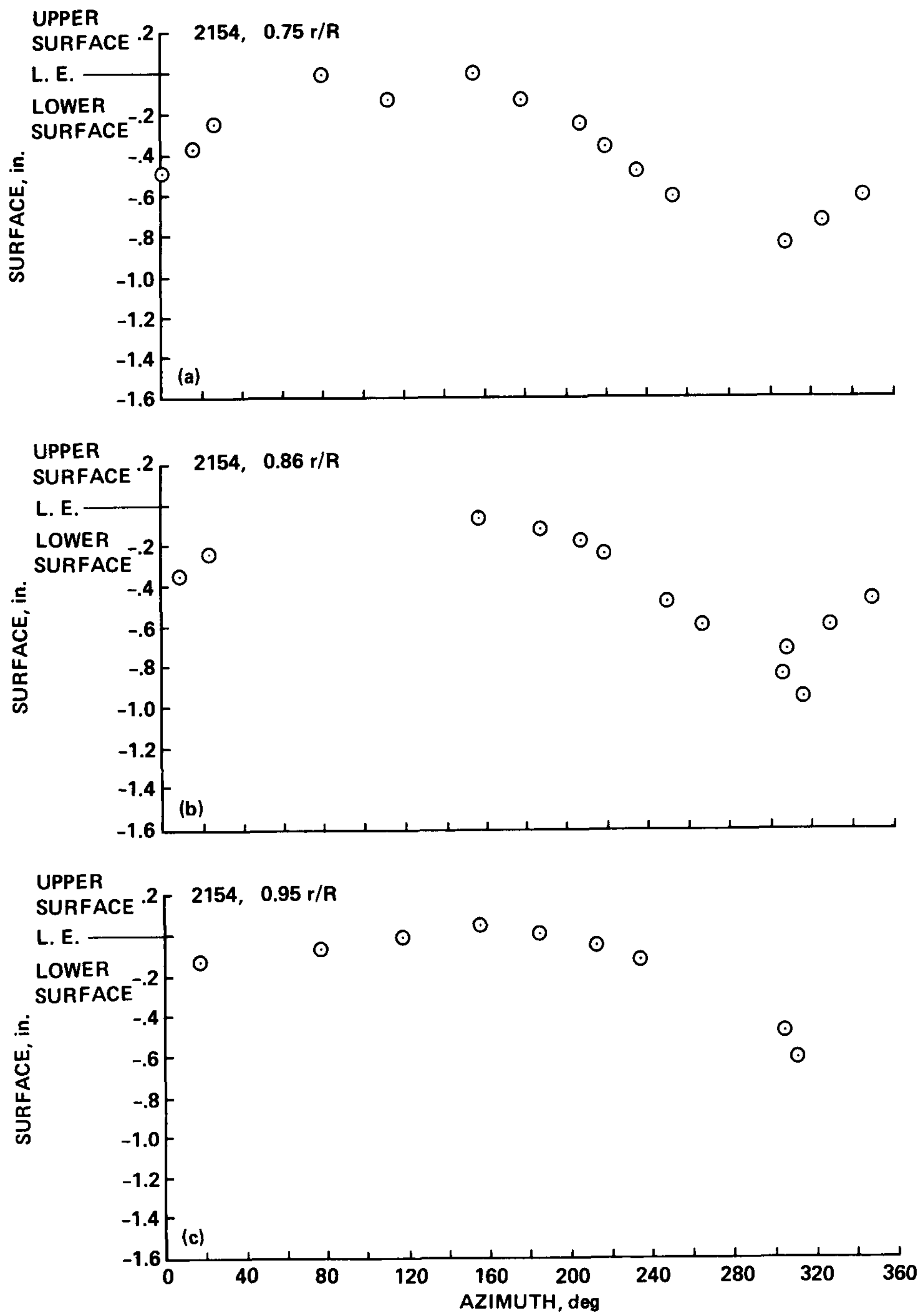

Figure 105.- Hot-wire stagnation point versus azimuth at 129 KTAS. (a) 75% radius; (b) 86% radius; (c) 96% radius.

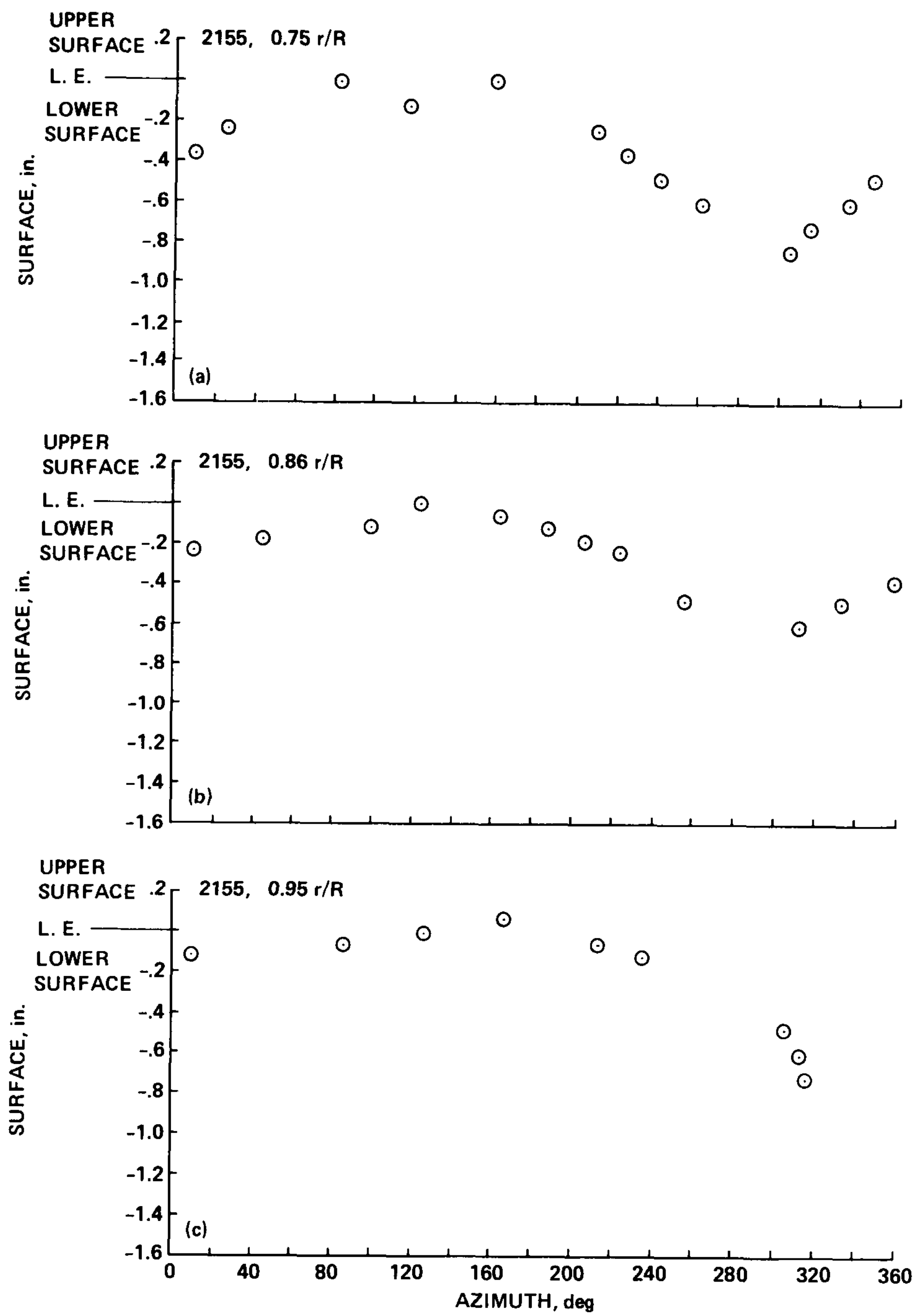

Figure 106.- Hot-wire stagnation point versus azimuth at 116 KTAS. (a) 75% radius; (b) 86% radius; (c) 96% radius.

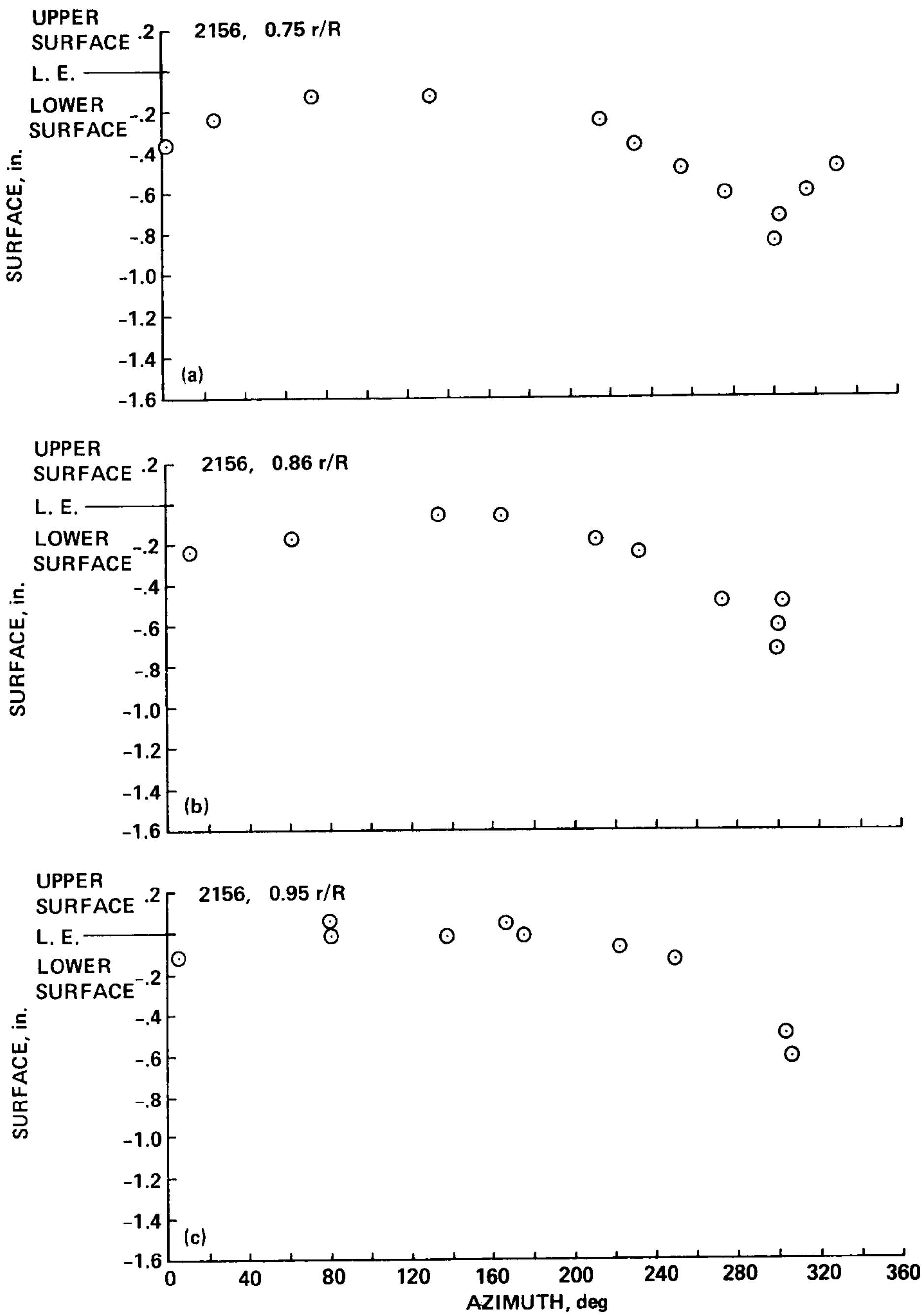

Figure 107.- Hot-wire stagnation point versus azimuth at 98 KTAS. (a) 75% radius, (b) 86% radius, (c) 96% radius.

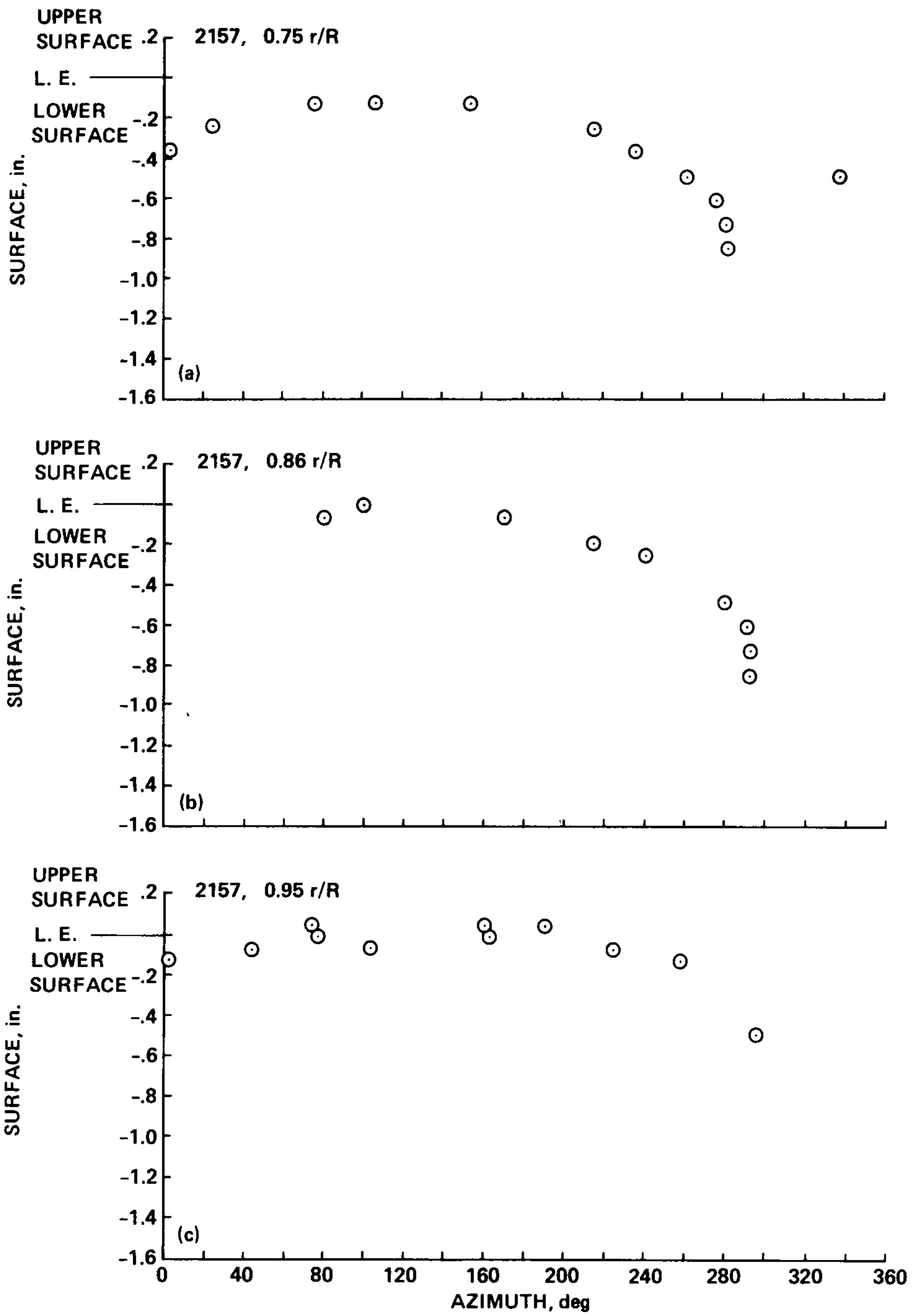

Figure 108.- Hot-wire stagnation point versus azimuth at 82 KTAS. (a) 75% radius, (b) 86% radius; (c) 96% radius.

ORIGINAL PAGE IS
OF POOR QUALITY

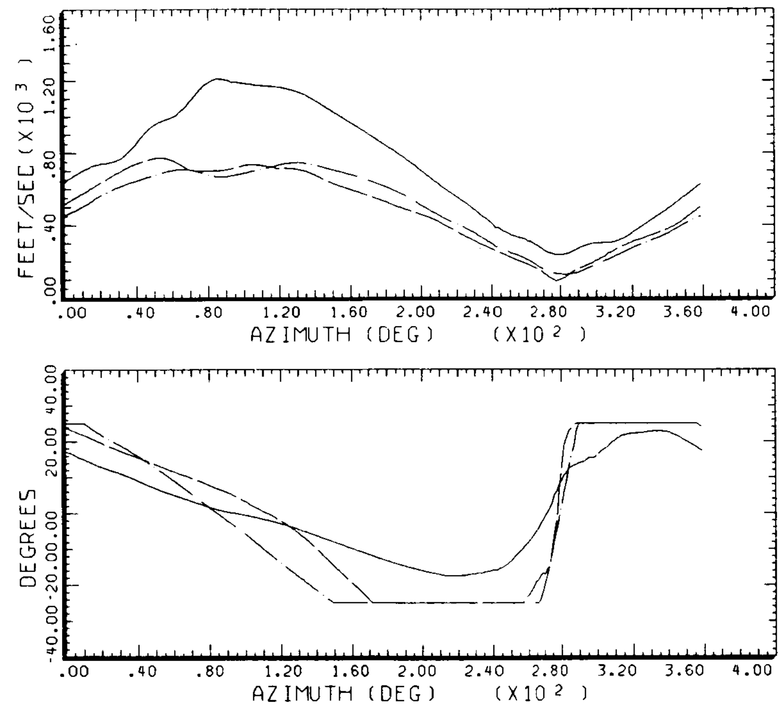

STRAIGHT AND LEVEL, 159 KNOTS, TOP SURFACE

CYCLE AVERAGE: BOUNDARY LAYER FLOW MAGNITUDE

COUNTER .75 2152 R/RADIUS GROSS WT LONG CG SHIP MODEL SHIP ID AH-1G 20004

.30 X/CHORD
.60 X/CHORD
.90 X/CHORD

DATAMAP (VERS 4.0 - 09/01/86) 23SEP'86 NASA ARC

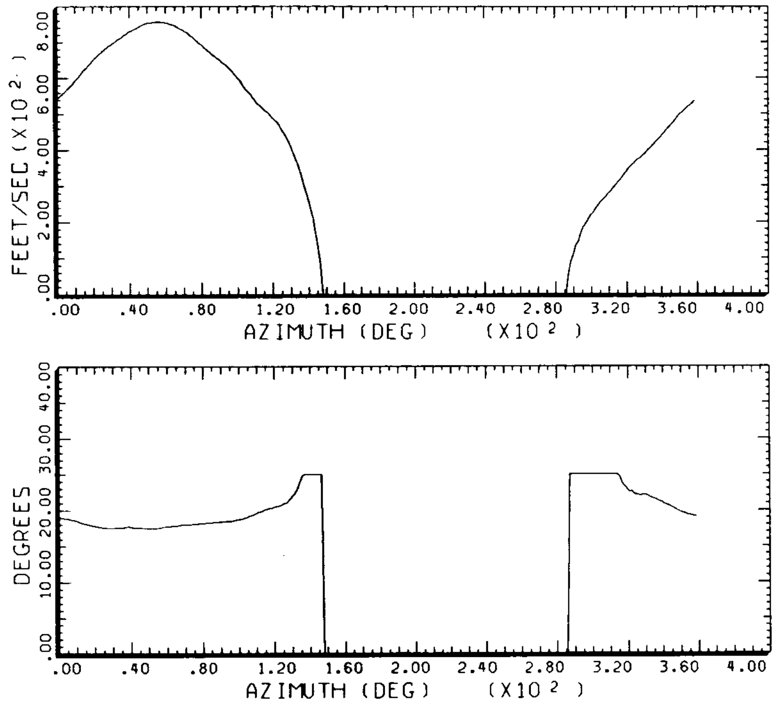

STRAIGHT AND LEVEL, 159 KNOTS, BOTTOM SURFACE

CYCLE AVERAGE: BOUNDARY LAYER FLOW MAGNITUDE

COUNTER .75 2152 R/RADIUS GROSS WT LONG CG SHIP MODEL SHIP ID AH-1G 20004

.60 X/CHORD

DATAMAP (VERS 4.0 - 09/01/86) 23SEP'86 NASA ARC

Figure 109.- At 159 KTAS, 75% radius, BLB flow magnitude and direction.

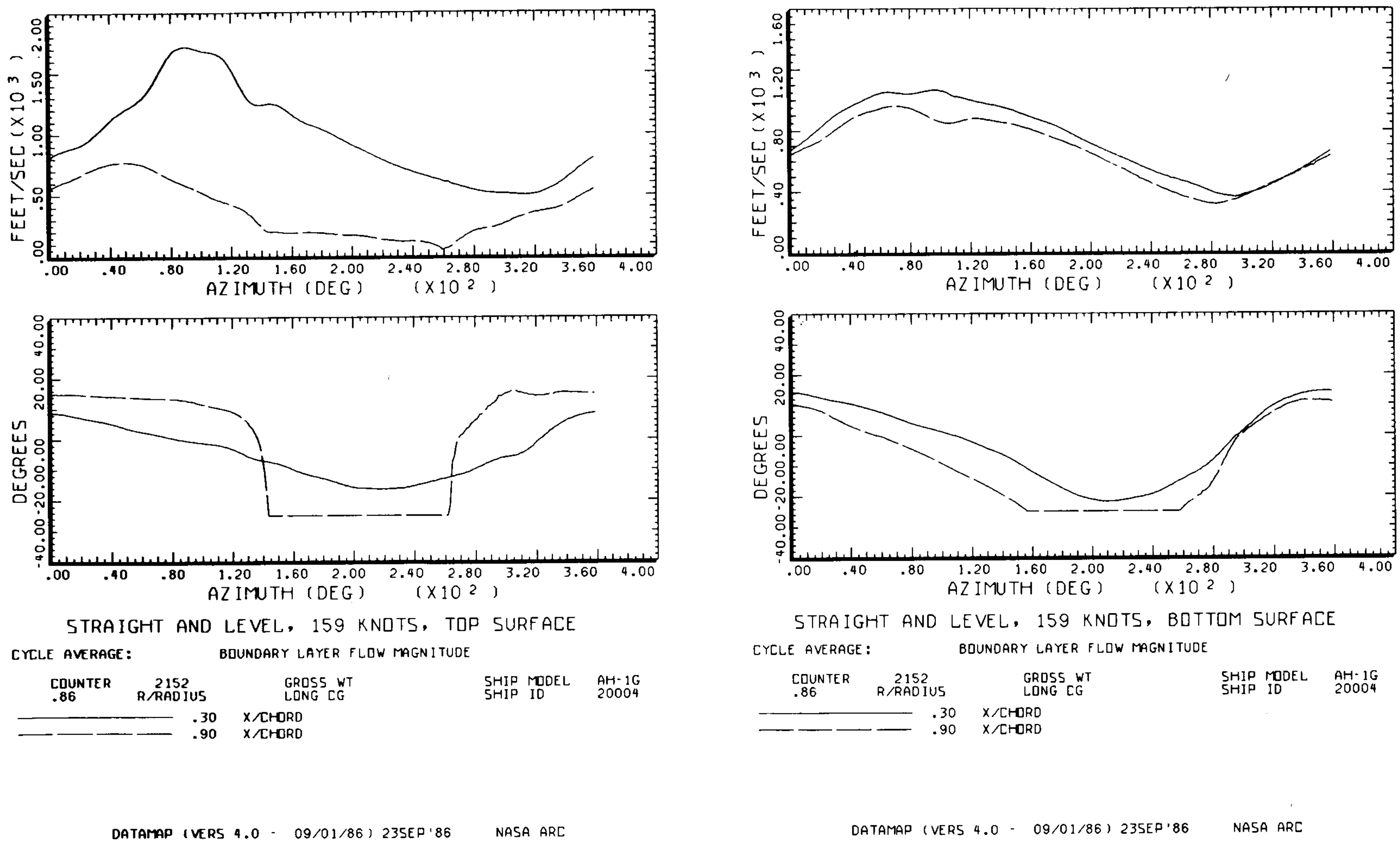

Figure 110.- At 159 KTAS, 86% radius, BLB flow magnitude and direction.

ORIGINAL PAGE IS
OF POOR QUALITY

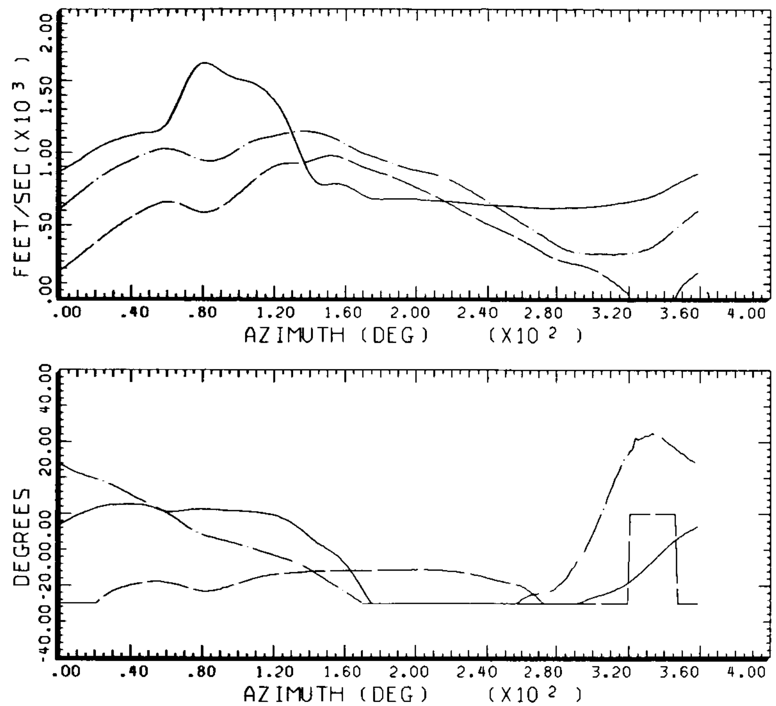

STRAIGHT AND LEVEL, 159 KNOTS, TOP SURFACE

CYCLE AVERAGE: BOUNDARY LAYER FLOW MAGNITUDE

COUNTER .96 2152 R/RADIUS GROSS WT LONG CG SHIP MODEL SHIP ID AH-1G 20004

.30 X/CHORD
.60 X/CHORD
.90 X/CHORD

DATAMAP (VERS 4.0 - 09/01/86) 23SEP'86 NASA ARC

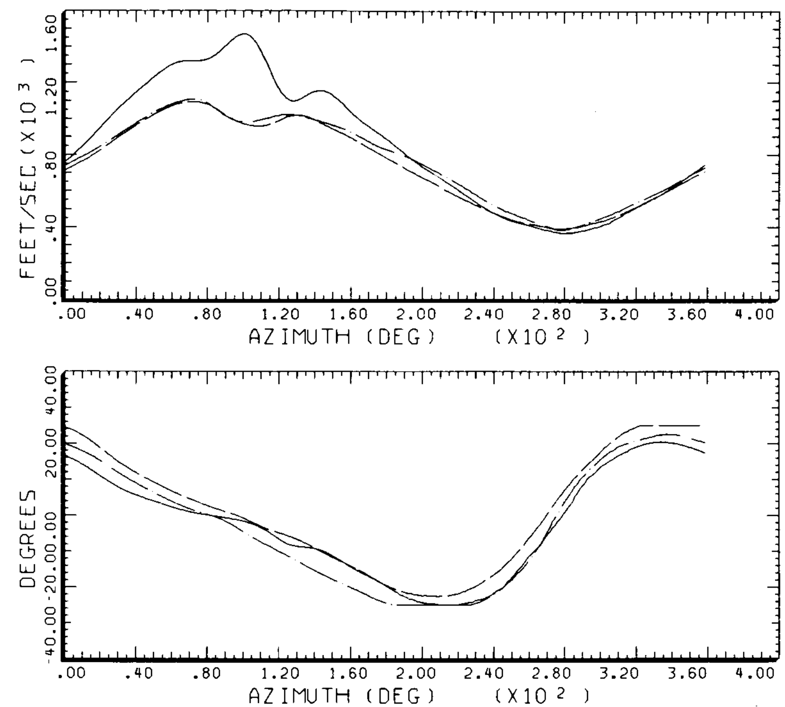

STRAIGHT AND LEVEL, 159 KNOTS, BOTTOM SURFACE

CYCLE AVERAGE: BOUNDARY LAYER FLOW MAGNITUDE

COUNTER .96 2152 R/RADIUS GROSS WT LONG CG SHIP MODEL SHIP ID AH-1G 20004

.30 X/CHORD
.60 X/CHORD
.90 X/CHORD

DATAMAP (VERS 4.0 - 09/01/86) 23SEP'86 NASA ARC

Figure 111.- At 159 KTAS, 95% radius, BLB flow magnitude and direction.

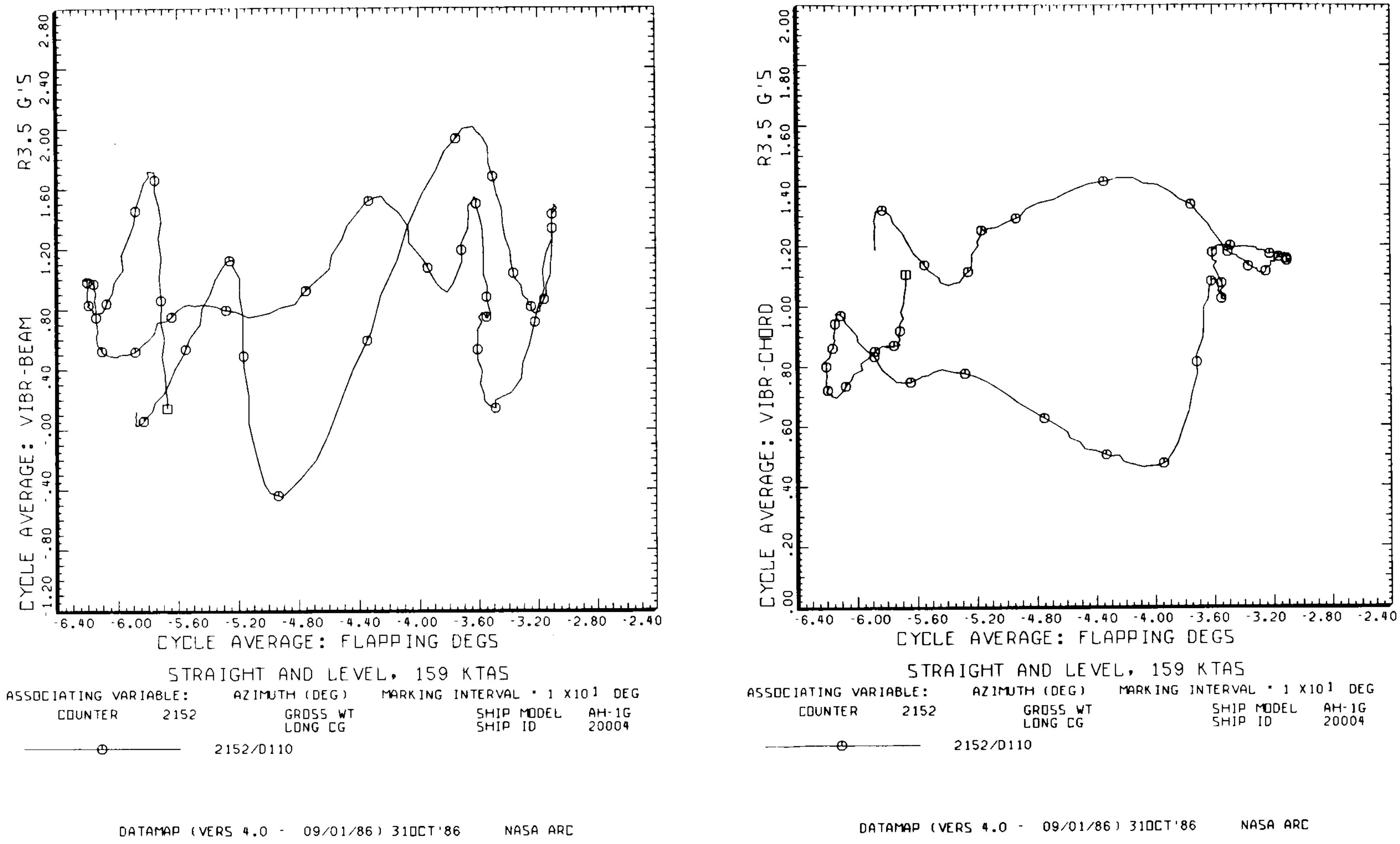

Figure 112.- Acceleration flapping crossplot at 1% radius.

ORIGINAL PAGE IS
OF POOR QUALITY

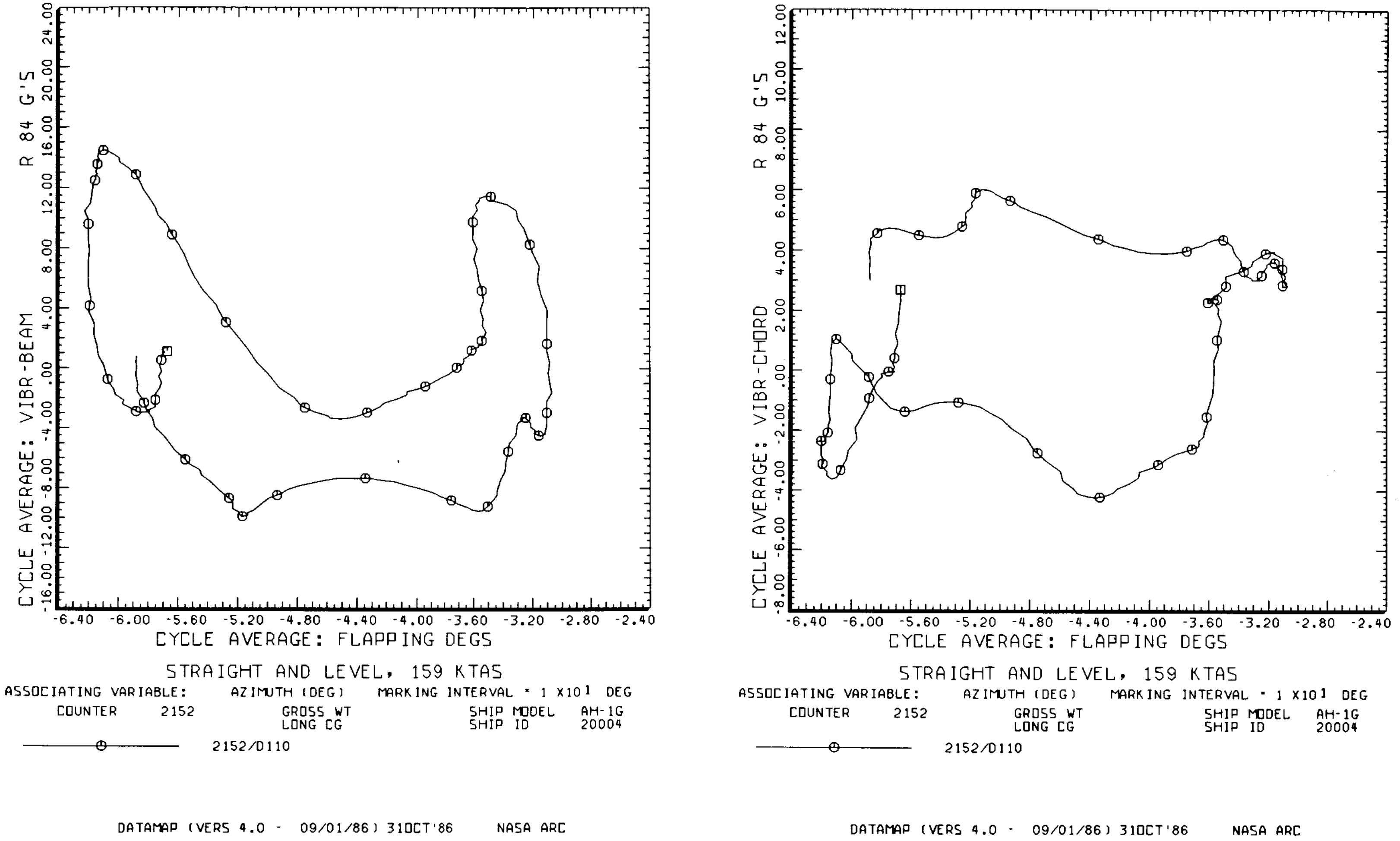

Figure 113.- Acceleration flapping crossplot at 50% radius. (a) Beamwise; (b) chordwise.

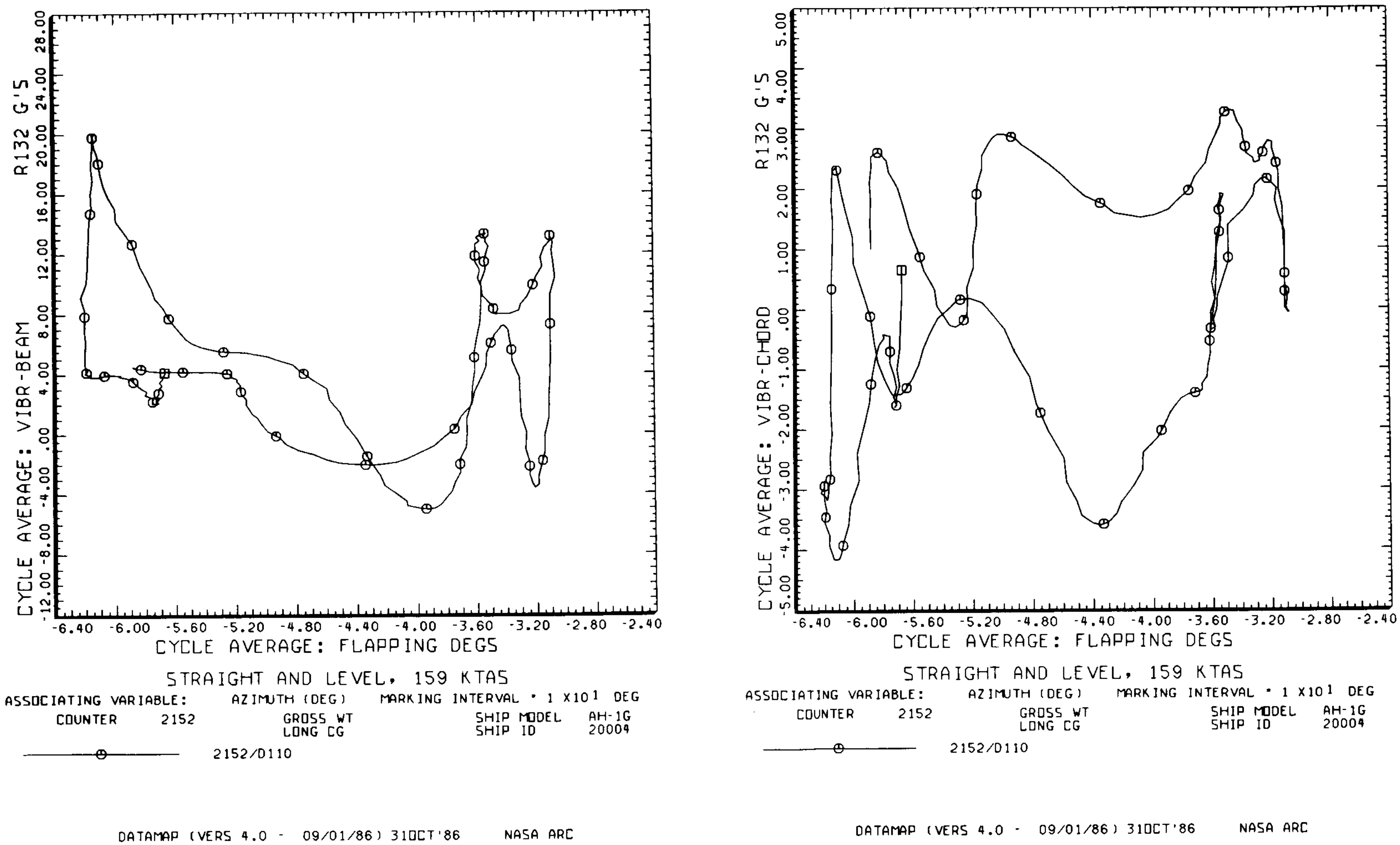

Figure 114.- Acceleration flapping crossplot at 59% radius. (a) Beamwise; (b) chordwise.

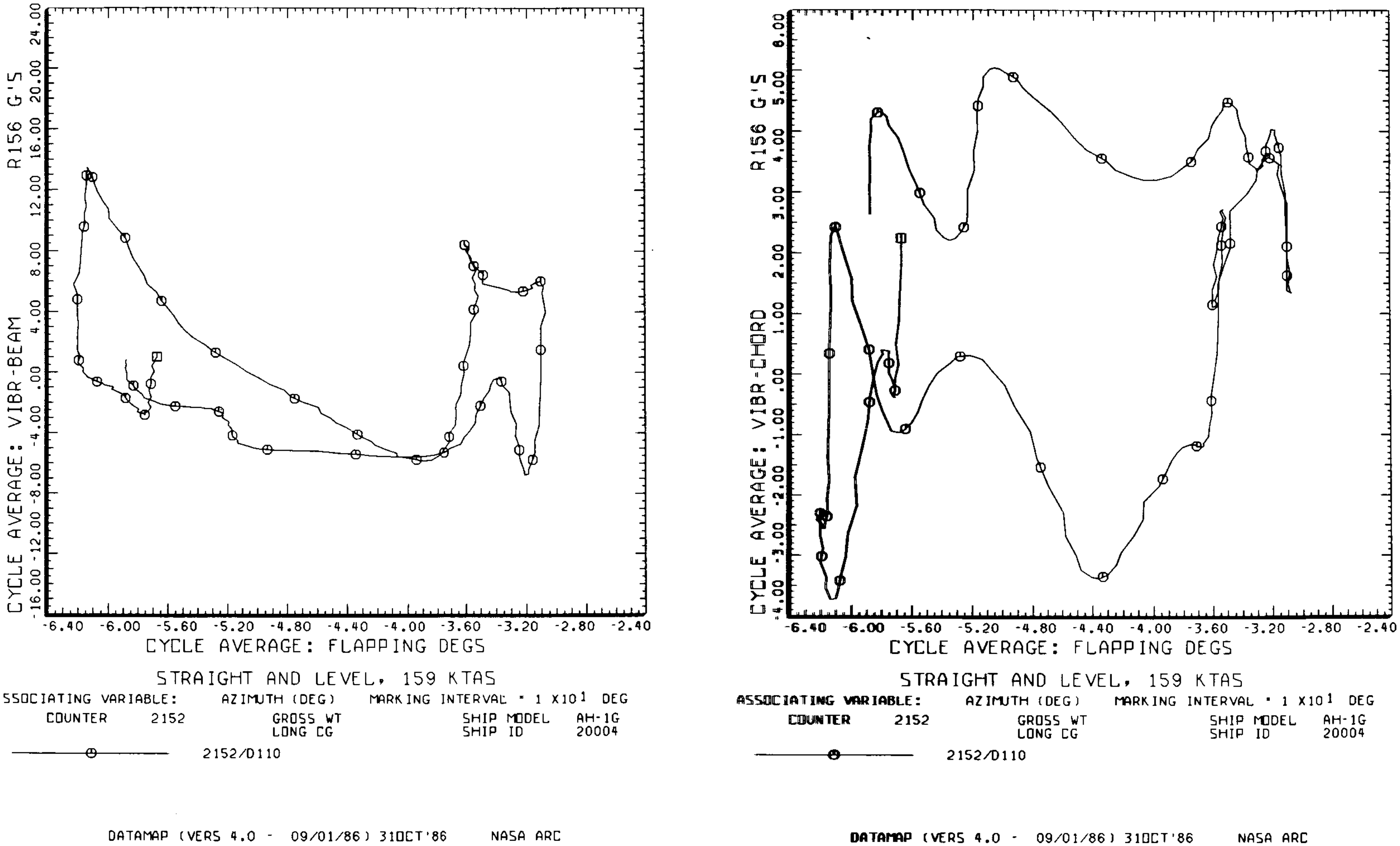

Figure 115.- Acceleration flapping crossplot at 70% radius. (a) Beamwise; (b) chordwise.

ORIGINAL PAGE IS
OF POOR QUALITY

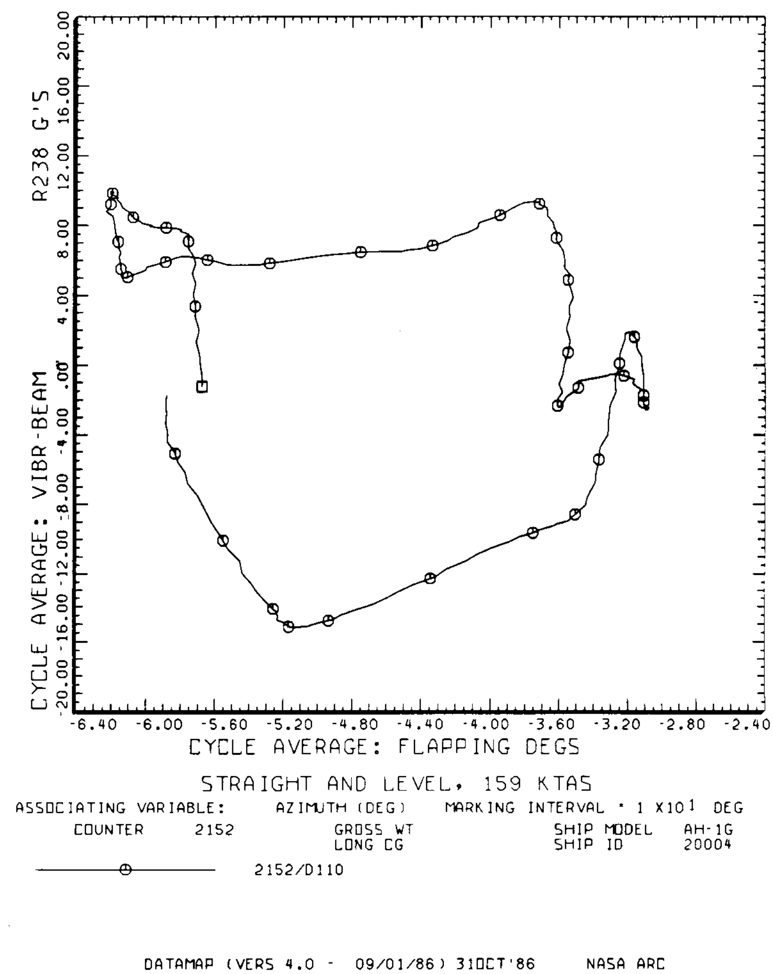

Figure 116.- Acceleration flapping crossplot at 90% radius.

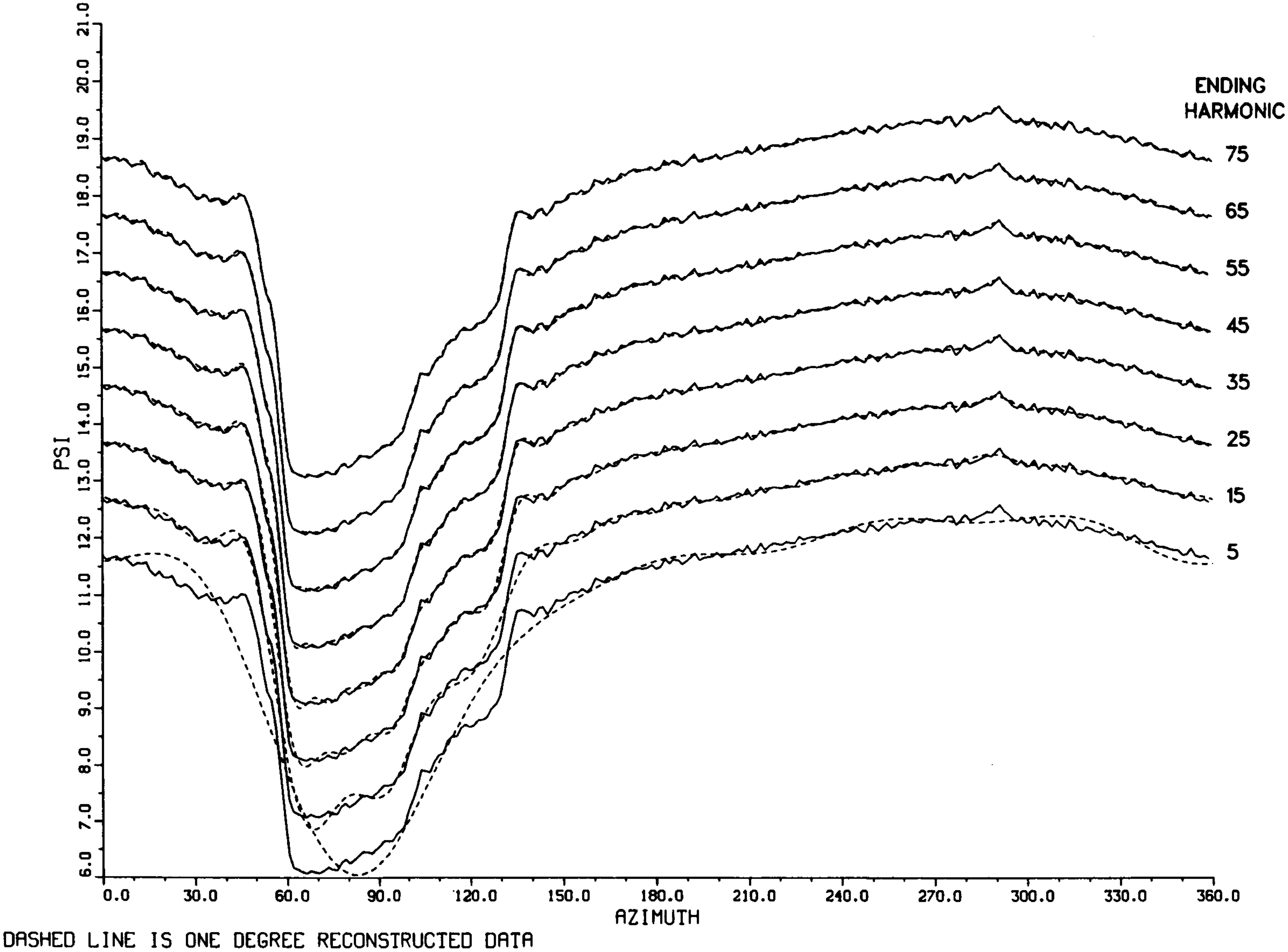

Figure 117.- At 159 KTAS, comparison of harmonic content with time history.

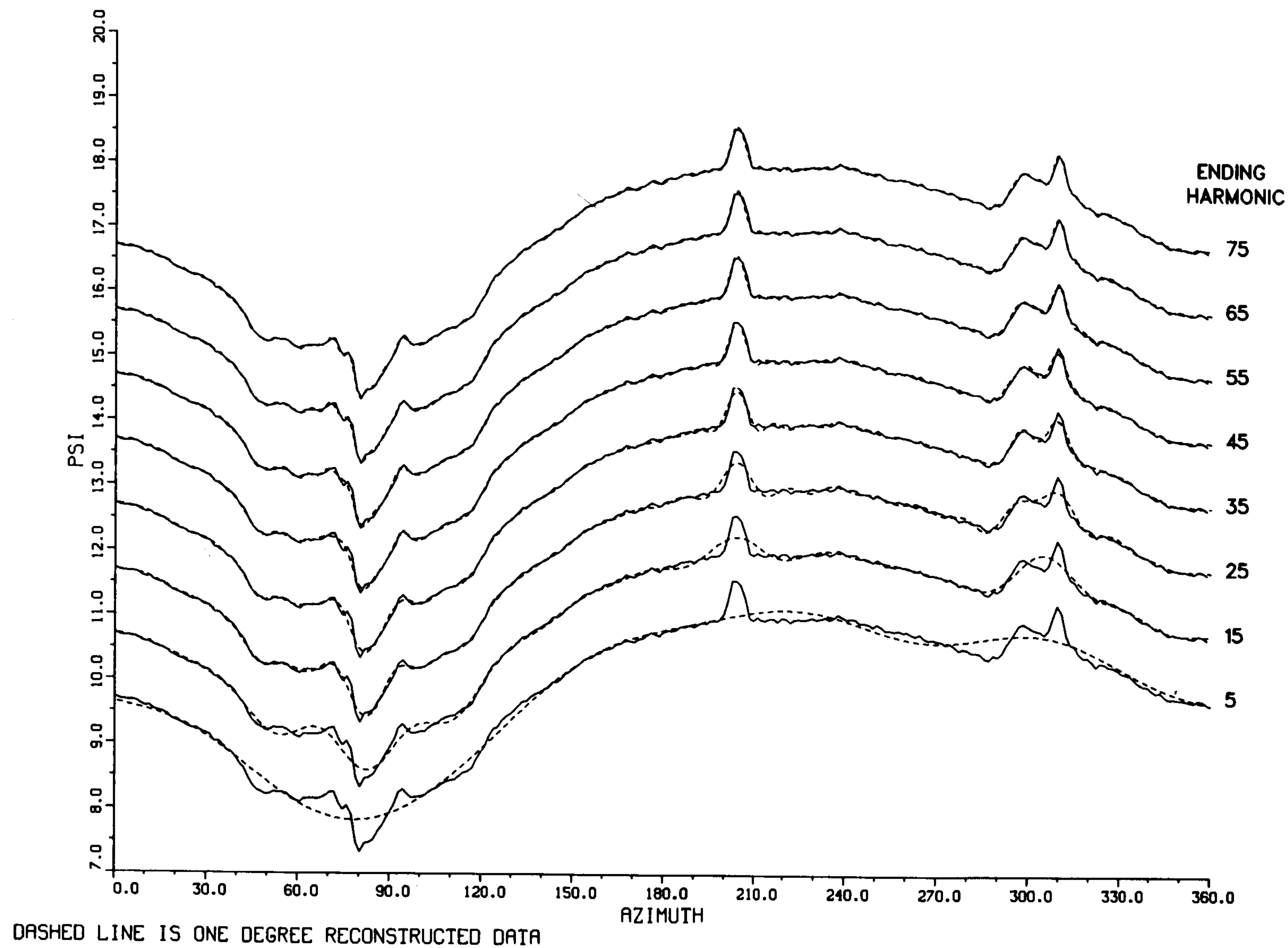

Figure 118.- At 82 KTAS, comparison of harmonic content with time history.

NASA
National Aeronautics and Space Administration

Report Documentation Page

1. Report No.	2. Government Accession No.	3. Recipient's Catalog No.
NASA RP-1179		

4. Title and Subtitle	5. Report Date
Tip Aerodynamics and Acoustics Test--A Report and Data Survey	December 1988
	6. Performing Organization Code
7. Author(s)	8. Performing Organization Report No.
Jeffrey L. Cross and Michael E. Watts	A-87128
	10. Work Unit No. 505-61-51
9. Performing Organization Name and Address Ames Research Center Moffett Field, CA 94035	11. Contract or Grant No.
	13. Type of Report and Period Covered Reference Publication
12. Sponsoring Agency Name and Address National Aeronautics and Space Administration Washington, DC 20546-0001	14. Sponsoring Agency Code

15. Supplementary Notes

Point of Contact: Jeffrey Cross, Ames Research Center, MS 237-5
Moffett Field, CA 94035 (415) 694-6571 or FTS 464-6571

16. Abstract

In a continuing effort to understand helicopter rotor tip aerodynamics and acoustics, a flight test was conducted by NASA Ames Research Center. The test was performed using the NASA White Cobra and a set of highly instrumented blades. All aspects of the flight test instrumentation and test procedures will be explained. Additionally, complete data sets for selected test points will be presented and analyzed. Because of the high volume of data acquired, only selected data points can be presented here. However, access to the entire data set is available to the researcher upon request.

17. Key Words (Suggested by Author(s))	18. Distribution Statement
Helicopter flight test AH-1g YO-3A Rotor airloads Rotor aerodynamics	Unclassified-Unlimited Subject Category - 02

19. Security Classif. (of this report)	20. Security Classif. (of this page)	21. No. of pages	22. Price
Unclassified	Unclassified	468	A20

NASA FORM 1626 OCT 86

☆U.S. GOVERNMENT PRINTING OFFICE:1989 -627-064/86012